

Some pages of this thesis may have been removed for copyright restrictions.

If you have discovered material in AURA which is unlawful e.g. breaches copyright, (either yours or that of a third party) or any other law, including but not limited to those relating to patent, trademark, confidentiality, data protection, obscenity, defamation, libel, then please read our [Takedown Policy](#) and [contact the service](#) immediately

COST AND PERFORMANCE ANALYSIS OF NEW WOOD-FUELLED
POWER PLANT CONCEPTS

YRJÖ OLAVI SOLANTAUSTA

Doctor of Philosophy

The University of Aston in Birmingham

May 2000

This copy of the thesis has been supplied on condition that anyone who consults it is understood to recognise that its copyright rests with its author and that no information derived from it may be published without proper acknowledgement.

The University of Aston in Birmingham

**COST AND PERFORMANCE ANALYSIS OF NEW WOOD-FUELLED
POWER PLANT CONCEPTS**

YRJÖ OLAVI SOLANTAUSTA

Doctor of Philosophy

2000

SUMMARY

The objective of the thesis was to analyse several process configurations for the production of electricity from biomass. Process simulation models using AspenPlus aimed at calculating the industrial performance of power plant concepts were built, tested, and used for analysis. The criteria used in analysis were performance and cost.

All of the advanced systems appear to have higher efficiencies than the commercial reference, the Rankine cycle. However, advanced systems typically have a higher cost of electricity (COE) than the Rankine power plant. High efficiencies do not reduce fuel costs enough to compensate for the high capital costs of advanced concepts.

The successful reduction of capital costs would appear to be the key to the introduction of the new systems. Capital costs account for a considerable, often dominant, part of the cost of electricity in these concepts. All of the systems have higher specific investment costs than the conventional industrial alternative, i.e. the Rankine power plant. Combined heat and power production (CHP) is currently the only industrial area of application in which bio-power costs can be considerably reduced to make them competitive.

Based on the results of this work, AspenPlus is an appropriate simulation platform. However, the usefulness of the models could be improved if a number of unit operations were modelled in greater detail. The dryer, gasifier, fast pyrolysis, gas engine and gas turbine models could be improved.

DEDICATION

To Kirsti and Erkki

ACKNOWLEDGMENTS

I wish to acknowledge my family, Anja, Anna and Sampo, from whom the time to prepare this work was taken. This was a long journey, and I could never have completed it without the invaluable guidance and encouragement of Professor A.V. Bridgwater, a most pleasant and patient tutor. I also wish to acknowledge my employer VTT, and especially Kai Sipilä, who arranged financial support. The IEA Bioenergy and colleagues from several IEA projects should be acknowledged for financial and professional support. Many thanks are due to Björn Kjellström, Doug C. Elliott, Anders Östman, Dave Beckman, Jim Diebold, and Pat McKeough for their excellent advice and company. I also thank Esa Kurkela, Tiina Koljonen, and Tuula Mäkinen for the help with the gasification and pyrolysis models, and Richard Walker and Maija Korhonen for their practical help with the manuscript.

Helsinki, December 1999

Yrjö Solantausta

TABLE OF CONTENTS

SUMMARY.....	3
DEDICATION.....	4
ACKNOWLEDGMENTS	5
TABLE OF CONTENTS.....	6
LIST OF FIGURES	12
LIST OF TABLES.....	21
1. INTRODUCTION	24
1.1 Bioenergy	24
1.2 Markets for bioenergy	24
1.3 Electricity production.....	30
1.4 Proposed feasible production scales.....	33
1.5 Electricity from biomass, process concepts	34
1.5.1 Rankine cycle.....	36
1.5.2 Integrated Gasification Combined Cycle	37
1.5.3 Gasification and an internal combustion engine	37
1.5.4 Fast pyrolysis and engines	38
1.6 Development of biomass to electricity concepts.....	39
1.7 Bases for this work.....	41
1.8 Structure of the thesis.....	41
2 REVIEW OF PREVIOUS ASSESSMENTS ON ELECTRICITY FROM BIOMASS... 44	
2.1 Review criteria	44
2.2 Electricity from biomass based on the Rankine cycle.....	46
2.2.1 Introduction.....	47
2.2.2 Power production efficiency	50
2.2.2.1 Ekono Energy	50
2.2.2.2 Other work.....	53
2.2.3 Power plant investment cost.....	55
2.2.3.1 Ekono Energy	55
2.2.3.2 Other work.....	58
2.2.4 Cost of electricity.....	61
2.2.4.1 Ekono Energy	61
2.2.4.2 Other work.....	65
2.3 Electricity from biomass based on gasification	68
2.3.1 Introduction	68
2.3.2 Power production efficiency	70
2.3.2.1 Enviropower - Carbona	70
2.3.2.2 National Renewable Energy Laboratories (NREL).....	71
2.3.2.3 Princeton University	73
2.3.2.4 Electric Power Research Institute (EPRI)	76
2.3.2.5 IEA Bioenergy - Interfacing Activity	77
2.3.2.6 Aston University.....	79
2.3.2.7 University of Ulster	80
2.3.2.8 ECN - University of Utrecht.....	82
2.3.2.9 IEA Bioenergy - Pyrolysis Activity, 1992 - 1994	83
2.3.3 Gasification power plant investment costs	84

2.3.3.1	Enviropower - Carbona.....	85
2.3.3.2	NREL.....	86
2.3.3.3	Princeton University.....	87
2.3.3.4	EPRI.....	88
2.3.3.5	IEA Bioenergy Interfacing Activity.....	89
2.3.3.6	Aston University.....	89
2.3.3.7	University of Ulster.....	90
2.3.3.8	University of Utrecht.....	91
2.3.4	Cost of electricity.....	92
2.3.4.1	Enviropower - Carbona.....	92
2.3.4.2	NREL.....	93
2.3.4.3	Princeton University.....	94
2.3.4.4	Electric Power Research Institute (EPRI).....	95
2.3.4.5	IEA Bioenergy - Interfacing Activity.....	96
2.3.4.6	Aston University.....	96
2.3.4.7	University of Ulster.....	97
2.3.4.8	University of Utrecht.....	97
2.4	Electricity from biomass based on fast pyrolysis.....	98
2.4.1	Introduction.....	99
2.4.2	Power production efficiency.....	100
2.4.2.1	VTT Energy.....	100
2.4.2.2	IEA Bioenergy Interfacing Activity.....	101
2.4.2.3	Aston University.....	101
2.4.2.4	Institute Pyrovac Inc.....	102
2.4.3	Pyrolysis power plant investment cost.....	103
2.4.3.1	IEA Bioenergy Interfacing Activity.....	103
2.4.3.2	Aston University.....	103
2.4.3.3	Institute Pyrovac Inc.....	104
2.4.4	Cost of electricity.....	104
2.4.4.1	VTT Energy.....	104
2.4.4.2	IEA Bioenergy Interfacing Activity.....	104
2.4.4.3	Aston University.....	105
2.5	Summary.....	105
2.5.1	Tools and methods applied.....	105
2.5.1.1	General.....	105
2.5.1.2	Specific models developed for critical units.....	107
2.5.1.3	General-purpose modelling software.....	107
2.5.1.4	Spreadsheets.....	109
2.5.2	Summary of system efficiencies.....	109
2.5.3	Summary of capital costs.....	112
2.5.4	Summary of cost of electricity.....	114
2.6	Objectives of the thesis.....	116
3	MODELLING.....	120
3.1	Approach.....	120
3.2	Simulation tools.....	120
3.3	AspenPlus™.....	121
3.4	Bio-power models.....	125
3.5	Outcome of the models.....	125

4. STEAM CYCLES.....	127
4.1 Introduction	127
4.2 Model description of a Rankine boiler steam cycle	127
4.3 Model description of a steam cycle as part of a combined cycle	131
4.4 Using the Aspen model to study the performance of a boiler power plant.....	135
4.4.1 Flue gas final temperature.....	136
4.4.2 Steam turbine back-pressure	136
4.4.3 Excess combustion air.....	137
4.4.4 Steam conditions.....	138
4.4.5 Summary	139
4.4.6 Comparison of the model results with industrial data.....	140
4.5 Using the Aspen model to study the performance of the steam cycle of a combined cycle	141
4.5.1 Moisture at steam turbine exit.....	142
4.5.2 Steam cycle performance	143
4.5.3 Superheater investment cost.....	143
5. DRYING OF BIOMASS	146
5.1 Introduction	146
5.2 Drying equipment for woody biomass.....	147
5.3 Dryer performance	150
5.4 Dryer emissions.....	152
5.5 Conclusions as bases for the model design.....	153
5.6 Description of the models	154
5.6.1 Flue gas dryer.....	155
5.6.2 Steam dryer	157
6. FLUIDIZED-BED GASIFICATION OF BIOMASS	161
6.1 Introduction.....	161
6.2 State-of-the-art	161
6.3 Review of modelling of gasification.....	162
6.3.1 Biomass gasification	162
6.3.2 Coal gasification models with Aspen (MIT, METC)	164
6.3.2.1 MIT.....	164
6.3.2.2 Work supporting the GPGP	166
6.3.2.3 METC.....	167
6.3.3 Testing of the departure-from-equilibrium model	169
6.4 Description of the model developed in this work	171
6.4.1 Approach.....	171
6.4.2 Description of the semi-empirical model designed.....	171
6.4.3 Testing and verification of the model	173
7. FAST PYROLYSIS OF BIOMASS	176
7.1 Introduction.....	176
7.2 State-of-the-art	176
7.3 Review of modelling the fast pyrolysis of biomass	178
7.3.1 IEA Bioenergy - BLTF, DBL, and ALPS.....	178
7.3.2 WFPP - Black.....	180
7.3.3 Science International - Wan.....	180
7.3.4 Ensyn Technologies Inc - Zeton Inc	181
7.3.5 Aston University - IEA Bioenergy.....	181

7.3.6 NREL	182
7.4 Model development in this work.....	182
7.4.1 Biomass fast pyrolysis liquids.....	183
7.4.2 Calculation of physical properties in pyrolysis.....	184
7.4.3 Model description	185
7.4.4 Fast pyrolysis performance	188
7.4.5 An example of using the performance model	189
8. GAS TURBINE	191
8.1 Introduction.....	191
8.2 Gas turbine in an IGCC.....	192
8.3 Low-heating-value gas in gas turbines.....	193
8.3.1 Engines proposed	194
8.3.2 Technical uncertainties.....	195
8.3.3 Steam injection.....	199
8.4 State-of-the-art of gas turbine operation with pyrolysis liquid	199
8.4.1 Teledyne CAE.....	200
8.4.2 Orenda Corporation.....	200
8.5 Modelling of gas turbines with low heating value gas.....	200
8.5.1 Introduction.....	201
8.5.2 Review of previous work	205
8.5.2.1 Stanford University - GATE/CYCLE	205
8.5.2.2 METC	206
8.5.2.3 Princeton University	208
8.5.2.4 Enter Software - GATE/CYCLE.....	208
8.6 The gas turbine model built for this work.....	208
8.6.1 Model description	208
8.6.2 Model features.....	211
8.6.3 Summary	216
8.7 The gas turbine model using fast pyrolysis liquid	216
9. INTERNAL COMBUSTION ENGINES	217
9.1 Introduction.....	217
9.2 Using LHV gas as fuel in combustion engines	219
9.3 Using pyrolysis liquid as fuel in diesel engines.....	221
9.4 Model description for a gas engine using LHV gas.....	222
9.5 Model description for a diesel engine using pyrolysis liquid	224
9.6 Summary	225
10. RESULTS OF THE PERFORMANCE ANALYSIS	226
10.1 Introduction.....	226
10.2 Description of an IGCC model	227
10.3 Bases for the analysis	232
10.4 Pressurised gasification combined-cycle, concepts 1-4 (PCC).....	233
10.5 Atmospheric pressure gasification combined-cycle, concepts 5 - 8 (ACC).....	236
10.6 Pressurised gasification steam-injected gas turbine cycles, concepts 9 - 13 (STIG).....	238
10.7 Gasification internal combustion engine concepts 14 - 15 (GE)	241
10.8 Fast pyrolysis of biomass.....	243
10.9 Pyrolysis liquid - diesel engine, concepts 16 - 17 (PD)	244
10.10 Pyrolysis liquid - combined-cycles, concepts 18 - 21 (PyCC).....	246
10.11 The Rankine steam boiler power plant.....	248

10.12	Summary of power plant performance	249
10.13	Uncertainties in performance estimation.....	256
10.13.1	Gasification engine power plant concept	256
10.13.2	Pyrolysis power plants	258
10.14	Potential improvements in IGCC concepts.....	260
10.15	Performance of advanced co-generation power plants.....	265
10.15.1	Significance of co-generation of heat and electricity.....	265
10.15.2	Advanced co-generation concepts.....	267
10.15.3	Significance of dryer type in co-generation	270
10.16	Summary	270
11.	DETERMINATION OF CAPITAL COST AND CONTINGENCY.....	272
11.1	Introduction.....	273
11.2	Capital cost contingency	276
11.2.1	Definition	276
11.2.2	Cost growth and contingency in investment cost estimation.....	277
11.2.3	Review of methods used to estimate contingency	279
11.2.4	Cost growth and the model used for contingency.....	281
11.3	Potential for cost improvement	283
11.4	Capital costs estimated for this work	286
11.4.1	Base capital cost investment estimates	286
11.4.2	Contingency and cost improvement in cost estimates	289
11.5	Summary	292
12.1	Electricity production modes	294
12.2	Calculation of COE.....	295
12.3	Bases for operating costs.....	297
12.3.1	Feedstock	297
12.3.2	Labour	298
12.3.3	Utilities.....	298
12.3.4	Maintenance and insurance	299
12.3.5	District heat.....	299
12.4	Production cost of fast pyrolysis liquid.....	299
12.5	Cost of electricity (COE)	302
12.5.1	Summary	303
12.5.2	Gasification and pyrolysis.....	306
12.5.3	Small, medium, and large scale	309
12.5.4	Annual operating time.....	311
12.5.5	Fuel cost	315
12.5.6	Rate of interest and contingency	323
12.5.7	Combined heat and power (CHP)	326
12.5.8	Scale of pyrolysis liquid production	328
12.6	Examples of using the cost and performance models in an industrial evaluation	330
13.	CONCLUSIONS	334
13.1	Modelling.....	334
13.2	Technologies studied.....	337
13.3	Further modelling work.....	342
13.4	Use of the models prepared.....	344
	REFERENCES	345

APPENDICES

1. Deriving the correlations for the steam dryer	365
2. AspenPlus input file for the steam dryer	373
3. AspenPlus input file for a steam boiler power plant	376
4. Testing of the departure from equilibrium model	384
5. AspenPlus input file for the gasifier	389
6. Physical property calculation for pyrolysis	395
7. AspenPlus input file for the pyrolyser	399
8. AspenPlus input file for the gas turbine	410
9. AspenPlus input file for an internal combustion engine	412
10. Basis for estimating capital investment costs	417
11. The capital investment costs estimated	423
12. Testing of the METC gas turbine model	424
13. AspenPlus flow diagram and the input file for an IGCC plant	426
14. An example of building an AspenPlus model	435
15. Solantausta, Y., Bridgwater, A., Beckman, D., Feasibility of power production with pyrolysis and gasification systems	446

LIST OF FIGURES

Figure 1-1. World primary energy production in 1980 and 1990, and four scenarios for the year 2020 /3/. CW conventional wisdom, BF battlefield, CO co-operation, HM hypermarket.

Figure 1-2. European Union primary energy production by the year 2020, conventional wisdom scenario /3/.

Figure 1-3. Average growth rates of different energy sources in world primary energy production over the years 1990 - 2020, average of four scenarios /3/.

Figure 1-4. A scenario for future energy sources, presented by Shell /2/.

Figure 1-5. A scenario for renewable energy, estimated from the data in Figure 1-4.

Figure 1-6. Number of potential power plants by 2025 according to the type of biomass fuel /1/. Data in reference is based on /7/.

Figure 1-7. Potential number of 50 MWe IGCC plants within the pulp and paper industry in 1993 based on residue availability.

Figure 1-8. Global potential number of biomass power plants by 2025 /20/.

Figure 1-9. Process configurations studied. A thick boundary denotes commercial applications, a thin boundary denotes applications at an advanced development stage, and a dotted boundary denotes early developments.

Figure 1-10. Boiler power plant.

Figure 1-11. Principle of an IGCC.

Figure 1-12. Gasification coupled to an internal combustion engine.

Figure 1-13. Principle of a pyrolysis oil combined cycle.

Figure 1-14. Use of pyrolysis oil in an internal combustion engine.

Figure 2-1. A co-generation steam boiler power plant /32/.

Figure 2-2. Thermal efficiency of steam boilers as a function of capacity. Location Finland 1994-96, data provided by Ekono /33/.

Figure 2-3. Power-to-heat ratio as a function of power output.

Figure 2-4. Net electric efficiency as a function of plant size.

Figure 2-5. Efficiencies employed for conventional wood-fired biomass power plant analysis (0.3 to 100 MWe) by Mitchell et al. /35/, McMullan et al. /36/, and Toft /37/. Ekono co-generation data as reference /34/.

Figure 2-6. Efficiencies employed for conventional wood-fired biomass power plant analysis (3 to 600 MWe) by Mitchell et al. /35/, McMullan et al. /36/, and Toft /37/. Ekono co-generation data as reference /34/.

Figure 2-7. Efficiencies employed for conventional wood-fired biomass power plant analysis by Marrison and Larson /38/ and EPRI /39/. Conversion from hhv to lhv efficiencies by the author. Ekono co-generation data as reference /34/.

Figure 2-8. Co-generation plant investments. Location Finland 1994-96, data provided by Ekono /34/. 1 US\$ = 5 FIM.

Figure 2-9. Specific investments for co-generation plants. Location Finland 1994-96, data provided by Ekono /347/. 1 US\$ = 5 FIM.

Figure 2-10. Capital costs of power plants according to Mitchell et al. /35/, McMullan et al. /36/, Marrison and Larson /38/ and EPRI /39/. Ekono data as reference /34/. £1= US\$ 1.7, \$ 1= FIM 5.

Figure 2-11. Correlations in Figure 2-10 shown for a range from 5 to 100 MWe. Toft /37/ included.

Figure 2-12. Specific capital costs of power plants according to Mitchell et al. /35/, McMullan et al. /36/, Marrison and Larson /38/, Toft /37/, and EPRI /39/. Ekono data as reference /34/.

Figure 2-13. Cost of electricity as a function of annual operating hours. 3/9 CHP denotes 3 MWe of electricity and 9 MWth of heat in co-generation. Location Finland 1994-1996, data provided by Ekono/34/, fuel 2.5 US\$/GJ, 20-year service life, 5% real interest rate, value of heat calculated using a tariff with the fixed cost component as 30US\$/MW,a and the variable cost component 11 US\$/MWh.

Figure 2-14. Cost of electricity as a function of power plant output. Location Finland 1994-1996, data provided by Ekono/34 /, fuel 2.5 US\$/GJ, 20-year service life, 5% real interest rate, value of heat calculated using a tariff with the fixed cost component as 30 US\$/MWa and the variable cost component 11 US\$/MWh. Condensing COE calculated from the Ekono data by the author.

Figure 2-15. Effect of value of district heat in co-generation. Location Finland 1994-1996, data provided by Ekono/34/, fuel 2.5 US\$/GJ, 20-year service life, 5% real interest rate. Value of heat defined in text.

Figure 2-16. Effect of fuel cost in co-generation. Location Finland 1994-1996, data provided by Ekono /34/, fuel 2.5 US\$/GJ, 20-year service life, 5% real interest rate.

Figure 2-17. COE at three locations with a Rankine-steam cycle, Marrison & Larson /38/. Utility financing: interest rate 8%, service life 20-years, annual operating time 6 570 h. NC = north central, SE = south east.

Figure 2-18. COE for different biomass technologies, EPRI /39/, location USA. Wood Fluidised Bed Combustion (FBC) and a Stoker boiler at 50 MWe, wood retrofit: co-fired 15% in a utility boiler (200 MWe). Wood 2.1, coal 1.1 \$/GJ, levelized cost according to the EPRI TAG /60/.

Figure 2-19. COE in a Rankine-steam cycle, Mitchell et al. /35/. Location Western Europe 1994, fuel 2.9 - 3.4 US\$/GJ. 20-year service life, 10% nominal interest rate, 5% inflation.

Figure 2-20. COE in a Rankine-steam cycle, McMullan et al. /36/. Location Western Europe 1995, fuel 1.0 – 2.8 US\$/GJ, break-even selling price estimated with 7.5% discounted cash flow.

Figure 2-21. Sydkraft IGCC plant at Värnamo, Sweden /40/.

Figure 2-22. IGCC efficiencies based on lower heating value /46/.

Figure 2-23. IGCC efficiencies according to NREL /47/; conversion from higher to lower heating values by the author.

Figure 2-24. Biomass IGCC efficiencies /48/, correlation based on /46/.

Figure 2-25. Power plant efficiencies according to Marrison and Larson /38/, conversion from hhv to lhv efficiency by the author. EP = Enviropower, Figure 2-22.

Figure 2-25. Power plant efficiencies according to EPRI /39/ with a correlation derived from Enviropower (EP) IGCC and Ekono (Rankine cycle) data as references. FBC = fluidised-bed combustion Rankine cycle, IGCC = integrated gasification combined cycle.

Figure 2-27. Power plant efficiencies, the IEA Interfacing Activity /35/. Enviropower (EP) IGCC /46/ and Ekono co-generation Rankine data /34/ as references.

Figure 2-28. Gasification power plant efficiencies according to Toft /37/ with Enviropower IGCC data /46/ as a reference.

Figure 2-29. IGCC power plant efficiencies by McIlveen et al. /50/ with Enviropower (EP) IGCC data /46/ as a reference. PGF pressurised gasification with ceramic filters, PGS pressurised gasification with water wash of fuel gas, and AGS atmospheric pressure gasification with water wash of fuel gas.

Figure 2-30. Gasification/gas engine power plant efficiencies by McIlveen et al. /50/ with data by Toft /37/ and Mitchell et al. /35/.

Figure 2-31. IGCC power plant efficiencies by van Ree and Faaij et al. /51/, /52/ atmospheric pressure gasification. EP = Enviropower /46/, pressurised gasification.

Figure 2-32. Gasification power plant efficiencies, IEA Pyrolysis /31/. A-IGCC = atmospheric pressure gasification IGCC, P-IGCC = pressurised gasification, Gas-Eng = atmospheric gasification and internal combustion engine. EP = Enviropower (P-IGCC)/46/, Toft= gasification and combustion engine /37/.

Figure 2-33. Specific investments for IGCC /46/, Scandinavia 1995.

Figure 2-34. Biomass IGCC capital cost estimates from several studies, USA 1990 /55/, /56/, /57/, /58/, /38/. EP correlation /46/ as a reference (a specific scale factor, equation 2-3, of -0.59).

Figure 2-35. Biomass IGCC capital cost estimates for two concepts by Marrison & Larson /38/ (1994), EP correlation /46/ as a reference.

Figure 2-36. Wood gasification power plant capital cost estimates by Toft /37/ 1995, Enviropower correlation /46/ as a reference.

Figure 2-37. IGCC power plant capital cost estimates by Faaij et al. /52/ in 1995. Enviropower (EP) data as a reference /46/.

Figure 2-38. Power production costs with IGCC and fluidised-bed combustion power plants, 1st and 10th plant costs shown for the IGCC /46/. Wood 2.8 US\$/GJ, Scandinavia 1994.

Figure 2-39. Levelized power production costs by NREL /55/, USA 1990. Levelized costs by EPRI TAG /60/, wood 2.6 US\$/GJ.

Figure 2-40. COE for different biomass technologies, EPRI /39/, USA 1994. IGCC cases at 100 MWe, wood retrofit: co-fired 15% in a utility boiler (200 MWe). Levelized costs by EPRI TAG, wood 2.1 US\$/GJ.

Figure 2-41. Production cost of electricity estimated by Toft /37/, wood 3 US\$/GJ.

Figure 2-42. Production cost of electricity estimated by Faaij et al. /52/. Location the Netherlands, rate of interest 4-6%, annual operating time 6570-7400 h/a.

Figure 2-43. ENEL RTP-system in Bastardo, Italy/65/.

Figure 2-44. Engine power production efficiency, pyrolysis oil to electricity with a diesel engine power plant /35/.

Figure 2-45. Overall power production efficiency, wood to electricity through fast pyrolysis and a diesel engine power plant /37/.

Figure 2-45. Specific capital costs for a close-coupled fast pyrolysis diesel power plant according to Toft /37/ , 1995 basis. Data from Roy /68/ as a reference.

Figure 2-47. Efficiencies (based on fuel lhv) of state-of-the-art power production technologies, the arrows showing near-future developments. IGCC correlation from EnviroPower /46/, NGCC = natural gas combined cycle, PC = pulverised combustion, HFO = heavy fuel oil, CFB = circulating fluidised-bed boiler.

Figure 2-48. A summary of predicted IGCC system efficiencies (based on wood lhv).

Figure 2-49. Specific capital costs for power plants using biomass fuels, 1994 (all nth plants).

Figure 2-50. COE for several alternatives, EPRI data 1994 /39/. Wood 2.1, Gas 2.4, Coal 1.1 US\$/GJ, levelized cost according to the EPRI TAG.

Figure 2-50. COE for several alternatives, EPRI data 1994 /39/. Wood 2.1, Gas 2.4, Coal 1.1 US\$/GJ, levelized cost according to the EPRI TAG.

Figure 4-1. A simplified Aspen block flow diagram of a small Rankine cycle power plant, 1 = boiler, 2 = heat recovery, 3 = steam turbine, 4 = deaerator. See Table 3-1 for explanation.

Figure 4-2. A simplified Aspen block flow diagram of the steam cycle of a combined-cycle power plant

Figure 4-3. Temperature - enthalpy diagram of a 10 MWe bottoming cycle of a wood-fuelled IGCC (boiler feed-water 105 °C, superheat steam 485 °C, 60 bar), approach and pinch points shown. SH = superheated steam, EVA = evaporating water, BFW = boiler feed-water.

Figure 4-4. Temperature - enthalpy diagram of the gasifier waste heat boiler as part of a 10 MWe bottoming cycle of a wood-fuelled IGCC. EVA = evaporating water.

Figure 4-5. The Rankine cycle electricity production efficiency at 2 MWe, flue gas temperature varied. Steam pressure 40 bar, superheat temperature 450 C, wood moisture content 45 wt%, LHV 9.35 MJ/kg.

Figure 4-6. The Rankine cycle electricity production efficiency at 2 MWe, condenser pressure varied. Steam pressure 40 bar, superheat temperature 450 C, wood moisture 45 wt%, LHV 9.35 MJ/kg.

Figure 4-7. The Rankine cycle electricity production efficiency at 2 MWe, excess air varied. Steam pressure 40 bar, superheat temperature 450 C, wood moisture 45 wt%, LHV 9.35 MJ/kg.

Figure 4-8. Effect of steam data on power plant efficiency (operation in condensing mode), capacity around 30 MWe.

Figure 4-9. Summary of model results, Rankine power plant efficiency as a function of capacity.

Figure 4-10. Biomass power plant efficiencies, no re-heating. Model results compared with industrial data.

Figure 4-11. Steam turbine exit moisture, IGCC using the GE LM2500 gas turbine. LM2500 gas turbine output 23.3 MWe, flue gas temperature 566 °C.

Figure 4-12. Steam turbine output as a function of superheat pressure and temperature, combined cycle. LM2500 gas turbine output 23.3 MWe, flue gas temperature 566 °C. Turbine moisture limit 10 wt%.

Figure 4-13. Temperature profiles for a combined-cycle hrsg superheater, pressure 60 bar, a) superheat temperature 485 °C and b) 530 °C .

Figure 4-14. Superheater area times heat transfer coefficient as a function of steam conditions, IGCC. LM2500 gas turbine output 23.3 MWe, flue gas temperature 566 C. Turbine moisture limit 10 wt%.

Figure 5-1. Principal dryer types and applicability for biomass with heat transfer medium.

Figure 5-2. A flowsheet of a suspension flue gas dryer, modelled later in the chapter.

Figure 5-3. A flowsheet of a rotary flue gas dryer.

Figure 5-4. A flowsheet of a steam dryer, modelled later in the chapter.

Figure 5-5. Energy consumption of dryers.

Figure 5-6. Release of organic compounds in a fluidized-bed batch steam drier /85/.

Figure 5-7. Aspen block diagram for the flue gas dryer. Aspen blocks listed in Table 3-1.

Figure 5-8. Aspen block diagram for the steam dryer. Aspen blocks listed in Table 3-1.

Figure 6-1. The BIGAS gasification process.

Figure 6-2. Aspen block diagram for the BIGAS reactor.

Figure 6-3. Aspen block diagram for the SLAGGER model (gasification section).

Figure 6-4. Aspen block diagram for a simple gasification model.

Figure 6-5. Aspen block diagram for the model developed in this work.

Figure 6-6. Use of the Aspen model for gasification.

Figure 6-6. Use of the Aspen model for gasification.

Figure 7-1. Flow diagram of the process model for the wood pyrolysis.

Figure 7-2. Energy balance of wood fast pyrolysis when the feed moisture content is varied. Moisture to pyrolyser constant at 10 wt%.

Figure 8-1. Block flow representation of the aero-derivative LM2500 engine.

Figure 8-2. An Aspen model for a gas turbine /118/.

Figure 8-3. Gas turbine block flow model built in Aspen.

Figure 8-4. LM2500 power output as a function of ambient temperature.

Figure 8-5. F6 power output as a function of ambient temperature.

Figure 8-6. LM2500 efficiency as a function of ambient temperature.

Figure 8-7. LM2500 efficiency as a function of ambient temperature.

Figure 8-8. Exhaust mass flow, gas turbine part-load operation with LHV gas, industrial F6 and aero-derivative LM2500.

Figure 8-9. Exhaust temperature, gas turbine part-load operation with LHV gas, industrial F6 and aero-derivative LM2500.

Figure 9-1. AspenPlus Block flow diagram of the gas engine model. Design specifications shown.

Figure 10-1. Flow diagram of an IGCC.

Figure 10-2. An example of a simulation input.

Figure 10-3. An example of the simulation results.

Figure 10-3. Block flow diagram of the pressurised gasification combined-cycle configurations. A flue gas dryer is shown. Concepts 1, 2 and 4.

Figure 10-5. Block flow diagram of the atmospheric pressure gasification combined-cycle configurations, concepts 5-8.

Figure 10-6. Block flow diagram of the pressurised gasification steam-injected gas turbine cycle concepts.

Figure 10-7. Block flow diagram of atmospheric pressure gasification - internal combustion engine concept.

Figure 10-8. Block flow diagram of fast pyrolysis.

Figure 10-9. Block flow diagram of a diesel power plant using fast pyrolysis liquid as fuel.

Figure 10-10. Block flow diagram of a combined-cycle diesel power plant using fast pyrolysis liquid as fuel.

Figure 10-11. Block flow diagram of the steam boiler power plant.

Figure 10-12. The calculated electricity production efficiencies of advanced biomass systems. Pyrolysis power plant efficiencies reported also from wood to electricity. Concept numbers shown as in Table 10-1. GE = Gasification engine, STIG = Steam injected gas turbine, PCC = Pressurised gasification combined-cycle, ACC = Atmospheric pressure CC, PD = Pyrolysis diesel, PyCC = Pyrolysis CC.

Figure 10-13. Power production efficiencies from wood. GE = Gasification engine, STIG = Steam injected gas turbine, PCC = Pressurised gasification combined-cycle, ACC = Atmospheric pressure CC, PD = Pyrolysis diesel, PyCC = Pyrolysis CC.

Figure 10-14. Power plant efficiencies using gasification. GE = Gasification engine, STIG = Steam injected gas turbine, PCC = Pressurised gasification combined-cycle, ACC = Atmospheric pressure CC.

Figure 10-15. Power plant efficiencies using fast pyrolysis. PD = Pyrolysis diesel, PyCC = Pyrolysis CC.

Figure 10-16. Sensitivity of power plant efficiencies using fast pyrolysis, the power plant efficiency varied $\pm 10\%$. The solid line depicts the efficiency of the Rankine cycle. PD = Pyrolysis diesel, PyCC = Pyrolysis CC.

Figure 10-17. Sensitivity of power plant efficiencies using fast pyrolysis. The power plant and pyrolysis efficiency varied $\pm 10\%$. The solid line depicts the efficiency of the Rankine cycle.

Figure 10-18. Potential improvements in IGCC performance. Enviropower (EP) /46/ as a reference for existing technology (industrial turbines, note that 6.8 MWe 40% is outside the figure area), Consonni & Larson /48/ for both current (aero-derivative) and future (inter-cooled) technologies

Figure 10-19. Comparison of (conventional) co-generation and power-only production from wood. Fuel to the power plant = 100%..

Figure 10-20. Co-generation system efficiencies. Note: PyCC power plant only without considering pyrolysis liquid production.

Figure 10-21. Advanced and new co-generation system efficiencies, the α -value is shown above the bars.

Figure 10-22. Power-to-heat ratios of the Rankine /34/ and advanced systems. Data for advanced systems around 60 MWe extrapolated from smaller concepts.

Figure 10-23. Two dryer types in co-generation, production efficiency. sd = steam dryer, fdg = flue gas dryer.

Figure 11-1. Comparison of cost overrun by project stage /216/.

Figure 11-1. Comparison of cost overrun by project stage /215/.

Figure 11-3. Reported cost estimates for coal-to-SNG plants discounted to 1982 dollars /215/, same capacity for all estimates.

Figure 11-4. Potential for cost improvement, two concepts compared in SNG production from coal, moderately and highly innovative technologies /215/.

Figure 11-5. Summary of specific investment costs. No contingency applied, location Western Europe 1998. Note: Pyrolysis plant included.

Figure 11-6. Summary of specific investment costs, contingencies included. RAND contingency applied, location Western Europe, 1998. Note: Pyrolysis plant included.

Figure 11-7. Summary of specific investment costs, contingencies and potential cost improvement included, pyrolysis both with and without liquid production plant. RAND contingency and potential cost reduction applied, location Western Europe, 1998.

Figure 12-1. Personnel per shift as a function of power plant capacity.

Figure 12-2. Fast pyrolysis liquid production cost as a function of fuel cost. Plant size in MW_{th} input as a parameter. 2.8 US\$/GJ corresponds to 10 US\$/MWh. Annuity factor 0.08, annual operating time 7 000 h/a.

Figure 12-3. Fast pyrolysis liquid production cost as a function of fuel feed capacity. Fuel cost as a parameter. 70 MW_{th} feed corresponds to a feed of 215 000 t/a 50% wet wood, and a liquid production of 87 000 t/a. Annuity factor 0.08, annual operating time 7 000 h/a.

Figure 12-4. COE as a function of power plant capacity, annual peak operating time as a parameter. Wood 2.8 US\$/GJ, pyrolysis liquid 8.6 US\$/GJ, annuity factor 0.08 corresponding to a 5 % rate of interest and a 20-year service life.

Figure 12-5. COE for gasification power plants, annual peak operating time as parameter. Wood 2.8 US\$/GJ, annuity factor 0.08 corresponding to a 5 % rate of interest and a 20-year service life.

Figure 12-6. COE for pyrolysis power plants, annual peak operating time as parameter. Wood 2.8 US\$/GJ, pyrolysis liquid 8.6 US\$/GJ, annuity factor 0.08 corresponding to a 5 % rate of interest and a 20-year service life.

Figure 12-7. COE for small-scale power plants as a function of annual peak operating time. Capacities of concepts shown in the legend in MWe. Wood 2.8 US\$/GJ, pyrolysis liquid 8.6 US\$/GJ, annuity factor 0.08.

Figure 12-8. COE for medium-scale power plants as a function of annual peak operating time. Capacities of concepts shown in the legend in MWe. Wood 2.8 US\$/GJ, pyrolysis liquid 8.6 US\$/GJ, annuity factor 0.08.

Figure 12-9. COE for larger-scale power plants as a function of annual peak operating time. Capacities of concepts shown in the legend in MWe. Wood 2.8 US\$/GJ, pyrolysis liquid 8.6 US\$/GJ, annuity 0.08.

Figure 12-10. COE for peak operating time, 660 h/a. Wood 2.8 US\$/GJ, pyrolysis liquid 8.6 US\$/GJ, capital cost recovery factor 0.08.

Figure 12-11. COE for intermediate operating time, 3000 h/a. Wood 2.8 US\$/GJ, pyrolysis liquid 8.6 US\$/GJ, annuity factor 0.08.

Figure 12-12. COE for intermediate operating time, 5000 h/a. Wood 2.8 US\$/GJ, pyrolysis liquid 8.6 US\$/GJ, annuity factor 0.08.

Figure 12-13. COE for base load, 7000 h/a. Wood 2.8 US\$/GJ, pyrolysis liquid 8.6 US\$/GJ, capital cost recovery factor 0.08.

Figure 12-14. A summary of power production costs as a function of power plant capacity at 7000 h/a. Production in condensing mode. Wood cost varied from 2.8 (top) to 5.6 (bottom) US\$/GJ (corresponding pyrolysis liquid costs 8.6 and 11.8 US\$/GJ), annuity for capital costs 0.08 (20-year service life, 5% rate of interest).

Figure 12-15. Power production costs as a function of power plant capacity at 4 700 h/a. Fuel cost varied from 2.8 (top) to 5.6 (bottom) US\$/GJ (corresponding pyrolysis liquid costs 8.6 and 11.8 US\$/GJ), annuity factor for capital costs 0.08 (20-year service life, 5% rate of interest).

Figure 12-16. Power production costs, small-scale power plants (capacity shown in the legend), effect of variation in fossil fuel cost, natural gas 2.8 (top), 5.6 (bottom) US\$/GJ in gas turbine and gas engine power plants. COE as a function of annual peak operating time. Wood 2.8 US\$/GJ, pyrolysis liquid 8.6 US\$/GJ, annuity factor 0.08.

Figure 12-17. Power production costs, medium-scale power plants (capacity shown in the legend in MWe), effect of variation in fossil fuel, cost natural gas 2.8 (top), 5.6 (bottom) US\$/GJ in gas engine power plant. COE as a function of annual peak operating time. Wood 2.8 US\$/GJ, pyrolysis liquid 8.6 US\$/GJ, annuity factor 0.08.

Figure 12-18. Power production costs, large-scale power plants (capacity shown in the legend in MWe), effect of variation in fossil fuel cost (natural gas 2.8, coal 1.9 (top), 5.6 and 3.8 (bottom) US\$/GJ). COE as a function of annual peak operating time. Wood 2.8, pyrolysis liquid 8.6 US\$/GJ, annuity factor 0.08.

Figure 12-19. Power production costs, medium-scale power plants (capacity shown in the legend in MWe), effect of increasing the rate of interest from 5 % (top) to 15 % (bottom) in the annuity method, annuity factors 0.08 and 0.16, respectively. COE as a function of annual peak operating time. Wood 2.8 US\$/GJ, pyrolysis liquid 8.6 US\$/GJ, natural gas 2.8 US\$/GJ.

Figure 12-20. Power production costs, medium-scale power plants (capacity shown in the legend in MWe), effect of increasing the rate of interest from 5 % (top) to 15 % (bottom) in the annuity method, annuity factors 0.08 and 0.16, respectively. No contingencies applied for the bottom case. COE as a function of annual peak operating time. Wood 2.8 US\$/GJ, pyrolysis liquid 8.6 US\$/GJ, natural gas 2.8 US\$/GJ.

Figure 12-21. COE in power-only and co-generation. Rankine cycle 17 MWe, in co-generation 17 MWe and 40 MW_{th}. IGCC 32 MWe, in co-generation 30 MWe and 33 MW_{th}. Wood 2.8 US\$/GJ, annuity factor 0.08.

Figure 12-22. COE in power-only and co-generation. Rankine cycle 17 MWe, in co-generation 17 MWe and 40 MW_{th}. IGCC 32 MWe, in co-generation 30 MWe and 33 MW_{th}. Wood 2.8 US\$/GJ, annuity factor 0.08.

Figure 12-23. Comparison of conventional and IGCC co-generation. Power production costs, co-generation of power and district heat. Biomass 50 FIM/MWh (2.8 US\$/GJ), annuity factor for capital costs 0.08.

Figure 11-24. Comparison of conventional and IGCC co-generation. Annual operating savings compared with the Finnish purchase tariff for electricity in 1995, co-generation of power and district heat. Biomass 50 FIM/MWh (2.8 US\$/GJ), annuity factor for capital costs 0.08.

Figure 12-25. Annual operating savings (compared with the Finnish purchase tariff for electricity in 1995) in co-generation of power and district heat, when different service lives are assumed for the gas cleaning catalyst. Biomass 50 FIM/MWh (2.8 US\$/GJ), annuity factor for capital costs 0.08.

LIST OF TABLES

- Table 1-1. Summary of biomass power plant technologies. ICE = internal combustion engine, CC = combined cycle, co-gen = co-generation of power and heat, * = in operation, ** = tested.
- Table 2-1. IGCC efficiencies (based on hhv values) reported by NREL /47/.
- Table 2-2. Base IGCC efficiencies (based on lhv values) reported by Consonni and Larson /48/.
- Table 2-3. Advanced IGCC concept efficiencies (based on lhv values) reported by Consonni and Larson /48/.
- Table 2-4. Biomass power plant data employed by Marrison and Larson /38/.
- Table 2-5. Power production technologies reported by EPRI /39/.
- Table 2-6. Biomass power plants concepts at 20 MWe (efficiencies based on lhv values) reported by Mitchell et al. /35/.
- Table 2-7. IGCC plant efficiencies /36/.
- Table 2-8. IGCC plant investment cost by EPRI /39/.
- Table 2-8. IGCC plant investment cost by EPRI /39/.
- Table 2-10. IGCC power plant concepts reported by McMullan et al. /36/ in 1989.
- Table 2-11. Biomass gasification power plant COE at 20 MWe reported by Mitchell et al. /35/ 1994.
- Table 2-12. Estimated cost correlations based on reviewed data, $y = a x^b$
- Table 3-1. Summary of unit operation models in AspenPlus version 9.3.
- Table 4-1. Some steam cycle model inputs and outputs.
- Table 4-2. Steam data used in each capacity (Figure 4-9) for the industrial correlation
- Table 5-1. Performance data for rotary dryers, flue gas as a drying medium /84/.
- Table 5-2. Performance data for other dryers /84/.
- Table 5-3. Some flue gas dryer model inputs and outputs.
- Table 5-4. Some steam dryer model inputs and outputs.
- Table 6-1. Some gasifier model inputs and outputs.
- Table 6-2. Model results compared with experimental data.
- Table 7-1. Comparison of mineral heating oils and fast pyrolysis liquid /143/.
- Table 7-2. Some pyrolyser model inputs and outputs.
- Table 7-3. Overall mass balance for fast pyrolysis.
- Table 7-4. Overall energy balance for fast pyrolysis. Auxiliary power for compressors, fans, pumps, mill, and conveyor motors.
- Table 8-1. Comparison of the advantages of industrial and aero-derivative engines /166/.
- Table 8-2. Predicted gas turbine performance with coal-derived syngas /190/.

Table 9-1. Energy balance around a state-of-the-art gas engine /210/.

Table 9-2. Engine performance with LHV gas. Operation with natural gas = commercial operation. BMEP = Brake mean effective power.

Table 9-3. Gas engine model inputs and outputs.

Table 10-1. Power plant concepts modelled.

Table 10-2. Characteristics of unit models in an integrated IGCC model.

Table 10-3. The most important inputs and outputs in an integrated IGCC model using a flue gas dryer.

Table 10-4. Energy balance for IGCC concept No 8 (section 10.4) in MW.

Table 10-5. Analysis of the wood feedstock employed, a wood fuel analysis at VTT /8/ (a mixture of Nordic hard and soft wood).

Table 10-6. Pressurised gasification combined-cycle configurations.

Table 10-7. Major process flow rates and conditions, concepts 1-4. Steam cycle conditions 60 bar and 485 °C. Internal power consumption breakdown in Table 10-9.

Table 10-8. Gas turbine characteristics, concepts 1-4.

Table 10-9. Plant's internal power consumption summary (kW), concepts 1-4.

Table 10-10. Overall efficiencies, concepts 1-4.

Table 10-11. Atmospheric pressure gasification combined-cycle configurations.

Table 10-12. Major process flow rates and conditions, concepts 5-8. Steam cycle conditions 60 bar and 485 °C..

Table 10-13. Gas turbine characteristics, concepts 5 - 8.

Table 10-14. Power consumption summary (kW), concepts 5 - 8.

Table 10-15. Overall efficiencies, concepts 5-8.

Table 10-16. Pressurised gasification combined-cycle configurations.

Table 10-17. Major process flow rates and conditions, concepts 9-13.

Table 10-18. Gas turbine characteristics, concepts 9 - 13

Table 10-19. Power consumption summary (kW), concepts 9 - 13.

Table 10-20. Overall efficiencies, concepts 9-13.

Table 10-21. Major process flow rates and conditions, concepts 14 - 15.

Table 10-22. Engine characteristics, concepts 14 - 15.

Table 10-23. Overall efficiencies, concepts 14 - 15.

Table 10-24. Major process flow rates and conditions, fast pyrolysis.

Table 10-25. Overall efficiency.

Table 10-26. Major process flow rates and conditions, concepts 16 - 17.

Table 10-27. Efficiencies, concepts 16 - 17. The overall figure includes pyrolysis liquid production.

Table 10-28. Pyrolysis liquid - combined-cycle configurations.

Table 10-29. Major process flow rates and conditions, concepts 18 - 21. HP superheat temperature 485 °C, pressure 60 bar.

Table 10-30. Gas turbine characteristics, concepts 18 - 21.

Table 10-31. Efficiencies, concepts 18 - 21. The overall figure includes pyrolysis liquid production.

Table 10-32. Major process flow rates and conditions, conventional power plants.

Table 10-33. Overall efficiencies, conventional power plants.

Table 10-34. Summary of electricity production efficiencies (% based on the lhv of the fuel) of advanced systems, efficiency of pyrolysis liquid production taken into account. Cogen = co-generation of power and heat.

Table 10-35. Estimated feasible production ranges for different technologies.

Table 10-36. Constants for different technologies in Equation (10-2).

Table 10-37. Sensitivity study with engine efficiency. Bold values used as input data; other values are results from simulation.

Table 10-38. Technical sensitivity studies; change in power plant performance. CC = combined cycle.

Table 10-39. Potential improvements in IGCC performance, concept 1. GT = gas turbine.

Table 10-40. Potential improvements in IGCC performance, concept 4.

Table 11-1. Summary of contingency (cont) methods /215/.

Table 11-2. Unit processes used in capital cost estimation, process parameters used for sizing processes, and the development stage of the unit (D = under development, I = industrial).

Table 11-3. Summary of the investment costs for the plants, no contingency applied. Costs as in 1998, Western Europe. Note that the pyrolysis cases include both liquid production and the powerplant. P-IGCC pressurised gasification combined cycle, A-IGCC atmospheric P-STIG pressurised STIG cycle, GE gasification and engine, Py-DP pyrolysis diesel power plant, Pyro-CC pyrolysis combined cycle.

Table 11-4. Estimation of process contingencies. Def. = definition, Dev. = development, CGF = cost growth factor. Py-DP ja Py-GTCC power plant section only.

Table 11-5. Summary of investment costs for the plants; average contingency applied for each technology, 1998, Western Europe. Final estimate = in addition to contingency, potential cost improvement included, corresponds to the 16th plant.

Table 12-1. Fast pyrolysis liquid production cost, feed capacity 70 MW_{th}, feed cost 2.8 US\$/GJ.

Table 12-2. Summary of power production costs. Nomenclature as in Table 11-3. Capital costs determined with the annuity method, service life 20 years, rate of interest 5%, 5 000 annual operating hours. Wood cost 10 \$/MWh or 2.8 \$/GJ, pyrolysis liquid 31 \$/MWh or 8.6 \$/GJ.

1. INTRODUCTION

In this chapter the opportunities for bioenergy are presented. Bioenergy is important because, unlike fossil fuels, biomass used as a fuel is renewable. The contribution that bioenergy can make to the energy market is summarised; electricity production is emphasised, and the justification for this is explained; the market and production scales are explained and justified; technologies are outlined as a means of defining the scope for the thesis; the criteria used in the process development are summarised; and, finally, the structure of the thesis is presented.

1.1 Bioenergy

The current bioenergy industry is integrated with forest products industries, which use wood wastes on a large scale for co-generation of electricity and process steam. Examples are found especially in Scandinavia and North America. Crop-processing residues also provide markets for bioenergy systems particularly in temperate climates. The sugar cane industry, for example, uses its bagasse residues for energy production.

Discussions on global warming have also fuelled the debate on the feasibility and viability of bioenergy systems. Whilst bioenergy clearly has much potential, it also involves great economic and technical uncertainties.

In the industrialised countries, the most vigorous growth in the energy sector is in electricity production. Hence, this will be the focus of the work in this thesis. In addition, of all the energy markets it is electricity that provides the greatest added value.

1.2 Markets for bioenergy

In this section, some aspects of global and European energy markets are discussed to emphasise the opportunities for bioenergy over the coming decades.

Initially, the key issues for the future of bioenergy are the environmental concerns. If the problem of global warming becomes more widely accepted in the political arena, the use of

biomass in the energy sector will no doubt provide one solution. However, without subsidies or tax breaks it is currently hard for bioenergy to compete with the fossil fuels on the market. For these reasons it is difficult to predict markets for bioenergy systems, even in the short term. Some of the markets referred to above already exist. The amount of energy recovered with biomass-fuelled boilers is already significant in a number of countries where the pulp and paper industry is important. For example, in Finland and Sweden 17 and 15% respectively of total primary energy production was derived from waste wood and other pulp mill residues in 1996 /1/.

Environmentally acceptable sustainable schemes for employing biomass as a fuel on a large scale may be envisioned. Global energy scenarios in which biomass plays a considerable part have been presented, for example, by Shell, the EU, the UN Rio de Janeiro Conference 1992, IIASA (International Institute for Applied Systems Analysis), and WEC (World Energy Council) /2/, /3/, /4/, /5/, and /6/.

The European Commission (EC) has recently published scenarios for energy production and consumption until the year 2020 /3/. The emphasis is on the European Union itself, but global analyses are also included. Four scenarios are envisioned:

- Conventional wisdom (CW) denotes the "business as usual" world
- Battlefield (BF) assumes a world with isolationism and protection
- Forum (FO) assumes co-operative international structures with a strong role for public administration
- Under hypermarket (HM) the predominant themes are market forces and free trade

A summary of world primary energy production in 1980 and 1990, and the four scenarios for 2020 are shown in Figure 1-1. Primary energy production from 1990 to 2020 is presented for the EU employing the "conventional wisdom" scenario (Figure 1-2).

The overall average global growth for the four scenarios from 1990 to 2020 is about 50%. The growth in the individual scenarios varies from about 40% (battlefield) to about 60% (hypermarket). Besides natural gas, renewables have higher than average growth rates. The global average growth in the four scenarios for energy sources is shown in Figure 1-3.

Changes in the relative shares of energy sources are anticipated. Biomass will increase its share as a primary energy source from the present 8% to 10 - 12% in the scenarios. This corresponds to doubling the amount of renewable energy used. In the EU, primary energy production is projected to increase by 23% in CW from 1990 to 2020, while the amount of renewable energy used is projected to increase by 170% over this period.

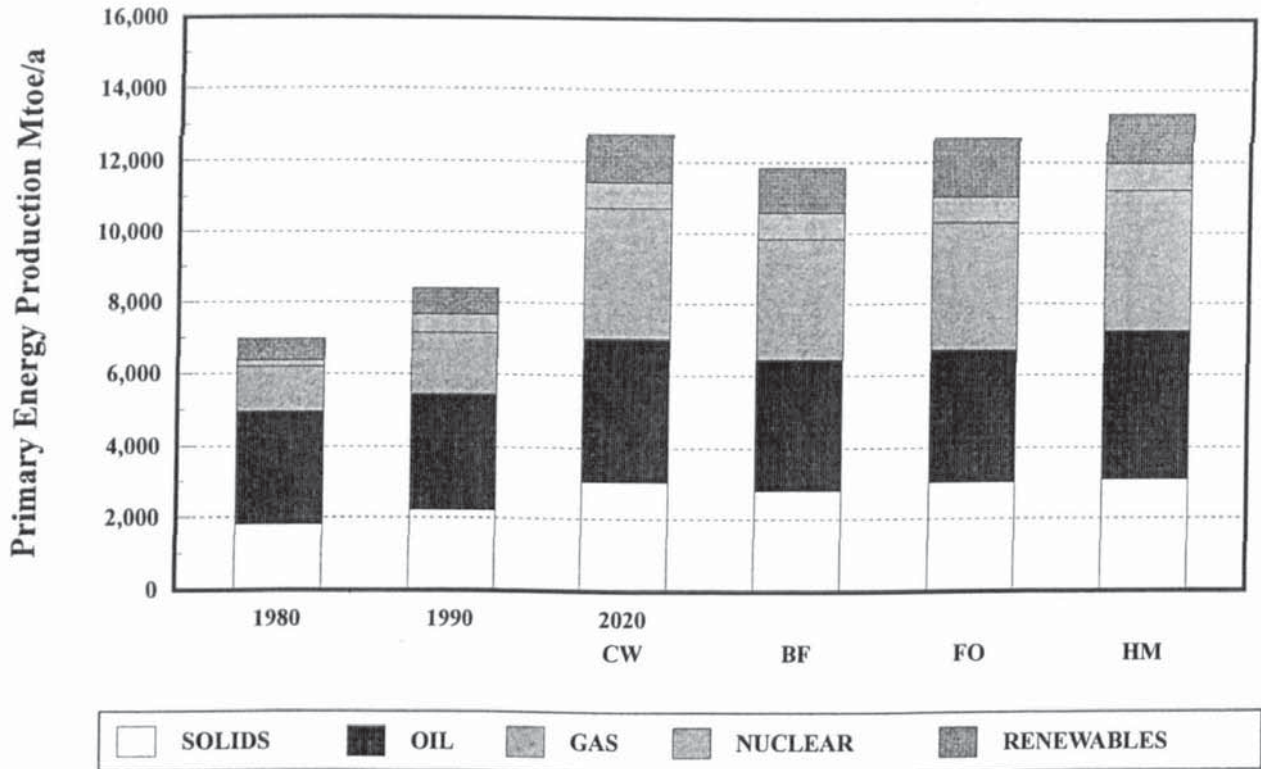
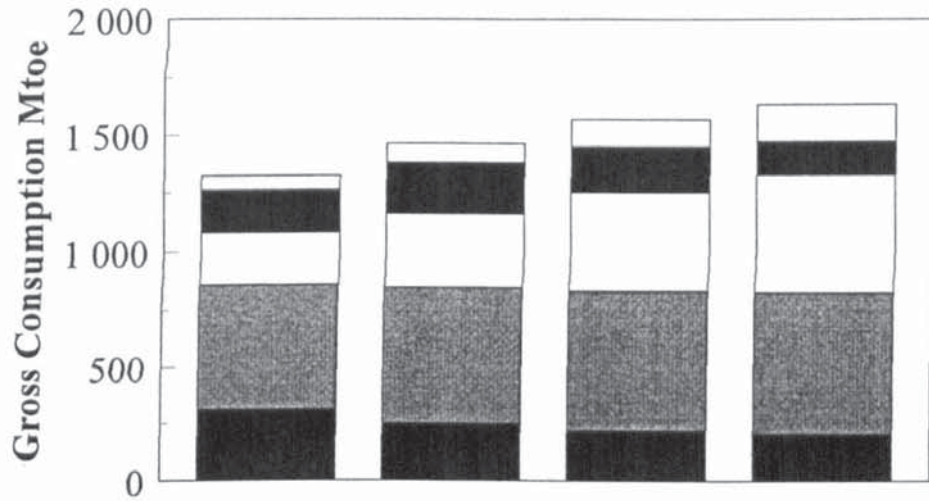


Figure 1-1. World primary energy production in 1980 and 1990, and four scenarios for the year 2020 [3]. CW conventional wisdom, BF battlefield, CO co-operation, HM hyper-market.



	1990	2000	2010	2020
Solids	311.37	247.31	216.83	200.98
Oil	546.75	598.06	613.40	622.71
Gas	222.35	315.20	421.00	501.76
Nuclear	181.31	218.08	197.30	145.81
Renewables	61.05	83.04	120.97	164.47

Figure 1-2. European Union primary energy production by the year 2020, conventional wisdom scenario /3/.

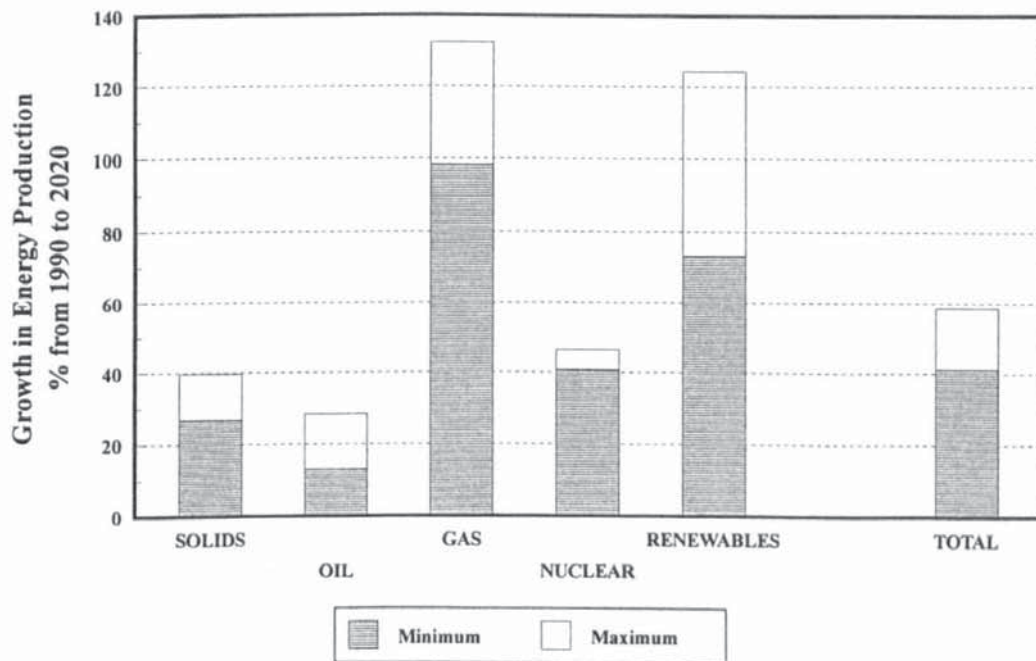


Figure 1-3. Average growth rates of different energy sources in world primary energy production over the years 1990 - 2020, average of four scenarios /3/.

Another scenario is presented by Shell (Figure 1-4) /2/. From this scenario it may be seen that renewables are predicted to provide a major share of total energy production in the future (Figure 1-5) if energy consumption continues to grow /2/. The study suggests that biomass may have a major role to play in global energy production, beginning within the next 20 - 30 years.

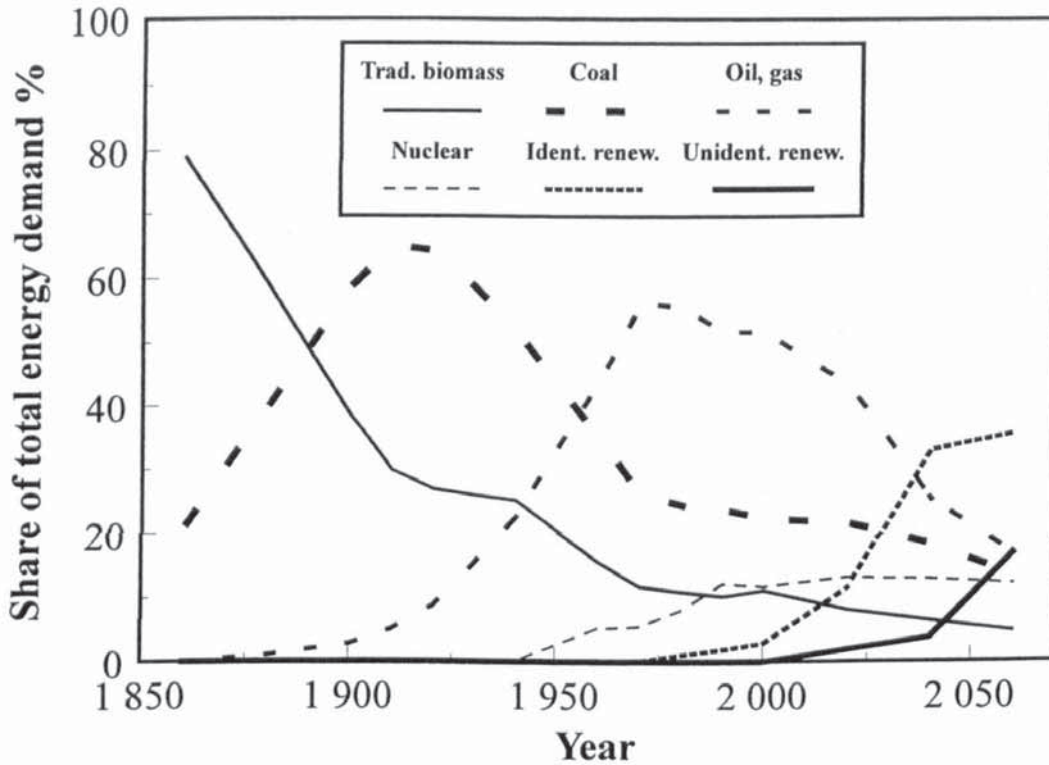


Figure 1-4. A scenario for future energy sources, presented by Shell /2/.

Many types of material fall within the category of biomass. The potential for bioenergy is presented from a different perspective in Figure 1-6. The number of potential power plants using biofuels by the year 2025 is shown according to the scenario in /7/. The biofuels include industrial residues like sugar cane bagasse and wood residues from pulping, the utilisation of which is often already now economically feasible. On the other hand, the utilisation of residues from farm products, although readily available, is usually not viable. Neither is the use of biomass specifically grown for energy production currently feasible. The two major industrial sources of biomass for energy production are sugar cane bagasse, and pulp and paper industry residues.

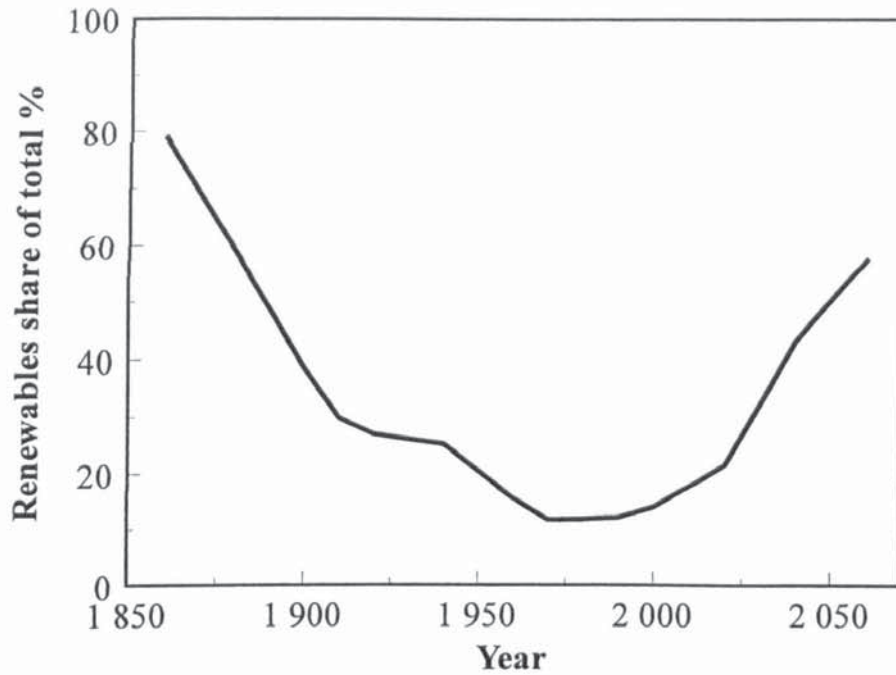


Figure 1-5. A scenario for renewable energy, estimated from the data in Figure 1-4.

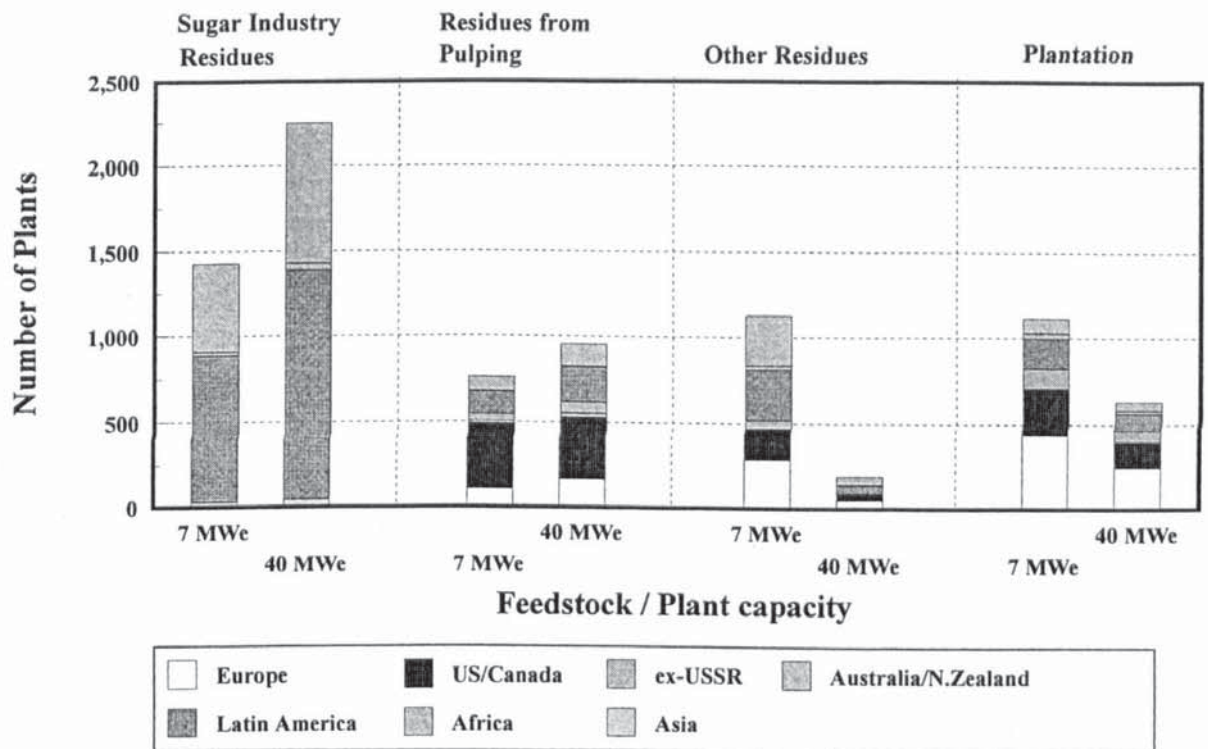


Figure 1-6. Number of potential power plants by 2025 according to the type of biomass fuel /8/. Data in reference is based on /7/.

1.3 Electricity production

Solid, gaseous and liquid fuels are used for generating electricity in thermal power plants. Coal and natural gas dominate the market, although distillate fuels are also still used in many countries. Natural gas has been increasing its market share in recent years, largely due to economic reasons, but also because of environmental considerations. A combined-cycle power plant employing natural gas as fuel has a low specific investment and high efficiency. It also has a short construction period compared, for example, with coal-fired power plants. Natural gas produces less carbon dioxide per produced electricity unit than other fossil fuels due to a lower carbon-to-hydrogen ratio. Combined cycles also have low emissions of nitrogen and sulphur oxides, and low particulate emissions.

Electricity consumption is constantly increasing in the industrialised countries. All of the available large-scale production options have some complications: nuclear, which is neutral towards global warming and often the choice of the industry, is politically questionable and unacceptable in many countries; coal, although generally regarded as economical, is considered environmentally doubtful; and reserves of natural gas, although more environmentally satisfactory than its competitors, are limited.

Global warming may be a problem in the future /9/. Global warming is intensified by carbon dioxide (CO₂) and some other gases released, for example, during the combustion of fuels in electricity production. Most of the man-made CO₂ emissions are generated in power and heat production, and in the transportation sector. In addition, there are several more or less natural players in the greenhouse gas balance (water reservoirs, soil, peat bogs, human & animal wastes, etc.). Renewable energy sources like wind, hydro, solar photovoltaics, geothermal, and biomass are examples of alternatives which do not release net CO₂ into the atmosphere. In this work, the use of biomass for electricity production is investigated. Besides liquid fuels, electricity production is the largest market sector expected to employ biomass fuels.

The US Department of Energy (DOE) /10/ and the EC DGXVII /11/ have proposed that new high-efficiency and low-emission systems using biomass as a fuel should be developed for future electricity production. Public funding has been considered necessary for the

R&D of high-efficiency and initially capital-intensive biomass concepts. Low fossil fuel costs do not justify the relatively high specific capital costs of high-efficiency concepts (high-efficiency processes are more economic than low-efficiency systems only if fuel costs are relatively high. At low fuel costs their share in the total product cost is low, and other cost components, e.g. capital and fixed costs, dominate). European Union R&D programmes such as JOULE/THERMIE and FAIR are striving to develop new technologies for utilities and industry /12, 13/.

Larson /14/ has assessed the potential of the Integrated Gasification Combined Cycle (IGCC) in the pulp and paper industry in the USA, and claims a potential co-generation capacity of 30 GW by the year 2020. Later he expanded his analysis world-wide, and suggested a potential equivalent to 10% of today's electricity production from fossil fuels /15/. Larson's potential in 2020 for Western Europe corresponds to about 10 GW. Although no detailed biomass potential assessment for Europe is available, a considerable amount of biomass is reported to be accessible for power production after the year 2000 /16/.

Keränen and Salo /17/ have estimated a world-wide potential for biomass IGCC using the information provided by the US DOE /10/, WEC /18/, and CEC /19/. Keränen and Salo report the following potentials by the year 2010 for the NAFTA countries, Brazil, South-east Asia, and Western Europe: 12, 5, 10, 3.5 GW_e, respectively. It is estimated that the potential corresponds to about 600 (each 80 MWe) IGCC plants world-wide.

Considerable potential exists within the pulp and paper industries. Taking into account only pulp and paper mill residues, and using this as a fuel feed capacity for a pulp mill IGCC, Keränen and Salo have estimated a global potential of about 80 plants, each of 50 MWe (Figure 1-7).

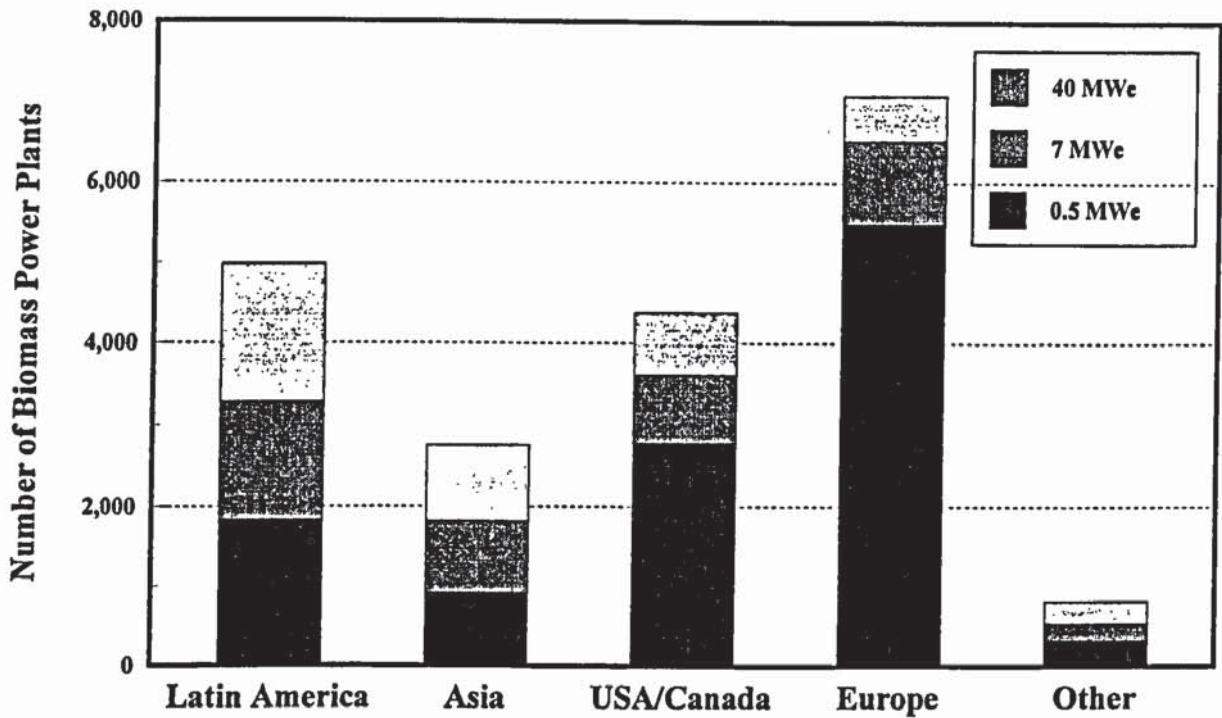


Figure 1-8. Global potential number of biomass power plants by 2025 /20/.

1.4 Proposed feasible production scales

The potential scale of bioenergy systems is uncertain because of scattered biomass availability (which tends to reduce the feasible plant size) and the capital-intensive production cost structure (which tends to increase the feasible plant size). Applications in which biomass could be used as a fuel are generally considered to be relatively small-scale, at least in Europe. Due to the inadequate availability of biomass, power production will probably be below 20 to 30 MWe, except in the pulp and paper industry, where it could be up to about 50 - 70 MWe /23/. On the other hand, it has been reported that the scale of viable operation may be as low as below 500 kW_e in Italy /22/. However, this was influenced by the very favourable electricity tariff applied in Italy.

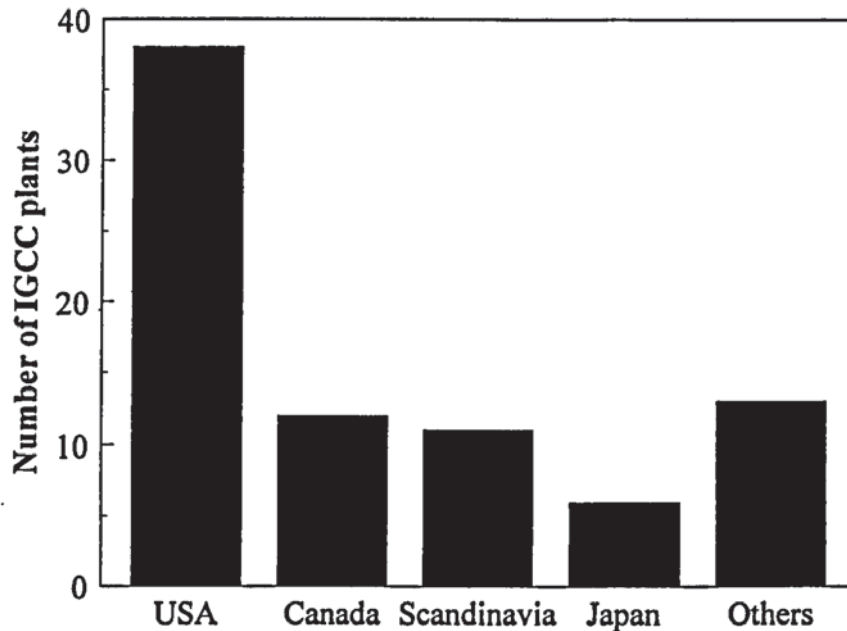


Figure 1-7. Potential number of 50 MWe IGCC plants within the pulp and paper industry in 1993 based on residue availability.

Even larger potential markets for biomass power technologies have been proposed /20/. Hislop and Hall present a scenario, where the potential additional capacity for biomass power is given for 2025 in three capacity classes, 0.5, 7 and 40 MWe (Figure 1-8). The scenarios are not considered by Hislop and Hall to require major changes in current energy policies. Even if the smallest-size power plants were excluded as doubtful, either technically or economically, the potential number remains considerable.

Small power plants rarely compete economically with large utility-scale production units, largely because of high specific investment costs. Personnel costs are also often high. However, the practical reason why small-scale production has, so far, been plagued with failures is the error-prone handling of heterogeneous biomass on a small scale.

Therefore, small-scale power plants (below 1 MWe) employing solid biomass as fuel are subject to considerable technical and economic uncertainties. They rarely meet the reliability required for power plants connected to the grid. The technical feasibility of the smallest-size capacity is often questioned, and their economic viability is a greater uncertainty /21/. However, they have frequently been proposed /22/. This is probably because in many cases only small amounts of biomass are available in one location.

The following scales for biomass electricity are distinguished in this study:

- Large scale

Condensing power plants of 50 - 150 MWe, suggested by the US DOE /10/. Short rotation forestry or other fast-growing species are proposed as fuel.

- Medium scale

Industrial and residential co-generation of about 15 - 50 MWe (state-of-the-art especially in the Nordic countries.) Condensing, power only, power plants were built in the US, especially in the 1980s because of a public utility regulatory act which was favourable for renewables.

- Small scale

Industrial and residential co-generation of 1 - 15 MWe (often uneconomical below approximately 3 - 5 MWe). Co-generation plants down to about 3 MWe employing biomass as fuel have recently been built in Finland. However, investment grants have been given to make the plants viable.

- Farm scale

Proposed to be as low as 50 kW_e at user sites /22/. Farm-scale cases are beyond the scope of this work because of the different technical and logistic problems associated with them compared to the larger-scale alternatives. Farm-scale systems are therefore not discussed further.

1.5 Electricity from biomass, process concepts

In this section, a brief overview of the process concepts proposed, developed or implemented for the production of electricity from biomass is given. Process alternatives employing combustion, gasification and fast pyrolysis as fundamental unit processes are included. While power plants based on boilers are already in commercial operation, systems based on gasification and pyrolysis are considered as promising for further development /24/, /25/, /26/, /27/, /28/, /29/.

A summary of the process configurations considered is shown in Figure 1-9 and Table 1-1. Concise descriptions of base alternatives are given. Process configurations of all the concepts analysed are described in more detail in Chapter 10.

It is necessary to define one biomass as the fuel for this study in order to make it possible to compare process concepts with each other and with existing technology. Woody biomass is selected because:

- woody biomass is already an important fuel in countries where modern bioenergy applications are available (e.g. in Scandinavia), and
- reliable and comparable data for model verification, when processes at an early development stage are considered, is often only available for wood fuel applications.

Wood analyses are shown in chapter 10, in which process descriptions are also presented.

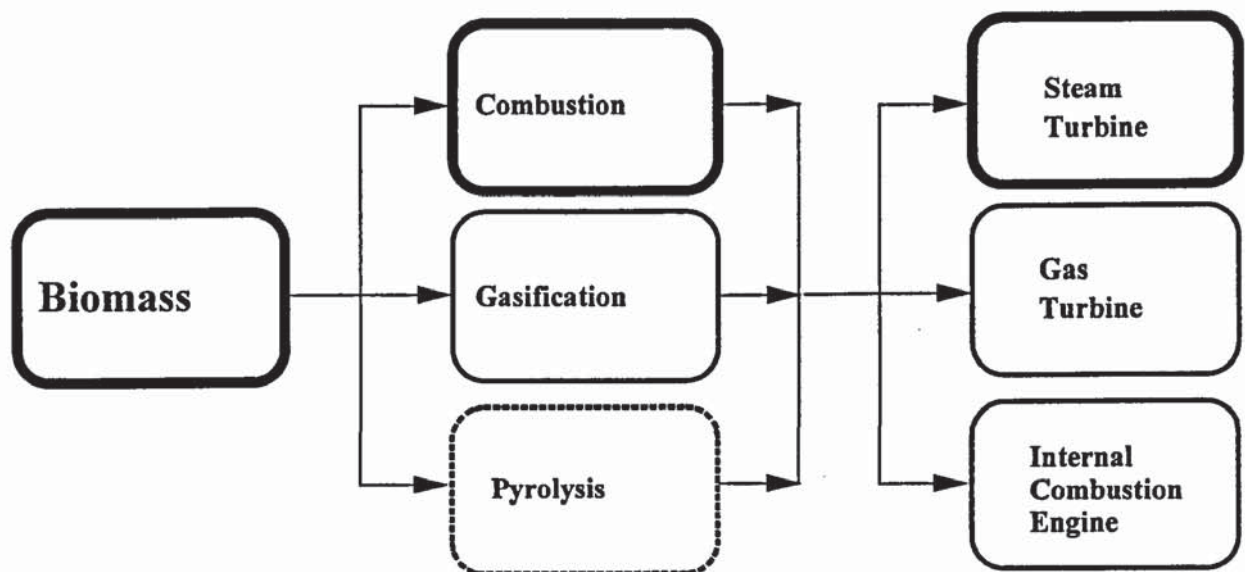


Figure 1-9. Process configurations studied. A thick boundary denotes commercial applications, a thin boundary denotes applications at an advanced development stage, and a dotted boundary denotes early developments.

Table 1-1. Summary of biomass power plant technologies. ICE = internal combustion engine, CC = combined cycle, co-gen = co-generation of power and heat, * = in operation, ** = tested.

Described in section	Concept	Stage of development	Largest unit MWe	Characteristic application
1.5.1	Boiler plant	Fully commercial	50*	Pulp & paper industry co-gen
1.5.2	IGCC	Demonstration	6*	Industry co-gen
1.5.3	Gasification - ICE	Demonstration	0.5** - 0.1*	Off-grid sites
1.5.4	Pyrolysis CC	Conceptual	2.5**	Co-generation
1.5.4	Pyrolysis ICE	Conceptual	1.5**	Co-generation

1.5.1 Rankine cycle

The principle of a conventional biomass-fuelled power plant is shown in Figure 1-10. Grate, fluidised-bed and other boilers are employed for biomass. Steam is raised in the boiler and expanded through a steam turbine connected to a generator producing electricity. The steam may be condensed with cooling water, or if condensed at a higher pressure, useful heat may be recovered. In the former case, more power will be produced, and in the latter case, by-product heat (process or district heat) is available.

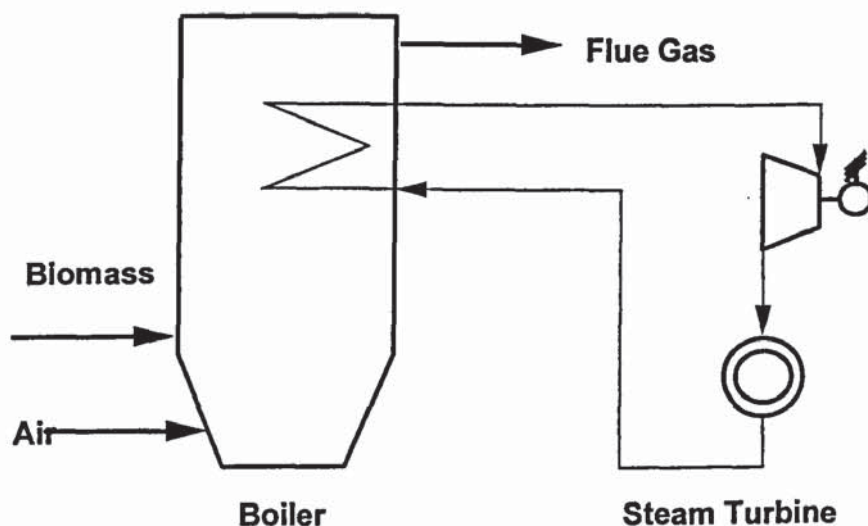


Figure 1-10. Boiler power plant.

1.5.2 Integrated Gasification Combined Cycle

The principle of an Integrated Gasification Combined Cycle (IGCC) is depicted in Figure 1-11. Dried biomass is fed into a gasifier, where fuel gas is produced. The fuel gas is cleaned of alkali metals and solid particulates at an elevated temperature. The clean fuel gas is combusted, and hot pressurised flue gases are expanded in a gas turbine connected to a generator producing electricity. The sensible heat in the flue gas after the gas turbine is used to raise steam for a steam cycle. A steam turbine connected to a generator produces additional electricity. The steam turbine may be either condensing, in which case only power is produced, or back-pressure, in which case co-generation of heat is possible.

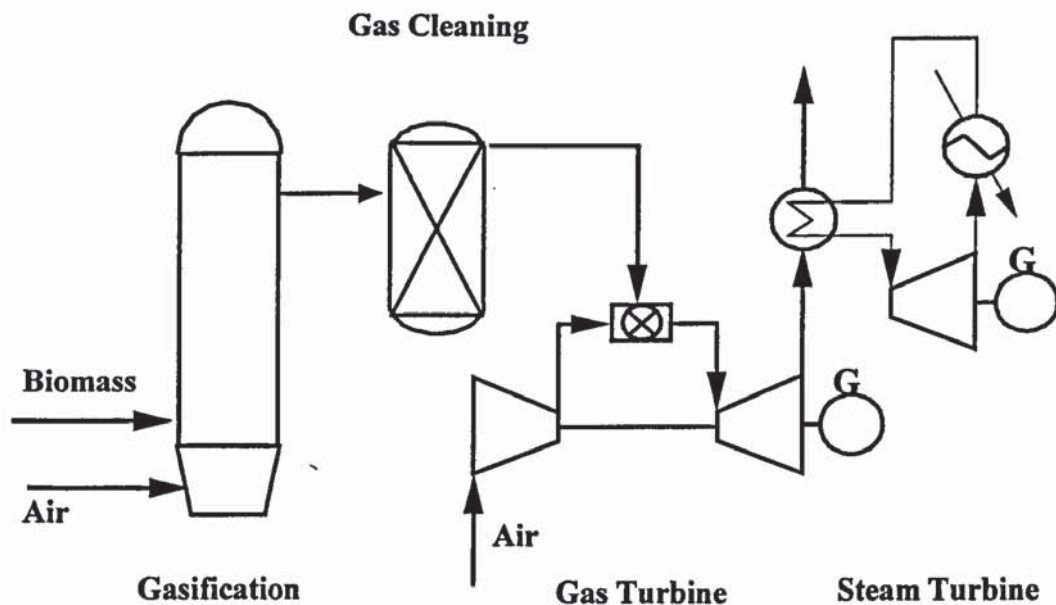


Figure 1-11. Principle of an IGCC.

1.5.3 Gasification and an internal combustion engine

The principle of gasification - internal combustion engine power plant concept is depicted in Figure 1-12. Dried biomass is fed into a gasifier, where fuel gas is produced. The fuel gas is cleaned of tars and solid particulates. The clean fuel gas is combusted in an internal combustion engine connected to a generator producing electricity. Co-generation of heat is also possible.

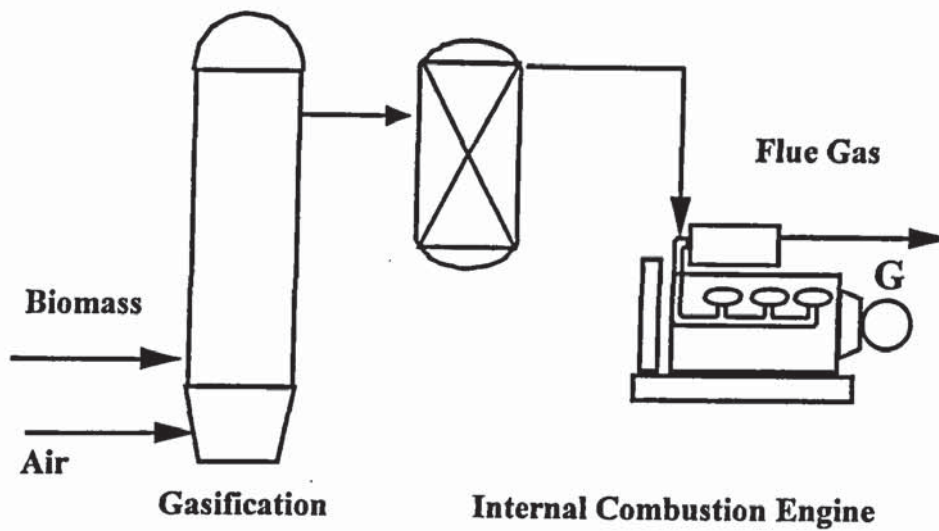


Figure 1-12. Gasification coupled to an internal combustion engine.

1.5.4 Fast pyrolysis and engines

The principle of a combined cycle employing fast pyrolysis oil as a fuel is depicted in Figure 1-13. Dried biomass is fed into a pyrolyser, where fast pyrolysis oil vapours are produced. Solids are removed from the vapours, which are condensed, and an oil is recovered.

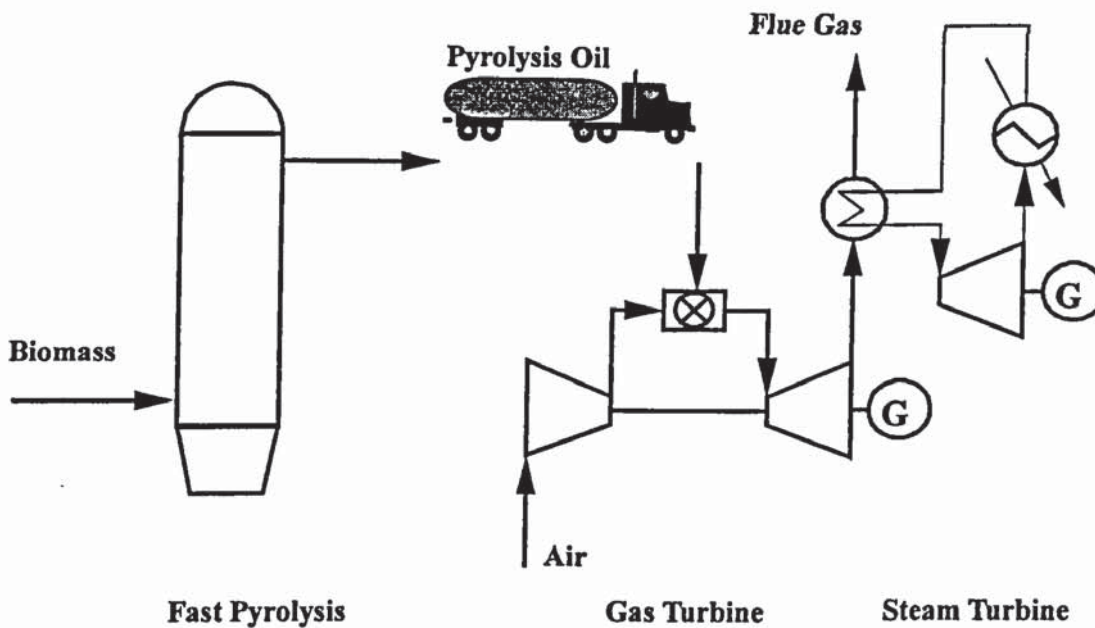


Figure 1-13. Principle of a pyrolysis oil combined cycle.

Oil production and electricity generation may be de-coupled. A central oil production plant feeding several oil users may be envisioned. Pyrolysis oil is combusted, and hot pressurised flue gases are expanded in a gas turbine connected to a generator producing electricity.

The sensible heat in the flue gas after the gas turbine is used to raise steam for a steam cycle. A steam turbine connected to a generator produces additional electricity. The steam turbine may be either condensing, in which case only power is produced, or back-pressure, in which case co-generation of heat is possible.

The principle of a concept where fast pyrolysis oil is employed as a fuel in an internal combustion engine is depicted in Figure 1-14. Dried biomass is fed into a pyrolyser, where fast pyrolysis oil is produced. The cleaned pyrolysis oil is combusted in an internal combustion engine connected to a generator producing electricity. Co-generation of heat is possible. Oil production and electricity generation may be de-coupled.

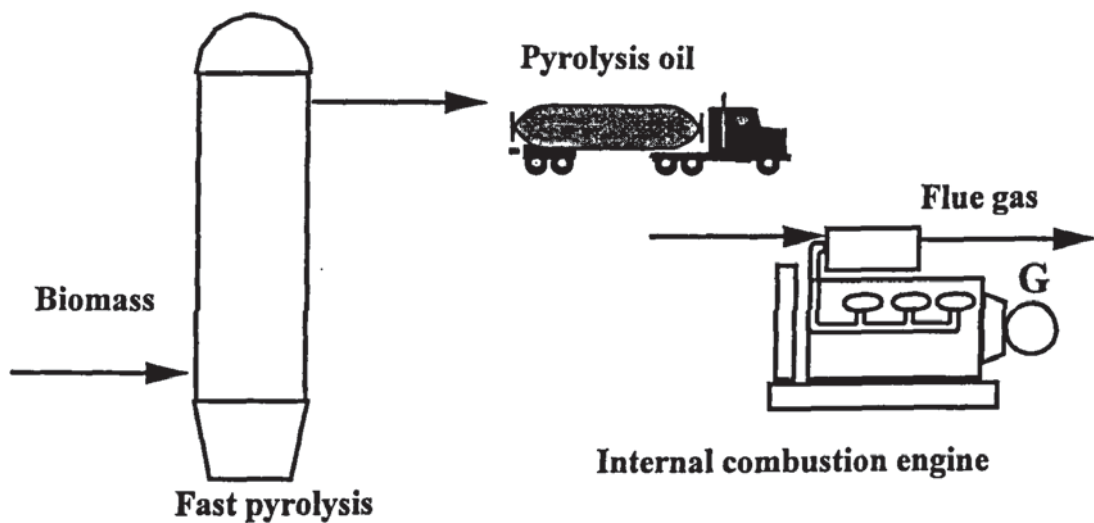


Figure 1-14. Use of pyrolysis oil in an internal combustion engine.

1.6 Development of biomass to electricity concepts

Essentially, all commercial biomass systems in electricity production currently employ a boiler and a steam cycle (Rankine cycle). However, to be able to improve the competitiveness of bioelectricity in the marketplace, and to exploit the opportunity presented in the

scenarios summarised in section 1.2, advanced bioenergy systems must be developed. A high number of new thermo-chemical process configurations have been proposed for power production from biomass. The alternatives were summarised in the previous section.

Minimising the cost of electricity (COE) is the objective of developing the biomass to electricity (bio-power) process. Therefore, there is a need to compare different bio-power plant configurations based on their estimated COE. While the existing Rankine cycle technology is being improved, new systems based on gasification and fast pyrolysis are being introduced to the market.

Process comparison includes two major elements: cost and performance analysis. Note that the process plant cost analysis, including the investment and operating cost estimates, is based on performance analysis, as units are sized and priced on the basis of mass and energy balances. However, it has been shown by RAND /30/ that cost estimates for concepts at an early stage of development may be misleading, due to the great uncertainties related to investment cost estimation. For these cases, performance analysis is a better measure of the potential competitiveness of a concept /30/.

Many of the proposed plant concepts reviewed here are at a rather early stage of development. Estimating the COE for these systems is uncertain. Although process economics are also eventually estimated in this work, it is recognised that they are always site-specific, vary from time to time, and from place to place. There is more uncertainty related to estimating the investment costs of new systems than there is in estimating their performance.

A robust performance analysis is therefore emphasised in this work. It is believed that the results from a rigorous performance study are more permanent than cost estimates. A rationale for this is presented in detail in Chapter 11. The performance analysis may be useful later, e.g. as an input to other studies. A cost analysis is closely associated with place and time, while an investment cost estimate is dependent on the market situation and may not be easily applied in other conditions.

1.7 Bases for this work

The key process concepts that formed the initial basis of this thesis were first designed and their cost and performance assessed within an IEA Bioenergy project over the years 1992 - 1994 /31/. The process models designed have since been developed further and validated within the thesis. An article summarising the results of the IEA project is attached as Appendix 15.

Advanced bioenergy systems are studied within IEA Bioenergy. IEA Bioenergy is an international collaboration in bioenergy within the International Energy Agency – IEA, an autonomous body within the framework of the Organisation for Economic Co-operation and Development (OECD) working on the implementation of an international energy programme.

1.8 Structure of the thesis

The structure of this thesis is summarised in this section.

This chapter has explained why it is important to develop electricity production systems employing biomass as a fuel. The principles of some base concepts have been presented. Several alternative configurations of these base cases are eventually modelled and analysed. Models may be used in supporting the development of these systems.

Chapter 2 is a review of earlier work on bio-power systems. Numerous feasibility studies concerning new bioelectricity systems have been carried out. However, few studies compare different technologies. A few satisfactory studies concerning biomass to power systems based on gasification, pyrolysis and combustion have been published. The competitiveness of the conventional steam boiler power plant has often been underestimated. Two principal objectives for the review are to collect reference data and to analyse tools and methods employed in earlier studies.

Chapter 3 explains the modelling approach applied in this thesis. It summarises the use of the modelling tool, AspenPlus, gives an example of building models, and outlines model outputs.

The structure of chapters 4 - 9 is essentially similar, presenting basic power plant unit operations. These chapters include reviews of critical unit operations and processes applied within the studied concepts. Firstly, the state-of-the-art of the technology is briefly summarised and major technical uncertainties are described. Secondly, earlier modelling work relevant to this thesis is reviewed. Work carried out with Aspen is especially emphasised. However, in many cases there is little available published modelling work with Aspen, particularly for biomass conversion. Thirdly, the model developed within this thesis is described, and a validation of the model, if possible, is carried out. However, validation of the industrial performance of process units is not always possible, either due to a lack of data on a large scale, or because of the proprietary nature of such data. In these cases an example using the model is presented.

In the review, particular emphasis has been given to three critical processes within power plant concepts: gasification, pyrolysis and gas turbines. These units are particularly important in determining the performance of advanced processes.

Chapter 4 describes the steam cycle models employed in this work. The Rankine cycle is primarily included in this work as a reference. It is also included in combined cycles as a bottoming cycle.

Chapter 5 deals with biomass drying, an essential pre-treatment step in all advanced conversion technologies dealt with in the thesis.

Chapter 6 includes a review of biomass gasification. Gasification is a critical step in many of the advanced systems proposed. The focus in many of the North American and European public R&D bioenergy programmes during the last two decades has been on gasification.

Chapter 7 includes a review of fast pyrolysis of biomass. The R&D on fast pyrolysis has begun relatively recently compared to gasification.

Chapter 8 summarises developments related to using biomass-derived fuel in gas turbines, and modelling of gas turbine performance. This is an especially critical stage in the IGCC concepts.

Chapter 9 reviews the utilisation of biofuels in internal combustion engines: diesel and gas engines.

Chapter 10 summarises the process performance models: processes are described and performance balances are presented. A summary of process efficiencies is presented. Technical sensitivity studies related to IGCC and gasification engine power plant concepts are presented.

Chapter 11 describes the method employed in this thesis for determining capital costs. Capital costs for the process concepts analysed will be presented. The uncertainties in investment cost estimation are reviewed.

Chapter 12 gives estimated electricity production costs for the advanced concepts. Sensitivity studies are included. Discussion of the results is included.

Chapter 13 summarises the conclusions and outlines recommendations for further work.

2 REVIEW OF PREVIOUS ASSESSMENTS ON ELECTRICITY FROM BIOMASS

A literature review of studies comparing the production of electricity from biomass through thermo-chemical processes is presented in this chapter. The two key objectives of the review are to collect reference data and to analyse the tools and methods employed in previous studies.

Three main process criteria in the review are:

- Thermal efficiency
- Power plant specific investment
- Cost of electricity

The criteria are employed for the three bio-power technologies presented in sections 1.5.2 - 1.5.4: the Rankine cycle, cycles using gasification, and cycles using fast pyrolysis. The results of the review are summarised. The methodologies employed in the reviewed studies are examined and summarised. The objectives for the thesis are outlined on the basis of these summaries.

2.1 Review criteria

Previous bio-electricity system analyses, based on the Rankine cycle (section 2.2), gasification (section 2.3), and fast pyrolysis (section 2.4), are reviewed. An overview of the process concepts is presented in sections 1.5.2 - 1.5.4. The review was carried out in order to study which methodologies and simulation tools have been employed earlier in related work. Another objective is to obtain data for comparison and validation of the models to be built. The methodologies used in previous studies are separately reviewed at the end of Chapter 2.

In particular, studies concerning more than one power plant concept are included. Many other studies of individual bio-power cases have been published but are not included in this

review. The contribution of such case studies to this work would be limited if no reference system or comparison to other systems were included in the study.

Three criteria are emphasised in the review: power plant thermal efficiency, power plant specific investment, and cost of electricity. The justification for choosing the criteria and the emphasis on their use are explained below.

The ultimate objective in the development effort of new power plant concepts is the minimised predicted cost of electricity (COE). Other criteria may also be considered (for example, minimising emissions or minimising the cost of selected emissions such as CO₂). However, COE is the factor on which investment decisions are based in the power production industry.

A general representation of calculating the COE is shown in equation (2-1). The main elements in COE are operating costs (fixed and variable costs), fuel costs, and capital costs.

$$\begin{aligned} \text{Unit product cost} = & \\ & \frac{\text{Annual CCR} \times \text{Capital cost} + \text{Annual O\&M cost} + \text{Annual Feedstock Cost}}{\text{Annual plant output}} \end{aligned} \quad (2-1)$$

where CCR = Capital charge rate

O&M = Operation and maintenance

All elements in the unit product cost are influenced directly or indirectly by process performance, as described in section 1.6. Process performance (and hence efficiency) determines fuel costs directly. Capital costs are a function of process performance too, because units are sized on the basis of performance analysis results. Plant output is also directly correlated to efficiency.

Hence, process performance is the most important criterion in comparing earlier assessments. This is also emphasised in section 1.6, in which issues related to cost and performance data are reviewed. It is concluded that power plant efficiency is the most reliable criterion of the published data. Power plant specific investment and cost of electricity are less reliable. This issue is discussed and the conclusion justified in chapters 11 and 12.

Efficiency may be defined on the basis of either the lower heating value (lhv) or the higher heating value (hhv) of the fuel. The difference between the two is related to the water vapour generated in combustion. In hhv, it is assumed to be condensed (and the corresponding heat recovered), whereas in lhv it is assumed to be vapour (and the heat lost).

Throughout this thesis, efficiency based on lhv values is employed (the European preference) unless otherwise noted. In the US, hhv efficiency is more common. Efficiency is defined in equation (2-2):

$$\text{Power production efficiency \%} = \frac{(\text{Gross power output} - \text{Internal consumption})}{\text{Energy input as fuel}} * 100 \quad (2-2)$$

Circumstances in Europe and North America are different, and this is reflected in performance and cost analysis. For example, power plants have been designed to a lower efficiency in North America because of the lower fuel costs. The different design principles can be seen when comparing corresponding studies in these regions.

2.2 Electricity from biomass based on the Rankine cycle

Results of the analysis of combustion systems using woody biomass as fuel are reviewed in this section. The structure is similar in sections 2.2 (Rankine power plant), 2.3 (gasification power plant), and 2.4 (fast pyrolysis power plant). Three important topics are discussed separately in each of these sections:

- Power production efficiency
- Specific investment cost
- Cost of electricity

The state-of-the-art in conventional power plant technology is summarised in the next section. The performance of both co-generation and condensing power plants is reviewed, based on existing plant data and literature. The justification for including co-generation systems is presented. The investment and production costs of these systems are also reviewed.

2.2.1 Introduction

When comparing different power production systems, the same methods should be applied to all alternatives. When systems under development are included, the task becomes more complex.

New systems have to be economically superior to existing ones to find markets. A common pitfall when comparing new and existing systems is related to efficiency. A new system proposed in the literature is usually designed for a high efficiency. This technology may be ready for industrial application after 10 years of continuous R&D work and considerable expense. Therefore, the design efficiency of the new system will be available 10 years into the future. In studies, however, this future efficiency may be compared with the efficiency of a relatively modern existing power plant, which may have been in operation for say 10 years. This power plant was therefore designed about 15 years ago. In fact, a potential process for 10 years ahead is being compared with something which was state-of-the-art 15 years ago.

In many studies reviewed, the conventional Rankine power plant is not analysed in a comparable way with the new systems. As an example, in /48/ efficiencies of IGCC systems under development are compared with the low efficiencies of existing biomass boiler power plants in the U.S. While the efficiencies measured at the U.S. biomass power plants may be below 25%, a modern design efficiency for such plants in Scandinavia would be closer to 30 - 35% (for discussion, note section 2.2.2). The power plants employing biomass fuels in California may have low efficiencies, but comparing those with the projected efficiencies of advanced systems is not appropriate.

Additionally, in many published studies the nominal design efficiency of a new power plant concept with a specified biomass fuel is compared with measured efficiencies of conventional plants, sometimes using various biomass fuels. Efficiency is typically reduced when other than design fuels are used. Only design efficiencies for process concepts using the same fuel should be compared. This is even truer if concepts with no existing industrial units are compared with commercial technology.

As an example, the power plants in California often use a variety of waste biomass, not all of which are well suited to the boilers in which they are used. The plants may be operated, for example, under less than optimum conditions due to potential ash slagging, which may occur if the plant is operated under boiler design conditions.

Steam boiler co-generation power plants have been standard especially in forest products industries for decades. There is an abundance of industrial experience available in North America and Northern Europe. Bark and wood wastes are used as fuel.

In addition to the forest products sites, co-generation plants using wood for community district heating have been built in recent years, principally in the Nordic countries. Co-generation, or combined heat and power (CHP), is included in this review due to its superior economics compared with the power-only mode.

Electricity is also produced from woody biomass in condensing power plants in the United States. A Public Utility Regulatory Policies Act created a favourable electricity tariff for renewable power plant projects in 1978. Several thousand megawatts of bio-power capacity were built in the 1980s. However, power production in biomass-fuelled condensing plants is rarely economic without subsidies or tax breaks. Once the favourable tariff was removed, many of the power plants built in the U.S. became uneconomic and were shut down.

In order to explain the scope and the power plant concept, a description of a commercial Rankine cycle is given. A power plant has three main sections: fuel handling, boiler plant, and steam and power section. As an example of a modern power plant, a flowsheet of the steam and power section of a district heat co-generation plant is shown in Figure 2-1. The co-generation power plant, which produces 17 MWe of electricity and 48 MWth of district heat, has been in operation in the city of Forssa in southern Finland since 1996 /32/.

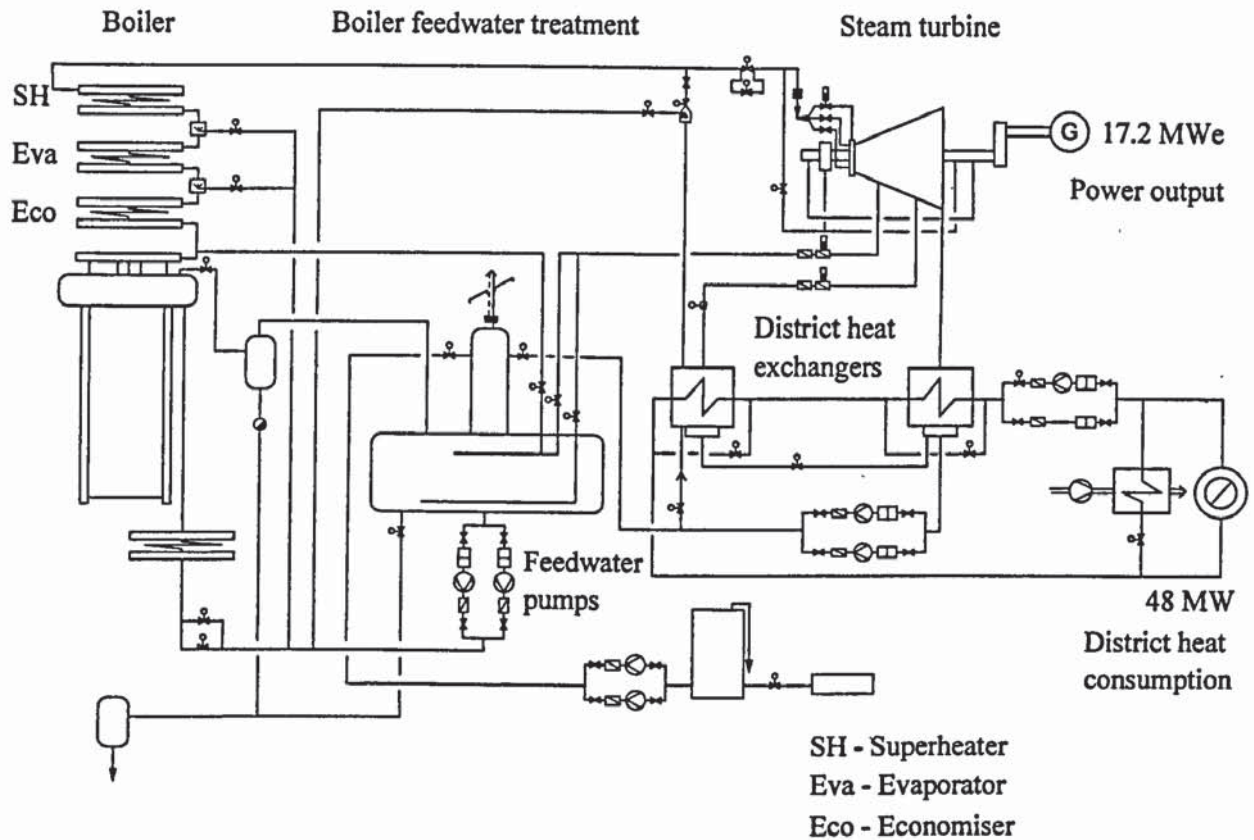


Figure 2-1. A co-generation steam boiler power plant [32].

Note that co-generator and condensing power plants are very similar, the major difference being in the condensing pressure after the steam turbine (see section 2.2.2.1).

Forest residue wood chips and wood wastes are used at this power plant. Wood chips are loaded from trucks into receiving bunkers. Belt conveyors carry the fuel to metal separators and screens, and oversize pieces are introduced to a hammer mill. The fuel is further conveyed to the boiler, which nowadays is typically either a bubbling or circulating fluidised-bed boiler (BFB or CFB, respectively). These boilers can burn several types of fuels from coals to bio-sludges, which is the main reason for their popularity. Superheated steam (60 bar, 510 °C) is generated in the boiler. Steam is expanded through a steam turbine, which drives the generator. The turbine is a back-pressure unit, where the steam is condensed while generating steam (industrial CHP) or heating district heat water. Condensates are treated in the deaerator and returned through the boiler feed-water pump to the boiler.

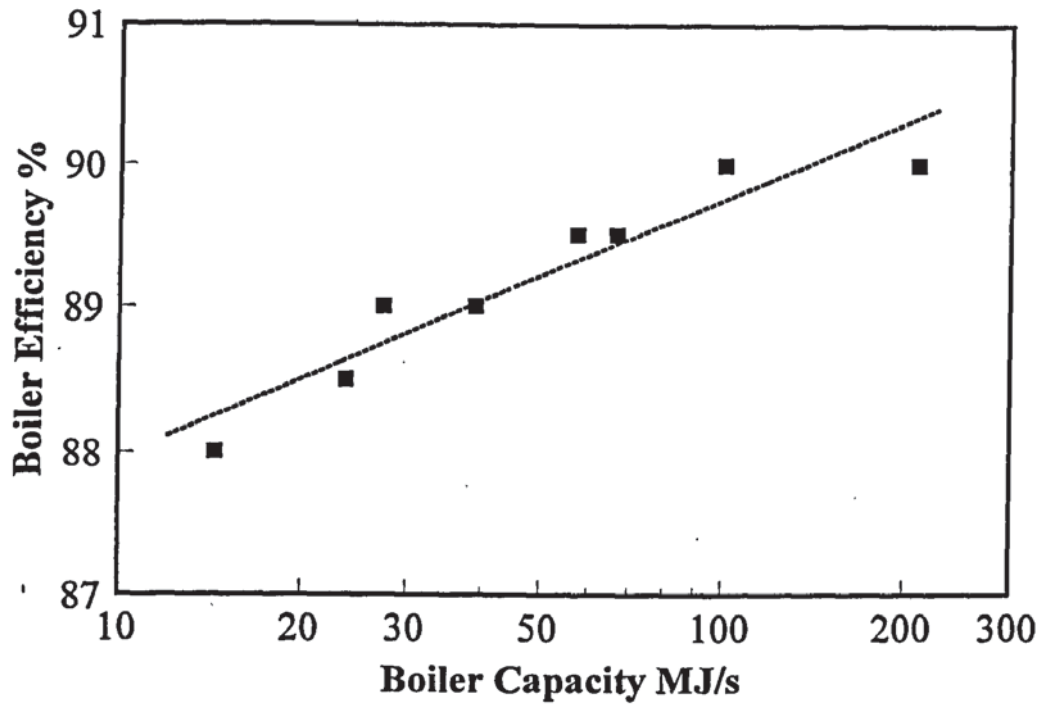


Figure 2-2. Thermal efficiency of steam boilers as a function of capacity. Location Finland 1994-96, data provided by Ekono /33/.

An important CHP parameter, the power-to-heat ratio (α -value, for an explanation, see section 10.15.1), is shown in Figure 2-3 as a function of plant size for power outputs currently considered economic. The significance of this is discussed in section 12.4. A higher α -value improves the economy of co-generation facilities, because electricity is usually more valuable than heat. The higher the α -value, the more power may be produced at an existing heat load. This is important because co-generation plants are sized on the basis of the heat load.

The α -value reaches 0.5 with the Rankine cycle, when power production is about 60 MWe. For smaller plants (around 3 to 5 MWe) the ratio is close to 0.3. The increasing α -value is primarily due to higher steam temperatures and pressures, and to the more complicated designs that are employed in larger plants. Advanced bio-power concepts often have a high α -value.

2.2.2 Power production efficiency

2.2.2.1 Ekono Energy

The cost and performance of the commercial Rankine cycle is first analysed on the basis of authoritative reports by Ekono Energy /33/, /34/. Note that the data presented is based on realised power plant projects. The data represents the current industrial state-of-the-art in wood-fired Rankine power plants. Other publications are also reviewed, especially those including comparisons between conventional and advanced power plant cycles.

Ekono Energy is a subsidiary of Jaakko Pöyry Engineering, which is globally the leading forest products engineering company. Ekono Energy has acted either as an engineering or turnkey contractor in tens of bioenergy co-generation projects, both industrial and residential, in Finland and elsewhere during the past 30 years. As bio-power accounts for a considerable share of Finnish generation capacity, the references of Ekono Energy are numerous. The data provided by Ekono is consistent and representative.

Most of the Ekono data is valid for co-generation facilities. Co-generation data may also be employed as a reference for power-only production. The difference between a co-generation facility and a plant producing only electricity is the steam turbine condensing pressure. In a condensing power plant, a typical pressure for the condensing steam is from 0.04 to 0.2 bar. In a district heating power plant a typical back-pressure is from 0.6 to 0.8 bar. A higher back-pressure in the steam turbine reduces power output by producing heat. However, there are no other differences for the purposes of this analysis between condensing and CHP plant performance. CHP data may therefore be employed as a reference, bearing this difference in mind. This aspect is justified in section 4.4.6.

First, boiler thermal efficiency [defined as $(\text{lhv energy in fuel} - \text{sensible heat in flue gas}) / (\text{lhv energy in fuel})$] is shown as a function of boiler capacity in Figure 2-2. It can be seen that an efficiency of 90% is reached at a capacity of around 100 MW_{th}. Even higher efficiencies would be possible if the flue gases were cooled to a lower temperature. However, this is not usually economic.

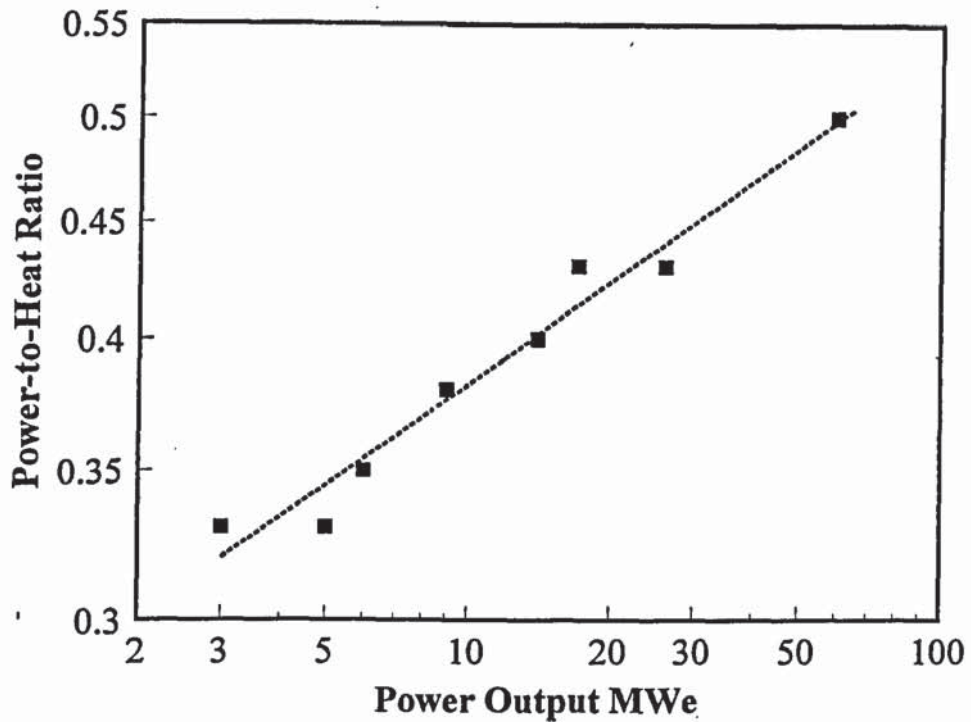


Figure 2-3. Power-to-heat ratio as a function of power output.

In co-generation, the higher the steam demand temperature, the lower the electricity yield. In industrial CHP higher temperatures are usually required than in district heating, where steam is typically condensed at around 85 to 90 °C, corresponding to a back-pressure of about 0.7 bar. The higher the temperature requirement, the higher the back-pressure. Increasing the back-pressure reduces the power output from the steam turbine.

The efficiency of electricity production in co-generation is, therefore, lower than in the condensing mode of production. The net efficiency of electricity production in district heating plants is shown in Figure 2-4. It is seen that the efficiency of electricity production ranges from about 20 to about 30% for the co-gen. plants built recently. These values may also be employed as references for condensing power production.

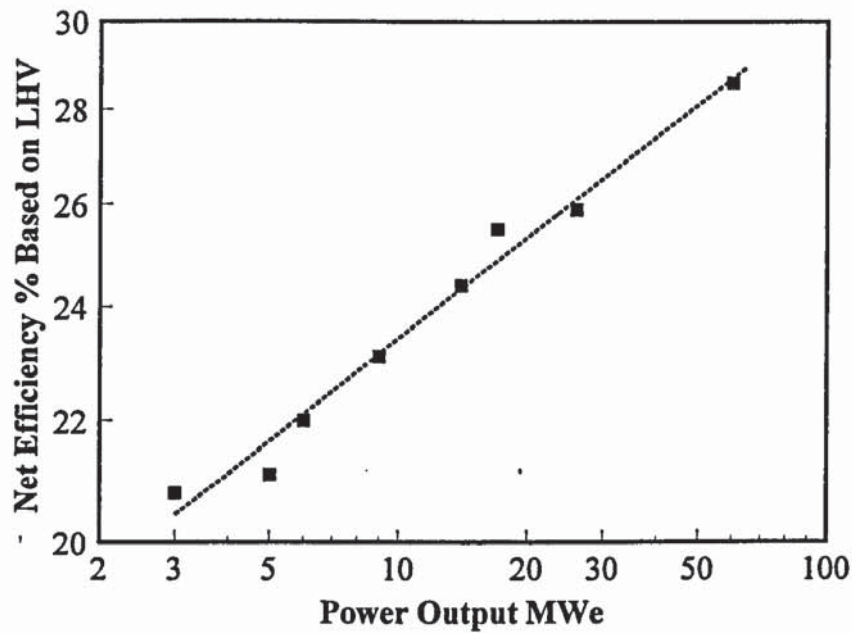


Figure 2-4. Net electric efficiency as a function of plant size.

2.2.2.2 Other work

The steam boiler power plant efficiencies employed in the studies by Mitchell et al. /35/, McMullan et al. /36/, and Toft /37/ are shown in Figures 2-5 and 2-6. The data is presented at two different scales. Figure 2-6 displays the entire upper range presented in the references, and Figure 2-5 depicts a range which is believed to be more reasonable for bio-power plants. The two figures are included to highlight the differences between the references.

The cycle efficiency relationships presented are lower at small scale and higher at large scale than the industrial practice today. The industrial data is represented by values from Ekono. Power production in the condensing mode has a higher efficiency than in co-generation (represented by the Ekono data).

It appears that the data presented by McMullan et al. approximately below 20 MWe, and the data presented by Mitchell approximately above 20 MWe are reasonable. However, none of the reviewed data appears to be accurate over a wide range of capacities. Neither do they agree with what is the industrial practice /34/.

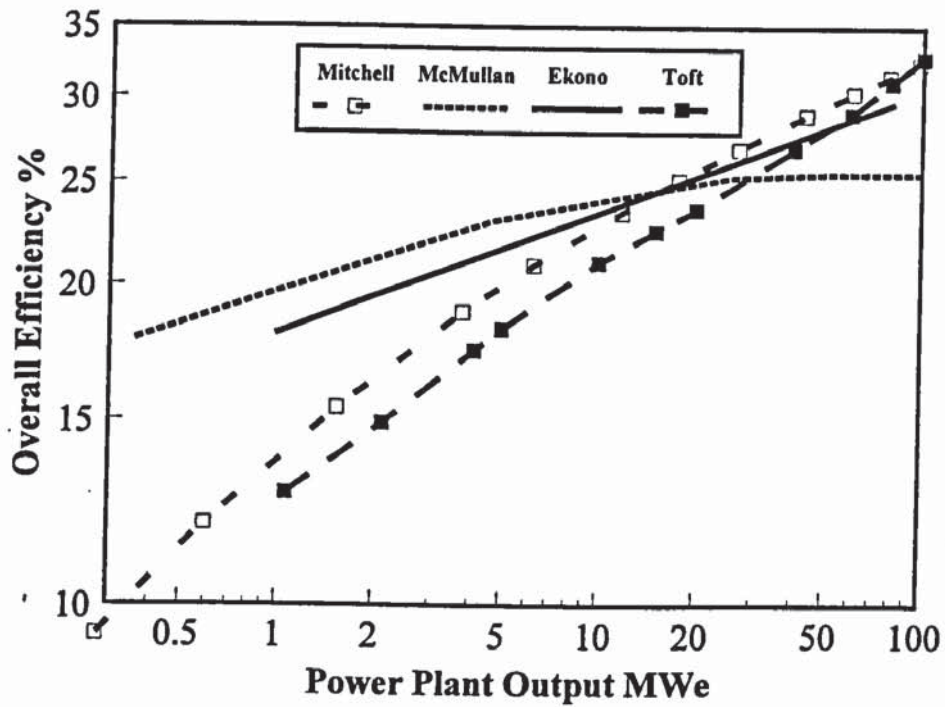


Figure 2-5. Efficiencies employed for conventional wood-fired biomass power plant analysis (0.3 to 100 MWe) by Mitchell et al. /35/, McMullan et al. /36/, and Toft /375/. Ekono co-generation data as reference /34/.

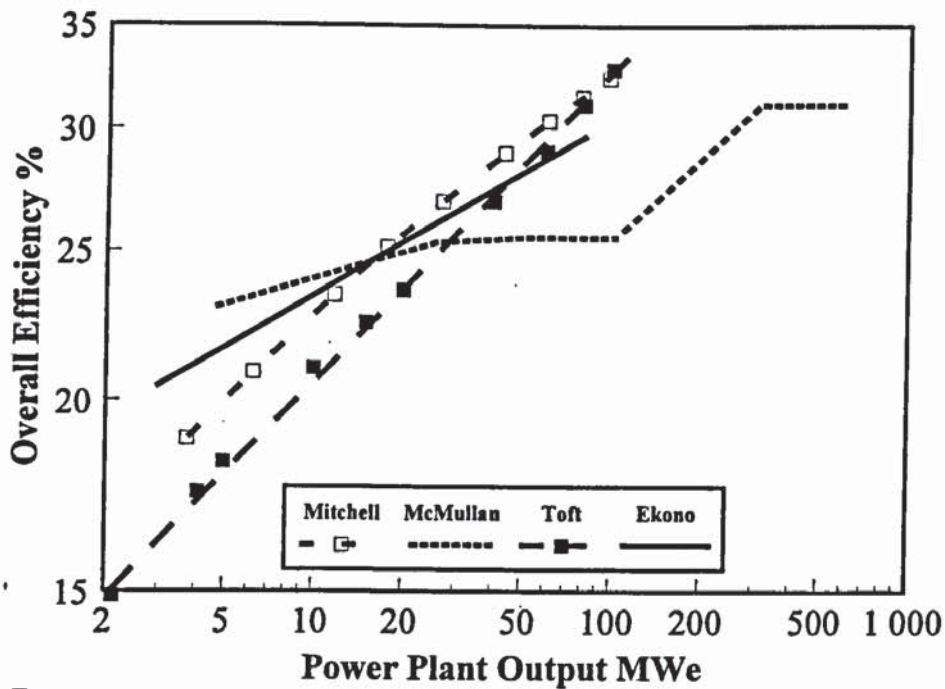


Figure 2-6. Efficiencies employed for conventional wood-fired biomass power plant analysis (3 to 600 MWe) by Mitchell et al. /35/, McMullan et al. /36/, and Toft /37/. Ekono co-generation data as reference /34/.

The data presented in two US studies is shown in Figure 2-7, together with Ekono data. It can be seen that the values used by Marrison and Larson /38/ agree well with the CHP data of Ekono. The data presented by Marrison and Larson is therefore low, as it is valid for the condensing mode of operation. The efficiency used by EPRI /39/ is even lower than this. It may be seen that these studies use lower efficiencies than previous references. The results suggest different design principles: when fuel costs are low (as in the US), it is not economic to invest in higher efficiency. This aspect is discussed further in section 2.6.

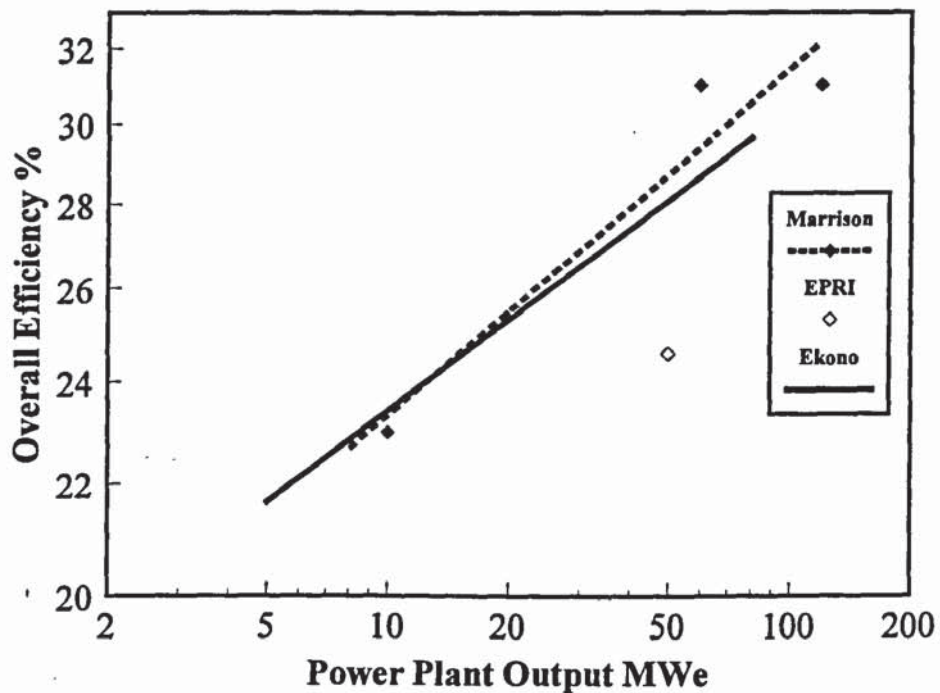


Figure 2-7. Efficiencies employed for conventional wood-fired biomass power plant analysis by Marrison and Larson /38/ and EPRI /39/. Conversion from hhv to lhv efficiencies by the author. Ekono co-generation data as referencee /34/.

2.2.3 Power plant investment cost

2.2.3.1 Ekono Energy

Power plant investment costs are shown for plants from a review by Ekono in Figure 2-8 /34/. Note that the data presented is based on recently realised power plant projects. Therefore, these costs represent accurately those of state-of-the-art technology.

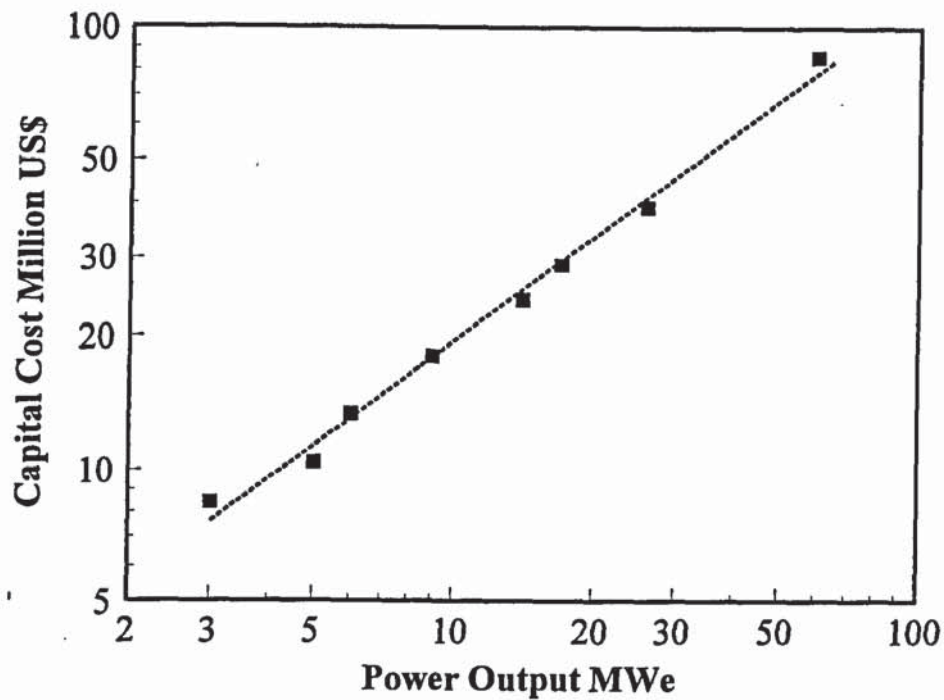


Figure 2-8. Co-generation plant investments. Location Finland 1994-96, data provided by Ekono /34/. 1 US\$ = 5 FIM.

The investment cost is the total cost paid by the customer for a fully operational power plant. It includes:

Main equipment

- Boiler plant (fuel delivery system, boiler, ash handling, pumps, heat exchangers, flue gas cleaning, steel parts of the stack, boiler instrumentation and electrical system)
- Turbine plant (steam turbine and generator, boiler feedwater system, internal piping, cooling water system)
- Fuel handling (fuel receiving station, intermediate silo, conveyor belts)
- Water treatment plant
- Piping and insulation
- Auxiliary equipment (instrument air, fire extinguishing equipment etc.)
- Automation
- Electrical equipment
- Spare parts for two years operation

Buildings

- Buildings and structures (boiler building, concrete stack, turbine building, service and office building, fuel handling building)
- Land and site preparation
- Connections (electrical network, water and waste water piping)

Other costs

- Design and control (costs for the power plant operator: general, process, architect, structural, instrumentation, and equipment design, control, and administrative costs, environmental licensing procedures, and other miscellaneous costs)
- Costs during construction (temporary buildings, structures, construction administration, services, insurance)
- Contingency (5% used by Ekono for mature technology)
- Interest during construction

Although the costs in Figure 2-8 are for co-generation plants, they also serve as good first estimates for condensing biomass power plants. In practice, the difference in investments between a co-generation and a condensing power plant is typically less than 5 % of the overall cost /34/.

Note that the scales are logarithmic. The same data as in Figure 2-8 is used in designing Figure 2-9, which shows specific investment as a function of power output. Specific investments decrease from about 2500 to 1400 USD/kW, as power output is increased from 3 to 60 MWe.

The costs are valid for 1994 - 1996 in Finland. Note that inflation during these years was very low, and has since been about 2% p.a. The capital cost reported in this section, and also in subsequent sections, represents the total installed plant investment cost, unless otherwise stated.

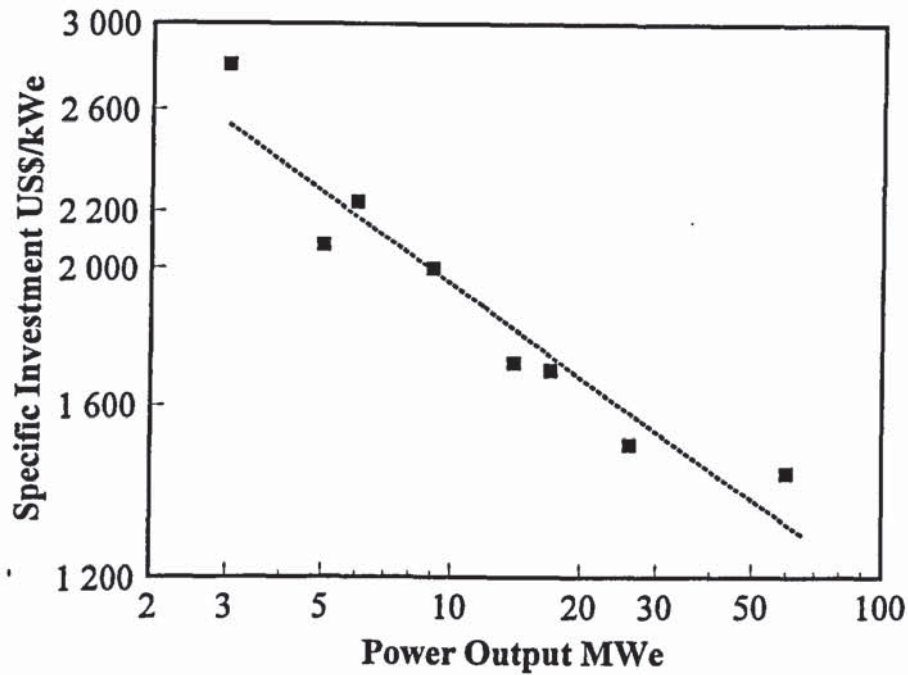


Figure 2-9. Specific investments for co-generation plants. Location Finland 1994-96, data provided by Ekono /34/. 1 US\$ = 5 FIM.

If the investment cost follows the power law of equation 2-3, the scale factor (b in equation 2-3) for the Ekono data is 0.78. A similar power law yields a specific scale factor of -0.21 , when equation 2-3 is fitted for the specific investment (Figure 2-9).

$$y = a * x^b \tag{2-3}$$

where y = Capital investment cost, million US\$

x = Plant capacity, MWe

a = Constant

b = Scale factor

2.2.3.2 Other work

The investment cost data by: Mitchell et al. /35/ (cost bases 1994), Marrison & Larson /38/ (1994, EPRI /39/ (1994), Toft /37/ (1995) and McMullan et al. /36/ (1989) is reviewed and compared with the data presented by Ekono over a wide range of capacities in Figures 2-10 and 2-11. According to the reports, the investment costs are total investment costs paid by the customer for a fully operational power plant. These estimates may be compared with

the data presented in the Ekono report, although it is accepted that the scope of all the studies may not be precisely the same. It appears, for example, that some of the data in the references is valid for older technology.

The data is presented at two different scales. Figure 2-10 displays the entire range presented in the references, and Figure 2-11 depicts a range which is believed to be more reasonable for bio-power plants. The two figures are included to highlight the differences between the investment costs in the references.

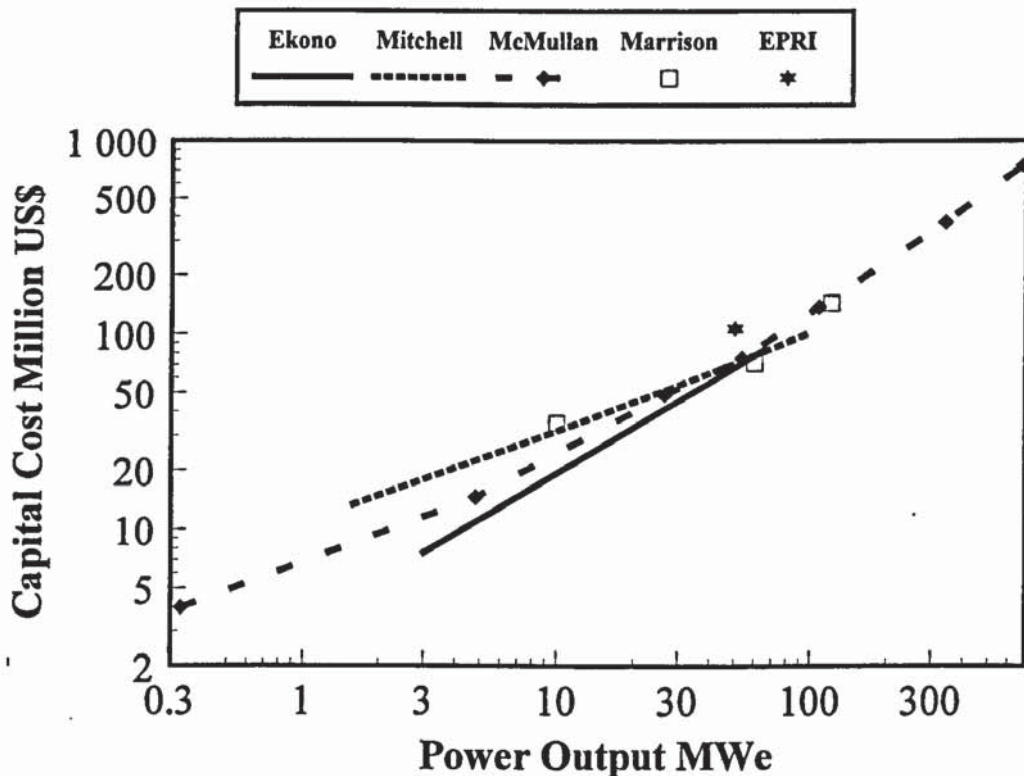


Figure 2-10. Capital costs of power plants according to Mitchell et al. /35/, McMullan et al. /36/, Marrison and Larson /38/ and EPRI /39/. Ekono data as reference /34/. £1= US\$ 1.7, \$ 1= FIM 5.

If the investment cost is assumed to obey the power law of equation 2-3, the following scale factors (b in equation 2-3) may be derived from the published data: Ekono 0.78, Mitchell et al. 0.49, McMullan et al. 0.69, Marrison & Larson 0.53. The variation in the reported investment costs is rather wide. Serious disagreement occurs especially at lower capacities, where bio-power concepts have often been suggested as feasible.

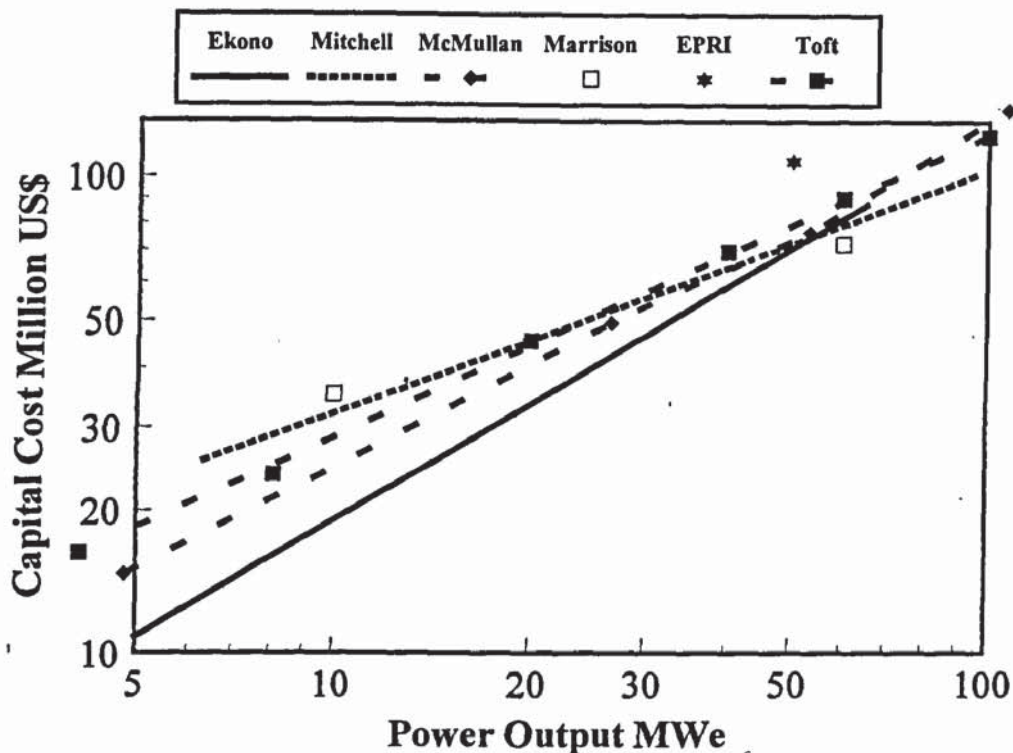


Figure 2-11. Correlations in Figure 2-10 shown for a range from 5 to 100 MWe. Toft /37/ included.

In addition to the references quoted in Figure 2-10, data by Toft /37/ is included in Figure 2-11. The work by Toft is a continuation of the work previously reported by Mitchell et al. /35/. Investment cost by Toft is not shown in Figure 2-10, because the correlation is close to that of McMullan et al. The scale factor derived from the data of Toft is 0.63.

It is seen from Figure 2-11 that most of the studies agree reasonably well around 50 MWe. The only data in disagreement even on that scale is that of EPRI /39/. The reason for this is the low power production efficiency used by EPRI.

Specific investments for the same studies are shown in Figure 2-12. The following specific scale factors (equation 2-3) can be estimated from the data: Ekono - 0.22, Mitchell et al. - 0.51, McMullan et al. - 0.30, Marrison & Larson - 0.34, and Toft - 0.37. It may be concluded that agreement between the studies is not particularly good. It should also be noted that the data by McMullan et al. and Marrison & Larson do not follow the same equation for scale as the other three sets of data.

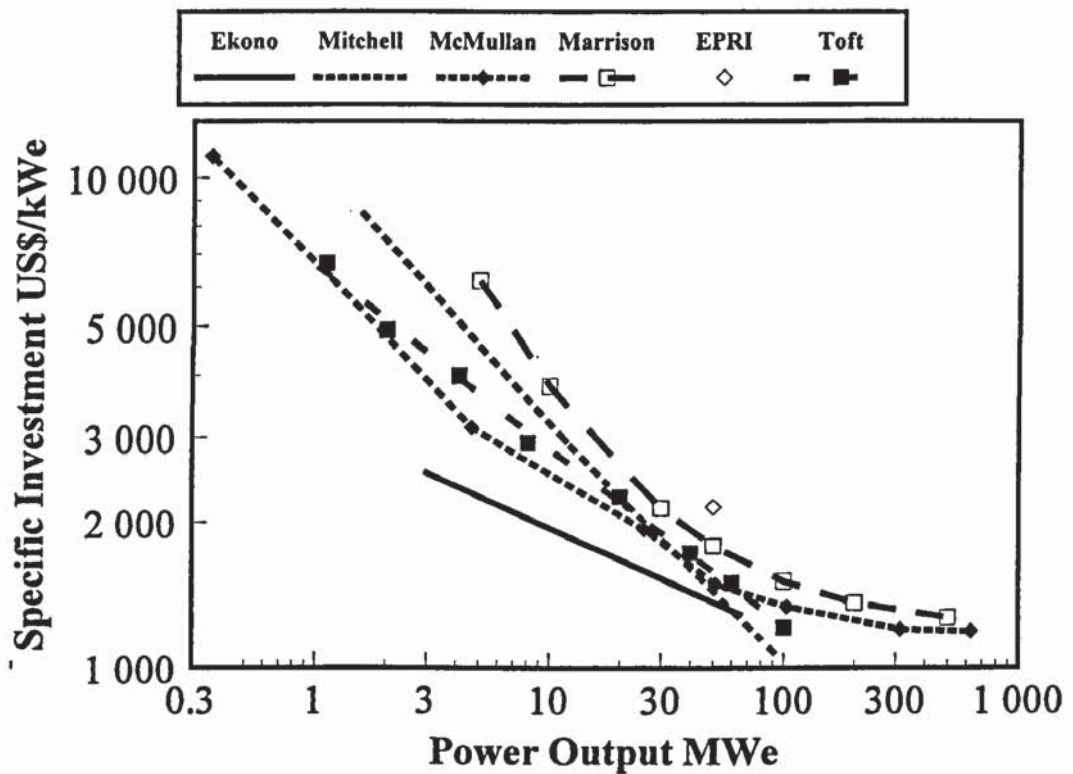


Figure 2-12. Specific capital costs of power plants according to Mitchell et al. /35/, McMullan et al. /36/, Marrison and Larson /38/, Toft /37/, and EPRI /39/. Ekono data as reference /34/.

2.2.4 Cost of electricity

2.2.4.1 Ekono Energy

The cost of electricity (COE) published by Ekono Energy /34/ is presented in this section. COE is presented first as a function of the annual operating time for four different capacity co-generation plants. Co-generation and power-only production are then compared over a wide capacity range. The effect of fuel cost on COE is shown next as a function of annual operating time. Finally, COE is shown using two heat prices, and also in the power-only production mode, to illustrate the difference between condensing and co-generation power production.

COE is calculated according to equation (2-1). The COEs for four conventional co-generation plants are shown in Figure 2-13 /34/. COE is estimated assuming a plant life-

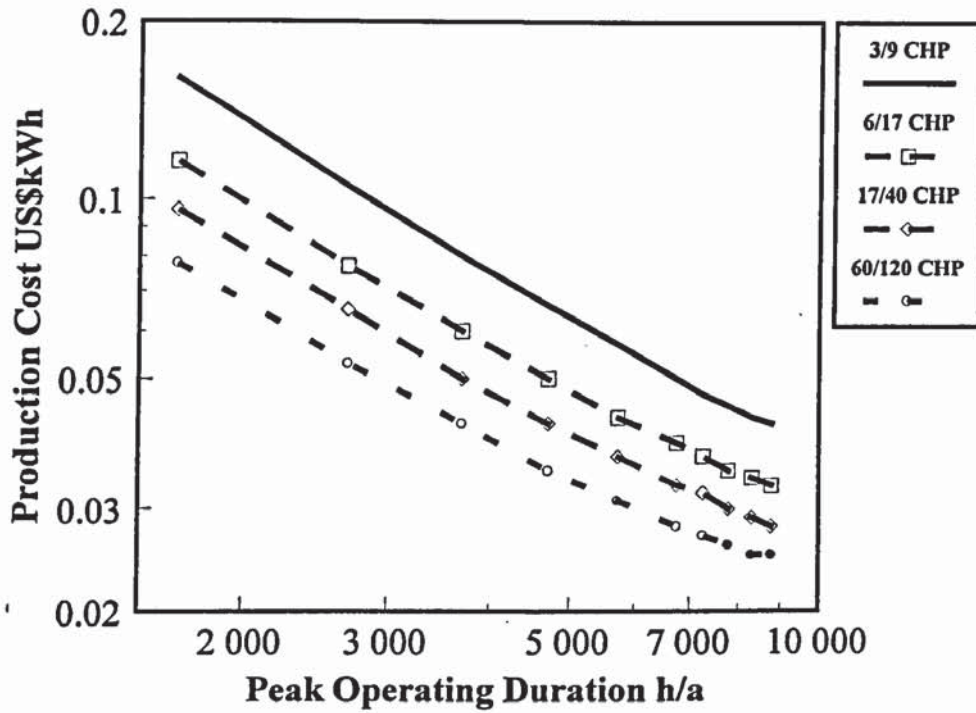


Figure 2-13. Cost of electricity as a function of annual operating hours. 3/9 CHP denotes 3 MWe of electricity and 9 MWth of heat in co-generation. Location Finland 1994-1996, data provided by Ekono/34/, fuel 2.5 US\$/GJ, 20-year service life, 5 % real interest rate, value of heat calculated using a tariff with the fixed cost component as 30US\$/MW,a and the variable cost component 11 US\$/MWh.

time of 20 years and using a 5% interest rate, which have been standard for the industry /34/. The respective annuity factor, which corresponds to CCR in equation (2-1), is 0.08. The capacities shown are typical of the bio-power plants built in recent years. However, the largest plant (60 MWe/120 MWth) shown is actually fuelled by peat, although the technology is the same as for woody biomass. Plants smaller than 3 MWe have, at least so far, been uneconomic. On the other hand, the fuel supply will set a limit for larger plants. Both the upper and lower limits are very site-specific. The COE values shown may be regarded as the lowest possible for bio-power at present time due to co-generation.

Co-gen. and condensing modes are compared in Figure 2-14. In co-gen. the COE at 4 700 h/a ranges from 0.066 (3 MWe/9 MWth) to 0.035 (60 MWe/120 MWth) US\$/kWh. A typical peak (annual) operating time for these co-gen. plants is around 4 000 - 5 000 h/a. The respective range in condensing mode production is from 0.118 to 0.070 US\$/kWh. The relevance of peak operating time in power production is discussed further in Chapter 12.

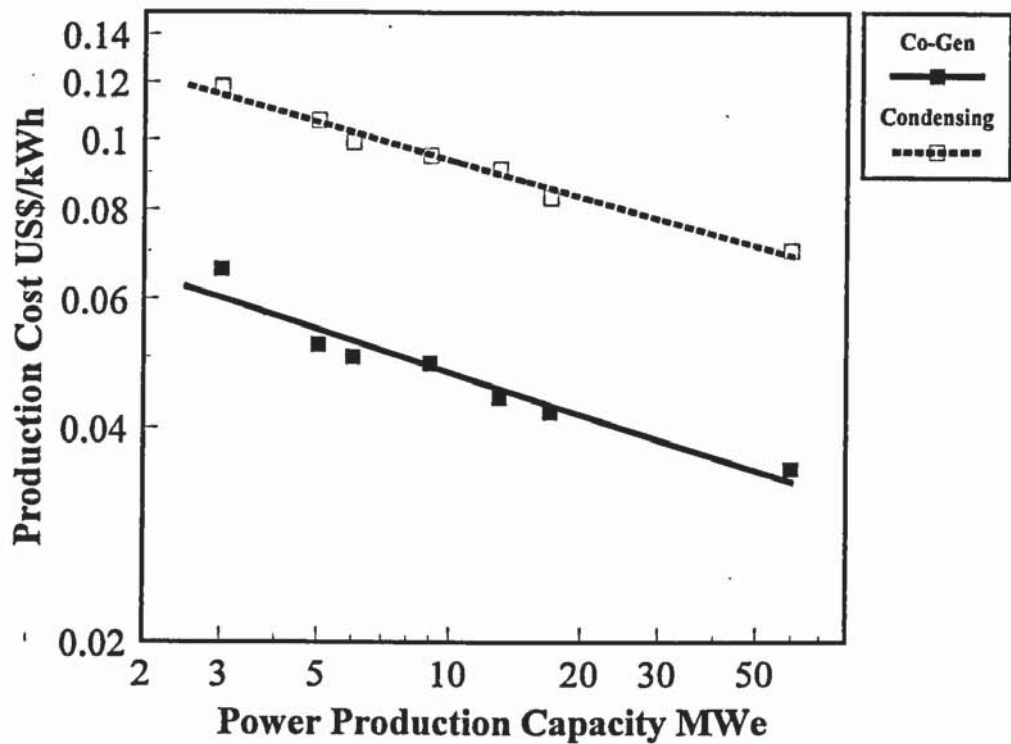


Figure 2-14. Cost of electricity as a function of power plant output. Location Finland 1994-1996, data provided by Ekono/34 /, fuel 2.5 US\$/GJ, 20-year service life, 5% real interest rate, value of heat calculated using a tariff with the fixed cost component as 30 US\$/MWh and the variable cost component 11 US\$/MWh. Condensing COE calculated from the Ekono data by the author.

The value of district heat for COE is shown in Figure 2-15. Heat production has a cost structure similar to that of power production, where increasing the annual operating time reduces the production costs. A comparison between co-generation (two heat prices) and power-only production is presented. District heat has been calculated with fixed operating costs of 16 000 and 36 000 US\$/MWh, and variable operating costs of 11 and 16 US\$/MWh for low and high heat cost, respectively. At 4700 h/a, the COEs are 0.03, 0.06, and 0.11 US\$/kWh with high and low heat cost in co-generation, and in condensing mode, respectively. It may be concluded from Figure 2-15 that heat cost has a decisive effect on the overall competitiveness of bio-power.

The effect of fuel cost on COE is shown in Figure 2-16, which shows three fuel costs corresponding to a range of 1.7-3.3 US\$/GJ. The COE is for a co-generation plant producing 5 MWe of electricity and 15 MWth of heat. At 4700 h/a, the COE ranges from 0.066 to 0.037 US\$/kWh.

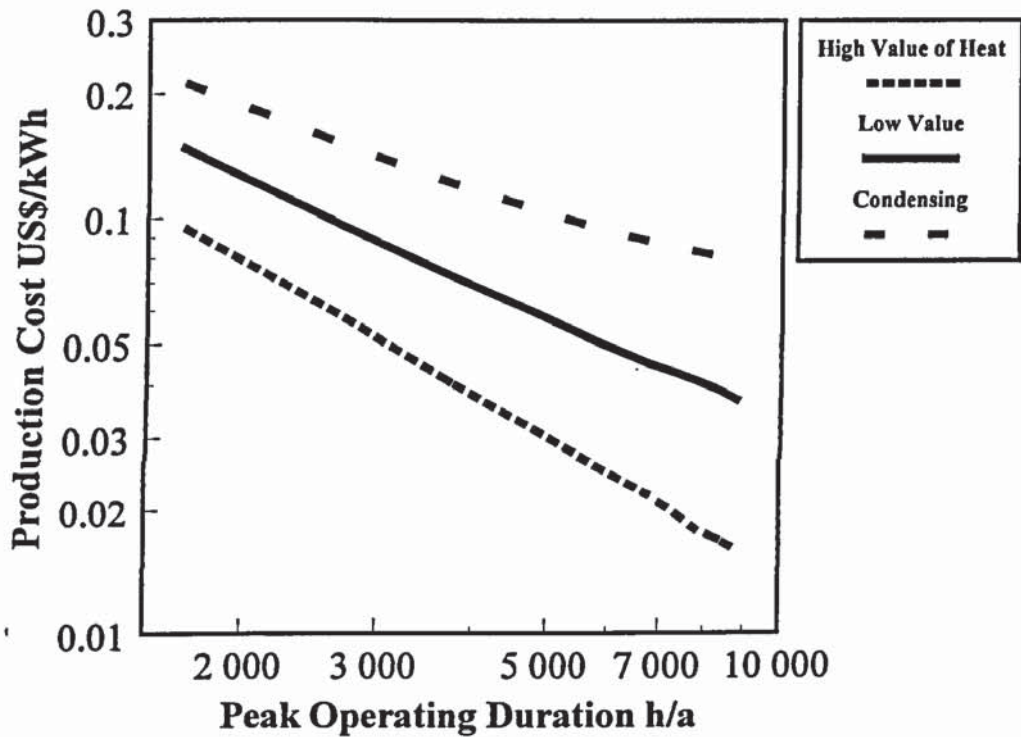


Figure 2-15. Effect of value of district heat in co-generation. Location Finland 1994-1996, data provided by Ekono/34/, fuel 2.5 US\$/GJ, 20-year service life, 5% real interest rate. Value of heat defined in text.

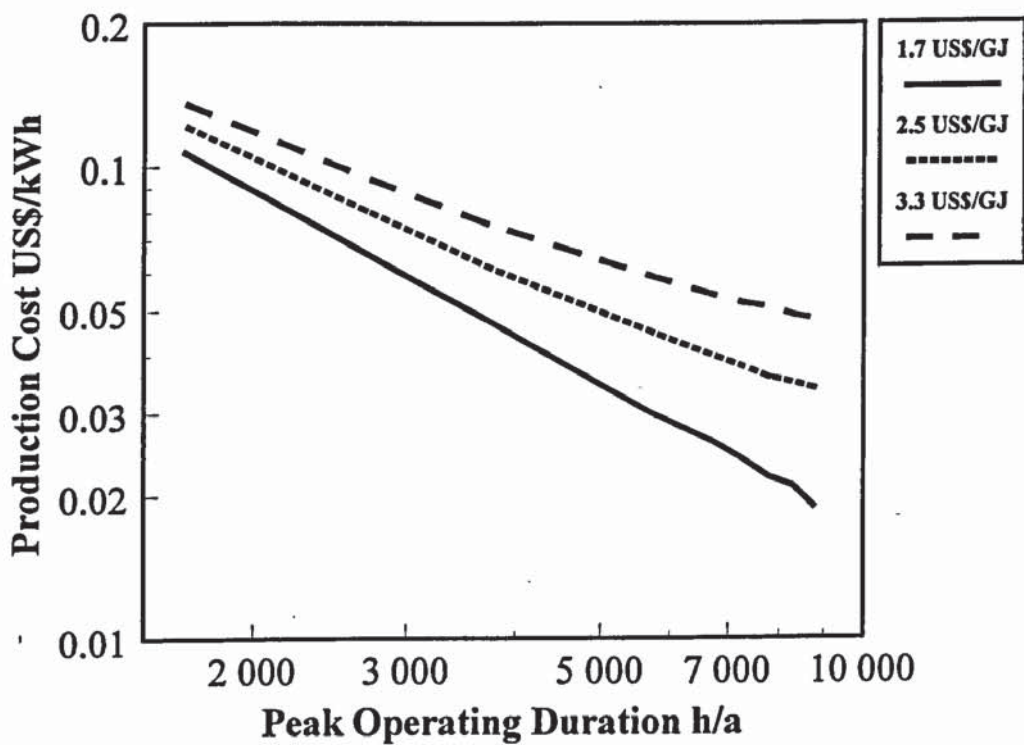


Figure 2-16. Effect of fuel cost in co-generation. Location Finland 1994-1996, data provided by Ekono /34/, fuel 2.5 US\$/GJ, 20-year service life, 5% real interest rate.

2.2.4.2 Other work

Marrison & Larson /38/ have studied cost versus scale for plantation-based bio-electricity systems at three locations: north central USA, southeast USA (switchgrass), and southern Bahia, Brazil (eucalyptus). In addition to advanced IGCC systems (section 2.4), they also show estimates for steam-Rankine cycles. The COEs for the years 2000 and 2020 are shown in Figure 2-17. The levelled COE is estimated at around 0.065 - 0.090 US\$/kWh in 2000. The assumed annual operating time is 6570 h/a. A lower COE is estimated in 2020 than in 2000, largely because of the expected lower biomass cost at that time. The biomass costs range from 5.2 US\$/GJ (2000 NC USA) to 2.6 US\$/GJ (2020 SE USA). In Brazil, the average cost is close to 3.0 US\$/GJ.

According to /38/ the minimum COE is achieved at very large capacities, around 400 MWe. However, the COE is within 5% of this minimum already at 100 - 110 MWe. Specific biomass supply curves but the same cost equation are used for each location. The investment cost equation (section 2.3.3.2) used by Marrison & Larson is rather different from those employed in most other studies, so the estimated COE includes considerable uncertainties.

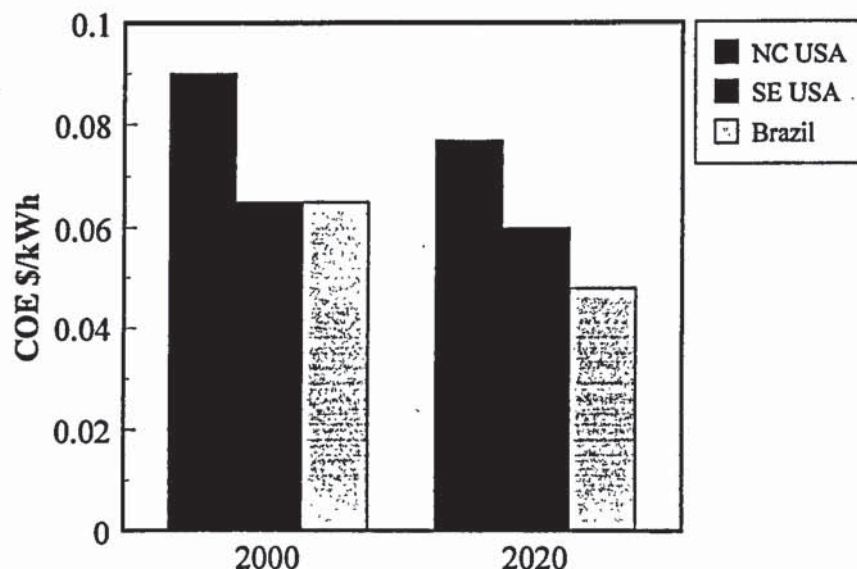


Figure 2-17. COE at three locations with a Rankine-steam cycle, Marrison & Larson /38/. Utility financing: interest rate 8%, service life 20-years, annual operating time 6 570 h. NC = north central, SE = south east.

EPRI has included SO₂, NO_x and even CO₂ emission charges in their economic assessment /39/. Nevertheless, the low cost of fossil fuels makes it difficult for biomass to compete economically (Figure 2-18). Overall, EPRI suggests co-firing in a utility boiler to be the lowest cost alternative for wood biomass. The relatively high efficiency steam cycle of a larger power plant may be used, and the retrofit investment is low. The estimated COE for production with specific wood-fired boilers is around 0.08 \$/kWh, which may be compared with the co-firing COE of below 0.04 \$/kWh.

The IEA interfacing activity has also included a Rankine steam cycle in their assessment of advanced systems /35/. The analysis is discussed in more detail in Section 2.4. This work studied the interaction between plant capacity and fuel cost. Their correlation for the COE of the Rankine power plant is shown in Figure 2-19. The values reported agree with the estimate by EPRI at 50 MWe, although the biomass cost is higher than that used by EPRI, 2.9-3.4 US\$/GJ versus 2.1 US\$/GJ. The investment cost in this work is based on EPRI data.

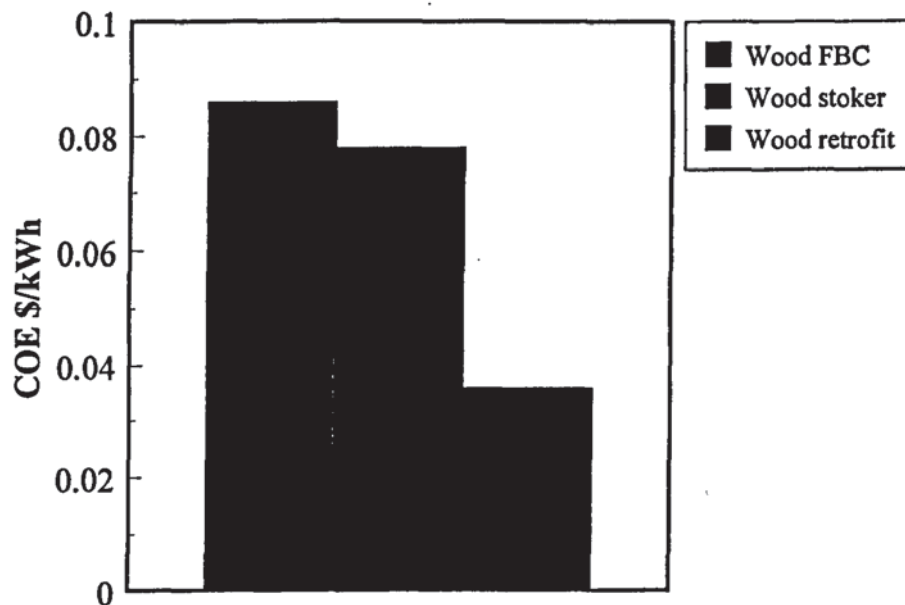


Figure 2-18. COE for different biomass technologies, EPRI /39/, location USA. Wood Fluidised Bed Combustion (FBC) and a Stoker boiler at 50 MWe, wood retrofit: co-fired 15% in a utility boiler (200 MWe). Wood 2.1, coal 1.1 \$/GJ, levelized cost according to the EPRI TAG /60/.

The estimated COE is higher than in the results of Ekono for similar plants, especially in the lower capacity range.

McMullan et al. /36/ also included a Rankine-steam cycle as part of their assessment of advanced systems. This work is also discussed in more detail in section 2.4. The correlation with the steam-cycle COE is shown in Figure 2-20. The capacity range considered is large, taking into consideration the potential availability of woody biomass in Europe. The cost of wood ranges from 1.0 to 2.8 US\$/GJ (as a function of capacity), which is lower at small capacities than other sources have used. Their estimation method for COE is different from that employed in other studies reviewed. Typically, COE based on a levelized or annuity costs is reported /34/, /39/. McMullan et al. employ a break-even electricity selling price calculated with a discounted cash flow. Therefore, the values cannot be directly compared with those in other references. However, McMullan et al. /36/ find a minimum for the COE at capacities of around 50 to 150 MWe. This may be compared with the findings of Marri-son & Larson /38/, who report a practically constant COE at higher capacities.

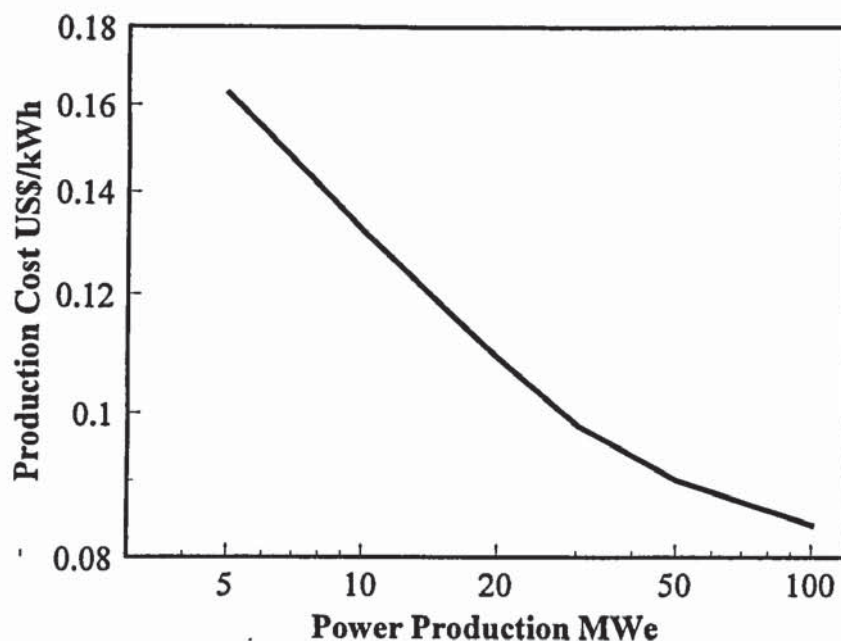


Figure 2-19. COE in a Rankine-steam cycle, Mitchell et al. /35/. Location Western Europe 1994, fuel 2.9 - 3.4 US\$/GJ. 20-year service life, 10% nominal interest rate, 5% inflation.

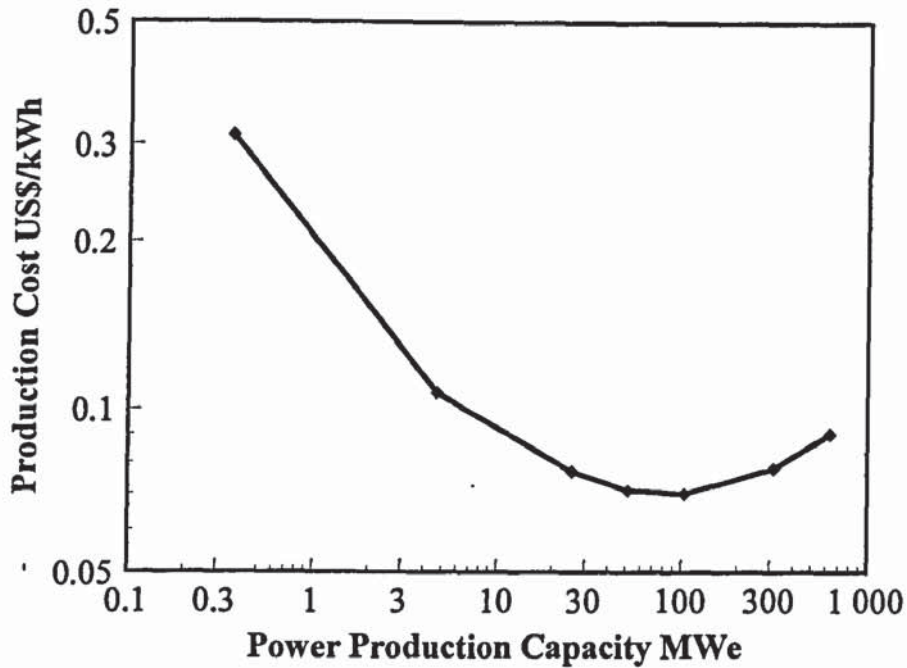


Figure 2-20. COE in a Rankine-steam cycle, McMullan et al. /36/. Location Western Europe 1995, fuel 1.0 – 2.8 US\$/GJ, break-even selling price estimated with 7.5% discounted cash flow.

2.3 Electricity from biomass based on gasification

In this section, results from the analysis of gasification systems using woody biomass as fuel are reviewed. Three important topics are again reviewed:

- power production efficiency
- specific investment cost
- cost of electricity

The state-of-the-art of gasification power plant technology is concisely summarised in the next section. The performance of power plants is reviewed on the basis of the literature. Estimated investment and production costs for these systems are also reviewed.

2.3.1 Introduction

Various Integrated Gasification Combined Cycle (IGCC) concepts have been proposed during this decade, as IGCC has evolved as one of the leading candidates for electricity

production from biomass. A simplified flowsheet of an IGCC was presented in section 1.5.2. Biomass IGCC technology has advanced to a point where one 6 MWe demonstration plant has been operating in Sweden since 1996 /40/, /41/ (Figure 2-21). Pressurised circulating fluidised-bed (CFB) gasification is employed. Three other biomass IGCC demonstration projects on approximately the same scale were pursued in Europe with partial funding from the EU Thermie Programme /42/. One pressurised bubbling fluidised-bed (BFB) and two atmospheric CFB gasifiers were initially selected for the projects. Only the two latter projects were active in 1999. In the U.S., two biomass gasification projects in progress in 1997 had plans to install gas turbines at a later stage /43/, /44/. However, only one of them was active in 1998 - 1999 /45/. Both of these applications have had partial funding from the U.S. DOE. A pressurised BFB and an indirectly heated double fluidised-bed gasification technology are employed. Fluidised-bed gasification is reviewed in Chapter 6.

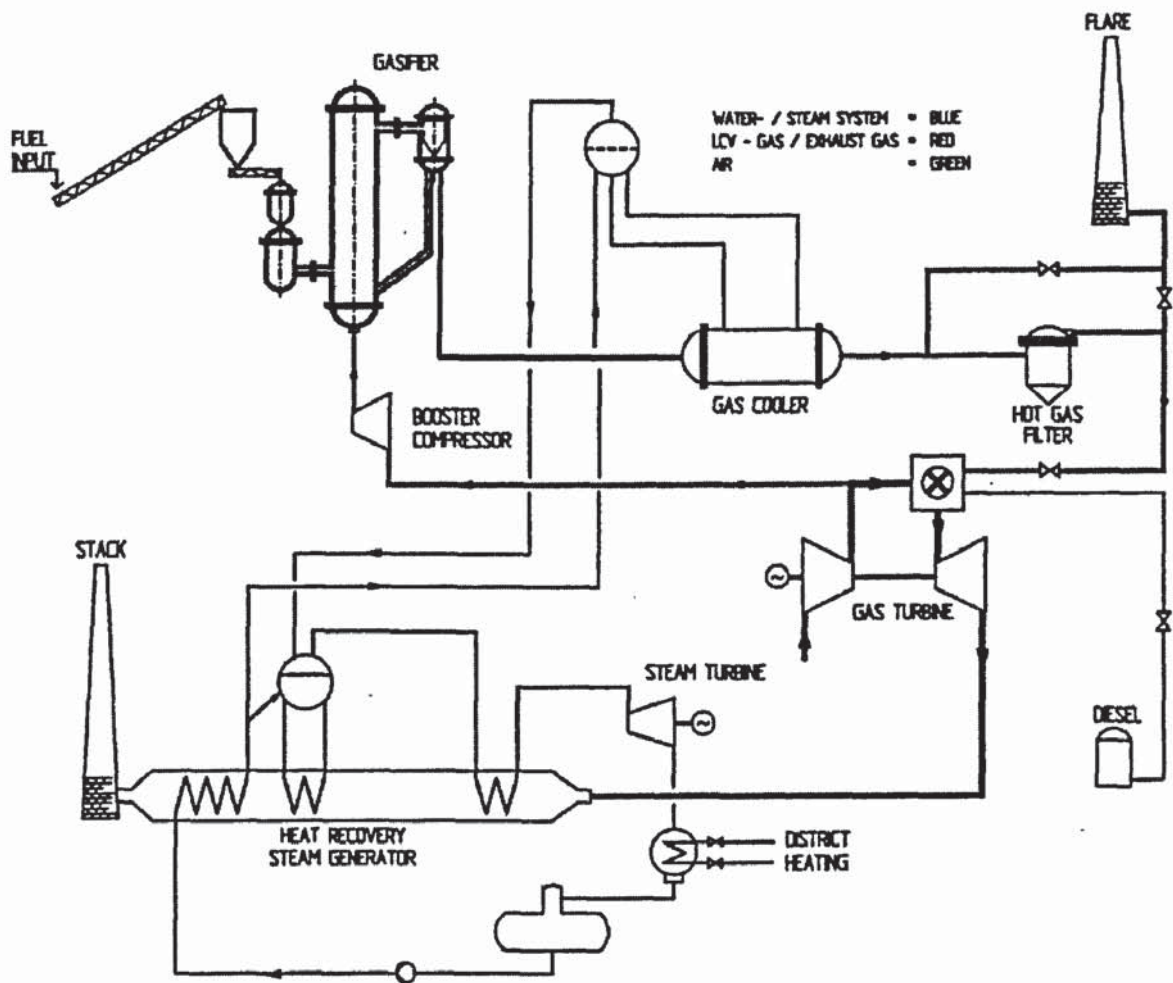


Figure 2-21. Sydkraft IGCC plant at Värnamo, Sweden /40/.

Other power production concepts employing gasification are also being developed. There are numerous projects in which gasifiers are coupled to internal combustion engines (ICE). However, most of the projects are on a relatively small scale, up to 200 kWe, and often below 100 kWe. As pointed out in section 1.4, these concepts are excluded from this study.

2.3.2 Power production efficiency

2.3.2.1 Enviropower - Carbona

Salo and Keränen of Enviropower Inc. (today Carbona Inc.) have reported on the feasibility of biomass-fuelled IGCC /46/. This study is important because their analysis, as opposed to many other studies reviewed, is based on actual detailed plant design by an engineering contractor, Tampella Power (today Kvaerner Pulping), together with Enviropower for commercial projects. Carbona Inc. proposes building Integrated-Gasification Combined Cycle (IGCC) plants.

Efficiencies for IGCC concepts reported in /46/ are presented in Figure 2-22. Performance calculations are based on the European Gas Turbines (EGT) Typhoon, the Mitsubishi Heavy Industries (MHI) MW151, the General Electric (GE) F6B and the Westinghouse (WH) W251B11 gas turbines. Note that recently EGT and WH have merged with other companies. The gas turbine is a critical unit operation in an IGCC, as the plant design is based on gas demand by the gas turbine. All other plant sections are designed and sized accordingly. The selection of a specific engine is of great importance, as Chapter 8 will show that only a few engines on the market may be employed with the low heating value (LHV) gas produced in biomass gasification.

The concepts presented by Salo and Keränen are important because they are based on gas turbines guaranteed by their manufacturers to operate with LHV gas. It is believed that the performance data is accurate. The performance of the gas turbine has been estimated by their manufacturers, and the overall performance calculation has been carried out by a large engineering company. The study also included a suitable capacity range for this work.

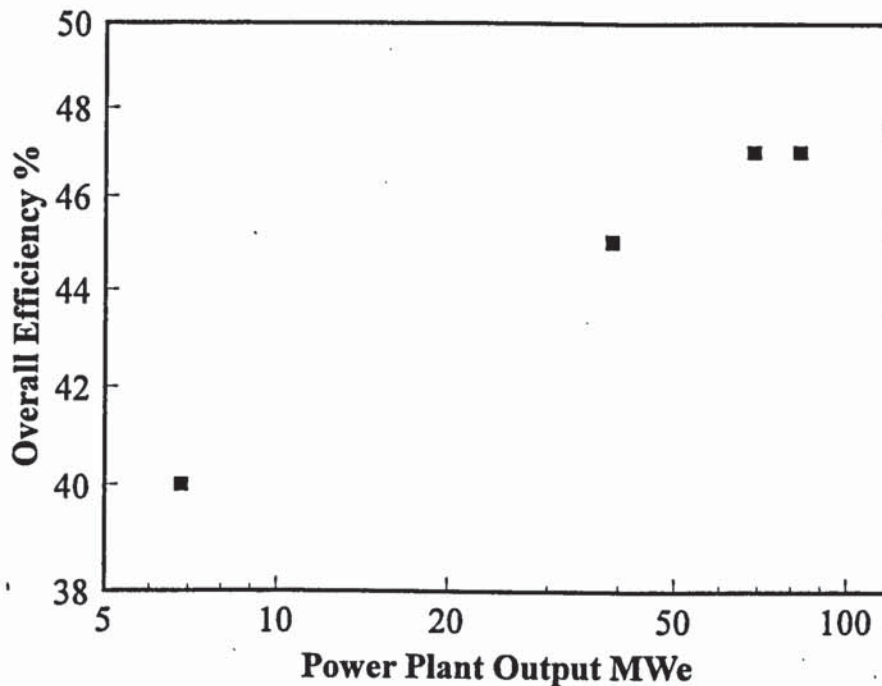


Figure 2-22. IGCC efficiencies based on lower heating values /46/.

The data presented in /46/ is used as a reference for other studies reviewed in the following sections.

Overall plant efficiencies range between 40 and 47% based on the lhv of the fuel (equation 2-2). Higher efficiencies appear more technically feasible for the biomass IGCC than for state-of-the-art steam-boiler power plants (approx. 45% versus 30%) (note section 2.3 describing steam-boiler power plants).

2.3.2.2 National Renewable Energy Laboratories (NREL)

Craig and Mann /47/ report efficiencies for four IGCC systems employing two gas turbines, in one case an aero-derivative and in three cases an industrial engine. Three gasification processes are included: the air-blown pressurised Institute of Gas Technology (IGT) RENUGAS®, the air-blown indirectly heated Battelle Columbus Laboratory (BCL) gasifier, and the air-blown atmospheric pressure Termiska Processer (TPS) gasifier. Aspen simulation software is used to derive the mass and energy balances. However, very little information is available concerning the models built.

As may be seen from Table 2-1, the concept with the advanced industrial turbine (6FA) yields a higher efficiency than the same concept with an aero-derivative engine (LM5000). Gas turbines are discussed in Chapter 8. Normally, aero-derivatives yield higher efficiencies, because of the higher pressure ratios and higher firing temperatures employed. How-

Table 2-1. IGCC efficiencies (based on hhv values) reported by NREL /47/.

Gasifier Pressure Gas turbine	Renugas Pressurised LM5000 ^a	Renugas Pressurised 6FA	BCL Atmospheric 6FA	TPS Atmospheric 6FA
Net output MWe	56	132	122	105
Net efficiency %	35.8	39.7	35.4	37.9

^a Efficiency corrected from the reference 36.7 to 35.8% is based on a discussion with one of the authors (M. Mann, 28 October 1996).

ever, the apparently unexpected result is probably due to the lower firing temperature assumed for the aero-derivative engine. A lower firing temperature reduces efficiency. There is some uncertainty as to which firing temperature may actually be employed industrially (note discussion about this aspect in Chapter 8).

IGCC with an industrial turbine employing pressurised gasification has the highest efficiency (about 40% based on hhv), followed by the direct atmospheric (38%) and indirect (35%) systems. The system efficiencies based on lower heating values cannot be compared with each other directly due to the different feedstock moisture contents assumed (38% for a pressurised system, and 50% for air-blown systems). However, an approximate conversion to lhv values is shown in Figure 2-23. The values are compared with a correlation from Figure 2-22. Although engines are not available at all points of this curve, such a presentation helps to highlight the differences between the studies.

The efficiency of an IGCC at 130 MW with pressurised gasification and an industrial turbine is estimated by NREL to be about 46%, based on lhv. The concept is similar to that presented by Enviropower. The value is lower than an efficiency extrapolated from the Enviropower data /46/ at the same capacity. However, different fuel moisture contents in the studies hamper direct comparison. It is concluded that the NREL work is consistent, but the dissimilarity to the Enviropower study is probably due to different design principles.

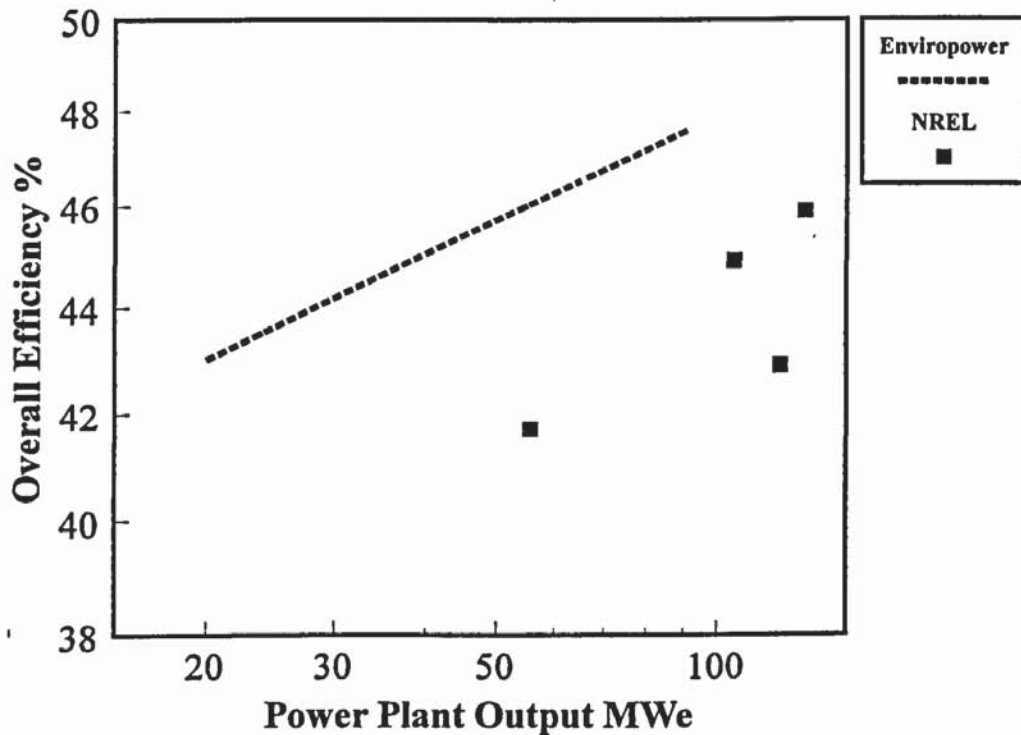


Figure 2-23. IGCC efficiencies according to NREL /47/; conversion from higher to lower heating values by the author.

2.3.2.3 Princeton University

Consonni and Larson have developed an advanced and detailed simulation tool to describe gas turbine performance (further discussion in section 2.6 and Chapter 8) /48/. They have analysed three base biomass IGCC concepts which are currently being proposed for commercial development and demonstration. The emphasis of the work is on the prediction of gas turbine performance. The IGCC concepts employ aero-derivative gas turbines in the 20 - 30 MWe power output range.

The concepts analysed in /48/ are based on air-blown pressurised fluidised-bed gasification (IGT-Enviropower-Carbona, Bioflow), air-blown atmospheric pressure fluidised-bed gasification (TPS, Lurgi), and indirectly-heated atmospheric pressure fluidised-bed gasification (Battelle Columbus) (Table 2-2 and Figure 2-24).

Table 2-2. Base IGCC efficiencies (based on lhv values) reported by Consonni and Larson /48/.

Gasifier	IGT Pressurised Derated ^a	TPS Atmospheric Derated	BCL Atmospheric Derated
Gas turbine			
Net output MWe	28.8	25.9	24.5
Net efficiency %	45.2	41.9	41.1

^a Firing temperature of 1 100 °C.

Consonni and Larson also explored more advanced cycles based on a generic 25 MWe class engine and the GE LM1600, both employing pressurised gasification (Table 2-3 and Figure 2-24). Further, inter-cooled gas turbines were assumed on the basis of a development programme being jointly carried out by gas turbine manufacturers, U.S. DOE and EPRI /49/.

Table 2-3. Advanced IGCC concept efficiencies (based on lhv values) reported by Consonni and Larson /48/.

Gasifier	IGT Pressurised LM1600	IGT Pressurised Generic 25 MW	IGT Pressurised Intercooled	IGT Pressurised Intercooled
Gas turbine				
Net output MWe	21.6	39.6	42.4	78.6
Net efficiency %	45.8	47.3	49.4	50.5

A correlation based on the results presented in /46/ is again shown for reference. The efficiencies of "present" concepts with a gas turbine inlet temperature of 1100 °C agree with those presented in /46/. The performances predicted in /48/ for advanced turbines indicate that there is room for improvement in the biomass IGCC concept. The work of Consonni and Larson is valuable in that it studies in detail the critical unit in an IGCC, the gas turbine. The performance balances generated with the gas turbine simulation tool may be used in estimating the development potential of the IGCC technology.

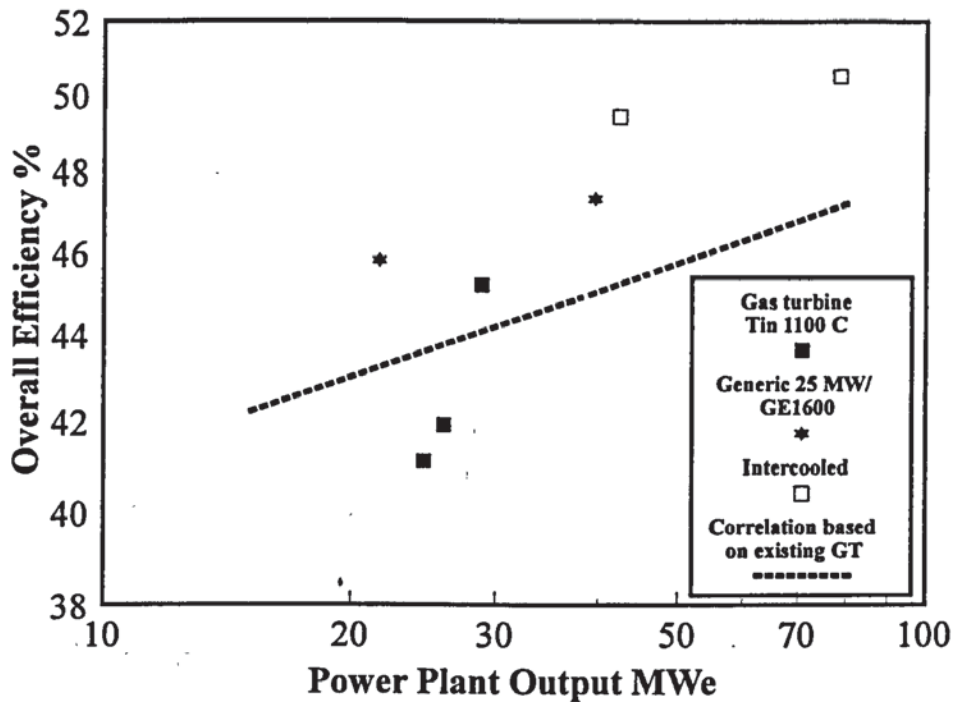


Figure 2-24. Biomass IGCC efficiencies /48/, correlation based on /46/.

Marrison and Larson have earlier studied the optimum size for power plants using plantation grown switchgrass as fuel /38/. The efficiency data employed is presented in Table 2-4 and Figure 2-25. The efficiencies presented for IGCC are constant, which is a serious flaw in an analysis which aims at studying capacity-related issues. The constant efficiency values may be compared with those shown previously in Figures 2-23 - 2-24 for the effect of scale on IGCC efficiency. Correlations are inadequate except for the Rankine cycle, the efficiency of which is close to the state-of-the art (note section 2.2.2).

Table 2-4. Biomass power plant data employed by Marrison and Larson /38/.

Production system	Capacity MWe	Efficiency	
		hhv	% lhv ^a
Rankine cycle	10	20	23
	high ^b	27	31
IGCC-atmospheric	10	37	42
	60	37	42
	high	37	42
IGCC-pressurised	30	40	46
	60	40	46
	high	40	46

^a Estimated from the hhv values given by the authors

^b "High" refers to the capacity at which minimum unit capital cost is reached

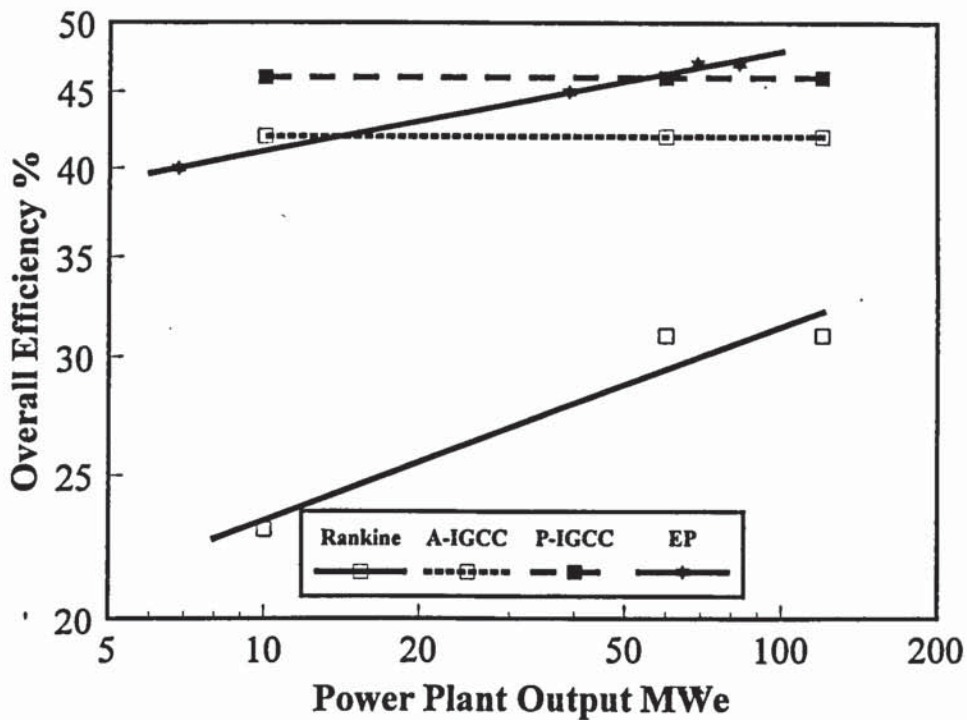


Figure 2-25. Power plant efficiencies according to Marrison and Larson /38/, conversion from hhv to lhv efficiency by the author. EP = Enviropower, Figure 2-22.

2.3.2.4 Electric Power Research Institute (EPRI)

EPRI has also analysed power production systems based on biomass /39/. A comparison of several technologies is presented in Table 2-5. EPRI reports lower efficiencies for IGCC than for other sources. The "existing" IGCC at 100 MWe has an hhv efficiency of only 28%, which may be compared to the 25% reported for a steam boiler plant at 50 MWe. An "advanced" IGCC has an efficiency of 35% at 100 MWe, which is still lower than those reported by others, including NREL. These efficiencies were converted to lhv efficiencies by the author, and are shown in Table 2-5 and Figure 2-26. EPRI data may be compared with that presented by both Enviropower (IGCC) and Ekono (Rankine). It is not possible to define sources of discrepancies between the EPRI study and others based on the EPRI publication.

Table 2-5. Power production technologies reported by EPRI /39/.

Power technology	Net capacity MWe	Efficiency	
		hhv %	lhv %
New coal	200	34.1	36.7
Natural gas CC	120	43.2	48.5
Wood FBC	50	24.6	28.3
Wood GCC ^a	100	28.1	32.3
Wood IGCC ^b	100	35.5	40.8

^a 1990 wood-fired IGCC, so-called existing technology, ^b An advanced IGCC

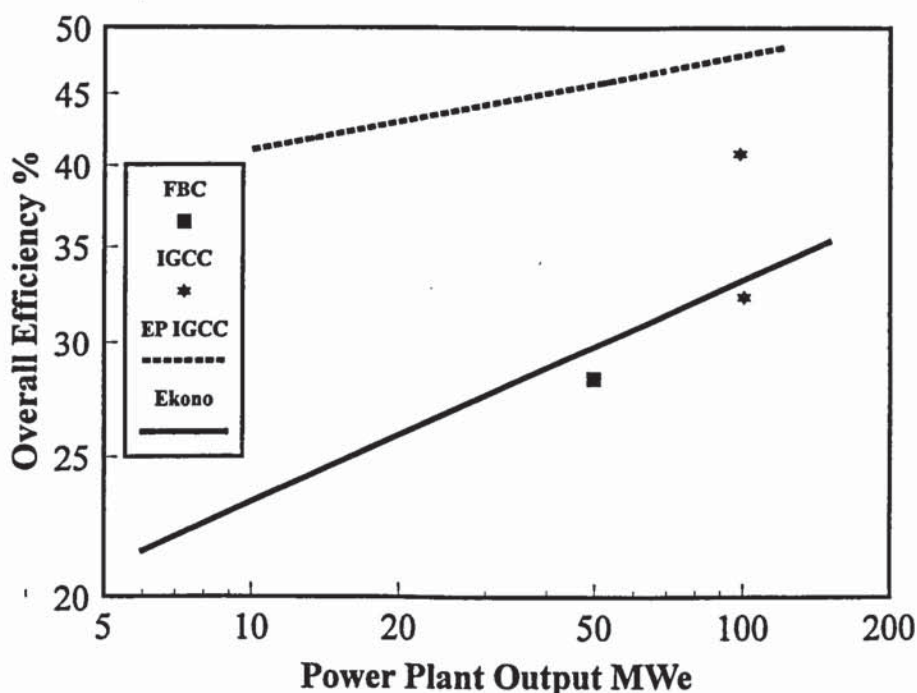


Figure 2-25. Power plant efficiencies according to EPRI /39/ with a correlation derived from Enviropower (EP) IGCC and Ekono (Rankine cycle) data as references. FBC = fluidised-bed combustion Rankine cycle, IGCC = integrated gasification combined cycle.

2.3.2.5 IEA Bioenergy - Interfacing Activity

Advanced bio-energy systems have been compared within the IEA Interfacing Activities, Mitchell et al. /35/. The emphasis in the study was on the overall bio-energy chain (feed-stock production, delivery, handling, conversion, power production) with the objective of examining relationships between the production of biomass and its conversion.

The results are summarised only for the capacity of 20 MWe (Table 2-6) in the report. However, efficiency correlations over a wide capacity range are also reported, and shown in Figure 2-27. The IGCC performance correlation does not match the data of Enviro-power. The Rankine cycle efficiency is close to that of Ekono, but since that is for co-generation facilities, the efficiency for the IEA condensing plant is too low. The two production modes are described and compared in section 4.4.6.

Table 2-6. Biomass power plants concepts at 20 MWe (efficiencies based on lhv values) reported by Mitchell et al. /35/.

Process concept	Efficiency % lhv
Boiler/steam cycle	23.5
IGCC	37.9
Gasification/diesel	27.6
Pyrolysis/diesel	29.8

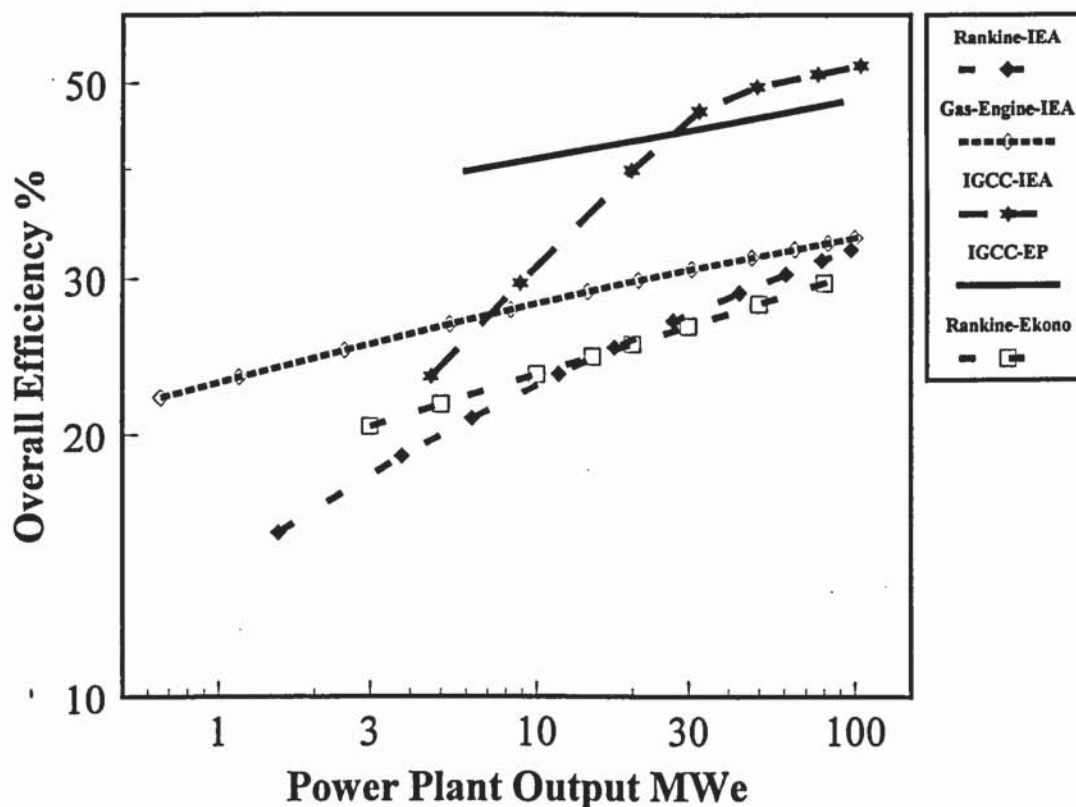


Figure 2-27. Power plant efficiencies, the IEA Interfacing Activity /35/, Enviro-power (EP) IGCC /46/ and Ekono co-generation Rankine data /34/ as references.

2.3.2.6 Aston University

Recently, Toft /37/ has analysed biomass power plants employing gasification (including pyrolysis and the Rankine cycle). The overall objective was to compare the whole utilisation chain from biomass to power, and to compare the main thermo-chemical processes.

Efficiencies for two bio-power systems based on gasification are shown in Figure 2-28. The IGCC performance correlation does not agree very well with the Enviropower reference data. The efficiency of the gasification/gas engine concept is slightly lower, especially above 5 MWe, than that reported in the IEA Interfacing work /35/.

Critical power plant prime movers are modelled in a simplistic manner by Toft /37/. Performance correlations for gas turbines using natural gas are used for LHV fuel gas. At the same time, the gas turbine outlet temperature is fixed. Studies carried out at Stanford and Princeton (see chapter 8 for details) describe more acceptable modelling procedures. The unacceptable modelling approach used by Toft reduces the value of the IGCC performance analysis carried out /37/.

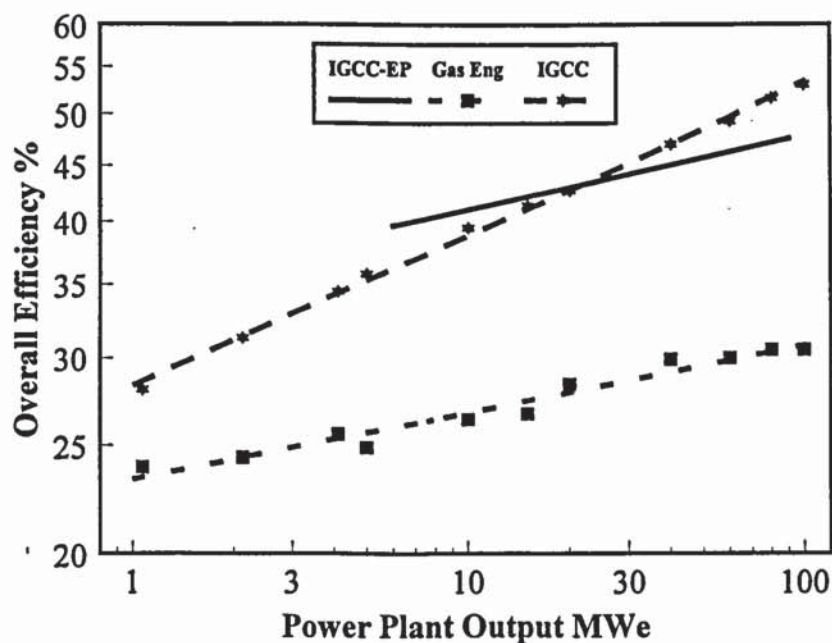


Figure 2-28. Gasification power plant efficiencies according to Toft /37/ with Enviropower IGCC data /46/ as a reference.

2.3.2.7 University of Ulster

McMullan et al. /36/ have assessed a large number of power plant configurations employing fossil fuels. Their modelling approach is summarised in section 2.6.

In /36/, four concepts using wood as fuel are included in a study for the EC DGXII:

- Wood combustion in a CFB with drying
- Wet wood CFB
- A hot gas filtration IGCC
- A wet gas scrubbing IGCC.

The efficiency of a wet wood combustion power plant at 25 MWe is reported as 25%, and of a hot gas clean-up IGCC as 42%. The IGCC results are summarised in Table 2-7.

Table 2-7. IGCC plant efficiencies /36/.

Concept	Capacity MWe	Efficiency %
IGCC		
- water scrubbing	38.6	38.4
- ceramic filter	42.7	42.4

In /36/, the gasification process assumed for the biomass IGCC is a pressurised circulating fluidised-bed, CFB. However, the concept includes some peculiar features. The IGCC concept employs cooling in the CFB reactor, much like in combustion. However, this cannot be realised, as heat cannot be removed from a biomass gasification reactor. Superheating steam with dirty product gas, another feature of the concept, is also ambitious due to dirty high-temperature fuel gas with a high hydrogen partial pressure. If technically feasible, the latter feature should raise the efficiency of an IGCC. However, the efficiencies reported are lower than in most other studies.

McIlveen et al. /50/ have later continued the analyses of power plants fuelled with short-rotation willow by adding more process concepts. Several IGCC concepts are evaluated, and efficiencies for pressurised hot gas clean-up gasification systems range from 40.4% (employing the industrial MS6001 with a total plant output of 74 MWe) to 42.6%

(MS9001FA with a total IGCC output of 435 MWe). Concepts employing atmospheric gasification give efficiencies ranging from 31.3 to 35.1%. The performance of all the concepts is shown in Figure 2-29. In spite of the enormous size of several concepts, the efficiencies are lower than in most other reports (except EPRI). It may also be seen that unlike in other studies, there is not a correlation between plant size and efficiency. The reason for these exceptional features cannot be deduced from the publication.

Gasifier/gas engine systems were also included at capacities from 0.2 to 2.3 MWe. Efficiencies for these small-scale systems ranged from 22.6 to 29.7%. The performances of the concepts analysed by McIlveen et al. /50/ are shown together with data by Mitchell et al. /35/ and Toft /37/ in Figure 2-30. The performance data of McIlveen agrees reasonably with the data of Mitchell et al. and Toft, except for two engines. However, at around one megawatt, efficiencies of about 22 to 30% may be seen, which is a rather wide variation.

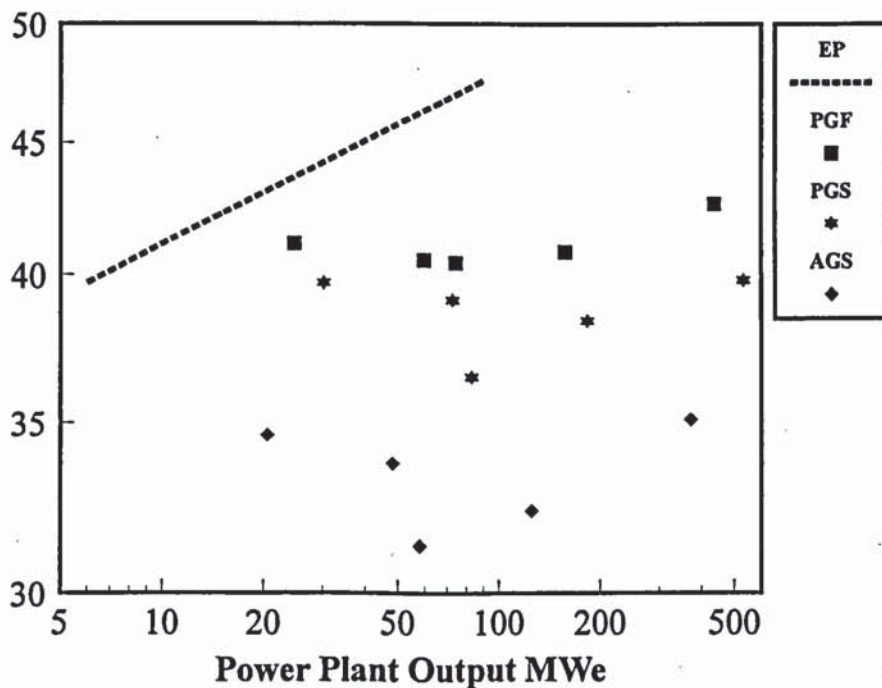


Figure 2-29. IGCC power plant efficiencies by McIlveen et al. /50/ with Enviropower (EP) IGCC data /46/ as a reference. PGF pressurised gasification with ceramic filters, PGS pressurised gasification with water wash of fuel gas, and AGS atmospheric pressure gasification with water wash of fuel gas.

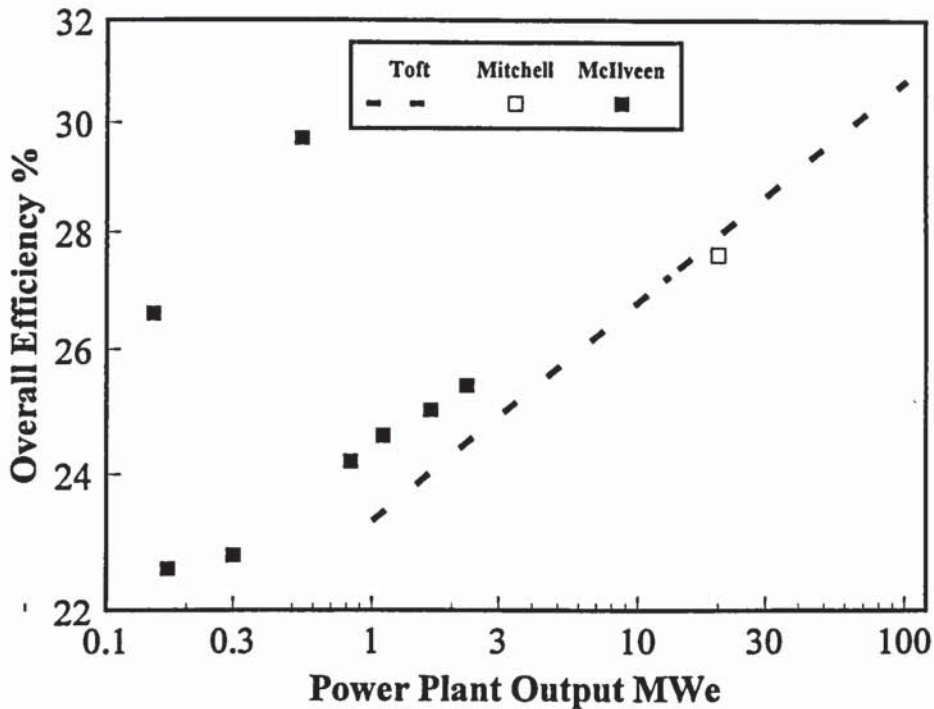


Figure 2-30. Gasification/gas engine power plant efficiencies by McIlveen et al. /50/ with data by Toft /37/ and Mitchell et al. /35/.

2.3.2.8 ECN - University of Utrecht

Van Ree et al. /51/ and Faaij et al. /52/ have analysed biomass-fuelled IGCC concepts with AspenPlus simulation software. Van Ree presents a detailed model built with AspenPlus. A simple gasifier model is used with the gas composition determined outside the model by the gasifier developer (Termiska Processer AB, TPS, Nyköping, Sweden). The gas turbine section is analysed properly with GTPRO (by Thermoflow Inc., Wellesley, MA 02181, USA). Particular emphasis is placed on analysing the environmental performance of the systems. In addition to the performance analysis, technical alternatives and uncertainties are discussed.

The efficiencies in the two studies are nearly identical. There is only a small systematic difference between them /51/, /52/: Faaij reports a slightly higher efficiency with a slightly higher output for each case. The performance of the cycles is shown in Figure 2-31. The IGCC concepts are based on atmospheric pressure CFB gasification and the GE LM2500 gas turbine. Several biomass types are considered (demolition wood, poplar wood, verge

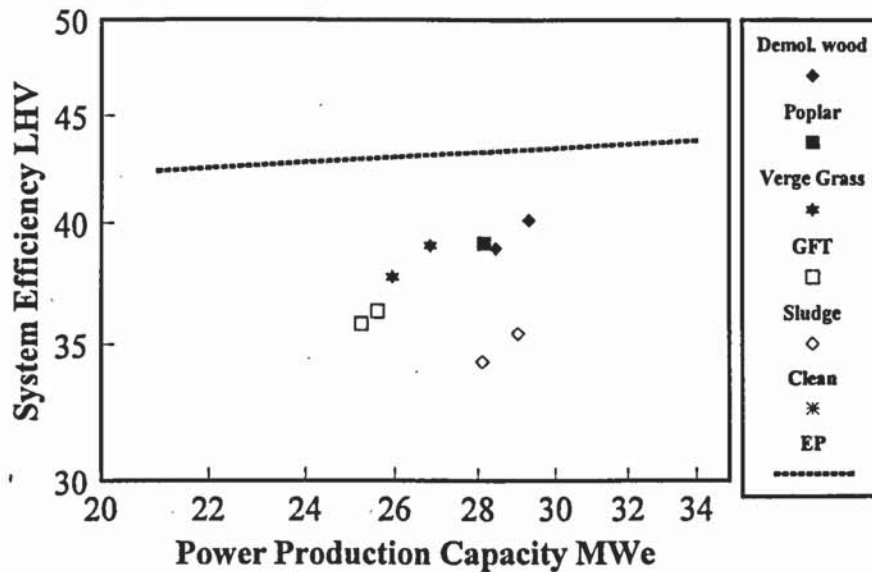


Figure 2-31. IGCC power plant efficiencies by van Ree and Faaij et al. /51/, /52/, atmospheric pressure gasification. EP = Enviropower /46/, pressurised gasification.

grass, and vegetable, fruit and garden waste). The reported efficiencies (36 - 40%, excluding sludge) are about two percentage points lower than the efficiency reported by Marrison & Larson /38/ for a similar concept and capacity.

2.3.2.9 IEA Bioenergy - Pyrolysis Activity, 1992 - 1994

Several concepts producing power from biomass based on gasification were assessed as part of an IEA activity /31/. An outline of the concepts that formed the basis of this thesis was first designed, and their cost and performance assessed within the IEA Bioenergy project. The concepts and the process models designed have since been developed further and validated within this thesis. An article, summarising the results of the IEA project /53/ is attached as Appendix 15.

IGCC concepts based on both atmospheric and pressurised gasification were included. Gasification coupled to an internal combustion engine was also estimated. Efficiencies for these systems are shown in Figure 2-32. Data by Enviropower /46/ and Toft /37/ are employed as references. There is reasonable agreement between the IEA data and the Enviro-

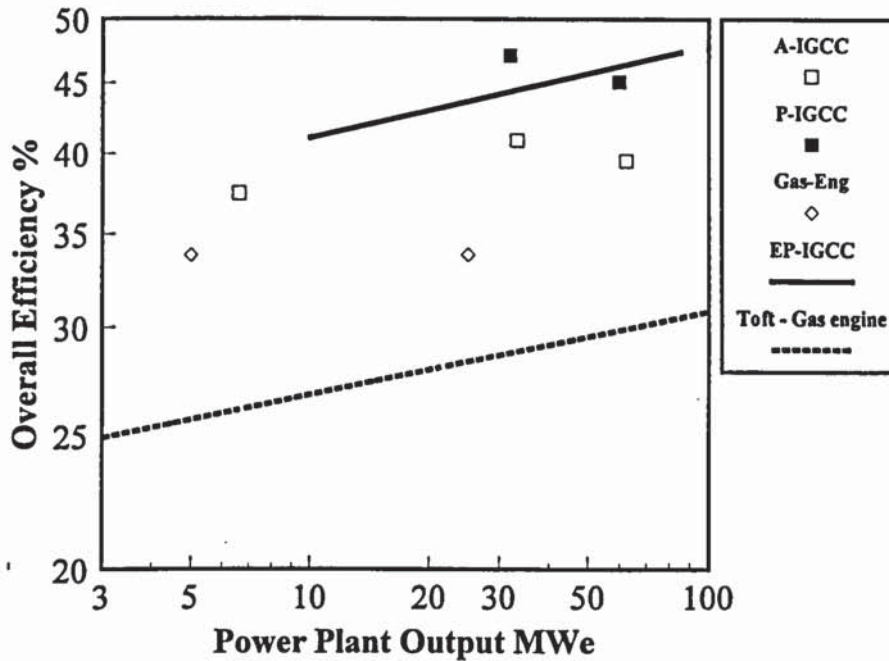


Figure 2-32. Gasification power plant efficiencies, IEA Pyrolysis /31/. A-IGCC = atmospheric pressure gasification IGCC, P-IGCC = pressurised gasification, Gas-Eng = atmospheric gasification and internal combustion engine. EP = Enviropower (P-IGCC)/46/, Toft= gasification and combustion engine /37/.

power data concerning the pressurised IGCC. In the IEA data, atmospheric IGCC is estimated to have an efficiency about five percentage points lower than that of the IGCC based on pressurised gasification. The efficiencies for gasification and the internal combustion engine concepts are considerably higher than those reported by Toft /37/. In the IEA report /31/, overly optimistic efficiencies have been used for the operation of combustion engines, which explain the high efficiencies estimated (note Chapter 9 for discussion).

2.3.3 Gasification power plant investment costs

Investment cost estimates for gasification power plants presented in the literature are reviewed in this section.

An important difference between the investment cost data reviewed here and the cost data of the Rankine power plant investment presented in section 2.3.3 should be borne in mind. There are no known reports based on real plant data for the investment costs of gasification

power plants. Some are estimates by engineering contractors, whereas in many cases the costs reported in the literature are derived from generalised correlations. The accuracy of the investment cost estimate is related to the development stage of the process, the definition stage of the power plant project, and the man-months used for engineering. Detailed sizing and costing of a power plant, which is needed for accurate investment estimates, may be as much as 5% of the total plant cost. Even a preliminary estimate at an early stage of a project is a considerable task, easily worth 10 man-months of effort.

It is therefore concluded that investment cost estimates presented for gasification power plants need to be viewed with caution. Enviropower (EP) /46/ data is also used as a reference in this section to compare the various studies with each other. However, unlike the performance analysis of EP /46/, which is used as a reference and considered accurate (see section 2.4.2.1), the accuracy of the investment cost is unknown. It is therefore used as a reference only to facilitate comparison.

Inflation was very low in the industrialised countries when all the reviewed estimates were carried out in the early 1990s. Hence, no correction due to inflation has been considered necessary when comparing different studies. An effort has been made to report the investment costs as the total cost paid by the customer for a fully operational power plant. The cost positions for a complete estimate are listed in section 2.2.3.1. However, it is evident that some discrepancy in scope exists between different studies.

2.3.3.1 Enviropower - Carbona

Capital costs for the IGCC concepts by Salo and Keränen /46/, presented in section 2.3.2.1, are shown in Figure 2-33. A green-field plant with turnkey costs in Scandinavia in 1995 is assumed. When the output is increased from 39 to 83 MWe the specific capital cost is reduced from 2300 to 1500 \$/kW. A specific scale factor (equation 2-3) of -0.59 may be estimated from the data.

Salo and Keränen conclude, largely on the basis of the specific investment cost, that IGCC is only feasible above approximately 50 MWe. Below about 30 MWe the investment cost is unacceptably high compared with the Rankine investments in section 2.2.3.

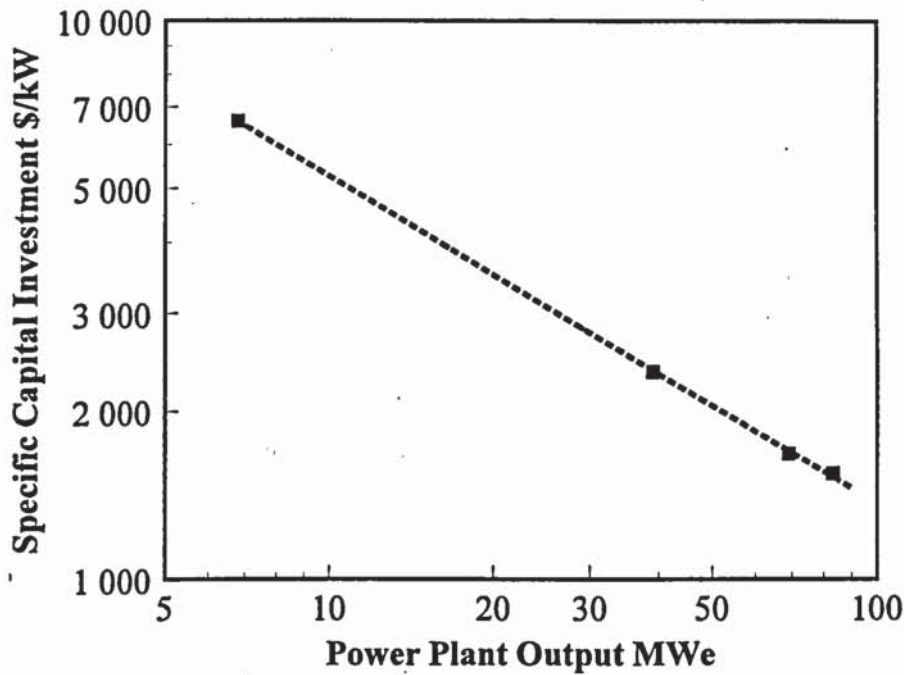


Figure 2-33. Specific investments for IGCC /46/, Scandinavia 1995.

2.3.3.2 NREL

Craig et al. have summarised several studies on IGCC systems carried out in the USA /54 - 55/. Their summary of IGCC capital cost estimates is shown in Figure 2-34, where the plots are individual studies and the correlations are made by the author. Both estimates for the 1st plant investment (specific scale factor, equation 2-3, of -0.37) and nth plant investment (specific scale factor -0.24) are shown. For a discussion about the first and nth plant cost, see section 11.2. The date of the investment cost estimates is 1990. More details concerning the cases may be found in /55/, /56/, /57/, /58/, /38/. These costs may be compared with those presented above by Salo and Keränen /46/. If it is assumed that the costs of Salo and Keränen are for the 1st plant (Figure 2-32), the cost summarised by NREL and the Enviropower costs are close to each other, around 30 to 60 MW_e.

In the U.S., dedicated feedstock supply systems (DFSS), developed by the U.S. DOE, NREL, and ORNL, are assumed to be used in the production of the fuel for biomass IGCCs. Large capacities, between 60 and 150 MW_e, are envisioned in the U.S. /10/. Graig et al. /55/ conclude that to reduce costs for electricity (COE), it is necessary to increase both

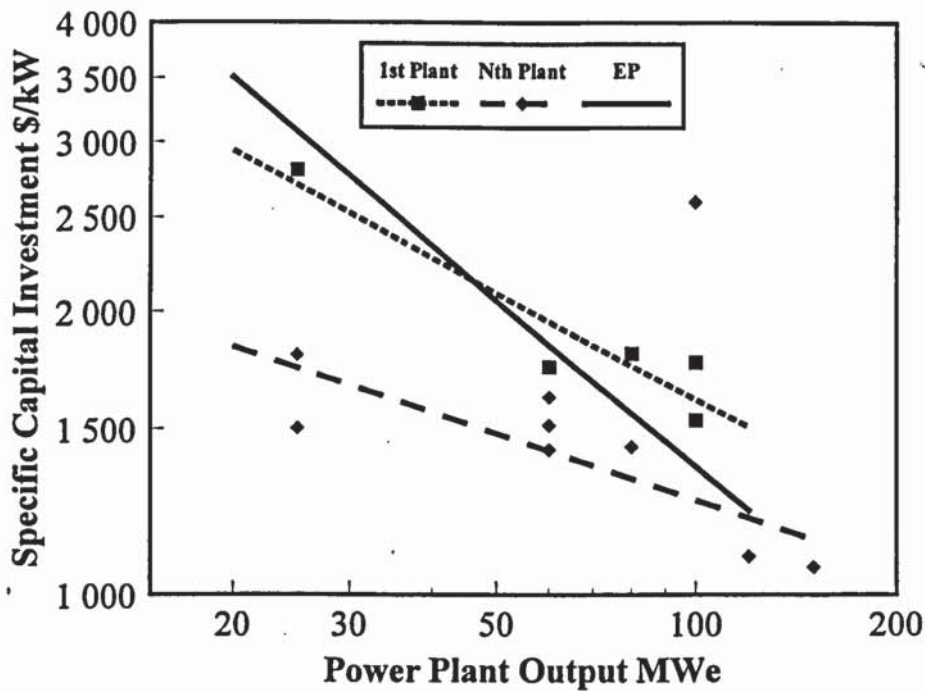


Figure 2-34. Biomass IGCC capital cost estimates from several studies, USA 1990 /55/, /56/, /57/, /58/, /38/. EP correlation /46/ as a reference (a specific scale factor, equation 2-3, of -0.59).

the system efficiency and the system size. They appear to agree with Keränen and Salo /46/, who also found that a large capacity is necessary for the competitiveness of a biomass IGCC.

2.3.3.3 Princeton University

Marrison and Larson /38/ used the correlations for capital investment shown in Figure 2-35 in their study on the optimum size of a biomass IGCC. The cost data is for 1994. Two concepts were assessed: atmospheric pressure (the specific scale factor -0.58) and pressurised gasification (the specific scale factor -0.78) combined cycles. However, R-square for the correlation is lower (0.76 and 0.87, respectively) in both cases than that for other studies reviewed. The shape of the function is different from those used by other sources, suggesting a different economy of scale. The pressurised Enviropower concept cost data is again shown as a reference (the specific scale factor -0.59, $R=0.9997$). It may be concluded that the cost correlations used by Marrison and Larson are not reasonable, and do not agree with data presented by other sources.

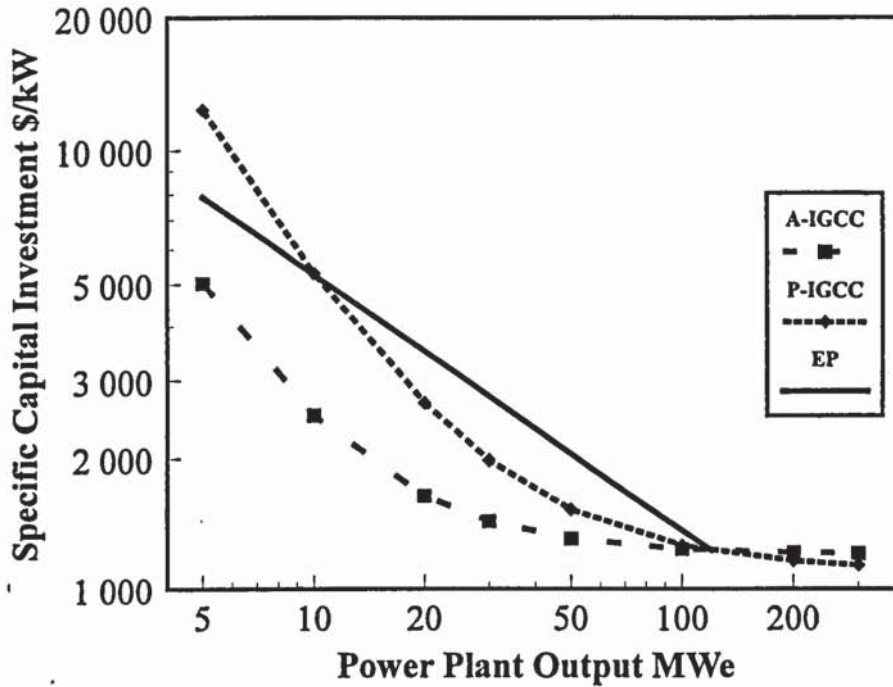


Figure 2-35. Biomass IGCC capital cost estimates for two concepts by Marrison & Larson /38/ (1994), EP correlation /46/ as a reference.

2.3.3.4 EPRI

The specific investment cost of two IGCC concepts assessed by EPRI are shown in Table 2-8 /39/. The costs are shown for 1994. The two concepts are referred to by McGowin and Wiltsee /39/ as 1990 technology and advanced technology.

Table 2-8. IGCC plant investment cost by EPRI /39/.

Concept	Net capacity MWe	Specific investment US\$/kW
IGCC		
- 1990	100	2600
- Advanced	100	1765

EPRI cost estimates are higher than in other reports. The cost of installed IGCC at 100 MWe ranges from 1250 \$/kWe (Williams and Larson /59/) to 2600 \$/kWe (EPRI /39/) for the first plant (see chapter 11 for discussion) and 1800 \$/kWe for the nth plant (EPRI). Enviropower reports 1400 \$/kWe, NREL 1600 \$/kWe for the first plant (see chapter 11 for discussion) and 1300 \$/kWe for the nth plant at this capacity. All except the 1st EPRI con-

cept are approximately similar. It is not possible to analyse the sources of the differences on the basis of these reports. All the investments reported are estimates for a fully operational power plant.

2.3.3.5 IEA Bioenergy Interfacing Activity

Capital costs for gasification electricity systems have been reported by Mitchell et al. /35/ at 20 MWe in Table 2-9. The costs reported by Mitchell are on a 1994 basis. The data is compared with other references in the Table. It may be concluded that at low capacity the disagreement between IGCC estimates is even larger than at 100 MWe (see previous section). All the investments reported are estimates for a fully operational power plant. There are numerous potential sources of cost variation (scope, development stage, location, etc.), and it is not possible to identify any single reason for the differences in IGCC cost estimates.

Table 2-9. Biomass power plant concepts at 20 MWe reported by Mitchell et al. /35/ 1994 compared with other references.

Source	Process concept	Specific investment \$/kWe
IEA Interfacing	IGCC	3820
	Gasification/diesel engine	2760
Enviropower /46/	IGCC	3500
NREL /55/	IGCC - 1st	3000
	IGCC - nth	2000
Marrison & Larson /38/	IGCC	2700

2.3.3.6 Aston University

Toft has also estimated the investment costs of bio-electricity power plants /37/. His nth plant specific investments for concepts employing gasification are shown in Figure 2-36.

The costs are given on the basis of 1995 US\$ for a plant located in the U.K. The specific scale factor (equation 2-3) for the Toft IGCC is -0.35, which may be compared with -0.59 for Enviropower. The specific investment reported by Toft is 4000 \$/kWe for 20 MWe,

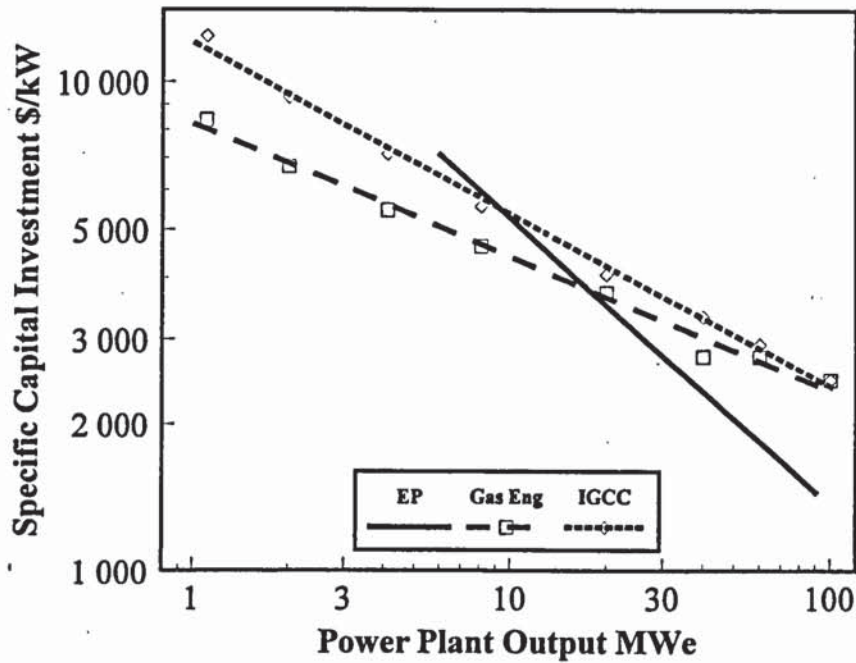


Figure 2-36. Wood gasification power plant capital cost estimates by Toft /37/ 1995, Enviro-power correlation /46/ as a reference.

and 2500 \$/kWe for 100 MWe. Toft's specific investment cost is therefore even higher than the 2600 \$/kWe reported by McGowin and Wiltsee /39/.

The specific investment in a gasification/engine power plant is 3700 \$/kWe, which is higher than the IEA data (previous section). The same cost database was used in both studies. The specific scale factor is -0.27 for this concept.

2.3.3.7 University of Ulster

McMullan et al. /36/ report the specific costs of IGCC systems shown in Table 2-10. The costs are slightly higher than those reported by Enviro-power, and close to the 1st plant costs reported by NREL. However, McMullan et al. do not specify whether their capital cost is for the 1st or the nth plant.

Table 2-10. IGCC power plant concepts reported by McMullan et al. /36/ in 1989.

Process concept	Power output MWe	Specific investment \$/kWe
Wet scrubber	38.6	2655
Ceramic filter	42.7	2353

2.3.3.8 University of Utrecht

Faiij et al. /52/ have reported on the results of the same JOULE project as Van Ree above /51/ (performance in section 2.3.2.8). Faiij reports the minimum and maximum investment costs for the power plant concepts shown in Figure 2-37. Specific investments range from 1800 to 2800 US\$/kWe. The data is compared with Enviropower cost data in the figure. It should be noted that the costs reported by Faiij are for atmospheric-pressure IGCC concepts, whereas the EP case is for a pressurised system. Faiij's data appears to agree with NREL /55/ and Princeton /38/ data, and is lower than other European estimates (Aston, EP, IEA interfacing) reviewed in previous sections. However, it should be noted that the range of the data is rather wide.

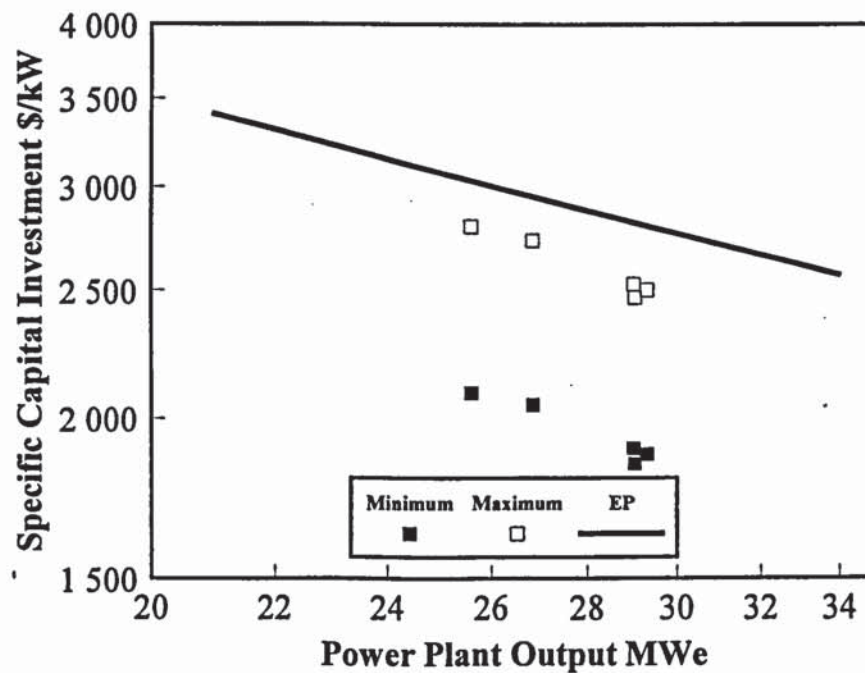


Figure 2-37. IGCC power plant capital cost estimates by Faiij et al. /52/ in 1995. Enviropower (EP) data as a reference /46/.

2.3.4 Cost of electricity

Estimates for the cost of electricity, COE, are presented in this section. Due to the many parameters (with several possible values for each) used in the estimates reviewed (including annual operating time, fuel cost, rate of interest, service life, assumed specific investment, return on investment, maintenance costs, etc.), direct comparison between the different studies is often not meaningful. Although there are standards for calculating COE (for example, EPRI TAG /60/), only the North American studies generally employ it.

The COEs reported are employed in reviewing the competitiveness of different concepts within a study. No direct comparison between different studies is made, unless methods and all their parameters are equal.

Of the three criteria employed in the review in Chapter 2, i.e. efficiency, specific capital cost, and cost of electricity, COE shows the widest variation among the studies reviewed.

2.3.4.1 Enviropower - Carbona

Salo and Keränen (Figure 2-38) compare IGCC and conventional FBC boiler plants in condensing power production /46/. In power production the IGCC is cheaper than the Rankine cycle at power outputs above approximately 40 MWe, when the fuel cost is about 10 US\$/MWh (2.8 US\$/GJ). At integrated pulp and paper mills, where wood IGCC plants are suggested, the IGCC also yields a lower cost of electricity on a larger scale. According to Salo and Keränen, IGCC is clearly suitable for relatively large scales.

The so-called learning effect (1st and nth plant cost) shown in Figure 2-38 will be considered in further detail in section 11.2.

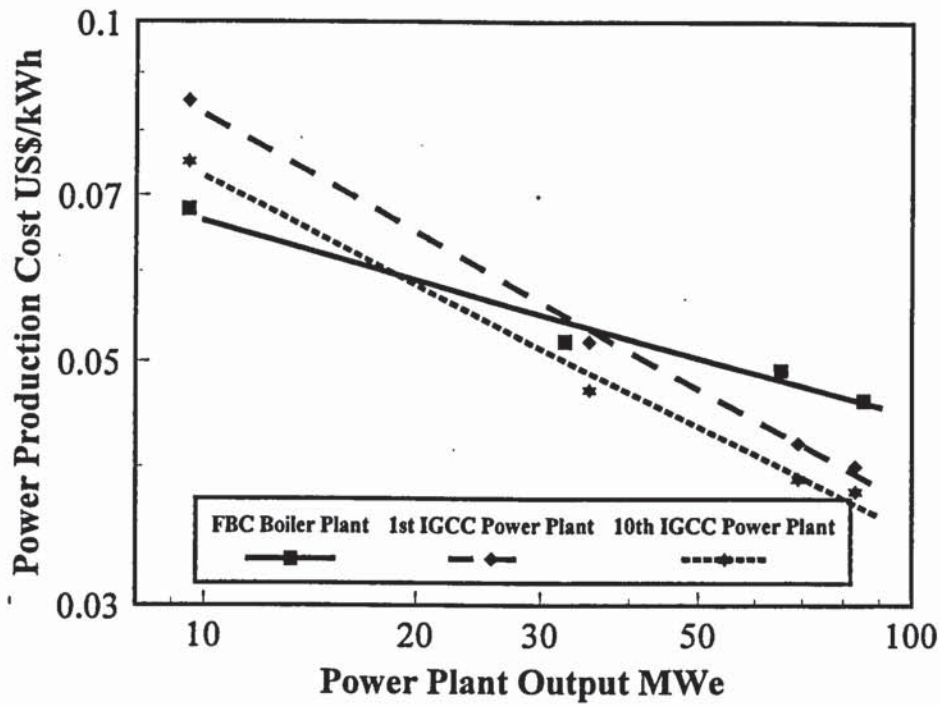


Figure 2-38. Power production costs with IGCC and fluidised-bed combustion power plants, 1st and 10th plant costs shown for the IGCC /46/. Wood 2.8 US\$/GJ, Scandinavia 1994.

It is known that cost reductions are realised when consecutive plants of a new technology are built. Enviropower's suggestion for the capital cost reduction in the cost of electricity is also shown in Figure 2-38. Salo and Keränen report /46/ that a considerable cost reduction is possible when consecutive plants are brought into operation, but their data suggests only a 10 % reduction.

2.3.4.2 NREL

Graig and Mann /55/ have estimated the cost of electricity for the IGCC systems presented in Table 2-1. Both COEs are estimated on the basis of the levelized cost defined by EPRI TAG /60/. The costs are shown in Figure 2-39. Only the smallest pressurised IGCC has a higher COE than the other concepts. There is no practical difference between the three other cases. The prices are not competitive with current prices in the USA, and are higher than the COE with the Rankine cycle.

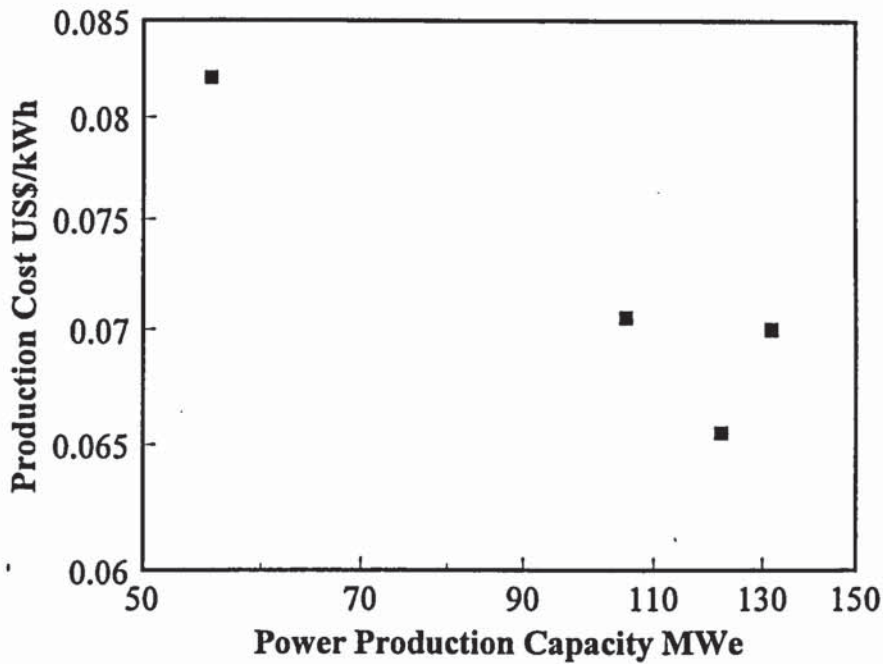


Figure 2-39. Levelized power production costs by NREL /55/, USA 1990. Levelized costs by EPRI TAG /60/, wood 2.6 US\$/GJ.

2.3.4.3 Princeton University

Marrison and Larson /38/ estimated the COE for the systems presented in section 2.3.2.3. The pressurised IGCC yields the lowest power production costs. The minimum COE is projected to be around 0.043 - 0.046 \$/kWh for biomass IGCC by 2020, by which time power production from coal is projected to cost 0.049 \$/kWh in the southeast USA (estimated in /60/). The fuel cost is about 3 US\$/GJ.

The authors conclude that IGCC will yield a lower COE than the steam Rankine cycle both in 2000 and 2020, and that IGCC technology has the potential to compete with coal COE by the year 2020. This conclusion appears rather optimistic, taking into account other studies in this review. Although most studies agree that the IGCC will be competitive compared with the Rankine cycle (EPRI being a notable exception), none of the other studies claim competitiveness against fossil alternatives.

2.3.4.4 Electric Power Research Institute (EPRI)

EPRI has also estimated the economics of different bio-power technologies, which have been referred to in section 2.3.2.4 previously. The COE for the IGCC cases is shown in Figure 2-40. The COE of “advanced IGCC” agrees with the estimate of NREL.

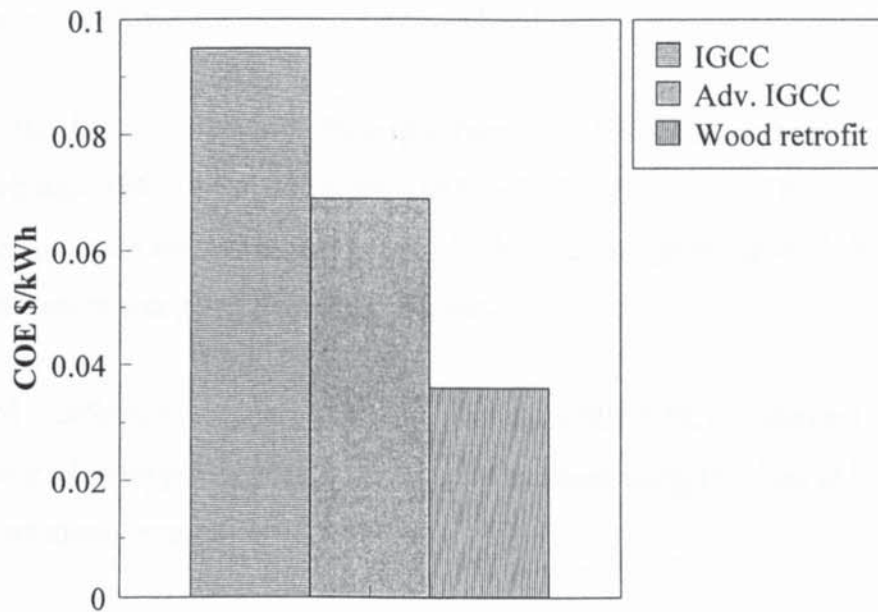


Figure 2-40. COE for different biomass technologies, EPRI /39/, USA 1994. IGCC cases at 100 MWe, wood retrofit: co-fired 15% in a utility boiler (200 MWe). Levelized costs by EPRI TAG, wood 2.1 US\$/GJ.

Comparing the COE of co-firing in an existing boiler with the COE of new power plants is not really appropriate. Marginal costs in production, which co-firing effectively represents, are typically lower than green-field plant costs. However, the example illustrates the real market situation, and emphasises the difficulty of new processes entering the market place. Experience in Europe appears to verify this, as co-firing of waste wood and other biomass is taking off in 1999 /61/, whereas no large-scale wood-to-electricity plants have been announced.

2.3.4.5 IEA Bioenergy - Interfacing Activity

Electricity costs of 20 MWe power plants employing gasification are shown in Table 2-11. The fuel wood costs range from 47.2 to 49.4 \$/odt, depending on plant efficiency (and corresponding amounts of fuel), which corresponds to approximately 3.3 US\$/GJ. The difference between the two gasification cases is probably not significant.

Table 2-11. Biomass gasification power plant COE at 20 MWe reported by Mitchell et al. /35/ 1994.

Process concept	Electricity costs \$/kWh
IGCC	0.102
Gasification/diesel	0.096

2.3.4.6 Aston University

Toft /37/ has analysed the biomass power plants employing gasification listed in section 2.3.2.6. The COEs for these systems are summarised in Figure 2-41. The IGCC appears to be preferable to the gasification/engine power plant over the whole capacity range of 5 to 100 MWe.

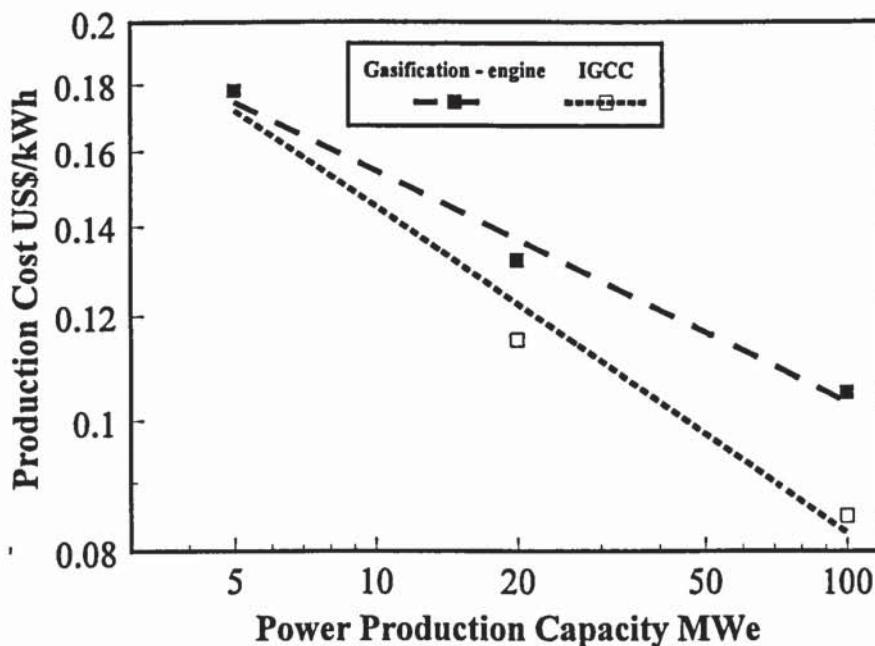


Figure 2-41. Production cost of electricity estimated by Toft /37/, wood 3 US\$/GJ.

2.3.4.7 University of Ulster

McIlveen et al. /50/ have calculated break-even electricity selling prices (BEESP) for power plant concepts using gasification, see section 2.3.2.7. The rate of interest employed is 10%. The costs of BEESP for gasification/engine systems (capacities between 0.2 and 2.3 MWe) were estimated between 0.085 and 0.12 US\$/kWh. Because the return on investment is included, the BEESP may be considered low.

The values may be compared with those determined for IGCC systems between 25 and 160 MWe, which had BEESPs ranging from 0.088 to 0.136 US\$/kWh. These appear realistic, considering the return on investment included. The price range is higher than that currently accepted for new power plant projects in Europe.

The costs of gasifier/gas engine systems appear especially low, considering the extremely small capacity of these power plants. Small-scale systems using biomass as fuel are usually considered relatively expensive.

2.3.4.8 University of Utrecht

Faiij et al. /52/ have analysed biomass-fuelled IGCC concepts, as described in section 2.3.2.8. Many feedstocks are included, and the economic analysis employs several sensitivities. Some COE values determined by Faiij et al. /52/ are shown in Figure 2-42. The biomass fuel costs employed in the study are estimated to vary within a wide range. The economic analysis appears optimistic. The low COE is partly explained by the high annual operating time, typical of base load operation.

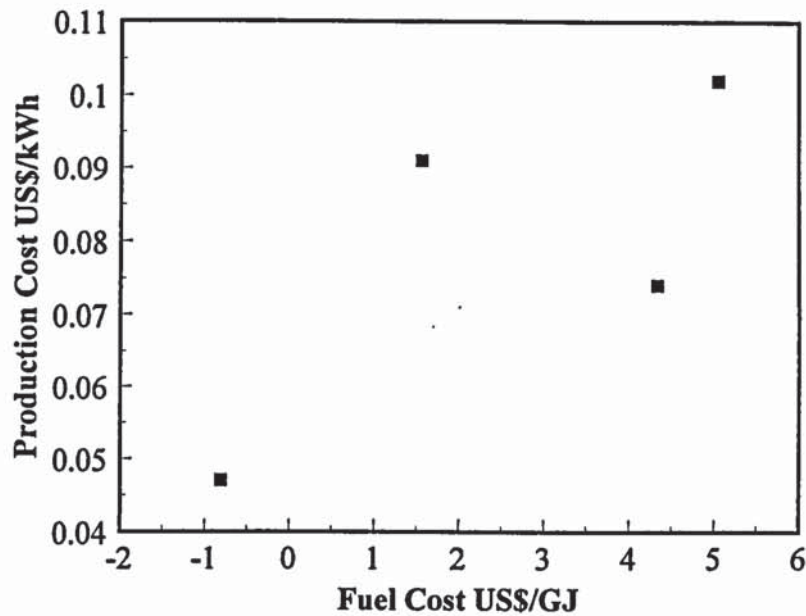


Figure 2-42. Production cost of electricity estimated by Faaij et al. [52]. Location the Netherlands, rate of interest 4-6%, annual operating time 6570-7400 h/a.

2.4 Electricity from biomass based on fast pyrolysis

Results of the analyses of systems employing fast pyrolysis as part of a power plant system with woody biomass as fuel are reviewed in this section. Three important topics are again reviewed:

- Power production efficiency
- Specific investment cost
- Cost of electricity

Note that the efficiencies are reported according to equation (2-4).

$$\eta_{TOT} = \eta_{py} \cdot \eta_{pp} \quad (2-4)$$

where η_{TOT} = overall efficiency, %

η_{py} = liquid production efficiency, %

η_{pp} = power plant efficiency, %

Note that the systems may integrate pyrolysis and power plants. However, fast pyrolysis also makes it possible to de-couple fuel production from the power plant. Here, to make a comparison with other systems possible, the overall efficiency from wood to electricity is reported.

2.4.1 Introduction

A concise analysis of fast pyrolysis power plant technology is presented in Chapter 7. A very brief state-of-the-art review is summarised below.

Very few performance or economic assessments have been published on fast pyrolysis of biomass, let alone on power production with pyrolysis. Some factors explaining this are:

- Fast pyrolysis is a recent development within the area of biomass conversion. Occidental Petroleum /62/ was the first documented attempt to apply fast pyrolysis to biomass, although their work focused on converting municipal solid waste (MSW). The system design owed much to fluidised-bed catalytic cracking of petroleum feedstock. However, the work, which commenced during the 1970s, was abandoned before the end of the decade.
- The next experimental work on fast pyrolysis of biomass, which had the stated objective of producing a low-cost liquid biofuel, was that of Scott and co-workers at the University of Waterloo, Canada /63/. Their first results were published in 1982. Around the same time, Diebold reported experiments in rapid pyrolysis of wood /64/. Since then, a considerable number of university research projects have been started in this area.
- Little performance data is published on pilots or larger-scale operation. No data is available in the public domain concerning the performance of larger fast pyrolysis units.
- There is only very limited data available on the utilisation of pyrolysis liquids.

An example of fast pyrolysis, the ENEL RTP pilot-plant, is shown in Figure 2-43.

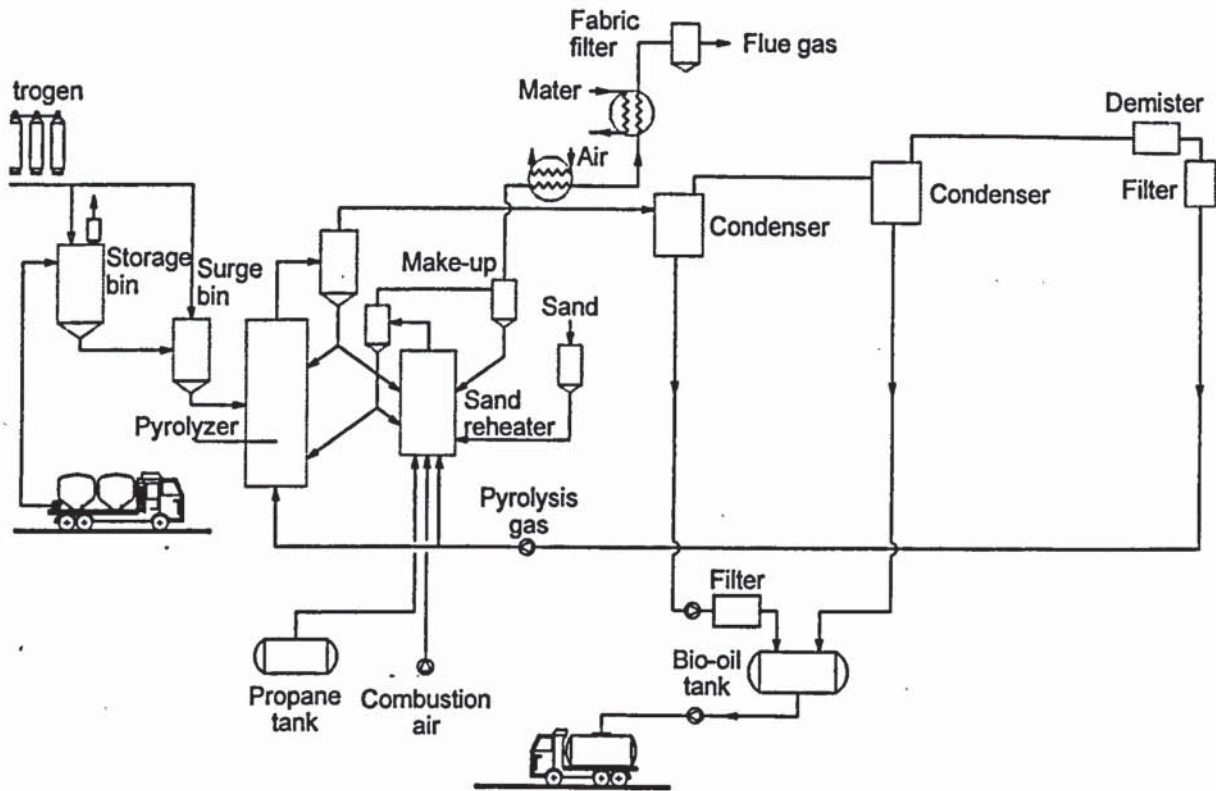


Figure 2-43. ENEL RTP-system in Bastardo, Italy /65/.

2.4.2 Power production efficiency

2.4.2.1 VTT Energy

The co-generation of power and heat in a diesel power plant using pyrolysis oil as fuel has been assessed at a Finnish location /66/. In the concept, pyrolysis oil is produced from sawmill waste and additional forest residues, as not enough wood waste was available at the sawmill to cover the steam demand of co-generation. The diesel engine selected has an output of 8 MWe power and 9 MWe heat.

The efficiency of oil production is 60%, which is based on the work by McKeough et al. /67/. The diesel power plant efficiency of oil to electricity was estimated at 41%. Hence, the overall efficiency used for the system is 25%.

2.4.2.2 IEA Bioenergy Interfacing Activity

The IEA Bioenergy Interfacing Activity has analysed power production with a diesel power plant using pyrolysis oil as fuel /35/. The conversion efficiency for fast pyrolysis without drying is reported as 71.1%. Two functions on different scales are reported for diesel power plant efficiencies. Because no dryer performance is given, it is not possible to combine the two into an overall efficiency. The engine efficiency used is plotted in Figure 2-44. At 20 MWe capacity the overall efficiency is reported as 29.8%.

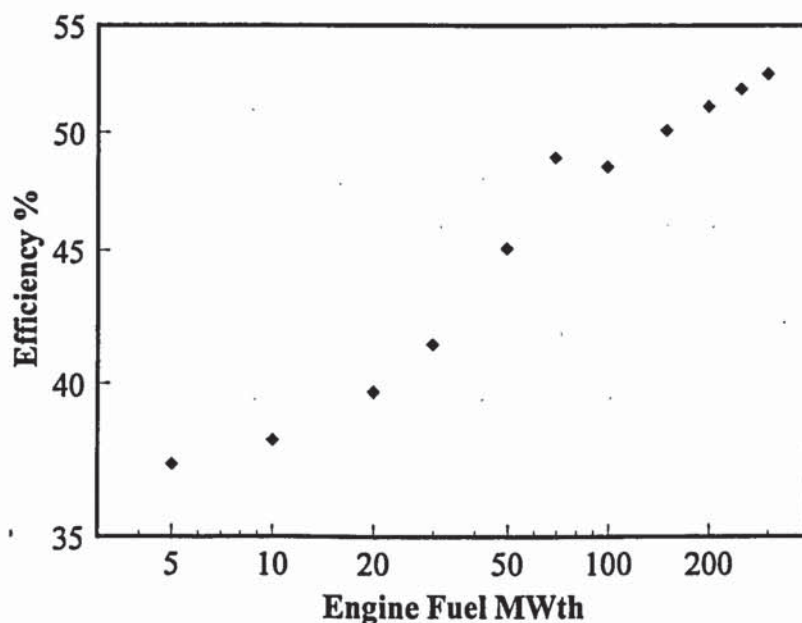


Figure 2-44. Engine power production efficiency, pyrolysis oil to electricity with a diesel engine power plant /35/.

Engine efficiencies of approximately above 50 MWth appear optimistic. Although slow speed diesel power plants have fairly high efficiencies (approaching 50%) on a large scale, it is not proven that the case remains the same with pyrolysis oils of lower energy density.

2.4.2.3 Aston University

Toft has continued where the previous project ended, and has analysed pyrolysis oil/diesel power plants in his work /37/. The correlation with the overall power plant efficiency is

shown in Figure 2-45. The overall power production efficiencies are lower than the correlation used by Mitchell et al. /35/ and the value presented in /31/.

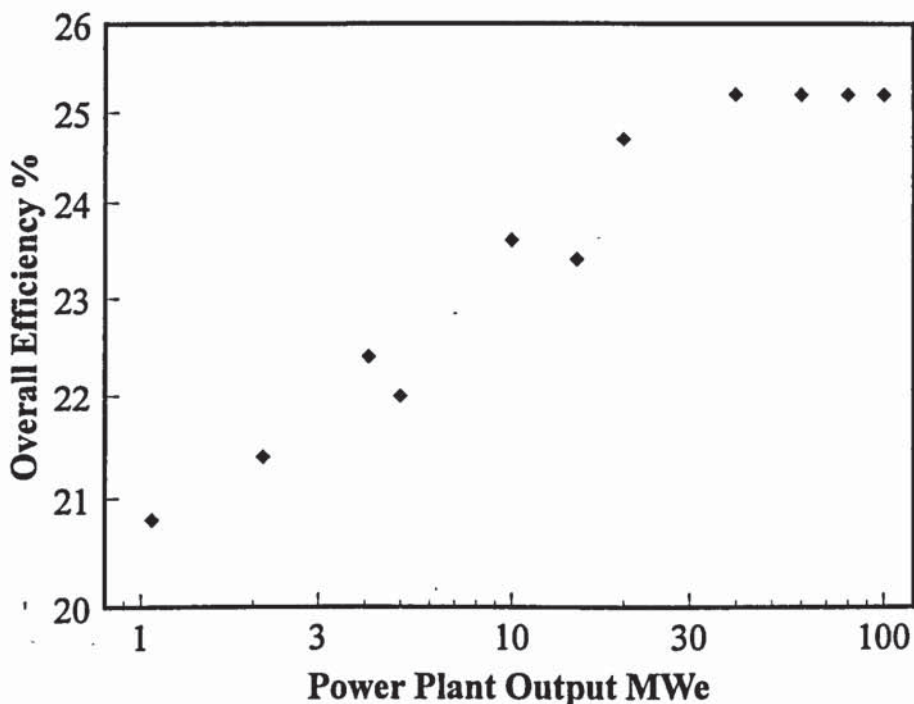


Figure 2-45. Overall power production efficiency, wood to electricity through fast pyrolysis and a diesel engine power plant /37/.

2.4.2.4 Institute Pyrovac Inc.

Roy et al. /68/ have analysed the performance of a 14 MWe concept, where pyrolysis oil is produced and used as a combined-cycle fuel. The concept is called Integrated Pyrocycling Combined Cycle, IPCC. Pyrolysis oil is produced in vacuum pyrolysis, the oil is used to fuel a gas turbine, the by-product char is used to fuel a boiler, and the steam generated in gas turbine heat recovery steam generator and char boiler are used to drive a steam turbine. An overall efficiency of about 37% based on the lower heating value of the bark fuel may be calculated using the data provided by Roy et al. /68/.

2.4.3 Pyrolysis power plant investment cost

2.4.3.1 IEA Bioenergy Interfacing Activity

Mitchell et al. /35/ report an overall specific capital cost for the total system (including fast pyrolysis oil production and a diesel engine power plant) of 2490 US\$/kWe at 20 MWe. The costs are on a 1994 basis.

2.4.3.2 Aston University

Toft has reported specific investment costs for an integrated system in which pyrolysis oil is used as diesel power plant fuel /37/. A summary of his results is shown in Figure 2-46. The specific capital cost for the system is 2890 US\$/kWe at 20 MWe. The costs are on a 1995 basis.

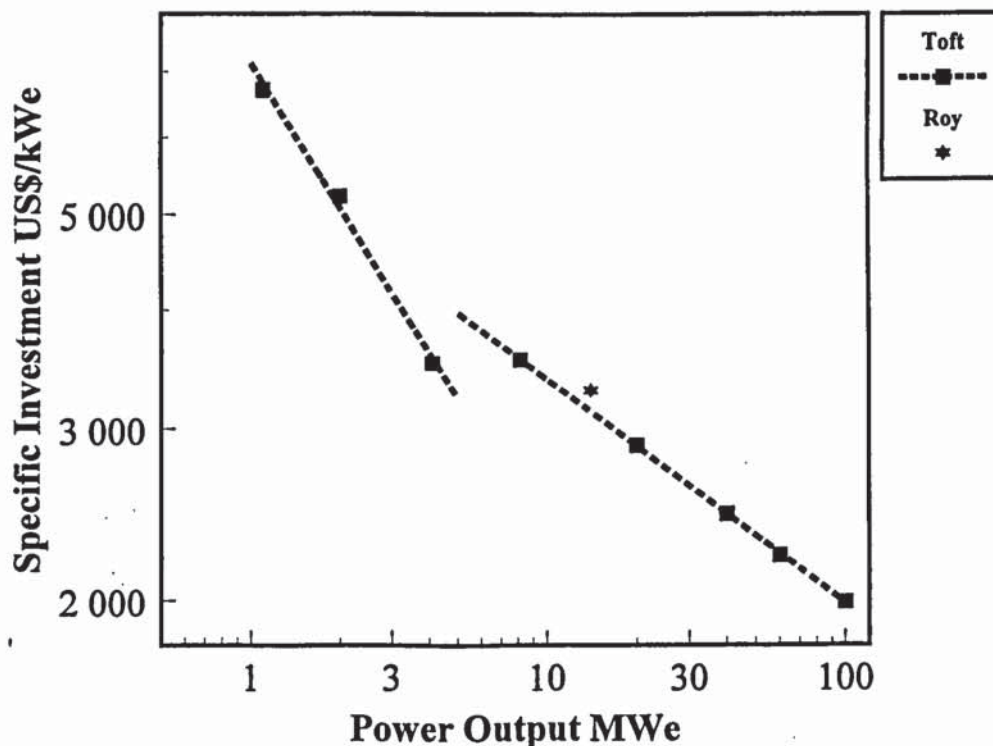


Figure 2-45. Specific capital costs for a close-coupled fast pyrolysis diesel power plant according to Toft /37/, 1995 basis. Data from Roy /68/ as a reference.

2.4.3.3 Institute Pyrovac Inc.

Roy et al. /68/ report an investment cost for the 14 MWe IPCC system described above as 3300 US\$/kW. This can be compared with the specific investment cost of 2080 US\$/kW reported for a Rankine cycle of the same size in the same publication. The costs are on a 1997 basis. The specific investment is shown for comparison in Figure 2-45 together with data from Toft, although it should be noted that the concepts are different.

2.4.4 Cost of electricity

2.4.4.1 VTT Energy

Power production costs were estimated in the study referred to in section 2.4.2.1 /66/. At a 4500 h/a peak operating time (a peak operating time of 3500 - 4500 h/a may be considered typical of a small co-generation facility) and a fuel cost of 2.8 US\$/GJ, a power production cost of 0.055 US\$/kWh with a 30% subsidy for the investment was determined in 1992.

This may be compared with a purchase tariff of 0.031 \$/kWh, which at the time would have been typical. However, it must be noted that the electricity tariff then applied in Finland represented one of the lowest prices for electricity in Europe. At the time concerned, investments in new technologies were being encouraged by giving, typically, a 20% subsidy to power plants employing new technology. It was found that an even higher investment subsidy would be required to make the concept feasible in Finland.

2.4.4.2 IEA Bioenergy Interfacing Activity

The analyses by Mitchell et al. /35/ conclude that the pyrolysis diesel power plant is the lowest cost alternative (gasification cases shown in Table 2-6) among the concepts studied, including the Rankine-steam cycle at 20 MWe. However, the differences between the concepts on this scale are not large. A wider range of costs is seen at lower capacities. At 20 MWe, the COE for a pyrolysis/diesel power plant is reported to be 0.094 US\$/kWh. The corresponding fuel cost is about 3 US\$/GJ.

2.4.4.3 Aston University

Toft /37/ reports for the nth plant that the fast pyrolysis diesel engine power plant is the most economic of the advanced systems up to 12 MWe, after which IGCC becomes less expensive. The combustion system yields the lowest cost on all scales. The COE for a pyrolysis/diesel power plant is estimated to be 0.166 US\$/kWh at 5 MWe, and 0.126 US\$/kWh at 20 MWe.

2.5 Summary

Results from previous studies are summarised in this section. Both methods and data are reviewed. First, the methods used in process assessments are summarised. The topic is broad, and can be approached from different angles. The advantages of the different approaches are discussed.

After reviewing the methods, the three criteria used previously are summarised: efficiency, specific investment, and cost of electricity.

2.5.1 Tools and methods applied

2.5.1.1 General

Different approaches and several modelling tools have been used in estimating the feasibility of advanced bio-power cycles. AspenPlus, ECLIPSE, specific simulation software for gas turbines, and user-designed spreadsheet models have all been used for performance analysis.

In this section the methods employed are organised into three classes:

- Specific models developed for critical parts of bio-power plants
- General-purpose steady-state modelling software
- Spreadsheet models

Determining the performance and the cost are two distinctive stages in assessing the feasibility of a power production system. The first one may be carried out with rigorous methods, routines and data banks. There are three basic methods of carrying out cost estimation. These methods use process steps, factors, or economies of scale as key inputs. The cost estimation method selected largely depends on the input data and resources available for the task.

Making a detailed plant investment cost estimate is a considerable task. Therefore most studies do not include detailed cost estimates, but rely instead on simple methods with rough building blocks. However, cost estimates play a critical role in estimating the viability of a process. The quality of the output from a cost analysis is directly related to the validity and accuracy of the input data, and to the amount and quality of the resources used for the analysis.

Most of the plant costs reviewed have been assembled using unit processes or operations as basic building blocks. Each of the unit processes incorporates several pieces of equipment. This approach is relatively easy, but it may be rather inaccurate, especially when a new application for an existing unit is considered.

An alternative method would be to size each piece of equipment individually, and to construct the plant cost using factors. This is the basis of most commercial plant estimates. The advantage is a more detailed cost estimate. However, the resources required for such an analysis may be considerable. This method also requires much more process and cost input data than the method employing unit processes.

The capital cost estimates for new operations include uncertainties /30/. Probably the greatest difficulty in any capital cost estimation method is the fact that a high proportion of the total capital cost often comprises equipment which has not been proven in a large-scale plant. Such investment costs cannot easily be derived from existing correlations for known units. For example, in a biomass IGCC more than 50% of the investment is related to unit operations not proven industrially (i.e. gasification, gas cleaning). These uncertainties should be taken into account. The issue is discussed in Chapter 11.

2.5.1.2 Specific models developed for critical units

Consonni and Larson have designed and used specific simulation software for gas turbines /48/. Their analysis clearly points out the special features of gas turbines, and why advanced simulation tools are needed for the analysis of gas turbine using unconventional fuels. This work is an invaluable addition to the few available publications related to the use of biomass-derived gas in a gas turbine.

Van Ree et al. /51/ used commercial software GT/PRO to simulate gas turbine performance. This is the second best alternative after the approach of Consonni and Larson, yet much better than the approach adopted in most of the other studies.

The modelling of a gas turbine is further discussed in Chapter 8, which concerns the construction and testing of a model. It becomes evident that a specific tool is needed for the performance analysis of biomass-derived gas in a gas turbine. This is also confirmed by ECN /51/ and by the IEA project /31/.

2.5.1.3 General-purpose modelling software

Two general-purpose modelling software applications have been used to model bioenergy systems: Aspen and Eclipse.

Aspen was used in the IEA project /31/, which is summarised in section 2.3.2.9. The overall conclusion was that this modelling software is quite suitable for advanced power plant concept comparisons, because all the units required could be modelled adequately with Aspen.

Van Ree et al. /51/ studied detailed emissions from several IGCC plant models fired with different bio-fuels. Their work shows an aspect of the versatile character of AspenPlus, as reducing plant emissions is one of the many areas in which this modelling tool may be applied successfully. However, they analyse different biomasses in one concept, and do not compare alternative concepts.

NREL has used Aspen to model both IGCC and pyrolysis systems /54/, /69/. However, they do not report the use of the modelling tool in detail, so it is not possible to estimate the accuracy of the models.

The performance balances calculated with AspenPlus are in agreement with the results produced with other tools (sections 2.3.2.3, 2.3.2.8, and 2.3.2.9).

A process simulator, ECLIPSE, has been developed at the University of Ulster for the assessment of fuel conversion systems /70/. Initially, the programme was developed for the Commission of the European Communities DGXII fossil fuel sector for evaluation of research proposals in the coal and hydrocarbon areas. Subsequently, the simulator has been employed to analyse power generation systems and even biomass conversion systems.

The program is a general-purpose chemical process simulator employing economic analysis with the emphasis on fuel conversion and power-generation. However, according to /70/, it includes only one enthalpy departure function (Lee and Kesler modification of the Benedict-Webb-Rubin equation of state). This feature limits the applicability of the program, as the BWR equation of state is best suited to hydrocarbon systems. Some of the advanced systems, including those analysed in /36/, include unit operations in which, for example, electrolytic properties of compounds are needed (water scrubbing of fuel gas). Although a number of concepts have been analysed so far, it is not likely that ECLIPSE would be easily applicable to fast pyrolysis analysis.

The performance balances reported with Eclipse disagree with other work (section 2.3.2.7).

A standard textbook approach (based on Peters & Timmerhaus /71/) is employed in the economic analysis section of ECLIPSE. Capital cost is derived on the basis of module costs. However, it appears that the factors employed in multiplying equipment costs are constants. This approach has been shown to be inaccurate, as the factors themselves are also a function of the base equipment cost /72/. The same inaccuracy is probably also true for Aspen, although the costing part of the software was not used in this work.

The chosen software is discussed in Chapter 3.

2.5.1.4 Spreadsheets

Spreadsheet models are easy to design and use. However, it is apparent from the studies in which this approach has been employed that the accuracy of determining performance for complete plants is not always as good as expected. An accurate performance analysis is the key to reliable process comparison.

Examples of spreadsheet models are reports by the IEA Interfacing Activity and Toft /35/, /37/. The overall performance analysis method is briefly reported. The estimation of individual modules (unit operations) is reported in /35/, but the integration of these into a process is not explained in detail. The process models are essentially linear, with no feedback of information on mass or energy flows to earlier process steps and fixed parameters being too frequently assumed.

Generalised performance correlations from existing applications are typically employed in spreadsheet models /35/, /37/. However, the performance of new applications with new fuels cannot be determined directly on the basis of existing operating data with existing fuels (compare gas turbines with biomass gas).

2.5.2 Summary of system efficiencies

Perhaps surprisingly, the efficiencies reported for commercial industrial Rankine systems vary a great deal in the studies reviewed. However, presenting performance and costs for advanced systems is insufficient if the commercial reference systems are poorly characterised. The development needs may be prioritised only by comparison with commercial systems.

As a reference, the efficiencies of state-of-the-art power production technologies using natural gas, coal, and heavy fuel oil in condensing mode are shown in Figure 2-47. The efficiencies shown for current technologies are based on data reported by manufacturers and engineering contractors /73/, /34/, /74/. Near-term improvements for conventional systems are shown to emphasise the importance of increasing the efficiencies of future biomass power systems.

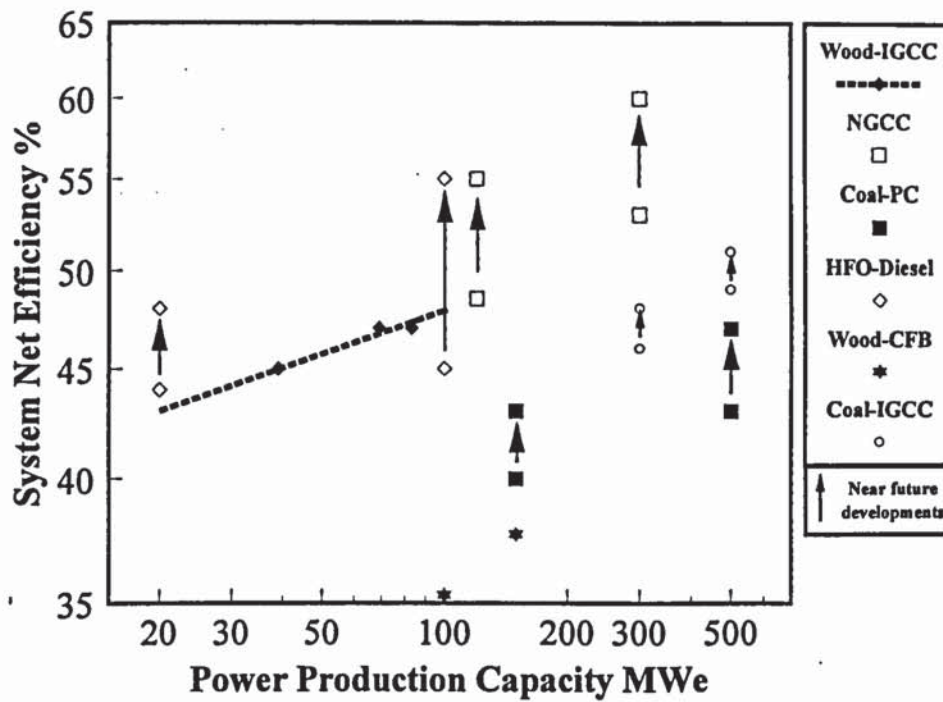


Figure 2-47. Efficiencies (based on fuel lhv) of state-of-the-art power production technologies, the arrows showing near-future developments. IGCC correlation from *Enviropower /46/*, NGCC = natural gas combined cycle, PC = pulverised combustion, HFO = heavy fuel oil, CFB = circulating fluidised-bed boiler.

It is important to note that the efficiency of the Rankine cycle power plant is increasing all the time, see, e.g. /76/; /75/. As an example, if fuel costs were higher, the efficiency of future Rankine cycle power plants could be improved with an appropriate increase in capital investment. Note that the modern large (500 MWe) pulverised coal-fired Rankine power plants recently built in Denmark and Finland have efficiencies of about 43% /75/, /76/. This is high considering the future projections for advanced IGCC coal power plant concepts (around 47 to 51% /77/).

Natural gas combined cycles (NGCC) are predicted to reach an efficiency of 60% /78/ in the near future. Today a modern NGCC plant has a typical efficiency range of 50 to 55% /78/. The efficiencies of pulverised-coal combustion power plants are being raised from about 40% to around 45% /75/. A diesel combined-cycle concept is entering the industrial stage, which will improve the efficiency from the present 46% to around 52%. Coal IGCC power plants are expected to reach an efficiency close to 50% in the future. The efficiencies predicted for wood-fired IGCC plants are shown in Figure 2-47.

It has already been seen (Figures 2-5 and 2-6) that the efficiencies reported for conventional Rankine power plants vary considerably in the reports reviewed. Data by Ekono /34/, which is presented in section 2.3.2.1, is believed to better represent the current state-of-the-art than the other publications reviewed here.

Several wood IGCC concepts have been proposed and evaluated in the literature, section 2.3. Three main alternatives have been assessed: the system based on pressurised gasification (IGCC-P), the system based on atmospheric pressure gasification (IGCC-A), and the system based on indirectly heated atmospheric pressure gasification (IGCC-I). The estimated efficiencies for these systems are shown in Figure 2-48. As one might expect, the figure shows that the IGCC-A systems have lower efficiencies than the IGCC-P systems. However, the range for IGCC-P systems is rather wide, although it should be re-called that some development trends are also included (e.g. Princeton University gas turbine performance improvements). The IGCC-A efficiencies are even more scattered. In both cases, the University of Ulster and EPRI data disagree the most with other data. There are only two estimates for the IGCC-I concept, and their efficiencies appear to fall in between the other two cases.

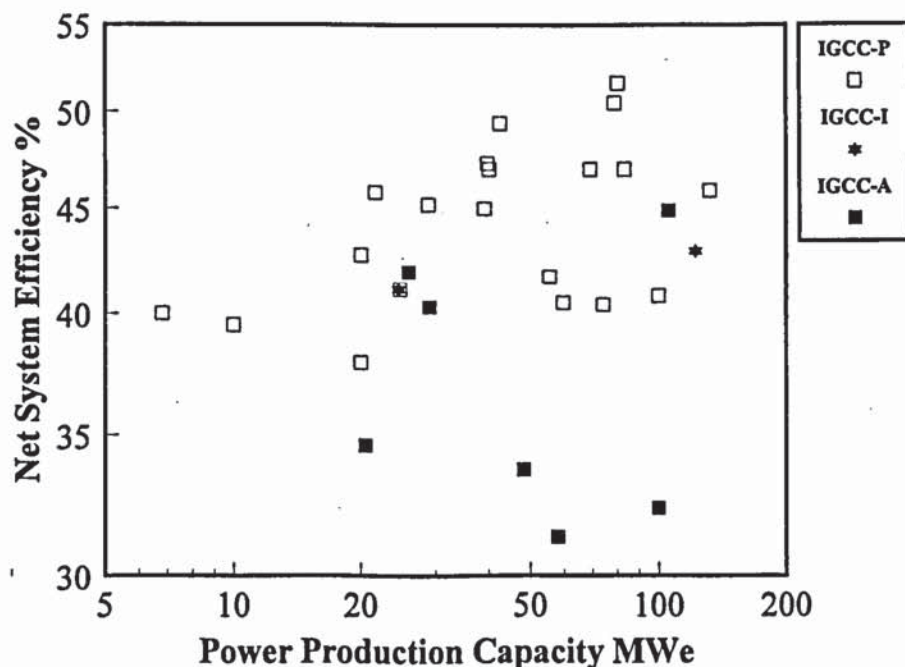


Figure 2-48. A summary of predicted IGCC system efficiencies (based on wood lhw).

Power plant concepts employing gasification/engine systems were compared in Figure 2-30. The agreement between the three studies reviewed is reasonable in most cases, although some peculiarities may be noticed. However, as will be described later in Chapter 9, estimating the performance of diesel or gas engines with low heating value gas is a difficult task.

The efficiencies of pyrolysis power systems have not been analysed satisfactorily. Only a few studies are published, and most of these are not documented in sufficient detail for analysis.

2.5.3 Summary of capital costs

A factor which is difficult to control in determining capital costs is the role of the estimator, whose data is used as basis for the estimation. Typically, process manufacturers tend to give too low cost estimates. Consultants tend to give what they consider reasonable estimates, and try to avoid too high or too low estimates. The source of the base cost data therefore affects the estimates. However, it is not always possible to know how the cost data used has been derived. This brings additional uncertainty into cost estimates.

There is a link between efficiency and investment costs. In general, increased capital spending raises process efficiency and reduces fuel costs. Thus, there is always a trade-off between efficiency and investment cost (between operating and capital costs). When comparing processes, care should be taken to derive the estimated investment cost from the estimated plant performance. High-efficiency concepts may be envisioned on paper, but it is important to include in the investment cost all the units needed to attain high efficiency. This aspect is emphasised when unproven technology is compared with commercial systems. It is a major challenge to determine capital costs for advanced systems with a similar rationale as for commercial systems.

A summary of the specific capital investment costs of power plant concepts reviewed is shown in Figure 2-49. This data set includes 28 IGCC, 8 gas/engine, and 8 pyro/engine

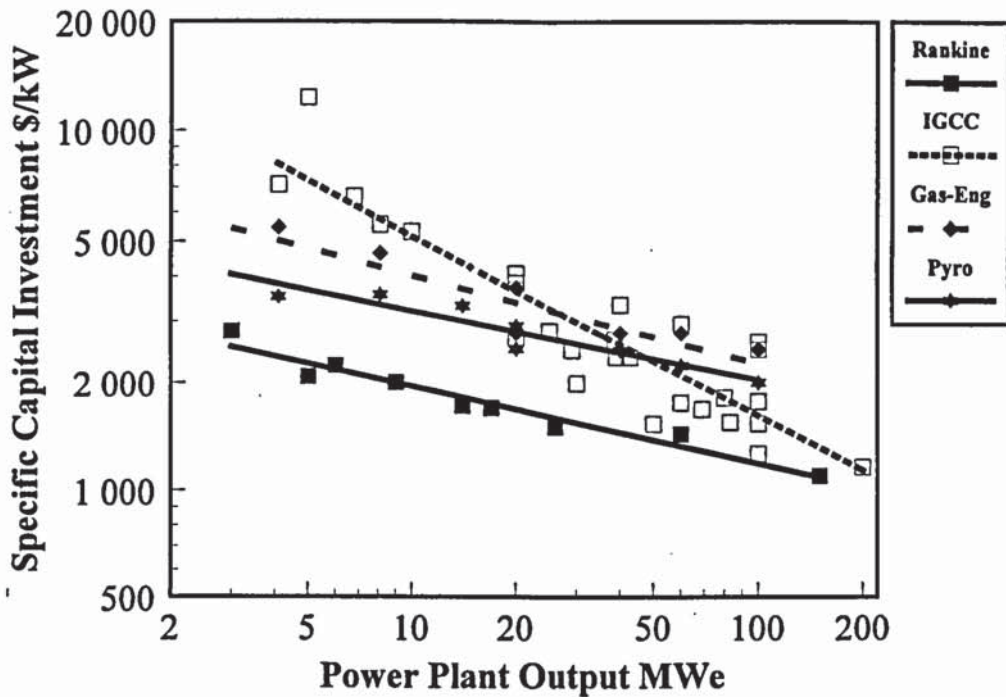


Figure 2-49. Specific capital costs for power plants using biomass fuels, 1994 (all nth plants).

power plant estimates. The Rankine cycle is shown as the reference case, and it is assembled from a database of more than 30 power plants that have been constructed /33, 34/. It has lower costs over the whole capacity range studied. The IGCC systems appear to have an advantage over other advanced systems at higher capacities, as its specific capital costs decline faster than with other concepts. The specific scaling factors for the different cases are shown in Table 2-12.

Table 2-12. Estimated cost correlations based on reviewed data, $y = a x^b$

Power plant type	Number of data points	R square	b	a
IGCC	28	0.82	-0.50	16400
Gasification engine	8	0.80	-0.25	7150
Pyrolysis engine	8	0.90	-0.20	5050
Rankine	>30	0.95	-0.22	3200

It can be seen that the scatter among cases of the same concept is considerable. At around 5 MWe, the approximate specific costs of each are: Rankine cycle 2500 US\$/kW, IGCC 7500 US\$/kW, gasification/engine concept 5000 US\$/kW, and pyrolysis concepts 3500

US\$/kW. At around 100 MWe the costs are: 1200, 1600, 2200, and 2000 US\$/kW, respectively. However, it may be concluded that the agreement between different studies is not very good.

An important element in the investment cost estimation of new systems is the so-called learning effect. This aspect is reviewed in Chapter 11.

2.5.4 Summary of cost of electricity

A drawback of most of the reviewed studies on advanced bio-power cycles is the lack of sufficient consideration given to the peak annual operating time of the power plant. This feature is one of the key considerations when power plant characteristics are reviewed. Production characteristics (base, medium, peak load operation, see chapter 12 for a description) are not considered at all in many of the reports reviewed. Even the assumed annual peak operating time is not always defined /35/. Often, fairly high annual operating times have been assumed (over 7000 h/a), which is typical of large, base load fossil power plants. Note that this is the lowest value market for electricity. However, the technical alternatives analysed often clearly suit different modes of operation. For example, diesel engines using liquid fuels may be employed for intermittent operation or at times of medium and peak load. Power plants employing gasification are more suitable for medium or base load, as they cannot be readily turned on and off.

It is seen from the review that the electricity (COE) from biomass power plants is more expensive than that from fossil fuel plants. A comparison of several alternatives from two independent sources is shown in figures 2-50 and 2-51, including the use of fossil fuels.

Some of the alternatives assessed by McGowin & Wiltsee /39/ have been presented in previous sections. The comparison reveals that:

- Natural gas is clearly the least costly if retrofits are excluded
- Only retrofitting fossil boilers will yield a competitive COE for bio-power
- IGCC concepts are not much better than the Rankine cycle

- COE from coal is rather high. This is probably attributable to the emission (SO_2 , NO_x , and CO_2) charges assumed in the study. However, this is not explicitly spelled out in /39/.

The differences between the alternatives are smaller in the Ekono study /34/. Natural gas CC is again the lowest-cost alternative, but the COE from coal is nearly as low. The biomass IGCC is considered fairly competitive, although the capacity considered is large for biomass (250MWe). The COE for Rankine cycles is 70 to 110% higher than with natural gas. The respective values in the previous publication are 100 and 120%.

It may be concluded that the COE will be quite different, even when obvious differences in the two studies (rate of interest, service life, fuel cost, annual operation time) are taken into account. Only natural gas combined cycle COEs are similar. It should also be pointed out that part of the difference in the results is related to distinct circumstances in Europe and North America. If it is assumed that price relations between fuels remain relatively stable over the next 20 years, the only way to realise bio-power projects is some form of subsidy, be it a CO_2 tax or something similar. Co-firing yields the lowest COE from biomass.

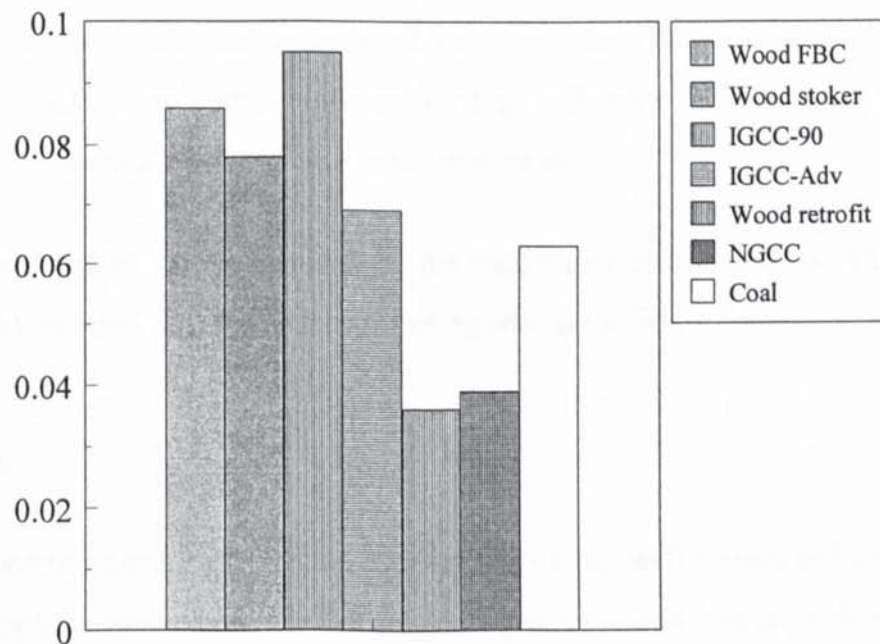


Figure 2-50. COE for several alternatives, EPRI data 1994 /39/. Wood 2.1, Gas 2.4, Coal 1.1 US\$/GJ, levelized cost according to the EPRI TAG.

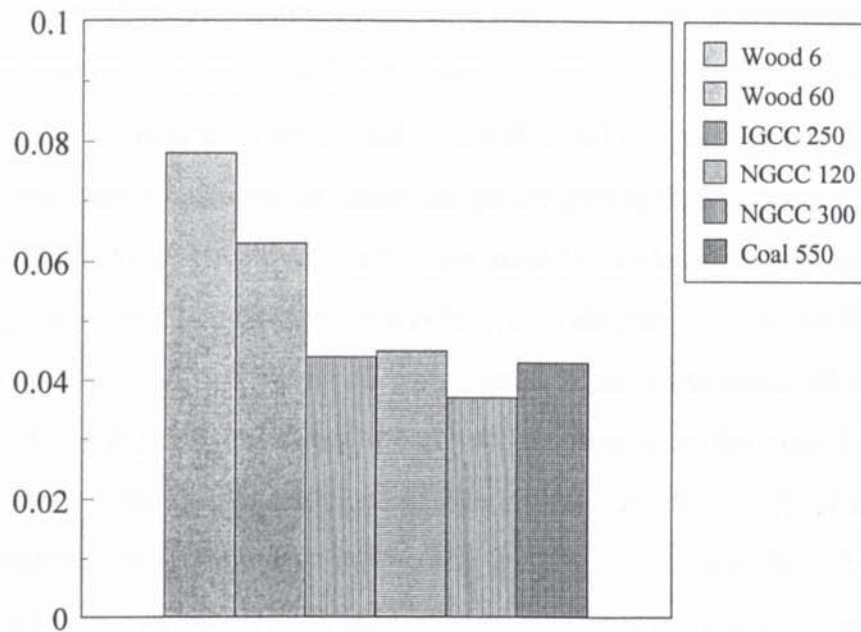


Figure 2-50. COE for several alternatives, EPRI data 1994 /39/. Wood 2.1, Gas 2.4, Coal 1.1 US\$/GJ, levelized cost according to the EPRI TAG.

2.6 Objectives of the thesis

The objective of this thesis is to study complete electricity and co-generation (of heat and power) bio-power concepts in order to support the development work related to new bio-energy systems. For example, new concepts under development may be ranked on the basis of cost and performance analyses. As already described in section 1.6, the performance balance will be emphasised because it is a more reliable criterion for future development potential than cost.

The content of this thesis is the construction of a set of development tools: computer models which may be employed in determining mass and energy balances for processes, in estimating their costs, in optimising them, and in defining further development needs for new systems. Of these four uses, the first has been carried out in detail. Cost estimation will be dealt with on a unit process level, some examples of using the models for process optimisation will be included, and further work will be suggested. Modelling is carried out using the AspenPlus™ process analysis software as a framework.

The emphasis in this work is on developing steady-state performance and cost models for complete biomass power plants. The models to be prepared in this study must be detailed enough to study the effects of critical process parameters, yet simple enough to construct the several process models needed for the overall assessment.

The following aspects are emphasised:

- Rankine cycle model
- Gasification model
- Gas turbine model
- Fast pyrolysis model.

Rankine cycle

Considerable differences exist between results concerning the performance of the conventional Rankine power plant. Based on the studies reviewed, this aspect needs further attention. The review indicated that most assessments did not include a detailed model for the boiler/steam cycle option. And when this is not done, there appears to be a danger of handling the conventional reference case differently from the new system being studied. For example, conservative efficiencies are used for conventional technology, while at the same time an advanced system may be designed for high efficiency without taking this properly into account in the respective increase in investment cost.

A performance model will be included for the Rankine cycle in this work. The cost model will be based on a real data from an engineering contractor /34/.

Gasification

The atmospheric-pressure gasification of biomass is fairly well known and industrially applied, although its applications are limited. Fuel gas for a lime kiln is produced from bark and wood residues at a few pulp mills (Finland, Sweden, Austria), and fuel gas is produced for residential heating boilers (Finland) and process heat (Sweden). In addition, numerous smaller-scale gasifiers are employed in the production of fuel gas for internal combustion

engines and other applications in many countries. Only one demonstration-scale pressurised gasifier is in operation (Sydkraft IGCC at Värnamo, Sweden), although several have been built over the years. There is experimental data published on gasification, and the prediction of mass and energy balances for industrial power production systems based on gasification may be carried out. However, gasification models employed in power plant analysis are often simplistic. Detailed gasification models (note chapter 6) have not been integrated into a power plant model. Only one of the biomass studies reviewed above includes a slightly more detailed gasification model that will do more than the most basic mass and energy balance, once the gas temperature is fixed. Craig and Mann report on a model in which experimental measurements from the IGT and BCL processes have been regressed and incorporated as a user model /55/. However, no details of the model are given.

A gasifier model, integrated with the power plant mode, will be included in this work. The cost model is based on /31/.

Gas turbine performance

Gas turbines using LHV gas have been analysed in just a few studies (detailed by Consonni and Larson /48/, to an extent by both Craig and Mann /55/, and by Van Ree /51/). Generalisations are employed in many studies, and some do not report their approach at all. It is concluded that many of the studies reviewed have weaknesses in their analysis concerning the IGCC, the performance of which is determined by the gas turbine. A gas turbine model based on correlations with data derived from Gate/Cycle, integrated into the gasifier model, will be included in this work.

Fast pyrolysis performance

There is reasonable agreement on IGCC efficiencies in the literature. There is less agreement on fast pyrolysis performance. It was already pointed out earlier that not many performance or economic assessments have been published on the fast pyrolysis of biomass or on power production with pyrolysis. None of the studies reviewed includes a model which could be used to predict the performance of an industrial pyrolysis reactor. No adequate performance balances have been published for industrial fast pyrolysis. A performance

model will be developed as part of this work. Special emphasis is put on modelling a pyrolysis system, as this issue has previously been poorly reported.

When a performance model validation becomes difficult or impossible, as with pyrolysis due to a lack of data, the calculation accuracy of physical properties of participating components is emphasised. Such a situation highlights the need to use robust modelling tools when calculating system performance.

Summary

It is believed that the Rankine cycle has been poorly represented in many studies, resulting in invalid comparisons with advanced concepts. There is a need for uniform performance analysis for biomass-to-power systems based on combustion, gasification and pyrolysis.

There appears to be a need for a modelling exercise, by which

- conventional technology is modelled and analysed similarly to the systems being developed,
- gasification and gas cleaning integration into the power module is analysed in more detail, and
- pyrolysis is modelled in greater detail.

3 MODELLING

In this chapter, the modelling approach is explained and the selection of a modelling tool is justified. The tool used to construct the simulations, AspenPlus™, is described. Model outputs are outlined.

3.1 Approach

The design of industrial units, or more accurately, the prediction of industrial plant performance is the aim of the present model development. The level of sophistication of the models to be built is ultimately determined by the overall objective, which in this case is to assess and compare several process alternatives. The models to be prepared in this study have to be detailed enough to study the effects of selected process parameters, yet simple enough to construct the several process models needed for the overall assessment.

The performance analysis carried out with the models will be employed in evaluating bio-energy systems. As explained in Chapter 1, a rigorous performance analysis is the key to a meaningful feasibility study. Performance analysis is essential in estimating system cost. Both operating and investment costs, key elements in feasibility studies, are determined on the basis of mass and energy balances. A rigorous mass and energy balance clearly improves the accuracy of cost estimation.

Verification of the models is essential. Simulated results should always be verified against experimental data. However, the scale on which some of the data used as a basis for the models is often quite small. In several cases there are no industrial-scale units operating for the assumed duty, and verification cannot be done. This is a distinct drawback with some of the models built in the present work.

3.2 Simulation tools

Both steady-state and transient-state modelling software applications are available for process simulation. For this study, steady-state simulation was considered appropriate, since the process concepts studied are at different stages of development. In many cases, not even the

steady-state condition of the processes under study is well understood. Therefore no further consideration was given to computer programmes that are able to model transient states of processes. These software programmes are needed, for example, in the development of power plant control systems, when the effect of changing process parameters during operation needs to be evaluated. Development is underway to integrate steady-state and dynamic modelling capabilities within one software application. Examples of this trend are DynaPlus (AspenTech) and Hysys (Hyprotech) /79/. The former is an integration of AspenPlus and Speedup. Hysys was introduced to the market in 1995.

A biomass power plant includes unit operations from both chemical processes and power plants. No process modelling tool is perfect for both applications. In the chemical process industry (CPI) only a few steady-state simulation tools are widely available on the open market with appropriate support service. In addition to AspenPlus (by Aspen Technology, Inc., Cambridge, MA), Design II (by WinSim Inc., Houston, Tex.), PRO/II (by Simulation Sciences Inc., Brea, Calif.), Hysim (Hyprotech Ltd., Calgary, Alta.), and CHEMCAD III (by Chemstations, Houston, TX) are all used within the CPI. However, none of these handles heterogeneous solid materials as well as Aspen. MASSBAL MK II (by SACDA, London, ONT) is also able to handle solids and model power production cycles, but it is designed especially for the pulping industry.

In analysing gas turbines using a low heating value (LHV) gas as fuel, GATE/CYCLE by Enter Software (Menlo Park, CA) is employed. Gas turbine performance is determined separately with GATE, and the results are then converted for use in Aspen. This procedure is used because of the special features of gas turbines, which are reviewed in Chapter 8.

Over the past 20 years AspenPlus has evolved into a sophisticated modelling tool and has a number of special features, described in section 3.3, that make it the most suitable modelling tool for this study.

3.3 AspenPlus™

A process analysis computer program, AspenPlus™, is used as the basic framework to perform material and energy balance calculations in this work. Aspen is a steady-state process

analysis program extensively employed in chemical engineering process modelling. It is used by the process industry, engineering contractors, and universities alike.

Aspen is qualified to simulate processes with both fluid and solid materials, which is a requirement when biomass conversion is studied. Aspen is employed in a range of applications from inorganic and organic chemical production, mineral processing, and oil refining to integrated gasification combined-cycle (IGCC) power production. The development of this flowsheeting package was started at the Massachusetts Institute of Technology (MIT) over a five-year period (1976 - 1981) under a grant from the US Department of Energy (DOE). Since then several versions have emerged: two commercial versions, Aspen/SP (by JSD, Inc., Denver, CO, no longer available) and Aspen Plus /80/. The Morgantown Energy Technology Center (METC) has kept up a DOE version, which has also been employed, for example, by the National Renewable Energy Laboratory (NREL). AspenTech version is the market leader in CPI process flowsheet simulation.

Although not developed for power plant design, features of gasification and pyrolysis make Aspen especially suitable for the design of power plants, where these critical technologies are included.

This program provides a convenient means of specifying flowsheet connectivity, material flows, equipment design information, and operating parameters through a graphical user interface, ModelManager. Aspen has a built-in expert system which determines when the model definition is complete. Thereafter, calculation may commence. After a sequential modular calculation routine with iterations (when necessary), Aspen produces a report with detailed data on all plant flows and equipment.

Aspen is a suitable modelling tool for the process concepts studied in this work for a number of reasons:

- It provides a comprehensive property data base for over 10 000 species.
- It includes an extensive collection of models to calculate physical properties for compounds being simulated. Its property data base and physical property calculation methods are widely considered appropriate for studies concerning the performance of proc-

ess plants. Complicated physical property calculation methods are needed in the study, e.g. for complex organic compound mixtures (pyrolysis oil) and for electrolyte systems (fuel gas wash with water). Aspen is fully capable of dealing with these systems.

- It includes built-in equipment models of varying sophistication to handle every process operation needed in the study. These include turbines, chemical reactors, absorber columns, heat exchangers, and many others.
- It allows the user to supplement or replace built-in models using FORTRAN statements or separate FORTRAN subroutines.
- It provides a variety of simulation convergence schemes to handle complicated recycle loops with a minimum of user input.

The construction of a simple AspenPlus model is presented in Appendix 14, which also includes examples of a Rankine cycle power plant model operation and its results.

The key steps in building a model are:

1. To define the process flowsheet to be modelled and the objectives for the model.
2. To select the units of measurement for input data and output reports.
3. To specify the chemical compounds which will be present in the streams of the flowsheet. There are two types of compounds, ordinary (known as mixed in AspenPlus) and non-conventional. The latter are not single chemicals and include solid fuels as an example. Only enthalpy and density are calculated for non-conventional compounds.
4. To specify the models and methods to be used for calculating the physical properties. Models and methods used to calculate thermodynamic and transport properties are packaged in AspenPlus in built-in option sets. Physical property parameters have to be supplied for the option sets, of which many are available directly in AspenPlus.
5. To establish flowsheet connectivity. Using built-in unit operation blocks, process model connectivity is established in a graphical user interface. Unit operation models (Table 3-1) include turbines, chemical reactors, absorber columns, heat exchangers etc.

Table 3-1. Summary of unit operation models in AspenPlus version 9.3.

Unit model	Description
HEATER	State changer. Models heaters, coolers, condensers, valves, etc.
FLASH2	2 outlet flash. Models flash drums, evaporators, etc. using rigorous VLE
FLASH3	3 outlet flash. Models flash drums, decanters, etc. using rigorous 3-phase VLE
DECANTER	2 phase liquid-liquid decanter. Models decanters, single stage separators with two liquid phases and no vapour phase
HEATX	2 stream cocurrent or countercurrent heat exchanger
MHEATX	Multistream heat exchanger. Model LNG exchangers, cold boxes, etc. or perform zone analysis
MIXER	Stream mixer. Also used to combine heat or work streams
FSPLIT	Flow splitter. All outlets have same composition, temperature, pressure, etc.
SEP	Component separator. Based on known split or flow for each component
SEP2	Two outlet component separator. Based on known splits, flows and purities
SSPLIT	Substream splitter. Divides feed based on splits specified for each substream
DSTWU	Shortcut distillation design using Winn-Underwood-Gilliland
DISTL	Shortcut distillation rating using Edmister
SCFRAC	Shortcut distillation for complex columns such as crude units and vacuum towers
RADFRAC	Rigorous 2 or 3-phase fractionation for single columns; distillation, absorption, reactive distillation, etc.
MULTIFRAC	Rigorous fractionation for complex columns such as crude units, absorber/strippers, etc.
PETROFRAC	Rigorous fractionation for petroleum applications
BATCHFRAC	Rigorous 2 or 3-phase batch distillation
RATEFRAC	Rigorous fractionation using the rate-based non-equilibrium model
EXTRACT	Rigorous liquid-liquid extractor
PIPE	Single segment pipe with constant diameter and rise; may include fittings
PIPELINE	Multiple segment pipeline; segments may have different diameters and elevations
VALVE	Control valve or pressure changer
PUMP	Pump or hydraulic turbine
COMPR	Polytropic or isentropic compressor, or isentropic turbine/expander
MCOMPR	Multistage polytropic or isentropic compressor, or multistage isentropic turbine
RSTOIC	Stoichiometric reactor based on known fractional conversions or extents of reaction
RYIELD	Nonstoichiometric reactor based on known yield distribution
RGIBBS	Rigorous reaction and/or multiphase equilibrium based on Gibbs free energy minimization
RCSTR	Rigorous continuous stirred tank reactor based on known kinetics
RPLUG	Rigorous plug flow reactor based on known kinetics
RBATCH	Rigorous batch or semibatch reactor based on known kinetics
CRUSHER	Models gyratory/jaw crusher, cage mill breaker, and single or multiple roll crushers
SCREEN	Models solids-solids separation using screens
FABFL	Models gas-solids separation using fabric filters
CYCLONE	Models gas-solids separation using cyclones
VSCRUB	Models gas-solids separation using venturi scrubbers
ESP	Models gas-solids separation using dry electrostatic precipitators
HYCYC	Models liquid-solids separation using hydrocyclones
CFUGE	Models liquid-solids separation using centrifuge filters
FILTER	Models liquid-solids separation using continuous rotary vacuum filters
SWASH	Models a single-stage solids washer
CCD	Models a multistage washer or a counter-current decanter
MULT	Stream multiplier. Used to multiply stream flows by a user supplied factor
DUPL	Stream duplicator. Used to copy a stream to any number of outlets
CLCHNG	Used to change stream class. Place between sections or blocks that use different stream classes
USER	Used to invoke a user-supplied model with up to 4 inlets and outlets
USER2	Used to invoke a user-supplied model with any number of inlets and outlets

6. To define input streams. This includes mass (or mole) flow, flow composition, temperature, and pressure.
7. To define unit operation model inputs. An example would be stream temperature out from a heat exchanger, or pressure after a pump.
8. To impose design specifications. An example is a heater in which heat input is varied to reach a specified outlet temperature.

Once the connectivity and definitions are complete, calculation may be carried out.

3.4 Bio-power models

The power plant concepts studied in this thesis comprise an integrated sequence of unit processes and operations, some of which are common to several process configurations. The unit processes are reviewed, and the construction of Aspen models is presented in Chapters 4 to 9. The basic unit processes are:

- steam cycles
- drying
- gasification
- fast pyrolysis
- gas turbine
- internal combustion engine

As an example, a gasification combined-cycle has the following basic unit processes: drying, gasification, gas turbine, and a steam cycle. Altogether 21 advanced concepts have been assessed, and are listed at the beginning of Chapter 10. In addition, the Rankine cycle is used as a reference case for all the scales studied.

3.5 Outcome of the models

Steady-state performance (Chapter 10) and cost (Chapter 11) models for complete biomass power plants are developed in this work.

The performance models will supply:

- Mass and energy flows in the process
- Energy demand and production in the process units/equipment
- Performance of unit operations
- Sizing data for unit operations

The models are used for:

- A robust cost and performance analysis of several bioenergy process configurations
- Technical sensitivity studies, in which some critical process parameters are varied to study their effects on the overall performance or cost

Performance model results are used for sizing of units, which is necessary for capital investment costs estimates. Using performance and investment costs, the cost of electricity may be calculated.

4. STEAM CYCLES

4.1 Introduction

In this chapter, models for Rankine steam-cycle power plants are presented. Two models are described, one for a wood-fuelled boiler, and one for the steam section of a combined cycle. Model execution is essentially similar in both cases, although more stages are required in the boiler plant because of the solids handling.

A summary of the conventional power plant technology employed for woody biomass fuels has been presented in sections 2.3.1 and 2.3.2. Power plant efficiency was presented in section 2.3.2.1, investment costs in section 2.3.3.1, and cost of electricity in section 2.3.4.1.

4.2 Model description of a Rankine boiler steam cycle

A model for a Rankine boiler steam cycle is described in this section. A flowsheet of a boiler plant steam cycle is shown in Figure 2-1.

An Aspen block flow diagram of a boiler power plant model is shown in Figure 4-1. The model is designed to calculate the output of electricity, when the mass flow of fuel wood to the boiler and steam parameters are given. The input file of the boiler model is shown in Appendix 3. Capital letters are used in the text when AspenPlus block models are referred to (SPLIT, RSTOIC-reactor etc., note table 3-1). In the blocks of Figure 4-1, the lower word refers to an Aspen keyword describing a unit block, while the upper word is user defined.

Examples of major user inputs and model results are presented in Table 4-1. In an integrated model, some input parameters are supplied by other power plant model sections, such as the inlet flue gas composition (all cases), or inlet flue gas mass flow (determined in an IGCC by the gas turbine).

The detail design will vary depending on the plant capacity. All steam cycles may be built by combining the basic sections and their elements. A simple boiler plant steam cycle is described.

There are five design specifications:

- Combustion airflow
- Heat loss
- Boiler feed-water mass flow
- Approach temperature
- Deaerator energy balance

First, water and dry solids are separated in a SEP block. The water is led directly to a RSTOIC block, which is used to model boiler combustion. The dry wood is broken down into its elements in a RYIELD block. The elements react in the RSTOIC reactor with oxygen to CO₂ and water vapour. Combustion air is introduced to the RSTOIC block. The model calculates the combustion airflow, once the user defines the percentage of flue gas oxygen (control of excess air). **The first design specification** varies combustion airflow to satisfy the excess air defined. Flue gas oxygen is fixed to 2 mol%, which corresponds to 13% of excess air. The adiabatic combustion temperature is calculated in the RSTOIC reactor, and the flue gas temperature is the adiabatic combustion temperature with boiler heat losses subtracted. Heat losses are defined as a fixed percentage of fuel input energy, and a **second design specification** varies adiabatic combustion temperature until the defined heat loss is reached.

The remaining three sections, heat recovery, steam turbine, deaerator, are parts of a steam cycle. The model ultimately calculates the steam turbine power output, once fuel into the boiler and steam parameters (boiler feed water pressure and superheat temperature) are defined by the user. The steam cycle is more complicated than the boiler model considering the model convergence. The steam cycle includes at least three design specifications, each of which causes one recycle loop in the model. The procedure may be rather slow in converging, because of the sequential modular approach used by AspenPlus. Typically, pure steam cycles are more conveniently modelled with a simultaneous equation-based solver.

The third design specification of the model varies the boiler feed-water mass flow to satisfy the flue gas exit temperature.

The boiler model heat recovery section has three MHEATX blocks to describe a boiler feed-water preheater, an evaporator, and a superheater. The assumed approach point temperature is 5 °C, which is set with the fourth design specification. In the boiler model there is no pinch point, a limiting temperature difference in steam-cycle design when the inlet flue gas temperature is low. Approach and pinch points, both important parameters in steam-cycle design, are explained in chapter 4.3.

Superheated steam is led to a steam turbine. The efficiency functions used for the steam turbine are shown in equations 4-2 and 4-3 /81/. If the volume flow is less than 600 m³/min, equation 4-2 is used. If the volume flow is more than 600 m³/min, equation 4-3 is used. Equations 4-2 and 4-3 are empirical, and they are based on equation 4-1.

$$v = (m_{st} * \Delta h_{is}) / (p_{in} - p_{out}) \quad (4-1)$$

where v = average volume flow, dm³/s
 m_{st} = steam mass flow, kg/s
 Δh_{is} = enthalpy difference across the turbine section, kJ/kg
 p_{in} = pressure at the inlet to the turbine section, bar
 p_{out} = pressure at the outlet from the turbine section, bar

$$\eta_{is} = 0.0517 * \ln(v) + 0.515 \quad (4-2)$$

$$\eta_{is} = 0.0071 * \ln(v) + 0.791 \quad (4-3)$$

where η_{is} = isentropic efficiency / 100
 v = average volume flow, m³/min

Turbines may operate either in back-pressure (in co-generation with heat recovery) or condensing mode (power-only production). The difference in terms of the model is the pressure at which the steam is expanded. In large condensing power plants a pressure of around

0.04 bar is employed. However, in small plants it is uneconomical to operate in such a high vacuum. A typical condensing pressure in a power plant of around 2 MW_e is 0.2 bar. In the condensing mode of operation, the steam exiting the last turbine stage is usually wet. For this section of the turbine, the isentropic efficiency function is corrected for moisture, using Equation 4-4:

$$\eta_{is} = \eta_{is,0} - (x_{in} + x_{out})/2 \quad (4-4)$$

where $\eta_{is,0}$ = isentropic efficiency for dry steam, %
 x_{in} = moisture fraction in steam entering the turbine section
 x_{out} = moisture fraction in steam exiting the turbine section

Steam is usually extracted at an intermediate pressure from the steam turbine to the deaerator for degassing. In Figure 4-1, which depicts a flow diagram of a small power plant, superheated steam is used. This arrangement makes the steam turbine investment lower, as no extraction is needed.

The fifth design specification varies the extract steam (or superheat steam) flow to satisfy energy balance requirements by making the deaerator adiabatic. Steam turbine condensates are pumped to the deaerator for treatment.

4.3 Model description of a steam cycle as part of a combined cycle

A model for a Rankine cycle employed as part of a combined cycle is described in this section. An Aspen block flow diagram of the model is shown in Figure 4-2. The model is designed to calculate the output of electricity, when the mass flow of flue gas to the heat recovery steam generator (hrsg) and steam parameters are given. When integrated as part of a gasification combined cycle, the gas turbine determines the flue gas mass flow.

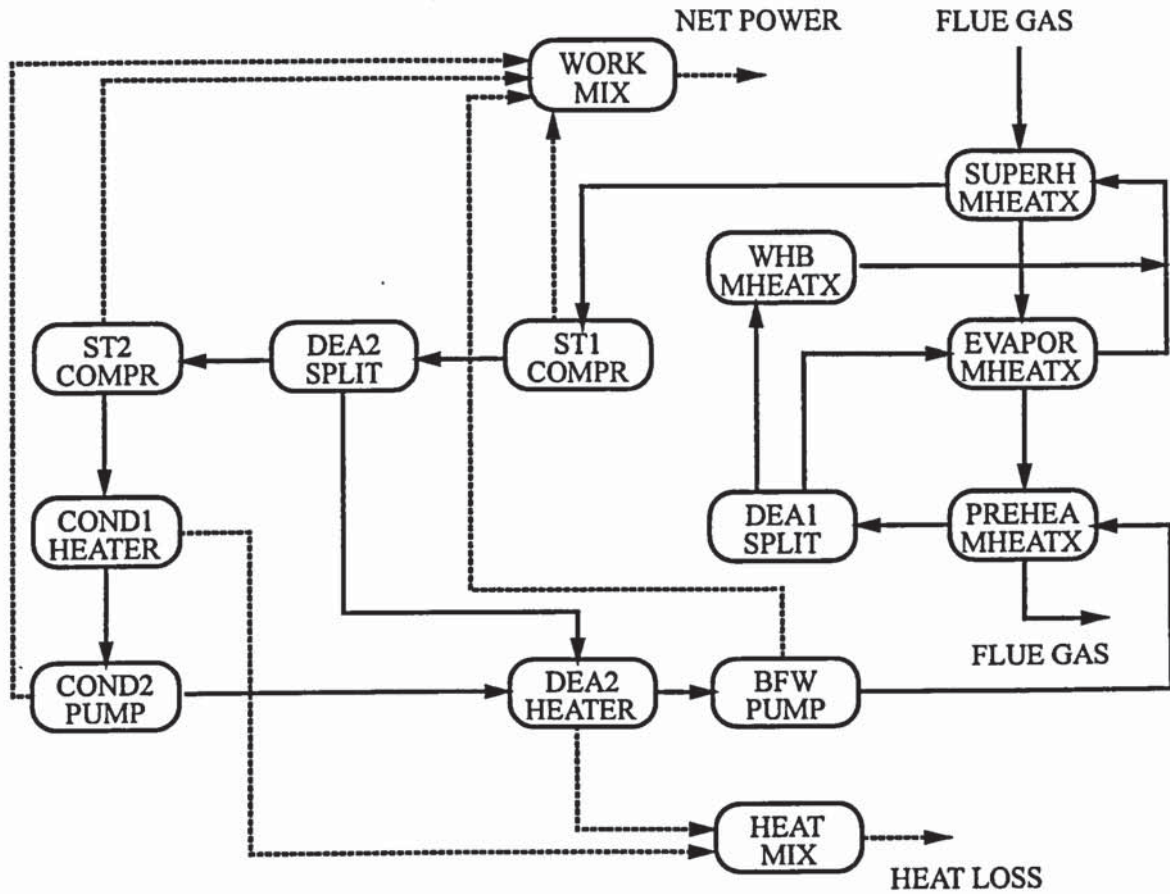


Figure 4-2. A simplified Aspen block flow diagram of the steam cycle of a combined-cycle power plant.

The model is very similar to that presented in the previous section. The differences between the models are described. The steam cycle model includes three major sections:

- Heat recovery steam generator (hrsg)
- Steam turbine
- Deaerator

The detailed design may vary depending on plant capacity.

The model ultimately calculates the steam turbine power output, once flue gas into the hrsg and steam parameters (boiler feed water pressure and superheat temperature) are defined by the user. The steam cycle includes four design specifications, each of which causes one recycle loop in the model.

There are four design specifications:

- Boiler feed-water mass flow
- Approach temperature
- Steam split to the gasifier waste heat boiler
- Deaerator energy balance

The first design specification of the model varies the boiler feed-water mass flow to satisfy the pinch point temperature. The pinch point is depicted in Figure 4-3. The pinch point temperature difference in actual plants usually ranges from 15 to 25 °C. The smaller the pinch point, the higher the heat recovery efficiency, and the higher the heat transfer area (and thus hrsg investment cost). In this work, a typical design value of 15 °C is used as the pinch point temperature.

The model hrsg has three MHEATX blocks to describe a boiler feed-water preheater, an evaporator, and a super-heater. The assumed approach point temperature (Figure 4-3) is 5 °C (a typical design value), which is set with the second design specification. The approach point is used in preheaters to prevent boiling.

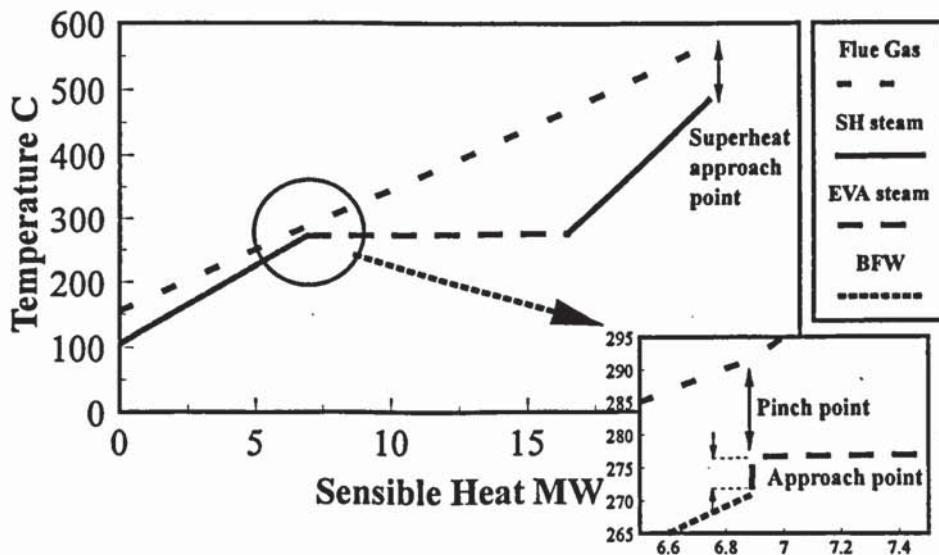


Figure 4-3. Temperature - enthalpy diagram of a 10 MWe bottoming cycle of a wood-fuelled IGCC (boiler feed-water 105 °C, superheat steam 485 °C, 60 bar), approach and pinch points shown. SH = superheated steam, EVA = evaporating water, BFW = boiler feed-water.

Part of the preheated feed-water is evaporated in the gasifier waste heat boiler (whb) in an IGCC. A temperature profile of the whb for the same bottoming cycle as above is shown in Figure 4-4. **The third design specification**, which controls stream splitting in DEA1 (Figure 4-2), is designed to determine the amount of water sent to the whb. Preheated water is evaporated in the whb. Saturated steam is led back to the hrsg, where it is superheated together with the remaining saturated steam.

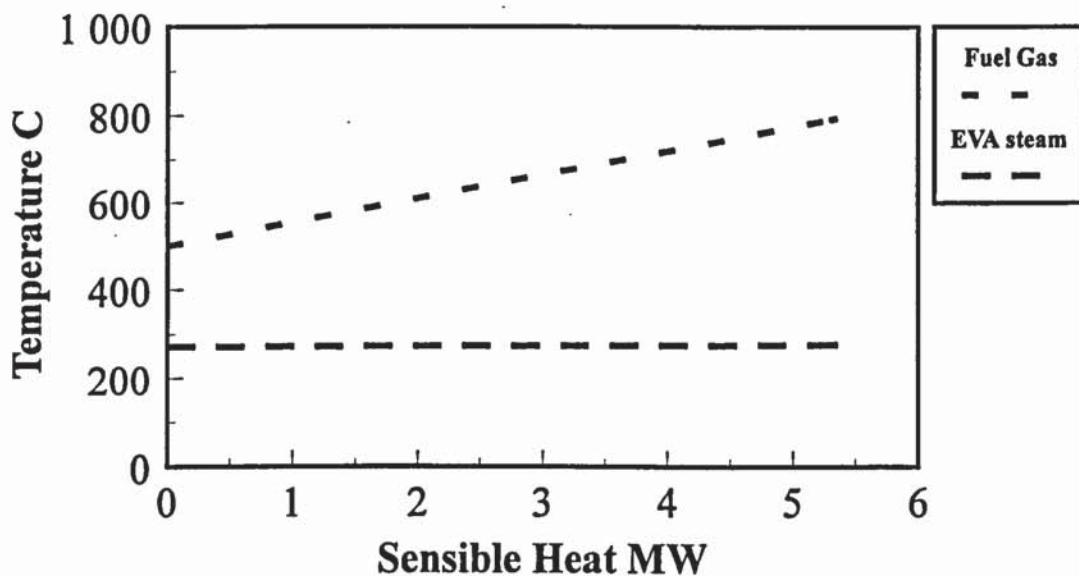


Figure 4-4. Temperature - enthalpy diagram of the gasifier waste heat boiler as part of a 10 MW_e bottoming cycle of a wood-fuelled IGCC. EVA = evaporating water.

Superheated steam is led to a steam turbine, which may operate either in back-pressure (in co-generation) or condensing mode (power-only production). Both modes are studied in connection with the IGCC.

Steam is extracted at an intermediate pressure from the steam turbine to the deaerator for degassing. **The fourth design specification** varies the extract steam flow to satisfy energy balance requirements by making the deaerator adiabatic. Steam turbine condensates are pumped to the deaerator for treatment.

When the flue gas temperature is low (as is typical in combined cycles), two or more steam pressure levels may be employed to improve heat recovery. The temperature of the exhaust

gas from a gas turbine or a combustion engine ranges from 400 to 550 °C. However, two pressure levels would increase the investment costs, and are not feasible in small-scale combined cycles.

Two pressure level steam generation improves efficiency considerably. In such a case at least two pinch points exist, and both of them are handled by a separate design specification.

4.4 Using the Aspen model to study the performance of a boiler power plant

In the following sections, critical process parameters are varied, and their effects on efficiency are studied. The parameters are flue gas final temperature, steam turbine back-pressure, the amount of excess combustion air, steam pressure and superheat temperature. Finally, model results are compared to state-of-the-art industrial data, and a summary of the results is presented.

The performance of a condensing power plant using wood is studied in this section with the model described in section 4.2. As explained in section 2.3.1, most existing modern wood-fuel-fired power plants are co-generation facilities, either industrial or residential. Condensing power plants have been built in the U.S., but their performance values are rather poor (note discussion in Chapter 2). Not much data concerning modern power production in condensing mode is available. Comparable reference data for process comparison is generated with the steam cycle model described in section 4.2. This data concerning the conventional Rankine cycle will be used as a reference to assess the performance of new systems under development. The importance of this data is emphasised by the results in Chapter 2, where a wide range of performance is reported in the literature for conventional power plants.

4.4.1 Flue gas final temperature

To study the effects of the final temperature of boiler flue gas on plant efficiency, temperatures between 160 and 200 °C were studied at a capacity of around 2 MWe. This capacity was selected to represent the smallest viable scale for the Rankine cycle.

The corresponding overall electricity production efficiency decreases from 21.7 to 21.1% (Figure 4-5) when the flue gas end temperature is increased. In practice, the actual flue gas temperature is a result of economic optimisation, as higher efficiency reduces operation costs (fuel costs), but increases investment costs (increased boiler heat surface area).

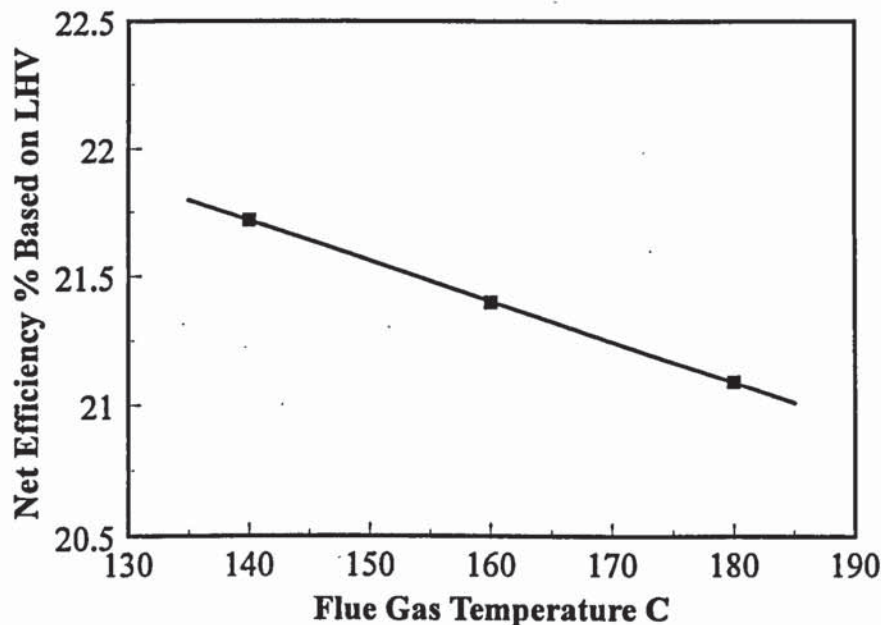


Figure 4-5. The Rankine cycle electricity production efficiency at 2 MWe, flue gas temperature varied. Steam pressure 40 bar, superheat temperature 450 C, wood moisture content 45 wt%, LHV 9.35 MJ/kg.

4.4.2 Steam turbine back-pressure

The significance of condenser pressure may be seen in Figure 4-6, where power production efficiency is shown as a function of turbine back-pressure. Again the capacity is around 2 MWe. On this small scale, a back-pressure lower than about 0.1 to 0.2 bar is not practical. However, efficiency is also shown for 0.04 bar to emphasise the importance of this parameter, because 0.04 is typical of large units. The efficiency ranges from 24 to 18% when

the back-pressure is increased from 0.04 to 0.8 bar. The latter is a typical pressure in residential combined heat and power production.

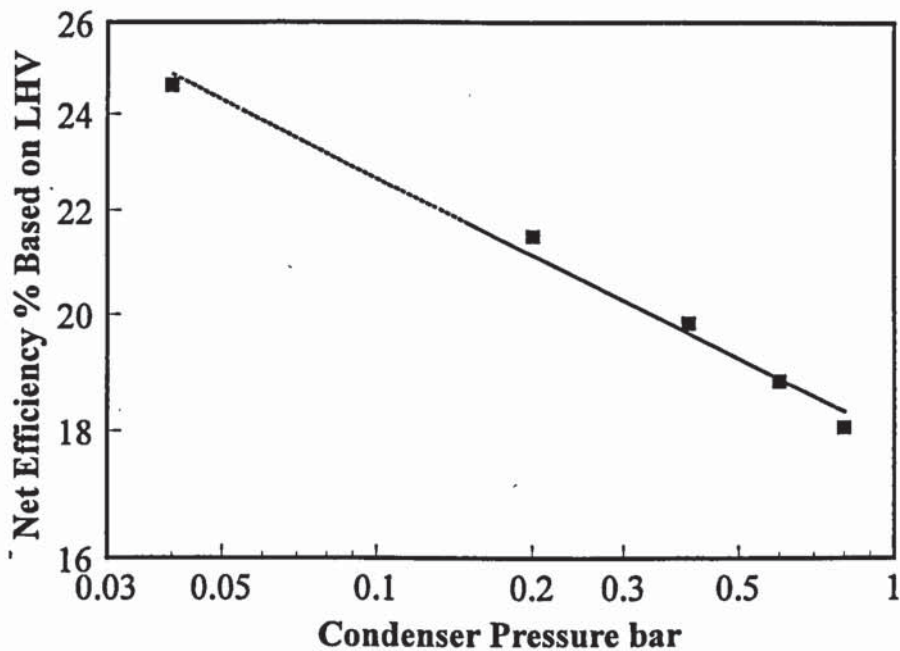


Figure 4-6. The Rankine cycle electricity production efficiency at 2 MWe, condenser pressure varied. Steam pressure 40 bar, superheat temperature 450 C, wood moisture 45 wt%, LHV 9.35 MJ/kg.

4.4.3 Excess combustion air

The effect of excess combustion air on power plant efficiency is shown in Figure 4-7. Oxygen in the flue gas is varied between 2 to 4 mol%, which corresponds to a variation of 13 to 30% excess air. Although an important process parameter in actual boiler operation, the calculated effect is not significant if a fixed final flue gas temperature is assumed, as it has been here. The result should not be confused with a situation in an existing boiler with fixed heat transfer surfaces. Varying excess air in an existing boiler would change the end temperature of flue gas, and the effect on efficiency would be different. However, in both cases the overall effect on power plant efficiency is relatively minor compared to other parameters varied here.

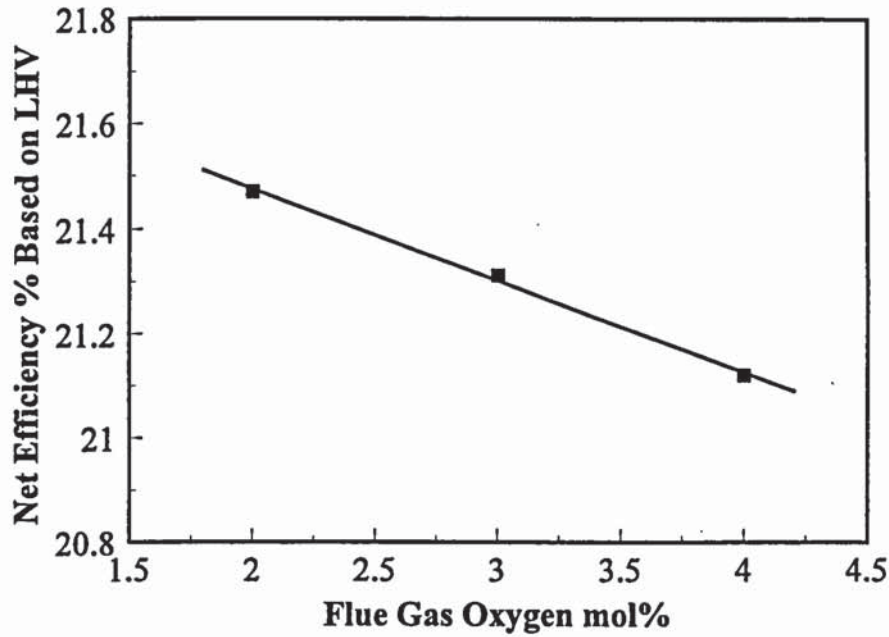


Figure 4-7. The Rankine cycle electricity production efficiency at 2 MWe, excess air varied. Steam pressure 40 bar, superheat temperature 450 C, wood moisture 45 wt%, LHV 9.35 MJ/kg.

4.4.4 Steam conditions

The superheat steam parameters (pressure, temperature) have a considerable effect on plant efficiency. These parameters are varied in Figure 4-8. The fuel input in each case is 12.8 kg/s of 50 wt% moist fuel, and the respective power outputs vary between 30.4 and 33 MWe. The capacity was selected because higher pressures and temperatures may already be feasible on this scale. High pressure and temperature become more economically viable as the plant size increases. Industrial practice with steam conditions is summarised in the next section.

Increasing both the superheat temperature and pressure raises power output and efficiency. However, raising the steam pressure increases the steam humidity after the turbine. The humidity in the steam turbine outlet should not exceed a certain value, which is defined by the turbine manufacturer. A water content of 10% has been used as a maximum in deriving Figure 4-8. The efficiency ranges between 28.9 and 31.3% when steam conditions are increased from 40 bar and 485 °C to 90 bar and 535 °C.

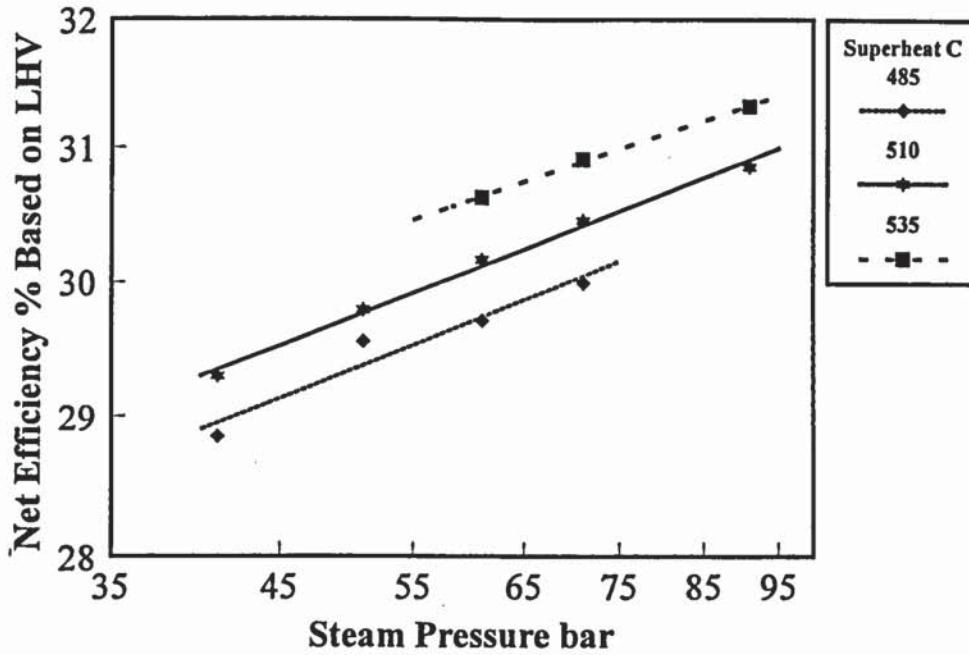


Figure 4-8. Effect of steam data on power plant efficiency (operation in condensing mode), capacity around 30 MWe.

4.4.5 Summary

A summary of model results is shown in Figure 4-9. The respective sensitivities of the parameters varied in the previous sections may be seen in the figure. Turbine back- pressure has a large effect on overall efficiency, whereas superheat steam pressure and temperature have a medium effect, and the flue gas final temperature has a small effect.

The industrial correlation shown in the figure is derived from steam data, which is representative of current industrial practise. The industrial steam data is summarised in Table 4-2.

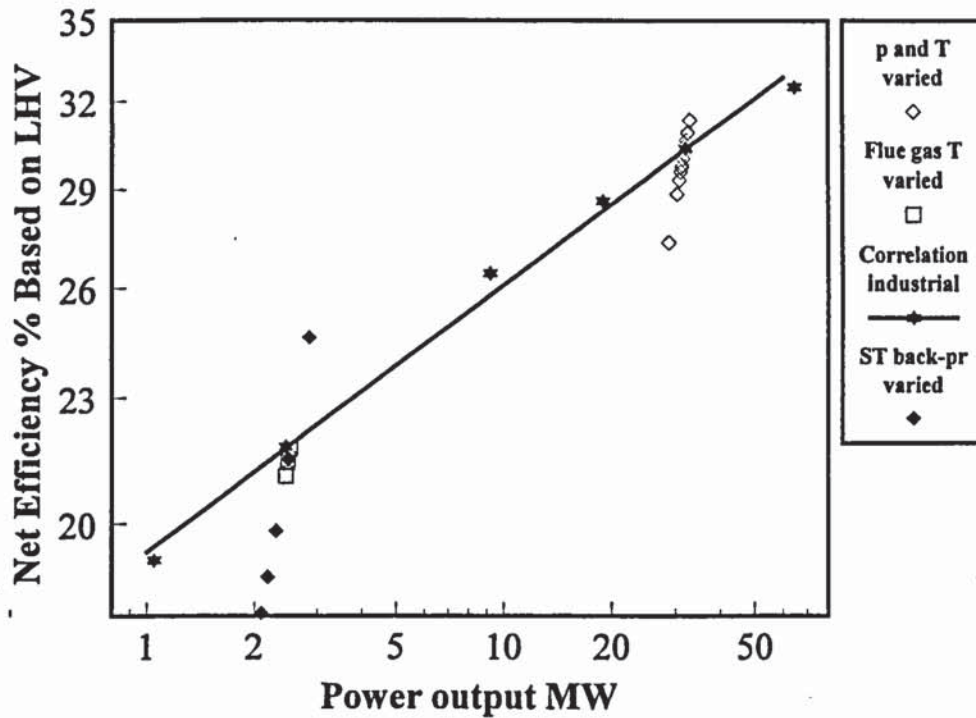


Figure 4-9. Summary of model results, Rankine power plant efficiency as a function of capacity.

Table 4-2. Steam data used in each capacity (Figure 4-9) for the industrial correlation.

Capacity MWe	Steam pressure bar	Superheat temperature °C	Turbine back-pressure bar
60	100	540	0.04
30	90	530	0.06
20	80	520	0.08
10	60	510	0.1
2	40	480	0.2
1	40	450	0.3

4.4.6 Comparison of the model results with industrial data

Model results which describe power production in the condensing mode are compared with industrial data in Figure 4-10. It should be noted that the industrial data presented earlier (Chapter 2) /34/ is for combined heat and power production, where the back-pressure is approximately 0.6 to 0.8 bar. One comparable data point is available for condensing power production /33/. It may be concluded that the AspenPlus model designed for a Rankine steam cycle is reasonable.

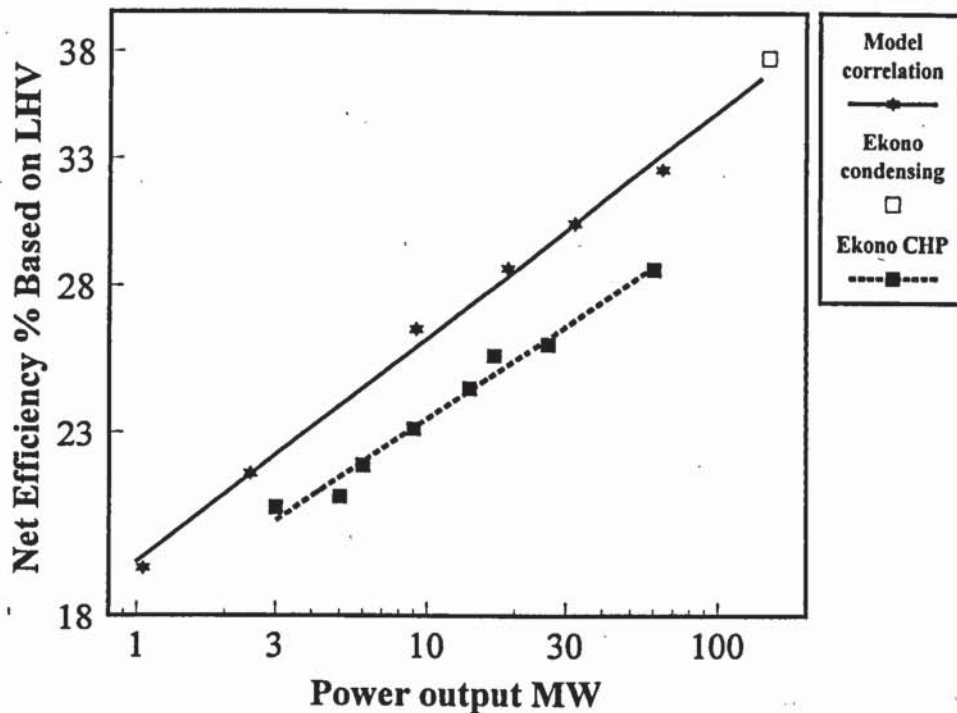


Figure 4-10. Biomass power plant efficiencies, no re-heating. Model results compared with industrial data.

4.5 Using the Aspen model to study the performance of the steam cycle of a combined cycle

The performance of the steam cycle of a combined cycle is studied in this section with the model described in section 4.3. The steam cycle is integrated later as part of gasification and pyrolysis combined cycles.

The steam cycle studied in sections 4.5.1 - 4.5.3 is part of an IGCC which uses the GE LM2500 gas turbine. The exit temperature from the hrsg is kept constant (at approximately 270 °C) to satisfy the energy demand for the fuel dryer.

Steam conditions (pressure, temperature) of the combined cycle are varied in this section. Generally, increasing the superheated steam pressure and temperature improves efficiency. However, it also increases the investment cost. Again, a trade-off between efficiency and capital cost is involved. These aspects are reviewed.

4.5.1 Moisture at steam turbine exit

Superheat steam conditions have to be selected in such a way that the conditions at the exit of the turbine are acceptable. A limiting factor is moisture, which should not be too high. The steam turbine manufacturer determines the acceptable value, but, typically, the steam moisture should not exceed 10 - 12 wt%. The value is equipment-specific, and only large turbines can tolerate a high water content.

Exit moisture is a function of steam superheat pressure, temperature, and isentropic efficiency of the turbine. Turbine efficiency is determined with equations 4-2 and 4-4 given earlier. An increased isentropic efficiency leads to a higher water content in the turbine exit, unless the superheat temperature is increased. The increase in superheat pressure also raises the water content in the turbine exit. Applying a higher superheat temperature may reduce the proportion of water in the turbine exit. A maximum of 10 wt% (water in exit) was selected for the relatively small steam turbine studied here (about 10 MWe).

The proportion of water in the steam as a function of superheat conditions is shown in Figure 4-11. It may be seen that when the pressure is increased from 60 to 90 bar the minimum superheat temperature rises from 485 to 545 °C.

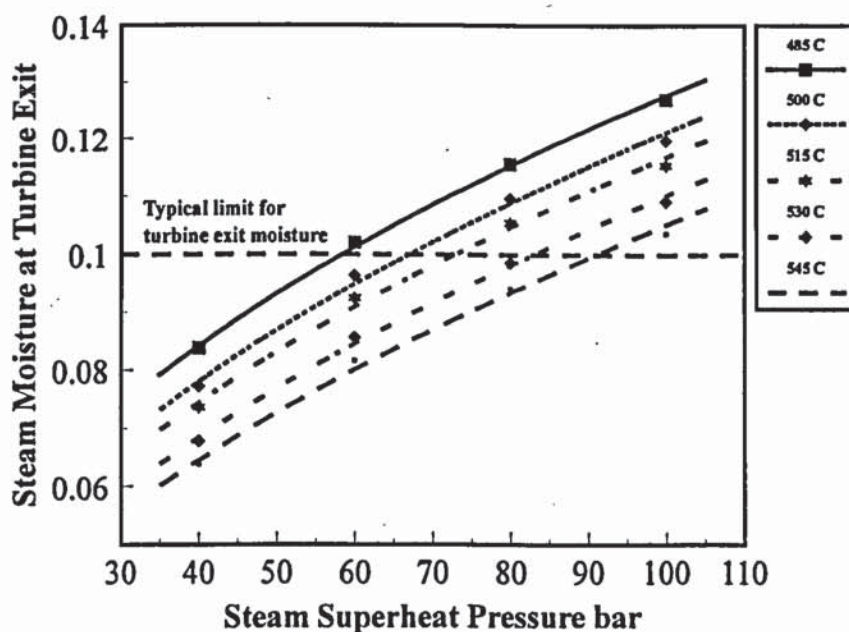


Figure 4-11. Steam turbine exit moisture, IGCC using the GE LM2500 gas turbine. LM2500 gas turbine output 23.3 MWe, flue gas temperature 566 °C.

4.5.2 Steam cycle performance

Figure 4-12 depicts the effects of varying steam properties on the power output of the steam turbine. Increasing the superheated steam pressure and temperature raises power output and improves efficiency. However, if the superheat pressure is 60 bar, the temperature has to be above 485 °C to prevent excessive moisture. If the pressure is 80 bar, the temperature has to be above 530 °C.

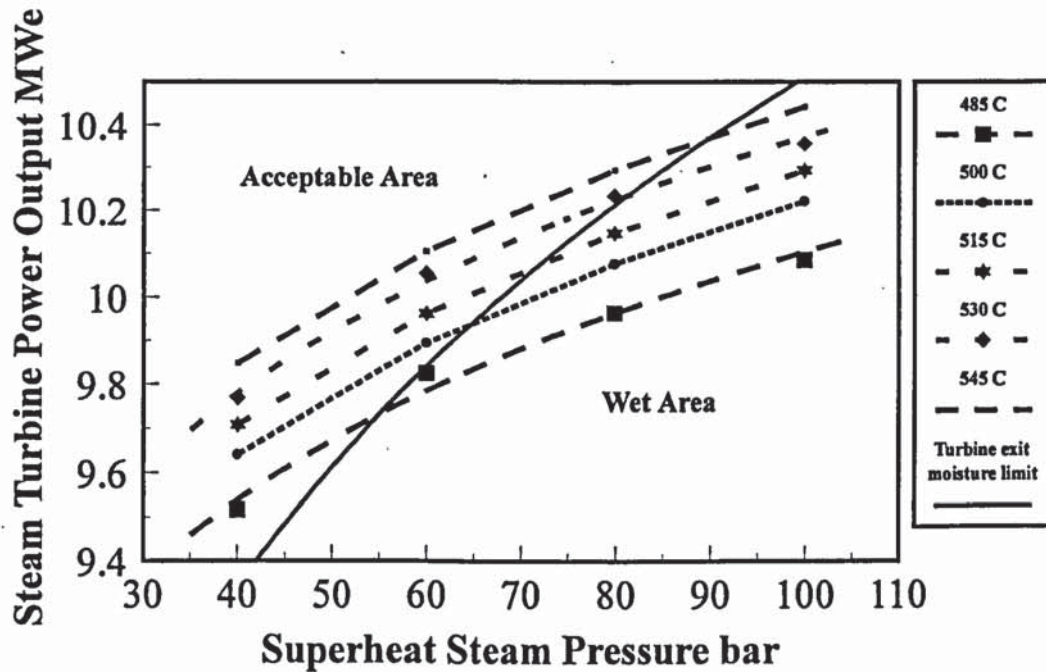
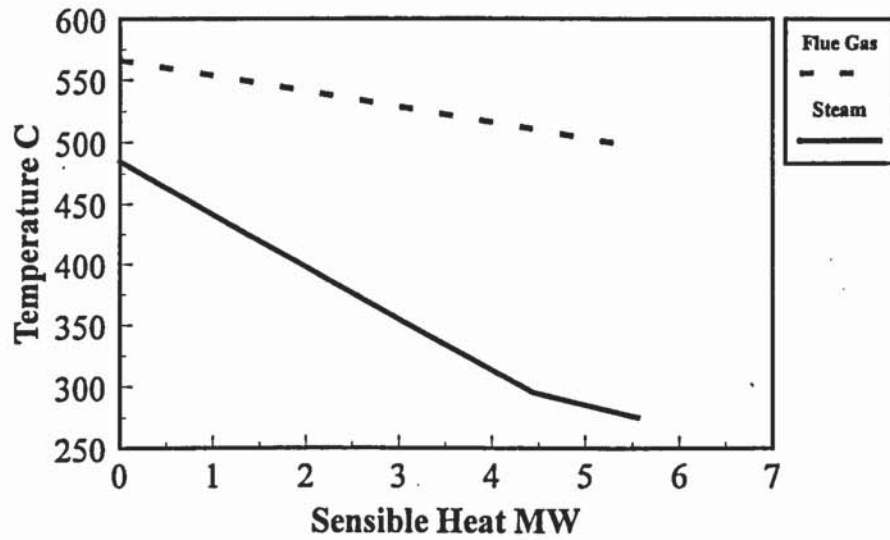


Figure 4-12. Steam turbine output as a function of superheat pressure and temperature, combined cycle. LM2500 gas turbine output 23.3 MWe, flue gas temperature 566 °C. Turbine moisture limit 10 wt%.

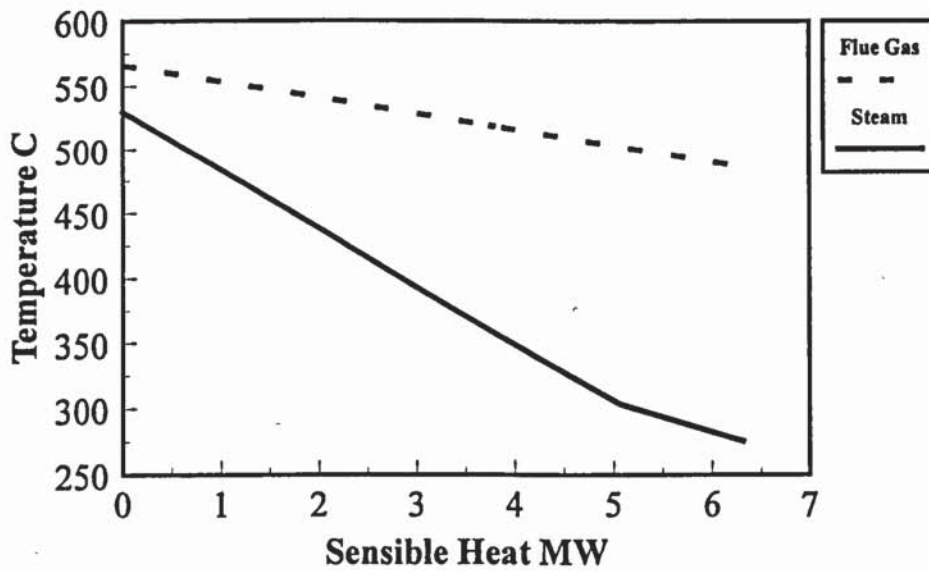
4.5.3 Superheater investment cost

When superheat pressure and temperature are increased, the cycle efficiency and the investment cost also rise. The cost is increased for two reasons: Firstly, more expensive materials have to be employed when pressure and temperature are raised. Secondly, the superheater surface area also increases due to the smaller temperature differences throughout the heat exchanger.

The situation depicted in Figure 4-13 shows superheater temperature profiles for two cases. In both cases the flue gas mass flow (69 kg/s) and temperature (566 °C) are the same, and the steam pressure is 60 bar. Two superheat temperatures, 485 and 530 °C, are compared. More heat is transferred from flue gas to steam when the steam superheat temperature is 530 °C.



4a)



4b)

Figure 4-13. Temperature profiles for a combined-cycle hrsg superheater, pressure 60 bar, a) superheat temperature 485 °C and b) 530 °C..

Specific superheater costs may be reviewed on the basis of Figure 4-14. Superheater AU is shown, where A is the heat exchanger area, and U is the overall heat transfer coefficient. If U is considered constant, it may be seen that when the pressure is increased from 60 to 80 bar and the temperature rises from 485 to 530 °C, the superheater area grows by about 65%. The corresponding increase in power output is about 4%. The trade-off between efficiency and cost may be studied on the basis of figures 4-12 and 4-14.

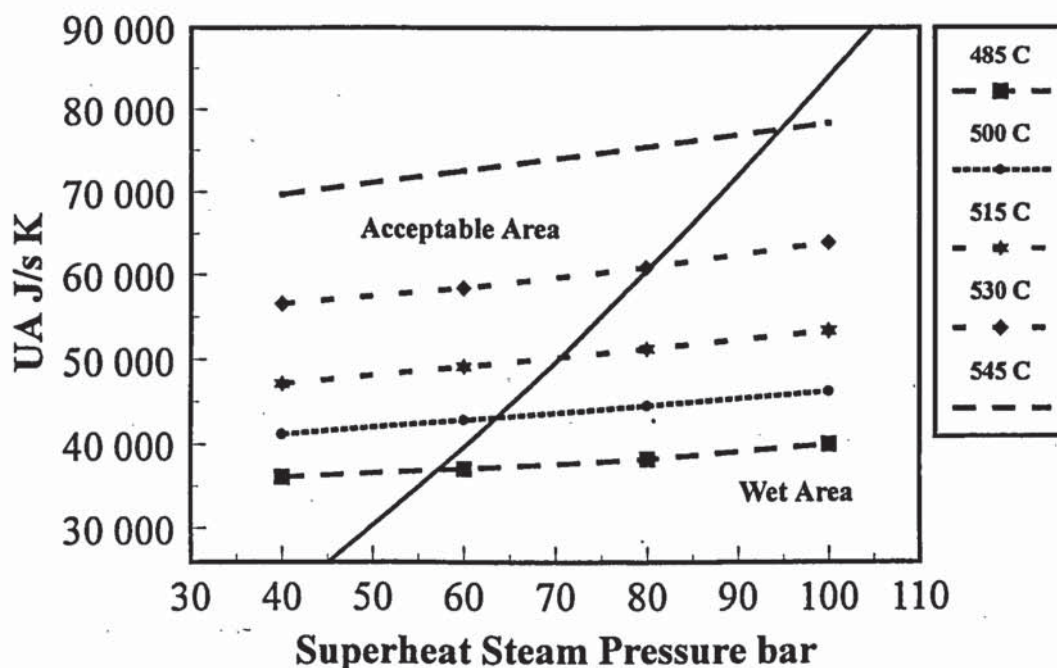


Figure 4-14. Superheater area times heat transfer coefficient as a function of steam conditions, IGCC. LM2500 gas turbine output 23.3 MWe, flue gas temperature 566 C. Turbine moisture limit 10 wt%.

5. DRYING OF BIOMASS

In this chapter industrial wood dryers are briefly reviewed. Dryer type, specific energy consumption, and emissions are considered the three most important aspects for drying model construction, and these are examined. These aspects impose the range of operation for the dryer models. Dryer models built with AspenPlus are presented.

5.1 Introduction

Most of the proposed thermochemical biomass conversion processes include drying of the feedstock. In gasification, wood typically contains 15 - 25 wt% moisture, and in pyrolysis the moisture content of wood should be less than 10 wt% to reduce the moisture content of the liquid product.

It is assumed in this work that wood is delivered to the plant as chips with a 50 wt% moisture content (the maximum dimension 20 - 40 mm), because chips are industrially the most important form of wood fuel at the present time. Although other wood forms can be delivered and produced, none are believed likely to replace chips in the foreseeable future.

Dryer performance should ideally be determined with a detailed simulation model, because modelling of mass and heat transfer during drying is a considerable challenge. Grønli /82/ has recently published a thesis in which a detailed model is presented. However, even a proper simulation model would probably have to be "tuned" for each type of equipment before it could be used in predicting performance. A predictive rigorous performance model is clearly beyond the resources of this work.

To properly describe an industrial process unit with the simulation model, the mass and energy balance for drying should be based on industrial data. Specific energy consumption (heat required to evaporate 1 kg of water), which is the most important dryer parameter determining dryer performance, is derived from industrial data. The dryer heat requirement is calculated with a linear approximation (Equation 5-1):

$$\text{Heat requirement (MW)} = \text{Specific energy consumption (MJ/kg)} * \text{Water evaporated (kg/s)} \quad (5-1)$$

where the data used for specific energy consumption is explained below. The amount of evaporated water may be calculated, once the feed to the plant and the final moisture content required are known.

The specific energy consumption presented in Figure 5-5, which is used in determining data for equation (5-1) above, is based on data from equipment vendors. The data was critically reviewed, and based on discussions with an engineering contractor /83/. 3.5 MJ/kg of evaporated water was selected. The reasoning for the selection of the value is explained in section 5.3.

Two models are included: a steam dryer and a flue gas dryer. These represent the two main energy input alternatives employed industrially: steam and hot flue gas. The two are analysed to determine whether either has specific advantages when integrated with bio-power concepts. The models calculate the mass and energy balances for an industrial dryer, once the input feed data and operation conditions have been established.

The dryer model determines the hot flue gas or steam requirements for the dryer, when integrated into a model of an advanced cycle. The calculated flows are then specified as a design specification for the respective units (heat recovery steam generator or steam turbine extraction), so that the required amount of flue gas or steam is available from these units to the dryer. An overview of the overall model operation is presented in Chapter 10, where the integrated model of an advanced cycle is presented.

5.2 Drying equipment for woody biomass

In this section, industrial dryers suitable for wood are reviewed. The review of drying systems is based on a report by Energy, Mines and Resources of Canada in 1983 /84/. The review is a comprehensive summary of equipment on the market. No significant modifications of dryer performance have taken place since then. The only important improvements are related to their environmental performance, which principally influences investment cost. The investment costs in this work are derived from other more recent sources.

In large-scale applications two general types of thermal dryers are employed for wood: rotary and suspension dryers. Suspension dryers include both fluidized-bed and transported beds. Some of the dryer characteristics are shown in Figure 5-1. Flue gases are most commonly used industrially as the heat transfer medium.

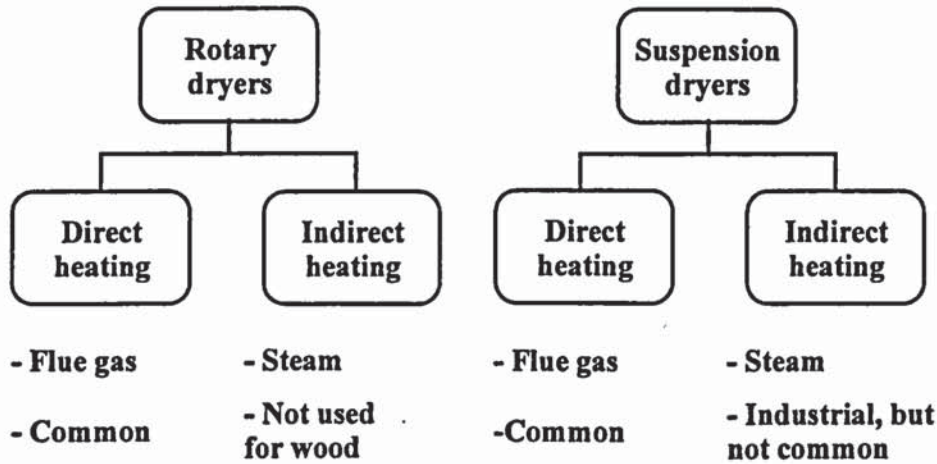


Figure 5-1. Principal dryer types and applicability for biomass with heat transfer medium.

According to the instructions of equipment vendors, the preferred feed particle sizes are typically 50-100 mm and 25-50 mm for rotary and suspension dryers, respectively. The particle retention time in rotary dryers is considerably longer than in suspension dryers, typically 20-30 min, although for smaller particles it may be considerably shorter. In suspension dryers the particle residence time is typically 30 s. In order to complete drying in the short time available in suspension dryers, some suppliers include a pulverizing mill in their system. Usually wood dryers employ direct contact between the solid and the heat source. Flue gas is the dominant source for the drying energy. Some suspension dryers also use steam.

A suspension dryer using direct heating with flue gas is depicted in Figure 5-2. A rotary dryer also heated with flue gas is shown in Figure 5-3. Typically, a bag-house filter is needed to remove solids from the flue gas exiting these dryers. A suspension dryer heated both directly and indirectly with steam is shown in Figure 5-4. Waste water, which is produced when the evaporated water is condensed, has to be treated.

Two suspension dryer models are presented later in the chapter. The rationale for this selection is presented in section 5.6.

The steam dryer (Figure 5-4), originally developed by MoDo Chemetics in Sweden, has also been built for pressurised operation. Niro A/S in Denmark has developed another version of a steam dryer. Drying under pressure in a steam atmosphere increases the drying rate. Another advantage in pressurised operation is the opportunity to recover heat from evaporated water in the condenser at a higher temperature. A pressurised dryer should also be suitable with a pressurised gasifier. A disadvantage is the more complicated and expensive feeding system.

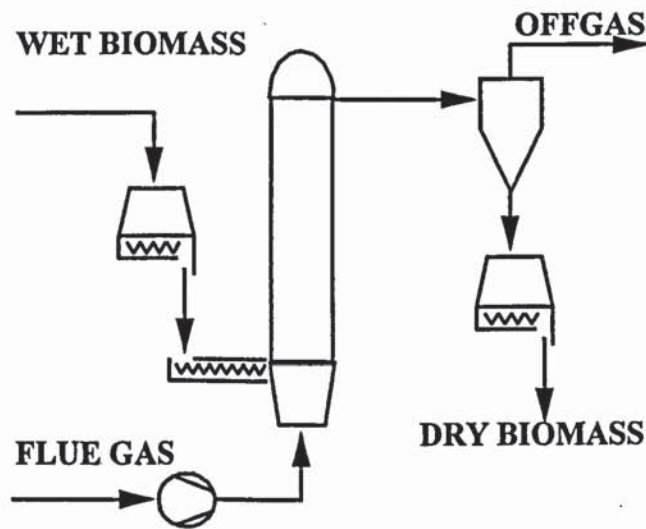


Figure 5-2. A flowsheet of a suspension flue gas dryer, modelled later in the chapter.

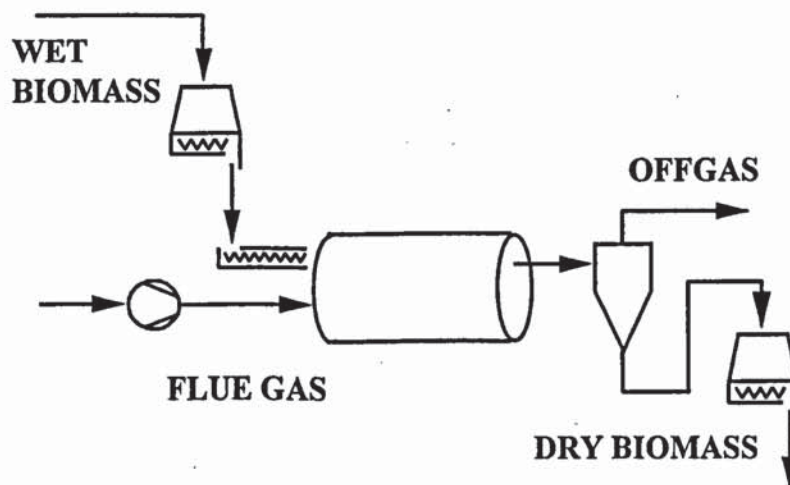


Figure 5-3. A flowsheet of a rotary flue gas dryer.

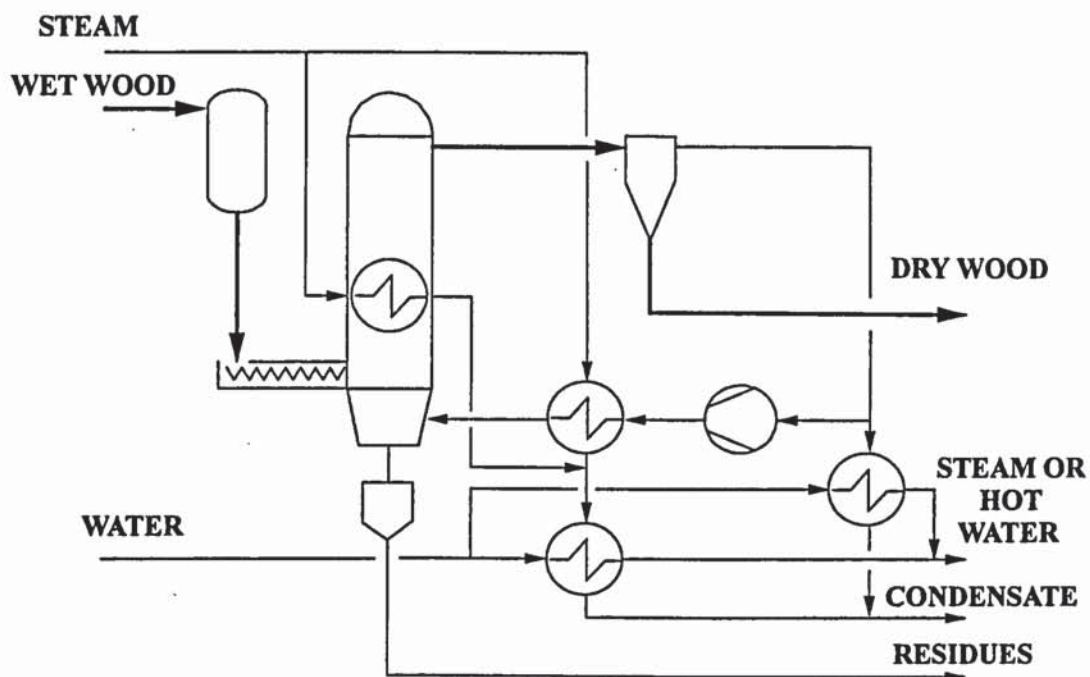


Figure 5-4. A flowsheet of a steam dryer, modelled later in the chapter.

5.3 Dryer performance

The performance data for dryers presented by Goater et al. /84/ is summarised in Tables 5-1, 5-2, and Figure 5-5. The specific energy consumption to be used in the simulation model is derived on the basis of the data in Figure 5-5 and discussions with an engineering contractor /83/.

Table 5-1. Performance data for rotary dryers, flue gas as a drying medium /84/.

Type of dryer	Single pass a	Single pass b	Triple pass b	Triple pass c	Single pass d	Single pass e
Feed rate, kg/s dry	1.80	2.87	3.89	2.52	5.78	6.80
Moisture of wet feed, wt-%	55	55	55	55	55	55
Moist. of dried biomass, wt-%	30	30	24	10-25	25	27
Gas inlet, °C	355	315	315	316	315	315
Gas outlet, °C	93	102	99.5	82	93	93
Evaporation rate, kg/s	1.43	2.27	3.50	2.45	5.04	5.04
Energy consumption, MJ/kg H ₂ O	3.9	4.5	3.8	2.9	3.1	3.1

^a C.E. Raymond, Brantford, Ontario, Canada

^b Guaranty Performance Co, Tigard, Oregon, USA

^c M.E.C Co, Neodesha, Kansas, USA

^d Rader Canada Ltd, Vancouver, British Columbia, Canada

^e Stearns-Roger Eng. Corp., Denver, Colorado, USA

Table 5-2. Performance data for other dryers /84/.

type of dryer	ascade ^a	lash dryer ^b	ill dryer ^c	team dryer ^d
Feed rate, kg/s dry	6.80	1.81	4.40	6.35
Moisture of wet feed, wt-%	55	55	55	55
Moist. of dried biomass, wt-%	32	30	12	10
Drying medium	Flue gas	Flue gas	Flue gas	Steam
Gas inlet, °C	233	538	371	150 ^e
Gas outlet, °C	93	107	93	120 ^f
Evaporation rate, kg/s	5.11	1.43	4.78	7.06
Energy consumption, MJ/kg H ₂ O	2.7	3.5	2.8	1.4

^a Bacho Systems Inc., Atlanta, Georgia, USA

^b C.E. Raymond, Brantford, Ontario, Canada

^c Flakt Canada Ltd., Vancouver, British Columbia, Canada

^d MoDo-Chemetics Div., Vancouver, British Columbia, Canada

^e Temperature of the steam used for drying

^f Temperature of the steam produced

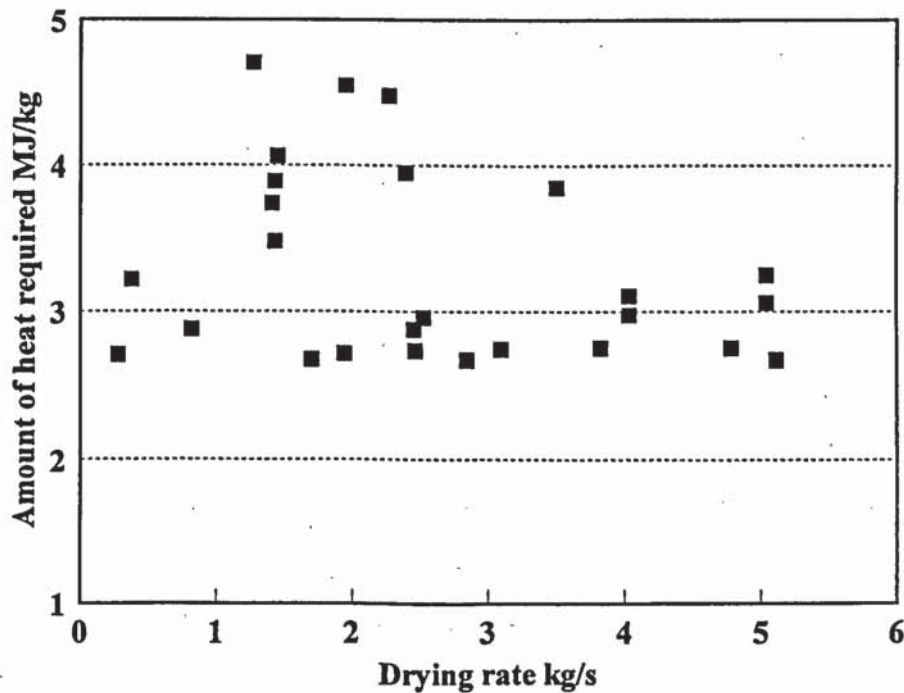


Figure 5-5. Energy consumption of dryers.

The data by Goater is employed, as it presents a consistent set of industrial data for flue gas dryers. A wide range of equipment is available. In the report, several sizes for each dryer are given. Both rotary and suspension dryers are included. The largest size available from each manufacturer was selected for the summary tables. The selection covers the North-

American market, so some European manufacturers are listed through their American offices.

The reported energy consumption ranges from 2.7 to 4.7 MJ/kg of evaporated water for flue gas dryers. However, the data presented was considered to be optimistic, as the theoretical minimum heat requirement is around 2.7 MJ/kg, depending on the operating temperature (and pressure) of the dryer and fuel feed. A conservative specific consumption of 3.5 MJ/kg is selected for this work to represent actual industrial practice /83/. The variation of this parameter is studied later in Chapter 10.

5.4 Dryer emissions

An important aspect in thermal drying is the amount of volatiles which are driven out of the biomass during drying and which cause environmental emissions. Drying temperature, vapour partial pressure, and solid residence time are key parameters related to pyrolysis. Fagernäs /85/ has studied the amount and composition of the volatile emissions in bark drying. The total amount of organic compounds released in an indirectly heated fluidised-bed steam dryer at 250 °C was about 3 wt% (dry ash-free basis) for pine bark. The effect of temperature on organic release is depicted in Figure 5-6. The correlation may also be used as an approximation for wood drying. Industrial wood fuels will contain a considerable amount of bark.

The wood temperature during drying has to be kept relatively low to prevent the release of organic vapours into the atmosphere. In this work, the dryers are designed to operate below 250 °C to reduce emissions. Dryers are equipped with bag-house filters to reduce dust emissions.

Gaseous emissions are usually not a problem with steam dryers. However, in a steam dryer the organic release ends up in the waste water. Therefore, waste water treatment needs to be included when a steam dryer is used.

An analogous correlation as in Figure 5-6 would exist for flue gas dryers, but no data was available. It is assumed that lowering of the drying temperature by recycling part of the off-gases is sufficient to reduce volatile emissions in flue gas drying. Should emissions still be unacceptably high, a scrubber would have to be installed after the dryer bag house.

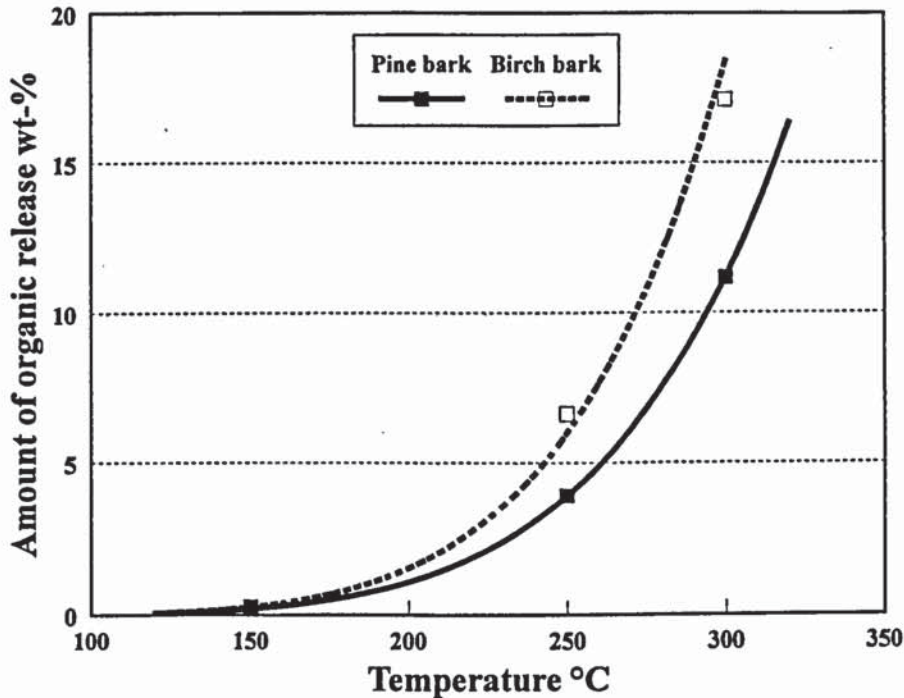


Figure 5-6. Release of organic compounds in a fluidized-bed batch steam drier /85/.

It is evident that with the resources available there is not enough data available to construct a model which would take account of the low-temperature pyrolysis occurring in dryers. As drying is an important step in advanced bio-power cycles, it is suggested that rigorous dryer models should be built in the future, for example, with AspenPlus.

5.5 Conclusions as bases for the model design

As a conclusion from the above, the following issues may be listed:

- A considerable amount of low temperature heat is available from the steam dryer. The dryer may be an interesting option if co-generation of heat and power is needed. Compared with other dryers, however, this type of dryer is relatively expensive due to its

more complicated design. Milling of wood chips to a smaller particle size may also be needed for successful operation.

- Flue gas dryers are generally fairly simple and cost slightly less than steam dryers. However, feed of a low moisture content is required for gasification (typically 15 to 25 wt%) and for pyrolysis (typically < 10 wt%). The final moisture content in rotary dryers usually ranges from 25-30 wt%, which is usually too high a feed moisture content for a conversion process. A lower moisture content is possible, but the relative investment increases considerably: the capacity of the dryer decreases when the final moisture content is lowered. According to Goater /84/, only one rotary dryer is reported to have a final design moisture content of 10%.
- The safety of flue gas dryers remains a problem. It is well known by dryer operators, and is described, e.g. by Burnett et al. /86/, that fires have caused occasional problems. The cause of these fires is usually related to air leakage into the hot flue gas stream.
- Volatilisation of organics is a problem in drying unless a sufficiently low temperature is used. However, relatively little actual plant data on emissions from these systems appears to exist.

5.6 Description of the models

In this section, the two models built for wood drying are presented. All advanced biomass power cycles studied in this work employ the drying of fuel. The dryer models are eventually integrated with other unit models, which together form the overall bio-power concept models. The principles of integration are explained in following sections.

Two models have been designed: a steam dryer and a generic flue gas dryer. Both models calculate the performance (mass and energy balances) of a dryer, once the amount of fuel and its final moisture content have been fixed.

Dryer models are summarised in the two following sections. The design of the steam dryer model is described in more detail and tested in Appendix 1. The AspenPlus input file is presented in Appendix 2.

5.6.1 Flue gas dryer

An AspenPlus block flow diagram of the dryer is shown in Figure 5-7 (the flowsheet is shown in Figure 5-2).

Examples of major user inputs and model results are presented in Table 5-3. In an integrated model, some input parameters are supplied by other power plant model sections, such as the inlet flue gas composition (all cases), or inlet flue gas mass flow (determined in an IGCC by the gas turbine).

Table 5-3. Some flue gas dryer model inputs and outputs.

INPUT DATA	Wet wood mass flow (kg/s) Feed moisture wt% Outlet wood moisture wt% Inlet flue gas mass flow (kg/s), pressure (bar), and composition mol-%
OUTPUT DATA	Dry wood mass flow (kg/s) Evaporated water mass flow (kg/s) Required flue gas temperature (°C) Outlet flue gas composition mol-% Blower power demand (MWe)

The user specifies the original and final wood moisture content and the wood mass flow, which determine the water evaporation rate, or dryer capacity. The investment cost is determined on the basis of the evaporation rate of the dryer.

The sensible heat in the flue gas stream entering the dryer delivers the heat needed to evaporate the fuel moisture. The specific energy consumption (section 5.3) and the water evaporation rate determine the total sensible energy required to operate the dryer. A specific energy demand of 3.5 MJ per evaporated kg of water is used. The final moisture content in the dryer is specified by the conversion process: 15 and 10 wt% has been used for gasification and pyrolysis, respectively. In principle the final moisture content of the fuel should be optimised by using the complete plant cost and performance models. However, the engine models (gas turbine, gas engine, diesel engine) were not rigorous enough to take the effect of fuel moisture on engine performance properly into account. For this reason optimization was not carried out.

Hot flue gas for drying may be taken from a heat recovery steam generator (gas turbine concepts), engine exhaust gas (engine concepts), or boiler flue gas (pyrolysis).

When gas turbine flue gases are used, the total sensible energy demand of the dryer determines the outlet temperature of the flue gas from the gas turbine heat recovery steam generator (hrsg). Hrsg steam production is reduced compared to operation without a dryer. The dryer exhaust flow is recycled to maintain the inlet flue gas temperature to the dryer at 250 °C, thereby reducing emissions.

There are three design specifications in the flue gas dryer model:

- Temperature of the flue gas into the dryer from another process section (mass flow DR19)
- Temperature of the flue gas into the dryer vessel (mass flow DR13)
- Heat loss from the dryer vessel (heat flow Q)

Inlet wood (DR11) is mixed with the flue gas in a MIXER. The mixture is led to a FLASH2 unit, where the necessary water is evaporated. Part of the flue gas out is recycled (FSPLIT) through a blower to reduce the inlet temperature of the flue gas. Recycled gas is first mixed with the flue gas from another process section, and then mixed with wet wood. Heat loss for the dryer is determined on the basis of two aspects. The dryer heat demand is derived from industrial practice, as explained above. Therefore the outlet flue gas temperature (DR15) is set to 95 °C, which is a typical industrial value (tables 5-1 and 5-2). To satisfy this requirement, heat loss Q is set with a design specification. Although the approach is not entirely satisfactory, it meets the most important requirement for a model: performance of industrial operation.

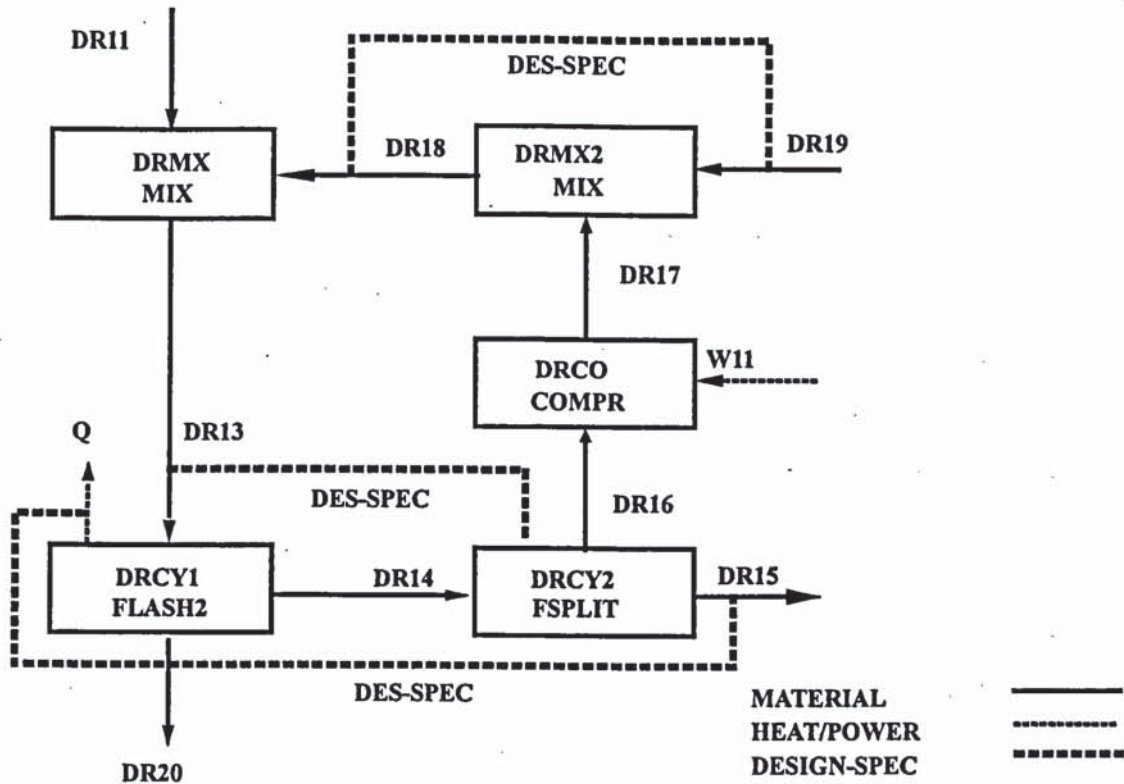


Figure 5-7. Aspen block diagram for the flue gas dryer. Aspen blocks listed in Table 3-1.

5.6.2 Steam dryer

An AspenPlus block flow diagram of the dryer is shown in Figure 5-8 (the flowsheet is shown in Figure 5-4). The dryer uses a fluidized-bed vessel, where sand is employed as a medium to enhance heat transfer.

Examples of major user inputs and model results are shown in Table 5-4.

The user specifies the original and final wood moisture contents and wood mass flow, which determine water evaporation rate, or dryer capacity. The investment cost is determined by dryer evaporation rate.

Steam entering the dryer provides the necessary heat to evaporate the fuel moisture. Medium pressure steam is used. The specific energy consumption (section 5.3) and water evaporation rate determine the total sensible energy required to operate the dryer. A specific energy demand of 3.5 MJ per evaporated kg of water is also used for the steam dryer.

The final wood moisture content from the dryer is selected by the conversion process: 15 wt% has been employed for gasification. Steam for drying is led from the steam turbine extract.

Table 5-4. Some steam dryer model inputs and outputs.

INPUT DATA	Wet wood mass flow (kg/s) Feed moisture wt% Outlet wood moisture wt% Steam pressure (bar) and temperature (°C)
OUTPUT DATA	Dry wood mass flow (kg/s) Evaporated water mass flow (kg/s) Required steam mass flow (kg/s) Recycle blower power demand (MWe) By-product steam or hot water mass flow (kg/s)

In addition to performance analysis, the steam dryer model is also used to size the dryer components. Optimising the dryer would also be possible with the model, although it is not applied in the present work. The AspenPlus block flow diagram of the model is shown in Figure 5-8. Model design and verification is presented in Appendix 1.

The following dryer components are sized and costed on the basis of the model performance results: recycling vapour blower, recycling vapour superheater, dryer reactor vessel, and cyclone. Once the dryer evaporation rate and final wood moisture content are fixed by the user, the model calculates the following (amongst other) data:

- Recycle mass flow, temperature, and pressure
- Exhaust mass flow, temperature, and pressure
- Recycle vapour blower power requirement
- Primary evaporator area requirement
- Recycle vapour superheater area requirement
- Dryer vessel size

The condensate from the dryer may include volatiles from the biomass. However, due to the relatively low drying temperature (below 200 °C) in the steam dryer it is assumed that the waste water is only neutralised, and it is fed to the normal waste water treatment plant of the power plant or to a municipal waste water treatment facility.

The dryer includes a vapour recycle, and for calculating the mass and energy balances, the heat exchanger in the fluidized-bed dryer vessel has to be dimensioned. According to Isoniemi et al. /87/, three conditions have to be met in sizing the fluidized-bed dryer:

- The gas velocity has to be high enough to maintain a steady fluidized bed.
- The residence time of particles to be dried has to be long enough to make it possible to reach the required final moisture content. The rate of drying is highly variable and too uncertain to model with confidence.
- The amount of heat required for drying has to be supplied with a heat exchanger in the fluidised bed.

Isoniemi /87/ points out that the first and the third terms are usually the critical ones. Simple correlations for both the minimum fluidisation velocity and the overall heat transfer coefficient as a function of pressure are derived. The derivation of the correlations employed for the model is presented in Appendix 1. The model validation is also shown.

The block diagram of the Aspen model is presented in Figure 5-8. Feedstock mass flow (DR11) and moisture content are required as inputs to the model. Once the input final moisture content is defined, the model calculates the area of the heat exchanger in the fluidized bed, steam consumption, steam or hot water heat production, and power requirement for the recycle blower. The Aspen model includes four MHEATX heat exchanger modules, one MIX mixer, one FLASH2 phase separator, and one FSPLIT flow splitter. The dryer model includes three design specifications with the following functions:

- Maintain the gas flow in the fluidised-bed vessel at three times the minimum fluidisation velocity by varying the recycle mass flow
- Maintain the recycle gas flow (DR18) at 200 °C by varying the steam consumption in the recycle heat exchanger (to control loss of organics and thus emissions in the dryer)
- Provide enough steam for the heat exchanger in the fluidised-bed vessel by maintaining the module DRHX1 adiabatic.

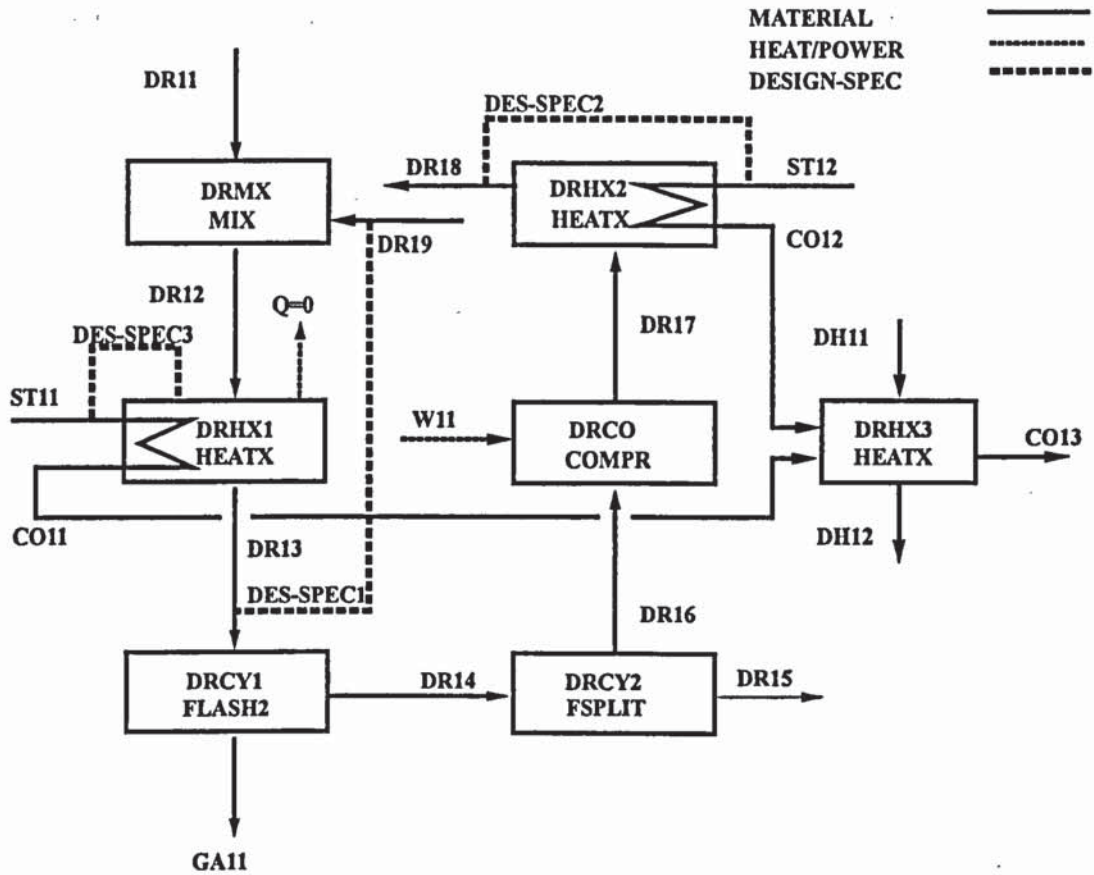


Figure 5-8. Aspen block diagram for the steam dryer. Aspen blocks listed in Table 3-1.

Because of the indirect heat transfer and the internal recycle, a fixed geometry was assumed for the dryer heater tubes in order to properly size the dryer. Once the dryer vessel pressure and temperature are known, the heat transfer coefficient is calculated. From this, Aspen calculates the respective heat transfer area for the fluidized-bed heat exchanger. With a fixed height for the exchanger, a cross-sectional area may be calculated for the fluidized-bed vessel. The volumetric gas flow through the dryer, used in design-spec 1, is derived from the area and the fluidization velocity. The calculation requires the fluidized-bed heat exchanger to be of a fixed geometry. It is assumed that the diameter of the exchanger tube is 42.4 mm, and the tubes are installed as squares 75 mm apart. The height of the bundle may be varied, and is typically 3 m. The steam dryer was evaluated at only one capacity, and one geometry was used.

6. FLUIDIZED-BED GASIFICATION OF BIOMASS

6.1 Introduction

In this chapter, the modelling of biomass gasification is reviewed. The model built with AspenPlus and its validation are presented. The model calculates the mass and energy balances for a fluidised-bed gasifier, once the input feed and operation conditions have been established.

6.2 State-of-the-art

It is generally accepted /88/ that fluidised-bed reactors are the most suitable ones for wood biomass gasification, when relatively clean fuel gas is needed, approximately >5 - 10 MWth. Fixed-bed updraft gasifiers, although simple and thus suitable for a small scale, yield a high tar content gas. Gas cleaning units needed for these concepts are considered expensive, and they are subject to large technical uncertainties. On the other hand, fixed-bed co-current gasifiers, yielding a reasonably clean gas, cannot be scaled up enough for the systems studied in this work. Pretreatment requirements, especially milling, are considered too expensive for entrained-bed gasifiers to be feasible for biomass.

Two general types of fluidised-bed reactors are often distinguished: a bubbling fluidised-bed (BFB) and a circulating fluidised-bed (CFB). They are employed commercially for biomass, both in combustion or gasification. It is reported /89/ that CFB should be the preferable choice for wood gasification, as otherwise carbon conversion remains too low (below 90%) because of the carry-over of fines. The same situation has been observed in an industrial-scale fluidised-bed peat gasifier, which suffered from fines carry-over /90/. Steam or pyrolytic or twin fluid bed gasifiers are not considered because of their low carbon conversion to fuel gas, complexity and hence high cost, poor quality of gas and low perceived advantage.

Although considerable R&D efforts have been devoted to biomass gasification, relatively few units are in actual industrial operation. The state-of-the-art has recently been summa

rised by Babu and Kaltschmitt /88/. Most of the biomass gasifiers in operation are of very small scale. Industrial scale units are employed in district and process heat production (about 10 atmospheric pressure fixed-bed reactors of around 5 to 10 MWth in Scandinavia /91/), at pulp and paper plants in the production of fuel gas for lime kilns (four atmospheric pressure fluidised-bed reactors of 15 to 25 MWth in Scandinavia and Austria /92/, and in IGCC co-generation (a pressurised CFB at the Värnamo IGCC in Sweden of about 25 MWth). A new application, which has received considerable interest, is biomass gasification integrated into a pulverised combustion (PC) boiler (which typically uses coal as the main fuel). The first atmospheric-pressure CFB has recently been brought into operation in Finland /61/. The main advantage of this approach is reduced investment, as no dryer is needed and a large existing steam cycle may be employed.

6.3 Review of modelling of gasification

The objective is to review those publications which are relevant for modelling of gasification with Aspen. A large number of models describing the gasification of biomass have been developed over the past 20 - 30 years. However, most of them are not suitable for integration into Aspen. The tool for predicting biomass gasifier performance has to be relatively simple, and should not rely on too many parameters to be fitted for versatile utilisation.

6.3.1 Biomass gasification

The chemical and physical aspects of modelling fluidised-bed gasification for coal are well covered in the literature (references 1-8 in Ma et al. /93/). However, as Bolthrunis /94/ points out, the lack of published data on any commercial fluidised-bed operations has prevented them from being validated for industrial applications.

This is even truer for biomass gasification, as only a few industrial biomass fluidised-bed gasifiers have ever been built. Thus, modelling the fluidised-bed gasification of biomass is an extremely complex task /95/, and model validation is difficult to carry out. Occurring within the reactor are pyrolysis, combustion and gasification reactions, both homogeneous gas-phase and heterogeneous gas-solid reactions, heating and mixing of incoming solids, mass transfer between the phases, and elutriation of solids etc. Pyrolysis alone is a very

complex series of ill-defined chemical reactions and not well-known physical interactions. This makes modelling all the more demanding, as it is known how important pyrolysis is for biomass gasification /96/, /95/.

The following processes occur simultaneously in a fluidised-bed wood gasifier:

- Fast pyrolysis of wood
- Partial oxidation of wood and pyrolysis products
- Gasification of pyrolysis char by means of reaction with CO_2 and H_2O
- Conversion of pyrolysis tar
- The possibility of a chemically enhanced mass transfer of reacting gases from the bubble phase to the dense phase

Buekens and Schoeters /96/ classify fluidised-bed gasification models in rising order of sophistication:

1. Thermodynamic models
2. Single phase models
3. Two or three phase models
4. Transient models

They review a number of models in /96/. An advantage of thermodynamic equilibrium models is that they are easy to construct and use. However, their usefulness is limited if the gas composition is not corrected for pyrolysis. The real gas composition deviates from the ideal one. Especially methane and higher hydrocarbon yields are much greater than those predicted by equilibrium models. This emphasises the need to take pyrolysis into account in biomass gasification modelling. Thermodynamic models do not consider the hydrodynamics of the reactor.

Single-phase models are based on either a well-mixed (CSTR) or a plug flow (PF) reactor. Two- or three-phase models feature a distinct type of gas flow in the dense and the lean phase, together with some interface mass transfer. There are fewer transient models than steady-state models. They are often fairly complicated, and their verification is even more demanding than that of steady-state models. They are, for example, used in studying the

load-varying, start-up, and shutdown characteristics of systems. A satisfactory general basis for the hydrodynamic scale-up of fluidised-bed reactors is not available at present /94/. However, the lack of a satisfactory hydrodynamic bed model has not prevented the successful scale-up of reactors, but scaling techniques are often empirical and tend to be process specific.

Although a number of gasification models for biomass have been published /95/, /97/, /98/, /99/, /100/, none of them can be applied when a simplified gasifier model has to be built for Aspen. It is necessary to study the Aspen models previously designed for coal gasification to see if they may be modified for biomass applications.

6.3.2 Coal gasification models with Aspen (MIT, METC)

Most of the Aspen modelling work published on coal gasification is for fixed-bed reactors. As these Aspen models are also relevant for gasification modelling generally, they are briefly summarised below.

Aspen was initially built to simulate the synfuels industry in the late 1970s. Great Plains Gasification Plant is one of the few synfuel plants still producing synthetic natural gas (SNG) and chemicals /101/. The huge plant, like most industrial gasification systems, employs Lurgi fixed-bed units. These models are of interest, as the operating plants provide an opportunity to validate the models developed.

6.3.2.1 MIT

Probably the first article on the use of Aspen in the simulation of coal gasification was published by Espenal et al. /102/ in 1980. At that time C.F. Braun Company was developing the BIGAS gasification process, which was modelled at MIT. The BIGAS gasification process is shown in Figure 6-1. It is an entrained flow slagging gasifier, where process energy is generated by combusting recycle char below the gasification section of the reactor.

The Aspen model of the system is shown in Figure 6-2. The main features of the model are summarised below. The model includes three reactor modules: RYIELD, RPLUG and RCSTR. Entrained-flow gasification has previously been successfully modelled with a well-stirred reactor model (RCSTR) for combustion, and a plug flow reactor model (RPLUG) for the gasification zone. Espenal et al. /102/ therefore selected a similar approach. Gasification kinetics is provided for both models. Because of the complexity of devolatilisation (pyrolysis) kinetics, the mass-yield-based reactor model RYIELD is employed in the modelling of the devolatilisation zone. Splitter and mixer modules are also used in the model.

The agreement between the reported model results and experimental data is good, especially when considering the general form of the rate expressions in the RPLUG and RCSTR modules. The parameters supplied by the user were chosen fairly arbitrarily. In the model, devolatilisation is assumed to be adiabatic, which may or may not be true in gasification. However, it does not seem to be of great importance in this model.

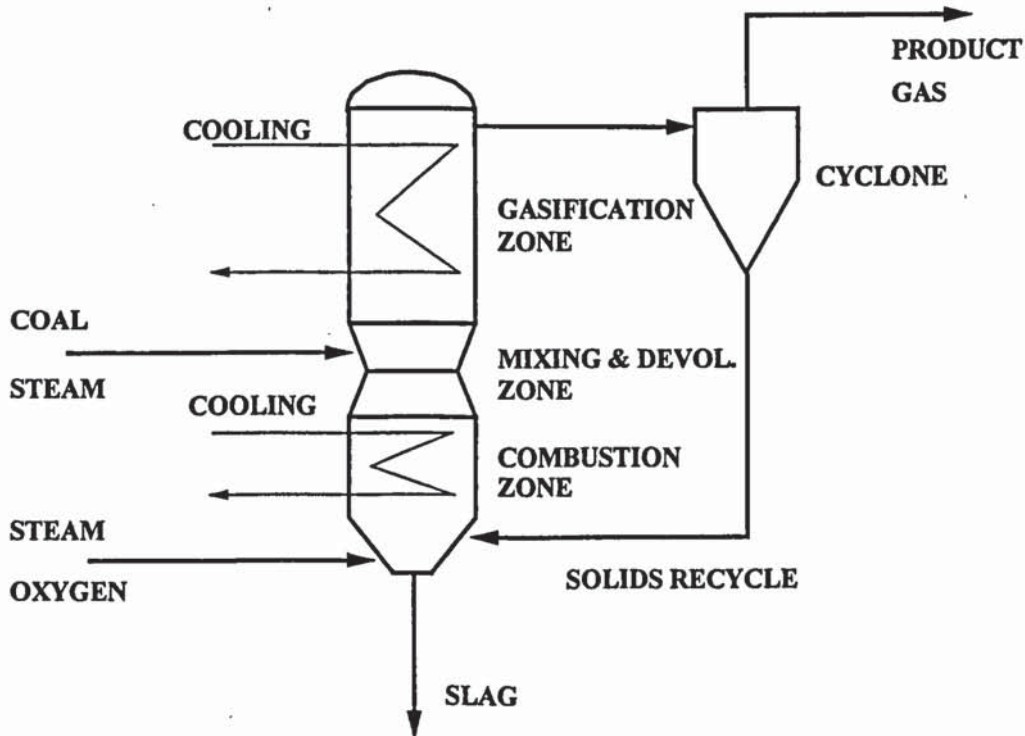


Figure 6-1. The BIGAS gasification process.

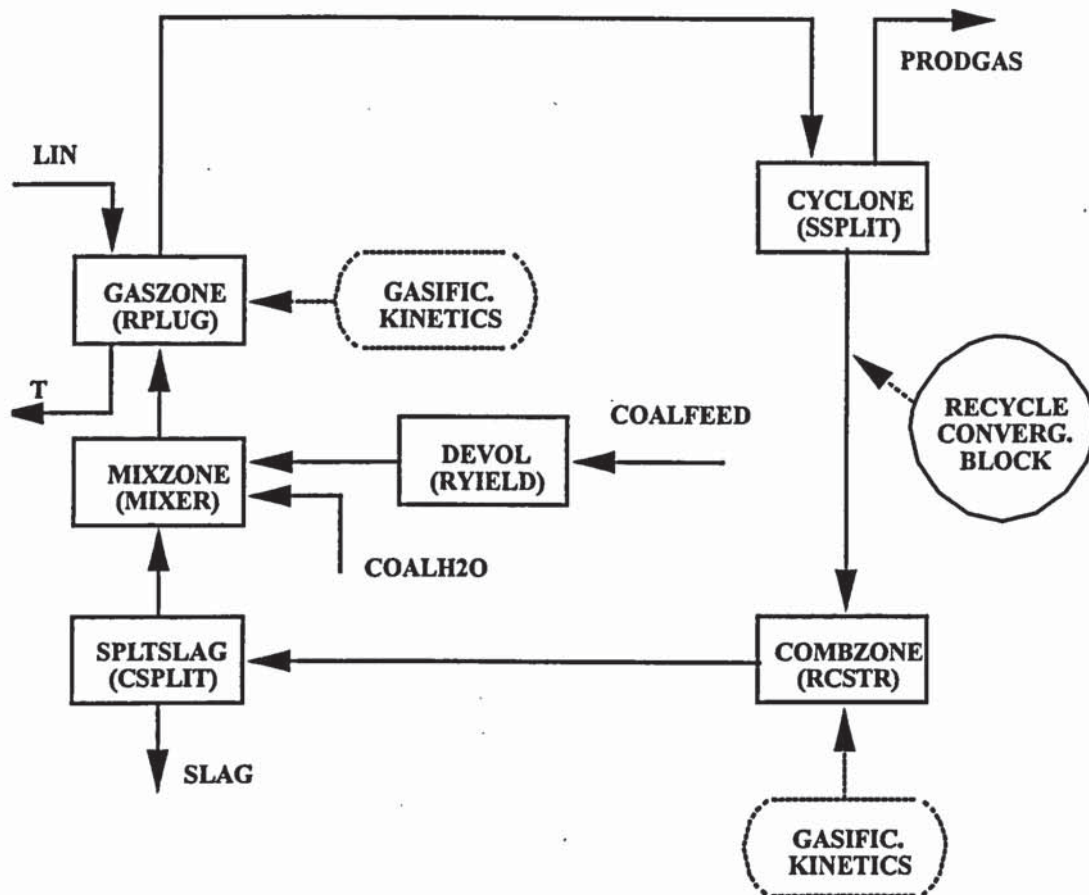


Figure 6-2. Aspen block diagram for the BIGAS reactor.

6.3.2.2 Work supporting the GPGP

As part of the task of developing an Aspen simulation model for the Great Plains Gasification Plant, Ringard and Benjamin /103/ have compared published coal gasification models for fixed-bed reactors. Six major modelling efforts were reviewed and analysed: the University of Delaware (UD) model by Denn and Wei and their students, e.g. /104/, /105/; the West Virginia University (WVU) model by Wen and his students /106/, /107/; the IBM model by Stillman /108/; the General Electric (GE) models by Daniel and Kosky /109/, /110/; the Washington University (WU) model by Joseph and his students /111/; and the University of Minnesota (UM) model by Amundson and his students /112/. Ringard and Benjamin /103/ summarise that the UM and IBM models involve the solution of complicated boundary value problems and do not appear to be robust or efficient enough to be installed in Aspen. Several models predict separate temperature profiles for the gas and the solids (IBM, UM, WU). This appears to be of limited value since there is no data to verify

such models. Including these features in the model does not appear justified, since it only adds to the complexity of the model without improving its usefulness. Appropriate documentation is only available for the UD and WVU models. Ringard and Benjamin /103/ conclude that the UD model is better suited for use as a basis for a moving-bed gasifier model in Aspen. They also describe specifications of a model for Aspen /103/. This model is referred to as RGAS in the next paragraph.

6.3.2.3 METC

Coal IGCC processes have been modelled with Aspen at METC. As part of this effort, four separate Aspen models for the fixed-bed gasification of coal have been reviewed by Stefano /113/: RGAS, a model developed by Halcon/Scientific Design Company /114/; USRWEN, Aspen model of the WEN II model originally developed by C. Wen at the West Virginia University /115/; the model developed by MIT /116/ to support the proposed design study by CONOCO; and the Oak Ridge National Laboratory (ORNL) model /117/. Essentially, the two first models are independent Fortran programs, which are employed in Aspen as user models. The models are kinetic, and thus coal-specific kinetic data is needed. Two latter models are non-kinetic. Although some of the models predicted reasonable gas compositions, none of them proved satisfactory. The major problems with the existing Aspen models were inaccurate material and energy balances, limitations of coal type, or long run times.

Significant modifications were therefore made in the MIT model, and a new model called SLAGGER was developed at METC. The Aspen block diagram of the model is depicted in Figure 6-3.

The basic logic of the SLAGGER model is similar to that of the MIT model, but is somewhat simpler and more flexible, making it suitable for use with an existing IGCC model. Experimental pyrolysis data is still needed to characterise the volatilisation of coal. Thus, the model is highly coal-specific. It should also be borne in mind that the model is designed for a fixed-bed gasifier, and hence cannot be directly employed in the modelling of other types of gasifiers.

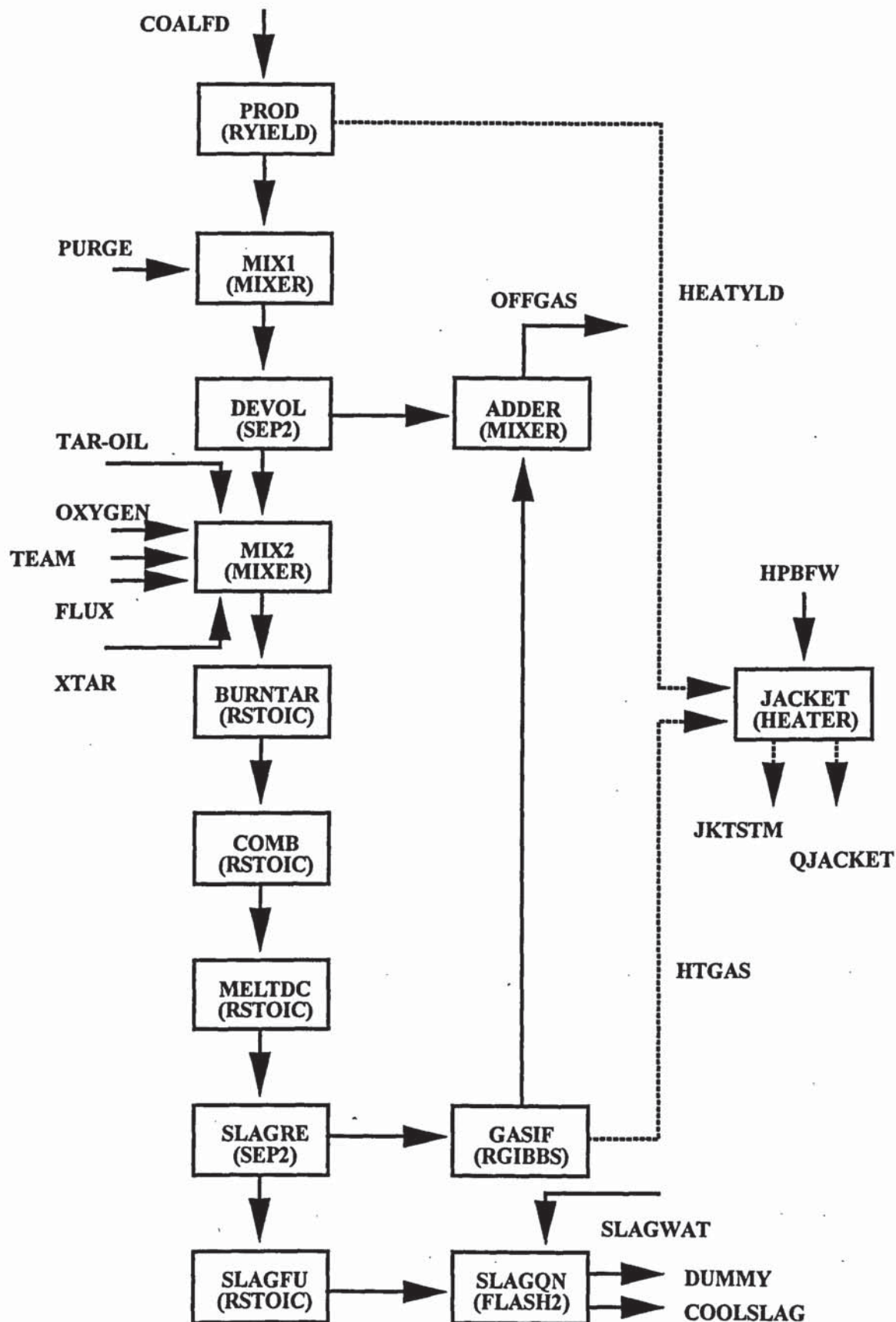


Figure 6-3. Aspen block diagram for the SLAGGER model (gasification section).

Stone /118/ has employed a semi-predictive model of gasification for analysing two integrated gasification combined-cycle power plant models. A similar model was employed both for a fluidised-bed gasifier and for an entrained-flow gasifier. The heart of this model is the Aspen module RGIBBS, which is used to minimise Gibbs free energy for a gas mixture. Departures from equilibrium temperature are determined for nine gasification reactions, and the composition of the product gas is calculated on the basis of the assumed departures. The departure temperatures are varied until the desired gas composition is reached.

The SLAGGER model has been employed by Stone /119/ in another analysis for an IGCC. Some modifications for the gasification model are reported. The most important modification is a new devolatilisation model in which errors found in the earlier model have been corrected. The gasification model includes a feature similar to the model described in a previous report by Stone /118/: departures from equilibrium temperature for the reactions are employed in the RGIBBS module.

6.3.3 Testing of the departure-from-equilibrium model

Stone /118/ reports an approach suitable for the analysis of gasification within Aspen. The model was also considered potentially suitable for biomass, and it is tested here for the gasification of biomass in a fluidised-bed reactor. The approach calls for determination of equilibrium reactions for the gas mixture. Departures from equilibrium are affected by departure from equilibrium temperatures, which may be defined for each reaction separately. The reactions employed here are listed below.





A simple model was designed on the basis of the Stone report (Figure 6-4), and the characteristics of the model were studied. The testing of the model is presented in Appendix 4.

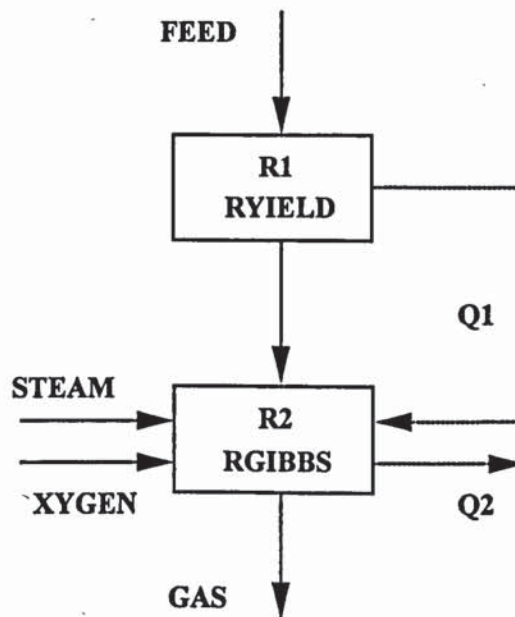


Figure 6-4. Aspen block diagram for a simple gasification model.

It is concluded (see Appendix 4) that the use of the equilibrium model is not practical, as many departures from equilibrium temperatures have to be selected by trial and error. Although the model predictions are within $\pm 5\%$ for the quantity of the main gas components, the inability to take pyrolysis into account is a major drawback. The pyrolysis products include 5 to 30% of the chemical energy of the product gas, so pyrolysis is an important feature in biomass gasification. As the experimental data available was insufficient to verify the sensitivity cases studied (such as effect of pressure, moisture content of feed), the appropriateness of the model remains questionable.

It was therefore considered necessary to construct a model that satisfies some basic criteria, for example:

- Minimum user input and ease of use when integrated into Aspen
- Accuracy in the quantity of the main gas components
- Versatility towards different fuel compositions
- Ease of modification of the model

6.4 Description of the model developed in this work

6.4.1 Approach

A detailed model including the phenomena affecting gasification is beyond the scope of this work. A semi-empirical model is developed. The operation and control of the model are presented in this section. The model calculates the performance (mass and energy balances) of a gasifier, once the input data has been fixed. The AspenPlus input file is shown in Appendix 5.

6.4.2 Description of the semi-empirical model designed

A relatively simple yet versatile model was designed. The model has two main sections: pyrolysis and equilibrium. The pyrolysis of biomass is first modelled, producing hydrocarbons and ammonia. The amount of these compounds is estimated with empirical functions, where the amount of hydrocarbons is a function of reaction temperature. After pyrolysis, the pyrolysis products (hydrocarbons) are led directly to the product stream, and the remaining components are led to an equilibrium reactor. The principal user input and outputs are presented in Table 6-1.

Table 6-1. Some gasifier model inputs and outputs.

INPUT	Wood ¹⁾ kg/s Air kg/s Carbon conversion % Heat loss % Departure from equilibrium temperature ²⁾ K
OUTPUT	Gas components kg/s Gas temperature °C Non-reacted solids kg/s

1) In an integrated model, determined in the previous model section

2) For the shift reaction $\text{CO} + \text{H}_2\text{O} \leftrightarrow \text{CO}_2 + \text{H}_2$

The block flow diagram of the Aspen gasification model designed in this work is shown in Figure 6-5. In this work it is used to describe a fluidised-bed reactor. However, with proper alternative input data, fixed-bed gasification and other systems may also be modelled. The model is semi-empirical, i.e. some of its features (for example, the departure from equilibrium temperature) require input data, supplied by the user, for the model to yield reasonable results.

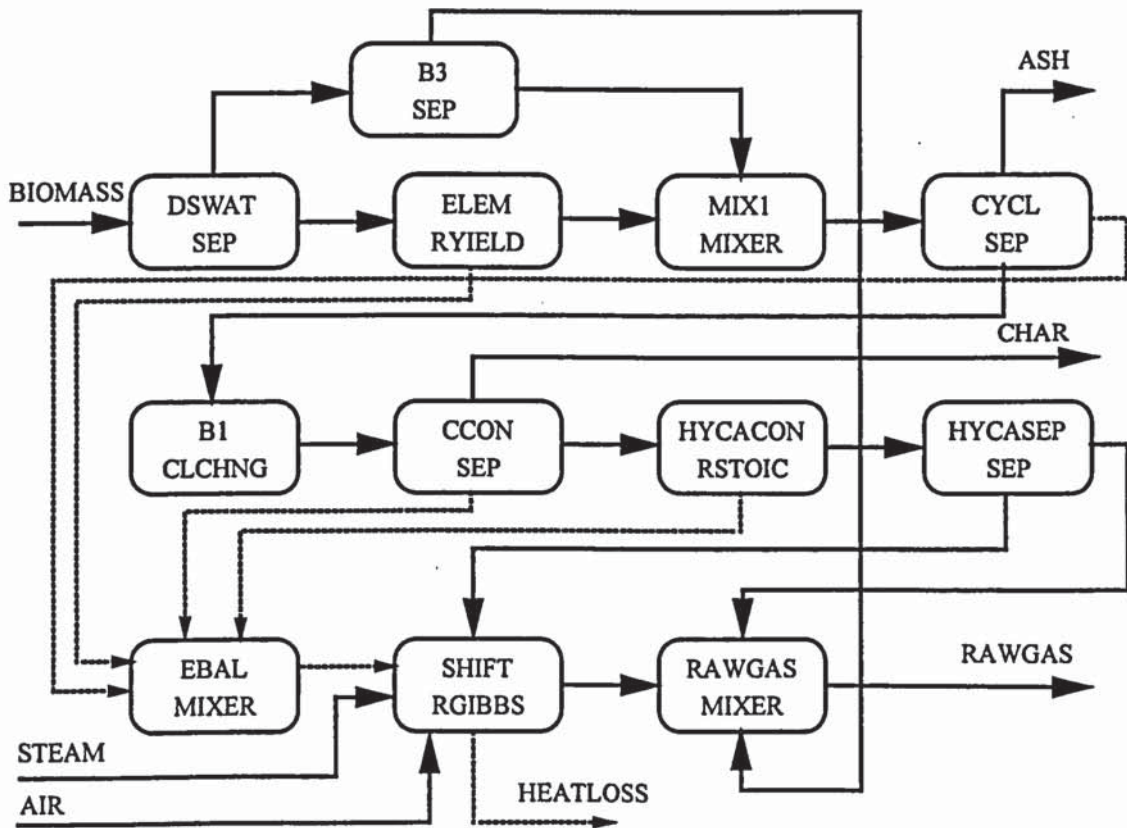


Figure 6-5. Aspen block diagram for the model developed in this work.

In the SEP block, an abundance of water is first sent directly to the product gas. It has been observed /120/ that above a certain threshold value, excess water does not participate in gasification reactions. In the next stage, the input wood is split into its elements in the RYILED block. Carbon conversion is an input to the SEP block. Ultimately, carbon conversion (to product gas) is a result of the interaction between fuel type, reaction temperature and pressure, fuel moisture content, reactor type, etc. In this model, carbon conversion is selected on the basis of fuel type. 99.5 wt% is used for the fluidised-bed gasification of wood biomass. Less reactive fuels (peat, lignite and coal) would have a lower conversion. Ash and non-reacted carbon are separated from the gas stream, and conveyed to ash handling.

The RSTOIC reactor is employed to describe the generation of pyrolysis products and ammonia (NH₃). Methane (CH₄), light hydrocarbons (C₂H₄, C₆H₆), and an oxygenate (C₆H₆O) are formed, together with ammonia. The reactions are shown below. These products are conveyed directly (past the equilibrium reactor) to the product gas stream. Pyrolysis reactions producing hydrocarbons (and tar) are a function of gasification temperature. Specific correlations are needed for different fuels. An iteration loop is generated, as gasification air is controlling the product gas temperature.



6.4.3 Testing and verification of the model

An example of the use of the model is shown in Figure 6-6. The amount of gasification air is varied, and the variation of gas composition is shown as a function of temperature. In Figure 6-7, the reaction temperature is shown as a function of air ratio.

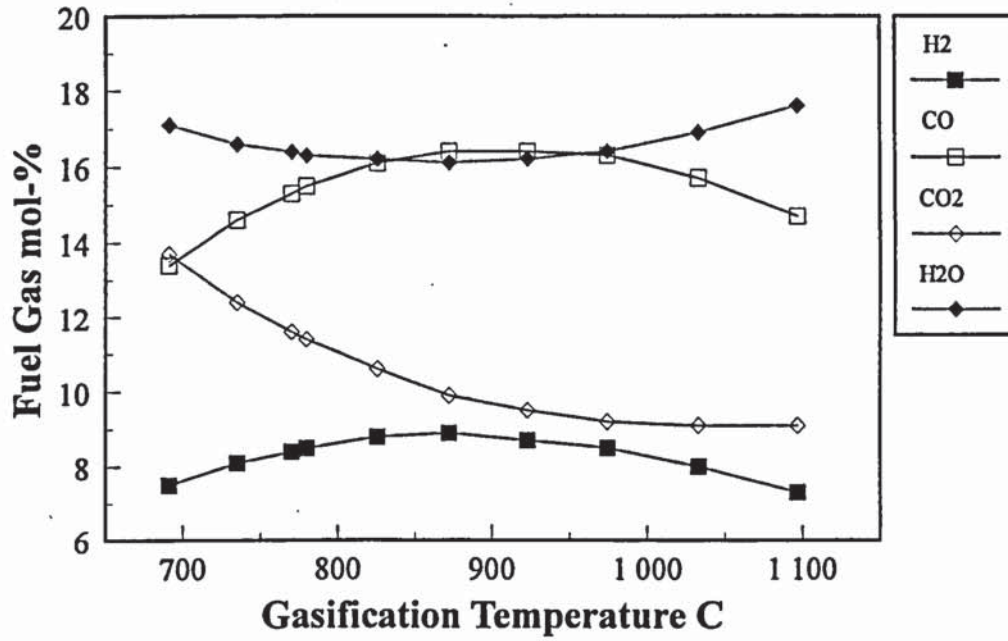


Figure 6-6. Use of the Aspen model for gasification.

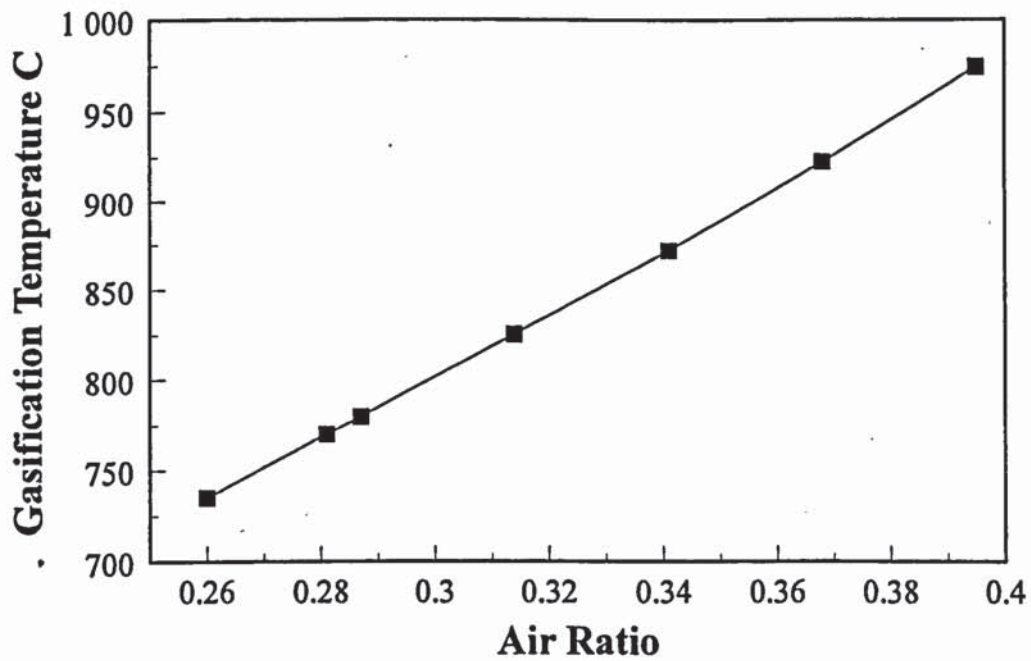


Figure 6-7. Gasification temperature as a function of air ratio.

Model results cannot be easily verified. Detailed industrial reference data on pressurised operation, which would be preferred, was not available. The verification is carried out by comparing published fluidized-bed process development scale (PDU) data using wood as feed for the gasification [121]. The comparison is shown in Table 6-2, where two set points for sawdust gasification are represented.

It may be seen that the fit is not as good as with the departure-from-equilibrium model (section 6.3.3 and Appendix 4). However, the current model is more practical to use, as only one departure from equilibrium temperature has to be specified. In addition, because of the functions employed for hydrocarbons, the tar content of the fuel gas is more in line with actual practice. It is concluded that the model is appropriate for describing pressurised wood gasification.

Table 6-2. Model results compared with experimental data.

	Experimental 1	Model 1	Error %	Experimental 2	Model 2	Error %
Input data						
Bed temperature C	775			814		
Fuel feed-rate kg/h	42.8			40		
Fuel moisture wt%	11.3			5.9		
Air feed kg/h	65.3			77.1		
Steam feed kg/h	2.9			12.8		
Nitrogen kg/h	2.5			4.4		
Results						
Gas flow Nm ³ /h	99.7	97.5	-2.2	117.6	117.0	-0.5
Composition mol%						
CO	14.3	15.2	6.5	10.8	10.9	0.9
CO ₂	11.5	11.6	1.3	12.0	12.5	4.2
H ₂	8.4	8.4	-0.5	9.0	8.3	-7.6
N ₂	42.3	43.1	2.0	43.5	43.4	-0.2
CH ₄	4.6	4.4	-3.3	2.8	3.4	22.6
Hydrocarbons	0.7	0.8	8.7	0.2	0.5	148.1
NH ₃	0.07	0.06	-11.1	0.020	0.051	157.2
H ₂ O	18.1	16.4	-9.3	21.7	20.9	-3.5

7. FAST PYROLYSIS OF BIOMASS

7.1 Introduction

In this chapter, the flash or fast pyrolysis of biomass is reviewed. The state-of-the-art of the technology is concisely summarized, and previous work is reviewed. The approach employed in this work is presented together with a brief description of pyrolysis liquids. Verification of the model developed is especially difficult, because only two plants of a reasonable scale (references given later in the chapter) have been built so far. However, no detailed operational data on these plants is available in the public domain.

7.2 State-of-the-art

It has been shown by Scott and Piskorz /63/ and later confirmed by others that the highest liquid yields from woody biomass can be produced with fast pyrolysis. An organic liquid yield of 60 - 75 wt% of dry wood was obtained /122/. It has later been shown /123/ that the critical process features in maximising the liquid yield are a rapid heat-up period and a short vapour-phase residence time. However, the scale-up of such a system poses challenges.

Pyrolysis liquids are a complex mixture of organic compounds. They contain hundreds of individual substances belonging to several chemical classes. Typically 30 - 40 wt% of the compounds have been identified with quantitative GC /124/.

Initially, the most important process development work in biomass fast pyrolysis was carried out in Canada. Two groups in particular, one at the University of Waterloo (Scott) and the other firstly at the University of Western Ontario and then later at Ensyn Technologies Inc. (Graham), developed systems which may be applied in liquid fuel production /125/, /126/. A bubbling fluidised bed is employed in the Waterloo Fast Pyrolysis Process (WFPP), whereas an entrained pyrolysis reactor is used in the Ensyn Rapid Thermal Process (RTP). In the USA a vortex reactor system was developed initially at the Solar Energy

Research Institute (today the National Renewable Energy Laboratory) for fast pyrolysis biomass /64/.

Ensyn has built the largest units presently in operation: two RTP reactors in the production of a food chemical with a feed capacity of 1 t/h /127/. However, in these plants the pyrolyser is not integrated into a char combustor, as envisioned in biofuel liquid production. There are no commercial biofuel liquid production plants on the energy market today. ENEL has operated an RTP pilot (500 kg/h) in Italy in 1996 - 1999 /128/. The Union Fenosa Waterloo Fast Pyrolysis Process (WFPP) plant (150 kg/h) /129/ was used in 1992 - 1998. Several PDU and laboratory-scale units are being operated both in Europe /130/, /131/, /132/, /133/, /134/, /135/ and in North America /136/, /137/, /138/. As an example, a flowsheet of the ENEL RTP system is shown in Figure 2-43.

The adverse properties of a fast pyrolysis liquid as fuel are well known /139/, /140/, /141/, /142/, /143/. The properties of a fast pyrolysis liquid as a fuel liquid were initially reviewed by Elliott /139/ in 1986, and several liquids were characterised in comparison with ASTM mineral oil specifications. Fuel specifications for pyrolysis liquids have more recently been discussed by Diebold et al /144/.

The use of pyrolysis liquid in medium-size boilers designed for light mineral fuel oil appears to be promising in locations where heating oil is expensive. However, this application is probably technically less demanding than the power production concepts suggested /145/. Technically easier but economically less attractive is the use of a pyrolysis liquid in a heavy oil boiler. Two large-scale combustion tests (40 and 20 tonnes) with a pyrolysis liquid have so far been carried out in 9 and 5 MW_{th} boilers /146/.

Various companies are developing modified diesel and gas turbine engines. The engine sets even more severe requirements /147/ for the fuel than the boiler applications, as the injection pressure is high. Two engine developers have studied the injection of pyrolysis liquids in diesel engines /148/, /149/. In addition to these, there has been some laboratory-scale work with engines /150/, /151/, /152/. A gas turbine has also been developed for pyrolysis liquid use /153/.

7.3 Review of modelling the fast pyrolysis of biomass

No models for complete fast pyrolysis plants are available. Some performance and cost analyses have been carried out, and they will be reviewed. In fast pyrolysis, numerous interrelated, simultaneous and consecutive physical and chemical phenomena take place. A detailed model taking these into account is beyond the scope of this work. The aim here is to be able to estimate the overall performance balance.

7.3.1 IEA Bioenergy - BLTF, DBL, and ALPS

The earliest assessment and performance models in the public domain on the fast pyrolysis of biomass to liquid fuel were published by an IEA Bioenergy Agreement activity /67/, /154/ in 1985. A fast pyrolysis process concept was designed by the IEA working group, and its cost and performance were assessed. The concept performance balance was largely based on the work by Scott and co-workers (for references see above) in their 3 kg/h reactor system. The concept included a flue gas dryer, bubbling fluidised-bed reactors for pyrolysis, an absorber/wash tower for vapour condensation, and a char gasifier for energy production. The reaction heat required was provided by recovering energy from char and non-condensable gases, and by introducing part of the non-condensable gases to the reactor as fluidising medium at a high temperature.

At the next stage of the IEA work /155/, two fast pyrolysis process concepts were assessed in 1990. The first concept was the same as in the previous work. The second concept was novel, because it included a circulating fluidised-bed for pyrolysis. Woody biomass was introduced and pyrolysed in the riser section of the reactor, where hot sand was flowing essentially in plug flow. Char was combusted in the lower part of the reactor (bubbling fluidised-bed) heating the recycle sand. Again, an absorber/wash tower for vapour condensation was employed. Whereas several reactors were estimated necessary in the "present" case (up to 20, as the feed capacity of the plant was 2 000 tpd wet wood), only one was needed for the "potential" case, because of the anticipated higher throughput of the reactor.

The performance balance was initially /67/ calculated (1983 - 1986) by generalised correlations and simple models. In the next stage of the IEA work /155/, spreadsheet models were employed to calculate the performance of processes of similar design as in the previous project, and essentially with similar correlations to calculate mass and energy balances. The IEA group also estimated the NREL pyrolysis concept, which employed a Vortex reactor /156/. Spreadsheet models were again employed to calculate the performance of the systems. The level of accuracy of the performance balances may be considered adequate considering the small scale of the experiments from which the model input data was derived.

An overall efficiency of 56% based on the lhv of wood was determined for pyrolysis liquid production in the initial work /67/. A more detailed basis are given in the performance analysis report /154/. In the next stage of the IEA Bioenergy work /155/, two fast pyrolysis systems were analysed. Energy efficiencies of 57% and 65% were determined for the concepts (the overall efficiency for the potential case should be 64% after an error in the original performance balance is corrected).

Within the first project /67/, the production cost for the liquid was estimated. Its relative value was assessed compared to a conventional fuel oil, which it was considered to replace. The pyrolysis liquid was estimated to cost 1.5 to 1.8 times more than the market price of number 4 fuel oil (light fuel oil, FO # 4) (9.1 - 10.5 USD/GJ), depending on the technical assumptions employed in the process evaluation. At the time of the estimate (1983), the value of FO # 4 was 6.0 USD/GJ. The feedstock cost used was 30 USD/wet ton (same as 60 USD/dry ton, which is equal to 3.5 USD/GJ). The capacity of the system was high, 2 000 tpd wet fuel.

Within the second IEA project /155/, production costs for pyrolysis liquids were again estimated. The pyrolysis liquid was estimated to cost 1.4 to 1.3 times more (present/potential) than the market price of number 4 fuel oil at the time of the estimate (1987). The value of FO # 4 was 6.7 USD/GJ. As previously, the feedstock cost employed was 30 USD/wet ton.

The third IEA study on pyrolysis /156/ concerned transportation fuel production with the Vortex concept, and it is not considered relevant for this work.

The three early IEA projects form the most comprehensive collection of consistent assessments and performance models on fast pyrolysis production technology in the public domain today.

7.3.2 WFPP - Black

In the early days of fast pyrolysis technology development, Black carried out a preliminary evaluation of the WFPP in 1986 /157/. He designed several alternative concepts, and analysed the most promising systems. An efficiency of about 78% based on lower heating values may be calculated from the mass and energy balance reported. Black also assessed the liquid production cost in two size classes. At 200 and 1 000 tpd (50% wet feed) the costs are 143 CAD/t and 92 CAD/t, respectively. These correspond to about 9.4 CAD/GJ and 6.0 CAD/GJ (about 7.5 and 5 USD/GJ). The fuel for the small plant was priced at 10 CAD/wet t, and 20 CAD/t for the larger plant size.

The efficiency appears rather high. However, this report is important because it directly compares different plant configuration concepts with each other.

7.3.3 Science International - Wan

In addition to Canada, the DOE in the United States has also supported pyrolysis development. An entrained-flow pyrolysis process developed at Georgia Tech was assessed in 1985 /158/. The products include, in addition to pyrolysis liquid, char as by-product. The residence time in the reactor was longer than in the fast pyrolysis processes, and the reported liquid mass yields were lower, about 49% based on dry feed (typical mass yields reported for other systems: Ensyn RTP, Union Fenosa - WFPP, and NREL ablative system are between 60 to 70% based on dry feed). The overall thermal efficiency of liquid production in the Georgia Tech process was reported to be 52% based on hhv. However, there is not enough data in the report to check the mass and energy balance. Liquid production

costs were determined for two capacities: 200 TPD and 1 000 TPD. With wood at 25 USD/dry ton, the liquid costs were 6.0 and 4.3 USD/GJ, respectively. Wan concludes that the production costs appear competitive with fuel oil selling prices /158/. The estimate appears rather optimistic compared with other studies, although the biomass cost is also relatively low, reducing product costs.

7.3.4 Ensyn Technologies Inc - Zeton Inc

Beckman and Graham have reported an economic analysis for Ensyn fast pyrolysis /159/. However, the analysis does not include an overall efficiency for liquid production, as only the energy balance of the reactor and recovery section, starting from dried wood, is given. The production costs are also determined without drying and milling costs, which is not satisfactory. If these costs are assumed to be 25 USD/t, the liquid production cost estimated by Beckman and Graham /159/ is about 5.7 USD/GJ, when wood is estimated at 30 USD/t. The costs reported appear rather low. However, there is some uncertainty about the drying and milling costs used. In any case, the data reported could be used to estimate the liquid production cost if the drying and milling costs were included.

7.3.5 Aston University - IEA Bioenergy

Cottam has reported on the technical and economic simulation of biomass pyrolysis /160/. The mass balance for pyrolysis is derived from the work of Scott and co-workers. However, there are serious flaws in determining the mass and energy balance. The author fails to distinguish between the mass balance reported for a bench-scale unit and the corresponding performance of an industrial unit. In fast pyrolysis, yields from a bench-scale unit can only be employed as a basis for deriving the industrial reactor performance. No performance data is available in the public domain on a vapour recovery section that could be employed to derive a mass and energy balance for an industrial vapour recovery section. It appears that Cottam assumes a 100% recovery of product vapours, which is, of course, impossible for an industrial unit.

Mitchell et al. /35/ report an efficiency of 71% for pyrolysis liquid production based on lhv. However, no bases or references are given. Therefore, this value is impossible to verify.

Recently, Toft /37/ has presented performance estimates for fast pyrolysis. The performance analysis is based on laboratory-scale data, and the industrial-scale performance is based on estimates and the use of engineering judgement. An efficiency of 62% is reported for pyrolysis liquid production. The accuracy of this estimate is uncertain due to the approach employed in deriving the performance.

7.3.6 NREL

Gregoire and Bain /69/ have modelled and assessed pyrolysis liquid production from wood based on the NREL vortex reactor system (see chapter 6). The process was simulated using the ASPEN/SP process simulator. They report that the bio-crude (pyrolysis liquid) contained 79.6% of the energy in the feed wood. Based on the flows reported and estimates for the heating value of wood, liquid production efficiencies of 64% and 78% may be calculated on the basis of lhv and hhv, respectively. The values agree with several other references. However, no details concerning the pyrolysis model are available, and its true applicability is thus unknown.

An extensive economic analysis has been carried out, and further research needs are listed. A product cost of 0.11 USD/kg has been reported (using a wood cost of 44 USD/dry tonne), which is equivalent to about 7.5 USD/GJ.

7.4 Model development in this work

It is seen from the previous review that no adequate process models are available for the fast pyrolysis of biomass. As an example, overall thermal efficiencies of about 55 to 75% are reported for a liquid product, often for basically the same process configuration. The fact that the variation between the reported results is so broad highlights the need for a robust performance model for a pyrolysis plant. It should be possible to determine a reliable energy balance for a plant, and to analyse the system performance within a certain range of

operating conditions. All plant investment costs are based on the results of a performance analysis.

No reliable balances for continuous large-scale pyrolysis liquid production are available in the public domain. Therefore, the model has to be developed largely on the basis of experimental work on a bench and available process development unit scale. The results presented by Scott and co-workers is especially useful /63, 122, 123/. It should also be borne in mind that verification of the industrial process models presented here remains impossible until data on at least a pilot scale is available. However, model results may be compared with the limited PDU data available /146/.

Before the Aspen pyrolysis plant model is presented, it is necessary to briefly summarise the characteristics of fast pyrolysis liquid. This is necessary because the properties of pyrolysis liquid are very different from those of mineral oil.

7.4.1 Biomass fast pyrolysis liquids

Fast pyrolysis liquids vary a great deal depending on numerous factors (feedstock, processing conditions, process type, etc.). Some properties of pyrolysis liquids are presented for reference in Table 7-1. The properties are shown in order to highlight the differences between mineral oils and pyrolysis liquids, which emphasise the importance of selecting model compounds (see next section and Appendix 6).

Table 7-1. Comparison of mineral heating oils and fast pyrolysis liquid /143/.

	PYROLYSIS LIQUIDS				MINERAL OILS	
	VTT/PDU Birch	VTT/PDU Pine	Ensyn Hard- wood	NREL Hot-filtered poplar	POK 14	POR 2000
Solids, wt%	0.06*	0.03*	0.3	0.045	-	-
pH	2.5	2.4	2.8	2.8	-	-
Water, wt%	18.9	17.0	23.3	18.9	0.025	0.3
Viscosity (50 °C), cSt	28	28	50	14	6	1 950
Density (15 °C), kg/dm ³	1.245	1.243	1.230	1.200	890	1.005
LHV, MJ/kg	16.5	17.2	16.6	17.4	40.3	39.5
Ash, wt%	0.004	0.03*	0.09	0.012	0.01	0.4
CCR, wt%	20	16	23	14	0.2	19
C, wt%	44.0	45.7	44.8	46.5	-	85.7
H, wt%	6.9	7.0	7.2	7.2	-	10.0
N, wt%	<0.1	<0.1	0.1	0.15	-	0.6
S, wt%	-	0.020	<0.01	0.02	0.2	2.5
O, wt%	49	47	48	46	0	0.7
Na, ppm	13	6	8	4	-	0.0015
K, ppm	16	16	320	4	-	-
Ca, ppm	50	23	195	1	-	-
Mg, ppm	12	5	30	1	-	-
Flash point, °C	-	-	>106	64	60	90
Pour point, °C	-24	-19	-9	-36	-15	10

*The low solid content is due to the combined effect of liquid-phase filtration and sedimentation

7.4.2 Calculation of physical properties in pyrolysis

The pyrolysis liquid is characterised as a model component mixture in the Aspen process model. The mixture consists of conventional and non-conventional components. The selection of the model compounds is based on the literature /161/, /162/ and experimental results /163/.

The following components are used in the process model:

- Non-condensable gases: nitrogen, oxygen, carbon dioxide, carbon monoxide, hydrogen, methane, ethane, propane, ethylene, propylene
- Organic compounds: formic acid, acetic acid, hydroxyacetaldehyde, acetol, glyoxal, ethyleneglycol, formaldehyde, levoglucosan, furfural, guaiacol, sorbitol, pyrene
- Non-conventional component, which is used to model the heavy fraction of the pyrolysis liquid

- Non-conventional component describing char
- Non-conventional component describing sand and ash
- Non-conventional component describing the wood feedstocks
- Elemental carbon
- Water

The selection of the physical property calculation method for the process is presented in Appendix 6. The model is presented in detail by Solantausta et al. /164/.

7.4.3 Model description

The flow diagram of the process model for the wood pyrolysis is shown in Figure 7-1. The model has three principal sections: pyrolysis reactor, vapour recovery, and energy generation. The principal user inputs and model outputs are shown in Table 7-2. The AspenPlus input file is shown in Appendix 7.

Table 7-2. Some pyrolyser model inputs and outputs.

INPUT	Wood ¹⁾ kg/s Reaction temperature °C Yield distribution ²⁾ wt% Liquid composition mol% Heat loss % Recovery stage temperature °C
OUTPUT	Product liquid kg/s Purge gas mass flow kg/s and composition mol% Fuel wood to the combustor kg/s

¹ In an integrated model, determined in the previous model section

² Temperature-dependent mass yields defined for organic liquid, water, non-condensable gases, and char

In this study, the Ensyn RTP process /165/ was modelled. The RTP process was selected because the author has got more data on this process than on the others. Some information about the process used in the model is confidential and hence will not be reported in this work.

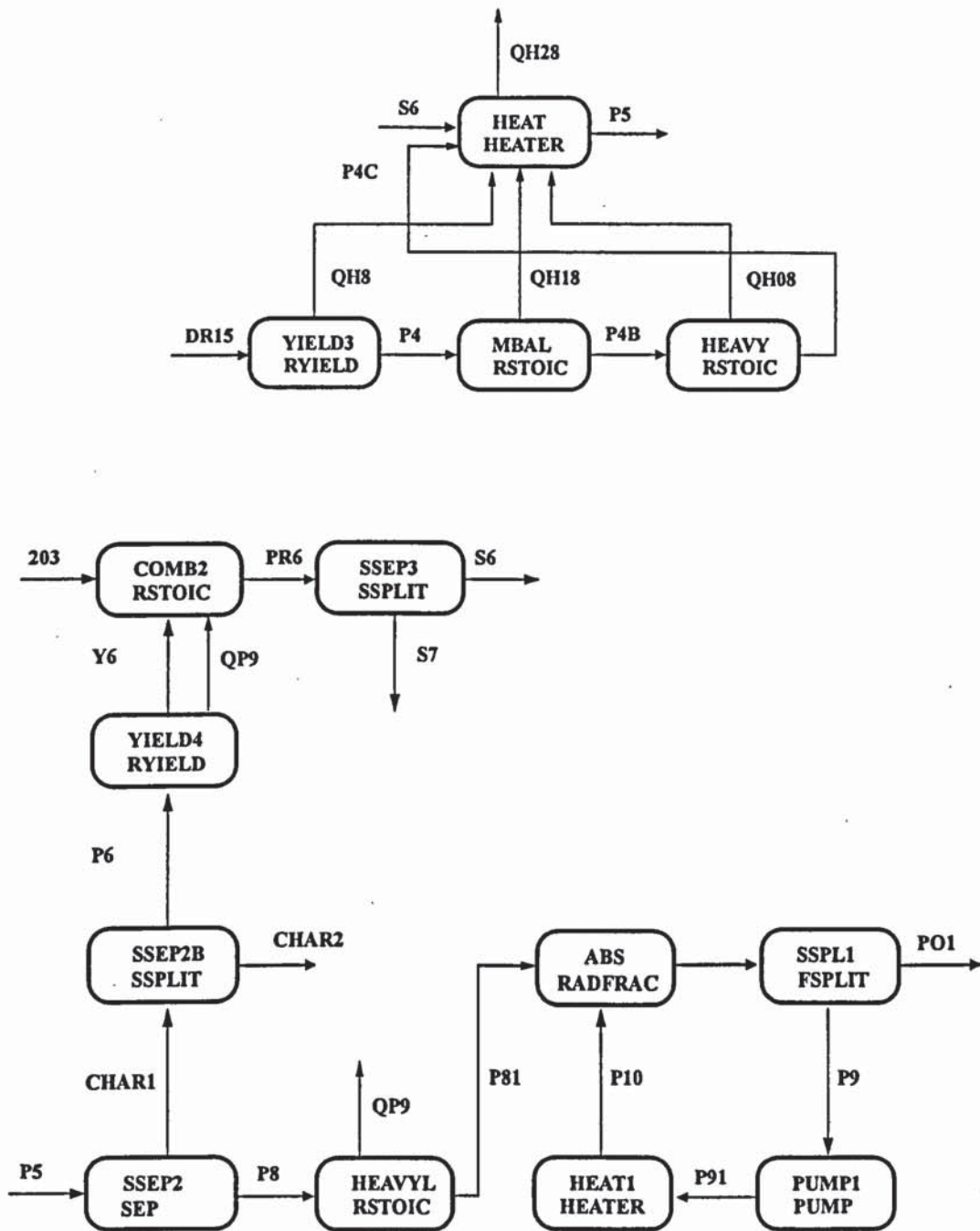


Figure 7-1. Flow diagram of the process model for the wood pyrolysis.

The particle size of the dried feed (DR15) is reduced from wood chips to 90% <5 mm in a hammer mill. The pyrolysis system comprises two reactors, a pyrolyser and a combustor, and sand is used as the heat carrier between the reactors. The pyrolyser (YIELD3, MBAL, HEAVY) is an entrained-flow reactor, and the combustor (COMB2) is a fluidised bed. Part of non-condensable gases from the liquid recovery unit (ABS) is used as fluidising gas in the pyrolyser.

Wood conversion in the pyrolyser is based on laboratory data /123/. The yields from a hardwood at 500 °C are as follows: organic liquid 64 wt%, non-condensable gases 12 wt%, pyrolytic water 12 wt%, and char 12 wt% of dry wood /123/. The mass yields for these compounds are temperature-dependent, and correlations from /123/ are used. Only hardwood yields are currently included in the model.

The yields are different for different wood species, and depend heavily on factors such as the amount of bark and foliage present in the feed (the feed composition employed in this study is presented in chapter 9). Feed moisture, particle size, and especially alkalis in ash all have a considerable effect on component yields. This is because the fast pyrolysis reactions depend greatly on the effectiveness of heat transfer, which is a function of wood moisture and particle size.

The yields of chemical compounds are based on the literature /123, 124, 126/ and experimental analytical data /143/. The relative yields of chemical compounds are assumed constant, which is a simplification. However, no data was available to improve this feature of the model. The elemental analysis of the char produced is also based on experimental results. The ash content of the char is calculated from the ash balance of the pyrolysis. An assumption is made that the char contains all the ash in the fuel feed. This simplification was made to ease convergence of the model.

The heating value of the heavy fraction (a non-conventional compound) is determined so that the selected heat of pyrolysis (see Appendix 6) is achieved. The elemental analysis of the heavy compound is calculated from the atom balance across the pyrolysis reactor.

The non-condensable gases that are not needed as fluidising gas, and part or all of the char formed, depending on the input wood moisture, are combusted in the combustor to supply heat for pyrolysis. The amount of the char needed is calculated by maintaining defined heat losses. Heat losses take place in two locations: a temperature drop of the heat carrier sand between the reactors (20 °C drop assumed), and a fixed percentage of the energy in the fuel in the reactors to account for radiation losses. These are determined using engineering judgement as 0.5 and 2% for the pyrolyser and the combustor, respectively.

The vapours from the pyrolyser are condensed in a wash tower (ABS), which is modelled using the Aspen RADFRAC column. The RADFRAC is a rigorous model for simulating all types of multistage vapour-liquid fractionation operations. A portion (P9) of the condensed pyrolysis liquid/water phase is recycled and used as the spray coolant in the column. The flow of the recycle stream is determined by specifying the temperature of the top stage of the column. 65 °C is assumed at the top stage. The liquid product (PO1) is withdrawn from the system.

7.4.4 Fast pyrolysis performance

A performance balance for a pyrolysis plant is presented in Tables 7-3 and 7-4. A sufficiently large capacity is selected for the plant principally to justify the equipment selected for energy recovery. The fluidised-bed combustors are not economic on a small scale. Note that the data includes a flue gas dryer and wood milling, which account for most of the power consumption in pyrolysis.

Table 7.3. Overall mass balance for fast pyrolysis.

		Mass flow, kg/h
IN	Wood to pyrolysis, m.f.	9 600
	Wood to combustion in the dryer, m.f.	1 054
	Wood moisture	10 654
	Air	20 387
	TOTAL	41 695
OUT	Product liquid (moisture 25.5 w-%)	7 651
	Ash	65
	Dryer flue gases	33 981
	TOTAL	41 697

Table 7-4. Overall energy balance for fast pyrolysis. Auxiliary power for compressors, fans, pumps, mill, and conveyor motors.

		HHV	Sensible	Power	Total
IN	Wood	59.78			59.78
	Auxiliary power			2.98	2.98
	TOTAL				62.76
OUT	Product liquid	41.43	0.34		41.77
	Ash, char losses	0.07	0.01		0.08
	Dryer flue gases		8.44		8.44
	Dryer heat losses		4.36		4.36
	Pyrolyser heat losses		1.36		1.36
	Heat losses in liquid recovery		6.64		6.64
	TOTAL				62.64
EFFICIENCY, %	HHV				66.0
	LHV				73.3

7.4.5 An example of using the performance model

As an example of using the model is shown in Figure 7-2. In the example the moisture content of wood fed to the dryer is varied between 10 and 60 wt%. Moisture to the pyrolyser is kept constant at 10 wt%. The left y-axis shows the energy content of the gas and char formed during pyrolysis. On the right y-axis the overall thermal efficiency is shown.

The example is selected to illustrate how important the feed moisture is in fast pyrolysis. The combustor duty increases from about 8 to 20 MW_{th} when the moisture content of the wood feed is increased from 10 to 60 wt%. The combustor provides heat for both the pyrolysis reactor (hot sand) and the dryer (flue gases). It is assumed that the pyrolysis off-gas is combusted first, after which the char is combusted to meet the process energy requirement. When the feed moisture content is increased from 10 wt% (= no dryer needed) to 30 wt%, the excess char decreases from about 3 MW_{th} to 0. This is a point at which the energy content of the by-products matches the energy requirement of the process. At >30 wt% feed moisture content, extra energy in the form of fuel wood has to be imported. At 60 wt% feed moisture content, some 10 MW_{th} has to be imported.

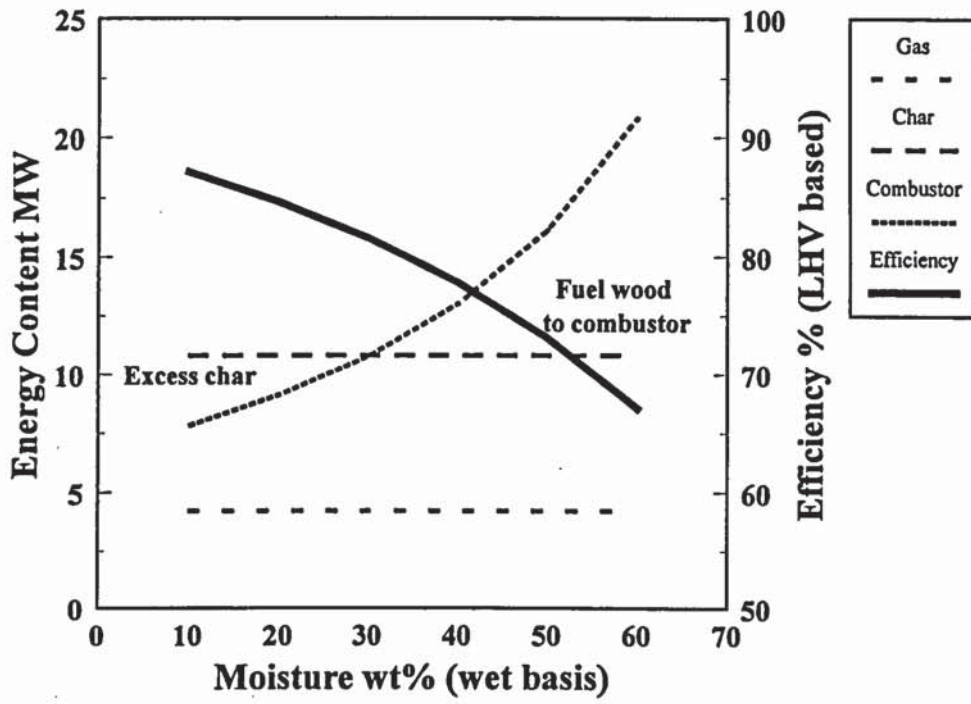


Figure 7-2. Energy balance of wood fast pyrolysis when the feed moisture content is varied. Moisture to pyrolyser constant at 10 wt%.

8. GAS TURBINE

Predicting the performance of gas turbines using low heating value (LHV) gas is critical in the IGCC concept. The characteristics of LHV-gas-fired gas turbines are reviewed in this chapter. The performance modelling of gas turbines in the literature is reviewed. It is concluded that specific performance software is required in modelling to estimate an engine operating with LHV gas. The modelling approach in this work is explained, and performance results using the models built are presented. The use of pyrolysis liquid in gas turbines is briefly summarised.

8.1 Introduction

The integrated gasification combined-cycle (IGCC) concept is believed to be one of the most promising candidates for the successful introduction of bio-power. The gas turbine is the critical power production unit within an IGCC.

Gas turbine modelling in order to determine engine performance is a specialised art, and there are not many predictive simulation tools in the literature or on the market. Modelling the performance of the gas turbine with a new fuel (LHV gas here) requires all the same modelling capabilities and information as the more usual industrial cases of predicting part-load performance or gas turbine capacity as a function of ambient temperature.

Limited industrial-scale data is available in this area. Because of recent industrial bio-energy projects as well as analogous work on coal-derived gas, there is some industrial-scale data available on LHV gas turbine operation. The published data is used in validating the models.

Two broad categories of gas turbines used in power production are industrial and aero-derivative engines. They have different characteristics in power plant operation. However, the performance of both types may be modelled in an analogous manner with similar modelling tools. Both types have been proposed for bio-power plants.

Typical features for the classes are summarised in Table 8-1. In commercial operation, natural gas or various distillate oils are used in gas turbines.

Table 8-1. Comparison of the advantages of industrial and aero-derivative engines /166/.

Aero-derivatives	Industrial
Higher efficiency	Wide fuel range capability
Smaller (up to 50 MW), lighter per kW	Somewhat higher reliability
Easily, quickly replaced	Can be repaired in-situ
Quicker starting	Power up to 250 MW
	Lower cost

In power production, gas turbines may be applied in all three modes of electricity production (see discussion in chapter 12). If in **peak service**, an open cycle is employed, and hot flue gases are released to the atmosphere without utilising the sensible heat in the flue gas. Both industrial and aero-engines are used in this duty. In **medium** and **base load**, the co-generation of steam and power is common, especially in industry. The sensible heat available in the gas turbine exhaust gas is used to raise steam. Both types are used, aero-engines being more common. In recent years, combined-cycle (CC) operation has become quite widespread, especially with natural gas, typically operated in **base load**. In this case a steam cycle utilises the gas turbine's sensible heat. The combined cycles are especially built upon industrial gas turbines, because of they are available on a larger scale and their specific investment is lower.

8.2 Gas turbine in an IGCC

A gas turbine determines the performance of an integrated gasification combined-cycle. The design of the whole IGCC system is based on the gas turbine characteristics, and all other plant units and components are sized accordingly. Once the gas turbine is chosen and its performance with the defined fuel is known, the plant feed-rate and several critical process design parameters are essentially fixed.

IGCC technology is being developed to utilise coal instead of natural gas as a gas turbine fuel. Because of the economy of large-scale heavy-duty industrial gas turbines (>150 MWe), they are employed in all the coal IGCC projects built, operated, and announced so far /167, 168, 169, 170, 171, 172/. Industrial turbines are also employed in heavy oil IGCC plants /173, 174/. Aero-derivatives are too small for coal IGCC projects, the biggest engines having a capacity of around 45 MWe.

The scale and thus the perspective for biomass IGCC is different. It is generally accepted that biomass power plants have to be smaller than coal plants, and thus smaller gas turbines are considered. Therefore, high-efficiency aero-engines have been proposed for bio-power projects /56, 48, 55, 31/. For example, the Brazilian project of GEF is based on the General Electric LM2500 gas turbine, which has a nominal power output of 21 MWe.

The Bioflow IGCC demonstration plant in Sweden employs the Typhoon engine from European Gas Turbine (EGT), which has a power output of approximately 4 MWe /175/. The Typhoon is of a demonstration scale for this application and is considered too small for economic industrial operation.

Most studies published on biomass IGCC cover a range from 20 to 60 MWe, although larger capacities are also suggested (100-150 MWe, especially in the USA) (see chapter 2.4). With biomass, fuel availability governs power plant scale and thus the selection of the gas turbine as well.

8.3 Low-heating-value gas in gas turbines

The review in this section serves as an introduction to gas turbine modelling using low heating value (LHV) gas. The main characteristics of gas turbines using LHV gas are reviewed. Because few large-scale experiences exist either with coal or biomass-derived gas, gas turbine performance modelling is a priority in the effort to model the whole biomass IGCC.

8.3.1 Engines proposed

Industrial engines are often classified as small and large engines, their capacities ranging approximately from 0.2 to 20 MWe and from 20 to 250 MWe, respectively. Aero-derivative engines currently have capacities of approximately 0.3 - 45 MWe.

The following engines on the market have been employed (Typhoon) or proposed (the rest) for biomass IGCC use: Ruston Typhoon /175/ (4 MWe), Allison 501 /46/ (4 MWe), GE LM2500 /56/ (21 MWe), Mitsubishi MW151 /46/ (21 MWe), GE Frame 6 /46, 176/ (38 MWe), Westinghouse CW251 /46/ (50 MWe), and GE Frame 6FA /46/ (70 MWe). All but the LM2500 are industrial engines.

It has been claimed /46/ that only industrial gas turbines are suitable for IGCC. First of all, the small combustors of aero-derivatives do not allow low-NO_x combustion for LHV fuel gas, which may be needed to reduce NO_x emissions. Secondly, the small combustors may not allow enough residence time for complete combustion of, e.g., carbon monoxide. In recent years, data on tests with LHV gas in gas turbine combustors have become available, and some of the critical issues have been addressed (see section 8.3.2).

Aero-engines are not built for power plant duty. Their construction is very compact. The firing of LHV fuel gas requires much larger volume flows than natural gas because of the lower energy density of the LHV gas. The installation of wider fuel piping (a requirement in LHV gas firing) is not necessarily technically feasible, as there simply may not be enough space. Generally speaking, the use of LHV gas in the aero-derivative engines (e.g., LM2500) is subject to greater uncertainties than in industrial engines.

LHV fuel gas (blast furnace gas and other process gases) has been employed in industrial engines in commercial service /i.a., 177/. Measured performance data with LHV gas for the GE Frame 6 was available for Enter Software /178/ in the construction of a simulation model used in this work (see chapter 8.5). It is therefore concluded that there is little uncertainty in using LHV gas as fuel in a Frame 6. The Typhoon, another industrial turbine, has been installed at the Bioflow IGCC demonstration plant in Värnamo, Sweden /175/, and has been in use for a few years. Although detailed data is not available, trouble-free engine operation has been reported /40/.

8.3.2 Technical uncertainties

A summary report on LHV gas in gas turbines discusses uncertainties in depth /179/. These uncertainties are reviewed in the following section based on Moses /179/, and they may be summarised as being associated with one of the following three issues:

- Fuel feeding and handling
- Combustor performance
- Durability and overall operation

Fuel feeding and handling

Larger or multiple-fuel systems will be needed for the combustion of LHV gases compared with natural gas. Aero-derivative systems are limited by the size of the injectors that can be located inside the housing. Modifications to industrial gas turbine systems using LHV gas are technically less demanding than in the case of aero-derivative engines. Industrial engines are therefore favoured in this respect.

Some technical uncertainty is related to the performance of the fuel feeding and handling unit because an elevated fuel gas temperature (compared with natural gas) is assumed in many IGCC concepts. The fuel control valve is especially affected. Temperatures around 400 to 500 °C have been proposed (hot fuel gas from filters), as a high fuel gas temperature increases the overall efficiency of the IGCC process. The present natural gas inlet temperatures are around 150 °C. It is reported /179/ that temperatures up to 370 °C are reasonable, and 550 °C is probably the maximum that can be handled in the control valve due to material limitations.

It can therefore be concluded that high inlet temperatures may be assumed with future gas turbines in the concepts to be assessed. However, it should be noted that high inlet temperatures are not available in current engines.

Combustor performance

One key issue is related to the low volumetric energy density of the gas employed (typically around 5 MJ/Nm³ from air gasification of biomass versus around 36 MJ/Nm³ for natural gas). This will affect the combustor performance in many respects: flame stability is affected, and the flammability limits of the gas are altered. The emissions will also be different with LHV fuel gas compared with natural gas. These issues are discussed below.

The rich and lean flammability limits are the major factors affecting the stability of combustion. Usually, the gas turbine has narrower stability limits when burning gaseous fuels than when burning liquid fuels. The lower the energy content, the narrower are the limits, and hence the less stable is the combustion. It appears that the use of LHV gas might reduce the range of engine operation, which usually extends from 30% to about 110% of the design output. As the steady-state condition with the design output is emphasised in this work, this aspect will not be studied further.

The emissions of concern are carbon monoxide (CO) and nitrogen oxides (NO_x). Generally speaking, LHV gases produce less thermal NO_x (which results from a high flame temperature) than natural gas does. However, fuel-bound nitrogen forms NH₃ in gasification, which is partly converted into NO_x in gas turbine combustion. The overall NO_x emissions are thus largely dependent on the amount of nitrogen in the fuel. The combustion of CO is of concern from the standpoint of both emission and combustion efficiency. CO oxidation is relatively slow, and especially aero-derivatives may face this problem with their shorter residence time.

There are apparently no superior technical reasons why a new combustor system could not be designed to burn LHV gases. However, this is typically much easier and thus less costly for industrial turbines. Few actual combustion tests at pressure have been reported for LHV fuels. Uncertainty is related especially to aero-derivative engine combustors.

Developments concerning the gas turbine combustor related to the British Coal Topping Cycle /180/ process is also relevant to biomass IGCC. The lower heating value of the LHV gas considered ranges from 3.6 to 4.1 MJ/m³. At the first stage of the development /181/

preliminary results for combustion efficiency, temperature distributions, and NO_x emissions with synthetic gas were encouragingly low. At the second stage, Kelsall and Cannon /182/ reported on the modifications needed for a conventional combustion chamber to function satisfactorily with LHV gas. The results showed that the combustion efficiency, exhaust temperature profile, and air pressure loss are all satisfactory with LHV gas. However, the conversion of fuel gas nitrogen to NO_x should be reduced in the future. The same applies to combustor surface metal temperatures, as these were higher than is industrially acceptable. The development work is continuing. The work is important as it has been carried out with a gas of lower heating value than the LHV gas from biomass gasification considered in this thesis. The work also shows that modifications are required for existing engines when fired with LHV gas.

GE has reported on the tests and modifications needed for the industrial MS5000 /183/, LM500 /184/, and aero-derivative LM2500 /185/ engines. The industrial MS5000 was rated at 27.6 MWe with a coal gas having a LHV from 3.9 to 5.8 MJ/m^3 . The LHV of the coal gas is in the same range as that of biomass-derived fuel gas. Output increased considerably from the 17 MWe achieved with distillate fuel. The increased power output with LHV gas is discussed in section 8.5.

The LM2500 combustor was tested using fuel gases with a heating value of 5.6 - 9.3 MJ/m^3 , which is not as low as the gas studied in this work. Sabla and Kutzko report /185/ that although some degradation of the pattern factor (=highest local temperatures divided by the average temperature in the combustor outlet) occurred because of higher volumetric gas flows, the operation of the engine at maximum power output with the tested combustion system appears viable. It is reported that the required modifications to the LM2500 combustors are considered achievable /56/. Recently, GE has reported on combustion tests with LM2500 combustors. However, no results from these tests have been published. No aero-derivative engines have so far been modified for LHV gas firing.

As part of an IGCC development effort, Karlsson /176/ and Salo & Keränen /46/ have reported on combustion tests carried out with a synthetic biomass-derived fuel gas in the GE Frame 6 combustor. Overall, the results were very positive. It was concluded that a modified combustor is well suited for biomass fuel gas. Temperatures and dynamic pressure

levels were within design limits and combustion characteristics were good. Thermal NO_x , CO and HC emissions were acceptably low. The conversion of fuel-bound nitrogen to NO_x was lower than expected on the basis of estimates concerning NH_3 conversion.

Based on this review it is concluded that both engine types are probably suitable for use with biomass-derived LHV gas. However, it appears that aero-derivative engine combustors are more difficult to modify than combustors of industrial engines, and are thus subject to more uncertainty.

Durability and overall operation

Most of the issues related to the durability of the engine concern gas cleaning. Contaminants (tar, particulates, alkalis) are substantially removed in gas cleaning, and the remaining impurities reduce the durability of the engine. Tar and char also affect combustion efficiency. Other particulate matter may cause erosion and hot corrosion, which may also be caused by alkali metals.

Compared with natural gas, the LHV gas flow needed to generate the same thermal effect is considerably larger. A flow mismatch between the compressor and the turbine reduces the compressor surge margin, i.e. reduces the operating range of the compressor. To address the complication, air may be bled from the compressor discharge air so as to reduce the turbine mass flow. The approach may be employed both in oxygen gasification coal IGCCs and in air gasification biomass IGCCs. The arrangement makes plant operation and control slightly more difficult due to the feedback loop being created.

In oxygen gasification, air is bled from the gas turbine compressor to the oxygen plant, where oxygen for gasification is produced. The by-product nitrogen may further be fed into the gas turbine combustion chamber to suppress the formation of nitrogen oxides. This alternative is feasible in large-scale plants.

In the second case of air gasification, extract air is fed to the gasifier through a booster compressor. The biomass demonstration IGCC plant at Värnamo has adopted this strategy. About 10% of the compressor air is bled off and led to a booster compressor, which feeds the air to gasification /175/.

8.3.3 Steam injection

Steam injection is employed in commercial gas turbine operation to reduce the NO_x emissions and increase power output. It is believed to be interesting for bio-power projects as well /186/. Steam injection also reduces the specific investment cost of a turbine. High specific investment is known to be the primary adverse feature of bio-power systems. However, there are technical uncertainties involved in employing steam injection with LHV gases.

Based on the results presented in the Enter reports /178,187/, it appears that less steam may be injected to gas turbines fired with LHV gas than with natural gas. This is particularly true with Frame 6, as it is a constant speed industrial engine. The additional steam injected reduces the compressor surge margin (= safe operation range), and hence relatively little steam injection is allowed (about 1.5 wt% steam of the airflow in the LHV gas-fired case versus about 4 wt% in the natural gas case). The situation is slightly better for aero-derivative engines, as part of the increased mass flow helps to increase the compressor speed, and only part reduces the surge margin. For the LM2500-PH engine, according to the Enter study /187/, about 4.5 wt% steam may be injected to the air flow in the LHV gas-fired case versus about 7.5 wt% in the natural gas case. In any case it seems that considerably less steam injection is allowed for LHV fuel gas fired turbines than in conventional operation with hydrocarbon fuels. Ultimately, this reduces the potential benefits reported for STIG systems when fired with LHV fuel gas.

STIG concepts are studied in this work to find out whether the advantages reported with hydrocarbon fuels are also obtainable with LHV gas operation.

8.4 State-of-the-art of gas turbine operation with pyrolysis liquid

There is little information available on the use of fast pyrolysis liquid (PL) in gas turbines. The issue has been seriously pursued only within two projects /188, 189/, of which the former effort used slow pyrolysis liquid. Although this fuel is different from fast pyrolysis liquid, the work will be reviewed because so little has been published on the topic.

8.4.1 Teledyne CAE

Teledyne CAE /188/ carried out a study using pyrolysis liquid which had been produced in slow pyrolysis. Such a liquid can be considered comparable to fast pyrolysis liquid, although it had a high water content of 33 wt% and a high percentage of suspended solids.

The results indicated that the use of pyrolysis liquid resulted in combustion efficiencies of >99%. Kaspar et al. /188/ concluded that pyrolysis liquid may be used as a supplement to fuel oils, and although pyrolysis liquid may be combusted, co-firing of diesel oil and pyrolysis liquid is required for adequate combustion.

8.4.2 Orenda Corporation

More recent work has been undertaken at Orenda Corporation since about 1993. The first laboratory work to characterise the combustion behaviour of fast pyrolysis liquid has been carried out /189/. Overall, the combustion and emissions were determined to be acceptable. Only particulate emissions were clearly higher than with reference mineral oil. Corrosion and erosion of the first turbine blades were studied under simulated conditions in a test boiler. Although ash deposits were found on the blades, the nature of the deposits was not considered damaging /189/.

An industrial 2.5 MWe Mashpoekt turbine has been modified for use with fast pyrolysis liquid. Some materials have been replaced and the firing procedure has been modified. A short full-scale test has been carried out. No major problems have been encountered and Orenda is continuing the development work /189/.

8.5 Modelling of gas turbines with low heating value gas

Based on the previous review and on the data available, the following GE engines were selected for modelling:

- LM2500 (aero-derivative)
- Frame 6 (industrial)

The first aero-derivative has been selected for several R&D projects. There are some experiences of the industrial engine in LHV gas operation, so it is subject to moderate technical uncertainty.

The task of predicting the maximum capacity performance characteristics of a gas turbine designed for natural gas or distillate oil when firing LHV gas is actually an off-design performance problem /190/, i.e. the turbine components are operated away from their design points. The modelling requires all the same modelling capabilities and information as the more usual cases of predicting part-load performance or maximum gas turbine capacity as a function of ambient temperature. The use of LHV gas is further complicated by the several strategies available to the gas turbine manufacturer for using this fuel.

8.5.1 Introduction

LHV gas is produced in the air gasification of biomass. Typically, a LHV fuel gas has a heating value of 4-5 MJ/m³n, whereas natural gas has a heating value of approximately 36 MJ/m³n. To maintain the same firing temperature in a gas turbine combustor with LHV fuel as with natural gas, more fuel has to enter the combustor, and consequently, more mass flow passes through the turbine expander. This causes the gas turbine to operate away from its design point, which is an important consideration when modelling these units.

Aero-derivative and industrial engines are not operated in the same way and their control systems are different. Even though the gas turbines operate well under a wide variety of conditions, control limits still exist due to effects such as compressor surging, overspeed, and shaft torque limits. For instance, compressor operation and control are more critical for aero-derivative engines than for industrial engines, since on aero-derivatives the compressor shaft is not connected to the generator, and therefore spins freely /187/.

Consonni /191/ has summarised the state-of-the-art of cooled turbine modelling. He points out that, due to the complexity of the task, the problem cannot be solved analytically without resorting to simplifying assumptions which compromise accuracy.

Two categories of models have been defined:

- Purely thermodynamic (zero dimensional) models, where cooling flows are calculated by referring only to the T, p history along the turbine. These are particularly suited to parametric analyses.
- One-dimensional models, whereby the cooling flows are calculated on the basis of the flow field and the geometry resulting from a "mean-line" design of the turbine. The required input data is hard to get, as the data is proprietary.

Consonni also points out that the two most popular codes on the market, GATE/CYCLE (by Enter Software Inc.) and GT/PRO (by Thermoflow Inc.) are provided with input data sets specifically calibrated to reproduce the behaviour of a number of commercial engines. This further illustrates the difficulty of modelling actual gas turbines.

A flow scheme for an engine is shown in Figure 8-1. LM2500 is shown, although the Figure serves as a generic flowsheet for a gas turbine.

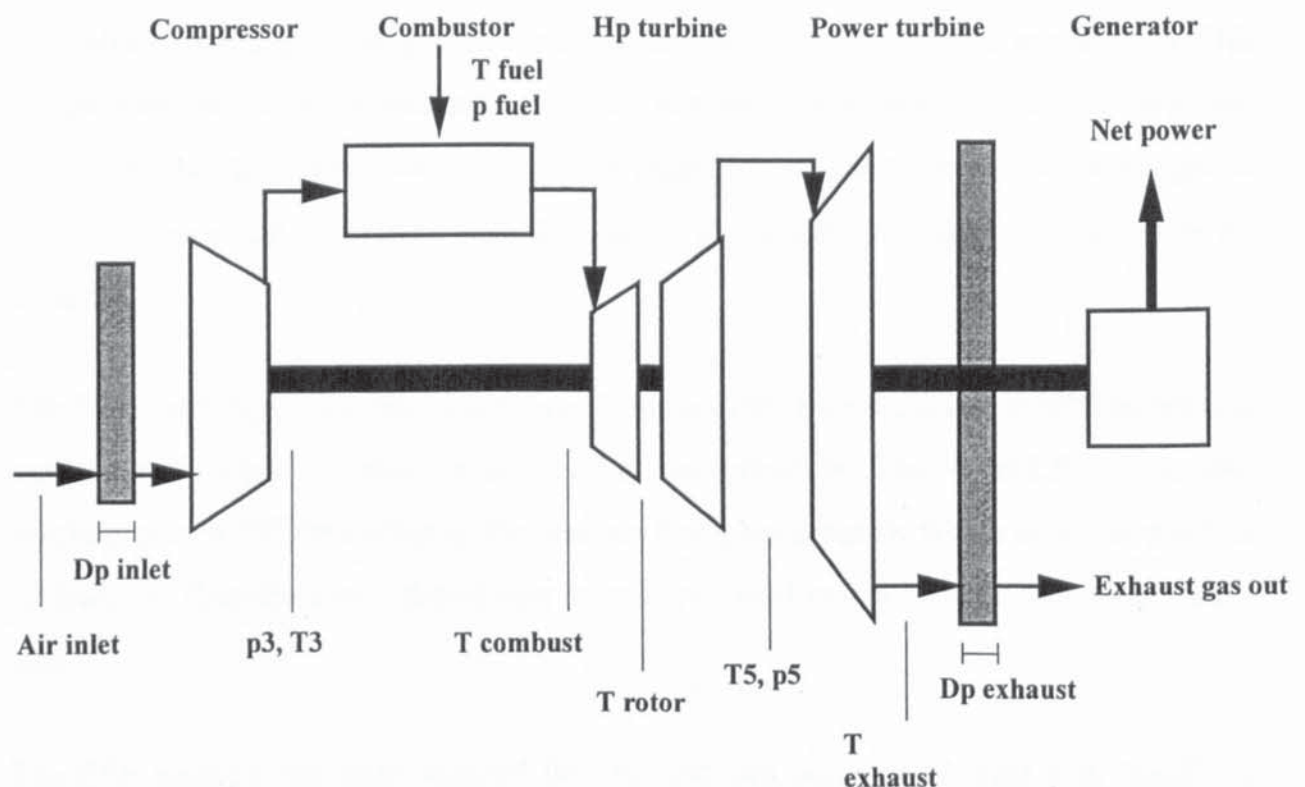


Figure 8-1. Block flow representation of the aero-derivative LM2500 engine.

The solution to the off-design performance of single shaft, constant speed gas turbines begins with the fact that the mass flow at the expander inlet (position at “T combust” in Figure 8-1) is choked. The mass flow relationship for choked flow of an ideal gas is shown in equation (8-1):

$$\dot{m} = pA^* \sqrt{\frac{M_w}{T_t}} \sqrt{\frac{\gamma}{R} \left(\frac{2}{\gamma + 1} \right)^{\frac{\gamma + 1}{\gamma - 1}}} \quad (8-1)$$

where

- \dot{m} = mass flow, kg/s
- p = total pressure, kPa
- A^* = critical area where the flow is choked, m²
- M_w = average molecular weight of the gas
- T_t = temperature, K
- γ = ratio of specific heats of the gas
- R = gas constant

all parameters at the expander inlet (position at “T combust”)

The term under the large right-hand radical may be considered constant as the first approximation. The importance of the molecular weight for the equation may be seen, as the products of natural gas firing are different from those of LHV gas firing. Choked mass flow is directly proportional to the total pressure and the critical flow area, and inversely proportional to the square root of the absolute total temperature. Variation in these parameters is discussed briefly below.

There are five principal strategies available to an engine manufacturer when dealing with a LHV gas. The strategies may be understood by examining their effects on equation 8-1, bearing in mind that the use of LHV gas increases the mass flow, \dot{m} .

Strategy 1: Operate the compressor at a higher pressure ratio (increase p).

Strategy 2: Reduce the compressor airflow, and consequently, \dot{m} .

Strategy 3: Increase A , the critical area (position at “T combust” in Figure 8-1).

Strategy 4: Reduce T_i (temperature), by reducing the combustor fuel flow. Both T_i and m are reduced.

Strategy 5: Bleed air from the compressor either to the oxygen plant (in the case of oxygen gasification), or to the gasifier (in the case of air gasification). This partly compensates for the larger fuel gas flow.

The first strategy is the most aggressive. Increasing the pressure ratio reduces the compressor surge margin (i.e. reduces the compressor operating range), increases the torque on the shaft, and increases the thermal loads on the turbine airfoils. The advantages of this approach would be increased output power and reduced heat rate (compared with natural gas firing).

The second option is less aggressive. The compressor inlet guide vanes are partially closed, and the expander mass flow are approximately equal to the natural gas case. The output power increases, but the gain is smaller than with the first strategy.

The third choice is to re-design the expander inlet nozzle to increase the critical area. This option is technically more demanding than the two previous strategies, and it would probably not be the first choice for a gas turbine manufacturer due to associated development costs. However, if development were undertaken, the nozzle would probably have to be re-designed.

The fourth strategy is the least attractive. Johnson /190/ points out that a 10% increase in mass flow (fuel gas and combustion air combined, which is close to the LHV-fired case) would require a 17% reduction in the absolute firing temperature, which is far too much to be feasible. Thus the fourth choice may only be practical in combination with other strategies.

The fifth strategy has been selected for the first two commercial-scale coal IGCCs in Europe /169, 170/ and in the biomass IGCC demonstration at Värnamo. Measures 1 to 4 above may also be employed in conjunction with this strategy.

8.5.2 Review of previous work

In addition to the work by Johnson /190/ referred to in the previous chapter and to the work of Consonni /191/ below, very little has been published on the modelling of gas turbines using LHV gas. In fact, there is little information available in the open literature on the off-design performance of gas turbines. The reports by Palmer and Erbes /178, 187/ are the only ones dealing directly with aero-derivative engine performance modelling with a biomass-derived LHV gas.

8.5.2.1 Stanford University - GATE/CYCLE

The pioneering (coal) IGCC analysis during the 1980s was carried out at Stanford University. The modelling tool applied was AspenPlus. The modelling of gas turbines using LHV gas was a central issue in these studies.

Johnson /190/ provides detailed performance simulation results using coal syngas with large industrial gas turbines. The work is a major contribution to publications on the modelling of gas turbines using LHV fuels. Five strategies for using coal-derived LHV fuel gases are described (see chapter 8.5.1), and modelling features for two of these cases are presented by Johnson.

The gas turbine performance analysis by Johnson /190/ was part of a work in which a complete IGCC was analysed with Aspen. The gas turbine performance was analysed with the GATE simulation software, and a set of gas turbine performance curves was produced for inclusion in the Aspen plant model. Johnson analysed three sets of industrial gas turbines, A, B, and C. Gas Turbine A was meant to be representative in the class of GE MS7001E or Siemens V84.2. Gas Turbine B is similar to GE MS7001F or Siemens V84.3. Gas Turbine C represents an evolved version of Gas Turbine B with a higher pressure ratio (14.5 versus 14.0) and a higher firing temperature (1370 versus 1260 °C). Johnson reports the performance increases shown in Table 8-2 for gas turbines using coal-derived fuel gas instead of natural gas. Strategy 1 is applied in all of the cases shown. The strategy is explained in chapter 8.5.1.

This analysis is important to the present work, as it points out two issues in LHV gas utilisation. The performance increase is considerable, as the output power is increased by 12 - 17% when LHV gas is used instead of natural gas. The efficiency is also increased: about 10% in all cases.

Table 8-2. Predicted gas turbine performance with coal-derived syngas /190/.

Gas turbine	Fuel	Efficiency %	Output power MW
A	Natural gas	32.6	83.5
	Coal gas	35.8	93.6
B	Natural gas	34.5	150.0
	Coal gas	38.1	174.5
C	Natural gas	35.1	173.2
	Coal gas	38.5	204.2

Earlier at Stanford University, Phillips /192/, Erbes /193/, and Paffenbarger /194/ employed another procedure for modelling a gas turbine in a study dealing with IGCC. Aspen was employed in the study as a modelling framework. A model was developed from performance data on the older GE Frame 7E turbines, since no data was available at that time for the new Frame 7F engine. The performance curves published by GE (Allen & Ross /195/) for the air and fuel flow of the Frame 7E were normalised, and curve fits were generated as a function of load fraction and ambient temperature. The design points for the Frame 7F were taken from the 59 F ambient air performance case published in a Fluor study /196/. Given the incoming fuel mass flow rate and ambient temperature, and using normalised relations, the model calculates the net gas turbine power and the required air-flow. The exhaust temperature and composition are then found using the Aspen reactor model RSTOIC and specifying the exhaust pressure and an energy withdrawal from the gas turbine control volume.

8.5.2.2 METC

Stone /118/ has published an Aspen model for the gas turbine (Aspen flowsheet in Figure 8-2). Isentropic efficiencies (for compressors and turbines), combustor pressure loss and heat losses, and turbine cooling flows are presented. These are parameters that are not

usually reported by engine manufacturers. The model includes three extraction points for the turbine cooling flows. A correlation for the cooling flows as a function of combustion temperature is presented in the report. However, the cooling flow requirements are, among other things, a function of temperatures in the turbine airfoils. These, on the other hand, are impossible to estimate without a complete thermodynamic analysis, like that described by Consonni /191/ (next section). Cooling flows (and other critical engine parameters listed above) are very much dependent on the gas turbine type concerned, and thus the correlation may only be valid for GE MS7001E (which appears to be the engine in question). However, because no validation for the model is presented, it is not known at this point how accurate the results are. Stone /119/ later modified some of the parameters in the model, and the engine is specified as MS7001F.

The accuracy of the model is tested in Appendix 12. The model is not appropriate for the task here, because it is only valid for a large industrial turbine. In the model, cooling mass flows are also needed and these are not available.

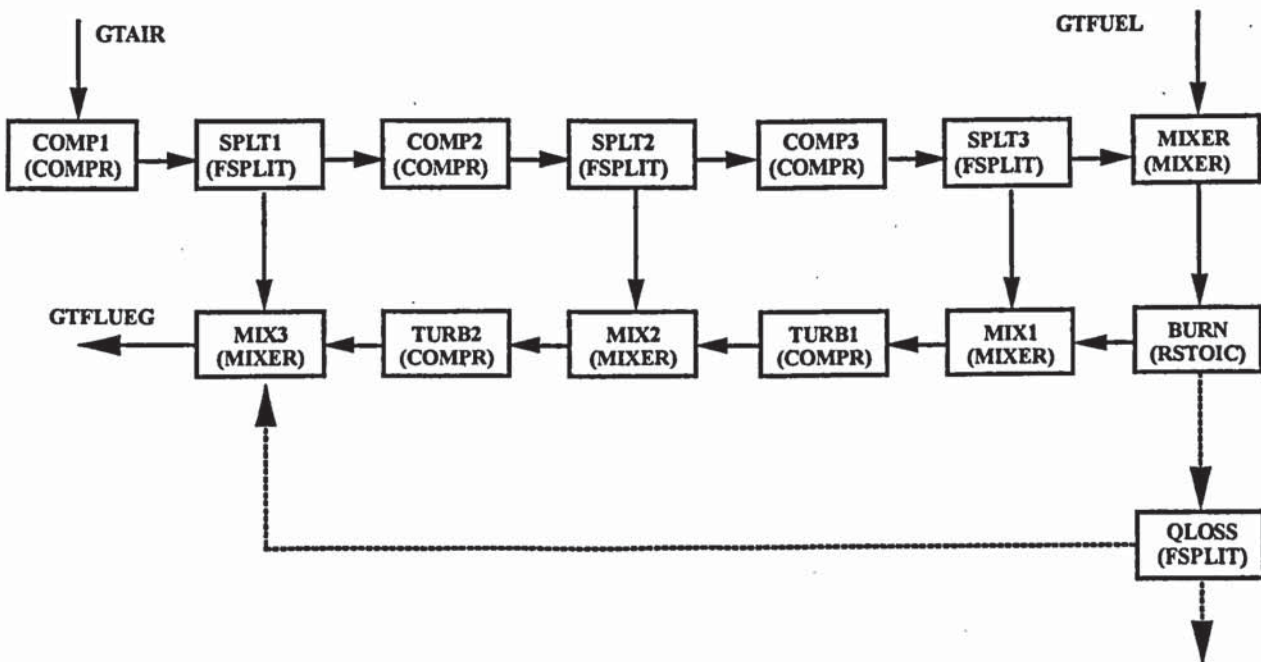


Figure 8-2. An Aspen model for a gas turbine /118/.

8.5.2.3 Princeton University

Consonni /191/ summarises the state-of-the-art of air-cooled turbine modelling. He presents a detailed model, which may be employed, in addition to current engines, in estimating the performance of future developments in gas turbines. The model is quite detailed. For example, cooling flows are calculated on the basis of the flow field and the geometry. The modelling tool built is among the most sophisticated in the public domain on gas turbines.

However, the model is too complex for this work. Results from IGCC analysis carried out with the model are presented in chapter 2.4.

8.5.2.4 Enter Software - GATE/CYCLE

Palmer and Erbes have employed the GATE modelling software /197/. The reported analysis deals only with thermodynamic performance issues. It does not address other critical issues relating to corrosion, emissions or combustor/fuel supply design. Palmer and Erbes /178/ predicted that the output power for a LM2500-PH may be increased from 18.9 MWe with natural gas to 24.2 MWe with LHV gas (ISO conditions). At the same time the efficiency of the engine is increased from 34.4 to 36.7%. They also report the off-design performance analysis of the engine with two different biomass-derived fuel gases. The results from the above report and another report by Enter /187/ are discussed in more detail in chapter 8.6.

8.6 The gas turbine model built for this work

8.6.1 Model description

The approach to the modelling of gas turbines chosen in this work is similar to that employed in the first Stanford studies /192, 193/ referred to previously. Gas turbine performance with a LHV gas is estimated with GATE/CYCLE, and the resulting performance is

transferred to the Aspen model. Because of the importance of the gas turbine model's accuracy for the overall performance of the IGCC, this approach was considered necessary.

The best thermodynamic models available, GT/PRO and GATE/CYCLE, are adequate for the purpose of this work. The inaccuracy due to the simplifying assumptions employed in these models is minor.

Neither GT/PRO nor GATE/CYCLE software was directly available for this work. However, as part of the IEA Bioenergy Pyrolysis Activity 1992-94 /31/, studies using LHV gas as feed for GATE/CYCLE were carried out to calculate the performances of two gas turbines: the aero-derivative LM2500 /187/ and the industrial Frame 6 /178/. These two reports were the only ones in the public domain, where the use of wood-derived LHV gases in both aero-derivative and industrial turbines were reported. Using comparable data for both engines types was considered critical, because the engine type is one of the crucial issues in an IGCC design.

An Aspen block flow model of a gas turbine is shown in Figure 8-3. The principal user input and outputs are presented in Table 8-3.

The following process parameters were transferred to the Aspen model from correlations /178, 187/ derived with GATE/ CYCLE for both LM2500 and Frame 6: fuel gas flow, air flow, air extraction for gasification, isentropic efficiency for compression, final (absolute) pressure of compression and expansion, pressure drop for air intake, and pressure drop for heat recovery. The model is tuned to reproduce reference data by:

- 1) isentropic efficiency for expansion (in C2) is varied until the required output power is reached, and
- 2) heat loss in DT1 is varied until the required flue gas temperature is reached.

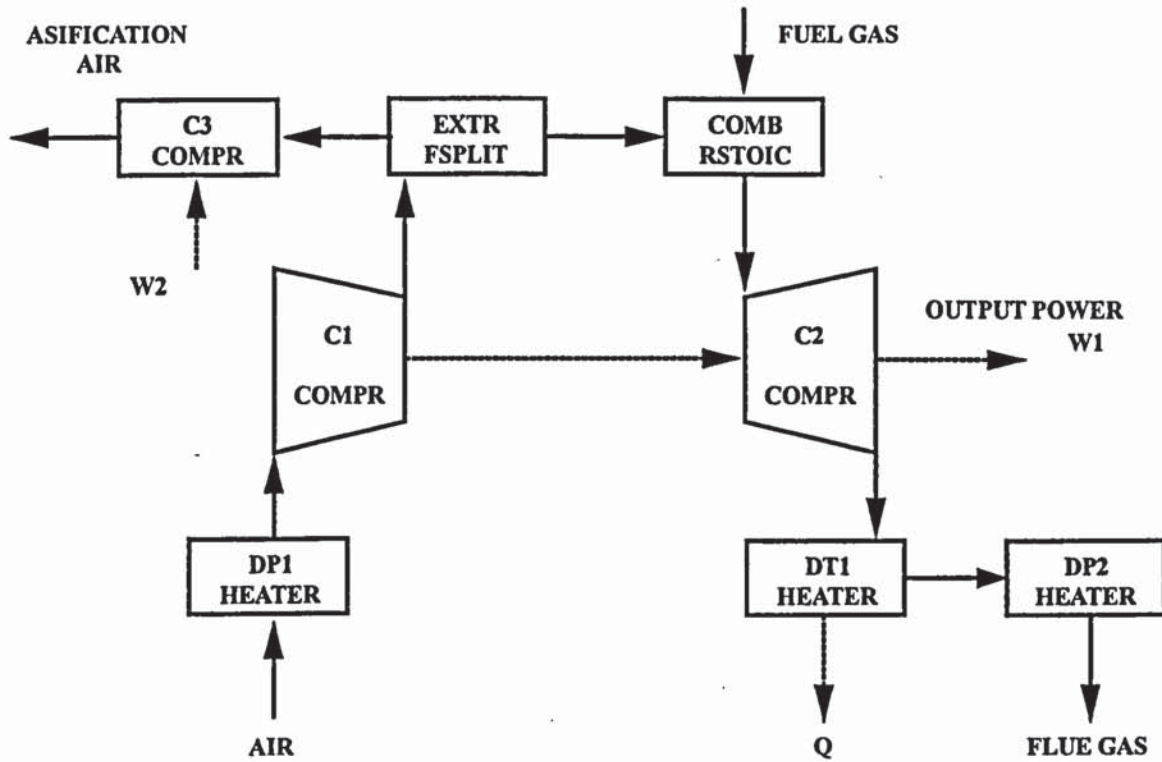


Figure 8-3. Gas turbine block flow model built in Aspen.

If part-load or off-ambient temperature (departing from the ISO 15 °C) performance analysis in Aspen is studied, specific Fortran correlations for the above parameters should be used.

Table 8-3. Gas turbine model inputs and outputs.

INPUT	Fuel gas ¹⁾ kg/s Air kg/s Pressure ratio in compressor Expansion ratio in turbine Isentropic efficiencies for compressor and turbine % Pressure losses in intake and out kPa Heat loss %
OUTPUT	Flue gas kg/s Flue gas °C Power output MWe

¹ Is fixed in an integrated model; the previous model sections (drying, gasification, gas cleaning) are sized accordingly

8.6.2 Model features

Some results from Palmer and Erbes /178, 187/ concerning the LM2500-PE and F6 gas turbines are reviewed below. These results are used as the basis of the Aspen gas turbine model developed in this work. Gas turbine characteristics are emphasised when illustrated as a function of ambient temperature. The current work deals with steady-state modelling, and a fixed ambient temperature is assumed. However, the following examples, where efficiency and power output are shown as a function of ambient temperature, are included to highlight the facts that:

- the performance of gas turbines when fired with LHV gas is different than when fired with natural gas. Using natural gas performance correlations for LHV gas leads to inaccurate results (note Figures 8-4 and 8-5)
- the performance of aero-derivatives and industrial engines is different due to their control systems, and
- the ambient temperature has a major effect on engine performance.

Power output as a function of ambient temperature is depicted in Figure 8-4 using natural gas and LHV gas as fuel in an LM2500. Features of the control system explain the shape of the curve. When the ambient temperature decreases, at higher temperatures the power turbine inlet temperature is kept constant, requiring less and less air flow, thus reducing compressor work and increasing power output. At lower temperatures the firing temperature is reduced, leading to a decreased power output. This is done since the compressor-corrected speed must not exceed a specified maximum value /187/. The point where the different control limits take precedence shifts from about 12 to 9 °C when the engine is fired with LHV gas instead of natural gas. The output for the LHV-fuelled case is higher over the whole range studied.

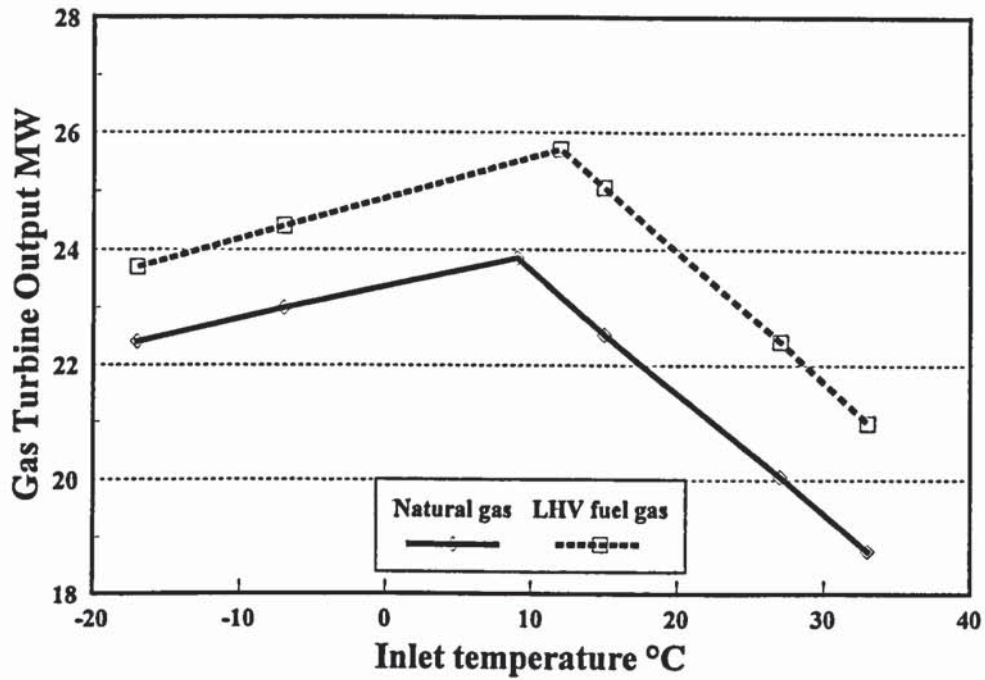


Figure 8-4. LM2500 power output as a function of ambient temperature.

The same curve is shown for the Frame 6 engine in Figure 8-5. The output continuously increases as the ambient temperature decreases, because F6 is a constant-speed engine. The firing temperature is kept practically constant over the whole operating range. Using LHV gas as fuel increases power output by 11% and 7% at 15 °C with the LM2500 and F6, respectively.

The efficiencies for the two engines are depicted in Figures 8-6 and 8-7 as a function of ambient temperature. In both cases, using LHV gas results in a higher efficiency. The increase in efficiency is 3% and 4% at 15 °C with the LM2500 and F6, respectively.

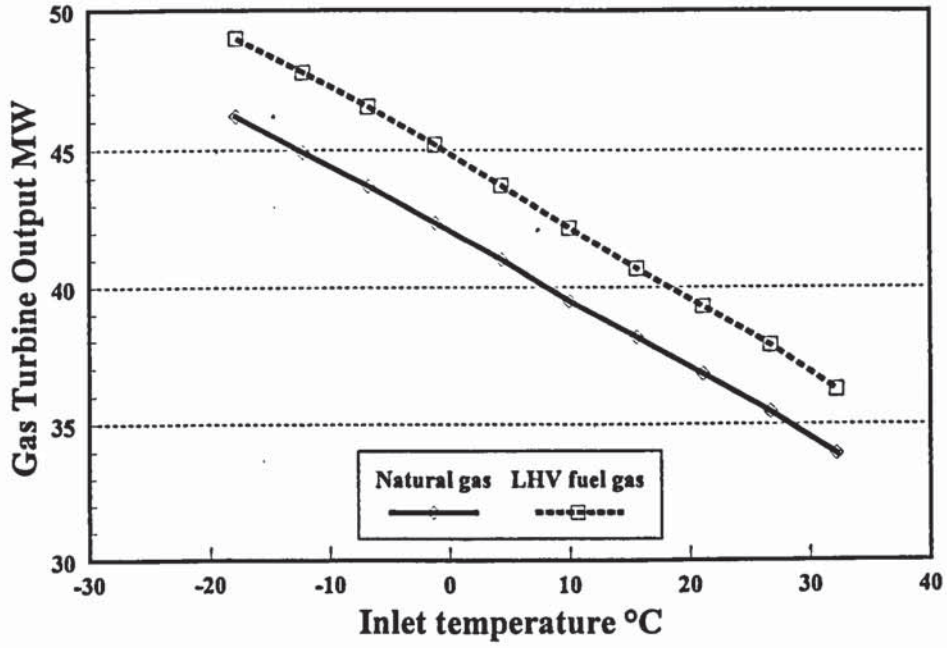


Figure 8-5. F6 power output as a function of ambient temperature.

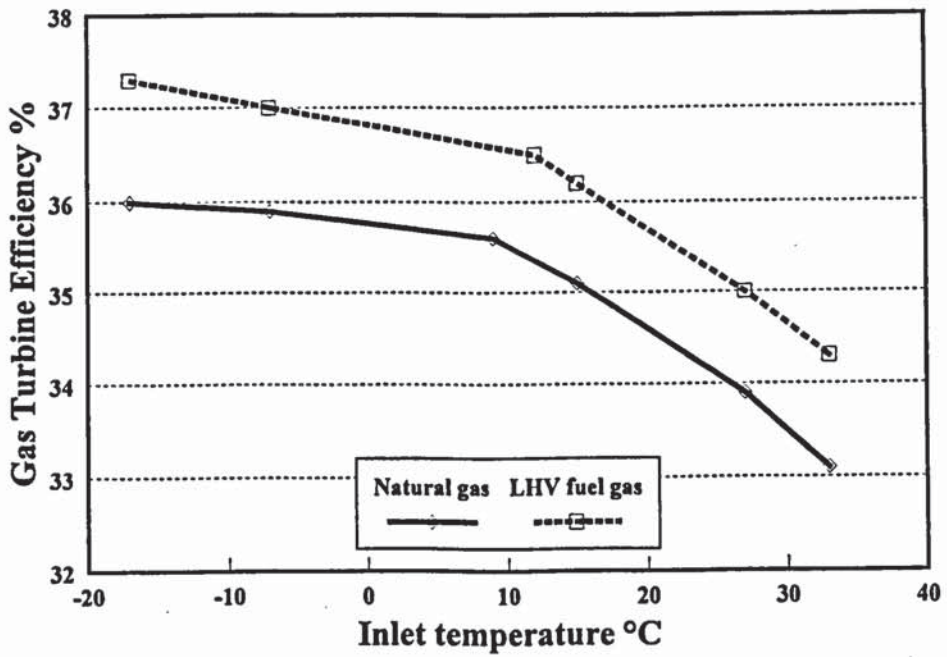


Figure 8-6. LM2500 efficiency as a function of ambient temperature.

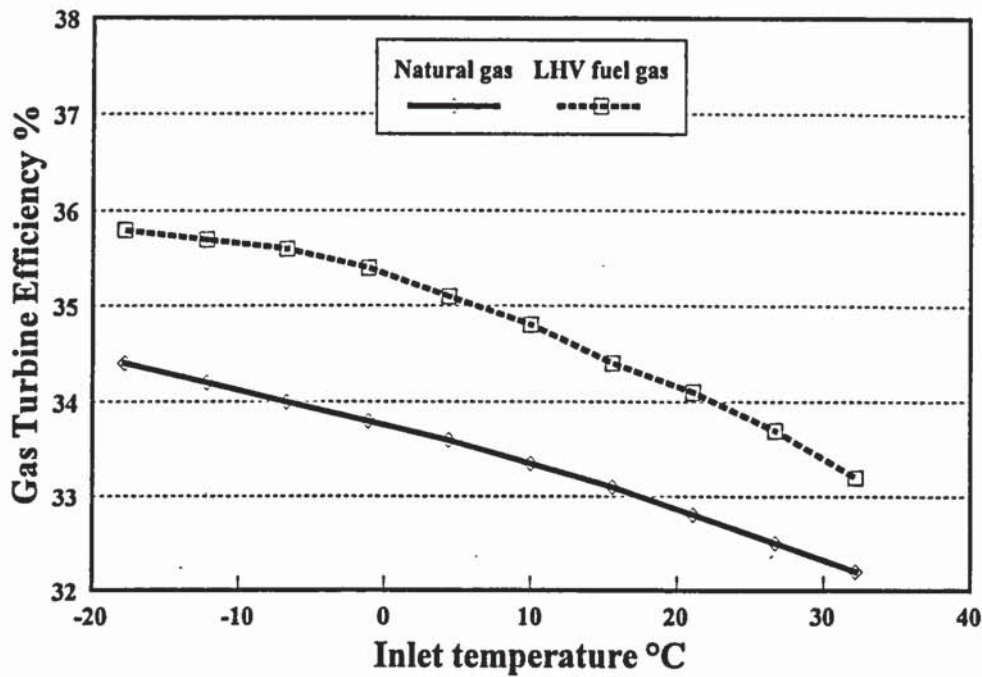


Figure 8-7. LM2500 efficiency as a function of ambient temperature.

The results presented in Figure 8-8 give a further example of the performance of gas turbines. The normalised exhaust mass flow is shown as a function of gas turbine load for both engines. It is seen how different engine types (industrial/aero-derivative) and operation control procedures influence gas turbine performance. Exhaust temperatures for the two cases are shown in Figure 8-9. These two results are especially important when the part-load characteristics of new power plant systems are studied. Although not critical in this study, the results again emphasise the need for accurate modelling of gas turbines. Without an attempt to include the control procedures for the engines, it is impossible to estimate their performance accurately. This is because a gas turbine performance analysis using LHV gas is, in fact, an analysis of off-design point operation.

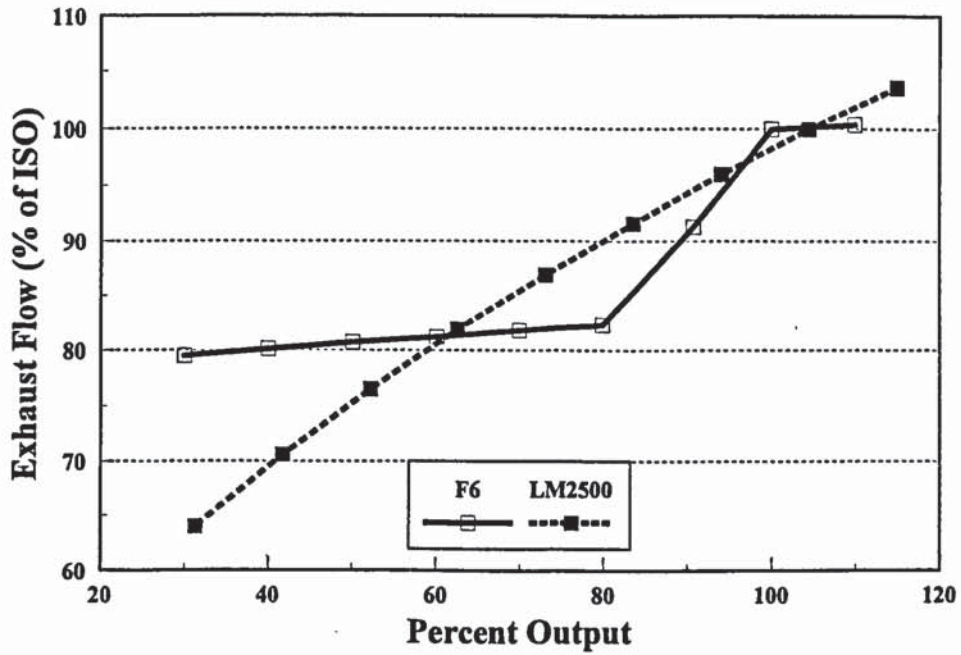


Figure 8-8. Exhaust mass flow, gas turbine part-load operation with LHV gas, industrial F6 and aero-derivative LM2500.

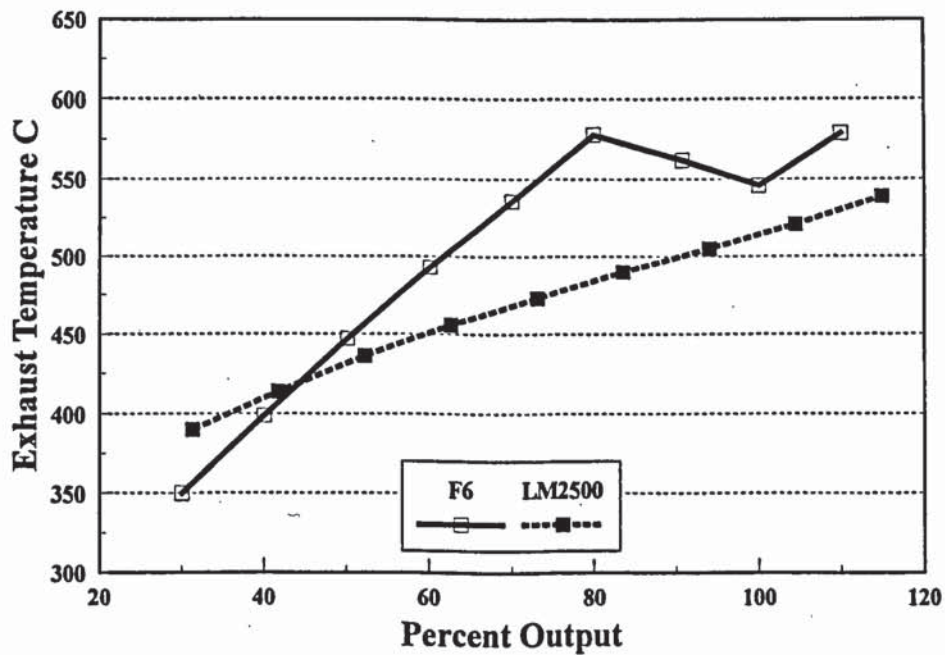


Figure 8-9. Exhaust temperature, gas turbine part-load operation with LHV gas, industrial F6 and aero-derivative LM2500.

8.6.3 Summary

The gas turbine modelling procedure used in this work is as follows:

- A gas composition is generated from the gasifier model.
- This gas is used as a fuel in a GATE/CYCLE gas turbine model.
- An Aspen model for a gas turbine is designed.
- The characteristic features of the gas turbine are copied to the Aspen model.
- When integrated into an IGCC plant model, the gas turbine model determines the amount of fuel gas fired, and therefore also the amount of biomass fed to the gasifier.

8.7 The gas turbine model using fast pyrolysis liquid

The gas turbine model described in the previous chapter was also used for fast pyrolysis liquid. The scant experimental data available did not suggest any major differences between the performance of fuel oil operation compared to pyrolysis liquid operation. Therefore, fast pyrolysis performance was based on using light fuel oil in both of the above engines. The models were used to reproduce engine performance when fired with fuel oil /198/. The engine parameters were fixed and the model was then employed for pyrolysis liquid. Hence, the engine efficiencies for pyrolysis liquid and fuel oil were the same.

9. INTERNAL COMBUSTION ENGINES

The use of fuel gas from gasification (low heating value, LHV gas) as fuel in internal combustion (IC) engines is reviewed in this chapter. The state-of-the-art of technology is presented, and the modelling approach and the Aspen model that was built are described.

9.1 Introduction

Modelling the performance of an internal combustion engine using a non-traditional fuel, in this work LHV gas instead of natural gas, is even more difficult than modelling the performance of a gas turbine. There are several reasons for this, but the overriding issue is the batch-wise combustion in the cylinder of an internal combustion engine. Combustion in a cylinder is a dynamic phenomenon and very difficult to model rigorously. In the public domain there are no modelling tools capable of estimating the performance of an internal combustion engine when a completely new fuel is used. Therefore, the model designed in this chapter is different from other unit operation models designed in this work in so far as it employs an assumed power production efficiency for the engine. The model designed in this work for an internal combustion engine fired with LHV gas is largely based on an analogy to an existing natural-gas-fired gas engine.

In this section the availability, experience and requirements relating to the use of LHV gas in engines is reviewed. Internal combustion engines (both diesel and Otto engines) may be fired with LHV gas in addition to liquid and gaseous hydrocarbon fuels. Although practised more or less successfully for the past 50 years with LHV gas produced mainly from coal but also from biomass, the gasification IC engine power plant concept still remains at the development stage. The power plants built so far, which can be described as demonstration plants, have been operated on a scale between approximately 20 and 150 kW_e /199/. For both co-generation and power-only projects, no gasification IC engine power plant concept can be said to be commercially available for biomass.

A typical problem has been the low availability of the engine power plant. All applications have encountered problems with gas cleaning. The engines require rather strict limits for impurities in the fuel gas, e.g. heavy tars, particulates, some residual compounds. It is difficult to establish limits for these impurities, as accurate limits exist only for natural gas operation. Despite numerous projects, so far there are no units using fuel gas derived from biomass gasification in continuous operation in the industrial countries.

In this thesis, the capacity range considered is 1 to 25 MWe. As already explained in section 1.3.6, small-scale concepts (below about 1 MWe) are excluded from this work. Small-scale biomass gasifier-engine systems have been extensively tested, but the results to date have been rather unfavourable /200/. Many of these installations have been located in developing countries.

Only some experimental work with gasification-engine concepts aimed at scales larger than about one MWe have been reported /201, 202/. The overriding problem in previous efforts has been the fuel gas quality: tar, dust, soot, and ash in the fuel gas are detrimental to engine operation. These reduce engine performance, increase maintenance costs, and may prevent operation altogether. If a turbo-charger is employed, deposits may form on the compressor blades /201/. Biomass fuel gas contains ammonia, which forms NO_x emissions in combustion. These emissions have been reported to be unacceptably high /203/. Water scrubbing to clean the fuel gas has been employed, which leads to a wastewater stream. This leads to higher investment and operating costs.

Diesel engines were mainly employed for LHV gas before this decade. However, the development of spark-ignition gas engines for natural gas made this engine type available for LHV gas. Nevertheless, as of spring 1998, only one European engine manufacturer is seriously considering using LHV gas in their engines /204/. Industrial-scale continuous experiences with LHV gas in gas engines have not been reported in the open literature.

In the next section, some characteristics of IC engine operation with LHV gas are briefly reviewed.

9.2 Using LHV gas as fuel in combustion engines

Recently, Herdin /205/ reported on the operation of an engine coupled to a gasifier. The overall power production efficiency was 26%. However, the size of the engine tested was not given, although it is believed to be around 200 to 500 kW_e. The test is important as it was carried out with a modern engine employing catalytic exhaust gas emission control devices. The tests confirm the gas cleaning problems previously encountered with this concept. Although NO_x emissions were acceptably low because of lean burn combustion, CO emissions exceeded the German emission standard by a factor of 3 to 5. And when an oxidizing catalyst was employed for the exhaust gases, the catalyst was soon poisoned by contaminants in the fuel gas tar. It is concluded that the gas cleaning stage is not yet proven in continuous operation, and that emissions have not yet been reduced to a satisfactory level.

In addition to the problem of fuel gas contaminants mentioned above, the second major issue related to IC engine operation with LHV gas is derating. This is the decreased maximum power output produced in an engine with an alternative fuel compared with that for which the engine was designed. Derating leads to an increased specific capital investment.

The derating is partially intrinsic because of the lower heating value of a stoichiometric mixture of LHV fuel gas and air compared with natural gas and air. The volumetric heating value of LHV gas from the air gasification of wood is typically about 10 to 15% of natural gas. However, the heating value of a stoichiometric mixture of LHV gas is only about 25% less than that of natural gas, and the intrinsic derating is thus about 25% /206/.

Derating may be partly overcome by three alternative actions:

- increasing the engine compression ratio,
- pressurizing the fuel gas by a turbo-charger, or
- using an additional fuel, i.e. dual-fuel operation.

The last alternative is technically the most attractive.

LHV gas has a relatively high octane number and is hence more suitable for Otto engines than diesel engines. The octane number describes the anti-knock quality of the fuel that is required for high compression ratio spark-ignited Otto engines. Knocking is a sudden and jerky pre-combustion taking place during the compression stage before (spark) ignition. It leads to irregular combustion and may ultimately damage the engine. The octane number of LHV gas is highly dependent on the hydrogen content of the gas. The higher the hydrogen content, the less suitable the gas is for high compression ratio engines. Pressure ratios of at least 11:1 have successfully been employed for typical air gasification fuel gas /206/.

Pressure charging increases the power output of the engine. However, there is very little experimental data available on turbo-charged engine operation with LHV gas. In principle, two alternatives are available for pressure-charging: LHV gas may be fed to the inlet of the engine combustion air compressor (as in /201/), or pressurised gasification may be applied to engine injectors (not reported in the open literature). In the latter case, part of the engine's turbo-charged compressor air may be used as the gasification air. However, both applications require modifications in existing engine configurations. The estimation of engine performance in such an operation is beyond the scope of this work. Such a system should be modelled with specific simulation modelling tool capable of predicting engine performance with different fuels.

Dual-fuel operation has been tested in diesel engines. Recently, as gas (Otto) engines have gained more popularity in LHV gas applications, dual-fuel operation has received less attention /206/.

The fuel gas / air mixture heating value before ignition, which has been referred to above, is only one factor controlling the power output of an engine. Stassen points out /206/ that it only fixes the limits of the maximum power output. Additional factors affecting the actual engine power output are the speed of flame propagation in the engine cylinders, mixture ignitability, and engine characteristics. The factors are interconnected /206/.

Differences in the flame propagation speeds of LHV gas components, especially hydrogen (H_2), carbon monoxide (CO) and methane (CH_4), complicate engine operation. The flame propagation speed of hydrogen is ten times higher than that of CO and CH_4 . At any rate,

the speed of flame propagation for a fuel gas will always be different compared with that of a gasoline-air mixture. If the speed of flame propagation is low compared with the average piston speed, part of the fuel gas air mixture may burn during the exhaust stroke, causing engine damage and a drop in power output. For this reason, relatively low piston speeds are usually preferred, and consequently slow-speed engines yield the best performance. This is true for both diesel and Otto engines.

The tendency of an engine to knock is mainly dependent on the compression ratio and on the composition of LHV gas, largely on its hydrogen content. Knocking may be reduced by a number of engine characteristics, but many of them are contradictory to achieving the maximum engine power output and minimal derating /206/. An optimum choice with regard to ignition timing, air-fuel ratio, engine speed, engine load, and mixture temperature/pressure may be established in engine experiments. Recent developments in engine simulation and engine control techniques provide new means of optimising the performance. However, numerical simulation has not been widely applied to improving LHV gas utilisation in engines.

9.3 Using pyrolysis liquid as fuel in diesel engines

There is very little data available on the industrial-scale operation of diesel engines with pyrolysis liquid. The largest-scale work has been carried out by Wärtsilä NSD Oy in a 1.5 MWe engine /207/. Ormrod has been operating one cylinder in a six cylinder 250 kW engine /149/. All other work has been carried out with smaller engines /150/, /151/, /152/.

According to the reported work, engine performance is close to the operation with heavy mineral oils. However, the injection system may consume more power than in fuel oil operation, and consequently overall power plant efficiency may be lower when firing pyrolysis liquid. Even less is known about the emissions from engines using pyrolysis liquid as fuel. There are indications that emissions of hydrocarbons and CO are higher in pyrolysis liquid operation than in diesel and heavy fuel oil operation /208, 209/. An oxidative catalyst is assumed for power plants employing pyrolysis liquid as fuel.

9.4 Model description for a gas engine using LHV gas

On the basis of the review presented above it is evident that a rigorous performance analysis is beyond the scope of this work. One engine manufacturer has at its disposal calculation routines to estimate engine performance with LHV gas /204/. However, this is the only known company to employ such routines. No modelling routines capable of a rigorous performance analysis once the fuel gas composition is known have been found in the public domain.

The engine is represented in this study essentially as a black box model. The model features are based on two sources of information:

- the energy balance of a commercial natural-gas-fired engine shown in Table 9-1 /210/
- two estimates of an engine manufacturer for a state-of-the-art gas engine performance with an LHV gas (Table 9-2) /211/.

Table 9-1. Energy balance around a state-of-the-art gas engine /210/.

	Energy kW
IN	
Fuel in	12 196
OUT	
Shaft power	5 000
Lube oil cooling	744
Jacket water	1 220
High temperature charge air cooling	228
Low temperature charge air cooling	647
Radiation losses	354
Flue gas sensible heat	4 003

Table 9-2. Engine performance with LHV gas. Operation with natural gas = commercial operation. BMEP = Brake mean effective power.

	Realistic estimate	Optimistic estimate	Operation with natural gas
BMEP bar	10	12	15.9
Efficiency %	30	37	43.3
Exhaust gas temperature °C	485	430	418
Exhaust gas mass flow kg/s	8.1	8.6	9.6
Power output per cylinder kW	200	240	315

The data shown in Table 9-1 is for natural gas, and is representative of a state-of-the-art gas engine. In the Aspen performance analysis, a similar distribution of energy is assumed for an engine using LHV fuel gas with the following corrections:

- Overall power production efficiency is lower than with natural gas operation. The optimistic estimate (Table 9-2) was employed as input for the AspenPlus model of an engine using LHV gas
- A corresponding exhaust gas temperature is selected on the basis of the data in Table 9-2.

The Aspen model for the gas engine is shown in Figure 9-1. The principal model user input and outputs are presented in Table 9-3. The model accepts power production efficiency (design specification EFF converts the defined quantity of fuel gas energy into power), and exhaust gas temperature as input, and calculates the composition of the flue gas. Based on a user-defined power output, the model finds the fuel gas feed required by the engine (design specification POWER). As the exhaust gas temperature is fixed, the model subtracts the power output and the sensible heat in the flue gas from the chemical energy in the fuel, and defines the remainder as heat losses (design specification FLTEMP). The AspenPlus input file is shown in Appendix 9.

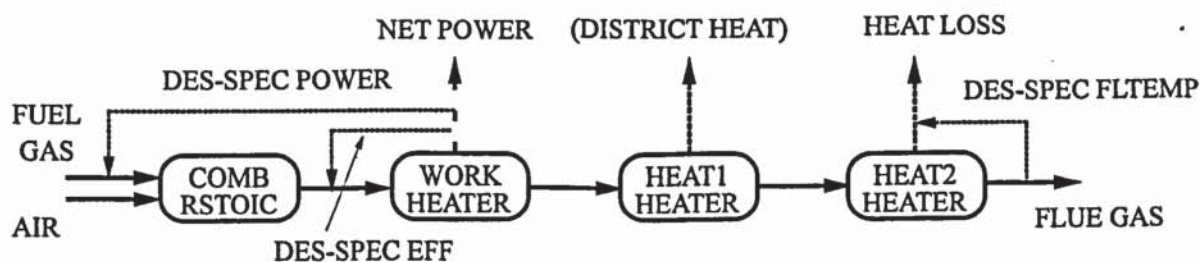


Figure 9-1. AspenPlus Block flow diagram of the gas engine model. Design specifications shown.

Table 9-3. Gas engine model inputs and outputs.

INPUT	Fuel gas composition ¹⁾ Fuel gas temperature and pressure °C/bar Combustion air kg/s Power production efficiency % Flue gas °C Power output MWe
OUTPUT	Fuel gas kg/s Flue gas kg/s Flue gas composition Heat loss %

¹⁾ Gas composition is determined in an integrated power plant model by the previous process stages, gasification and gas clean-up

As a summary, the following major parameters are different when the engine is fuelled with LHV gas than when operated with natural gas:

- Power production efficiency is reduced
- Exhaust temperature is increased
- Engine power output is reduced (de-rating).

The effects of the critical engine performance parameters listed in the previous section (ignition timing, air-fuel ratio, engine speed, engine load, and mixture temperature/pressure) on engine efficiency are not directly considered in the current model.

9.5 Model description for a diesel engine using pyrolysis liquid

The performance estimate for an engine fired with pyrolysis liquid is derived using an approach similar to that employed for LHV gas in the previous section:

- The energy balance is based on an industrial balance for a heavy fuel oil fired diesel engine.
- The energy balance is corrected to take account of the specific properties of pyrolysis liquid as a fuel.

The industrial energy balance is based on the reference /210/. The engine efficiency with pyrolysis liquid is assumed to be two percentage points below the efficiency in heavy fuel oil operation. This is because a modified injection system with an increased power consumption is required. A fuel homogenizer which also adds to the plant's internal power consumption is used. Depending on the engine capacity, the heavy-fuel-oil-fuelled power plant's efficiency ranges from 41 to 45% (plant output from 1 to 18 MWe) /212/. The AspenPlus model and derivation of the energy balance around the engine is calculated using an approach similar to that presented in the previous section.

9.6 Summary

Two performance models have been built: one for a gas engine using LHV gas, and one for a diesel engine using pyrolysis liquid. The models calculate the energy balance for the system when a number of engine parameters are fixed.

The models have been used to study the effect of injection pressure on gas engine power plant efficiency in chapter 10.13.1. No actual model verification can be done.

10. RESULTS OF THE PERFORMANCE ANALYSIS

The results of the performance analysis carried out with the models built are presented in this chapter. Firstly, one of the models built is reviewed and its features are explained. The next sections summarise the mass and energy balances of all the power plant process concepts estimated with the simulation models. The performance balances are eventually used to size and cost the systems. The system efficiencies calculated with models are summarised and compared. The effect of technical uncertainties on the overall efficiency is studied in connection with pyrolysis power plant concepts. Finally, two IGCC models are used to study potential improvements within the concepts. The results are compared with two published references. Unless otherwise stated, all of the values presented in the tables and figures of this chapter have been generated with the simulation models built.

10.1 Introduction

The mass and energy balances for the systems studied are presented in this chapter. Six advanced process configurations were analysed in addition to the Rankine cycle:

- Pressurised gasification combined-cycle
- Atmospheric pressure gasification combined-cycle
- Pressurised gasification Steam-injected-gas-turbine cycle
- Gasification - internal combustion engine
- Fast pyrolysis - internal combustion engine
- Fast pyrolysis - combined-cycle
- Rankine cycle - steam turbine

The concepts are summarised in Table 10-1. For each concept, two or more capacities were studied. The studied capacity ranged from 5 to 60 MWe, and the results of 21 advanced concepts are reported. In addition, the Rankine power plant was modelled and is employed as a reference over the whole capacity range.

Note that the efficiency based on the lower heating value (lhv) of the fuel is used. The corresponding value based on hhv is also shown in chapters 10.1 - 10.9, in which the individual concepts are presented. All of the performance balances were calculated with Aspen-Plus simulation software, as explained previously in chapters 1.6 and 3.

Table 10-1. Power plant concepts modelled.

Concepts	Number	Nominal capacity MWe
Pressurised gasification combined-cycle (PCC)	1-4	30, 60
Atmospheric pressure gasification combined-cycle (ACC)	5-8	5, 30, 60
Pressurised gasification Steam-injected-gas-turbine cycle (STIG)	9-13	5, 20, 40
Gasification - internal combustion engine (GE)	14-15	5, 20
Fast pyrolysis - internal combustion engine (PD)	16-17	5, 25
Fast pyrolysis - combined-cycle (PyCC)	18-21	5, 30, 60
Rankine cycle - steam turbine	22-24	5, 15, 60

10.2 Description of an IGCC model

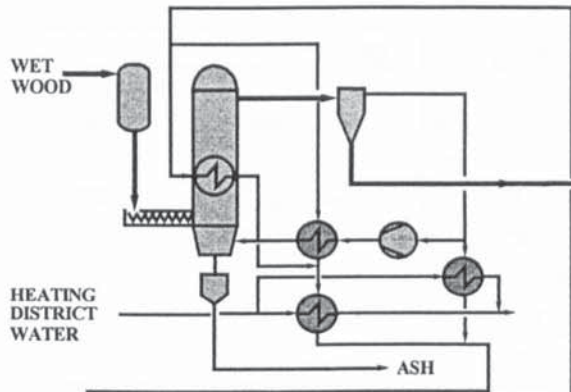
This section describes a power plant model. An atmospheric pressure IGCC (ACC) is used as an example. A flow diagram of the process is shown in Figure 10-1. A block flow diagram of the concept is shown in Figure 10-5.

The process model is built with the following unit operations:

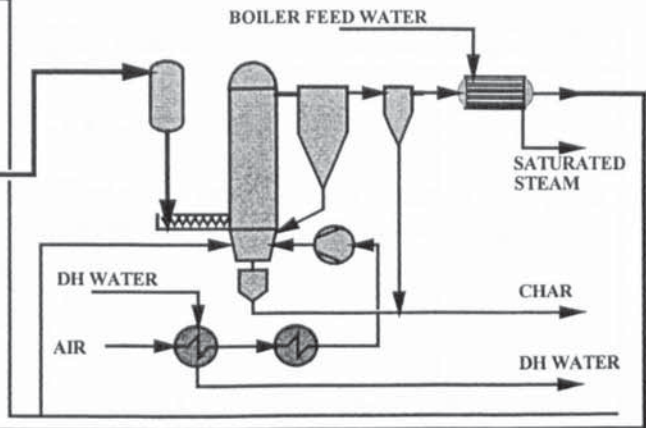
- Wood drying
- Gasification
- Gas cleaning and compression
- Gas turbine
- Steam cycle

The individual unit models were presented in Chapters 4, 5, 6, and 8. Table 10-2 summarises some of the modelling features of these units. The separately developed unit models are integrated to form an IGCC model. The significance of the design specifications and Fortran statements are explained in Chapter 3 and Appendix 14.

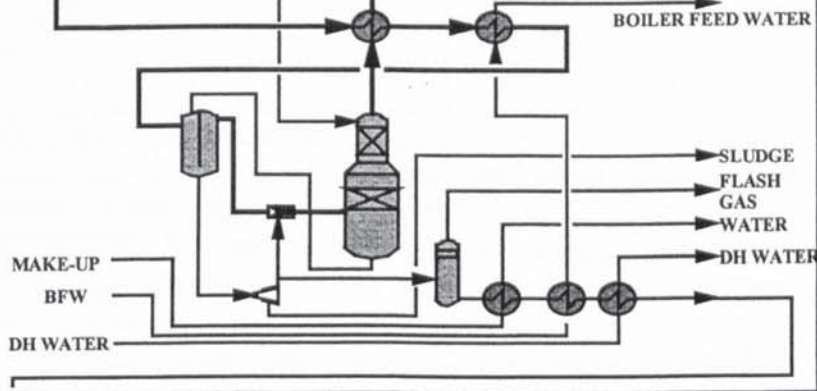
DRYING



GASIFICATION



GAS CLEANING



POWER CYCLE

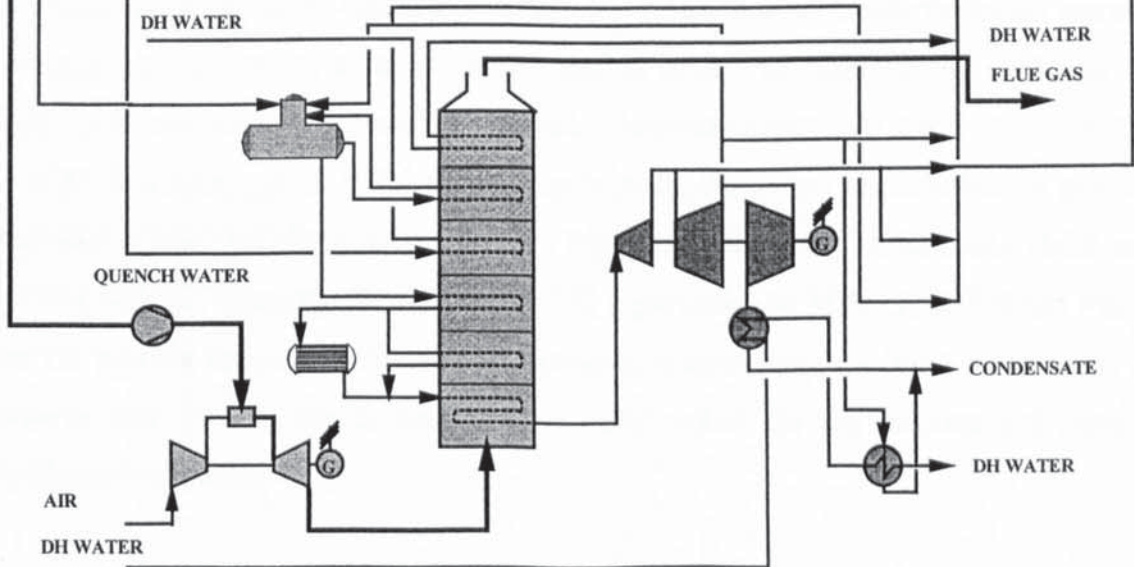


Figure 10-1. Flow diagram of an IGCC.

Table 10-2. Characteristics of unit models in an integrated IGCC model.

	Wood drying	Gasification	Gas cleaning	Gas turbine	Steam cycle
Components NC ¹⁾	Wood	Wood, char, ash	Char, ash		
Mixed	CO ₂ , N ₂ , Ar, O ₂ , H ₂ O	H ₂ , CO, CO ₂ , CH ₄ , N ₂ , Ar, O ₂ , NH ₃ , H ₂ O, C ₆ H ₆ , C ₂ H ₄ , C ₁₀ H ₈ , C ₆ H ₆ O	Those in gasification and H ⁺ , NH ₄ ⁺ , H ₂ CO ₃ , HCO ₃ ⁻ , NH ₂ CO ₂ ⁻ , OH ⁻ , CO ₃ ⁻²	Those in gasification	CO ₂ , N ₂ , Ar, O ₂ , H ₂ O
Physical properties	SYSOP ²⁾ STEAMNBS ³⁾	RK-Soave ⁴⁾	ELECNRTL ⁵⁾	RK-Soave	RK-Soave STEAMNBS
No. of design specifications	2	2	1	2	4
No. of FORTRAN statements	4	2			7

- 1) User defined non-conventional (NC) components
- 2) Ideal gas equation of state for vapour phase, ideal liquid activity coefficient model for liquid phase, Raoult's law for vapour-liquid equilibrium
- 3) The 1984 NBS/NRC /213/ equation of state for all thermodynamic properties of steam
- 4) The Redlich-Kwong-Soave equation of state for all thermodynamic properties except Rackett model for molar volume
- 5) RK-Soave for vapour phase, electrolyte NRTL (non-random two liquid) for heats of mixing

Convergence for the model calculation is typically good, in other words the model convergence takes place in a few minutes without manual input. The most difficult section is the steam cycle, because several iterative calculation loops are created. As always in sequential modular simulations, good initial values help to make the convergence faster. To give an impression of the size of the IGCC model, a typical running time for the model (built and operated with the AspenPlus™ version 9.3-1 in a portable 166 MHz, 32 MB RAM Pentium PC running under the Windows 95 operating system) requires about 1.5 minutes to converge with good (close to final results) initial values for tear streams and design-specification variables.

The most important inputs and outputs of the model are listed in Table 10-3.

Table 10-3. The most important inputs and outputs in an integrated IGCC model using a flue gas dryer.

	Wood drying	Gasification	Gas turbine	Steam cycle
Input	Wood ⁵⁾ and moisture Energy requirement Final moisture	Gasification air/feedstock-ratio Heat loss ¹⁾	Isentropic ef- ficiencies ²⁾ Pressure ratio	Superheat steam p, T Medium pressure Low pressure
Output	Flue gas ⁴⁾ Power consumption Co-gen heat	Fuel gas ⁴⁾ Co-gen heat Power consumption Waste water ³⁾	Power output Flue gas ⁴⁾	Superheat steam ⁵⁾ Power output Co-gen heat Power consumption

- 1) Estimated as 2% of feed LHV (a representative industrial value)
- 2) Are available from a GATE/CYCLE analysis, see Chapter 8
- 3) In atmospheric pressure gasification
- 4) Composition, amount, temperature, pressure
- 5) Mass flow

All the basic unit building blocks in the model (note Appendix 13, where each block is shown) have to be specified individually. Inputs are required for each block, and each block produces a report. An example of an input is presented in Figure 10-2, which shows the input form for a heater. An example of an output is presented in Figure 10-3, which shows the simulation results for a heat exchanger.

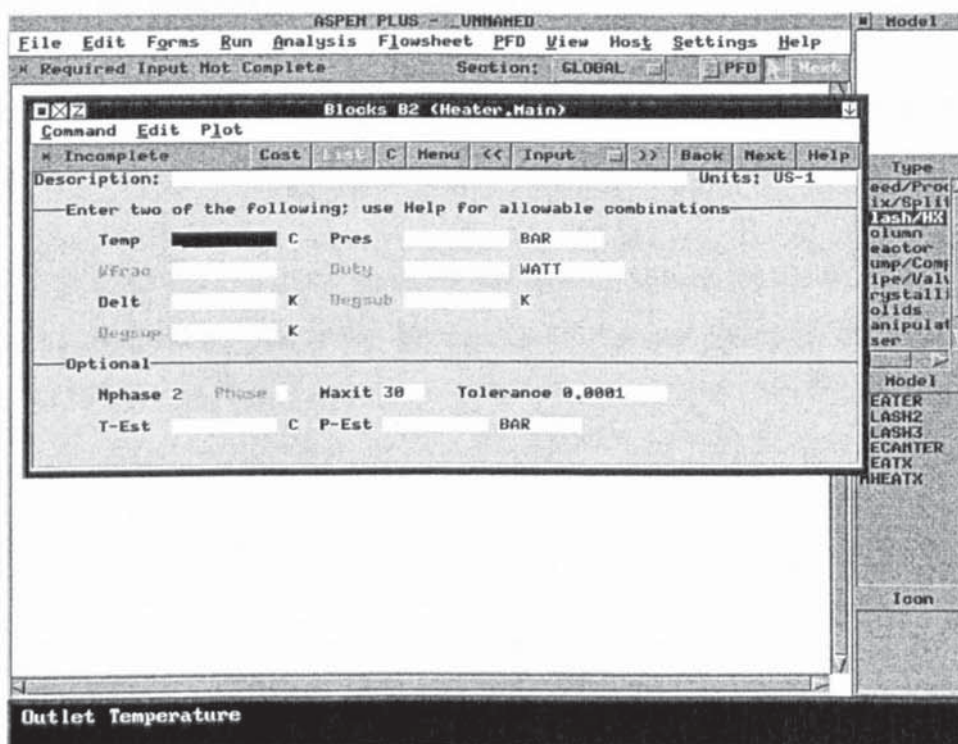


Figure 10-2. An example of a simulation input.

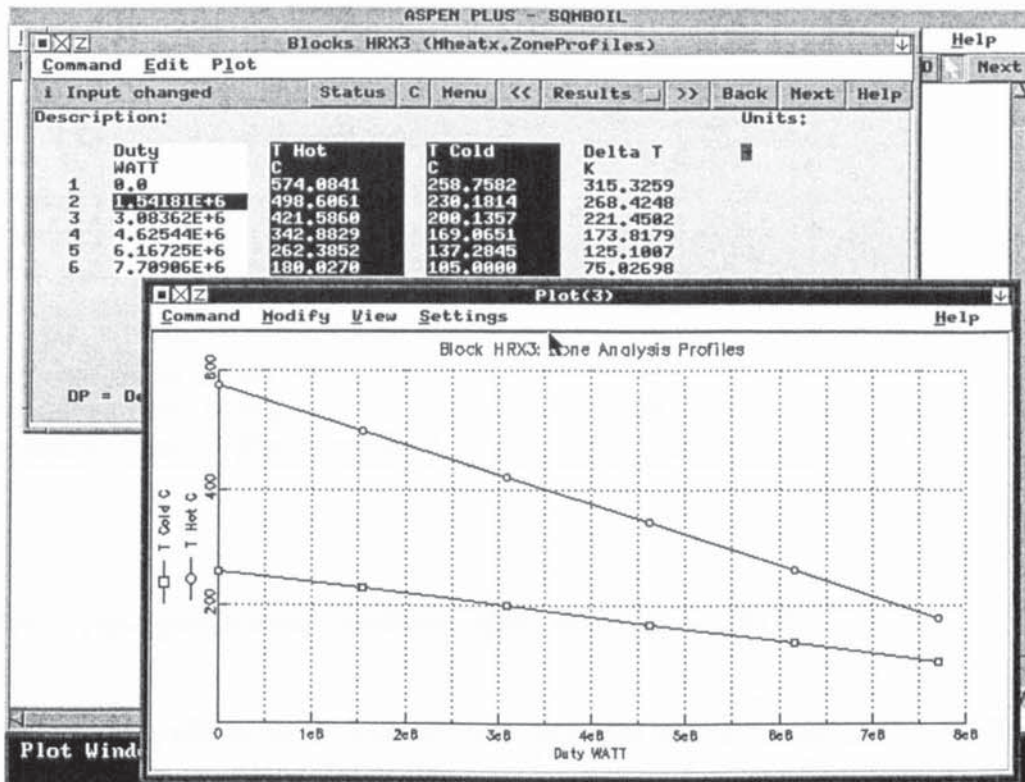


Figure 10-3. An example of the simulation results.

Energy balance closure for this IGCC model is 99.9%, defined as: (Energy in all flows out from plant model) / (Energy in all flows into plant model) * 100. An energy balance closure higher than 99.8% was specified as the requirement for a model to be considered adequate.

A summary of the energy balance from the simulation model for the IGCC system is shown in Table 10-4. The higher heating value (hhv)-based efficiency for this concept is calculated as follows: (power output - power input) / fuel hhv in, $(24.24+2.39+9.13-6.54-0.03-0.12) / 95.90 * 100 = 30.3\%$. Hhv-based values are used here as an example because the data is readily available from AspenPlus, and the above requirement for energy balance closure was practical to check from hhv data.

Table 10-4. Energy balance for IGCC concept No 8 (section 10.4) in MW.

IN	HHV	Sensible heat	Power	Total	% of input
Biomass	95.90			95.90	93.48
Gasifier			0.03	0.03	0.03
Fuel gas compression			6.54	6.54	6.37
BFW treatment			0.12	0.12	0.12
Total	95.90		6.68	102.59	100.00
OUT					
Gasifier air expander			2.39	2.39	2.33
Gas turbine			24.24	24.24	23.63
Steam turbine			9.13	9.13	8.90
District heat		30.31		30.31	29.55
Flue gas losses		25.45		25.45	24.80
Dryer losses		3.71		3.71	3.62
Gasification losses	1.92	2.04		3.96	3.86
Gas cleaning losses		1.74		1.74	1.70
Gas turbine losses		1.52		1.52	1.48
Steam cycle losses		0.03		0.03	0.03
Total		64.80	35.76	102.48	99.89
Unaccounted				0.11	0.11

10.3 Bases for the analysis

The process performance values reported in the tables below correspond to a 15 °C ambient rating.

Table 10-5 presents the elemental analysis and heating values for the wood feedstock employed in the evaluations. The wood feedstock to the power plants for each concept is assumed to be 50 wt% wet wood chips.

Table 10-5. Analysis of the wood feedstock employed, a wood fuel analysis at VTT /8/ (a mixture of Nordic hard and soft wood).

Component	wt% moisture-free wood
Carbon	50.4
Hydrogen	6.0
Nitrogen	0.1
Sulphur	-
Oxygen	43.0
Ash	0.5
Lower heating value MJ/kg (m.f.)	18.9
Higher heating value MJ/kg (m.f.)	20.2
Lower heating value MJ/kg (as received)	8.2

10.4 Pressurised gasification combined-cycle, concepts 1-4 (PCC)

Four pressurised gasification combined-cycle concepts are estimated (Table 10-6). Both power-only (two cases) and co-generation of heat and power (two cases) are included. A block flow diagram of the plant configuration is shown in Figure 10-4.

The nominal capacities of the concepts are 30 and 60 MWe. Plant output is determined by the gas turbine selection, which is established on the basis of the availability of gas turbine performance data on LHV fuel gas. Reliable data was available for only two engines: the General Electric (GE) LM2500 aero-derivative, and the GE Frame 6B industrial gas turbine /178, 187/. Turbine performance with LHV gas, a critical issue with the IGCC concepts, is reviewed in detail in Chapter 8. The LM2500 has a higher pressure ratio and a higher firing temperature, and consequently, a higher efficiency than the Frame 6.

Table 10-6. Pressurised gasification combined-cycle configurations.

Concept	Nominal capacity MWe	Gas turbine	Dryer type	Products
1	30	LM2500	Flue gas dryer	Power
2	30	LM2500	Flue gas dryer	Power and heat
3	30	LM2500	Steam dryer	Power and heat
4	60	Frame 6	Flue gas dryer	Power

Table 10-7. Major process flow rates and conditions, concepts 1-4. Steam cycle conditions 60 bar and 485 °C. Internal power consumption breakdown in Table 10-9.

	1	2	3	4
Gas turbine net power, MW	23.3	23.3	23.3	40.8
Steam turbine net power, MW	9.4	7.6	6.9	20.2
Internal consumption, MW	0.8	0.8	1.0	1.3
Net plant power output, MW	31.9	30.0	29.1	59.8
District heat, MW		23.0	33.3	
Wood feed (as received), kg/s	8.2	8.2	8.2	16.1
Ash produced, kg/s	0.02	0.02	0.02	0.04
Raw gas, kmol/s	0.48	0.48	0.48	0.94
Flue gases, kmol/s	2.37	2.37	2.37	5.02

Table 10-8. Gas turbine characteristics, concepts 1-4.

	1	2	3	4
Power output, MW	23.3	23.3	23.3	40.8
Compressor air flow, kg/s	64.1	64.1	64.1	136.3
Compressor pressure ratio	18.2	18.2	18.2	12.3
Fuel gas flow, kg/s	12.0	12.0	12.0	23.5
Combustion temperature, °C	1 240	1 240	1 240	1 100
Fuel gas temperature, °C	480	480	480	480
Flue gas flow, kg/s	68.9	68.9	68.9	145.7
Gas turbine exhaust temperature, °C	547	547	547	546

Table 10-9. Plant's internal power consumption summary (kW), concepts 1-4.

	1	2	3	4
Milling and feeding of wood	310	310	350	250
Drying	50	50	190	80
Gasification	350	350	350	770
Steam system & BFW treatment	100	100	120	180
Total kW	810	810	1 020	1 280

Table 10-10. Overall efficiencies, concepts 1-4.

		1	2	3	4
Electricity	LHV %	47.1	44.3	42.9	45.1
	HHV %	38.4	36.1	35.0	36.8
Heat	LHV %		33.9	47.2	
	HHV %		27.6	38.5	

10.5 Atmospheric pressure gasification combined-cycle, concepts 5 - 8 (ACC)

Four gasification combined-cycle concepts based on atmospheric pressure gasification are estimated (Table 10-11). Both power-only (three cases) and co-generation of heat and power (one case) are included. A block flow diagram of the plant configurations is shown in Figure 10-5. The greatest difference on the block level, compared with concepts 1 - 4, is a gas water wash prior to a compressor, which is needed to compress the fuel gas to gas turbine combustor pressure.

A complete AspenPlus flow diagram for the concept is shown in Appendix 13, which also includes a complete input file.

Table 10-11. Atmospheric pressure gasification combined-cycle configurations.

Concept	Nominal capacity MWe	Gas turbine	Products
5	5	Typhoon	Power
6	30	LM2500	Power
7	60	Frame 6	Power
8	30	LM2500	Power and heat

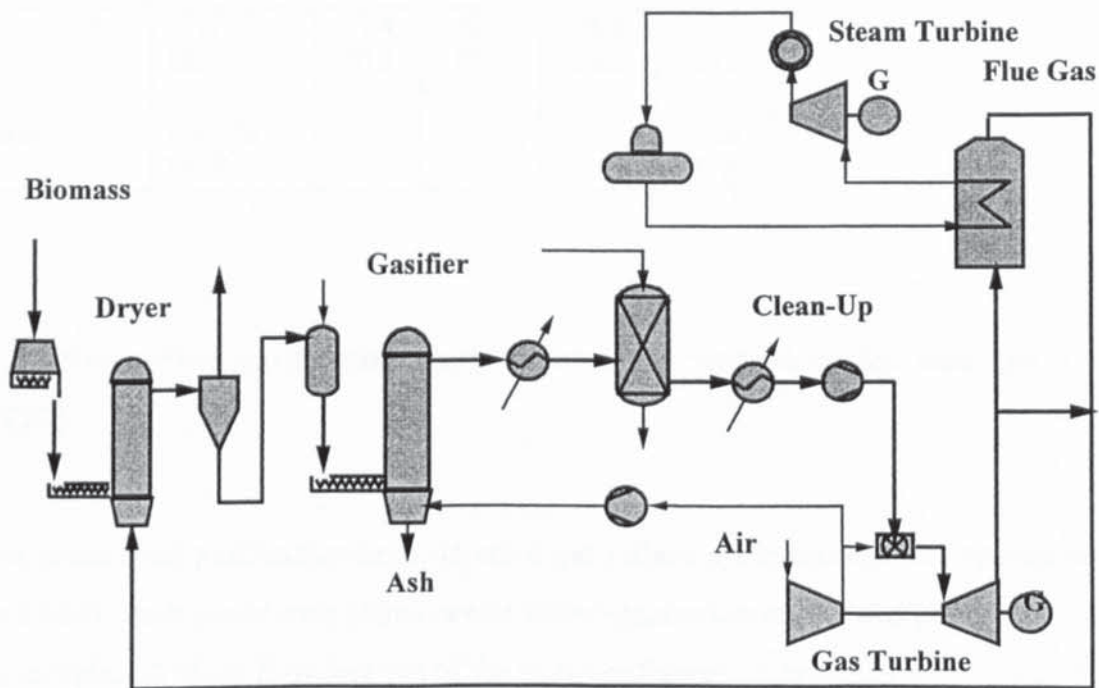


Figure 10-5. Block flow diagram of the atmospheric pressure gasification combined-cycle configurations, concepts 5-8.

The nominal capacities of the plants are 5, 30 and 60 MWe. As before, plant output is determined by the gas turbine selection. Concept 5 employs a European Gas Turbines (EGT) Typhoon engine, concepts 6 and 8 employ a GE LM2500 engine, and concept 7 employs a GE Frame 6B engine. Concept 8 applies co-generation of heat and power. There is reliable data for the GE engines /178, 187/. However, the performance of the Typhoon engine with LHV gas was estimated on the basis of the analogy with the other industrial turbine, Frame 6.

The plant consists of the following major units: wood receiving and storage, milling and flue gas drying, gasification, particulate removal, gas compression, and a combined-cycle power system. All of the units are single-train except for the dryer, which in concept 7 has two trains. In addition to the main processing units, the plant includes all necessary support facilities.

A summary of the process streams is given in Table 10-12. The gas turbine section's performance is summarized in Table 10-13. A summary of the plant's internal power consumption is shown in Table 10-14. The overall efficiencies for the concepts are shown in Table 10-15.

Table 10-12. Major process flow rates and conditions, concepts 5-8. Steam cycle conditions 60 bar and 485 °C.

	5	6	7	8
Gas turbine net power, MW	4.7	24.2	42.3	24.2
Steam turbine net power, MW	2.9	13.5	28.1	9.1
Expander, MW	0.5	2.4	3.5	2.4
Internal consumption, MW	1.4	6.9	11.6	6.7
Net plant power output, MW	6.6	33.2	62.3	29.1
District heat, MW				30.3
Wood feed (as received), kg/s	2.1	9.8	19.1	9.8
Ash produced, kg/s	0.005	0.02	0.05	0.02
Raw gas, kmol/s	0.11	0.58	1.94	0.58
Flue gases, kmol/s	0.47	2.44	5.1	2.44

Table10-13. Gas turbine characteristics, concepts 5 - 8.

	5	6	7	8
Power output, MW	4.7	24.2	42.3	24.2
Compressor air flow, kg/s	18.8	64.8	136.5	64.8
Compressor pressure ratio	14.5	18.7	12.5	18.7
Fuel gas flow, kg/s	2.9	13.5	26.2	13.5
Combustion temperature, °C	1 100	1 240	1 100	1 240
Fuel gas temperature, °C	255	255	255	255
Flue gas flow, kg/s	20.0	70.5	147.3	70.5
Gas turbine exhaust temperature, °C	511	543	547	543

Table10-14. Power consumption summary (kW), concepts 5 - 8.

	5	6	7	8
Gasification	10	40	90	30
Gas treatment	1 340	6 720	11 260	6 540
Steam system & BFW treatment	40	130	240	120
Total kW	1 390	6 900	11 590	6 680

Table10-15. Overall efficiencies, concepts 5-8.

		5	6	7	8
Electricity	LHV %	37.4	40.9	39.5	37.2
	HHV %	30.5	33.4	32.2	30.3
Heat	LHV %				38.8
	HHV %				31.6

10.6 Pressurised gasification steam-injected gas turbine cycles, concepts 9 - 13 (STIG)

Five pressurised gasification steam-injected gas turbine cycle concepts are estimated (Table 10-16). Both power-only (three cases) and co-generation of heat and power (two cases) are included. A block flow diagram of the plant configurations is shown in Figure 10-6.

The nominal capacities of the plants are 5, 30 and 60 MWe. As before, plant output is determined by selection of the gas turbine. Concept 9 employs the EGT Typhoon engine, concepts 10 - 12 employ a GE LM2500 engine, and concept 13 employs a GE Frame 6B engine. Reliable data was available only from Palmer and Erbes /178, 187/ for the two GE engines. GATE/CYCLE, a specific gas turbine modelling tool (note discussion in Chapter 8), was used to determine the amount of steam injection allowed. However, the Typhoon's performance was estimated with an analogy similar to that employed in the previous chapter. Concepts 11 and 12 employ co-generation of heat and power. Concept 11 has a steam dryer, and the other STIG concepts employ flue gas dryers.

Table 10-16. Pressurised gasification combined-cycle configurations.

Concept	Nominal capacity MWe	Gas turbine	Dryer type	Products
9	5	Typhoon	Flue gas dryer	Power
10	30	LM2500	Flue gas dryer	Power
11	30	LM2500	Steam dryer	Power and heat
12	30	LM2500	Flue gas dryer	Power and heat
13	60	Frame 6	Flue gas dryer	Power

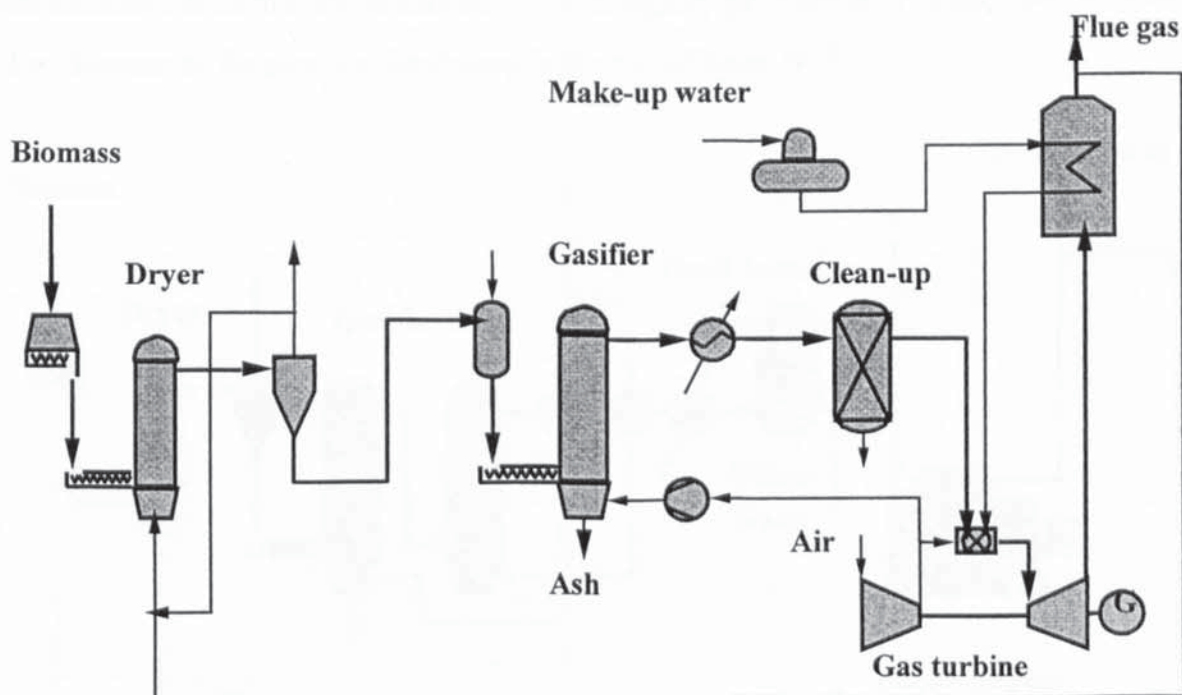


Figure 10-6. Block flow diagram of the pressurised gasification steam-injected gas turbine cycle concepts.

The plant consists of the following major units: wood receiving and storage, milling and drying, gasification, particulate removal, and a gas turbine power system. All of the units are single-train except for the dryer, which in concept 13 has two trains. In addition to the main processing units, the plant includes all necessary support facilities.

A summary of the process streams is given in Table 10-17. The gas turbine section's performance is summarised in Table 10-18. A summary of the plant's internal power consumption is presented in Table 10-19. The overall efficiencies for the concepts are presented in Table 10-20.

Table 10-17. Major process flow rates and conditions, concepts 9-13.

	9	10	11	12	13
Gas turbine net power, MW	5.0	24.5	24.5	24.5	41.6
Internal consumption, MW	0.2	0.9	0.9	0.9	1.6
Net plant power output, MW	4.9	23.6	23.5	23.6	40.0
District heat, MW			31.6	21.8	
Wood feed (as received), kg/s	2.1	8.2	8.2	8.2	16.2
Ash produced, kg/s	0.005	0.02	0.02	0.02	0.04
Raw gas, kmol/s	0.12	0.48	0.48	0.48	0.95
Flue gases, kmol/s	0.7	2.5	2.5	2.5	5.1
Steam injection, kg/s	0.3	2.5	2.5	2.5	0.8

Table 10-18. Gas turbine characteristics, concepts 9 - 13.

	9	10	11	12	13
Power output, MW	5.0	24.5	24.5	24.5	41.6
Compressor air flow, kg/s	18.7	64.6	64.6	64.6	136.3
Compressor pressure ratio	14.8	18.9	18.9	18.9	12.4
Fuel gas flow, kg/s	3.0	12.0	12.0	12.0	23.6
Combustion temperature, °C	1 100	1 180	1 180	1 180	1 100
Fuel gas temperature, °C	255	480	480	480	480
Flue gas flow, kg/s	20.2	71.9	71.9	71.9	146.6
Gas turbine exhaust temperature, °C	409	512	512	512	545

Table 10-19. Power consumption summary (kW), concepts 9 - 13.

	9	10	11	12	13
Milling and feeding of wood	50	350	350	350	330
Drying	50	180	140	180	430
Gasification	50	320	320	320	850
Steam system & BFW treatment	10	20	40	20	10
Total kW	160	870	840	870	1 630

Table 10-20. Overall efficiencies, concepts 9-13.

		9	10	11	12	13
Electricity	LHV %	28.9	34.9	34.9	34.9	29.9
	HHV %	23.6	28.4	28.4	28.4	24.4
Heat	LHV %			46.8	32.2	
	HHV %			38.1	26.3	

10.7 Gasification internal combustion engine concepts 14 - 15 (GE)

Two power plant concepts using atmospheric and pressure gasification coupled to an internal combustion engine are estimated. Only electricity production is considered. A block flow diagram of the plant configurations is shown in Figure 10-7.

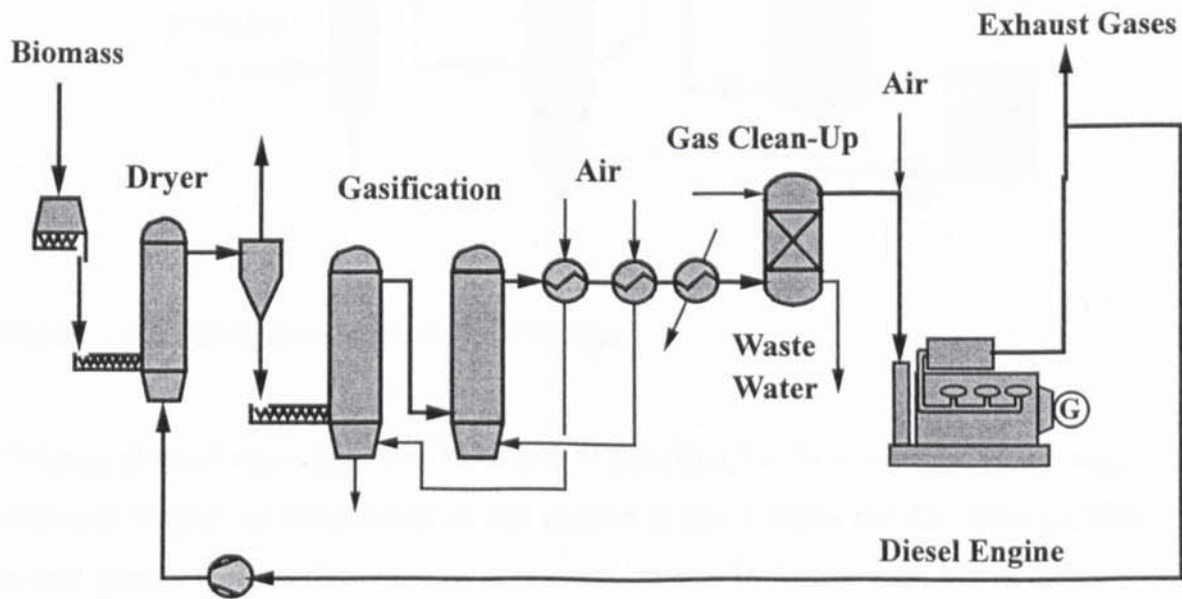


Figure 10-7. Block flow diagram of atmospheric pressure gasification - internal combustion engine concept.

The nominal capacities of the plant concepts are 5, and 20 MWe. The 5 MW concept uses atmospheric pressure gasification, whereas the larger concept employs pressurised gasification. The atmospheric gasification concept is principally based on the R&D work carried out at TPS /201/. A separate tar cracking reactor is installed after the gasifier. The engine performance balances are not based on actually existing engines. They were chosen to represent what was believed to be feasible for this technology (note Chapter 9 for discussion).

The plant consists of the following major units: wood receiving and storage, milling and drying, gasification, gas cleaning, and an internal combustion (gas engine) power system. All of the units are single train except for the engine section in the larger concept, which has two 10 MWe engines. In addition to the main processing units, the plant includes all necessary support facilities.

A summary of the process streams is given in Table 10-21. The engine section's performance is summarised in Table 10-22. The overall efficiencies for the concepts are presented in Table 10-23.

Table 10-21. Major process flow rates and conditions, concepts 14 - 15.

	14	15
Gas engine net power, MW	5.0	20.0
Internal consumption, MW	0.8	1.6
Net plant power output, MW	4.2	18.4
Wood feed (as received), kg/s	1.88	7.50
Ash produced, kg/s	0.02	0.08
Raw gas, kmol/s	0.109	0.440
Flue gases, kmol/s	0.350	1.37
Flue gases for dryer, kmol/s	0.250	0.854

Table 10-22. Engine characteristics, concepts 14 - 15.

	14	15
Power output, MW	5.0	10
Engine air flow, kg/s	7.63	15.1
Fuel gas flow, kg/s	2.60	5.02
Fuel gas temperature, °C	40	43
Flue gas flow, kg/s	10.2	20.1
Engine exhaust temperature °C	430	430

Table 10-23. Overall efficiencies, concepts 14 – 15.

		14	15
Electricity	LHV %	27.5	29.8
	HHV %	22.4	24.3

10.8 Fast pyrolysis of biomass

Fast pyrolysis liquid (PL) production and power generation are de-coupled. Power plants employing PL are served by transporting PL from centralised production units. This arrangement minimises the cost of pyrolysis liquid production. One fast pyrolysis concept is modelled. The concept's performance is based on data published by Scott et al. at the University of Waterloo (see Chapter 7). The concept design is close to that of the Ensyn RTP™ plant at the ENEL Bastardo power plant in Italy. A block flow diagram of the plant configuration is presented in Figure 10-8.

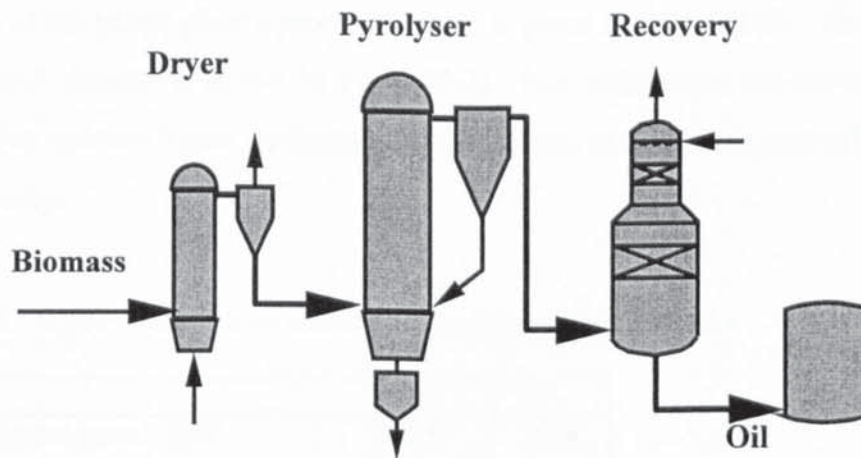


Figure 10-8. Block flow diagram of fast pyrolysis.

A range of plant capacities from 18 to 140 MW_{th} (feed l_{h_v}) is considered. This range corresponds roughly to the amount of fuel needed in the 5 MWe and 60 MWe gasification power plant concepts. The balance is presented for a 48 MW_{th} case, because this is believed to be a good compromise between small (at high operating and capital costs) and large size (with biomass supply problems). The concepts employ a flue gas dryer.

The plant consists of the following major units: wood receiving and storage, milling and drying, fast pyrolysis, particulate removal, vapour quench and product recovery, and storage system for PL. All of the units are single-train except for the dryer, which on a large scale (above 48 MWth) has two trains. In addition to the main processing units, the plant includes all necessary support facilities.

A summary of the process streams is given in Table 10-24. The overall efficiency for the concept is presented in Table 10-25.

Table 10-24. Major process flow rates and conditions, fast pyrolysis.

	1
Internal consumption, MW	3.0
Wood feed (as received), kg/s	5.9
PL, kg/s	2.1
Ash produced, kg/s	0.02
Dryer flue gases, kmol/s	9.4

Table 10-25. Overall efficiency.

		1
PL	LHV %	73.3
	HHV %	66.0

10.9 Pyrolysis liquid - diesel engine, concepts 16 - 17 (PD)

A block flow diagram of the plant configuration is presented in Figure 10-9. Two power plants with nominal capacities of 5 and 25 MWe are considered. The performance balances are not based on actually existing engines. They were chosen to represent what was believed to be feasible for this technology after the current R&D work. Only electricity production is considered.

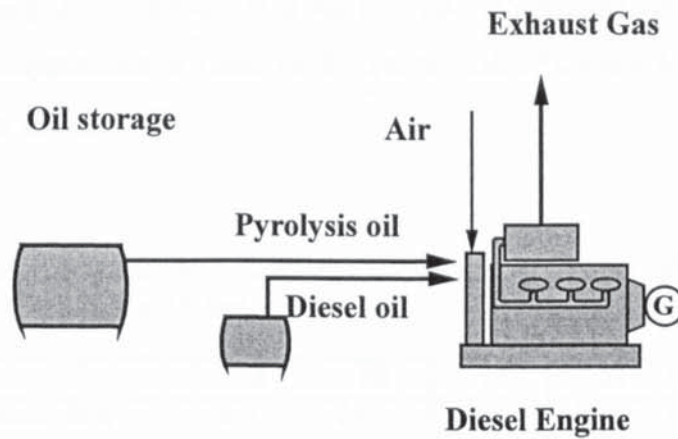


Figure 10-9. Block flow diagram of a diesel power plant using fast pyrolysis liquid as fuel.

The power plant includes liquid storage, a liquid handling unit, and a diesel engine generator set. All of the units for the 5 MWe plant are single-train, and the larger plant of 25 MWe has five engines and generators. In addition to the main processing units, the plant includes all necessary support facilities.

A summary of the power plant's process streams is given in Table 10-26. The overall efficiency for each concept is shown in Table 10-27. Two efficiencies are shown: an overall efficiency that includes liquid production and utilisation, and a power plant efficiency from PL to electricity.

Table 10-26. Major process flow rates and conditions, concepts 16 - 17.

	16	17
Diesel engine net power, MW	5.0	25.0
Pyrolysis liquid feed, kg/s	0.85	3.9
Diesel oil, kg/s	0.02	0.07

Table 10-27. Efficiencies, concepts 16 - 17. The overall figure includes pyrolysis liquid production.

		16	17
Electricity, overall	LHV %	26.6	28.7
	HHV %	22.2	23.9
Electricity, power plant	LHV %	38.0	41.0
	HHV %	34.1	36.8

10.10 Pyrolysis liquid - combined-cycles, concepts 18 - 21 (PyCC)

A block flow diagram of the plant configurations is presented in Figure 10-10. The nominal capacities of the plants are 5, 30 and 60 MWe (Table 10-28). The performance balances are not based on actually existing turbines. They were chosen to represent what was believed to be feasible for this technology. Both power-only (three cases) and co-generation of heat and power (one case) are included.

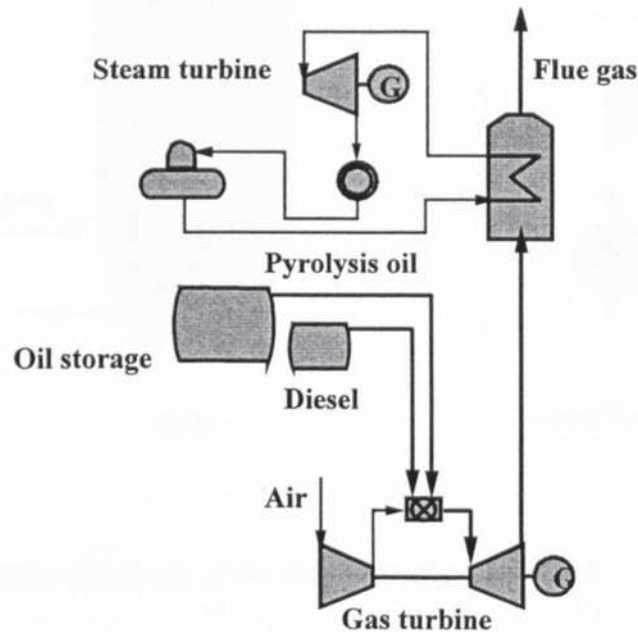


Figure 10-10. Block flow diagram of a combined-cycle diesel power plant using fast pyrolysis liquid as fuel.

The power plant consists of the following major units: liquid storage, a gas turbine, a heat recovery steam generator, and a steam cycle. All of the units are single train. In addition to the main processing units, the plant includes all necessary support facilities.

Table 10-28. Pyrolysis liquid - combined-cycle configurations.

Concept	Nominal capacity MWe	Gas turbine	Products
18	5	Typhoon	Power
19	30	LM2500	Power
20	30	LM2500	Power and heat
21	60	Frame 6	Power

A summary of the process streams is given in Table 10-29. The performance of the gas turbine section is summarised in Table 10-30. The overall efficiency for each concept is presented in Table 10-31.

Table 10-29. Major process flow rates and conditions, concepts 18 - 21. HP superheat temperature 485 °C, pressure 60 bar.

	18	19	20	21
Gas turbine net power, MW	4.4	24.5	24.5	40.6
Steam turbine net power, MW	2.1	9.5	6.9	20.9
Internal consumption, MW	0.02	0.1	0.1	0.2
Net plant power output, MW	6.4	32.0	29.4	60.1
District heat, MW			27.7	
Oil feed, kg/s	0.9	4.3	4.3	8.3

Table 10-30. Gas turbine characteristics, concepts 18 - 21.

	18	19	20	21
Net power output, MW	4.4	22.6	22.6	39.4
Compressor air flow, kg/s	18.8	64.1	64.1	136.3
Compressor pressure ratio	14.5	18.2	18.2	12.3
Fuel gas flow, kg/s	0.90	4.25	4.25	8.25
Combustion temperature, °C	1 150	1 240	1 240	1 100
Fuel temperature, °C	80	80	80	80
Flue flow, kg/s	19.7	68.4	68.4	144.6

Table 10-31. Efficiencies, concepts 18 - 21. The overall figure includes pyrolysis liquid production.

		18	19	20	21
Electricity, overall	LHV %	32.6	35.7	32.8	34.5
	HHV %	27.4	30.2	27.7	29.1
Electricity, power plant	LHV %	46.6	51.0	46.8	49.3
	HHV %	41.5	45.7	41.9	44.1
Heat, power plant	LHV %		44.1		
	HHV %		39.5		

10.11 The Rankine steam boiler power plant

The performance balance for the reference power plant concept (Figure 10-11) is shown at three capacities. As for the advanced cycles described in previous sections, the performance balance is calculated with a simulation model. However, in this case the balance is not only a prediction, but represents a commercially available process.

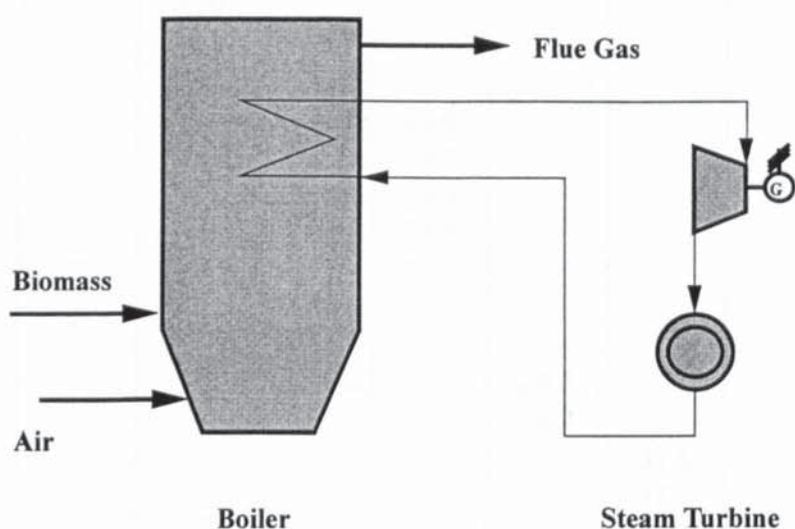


Figure 10-11. Block flow diagram of the steam boiler power plant.

The concept in each case is similar. Their different performances (overall efficiencies) are principally due to the steam turbine performance varying with mass flow. A summary of the process streams is given in Table 10-32. The overall efficiency for the concept is shown in Table 10-33. The Rankine power plant is described in more detail in Chapter 4.

Table 10-32. Major process flow rates and conditions, conventional power plants.

	22	23	24
Steam turbine net power, MW	3.7	16.0	68.3
Internal consumption, MW	0.2	0.6	2.4
Net plant power output, MW	3.5	15.3	65.9
Wood feed (as received), kg/s	1.60	6.40	25.60
Ash produced, kg/s	0.004	0.02	0.06
Flue gases, kmol/s	0.26	1.02	4.09

Table 10-33. Overall efficiencies, conventional power plants.

		22	23	24
Electricity	LHV %	26.8	29.1	31.2
	HHV %	21.9	23.7	25.4

10.12 Summary of power plant performance

A summary of the power plant concepts' performances calculated and reported in sections 10.3 - 10.10 is presented in this chapter. A comparison of the efficiencies for all of the configurations studied is reported.

In evaluating the potential competitiveness of proposed new processes, performance analysis is critical. It establishes the process parameters, on the basis of which the feasibility of a system is established. Both capital and operating costs are estimated on the basis of the mass and energy balance.

A performance summary of the alternative process configurations studied in this work is presented in Table 10-34 and Figure 10-12. The concepts analysed in sections 10.4 to 10.10 are labelled. Although pyrolysis concept efficiencies are reported for wood to electricity, there is no process integration between the pyrolysis liquid plant and the power plant. The combined efficiency shown is simply

$$\eta_{tot} = \eta_{pyr} * \eta_{pp} \quad (10-1)$$

where η_{tot} = overall efficiency, %

η_{pyr} = efficiency of pyrolysis liquid production, %

η_{pp} = efficiency of power plant, %

Table 10-34. Summary of electricity production efficiencies (% based on the lhv of the fuel) of advanced systems, efficiency of pyrolysis liquid production taken into account. Cogen = co-generation of power and heat.

Case	MW _e	PCC	ACC	GE	STIG	PD	PyCC	Cogen heat %
1	31.9	47.1						
2	30.0	44.3						33.9
3	29.1	42.9						42.1
4	59.8	45.1						
5	6.6		37.4					
6	33.2		40.9					
7	62.3		39.5					
8	29.1		37.2					38.8
9	4.9				28.9			
10	23.6				34.9			
11	23.6				34.9			46.8
12	23.6				34.9			32.2
13	41.0				30.3			
14	4.2			27.5				
15	18.4			29.8				
16	5.0					26.6		
17	25.0					28.7		
18	6.4						32.6	
19	32.0						35.7	
20	29.4						32.8	30.9
21	60.1						34.5	

An integrated pyrolysis liquid and power plant may have a higher overall efficiency. However, it is believed that the possibility of decoupling the solid fuel handling stage and the power plant is of special advantage to pyrolysis, and it is therefore the arrangement studied in this work.

A generalised correlation between plant capacity and efficiency for each technology may be derived from individual power plant efficiencies. It is recognised that such correlations cannot be employed as the basis for a rigorous analysis. However, the correlations are shown to emphasise differences between technologies, which may be observed more easily from continuous functions than individual data points.

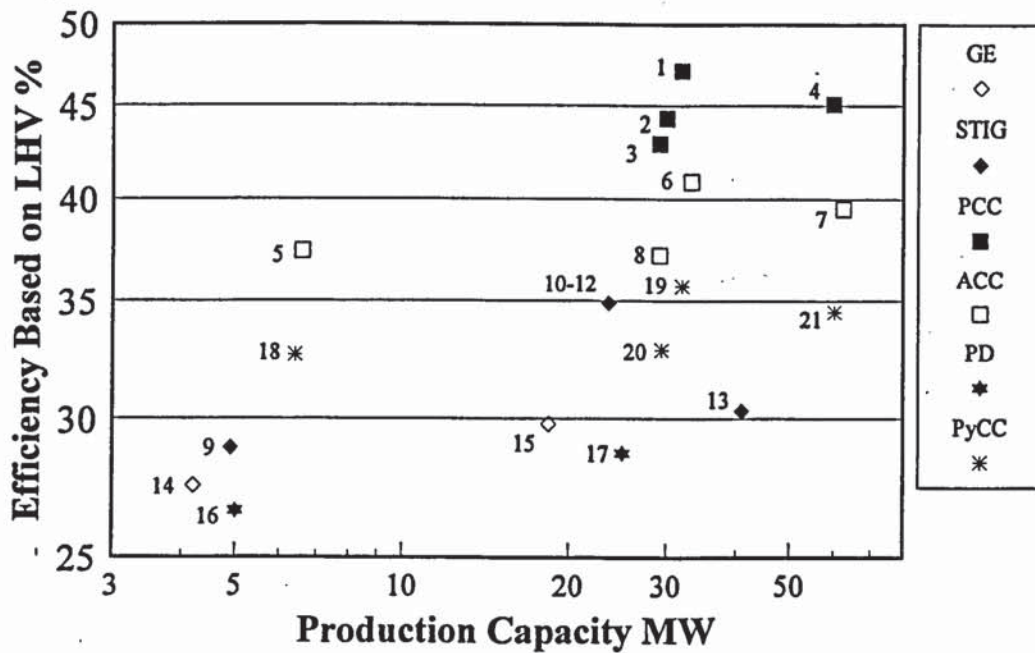


Figure 10-12. The calculated electricity production efficiencies of advanced biomass systems. Pyrolysis power plant efficiencies reported also from wood to electricity. Concept numbers shown as in Table 10-1. GE = Gasification engine, STIG = Steam injected gas turbine, PCC = Pressurised gasification combined-cycle, ACC = Atmospheric pressure CC, PD = Pyrolysis diesel, PyCC = Pyrolysis CC.

Generalised correlations are derived using the following procedure:

1. A power function (Equation 10-2) is fitted for each technology (Table 10-35) separately. The constants in Equation 10-2 are shown in Table 10-36. Although the quality of fit is poor, it will establish ranges for comparative purposes, as described below.

$$y = a * x^b \quad (10-2)$$

where y = efficiency, %
 x = capacity, MWe
 a, b = constants

2. A likely feasible output range is selected for each technology. These are shown in Table 10-35. It is recognised that the selection of a feasible range is somewhat subjective. Again, it is only done to facilitate the comparison of different technologies.

3. Ranges are made by drawing correlations $\pm 1.5\%$ below and above the correlation from Equation 10-2. This range was found to be adequate, considering the variation in the Rankine cycle efficiency when some process parameters were varied (Figure 4-9).

Table 10-35. Estimated feasible production ranges for different technologies.

Concept	Number	Feasible capacity range MWe
Pressurised gasification combined-cycle	1-4	20 - 70
Atmospheric pressure gasification combined-cycle	5-8	15 - 70
Steam-injected-gas-turbine cycle	9-13	5 - 50
Gasification - internal combustion engine	14-15	3 - 30
Fast pyrolysis - internal combustion engine	16-17	2 - 20
Fast pyrolysis - combined-cycle	18-21	5 - 70
Rankine cycle - steam turbine	22-24	5 - 70

Table 10-36. Constants for different technologies in Equation (10-2).

Concept	a	b	R ²
GE	25.3	0.056	0.99
STIG	27.6	0.044	0.24
PCC	39.4	0.040	0.62
ACC	35.6	0.031	0.61
PDI	24.5	0.050	0.99
PyCC	31.0	0.031	0.63
Rankine	19.8	0.123	0.99

Generalised correlations between plant capacity and efficiency for each technology are shown in Figure 10-13. The figure may be employed in estimating likely feasible output ranges for the technologies, where their efficiency appears to offer advantages over alternatives.

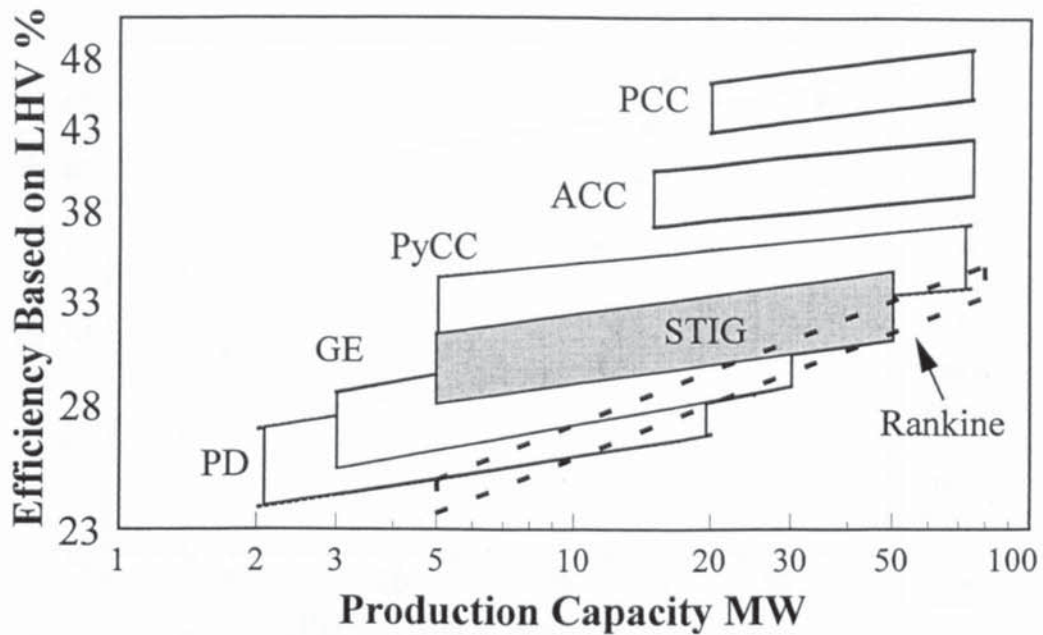


Figure 10-13. Power production efficiencies from wood. GE = Gasification engine, STIG = Steam injected gas turbine, PCC = Pressurised gasification combined-cycle, ACC = Atmospheric pressure CC, PD = Pyrolysis diesel, PyCC = Pyrolysis CC.

The following issues may be observed:

- The analysis is rigorous and is consistent for all cases compared.
- The Rankine power plant is generally the least efficient over most production capacities.
- Pressurised IGCC systems have the highest efficiencies of the concepts compared: 45 to 47% at 30-60 MWe.
- The highest power production efficiency is achieved with the medium-scale IGCC concept (employing the aero-derivative LM2500 engine): 47% based on the lower heating value (lhv) of wood fuel.
- There is a distinct difference between the IGCC concepts using aero-derivative and industrial gas turbines (Figure 10-12). The IGCC concepts employing aero-derivative engines have a higher efficiency than those using industrial engines. This was expected due to the respective efficiencies of the base engines.
- Pyrolysis diesel power plants have lower efficiencies than systems using gasification.
- In spite of de-coupling pyrolysis liquid production and the power plant, pyrolysis CC has a relatively high overall efficiency of around 35%.

- All the advanced systems appear to have higher efficiencies than the Rankine cycle. However, it should be noted that re-heating, which increases efficiency a few percentage points, has not been taken into account in estimating the Rankine performance. Re-heating of steam was not modelled in this work, as it becomes viable in large Rankine power plants. Re-heating is not usually practised within the capacity range studied here.

Implications for viability:

- Of all the new concepts, PCC systems appear to be most feasible because of their superior performance.
- Pyrolysis diesel may be interesting on a small scale (< 10 MW). It has a relatively high efficiency at small outputs, a considerable advantage over other bioenergy applications, especially compared with the Rankine cycle.
- Pyrolysis CC may be interesting below 30 MW, because the conventional cycle has a relatively low efficiency below this capacity.

Conventional technology appears to lose especially at the low end of the scale. However, the performances of new systems are estimates, and they have not been proven in industrial operation. Sensitivity studies are carried out later in the chapter to examine this topic. In the next chapter, investment cost contingency is used in dealing with this aspect.

Estimates in this work are also compared with a few other studies below. In Figure 10-14, gasification power plant performance estimates are compared with data provided by Salo and Keränen /46/, van Ree et al. /51/ (IGCC), and Toft /37/ (GE). It may be seen that the pressurised IGCC concepts agree well with the data of Enviropower, which is also estimated for pressurised gasification. The atmospheric IGCC agrees well with the data of van Ree et al. /51/, who estimated concepts employing atmospheric gasification. There is some difference between the gasification gas engine performance data of Toft and this work at 5 MW, but the difference is not significant at 20 MW. It may be concluded that the performance estimates for power plant concepts employing gasification agree reasonably well with the literature.

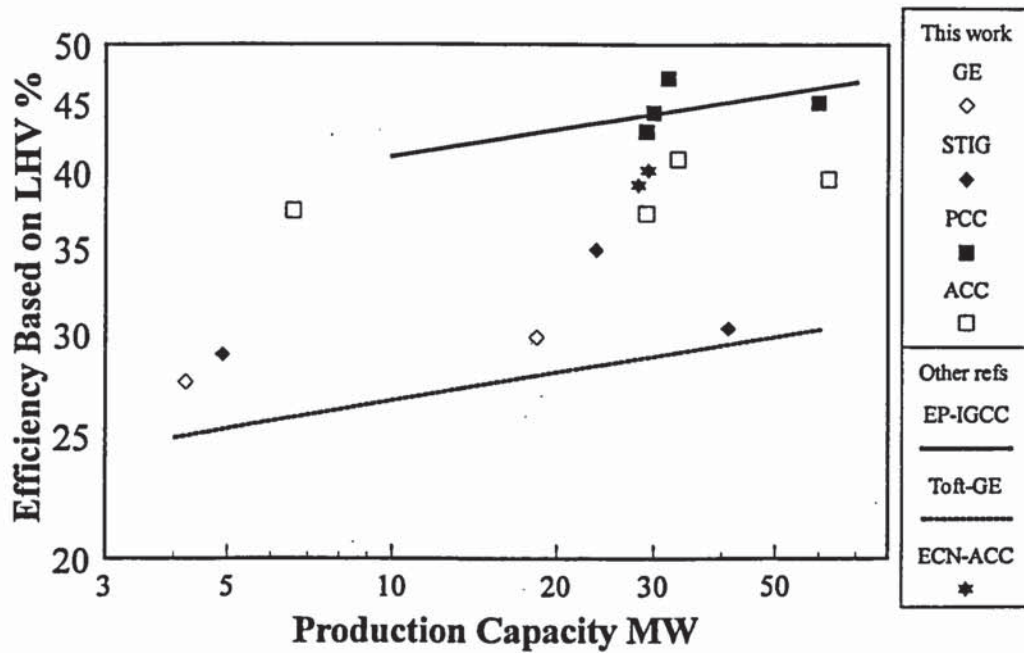


Figure 10-14. Power plant efficiencies using gasification. GE = Gasification engine, STIG = Steam injected gas turbine, PCC = Pressurised gasification combined-cycle, ACC = Atmospheric pressure CC.

The performance of the pyrolysis power plant concepts analysed are compared with other work in Figure 10-15. It may be seen that the performance of a diesel power plant does not agree with the values presented by Toft. This is due to differences in the pyrolysis plant efficiencies employed in each study. The efficiency used by Toft /37/ is 62%, whereas the efficiency estimated in this work (Chapter 7) is 73%. The power plant efficiencies in the two studies are similar.

The concept analysed by Roy et al. /68/ is a PyCC variant, in which pyrolysis liquid production is close-coupled to a combined-cycle. The efficiency of this concept may be compared with the PyCC concept in this work. The performances of the concepts are similar, and the somewhat higher efficiency reported in /68/ is plausible because of integrated operation. However, this concept does not have the advantage of de-coupling solid fuel handling from the power plant, which is probably the primary advantage of fast pyrolysis.

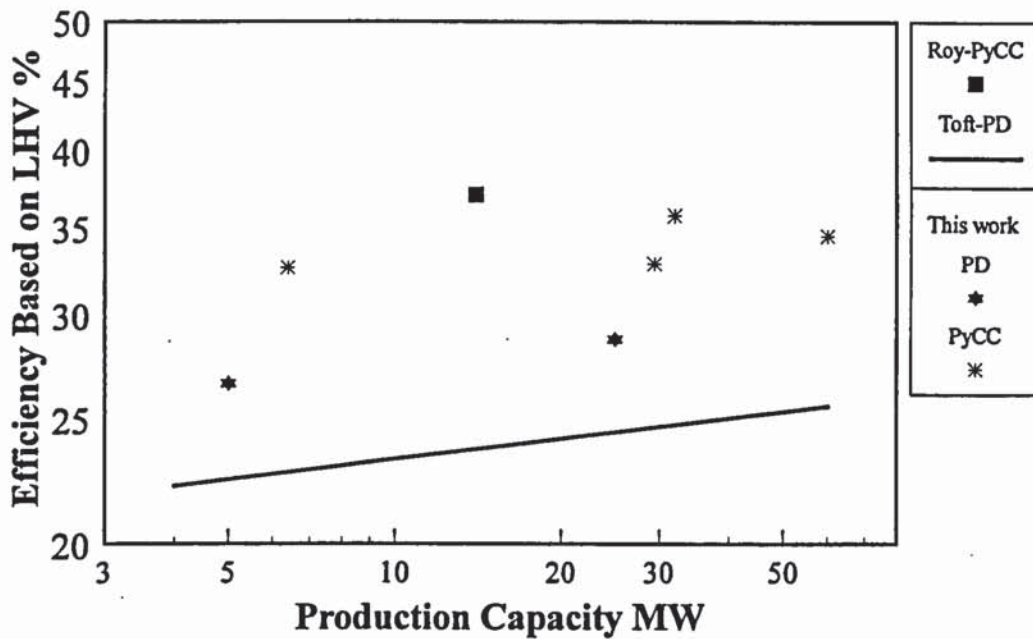


Figure 10-15. Power plant efficiencies using fast pyrolysis. PD = Pyrolysis diesel, PyCC = Pyrolysis CC.

10.13 Uncertainties in performance estimation

Performance estimates concerning new power plant concepts are subject to uncertainties. In this section some models are used to highlight the nature and effect of these uncertainties on overall process performance.

Both gasification and pyrolysis power plant models are studied. However, the pyrolysis concepts are subject to greater uncertainties than the gasification power plant concepts. First, there is far less large-scale data available for pyrolysis to verify the mass and energy balances. Secondly, neither of the two process stages in pyrolysis power plant concepts (the liquid production and the power plant) have been proven in continuous operation.

10.13.1 Gasification engine power plant concept

Gas engine parameters are varied in this section to study the effect of the uncertainties related to these values on overall power plant performance. The uncertainties are discussed in more detail in Chapter 9.

Results from varying the engine efficiency are presented in Table 10-37. The range of variation for the engine efficiency, the corresponding injection pressure, and the flue gas temperature were estimated by an engine manufacturer [211]. The sensitivity study was carried out for the concept with a 5 MWe engine and atmospheric gasification. Five cases are shown. The injection pressure is increased from 1 to 6 bar, while the engine efficiency rises from 30 to 40%. The “high 2” concept is an optimistic estimate for a case in which the engine has the same efficiency and injection pressure with LHV gas as with natural gas.

Table 10-37. Sensitivity study with engine efficiency. Bold values used as input data; other values are results from simulation.

	Low 1	Low 2	Base	High 1	High 2
Engine efficiency %	30	34	37	40	43
Injection pressure bar	1	4	5	6	4
Biomass feed kg/s dm	1.16	1.02	0.94	0.87	0.81
Engine output MWe	5.00	5.00	5.00	5.00	5.00
Internal consumption MWe	0.31	0.88	0.92	0.94	0.70
Net output MWe	4.69	4.12	4.08	4.06	4.30
Exhaust gas temperature °C	485	454	430	406	418
Overall efficiency %	24.6	24.5	26.4	28.4	32.4
Change %	-6.8	-7.2	0.0	7.6	22.6

The power plant efficiency rises from 24.6 to 28.4% when the engine efficiency is increased from 30 to 40%. The largest single internal power consumption is for the compressor, which raises the fuel gas pressure from atmospheric pressure to the injection pressure.

Because there is a considerable uncertainty related to the maximum feasible engine efficiency, the table may be used to estimate the potential overall power plant efficiency. It may be noticed that increasing the engine efficiency from 30 to 34% does not improve the power plant efficiency, provided that the assumptions concerning the required injection pressure are valid, i.e. 30% efficiency may be reached with a low injection pressure. The result highlights the importance of the injection pressure when LHV gas is used. A considerable amount of power is needed if the fuel gas is pressurised.

10.13.2 Pyrolysis power plants

In this section a review is carried out to reveal how technical uncertainties related to the components of the pyrolysis power plant concept may change the overall performance. Sensitivities in both liquid production and power plant efficiencies are studied.

The basic efficiencies used previously for pyrolysis power plants are presented in Table 10-38. There is uncertainty related to the operation of both the diesel engine and the gas turbine with fast pyrolysis liquid. To study the effects of the uncertainty, power plant efficiencies have been varied $\pm 10\%$ from their base values.

Table 10-38. Technical sensitivity studies; change in power plant performance. CC = combined cycle.

Concept	Power plant	Output MW _e	Base efficiency %	Efficiency variation	
				- 10 %	+10 %
16	Diesel	5	38.0	34.2	41.8
17	Diesel	25	41.0	36.9	45.1
18	CC - Typhoon	6.4	45.7	41.1	50.3
19	CC - LM2500	32.0	51.0	45.9	56.1
20	CC - Frame 6	60.1	49.3	44.4	54.2

Two sensitivity studies were carried out. First, the power plant efficiency was kept at its base value, and the pyrolysis efficiency was varied. A change of $\pm 10\%$ from the base value (73.3%) was used. The range for pyrolysis efficiency was therefore from 66% to 80%. In the second case, extreme combinations were studied: both low and high pyrolysis and power plant efficiencies were assumed simultaneously.

Results from the first technical sensitivity study are shown in Figure 10-16. The efficiency of pyrolysis liquid production was varied with the corresponding change in the overall power production efficiency shown in the figure. An estimated feasible capacity range was selected for each technology (diesel 5 - 25 , combined cycle power plant 10 - 70 MWe). Note that the ranges are slightly different from those used in Table 10-35. However, the present range is shown to highlight the trends studied.

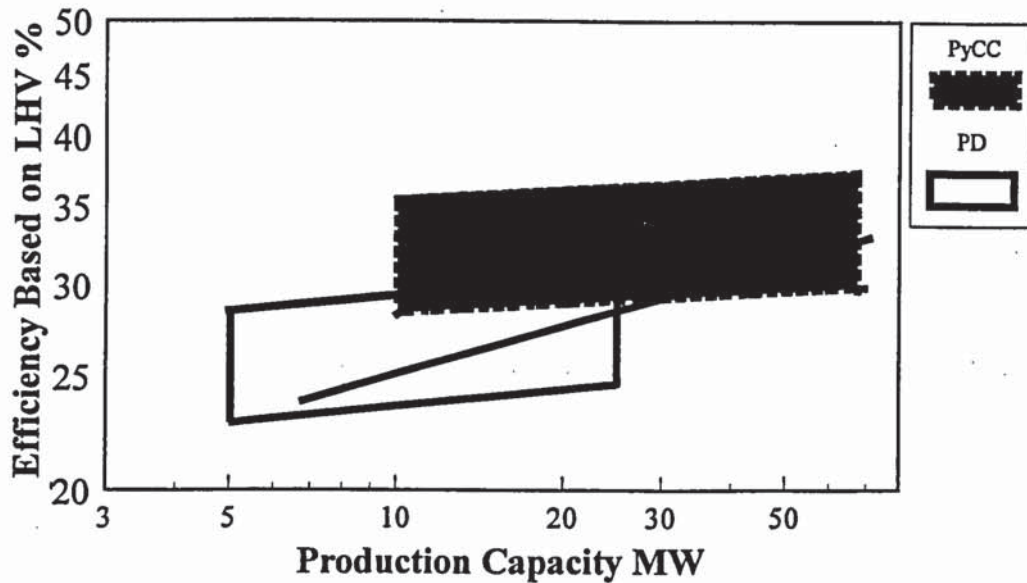


Figure 10-16. Sensitivity of power plant efficiencies using fast pyrolysis, the power plant efficiency varied $\pm 10\%$. The solid line depicts the efficiency of the Rankine cycle. PD = Pyrolysis diesel, PyCC = Pyrolysis CC.

Efficiencies are compared with those of the Rankine cycle. It may be seen that if the efficiency of pyrolysis liquid production is 66% instead of 80%, the diesel power plant competes with the Rankine cycle only on a small scale. CC has a higher efficiency than the Rankine cycle below 30 MWe. Both appear to compete better at the lower end of the scale.

In Figure 10-17 the most optimistic and pessimistic estimates for oil production and the power plant are combined. It may be seen from the figure that there appears to be a good chance that the overall efficiency of the pyrolysis diesel power plant is higher than that of the Rankine cycle. PyCC competes better even if pessimistic assumptions prove valid. However, there is a chance, especially at higher capacities, that the CC efficiency is not higher than with the Rankine cycle.

New processes are chosen for further development on the basis of their projected production costs. However, other criteria, notably projected efficiency, are also used, especially if technical uncertainties are high. If the expected efficiency of a new power plant concept is low, the likelihood of anybody funding such development is low. It may be seen that if the estimated performance values for pyrolysis power plant components are not reached, there is a chance that the efficiency of a new power plant concept is not higher than that of the

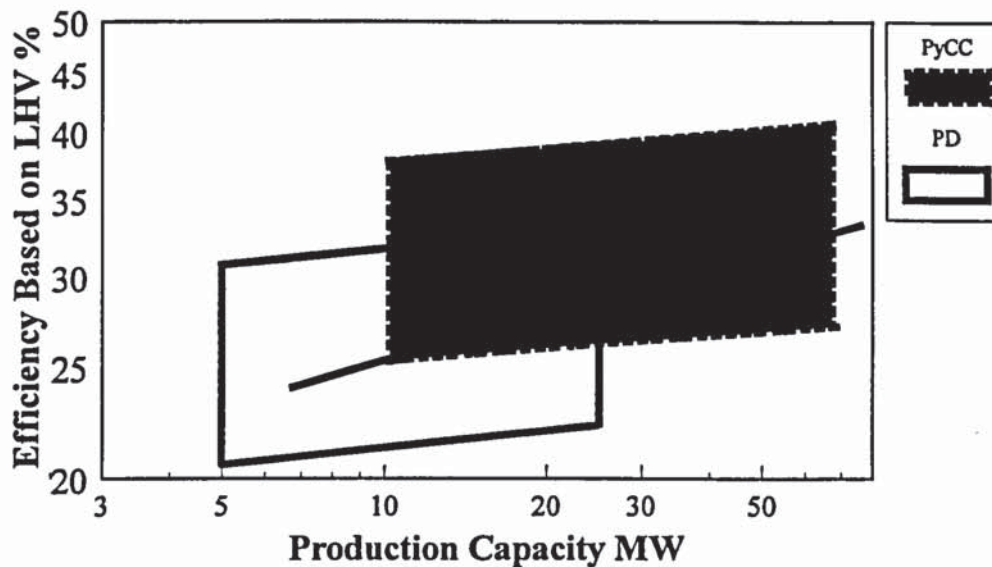


Figure 10-17. Sensitivity of power plant efficiencies using fast pyrolysis. The power plant and pyrolysis efficiency varied $\pm 10\%$. The solid line depicts the efficiency of the Rankine cycle.

Rankine cycle. The capacity for de-coupled operation with liquid fuel remains the strongest merit for pyrolysis systems, since their overall specific investment is not believed to be lower than that in the Rankine power plant.

10.14 Potential improvements in IGCC concepts

In this section, potential improvements in two IGCC concepts are studied by means of simulation models. The aims of this study are threefold:

- To present examples of using the power plant simulation models developed in this work
- To study the effects of potential improvements in several unit processes on overall power plant performance
- To estimate the development potential of IGCC technology

IGGC is used as an example because it has a high efficiency and it is projected to have a more short-term commercial potential. The development of this concept is supported by many organisations, US DOE and EC DGXVII included. It is also suitable for this study because it includes several unit processes that have further development potential.

The concepts considered are based on pressurised gasification, and employ flue gas dryers (section 10.4 concept 1 and 4). The first employs an aero-derivative LM2500, and the second an industrial F6 gas turbine. It should be noted that only performance improvements are reviewed here. The associated costs are not included in the analysis. Estimating the effect of a parameter change on the cost of electricity, although in principle more important than performance analysis, is beyond the resources of this work. Such a study would require, for example, very detailed cost models for individual steam cycle components.

Improvements in the performance of three unit processes within the IGCC are studied:

- Dryer
- Gas turbine
- Steam cycle

The reasons for selecting these units is explained below. The study carried out is not a sensitivity analysis, as there is less technical uncertainty associated with this concept than with the concepts studied in previous sections. The objective is to assess the development potential in the concept performance. The base case values for the process parameters (Table 10-39) are considered feasible, and the effect of potential improvements in these parameters on performance is studied. The improvements are not the same percentages for all parameters, as the industrial development potential of each parameter is different.

Commercially available dryers exhibit an exceptionally wide range of specific energy demands (see Figure 5-5). Their reported energy demands range from 2.8 to 4.5 MJ/kg water evaporated. Based on the literature, it is not possible to analyse the reasons for this variation. In the base case, a specific consumption of 3.5 MJ/kg evaporated water is selected for the dryer based on industrial experience. In the sensitivity study, an energy demand of 3.0 MJ/kg is assumed, which, considering the data in Figure 5-5, may be considered feasible.

Gas turbines are being improved and their efficiencies have been increased rapidly over the past ten years. The gas turbine performance analysis employed in this work (by Enter Software /178, 187/) is based on engines of a relatively old design. The LM2500-PE has been on the market for 13 years, and the Frame 6 for 21 years. Improvements in gas turbine

efficiencies used as the base case are therefore probable. In the study, improvements in gas turbine compressor and turbine isentropic efficiencies are used to raise the efficiency of the gas turbine.

Increasing the steam superheat temperature and pressure will improve the efficiency of the steam cycle (see discussion about steam cycle parameters in section 4.5). The higher pressures and temperatures are subject to only minor technical uncertainties. However, as shown in Figure 4-14, the increased steam parameters will increase superheater costs. Steam cycle parameters are varied to study the effects of varying the conventional power plant components on the overall efficiency of the plant.

Estimated improvements in process parameters and their effects on the performances of IGCC concepts 1 and 4 are shown in Tables 10-39 and 10-40, respectively. The first column depicts the parameters used in the base case, and the respective process performance. The parameters varied within the three units are shown in the next three columns in bold face. Each process parameter is first varied separately to display its individual effect on overall performance. The last column depicts a case in which all of the improvements in process parameters are applied simultaneously.

Table 10-39. Potential improvements in IGCC performance, concept 1. GT = gas turbine.

	Base case	Dryer	Gas turbine	Steam cycle	Combined
Varied parameters					
Dryer demand MJ/kg	3.5	3.0	3.5	3.5	3.0
GT compressor isentropic efficiency %	84.1	84.1	86.0	84.1	86.0
GT turbine isentropic efficiency %	86.6	86.6	88.0	86.6	88.0
Superheat steam temperature °C	485	485	485	530	530
Superheat steam pressure bar	60	60	60	80	80
Calculated values					
Biomass kg/s dm	4.16	4.16	4.16	4.16	4.16
Gas turbine MW	23.30	23.30	25.11	23.30	25.11
GT exit temperature °C	565	565	544	565	544
GT efficiency %	36.3	36.3	39.1	36.3	39.1
Steam turbine MW	9.81	10.46	9.16	10.23	10.22
Internal consumption MW	0.83	0.84	0.83	0.83	0.86
Net production MW	32.27	32.92	33.45	32.70	34.47
Net efficiency %	47.12	48.06	48.83	47.74	50.32
Improvement over base case %		2.0	3.6	1.3	6.8

Table 10-40. Potential improvements in IGCC performance, concept 4.

	Base case	Dryer	Gas turbine	Steam cycle	Combined
Varied parameters					
Dryer demand MJ/kg	3.5	3.0	3.5	3.5	3.0
GT compressor isentropic efficiency %	87.5	87.5	88.5	87.5	88.5
GT turbine isentropic efficiency %	85.0	85.0	86.5	85.0	86.5
Superheat steam temperature °C	485	485	485	530	530
Superheat steam pressure bar	60	60	60	80	80
Calculated values					
Biomass kg/s dm	8.04	8.04	8.04	8.04	8.04
Gas turbine MW	40.84	40.84	42.73	40.84	42.73
GT exit temperature °C	546	546	535	546	535
GT efficiency %	34.5	34.5	36.1	34.5	36.1
Steam turbine MW	20.17	21.30	19.52	20.93	21.48
Internal consumption MW	1.27	1.28	1.27	1.33	1.33
Net production MW	59.73	60.85	60.98	60.44	62.88
Net efficiency %	45.07	45.91	46.01	45.60	47.44
Improvement over base case %		1.9	2.1	1.2	5.3

The likelihood and significance of these potential improvements may be summarised as follows:

- A reduction in the specific energy consumption of the dryer is feasible. A dryer with a lower specific energy consumption probably has a higher investment cost. However, it was not possible to correlate the dryer cost and performance in this work.
- Gas turbines are being improved. However, it is not clear when advanced aero-derivative engines may be available for LHV gas.
- Improvements in steam cycle parameters are possible already now, but associated increases in cost may be relatively high on this scale compared with the performance gain. The component cost models employed for the steam cycle in this work are not detailed enough to optimise the system.

In Figure 10-18, potential improvements in IGCC performance estimated with the simulation models are compared with those presented in other studies. Two performance correlations for the current technology are shown, one for each class of gas turbines. The Enviro-power data is based on industrial turbines (section 2.4.2.1), and the data by Consonni and

Larson (section 2.4.2.3) is based on aero-derivative engines. The difference between these two technologies is, as expected, due to the higher efficiency of aero-derivative engines.

It may be seen that the LM2500 IGCC base performance estimated in this work is higher than the data reported by Consonni and Larson for “current” aero-engine technology. It is believed that the differences between the efficiencies in the two studies are related to units within the IGCC other than the gas turbine. The improvement in gas turbine performance estimated in this work brings the plant efficiency to the same level as an IGCC employing future gas turbines estimated by Consonni and Larson. If all of the improvements estimated for the concept in this work are applied simultaneously, the overall efficiency is more than 50% at 35 MWe. The same efficiency is reported by Consonni and Larson for an 80 MWe IGCC with an inter-cooled gas turbine. It may be concluded that simultaneous performance improvements in this work are optimistic for the aero-engine IGCC.

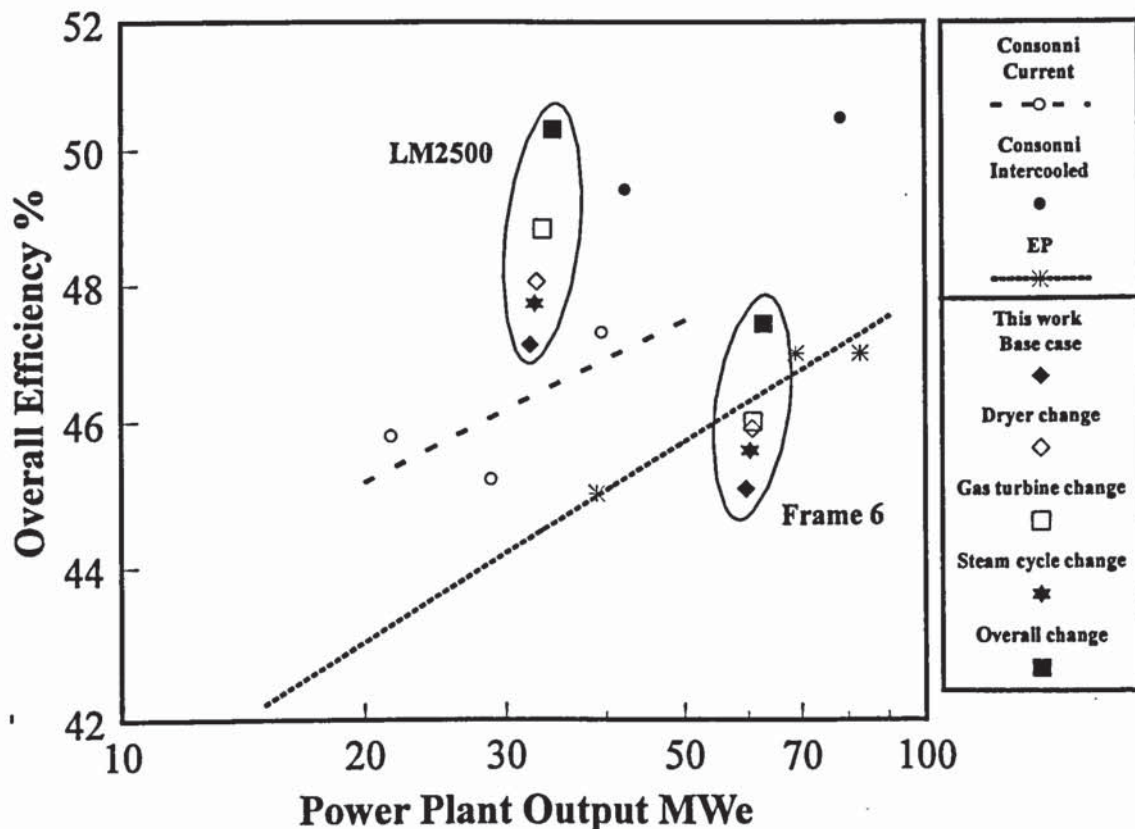


Figure 10-18. Potential improvements in IGCC performance. Enviropower (EP) /46/ as a reference for existing technology (industrial turbines, note that 6.8 MWe 40% is outside the figure area), Consonni & Larson /48/ for both current (aero-derivative) and future (inter-cooled) technologies.

The base efficiency of the Frame 6 IGCC concept evaluated in this work has a lower efficiency than that estimated by Enviropower /46/ for industrial gas turbines. Since the gas turbine performances in the two studies are close to each other, differences in other plant sections must principally contribute to the difference. It should be borne in mind that the case of applying all improvements simultaneously for the Frame 6 does not differ greatly from the Enviropower data.

It may be concluded that although the IGCC concepts have the highest efficiencies of the bio-power concepts, there is still potential for further development. As expected, improvements in gas turbine performance offer the greatest benefit. Because advanced gas turbines are not currently available for biomass power plants, the cost effectiveness of this approach cannot be estimated.

It appears that integration of the dryer into the IGCC concept should be done carefully. Selecting a design with a high-efficiency dryer may well be worthwhile. However, it was not possible to carry out a true optimisation in this work in the absence of a dryer model capable of detailed sizing of the dryer components and their investment cost.

It could reasonably be expected that all biomass concepts have similar potential for improvement. Because they start at a lower efficiency, the improvement is not dramatic.

10.15 Performance of advanced co-generation power plants

10.15.1 Significance of co-generation of heat and electricity

In this section the benefits of advanced power plant concepts in co-generation are reviewed.

If a heat sink (process steam/other heat demand, or district heat network) is available, co-generation should be considered. Co-generation of power and heat may become an important market for advanced bioenergy systems. Two reasons exist:

- Co-generation considerably improves the viability of otherwise uneconomic bio-power systems (note section 2.3.4.1), and may make an uneconomic case economic.
- The power-to-heat ratio (α value), an important parameter in co-generation, is much higher for many advanced generation systems than for the conventional Rankine cycle.

The importance of the latter factor is emphasised because co-generation facilities are sized on the basis of the heat load. Advanced systems allow an increased power output per heat load (high α value), and hence improved economy at a fixed heat load.

The efficiency of the co-generation plant is defined as

$$\text{Efficiency \%} = \frac{\text{Net power production} + \text{Heat production}}{\text{Energy input as fuel}} * 100 \quad (10-3)$$

where power, heat and fuel energy are expressed in MW.

The power-to-heat ratio (often referred to as the α value) is defined as

$$\text{Power-to-heat ratio} = \frac{\text{Net power production}}{\text{Heat production}} \quad (10-4)$$

where power and heat are expressed in MW.

Co-generation of power and heat helps to conserve energy, as a total of 80 - 90% of the fuel energy is utilised. This may be compared with about 43%, which is a representative electricity production efficiency for a large (around 300 - 500 MWe) modern condensing coal power plant, and 55%, which is the state-of-the-art with natural gas combined-cycles on the same scale (note discussion in section 2.6.2). The net power production efficiency is considerably lower for small units using wood as fuel: from 20 to 30%. An example of energy outputs from power plants is shown in Figure 10-19.

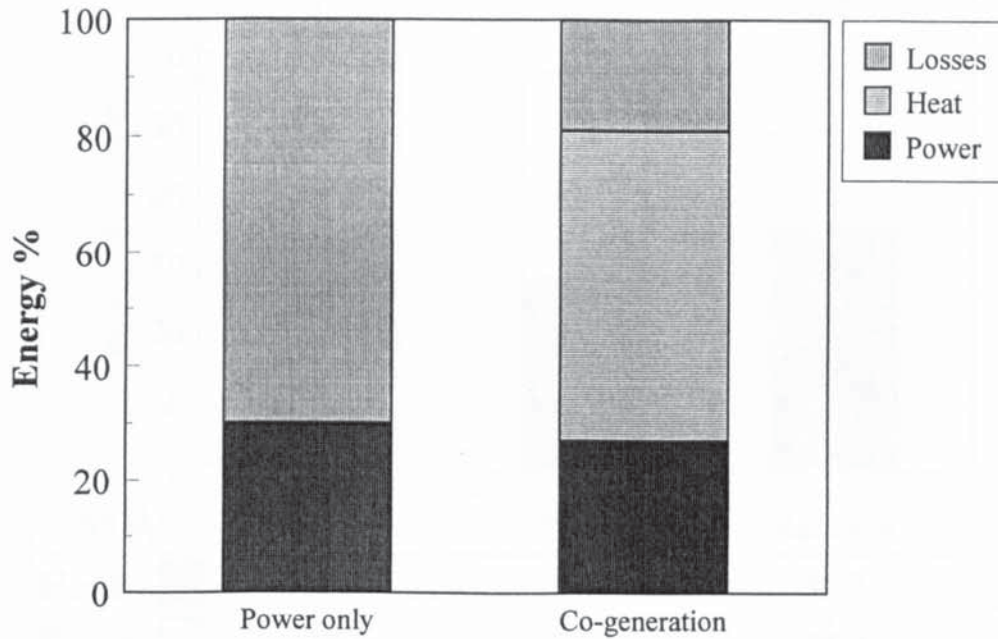


Figure 10-19. Comparison of (conventional) co-generation and power-only production from wood. Fuel to the power plant = 100%..

Co-generation of heat (steam or hot water) and power from biomass is widely applied industrially. Examples are forest products industries, especially in North America and Scandinavia, and co-generation of district heat, primarily in Scandinavia. Co-generation of district heat from straw is employed in Denmark, whereas wood is used in Finland.

10.15.2 Advanced co-generation concepts

Overall energy balances for three concepts based on gasification and fast pyrolysis are compared in Figure 10-20, in which efficiencies for district heat and power production are shown. In power-only production with a flue gas dryer, the electricity generation efficiency of the IGCC is about 47%. If a steam dryer is employed in co-generation, the overall efficiency is about 90%. The pyrolysis combined-cycle also has a high efficiency and power-to-heat ratio. Note, however, that only the power plant is considered in the figure. The STIG cycle has a lower α value than combined-cycles.

The high power-to-heat ratio is a considerable advantage for advanced systems. The α values of new systems are much higher than those of conventional technology, Figure 10-21. In the figure, two advanced concepts (IGCC and PyCC) are compared with the Rankine cycle, all at approximately the same heat production capacity (around 30 MWth). This a valid comparison because co-generation plants are sized on the basis of the heat load. Values are shown in megawatts to illustrate the significance of the power-to-heat ratio. Approximately twice as much power can be produced with advanced cycles compared with the Rankine cycle, when the heat load is the same. This is true over a wide range of capacities, as shown in Figure 10-22. The α values are shown as a function of plant size.

New systems have consistently about double the α -value compared with the existing technology. It is believed that this could be one of the key selling arguments for advanced bio-energy systems. However, finding suitable heat loads is known to be the key problem.

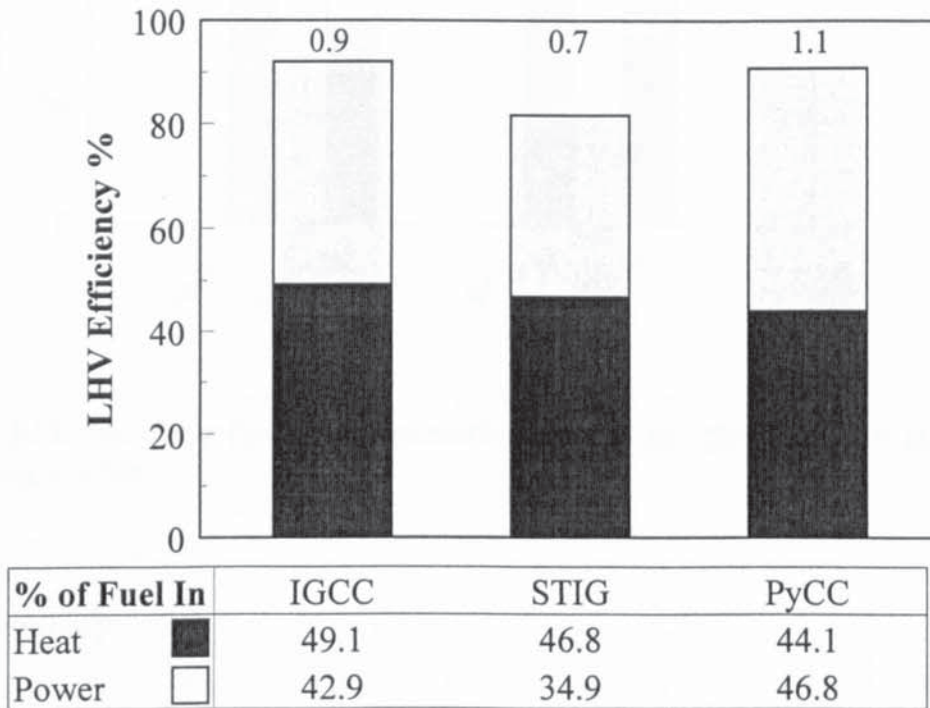


Figure 10-20. Co-generation system efficiencies. Note: PyCC power plant only without considering pyrolysis liquid production.

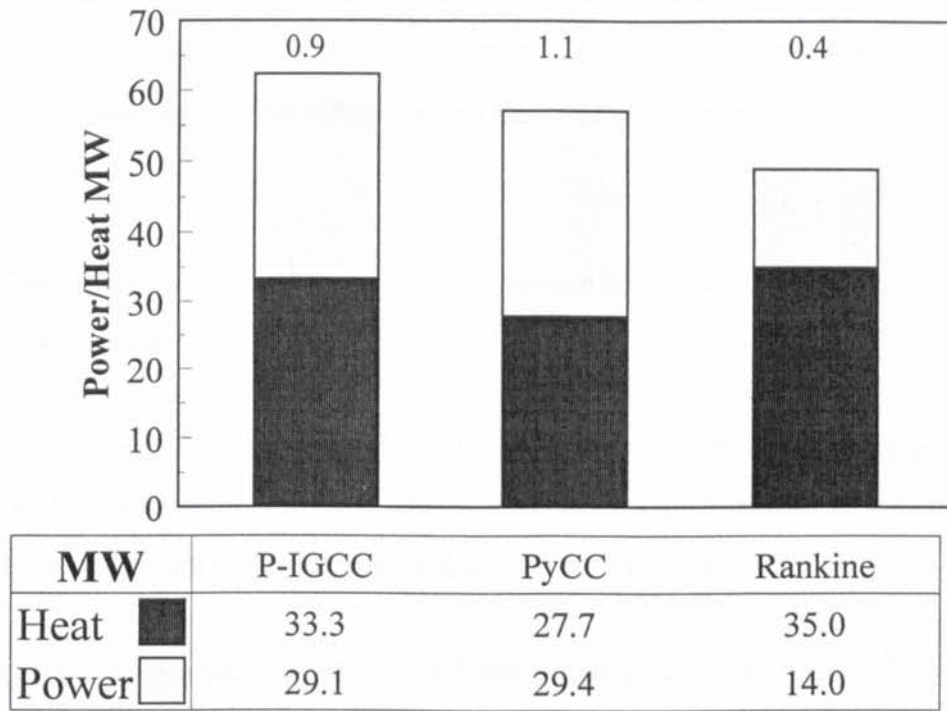


Figure 10-21. Advanced and new co-generation system efficiencies, the α -value is shown above the bars.

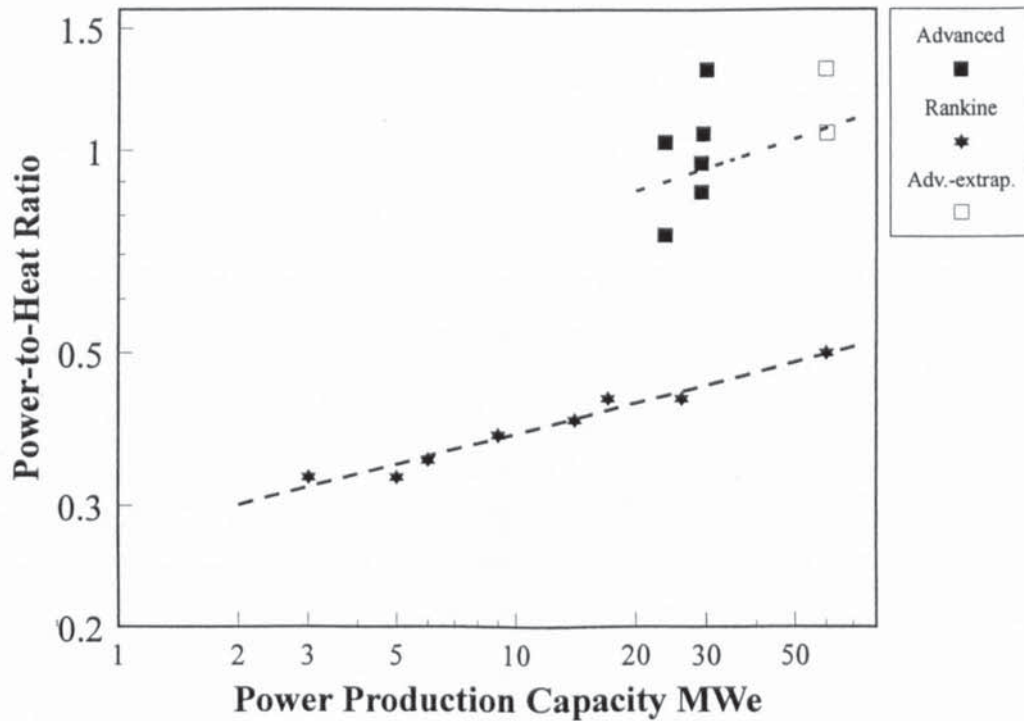


Figure 10-22. Power-to-heat ratios of the Rankine /34/ and advanced systems. Data for advanced systems around 60 MWe extrapolated from smaller concepts.

10.15.3 Significance of dryer type in co-generation

A flue gas and a steam dryer are compared in co-generation, Figure 10-23. 45% more heat may be produced in an IGCC and a STIG concept employing steam drying instead of flue gas drying. The overall efficiency using steam dryers is also considerably higher, 90 versus 80%. Therefore, it appears that the steam dryer would be preferable in district heat production. Ultimately, however, the dryer selection is based on economic considerations.

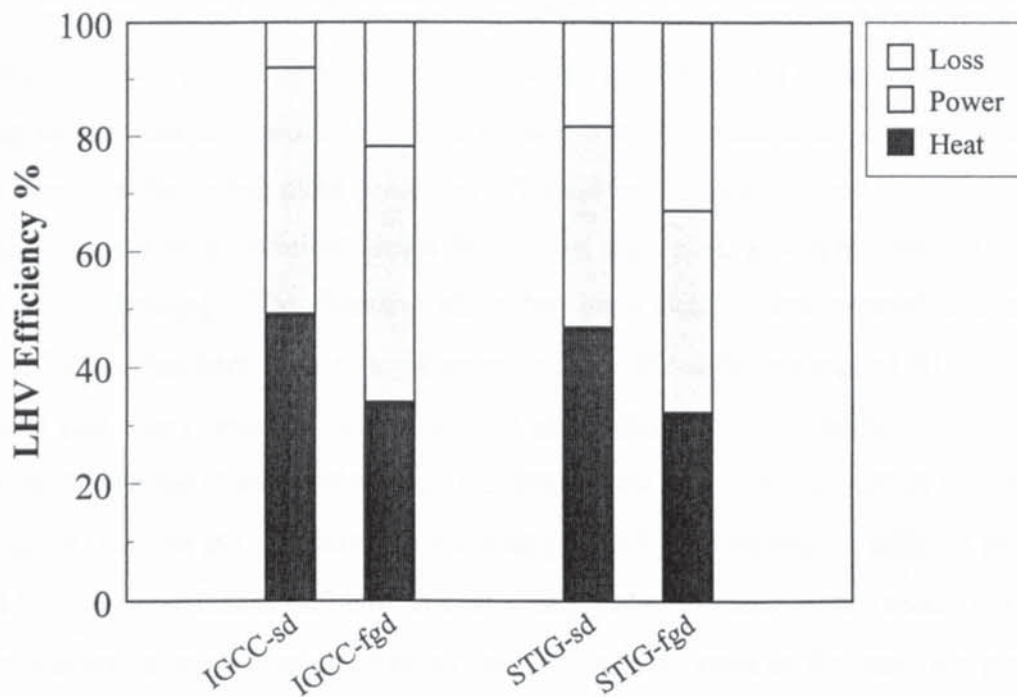


Figure 10-23. Two dryer types in co-generation, production efficiency. *sd* = steam dryer, *fdg* = flue gas dryer.

10.16 Summary

In addition to the Rankine cycle, six advanced process configurations were analysed. For each concept, two or more capacities were studied. The studied capacities ranged from 5 to 60 MWe, and the results of 21 advanced concepts are reported. In addition, the Rankine power plant was modelled and is employed as a reference over the whole capacity range.

The analysis carried out is rigorous and consistent for all cases compared. The Rankine power plant is generally the least efficient over most production capacities. Pressurised IGCC systems have the highest efficiencies of the concepts compared, 45 to 47% at 30 - 60 MW_e.

The performance estimates are compared to published data. There is a fair agreement with most reliable references.

Technical sensitivity studies are carried out for the power plant concepts using pyrolysis liquid as fuel. It is found that the concepts studied have a good chance of becoming more efficient than the current industrial standard, i.e. the Rankine cycle.

Selected parameters are varied to study the development potential of an IGCC concept. It is found that further development of this concept offers considerable potential.

Finally, dryer characteristics are studied. It is found that a steam dryer is quite suitable for co-generation service.

11. DETERMINATION OF CAPITAL COST AND CONTINGENCY

Determination of the capital investments for the systems modelled is described in this chapter. Firstly, investment cost contingency is described and reviewed. The contingencies required for capital investment estimation are derived using established methodologies. The potential for cost improvement is reviewed. The impact of both of these on system capital cost is evaluated.

Capital costs are subject to a wide range of modification over time, apart from the effect of inflation. Upwards pressures result from increasing environmental mitigation requirements and legislative controls, increasing labour costs and lower productivity, increasing costs of permitting, and increasing plant complexity. Downward pressures result from competition and the drive for more efficient and/or lower cost processes, and this overall is often referred to as "learning". This learning effect has been clearly demonstrated in chemicals prices /214/ and has been applied to bioenergy plants /56/ with an assumed 20 % reduction in capital cost every time the sales of a plant are doubled. 20 % is probably an optimistic figure. However, the overall effect of all the upward and downward pressures is impossible to calculate, and the use of optimistic learning effects by themselves is difficult to justify. An additional important contributor to cost estimates is the state of the market at the moment a budget estimate is made. Vendor quotes are often used as the basis for plant cost estimates. A manufacturer may give a higher estimate if its capacity is fully used, whereas it will give a lower budget estimate if it has capacity available.

The rest of this chapter is devoted to an explanation of the most comprehensive discussion of contingency and experience that has been found, and the application of the methodology to the prime capital costs employed.

11.1 Introduction

Hess and Myers /215/ write concerning cost estimates of new technologies:

During R&D and early design for a first commercial plant, capital costs have a near-universal tendency to be under-estimated.

The capital cost contingency is used to deal with uncertainty in cost estimation. The uncertainties may be estimated with a reasonable accuracy when plants employing conventional technology are designed. However, when technology at an early development stage is designed for scale-up, large uncertainties often have to be dealt with.

Investment cost estimates are always subject to uncertainties, and sometimes, when the technology being assessed is at a very early development stage, they may even be over-optimistic and misleading by having an unrealistically low contingency. Estimating costs for new systems not yet in continuous operation is a challenging task.

It is reported that the accuracy of investment cost estimates for pioneer plants of the chemical process industry (in many respects analogous to the technologies studied here), vary typically from $\pm 20\%$ (when full commercial operation experience is available) to 50-400% (with untested operation) /215/, Figure 11-1. Note that engineering contractors are able to reach the $\pm 20\%$ accuracy. The estimation of capital costs in this or any other similar work may be even less precise than the latter estimates, although proper consideration of the contingency will presumably improve the estimate accuracy.

If there is no industrial construction experience from most of the unit processes in the new process concept under study, cost estimates are seldom accurate. According to Merrow et al. /30/, the importance of such cost estimates should be downplayed as process selection criteria. A rigorous performance analysis may be a more useful indication of the potential competitiveness of such a process concept /30/. In other words Merrow et al. believe that a performance analysis may be a more useful tool than a cost estimate, when there is no industrial experience of the plants being assessed.

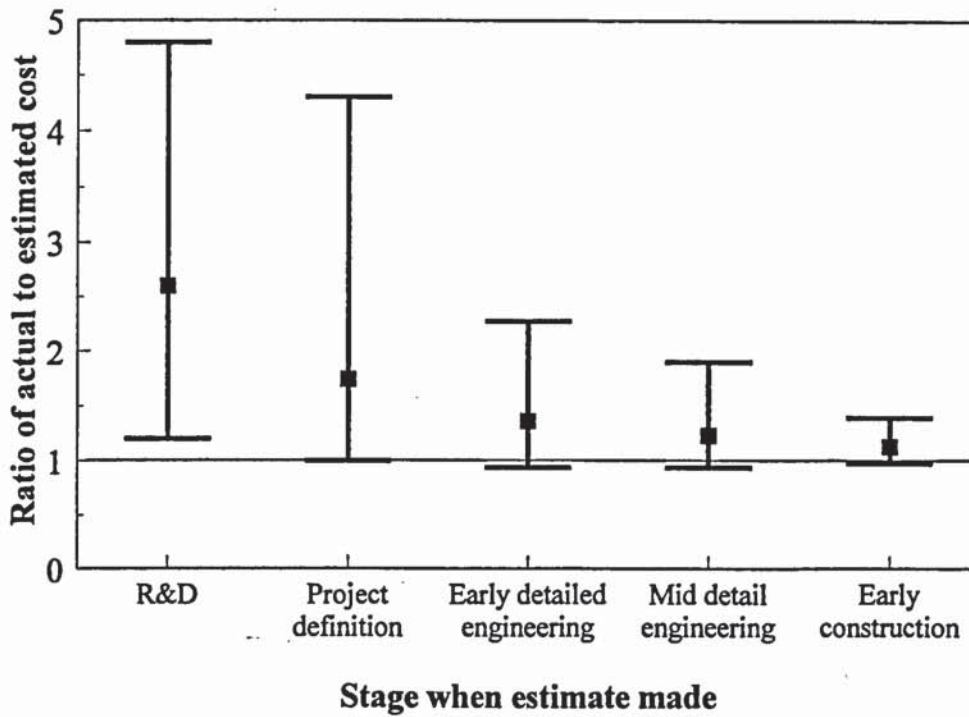


Figure 11-1. Comparison of cost overrun by project stage /216/.

Early estimates, and even estimates made well into the definitive design, concerning pioneer (first-of-a-kind) plants have been poor predictors of actual costs /30/. Merrow et al. /30/ list the following options for a research funding authority trying to improve the ranking of new process alternatives:

1. Downplay the importance of cost estimates when the uncertainties are very high. A wide "confidence" interval in cost estimate (values ranging from + 50 to + 400 percent are reported for early estimates) offers no guidance for decision-making. Premature estimates may be optimistic, as process definition is only partial. This typically results in the exclusion of essential equipment, leading to underestimation of the capital cost.
2. Attempt to control the scope of optimism when assessing new technology. Standards and procedures should be employed. These include standard quality requirements for the scope, process and project definitions underlying an estimate; standards for the completeness and thoroughness of estimates; and the use of independent consultants to review estimates.
3. Adjust for uncertainties. Traditionally, companies employed contingencies ranging from 10 to 30 percent when assessing investments for new technology. Such routine contin-

agencies clearly do not cope with the kind of uncertainty seen in cost estimates for many energy process plants. Note Figure 11-2, where contingencies employed are compared with the average overrun by project stage in the synfuel industry.

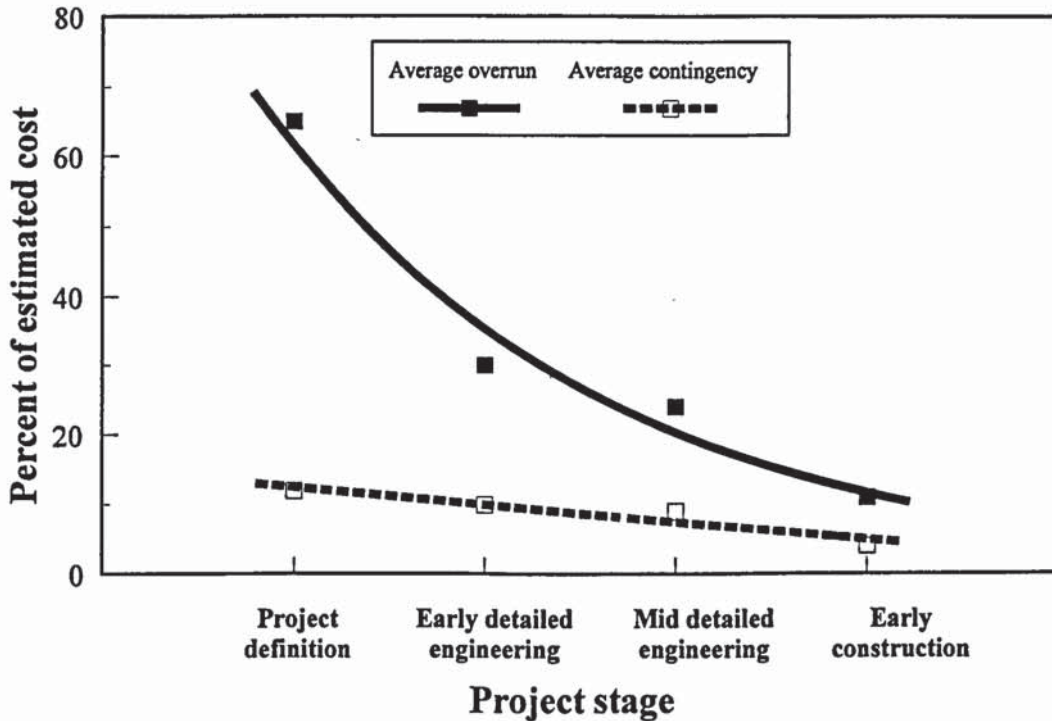


Figure 11-2. Comparison of cost overrun by project stage /217/.

An effort is made here to assess new power production processes using renewable fuel, i.e. woody biomass, and to compare these with the established technology, i.e. the Rankine cycle, also using wood as fuel. An attempt is made especially to address items 2 and 3 above: detailed performance models are designed for the processes, and contingency factors are estimated by established methodologies. The resulting investment costs are discussed and reviewed. Unfortunately, the necessary stage of employing independent consultants to review and improve estimates was not available for this work.

The findings of Hess and Myers /215/ are emphasised. Their work together with other related Rand Corp. reports were found to be the only completely relevant publications available on cost growth and cost reduction in the chemical process industries (CPI).

11.2 Capital cost contingency

11.2.1 Definition

Different companies and organisations employ contingencies in a diverse manner. Hess and Myers /215/ formulate a definition that is employed in this work:

Contingency is the amount of money that experience has demonstrated must be added to an estimate to provide for uncertainties in: (a) project definition and (b) the cost and performance of a commercially unproven process. It is selected such that the estimate including contingency is the most probable cost.

Two separate contingencies are often employed (for example, by EPRI /60/): a project contingency and a process contingency (or process development allowance). However, this definition is not suggested by Hess and Myers /215/.

Other definitions for contingency are given below for reference:

Specific provision for unforeseeable elements of cost, particularly in fixed investment estimates, which previous experience has shown to be statistically likely to occur. May include an allowance for escalation /218/.

Contingency is defined as a specific provision of money or time in an estimate for undefined items which statistical studies of historic data have shown will likely be required /219/.

A significant feature of the above definitions is how heavily the entire issue is related to past experience and statistical data, and how little such data is published.

And as Frey /220/ points out,

The contingency often is the single largest expense item in the cost estimate, and yet it is also the least documented.

11.2.2 Cost growth and contingency in investment cost estimation

An example presented by Hess and Myers /215/ is depicted in Figure 11-3, where historical investment cost estimates (discounted to 1982 US dollars) for coal-to-SNG (based on Lurgi gasification) plants are shown. It should be noted that the last estimate is the actual cost of the Great Plains facility.

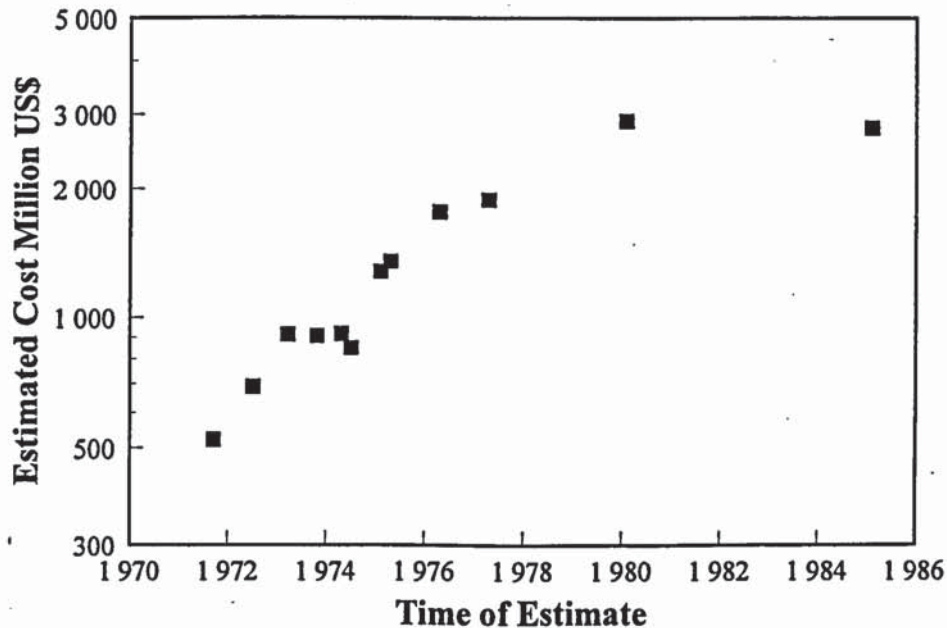


Figure 11-3. Reported cost estimates for coal-to-SNG plants discounted to 1982 dollars /215/, same capacity for all estimates.

Contingency may be used in estimating cost growth. However, the contingencies typically employed do not, on average, achieve this purpose. An example is from /215/ (Figure 11-2), in which contingencies employed are compared with average overrun by project stage. It may be seen that early cost estimates made during the project definition stage should have had contingencies averaging over 60%. In reality the average contingency used was close to 10%.

In another report, Merrow et al. /221/ demonstrate how difficult the estimation of capital cost for pioneer process plants is. The average cost overrun by project stage is depicted in Figure 11-1. Merrow et al. /220/ point out three distinct items based on the results:

1. In the early stages of project development, initial estimates capture only 40 to 60 percent of the ultimate cost (Figure 11-2).
2. Even though cost estimates for new technologies improve as a project develops, the final costs are still understated during the project engineering and early construction phases (Figure 11-1&2).
3. The accuracy of the estimates is subject to substantial variation. For example, some R&D estimates reflect only about 20 percent of the final costs, whereas others reflect over 80 percent of the final costs (Figure 11-1).

Clearly, both the systematic underestimation of costs, and the wide variation in accuracy are problems. It therefore becomes necessary to identify the factors that are responsible for the cost growth. Ideally, it would then be possible to determine appropriate contingency factors, given the particular characteristics of the project studied.

More recently, Merrow and Yarossi /222/ have expanded the analysis to cover a period of over 20 years. Sixteen general categories of CPI are included, from fine chemicals, fibers and fiber intermediates, minerals, refining, power plants, to waste treatment. Merrow and Yarossi report that from pre-1976 to post-1990 the ratio between the actual investment cost and the final estimate has decreased. This is, of course, a positive development, but a negative aspect is that the standard deviation of actual to authorised costs has declined only modestly. In the article only large US projects (above US\$ 10 million in 1988) were used in the database. However, they also report that the results are applicable for other areas (Europe, Asia) and for smaller-scale projects.

The results from /215/ are based on pioneer plants of the chemical process industries. However, they are also appropriate for the biomass power technologies studied in this thesis. Bio-power technologies largely employ CPI operations. In addition, bio-power has many features related to synfuel technologies, an area where relevant experiences have also been reported.

11.2.3 Review of methods used to estimate contingency

... (the) purpose of using these methods is to adequately compensate for the bias toward the underestimating characteristic of new technology cost estimates, and thus to provide realistic expectations about a technology and project's economic viability /215/.

Hess has reviewed six publicly available methods and one unpublished corporate method for estimating investment cost contingencies /215/. The methods presented and some of their features are shown in Table 11-1.

Table 11-1. Summary of contingency (cont) methods /215/.

Approach	Type of method	Level of detail	Empirical basis
GRI /223/	Separate project/process cont	Moderate	None
ESCOE /224/	Separate project/process cont	Low	Unknown
EPRI /60/	Separate project/process cont	Low	Unknown
Valle-Riesta /225/	Overall contingency	Low	Unknown
Industry example	Overall contingency	Low	Company experience
Hackney /226/	Overall contingency	High	29 estimates
PPS /215/	Overall contingency	Moderate	40 Projects/106 Estimates

GRI Gas Research Institute
 ESCOE Engineering Societies Commission on Energy, Inc.
 EPRI Electric Power Research Institute
 PPS Pioneer Plant Study

The accuracy of the different methods may be questioned. Only the last three methods have been validated with actual experience from process cost estimation. Of all the methods, only the last two offer a means of estimating the probable accuracy of the contingency.

Another issue is the reliability of the methods. For instance, the wide ranges of contingencies recommended by several methods must be determined subjectively. Most of the methods provide little or no guidance. Thus, their reliability is open to question. One issue is the practical application of the methods. Considerable ambiguity with the definitions of the terms used makes it difficult to employ many systems.

Three significant issues are emphasised by Hess and Myers /215/: one related to the stage of process development, another related to the effects of start-up, and the third related to the effects of project definition and process development.

The first important concern is the potentially misleading focus on individual stages of process development in some methods. Not only do the definitions vary across companies in the industry, but also across governmental agencies and research centres. *Identifying the development stage serves nothing more than a proxy for the level of process understanding achieved /215/.* Hess and Myers /215/ show, based on the PPS database, how the level of the most advanced unit operating at the time of the estimate does not explain the extra contingency that would have been needed to correct the estimate.

Another major concern is that most methods ignore the effects of start-up on the cost estimate accuracy. Hess and Myers /215/ report that a considerable part of the total project cost growth occurs during the start-up phase.

The third important consideration specified by Hess and Myers /215/ is the significance of jointly considering the effects of project definition and process development. These factors strongly interact, and their separation is unlikely to yield meaningful results. In effect, risk is taken into consideration by jointly considering these two aspects, as is shown in equation (11-1) for cost growth.

Two types of cost contingencies are compared by Hess and Myers /215/. The methods take either new sub-systems or the entire project estimate as their base.

... cost growth from early estimate to final costs is largely a function of (a) the degree of technological innovation involved and (b) the extent of project definition accomplished at the time the estimate was prepared /215/.

Firstly, they point out that:

The most striking result of (our) analysis of sub-system growth concerns the lack of data... /215/

Therefore the method that uses new sub-systems at its base will be difficult to verify, and will not be considered further.

11.2.4 Cost growth and the model used for contingency

Hess and Myers /215/ describe a system, which is validated. They propose a formula for calculating a contingency for a given process plant, which will be used in this work. Four factors are considered in the model:

1. The percentage of the estimated cost that involves commercially unproven technology.
2. The extent to which stream impurity problems are encountered during process development.
3. The level of project definition.
4. The stage of process development.

The model for cost growth prepared by Hess and Myers /215/ is shown as equation (11-1).

$$\begin{aligned} \text{Cost growth factor (CGF)} = & 1.08 - 0.0025 * \text{Percent New} \\ & - 0.0174 * \text{Impurities} \\ & - 0.0482 * \text{Project Definition} \\ & - 0.201 * (\text{Project Definition} * \text{Process Development}) \end{aligned} \quad (11-1)$$

Percent new refers to the percentage of the estimated costs that involves commercially unproven technology.

Impurities refer to the extent to which process stream impurity problems are encountered during process development. A six-point scale is employed, ranging from zero, indicating no problem, to five, indicating that impurities posed a major problem.

The level of **project definition** completed at the time of the estimate is prepared. Project definition is measured using the sum of two components. The first one assesses the level of process engineering completed on a four-point scale ranging from one, indicating design specifications, to four indicating a screening study. The second component measures the

average degree of definition corresponding to a number of informational categories about the specific plant site. The categories include on-site and off-site unit configurations, soils and hydrological data, health and safety requirements, and environmental requirements. Using four-point scales, the quality of information for each category is rated as having been based on 1) definitive work, 2) preliminary work, 3) assumed or implicit analysis, or 4) not used in the estimate at all. The resulting project definition variable ranged from two, indicating design specifications and definitive site information, to eight, indicating a screening study level of engineering and non-site-specific information is used.

The stage of **process development**. The effect of project definition on cost growth is found to depend on the process development stage. A binary indicator of the process development is used. If most process information is obtained from small-scale lab experiments and the literature, or a co-ordinated R&D program was under way at the time of the estimate, the indicator was assigned a value of one. If process development work focused on minimizing risk for commercial application with demonstration-scale pilot work, or major process uncertainties have been resolved and development work completed, the indicator was assigned a value of zero.

The role of project definition is especially important. Project estimates at a "medium" definition stage for processes still in the R&D stage require an average contingency that is two to three times that required for pre-commercial or commercially established technologies.

Contingency is defined in equation (11-2).

$$\text{Contingency \%} = \frac{1}{CGF - 1} * 100 \quad (11-2)$$

To illustrate the use of the method, a contingency for a pressurised gasification combined cycle is estimated.

Percent new: 67% (gasification and gas turbine investment are 67% of the total investment of concept 1)

Impurities: 3

The level of **project definition**

- the level of process engineering completed: 2
- the average degree of definition: $+(2+3+3+3)/4 = 2.8$

The stage of **process development: 1**

Cost growth factor =

$$1.08 - 0.025 * 67 - 0.0174 * 3 - 0.0482 * (2 + 2.8) - 0.201 * (2.8 * 1) = 0.58$$

$$\text{Contingency} = (1/0.58 - 1) * 100 \% = 74\%$$

11.3 Potential for cost improvement

It is accepted that costs of pioneer facilities are not necessarily representative of mature technology. Two tendencies, one increasing the investment (insufficient process definition) and, the other reducing it (cost improvement over time) in comparison with mature technology, should be understood in order to utilise preliminary cost assessments.

Cost improvement is defined as the reduction in a technology's unit product cost that occurs as experience with the technology is gained /215/.

A numbers of factors, which tend to occur over time, may push the costs of successive plants down:

1. Learning from experience by building successive plants
2. Plant and process optimisation
3. Evolutionary technical improvement

It may be seen from the simplified model shown in Equation (11-3) that improvement in the overall product cost may be obtained by:

1. Reducing the capital charge rate or the capital

2. Reducing operating and maintenance costs
3. Reducing feedstock costs
4. Increasing the plant output
5. Combinations of the above

$$\begin{aligned}
 & \text{Unit product cost} = \\
 & \frac{\text{Annual CCR} \times \text{Capital cost} + \text{Annual O\&M cost} + \text{Annual Feedstock Cost}}{\text{Annual plant output}} \quad (11-3)
 \end{aligned}$$

Studies dealing with diverse industries including aircraft, electricity, electronics, musical instruments, and clothing have been reviewed in /227/. The objective of the study was to provide a basis for assessing potential synthetic fuel process cost reductions. In addition to the few synthetic fuel facilities in existence, relatively analogous petroleum refining and CPI were therefore emphasised.

Improvements related to the overall unit product costs are available for petrochemical and chemical processes /214/, /228/, /229/. It should be noted that all of these studies use price data as recorded on the market rather than actual production cost data. However, if a long-run perspective is adopted, the price reduction acts as a rough substitute for cost improvement.

It is important to note that data concerning only the overall unit product cost was available. No data is available concerning the unit capital cost reduction for individual processes, which is often used in trying to estimate cost growth.

For estimating cost improvement, Hess and Myers 215/ prefer a method that aims at estimating the improvement in the original process. The approach presented in /227, 228/ has the disadvantage that it also captures effects of evolutionary technological change, which often results in a process that does not resemble the original.

The method in /215/ takes account of improvements in three broad areas:

1. Capital cost

2. O&M cost
3. Plant performance

Potential improvements for the pioneer, second, third, and “nth” plants are considered. The “nth” is included to reflect the costs associated with a mature process. Hess and Myers /215/ have selected the sixteenth plant as the “nth” unit. Two reasons were stated. Firstly, no more than 16 large synfuels plants were conceived on the basis of a single basic gasification process. Secondly, on the basis of the conventional assumption with respect to learning, the 16th plant is well past the point at which the majority of absolute improvements has been realised.

Hess and Myers /215/ conclude that between process introduction and process maturity, overall cost reductions of between 30 percent (for moderately innovative technologies) and 60 percent (for highly innovative technologies) are possible. Figure 11-4 depicts an example of such a cost reduction, where cost improvement potential has been estimated for two process concepts related to the Great Plains plant project. The cost reduction, however, should not be considered in any way automatic.

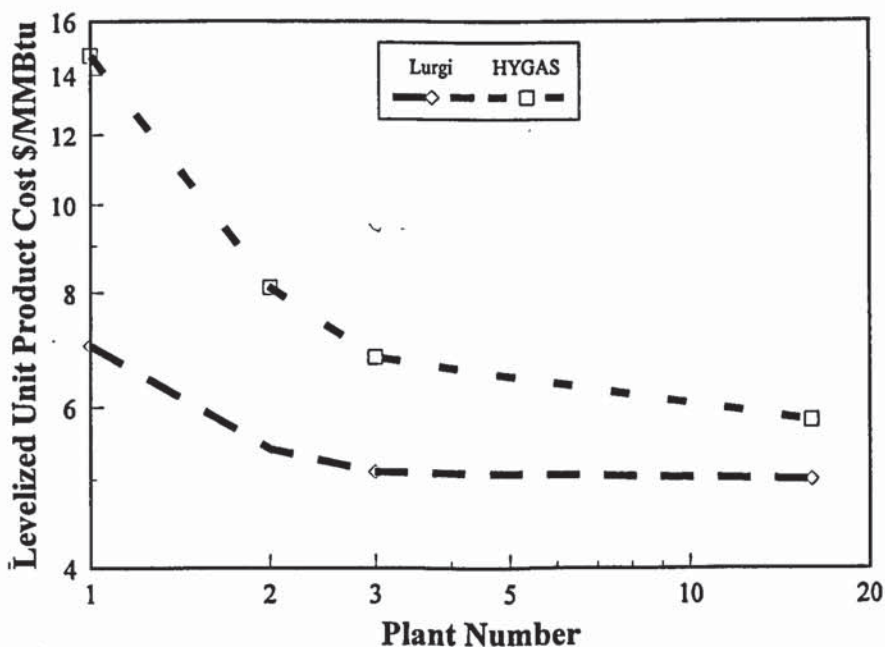


Figure 11-4. Potential for cost improvement, two concepts compared in SNG production from coal, moderately and highly innovative technologies /215/.

Cost improvement is described also by EPRI in /60/. No absolute data is given in the publication, and no actual method is described. However, several other related factors, e.g. the effects of market factors on investment costs, are reviewed and discussed.

11.4 Capital costs estimated for this work

The capital cost estimates used in this work are prepared at two stages: Firstly, estimates are made using principally the cost functions originating from an IEA Bioenergy project, in which contingency is specially excluded or deducted /31/. At the second stage, the contingency method presented in chapter 11.2.4 is applied. After this, the cost improvement is taken into account to produce the final capital cost estimate for the systems studied.

11.4.1 Base capital cost investment estimates

The costs used in this work are derived primarily from two sources: the International Energy Agency (IEA) Bioenergy Pyrolysis project 1992-1994 /31/, and an in-house database at VTT Energy. No contingencies are used at this stage. Many of the unit processes are at an early development stage, and the accuracy of the estimate used is difficult to assess.

The total capital investment costs of power plant are based on unit process investment costs. The units listed in Table 11-2 are considered. The unit process costs are derived on the basis of the performance analysis (Chapter 10). A parameter has been selected for each unit and used to scale the unit cost. The correlations between the parameter and cost employed, which form the bases for the total investment cost, are shown in Appendix 10.

Summaries of investment costs are shown in Table 11-3 and Figure 11-5 for all the concepts. The investment costs are presented in detail in Appendix 11. The Rankine cycle investments are shown in Figure 11-5 as the commercial reference. It may be seen that the conventional power plant technology has investment costs that are about one half to one third of those of new systems. Pyrolysis systems have slightly lower base investment costs than gasification power plants. Advanced systems appear to be closer to Rankine power plants at higher capacities.

Table 11-2. Unit processes used in capital cost estimation, process parameters used for sizing processes, and the development stage of the unit (D = under development, I = industrial).

Unit process	Parameter used in sizing	Development stage
Receiving, storage and handling of biomass	Dry biomass mass flow	I
Steam drying	Dry biomass mass flow	I
Flue gas drying to 15% (gasification)	Dry biomass mass flow	I
Flue gas drying to 10% (pyrolysis)	Dry biomass mass flow	I
Grinding	Dry biomass mass flow	I
Gasification, pressure	Dry biomass mass flow	D
Gasification, atmospheric	Dry biomass mass flow	D
Compressors/Expanders	Power demand	D
Pyrolyser	Dry biomass mass flow	D
Waste water incinerator	Waste water mass flow	D
Gas turbine-generator	Gas turbine power output	D
Heat recovery steam generator (HRSG)	HRSG steam mass flow	I
Boiler feed water system	De-aerator water mass flow	I
Steam turbine-generator	Steam turbine power output	I
Cooling water system	HRSG steam mass flow	I
Diesel-generator using gaseous fuel	Engine power output	D
DeNOx catalyst system	Engine power output	D
Diesel-generator using liquid fuel	Engine power output	D
Oxidising catalyst system	Engine power output	D
Co-generation unit (for CHP)	Heat output	I
Electricity connection	Electricity output	I

Table 11-3. Summary of the investment costs for the plants, no contingency applied. Costs as in 1998, Western Europe. Note that the pyrolysis cases include both liquid production and the powerplant. P-IGCC pressurised gasification combined cycle, A-IGCC atmospheric P-STIG pressurised STIG cycle, GE gasification and engine, Py-DP pyrolysis diesel power plant, Pyro-CC pyrolysis combined cycle.

	Concept	Capacity MWe	Investment Mill. US\$	Cost \$/kW
1	P-IGCC	31.9	87	2 730
2		30	88	2 920
3		29.1	89	3 050
4		59.8	134	2 240
5	A-IGCC	6.6	32	4 840
6		33.2	90	2 710
7		62.3	139	2 230
8		29.1	89	3 040
9	P-STIG	4.9	32	6 570
10		23.6	80	3 410
11		23.6	83	3 530
12		23.6	81	3 450
13		41	121	2 960
14	GE	4.2	23	5 420
15		18.4	60	3 230
16	Py-DP	5	21	4 180
17		25	63	2 520
18	Py-GTCC	6.4	27	4 230
19		32	69	2 140
20		29.4	69	2 350
21		60.1	105	1 760

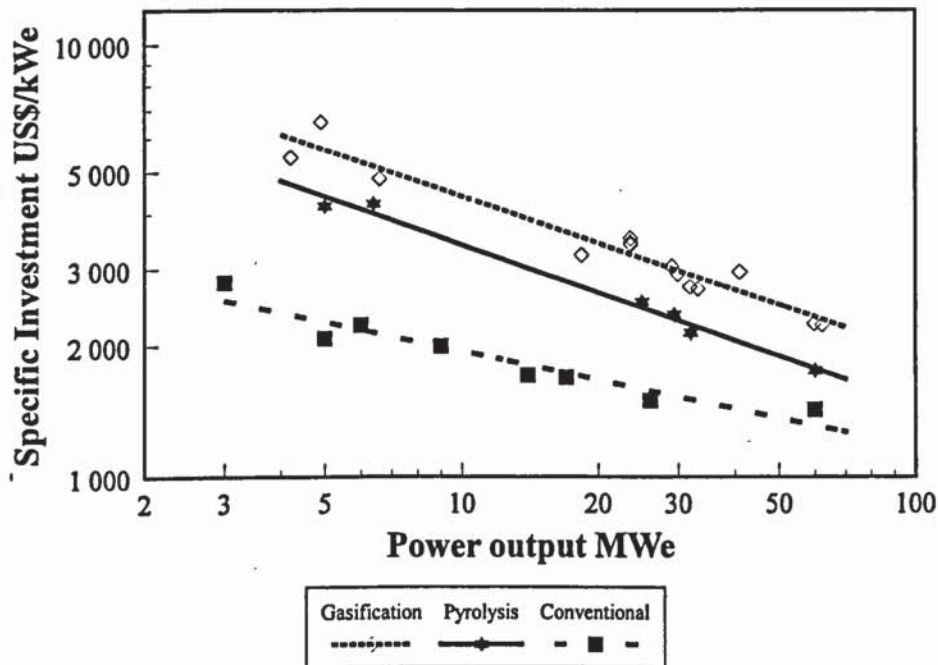


Figure 11-5. Summary of specific investment costs. No contingency applied, location Western Europe 1998. Note: Pyrolysis plant included.

11.4.2 Contingency and cost improvement in cost estimates

The investment cost estimates change considerably when contingency is taken into account. Contingencies are estimated on the basis of the method presented in chapter 11.2.4. The respective values used for each factor in formula 11-1 are presented in Table 11-4.

Using the average contingencies for each technology, revised investment cost estimates are presented in Table 11-5. Specific investments are compared with the Rankine cycle power plants in Figure 11-6.

Table 11-4. Estimation of process contingencies. Def. = definition, Dev. = development, CGF = cost growth factor. Py-DP ja Py-GTCC power plant section only.

Concept	Case	Percent new	Impurities	Project def. 1	Project def. 2	Process dev.	CGF	Contingency %	Average contingency %
P-IGCC	1	67	3	2	2.75	1	0.58	74	74
	2	67	3	2	2.75	1	0.58	73	
	3	66	3	2	2.75	1	0.58	73	
	4	68	3	2	2.75	1	0.57	74	
A-IGCC	5	53	2	2	2.75	1	0.63	59	65
	6	64	2	2	2.75	1	0.60	66	
	7	64	2	2	2.75	1	0.60	66	
	8	64	2	2	2.75	1	0.60	66	
P-STIG	9	69	3	2	2.75	1	0.57	75	78
	10	73	3	2	2.75	1	0.56	79	
	11	71	3	2	2.75	1	0.57	77	
	12	72	3	2	2.75	1	0.56	78	
	13	76	3	2	2.75	1	0.55	80	
GE	14	63	3	2	3.00	1	0.57	76	78
	15	69	3	2	3.00	1	0.56	80	
Py-DP	16	77	4	3	3.00	1	0.47	113	113
	17	76	4	3	3.00	1	0.47	112	
Py-GTCC	18	30	3	3	3.00	1	0.60	66	76
	19	49	3	3	3.00	1	0.56	80	
	20	48	3	3	3.00	1	0.56	79	
	21	50	3	3	3.00	1	0.55	81	
Rankine		0	0	1	2.25	0	0.92	8	8
Pyrolysis		70	4	3	3.00	1	0.49	106	106

Investment costs for advanced systems increase above the Rankine power plant investments because of the high contingencies applied. New systems now have specific invest-

ments which are between three to four times higher than those of conventional power plants. Overall investment costs for pyrolysis plants also increase more than gasification power plant costs, and pyrolysis and gasification power plant costs are quite close to each other. A higher contingency for pyrolysis reflects the higher uncertainties related to the technology.

Table 11-5. Summary of investment costs for the plants; average contingency applied for each technology, 1998, Western Europe. Final estimate = in addition to contingency, potential cost improvement included, corresponds to the 16th plant.

	Concept	Capacity MWe	Investment, no contingency \$/kW	Contingency %	Investment with contingency \$/kW	Final estimate \$/kW
1	P-IGCC	31.9	2 730	74	4 740	3 460
2		30	2 920	74	5 070	3 700
3		29.1	3 050	74	5 290	3 860
4		59.8	2 240	74	3 890	2 840
5	A-IGCC	6.6	4 840	65	7 970	5 820
6		33.2	2 710	65	4 450	3 250
7		62.3	2 230	65	3 670	2 680
8		29.1	3 040	65	5 010	3 660
9	P-STIG	4.9	6 570	78	11 670	8 520
10		23.6	3 410	78	6 060	4 420
11		23.6	3 530	78	6 270	4 580
12		23.6	3 450	78	6 130	4 480
13	GE	41	2 960	78	5 250	3 830
14		4.2	5 420	78	9 640	7 030
15		18.4	3 230	78	5 750	4 200
16	Py-DP	5	4 180	113	8 880	6 480
17	Py-GTCC	25	2 520	113	5 360	3 910
18		6.4	4 230	76	9 000	6 570
19		32	2 140	76	4 550	3 320
20		29.4	2 350	76	5 010	3 650
21		60.1	1 760	76	3 730	2 720

The potential for cost improvement is taken into account as suggested by Hess and Myers /215/ in the next stage. The specific investment costs are shown in Table 11-5 and Figure 11-7. "Learning" is assumed to reduce the investment cost by 10% between the pioneer plant and the second plant, 10% again between the second and the third, and a further 10% between the 3rd and the 16th plant, all of the reductions being based on the report by Hess and Myers /215/. Therefore, a reduction of 27% is assumed for all capital costs of advanced cycles to give the cost of the 16th or "nth" plant. This is consistent with the bases of the

reviews in Chapter 2. Note that no reduction is assumed for the Rankine cycle, as that technology is considered to have already passed the 16th plant stage.

Even the 27% reduction does not change the relationship between the alternatives. Pyrolysis and gasification investments are very close to each other. The new systems are estimated between 2.5 (large plants) to three times (small plants) more expensive than the Rankine cycle.

Note that investment for the pyrolysis oil production plant has been taken into account in Tables 11-3 and 11-5, and also in Figures 11-5 and 11-6, to correspond to the power plant fuel requirement. However, by using pyrolysis, the power plant may be de-coupled from solids handling, which may, among other positive aspects, increase power plant availability. The production of pyrolysis oil in a large centralised facility, instead of on-site for only one power plant fuel, would also reduce the cost of oil production. Investment costs for only the pyrolysis power plant are also shown in Figure 11-7. The investments for the oil-fuelled power plants are close to those of Rankine power plants.

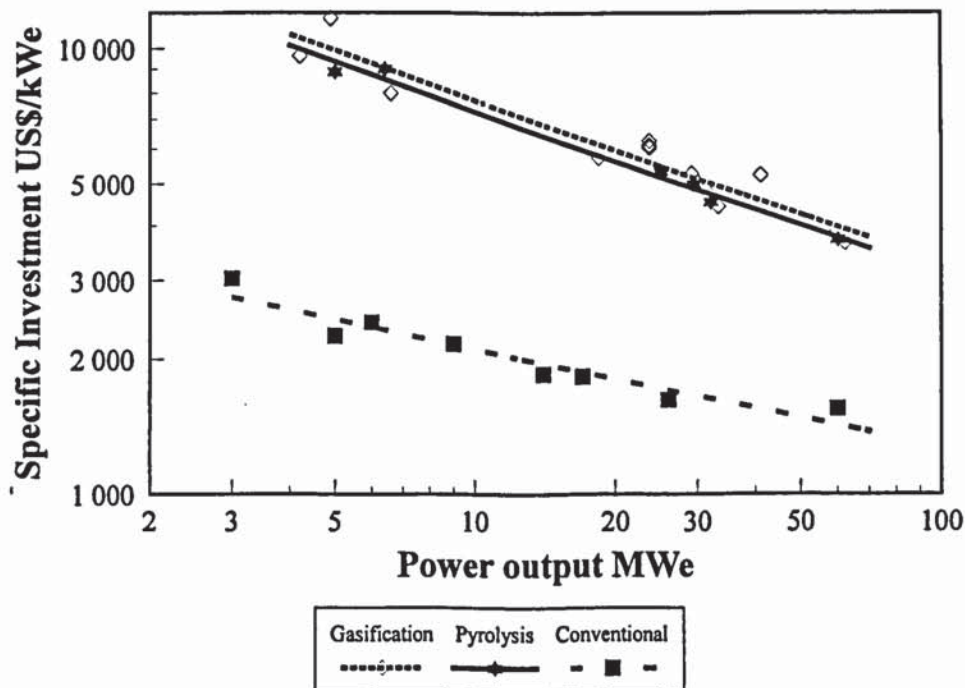


Figure 11-6. Summary of specific investment costs, contingencies included. RAND contingency applied, location Western Europe, 1998. Note: Pyrolysis plant included.

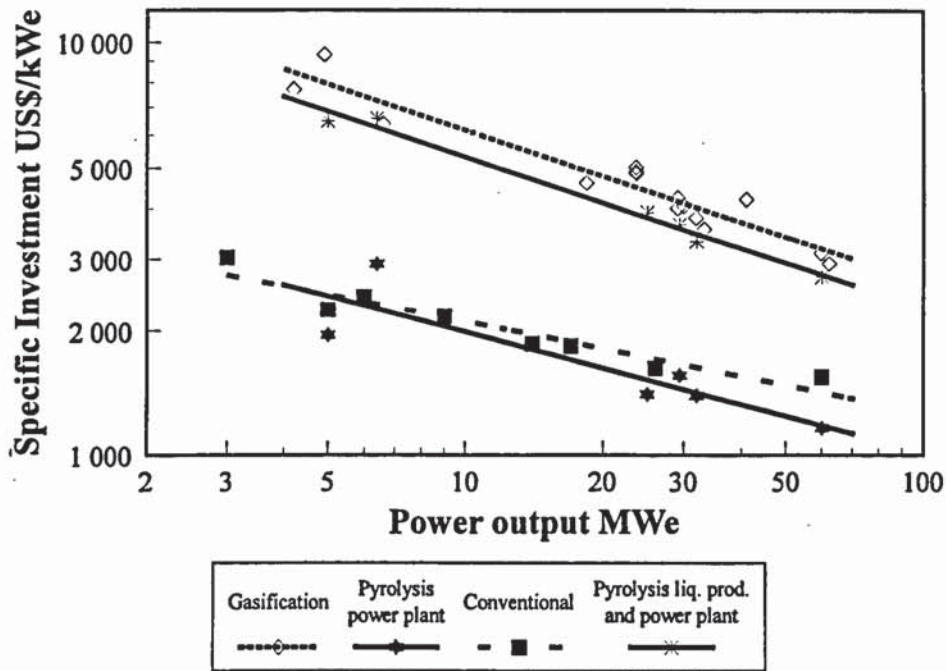


Figure 11-7. Summary of specific investment costs, contingencies and potential cost improvement included, pyrolysis both with and without liquid production plant. RAND contingency and potential cost reduction applied, location Western Europe, 1998.

All of the advanced cycles are estimated to be much more capital-intensive than the conventional Rankine cycle, which is currently the state-of-the-art in bio-power. It is estimated that the specific investments of advanced cycles are about three times higher than those of the Rankine cycle at around 5 MWe and about twice as high at around 50 MWe. However, advanced cycles are more efficient, and to compete with Rankine power plants the operating costs of advanced cycles have to be lower.

11.5 Summary

The capital costs of new biomass power plant concepts are estimated on the basis of standard engineering methods. Even though it is believed that the base investment costs used are authoritative, it is accepted that capital estimates concerning unproven processes are subject to uncertainty. The weakest point in the analysis carried out is therefore the base unit investment cost used. Any error in the base cost will be multiplied using the contingency estimation procedure.

The investment cost contingency, which experience has demonstrated must be added to an estimate to provide for uncertainties, was derived using established methodologies. The potential for cost improvement is also taken into account. The methods used are validated with industrial data.

Investment costs for the advanced bio-power concepts studied in this thesis are higher than those reported in many recent studies. However, this is not surprising considering the lack of data on CPI cost growth, which necessarily makes up the foundation for a proper cost contingency estimation.

Two conclusions from the above analysis are:

- For the new processes to be competitive, the present biomass fuel costs must be increased to make new high-efficiency processes competitive.
- The reduction of capital costs is imperative for the competitiveness of new technologies.

12. PRODUCTION COSTS OF ELECTRICITY

In this chapter, electricity production costs (or the cost of electricity, COE) are presented for each of the cases modelled. Comparisons are made between the cases, and again, new systems are compared with commercial technology.

12.1 Electricity production modes

The operation of power generation is classified by the amount of time the unit is on-stream. Three main modes are usually used. These differ in terms of their cost structures and periods of operation, as explained below. Power plants are operated in peak, medium or base load modes. The distinction between the three modes is based primarily on their capital cost, variable operating costs, and load variation characteristics. The cost structures dictate that a technology with a low operating cost (low fuel cost, medium or high capital cost) is operated in base load mode, and plants with a higher operating cost (usually low capital cost) are used in intermediate and peak load mode. Load variation is the primary requirement in peak load, and a reliable start-up is essential. The relative competitiveness of these power plant concepts varies considerably, depending on the annual operating time, because the three modes favour different cost structures.

Base load operation refers to power plants that are operated typically in excess of about 6000 hours annually, often more than 7 500 h/a. They are also often operated close to their design capacity. Nuclear power plants, combined-cycle plants using natural gas, and large conventional pulverised-coal-fired steam power plants are examples of this class.

Peak load plants are operated only over short periods (typically less than 500 - 1 000 h/a) and are characterised by low capital costs, higher fuel costs, and a quick start-up time. Gas turbines and diesel engines are examples of power plants employed in peak mode. These plants are typically smaller in capacity than base load units.

Power plants operated in **medium load** (around 1 000 - 5 000 h/a) may be of several types. Typically, old base-load power plants with some remaining service life are operated in me-

dium load mode. Their variable costs may be higher than those of new base-load plants, and therefore they are started up second after the new base-load capacity.

This aspect has implications for this work as well: for example, gasification power plants are capital-intensive and thus more economical in base load. Their limited load-following capacity also suggests base load service. Conversely, diesel power plants are most competitive in medium and peak load modes. With a relatively low investment cost but higher O&M costs, they are quick to start up and are good in load following.

12.2 Calculation of COE

In this work, COE is calculated by dividing the total production cost by the amount of production, equation (12-1). The equation is another version of equation (2-1).

$$COE \text{ (Electricity unit product cost)} = \frac{\text{Annuity} \times \text{Capital cost} + \text{Annual O\&M cost} + \text{Annual feedstock cost}}{\text{Annual plant net output}} \quad (12-1)$$

where Annuity = Interest and depreciation for capital investment (eq. 12-2)

O&M = Operation and maintenance

$$\text{Annuity} = \{(r/100)/(1-(1+(r/100))^a)\} \quad (12-2)$$

where r = Fractional interest rate

a = Service life in years

The structure of electricity demand requires some of the generating capacity to be load following, and this result in different modes of operation for power plants. Because of this feature of electricity production, COE is often expressed as a function of annual peak operating hours. Consequently, the competitiveness of power plant concepts may be readily assessed in different modes of operation.

Using the annuity method is a simplification, as interest and depreciation of the capital cost is defined for a typical average year with this method. However, the approach is particularly convenient when comparing several similar processes with each other. Traditionally, the Finnish power industry has most often used the average COE in initial concept comparisons. Profit is not included, but may be effectively taken into account by increasing the rate of interest in the annuity method. Most real investment projects calculate a net present value or an internal rate of return using the market price of electricity to justify an investment.

The base values for the annuity in this work, a 5% rate of interest and a service life of 20 years, have been used by the leading Finnish contractor when comparing power plant concepts /34/. The same values have also been employed in studies funded by the Ministry of Trade and Industry /33/. It is recognised that the rate of interest used is low for a commercial investment, although is more widely used for government-funded strategic investments. Using a higher rate of interest may be considered as a means of compensating for risks and including a profit. However, in this work capital cost contingency is employed to take account of risk. Using both contingency and a high rate of interest would in effect allow for process uncertainty twice. The sensitivity case for the rate of interest presented in section 12.5.6 may be considered as a means of studying the competitiveness of advanced cycles, when profit is taken into account. A comparison between contingency and a high interest rate is also carried out.

Other methods, in which funding arrangements and time value of money are taken into account, are also employed. EPRI uses a specified method for calculating the cost of electricity /60/. Although this is a more rigorous analysis and more acceptable to the financial community, it is only used widely in the U.S. This method, although rigorous and appropriate, does not offer any additional value for the analysis of this work, as it is the comparisons that are the focus of the analysis.

The internal rate of return (IRR) may also be calculated for the production of electricity. In this approach a price has to be established for the electricity sold. This method is necessary when analysing the commercial viability of a project. Different types of project may be compared with a common yardstick, the internal rate of return. However, this method is not

necessarily more informative for the purpose of this work. The IRR method is especially suitable for assessing projects ready for investment decision-making.

12.3 Bases for operating costs

In this section, the methods used in estimating operating costs are reviewed. All cost items are shown in Table 12-2, where a summary of the COEs is presented.

The operating costs include:

- Feedstock
- Labour
- Utilities
- Maintenance and overheads

For the cases in which district heat production is considered, the heat by-product income is deducted from the annual operating costs. The operating costs are then added to capital payments on an amortisation basis to derive production costs.

12.3.1 Feedstock

The feedstock considered is wood at a delivered base cost of US\$ 25 / wet (50% moisture) tonne. This corresponds to 2.8 US\$/GJ or 10 US\$/MWh. This base cost is a typical industrial cost for delivered fuel wood in Northern Europe 1999 /230/. The reference fossil fuel base prices for natural gas and coal for an industrial user are 2.8 and 1.9 US\$/GJ, respectively. These are average costs in Western Europe in 1999 /231/. Variations in fuel cost are considered in the sensitivity analyses.

12.3.2 Labour

A generalised correlation for the number of operating personnel per shift has been employed /31/. The correlation is shown in Figure 12-1. Five shifts are assumed. An annual man-year rate of US\$ 35 000 is assumed, including all direct payroll overheads.

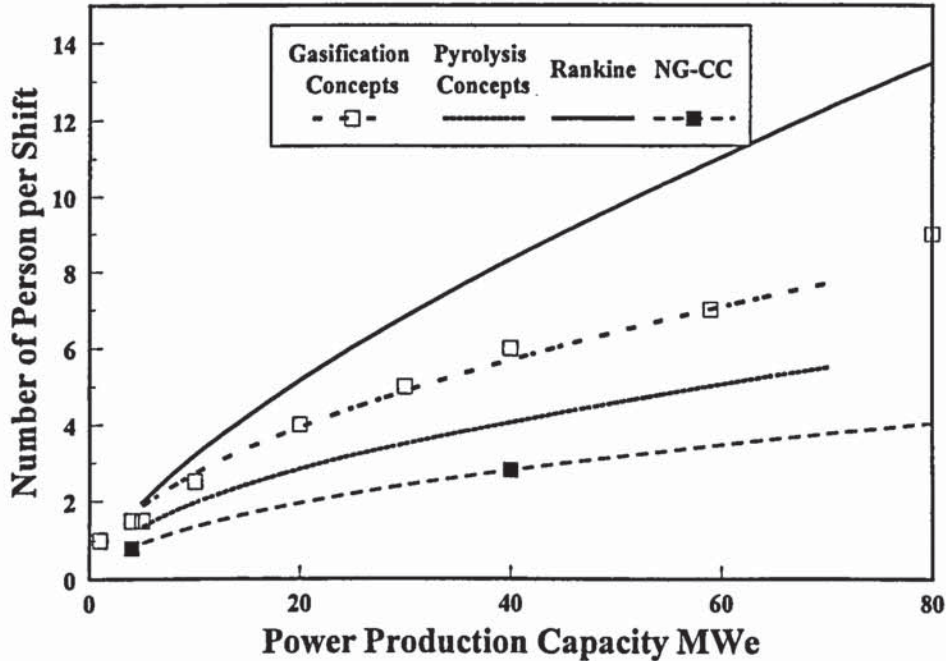


Figure 12-1. Personnel per shift as a function of power plant capacity.

12.3.3 Utilities

Performance calculations for utilities (power and water consumption), calculated with AspenPlus models, provide data for estimating the cost of the utilities. Electricity for pumps, blowers, feeding systems, etc., is subtracted from the plant's own production. Wash water for product gas scrubbers and cooling water is costed on the basis of consumption.

None of the processes require fuel gas or oxygen services. All other energy requirements are met in-house without requiring conventional fuels, except for start-up and where otherwise reported (pilot fuel for diesel engines).

12.3.4 Maintenance and insurance

The annual maintenance cost (including labour and materials) is usually estimated as a proportion of the system's capital cost. A maintenance and insurance cost of 1.6% on a total plant cost basis was used in the product cost calculations, and variations can be considered in a sensitivity analysis. The value used is slightly higher than that typically used in power production, 1.2% /34/. Using solid wood as fuel increases maintenance costs. Additionally, commercially unproven advanced processes are assumed to have higher maintenance costs than industrial plants.

12.3.5 District heat

District heat as a by-product is considered for some concepts. The total annual income from district heat production is deducted from the annual operating costs, when the by-product heat is considered. A typical cost structure employed in Finland for district heat is used (a fixed cost of 25 000 USD/MW_a and a variable cost of 10 US\$/MWh) /34/, and a rather wide range is used in sensitivity studies to cover a broad potential user-base for heat.

12.4 Production cost of fast pyrolysis liquid

The production cost of pyrolysis liquid is determined independently of power production. Pyrolysis liquid is produced separately, as explained in section 10.8, and the production capacity may be considered independent of power plant capacity. Therefore it is necessary to present the pyrolysis liquid production cost before considering the COE in a pyrolysis power plant.

The production costs of fast pyrolysis liquid are estimated on the basis of standard chemical engineering practise (Table 12-1) /31/. The parameters used in the table are: Fuel feed capacity 30.7 t/h 50% wet wood fuel (215 000 t/a), 7 000 hours of annual operation, capital cost annuity factor 0.08 (corresponds to a 5% rate of interest and a 20-years service life). In a later section the effect of a higher rate of interest is shown.

The liquid cost is shown as a function of fuel cost in Figure 12-2. A range for capacities is shown. The fuel cost is varied $\pm 40\%$ from the base value to cover the most probable industrial price range. Within the range studied, the liquid is 2.4 to 4.4 times more expensive than the wood fed into the pyrolyser. A similar presentation as a function of plant capacity is shown in Figure 12-3. It corresponds to the fuel feed range used for gasification power plants concepts. The fuel cost is shown as a parameter, and the sensitivity to biomass feed is shown. When the sensitivity analysis of the fuel cost is studied later, the solid line correlation in Figure 12-2 is used for the fuel costs of the pyrolysis power plant.

Table 12-1. Fast pyrolysis liquid production cost, feed capacity 70 MW_{th}, feed cost 2.8 US\$/GJ.

	M USD/a	USD/t	USD/GJ	USD/MWh
FIXED OPERATING COST				
Operating labour	0.4	5.0	0.3	1.1
Maintenance labour	0.3	3.1	0.2	0.7
Overheads	0.5	6.2	0.4	1.4
Maintenance materials	0.8	9.4	0.6	2.1
Taxes, insurance	0.5	6.2	0.4	1.4
Others	0.3	3.1	0.2	0.7
Sub-Total	2.9	33.1	2.1	7.4
VARIABLE OPERATING COST				
Feedstock	4.9	56.0	3.5	12.5
Electricity	0.9	10.8	0.7	2.4
Sub-Total	5.8	66.9	4.2	15.0
CAPITAL CHARGES	2.6	29.7	1.8	6.6
PRODUCTION COST	11.3	129.7	8.1	29.0

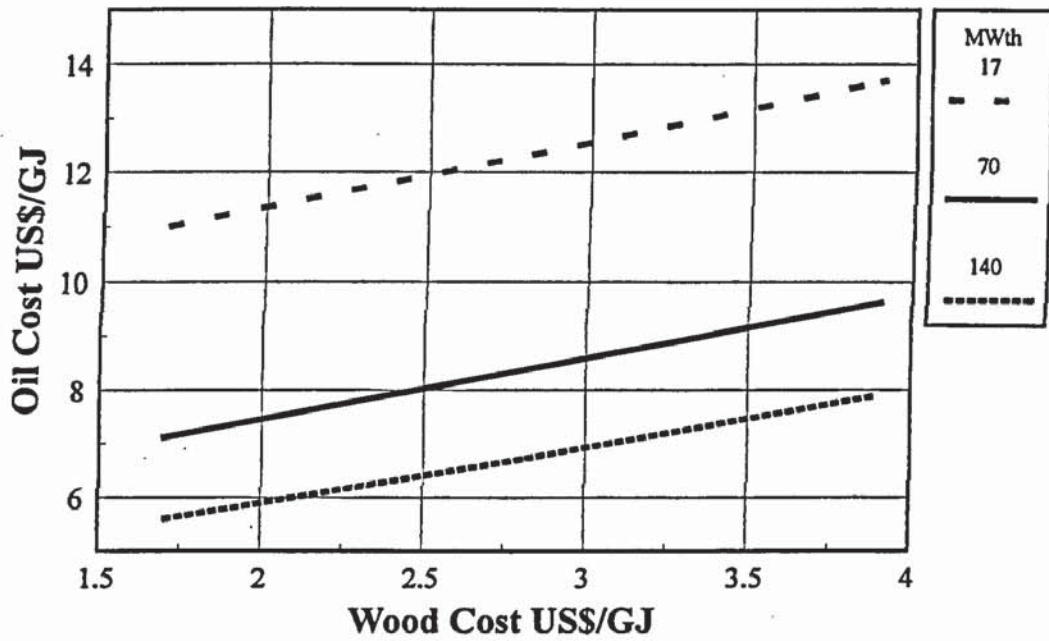


Figure 12-2. Fast pyrolysis liquid production cost as a function of fuel cost. Plant size in MW_{th} input as a parameter. 2.8 US\$/GJ corresponds to 10 US\$/MWh. Annuity factor 0.08, annual operating time 7 000 h/a.

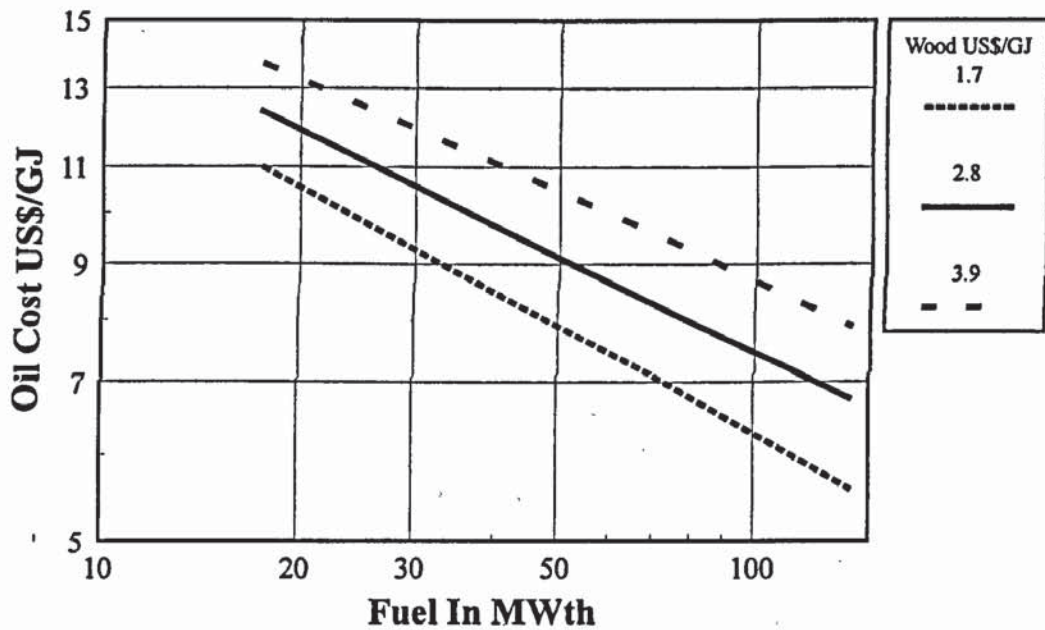


Figure 12-3. Fast pyrolysis liquid production cost as a function of fuel feed capacity. Fuel cost as a parameter. 70 MW_{th} feed corresponds to a feed of 215 000 t/a 50% wet wood, and a liquid production of 87 000 t/a. Annuity factor 0.08, annual operating time 7 000 h/a.

12.5 Cost of electricity (COE)

The COE is studied under several sub-sections:

- Summary of cost of electricity from advanced systems
- Gasification and pyrolysis presented separately
- Modes of operation: peak, medium, and base load operation
- Sensitivity to *fuel cost*
- Sensitivity to rate of interest
- Comparison with fossil fuel fired power plants
- Effect of CHP
- Effect of the scale of pyrolysis liquid production on the COE
- An example of using the cost and performance model in an industrial evaluation

Production capacity and annual operating time are used as variables in each sub-section for all concepts. These two parameters are considered critical for the analysis. In this section the COE is calculated for the proposed gasification, pyrolysis and conventional Rankine power plant concepts. The results are reviewed in several sections to study different aspects of power production. All of the concepts are analysed to study the *circumstances in which* new power plants may become competitive.

The principal criteria employed in the analyses include:

- Lowest COE overall. Intermediate or medium annual operating time (3 000 - 5 000 h/a) is considered technically the most suitable market for bio-power.
- Competitiveness on a small scale (< 5 MWe), a range where bio-power is often proposed. Although technically demanding, this scale is important because biomass is available in many places only in relatively small quantities.
- Competitiveness compared with the Rankine cycle. A new concept must offer a lower COE than the conventional alternative.
- The concept with the lowest COE in peak load operation. The Rankine cycle is not technically suitable.

12.5.1 Summary

A summary of power production costs for all alternatives is shown in Table 12-3 using the following values for the key parameters: rate of interest 5%, service life varies with technology (16 years for engine power plants, 20 years for others), annual operating time 5 000 h/a, biomass cost 25 \$/wet ton (10 \$/MWh or 2.8 \$/GJ), pyrolysis liquid 140 \$/ton (31 \$/MWh or 8.6 \$/GJ). These values have been standard for capital cost estimation in recent years in Finland /34/. Note also what was said in section 12.2 about a high rate of interest and contingency.

The wood cost is for industrial fuel wood in Northern Europe in 1999 /229/. The justification for base pyrolysis liquid cost is presented in section 12.4. The cost of electricity shown is for the "nth" or "16th plant", which corresponds to a mature technology. This practice has been proposed by Hess and Myers /215/.

Figure 12-4 presents the effect of annual operating hours on the COE for each technology at 3000, 5000 and 7000 h/a, respectively. These represent peak, medium and base load operating times. All gasification and pyrolysis concepts are lumped into two correlations, respectively. Note that a straight-line correlation is shown for all cases in the log-log presentation.

The competitiveness of gasification concepts improves at higher annual hours, and they are less expensive compared with pyrolysis concepts above 20 - 30 MWe. The pyrolysis concepts tend to compete better at low annual operating hours, when their COE is lower than that of gasification over the whole range (IGCC is an exception). The pyrolysis COE is only somewhat higher than that of the Rankine concept, which has the lowest COE over the whole range. Gasification is competitive on a larger scale (above 50 MWe) with the Rankine cycle, if the annual operation time is long. However, the cost of pyrolysis liquid is a strong function of plant capacity and annual operating time. When assumptions for these parameters change, the conclusions are also affected. A more detailed analysis is presented in the following sections.

Table 12-2. Summary of power production costs. Nomenclature as in Table 11-3. Capital costs determined with the annuity method, service life 20 years, rate of interest 5%, 5 000 annual operating hours. Wood cost 10 \$/MWh or 2.8 \$/GJ, pyrolysis liquid 31 \$/MWh or 8.6 \$/GJ.

CONCEPT	1	2	3	4	5	6	7
	P-IGCC	P-IGCC	P-IGCC	P-IGCC	A-IGCC	A-IGCC	A-IGCC
MWe	31.9	30.0	29.1	59.8	6.6	33.2	62.3
FIXED COSTS \$/kWh							
Salaries	0.003	0.004	0.003	0.003	0.007	0.003	0.002
Maintenance	0.011	0.012	0.012	0.009	0.019	0.010	0.009
VARIABLE COSTS \$/kWh							
Fuel	0.021	0.023	0.023	0.022	0.027	0.024	0.025
Fuel oil	0.000	0.000	0.000	0.000	0.000	0.000	0.000
CAPITAL COST \$/kWh	0.056	0.059	0.062	0.046	0.093	0.052	0.043
CREDIT FOR DH \$/kWh	0.000	-0.014	-0.021	0.000	0.000	0.000	0.000
TOTAL COST \$/kWh	0.091	0.084	0.080	0.079	0.146	0.090	0.079
CONCEPT	8	9	10	11	12	13	14
	A-IGCC	P-STIG	P-STIG	P-STIG	P-STIG	P-STIG	A-GDP
MWe	29.1	4.9	23.6	23.6	23.6	41.0	4.2
FIXED COSTS \$/kWh							
Salaries	0.003	0.009	0.004	0.004	0.004	0.003	0.011
Maintenance	0.012	0.027	0.014	0.015	0.014	0.012	0.023
VARIABLE COSTS \$/kWh							
Fuel	0.027	0.035	0.029	0.029	0.029	0.033	0.029
Fuel oil	0.000	0.000	0.000	0.000	0.000	0.000	0.005
CAPITAL COST \$/kWh	0.059	0.137	0.071	0.073	0.072	0.062	0.113
CREDIT FOR DH \$/kWh	-0.019	0.000	0.000	-0.024	-0.017	0.000	0.000
TOTAL COST \$/kWh	0.082	0.208	0.118	0.097	0.102	0.110	0.180
CONCEPT	15	16	17	18	19	20	21
	A-GDP	Py-DP	Py-DP	Py-CC	Py-CC	Py-CC	Py-CC
MWe	18.4	5.0	25.0	6.4	32.0	29.4	60.1
FIXED COSTS \$/kWh							
Salaries	0.003	0.006	0.002	0.005	0.002	0.002	0.002
Maintenance	0.013	0.006	0.005	0.009	0.004	0.005	0.004
VARIABLE COSTS \$/kWh							
Fuel	0.029	0.104	0.104	0.096	0.088	0.095	0.091
Fuel oil	0.006	0.002	0.002	0.000	0.000	0.000	0.000
CAPITAL COST \$/kWh	0.067	0.031	0.023	0.047	0.022	0.025	0.019
CREDIT FOR DH \$/kWh	0.000	0.000	0.000	0.000	0.000	-0.017	0.000
TOTAL COST \$/kWh	0.119	0.149	0.135	0.157	0.117	0.111	0.115

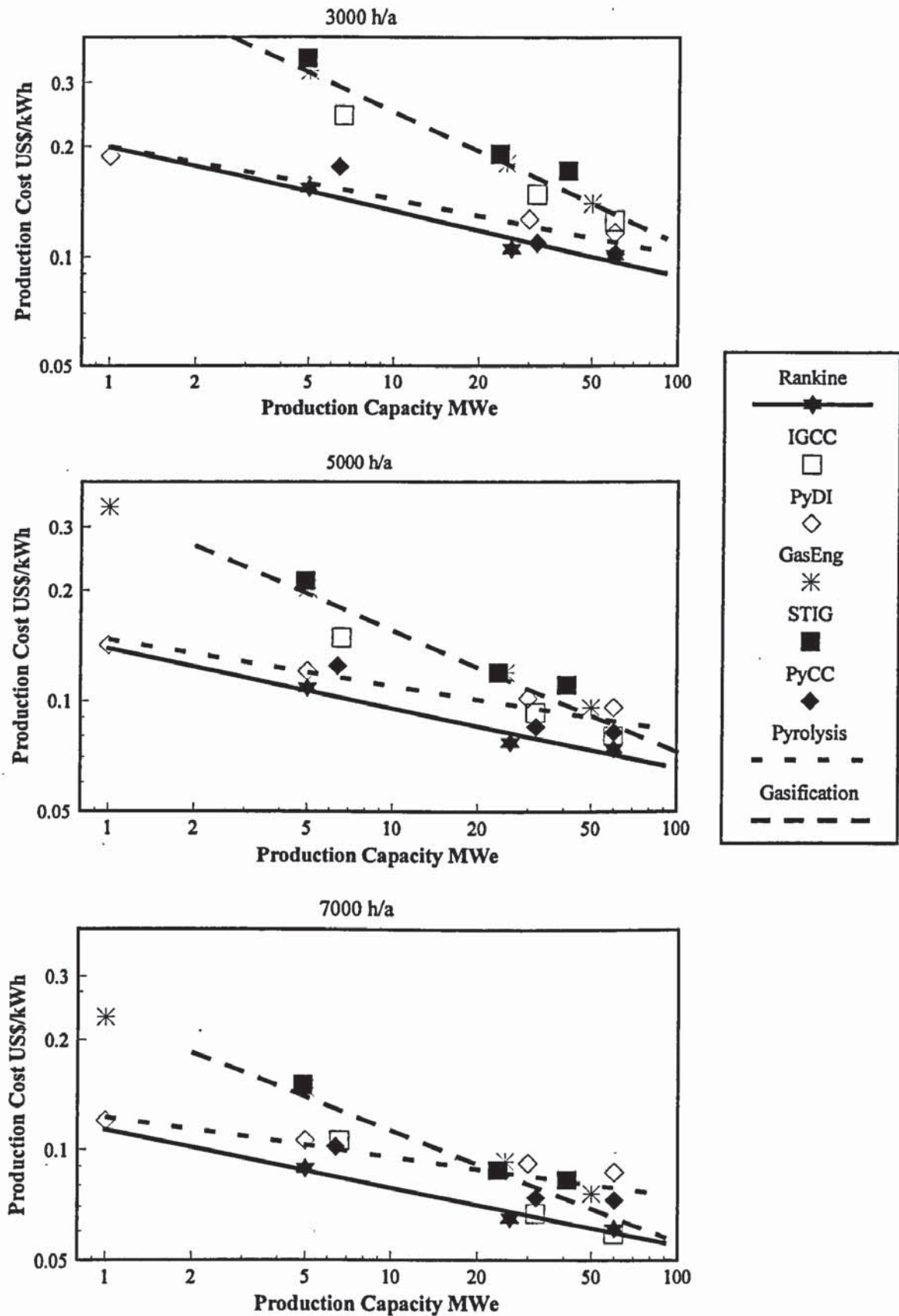


Figure 12-4. COE as a function of power plant capacity, annual peak operating time as a parameter. Wood 2.8 US\$/GJ, pyrolysis liquid 8.6 US\$/GJ, annuity factor 0.08 corresponding to a 5% rate of interest and a 20-year service life.

12.5.2 Gasification and pyrolysis

In this section, gasification and pyrolysis are presented separately to compare different concepts using these primary technologies. The COEs of gasification and pyrolysis are presented in Figures 12-5 and 12-6, respectively.

Different gasification concepts are compared in Figure 12-5 over a wide capacity range for three levels of annual operating hours. The IGCC appears to be the low-cost option of the concepts even at 3000 h/a, although differences at this operating time are probably not significant (< 10%), taking the uncertainties into account. The IGCC is clearly the most economical at high operating hours, and at 7000 h/a its COE is about 30% less than in the other gasification cases. STIG and gas engine concepts yield a higher COE than the IGCC at all capacities and annual operating times. The two concepts have COEs quite close to each other. The competitiveness of the IGCC is largely due to its higher efficiency.

Pyrolysis power plant concepts are compared in Figure 12-6. The diesel power plant is favoured over pyrolysis combined cycles (CC) on a small scale. The difference is pronounced at lower operating times. With high annual operating hours, PyCC has a lower COE throughout, except on a scale below 5 MWe. At 7000 h/a the COE for PyCC is about 20% lower than for PyDI. However, otherwise the differences between the pyrolysis power plant concepts are less than 20% over the whole capacity and operating range, and are probably not significant. Overall, the diesel power plant has a lower cost than the PyCC at low capacities. The competitiveness of PyCC improves with higher operating hours due to its higher efficiency.

The full potential economies of scale for pyrolysis power plants is not shown in Figure 12-6, as the cost of pyrolysis liquid is kept constant. However, it may be argued that pyrolysis power plant concepts will not become economic unless the production is carried out at a large capacity. The cost of pyrolysis liquid in such a situation will be close to constant for all users. The COE sensitivity of pyrolysis liquid production is presented in a later section.

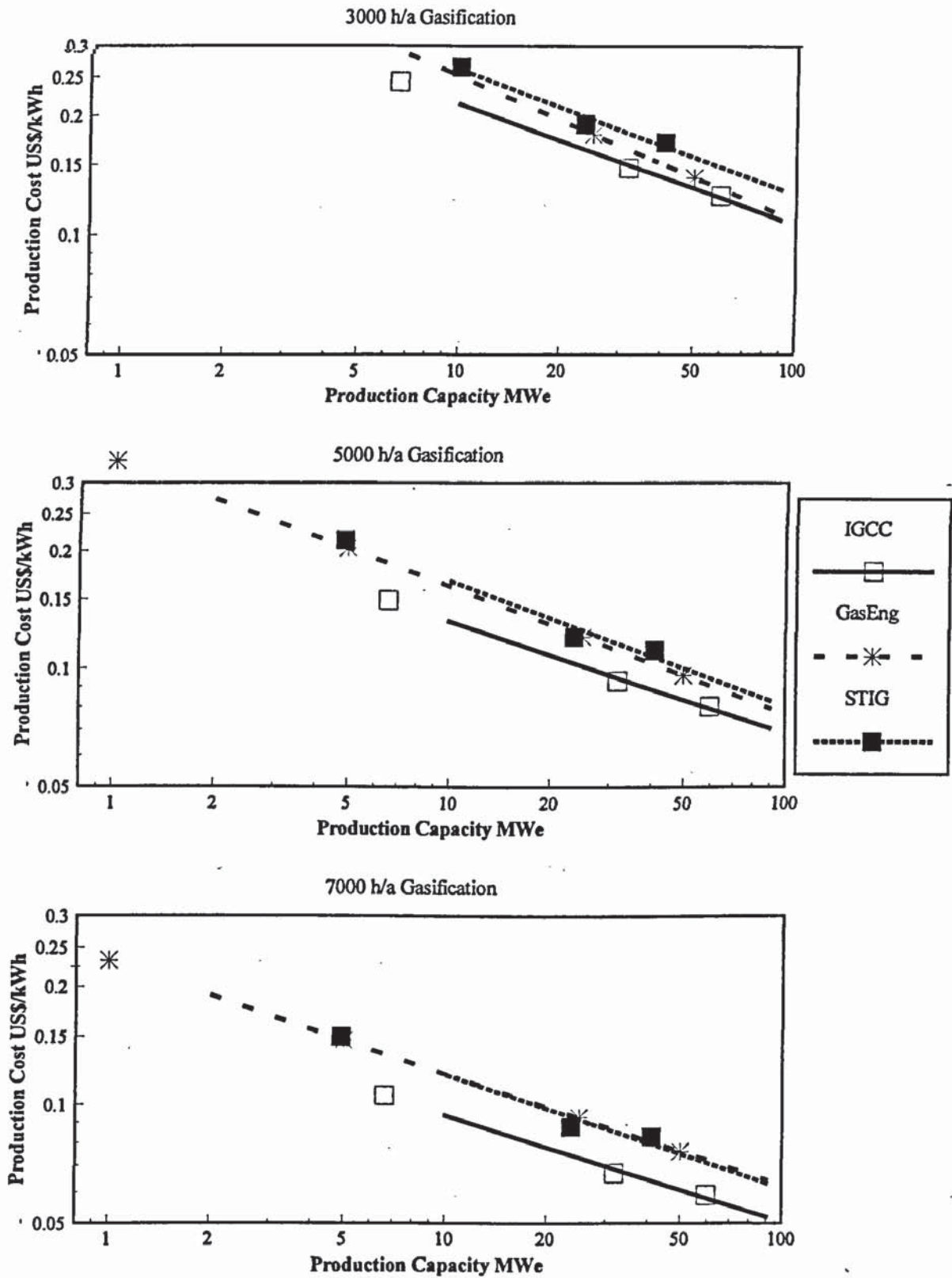


Figure 12-5. COE for gasification power plants, annual peak operating time as parameter. Wood 2.8 US\$/GJ, annuity factor 0.08 corresponding to a 5 % rate of interest and a 20-year service life.

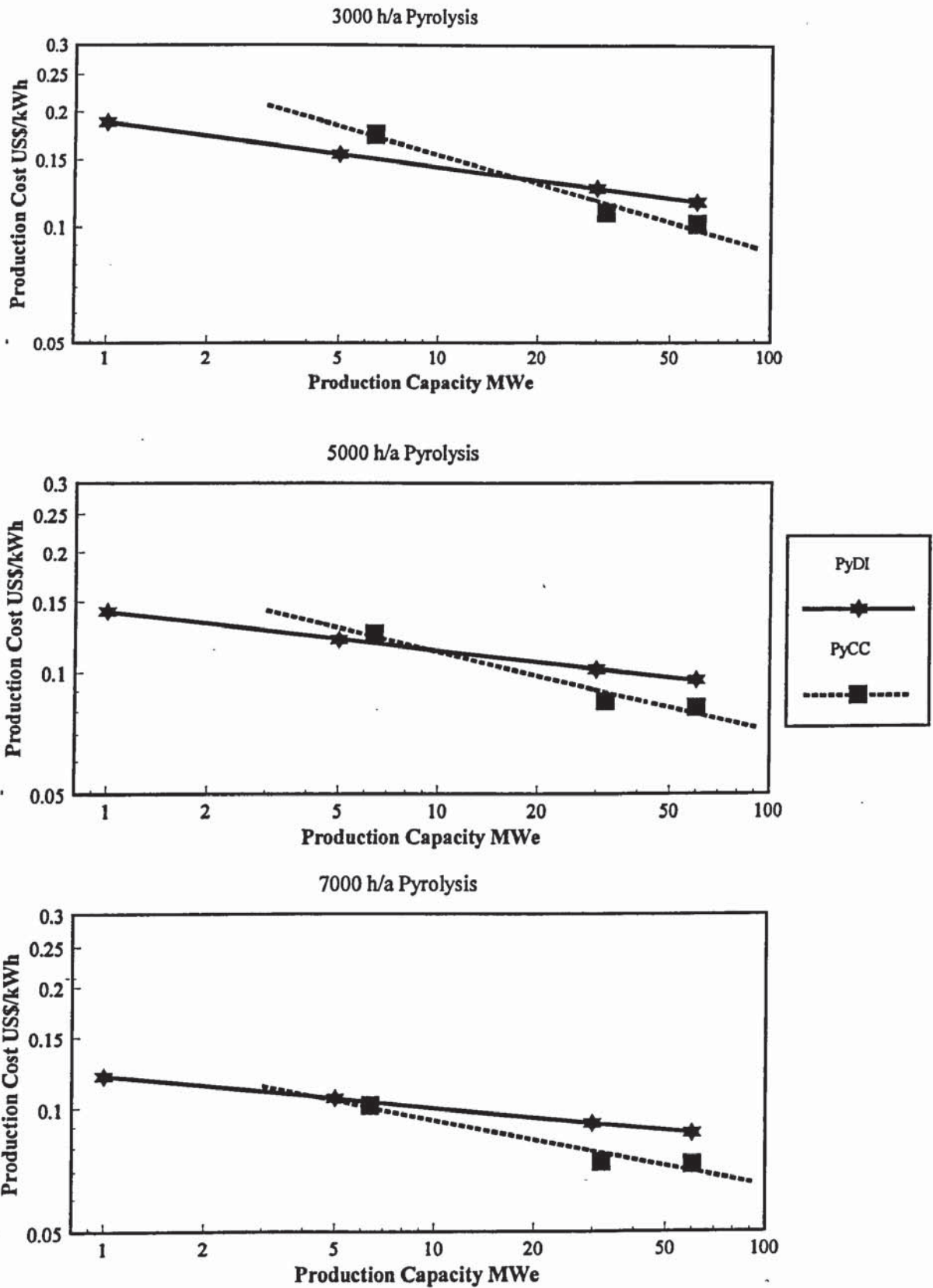


Figure 12-6. COE for pyrolysis power plants, annual peak operating time as parameter. Wood 2.8 US\$/GJ, pyrolysis liquid 8.6 US\$/GJ, annuity factor 0.08 corresponding to a 5 % rate of interest and a 20-year service life.

12.5.3 Small, medium, and large scale

The competitiveness of different concepts on three scales is studied in this chapter. Representative technologies are selected for comparison at capacities of 5, 25 to 30, and 50 to 60 MWe from each class: Rankine, pyrolysis, and gasification power plants.

The Rankine cycle appears to be competitive with the advanced concepts in most cases. However, the comparison with new proposed power plant concepts indicates when the new concepts may become competitive. Furthermore, the analysis reveals which concepts do not appear to be competitive under any conditions.

Small-scale plants are shown in Figure 12-7. Rankine has the lowest COE above 2 000 h/a operating time, and pyrolysis diesel the lowest below this operating time. However, the Rankine, pyrolysis diesel, and pyrolysis CC are quite close to each other. Only for high annual operating hours does Rankine clearly show the lowest cost. The gasification gas engine concept has a higher COE for all peak operating hours, and it does not seem to compete on this scale. It appears that both pyrolysis power plant concepts are relatively promising on a small scale. This is largely due to the non-integrated production of pyrolysis liquid. Handling of solids, an especially expensive stage on a small scale, is carried out on a larger scale in pyrolysis liquid production. The gasification engine power plant suffers especially from high specific capital costs.

Medium-scale concepts are shown in Figure 12-8. Rankine has the lowest COE across the whole range, although the pyrolysis CC is nearly the same cost. IGCC becomes competitive with the Rankine at high operating hours, above 6 000 h/a. The pyrolysis diesel does not compete with Rankine or pyrolysis CC above 1 000 h/a. The diesel concept is clearly most applicable on a small scale. On the other hand, the gas engine concept is not economic at any operating time. PyCC is especially promising for the medium scale for two reasons: handling of solids is avoided on this relatively small scale, and the efficiency is high.

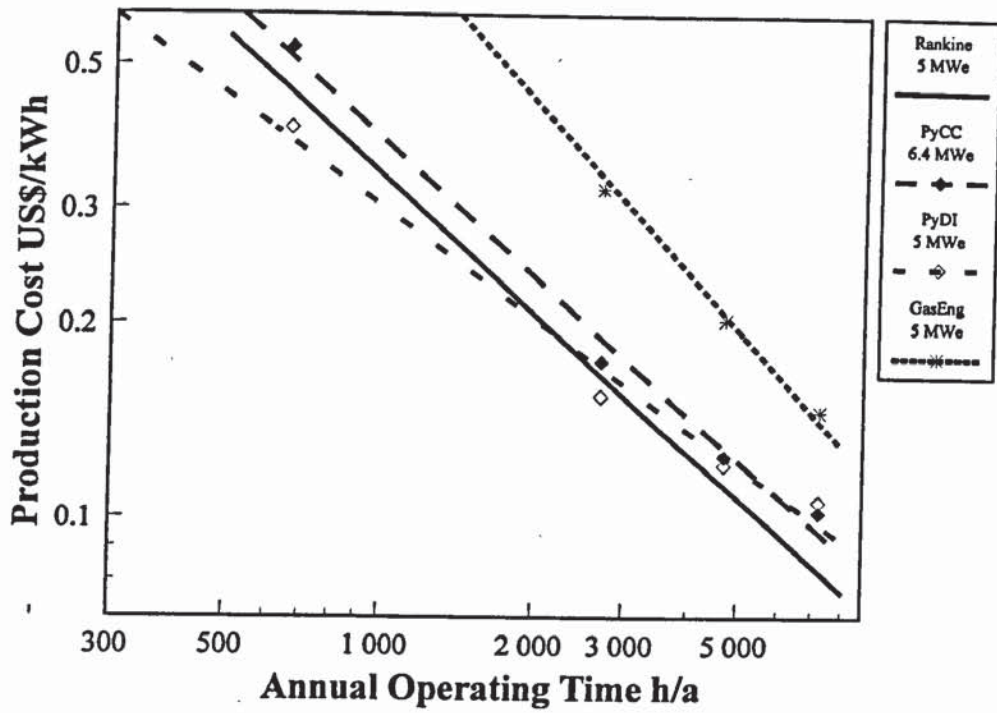


Figure 12-7. COE for small-scale power plants as a function of annual peak operating time. Capacities of concepts shown in the legend in MWe. Wood 2.8 US\$/GJ, pyrolysis liquid 8.6 US\$/GJ, annuity factor 0.08.

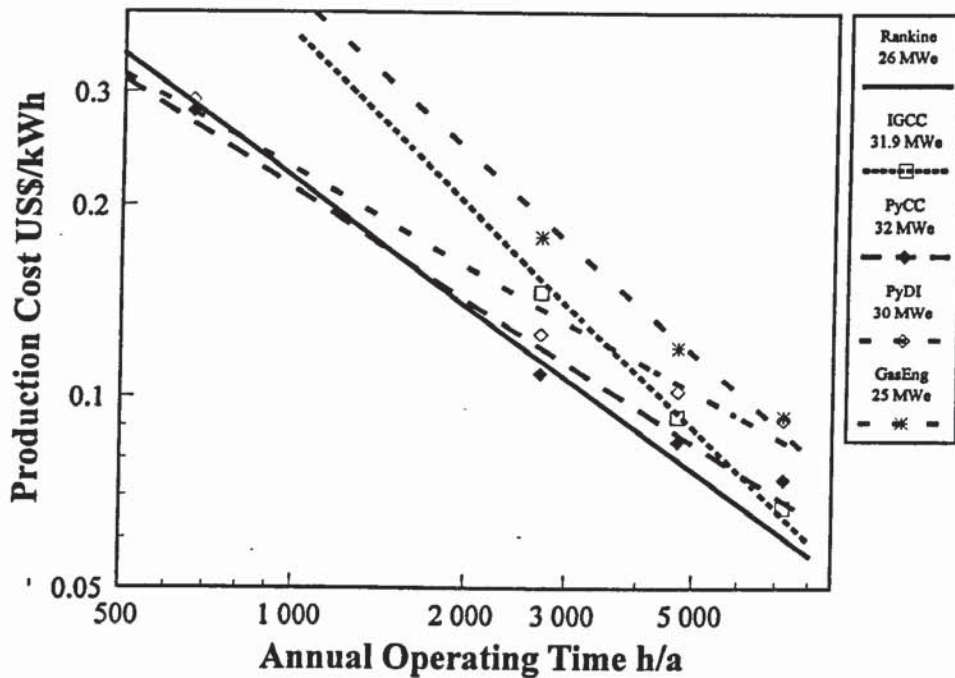


Figure 12-8. COE for medium-scale power plants as a function of annual peak operating time. Capacities of concepts shown in the legend in MWe. Wood 2.8 US\$/GJ, pyrolysis liquid 8.6 US\$/GJ, annuity factor 0.08.

“Large”-scale (from 50 to 60 MWe) concepts are compared in Figure 12-9. The Rankine cycle shows the lowest cost above 2500 h/a, while the pyrolysis CC has the lowest COE below 2500 h/a. IGCC has the lowest COE of the new concepts above 4000 h/a, and becomes competitive with the Rankine cycle at 7000 h/a. The comparison highlights the suitability of the IGCC concept for large-scale base load operation, which is due to its high specific investment. Note the logarithmic scale and the respective considerable differences between the alternatives at low operating hours. At 7000 h/a the COE of PyDI is more than 40% higher than that of the IGCC.

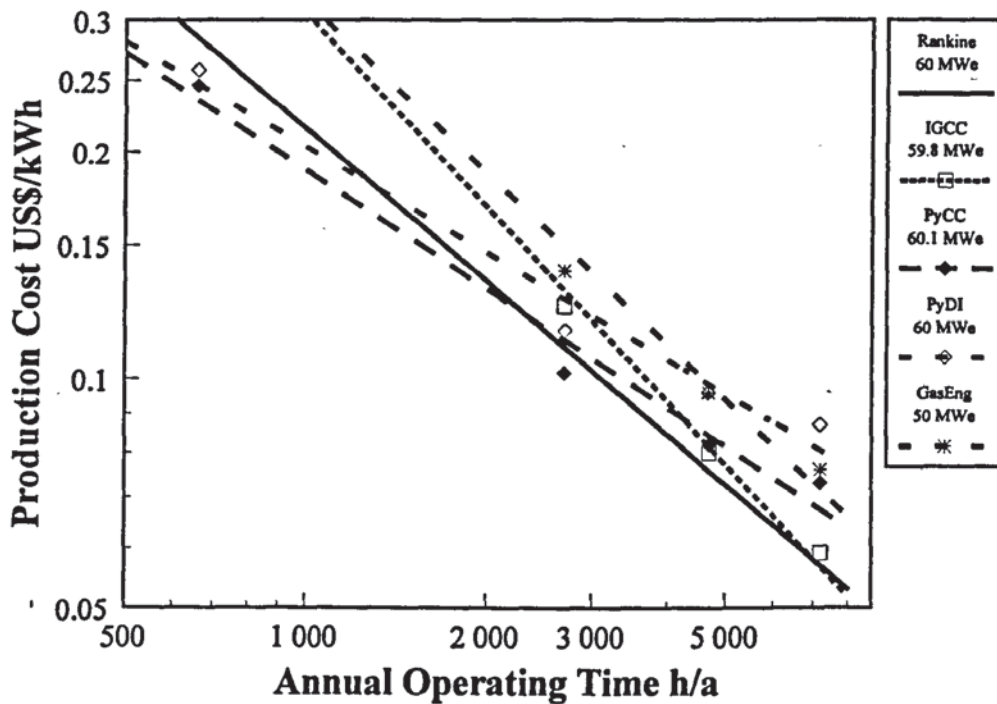


Figure 12-9. COE for larger-scale power plants as a function of annual peak operating time. Capacities of concepts shown in the legend in MWe. Wood 2.8 US\$/GJ, pyrolysis liquid 8.6 US\$/GJ, annuity 0.08.

12.5.4 Annual operating time

Different annual operating times are studied in this section. The analysis is done as a function of plant capacity for four cases: 700, 3000, 5000, and 7000 h/a, the first one representing peak, the next two intermediate, and the last one base load operation.

Peak load operation is shown in Figure 12-10. Only the pyrolysis concepts are technically well suited for peak load service. The other power plant concepts are not usually considered for peaking, as they cannot easily be started up quickly enough for peak load service. On the other hand, they cannot be technically ruled out completely either. Their costs are shown with thin lines to highlight that they are less suitable than the pyrolysis cases.

The diesel power plant is preferred over the combined-cycle concept in peak service. Only at > 40 MWe does the COE of the PyCC become lower than the COE of the PyDI concept. However, it is unlikely that biomass power plants will be built for large-scale peak service. Other applications, including small-scale peak service, are more likely if bio-power becomes competitive.

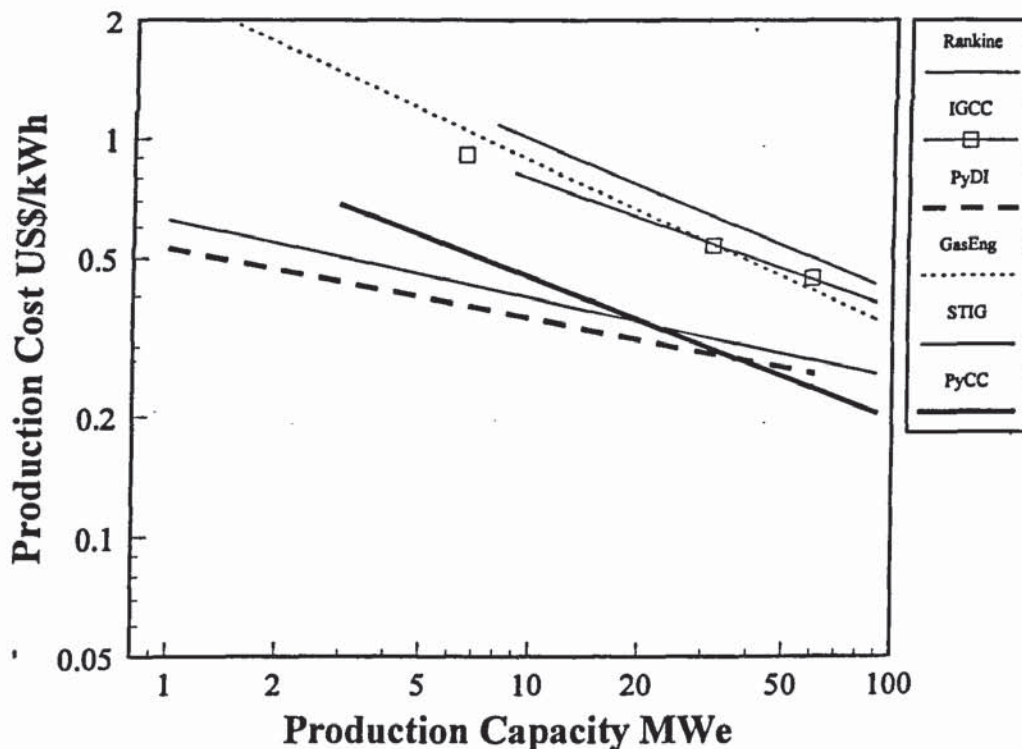


Figure 12-10. COE for peak operating time, 660 h/a. Wood 2.8 US\$/GJ, pyrolysis liquid 8.6 US\$/GJ, capital cost recovery factor 0.08.

Two intermediate times are shown for annual operating times, 3000 and 5000 h/a. The first intermediate operating time is depicted in Figure 12-11. The Rankine cycle is most economical, followed by pyrolysis diesel (below 20 MWe), pyrolysis CC (above 20 MWe), IGCC, gasification gas engine, and STIG. The gasification cases have a considerably

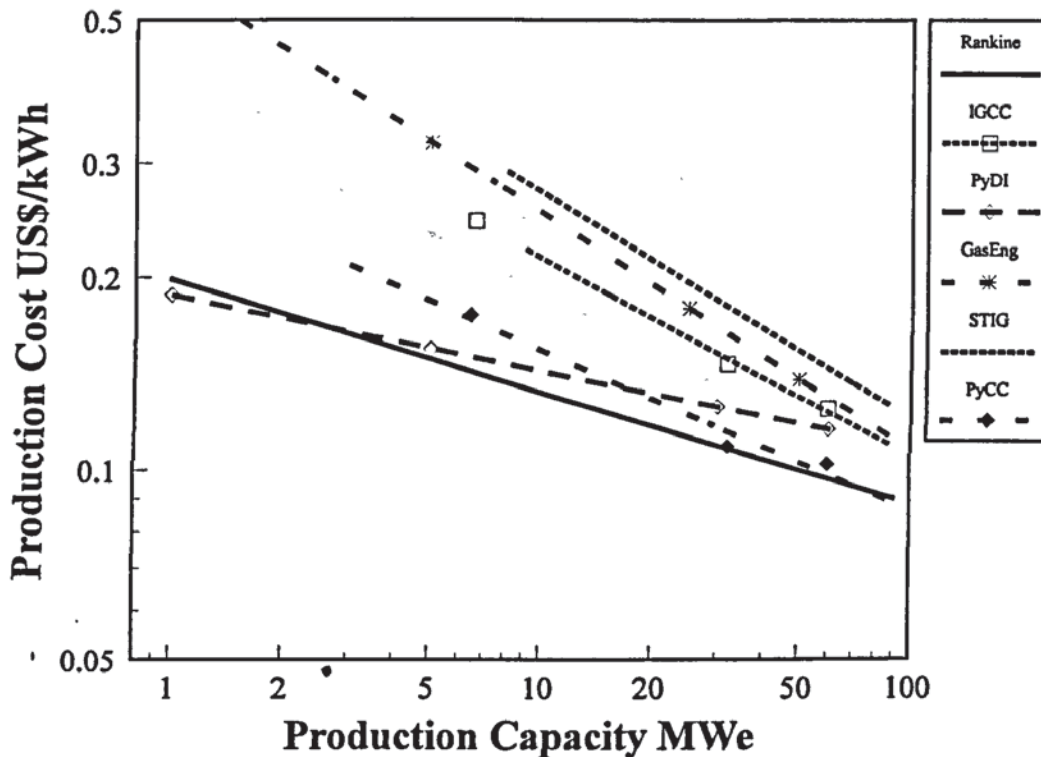


Figure 12-11. COE for intermediate operating time, 3000 h/a. Wood 2.8 US\$/GJ, pyrolysis liquid 8.6 US\$/GJ, annuity factor 0.08.

higher COE than pyrolysis, which highlights their capital-intensive production structure. It is seen that the COE of pyrolysis power plants is not much higher than the Rankine COE, which again suggests their suitability for low operating time service.

The second intermediate operating time is depicted in Figure 12-12. The competitiveness of IGCC improves considerable, especially at higher capacities, when the annual operating time is raised to 5000 h. This is because of the relatively high specific investment of IGCC and its high efficiency. The Rankine cycle improves even more, and it has a lower COE than the new cycles over the whole capacity range. However, at 1 MWe PyDI is competitive with Rankine, and at high capacities (closer to 100 MWe) the IGCC becomes competitive.

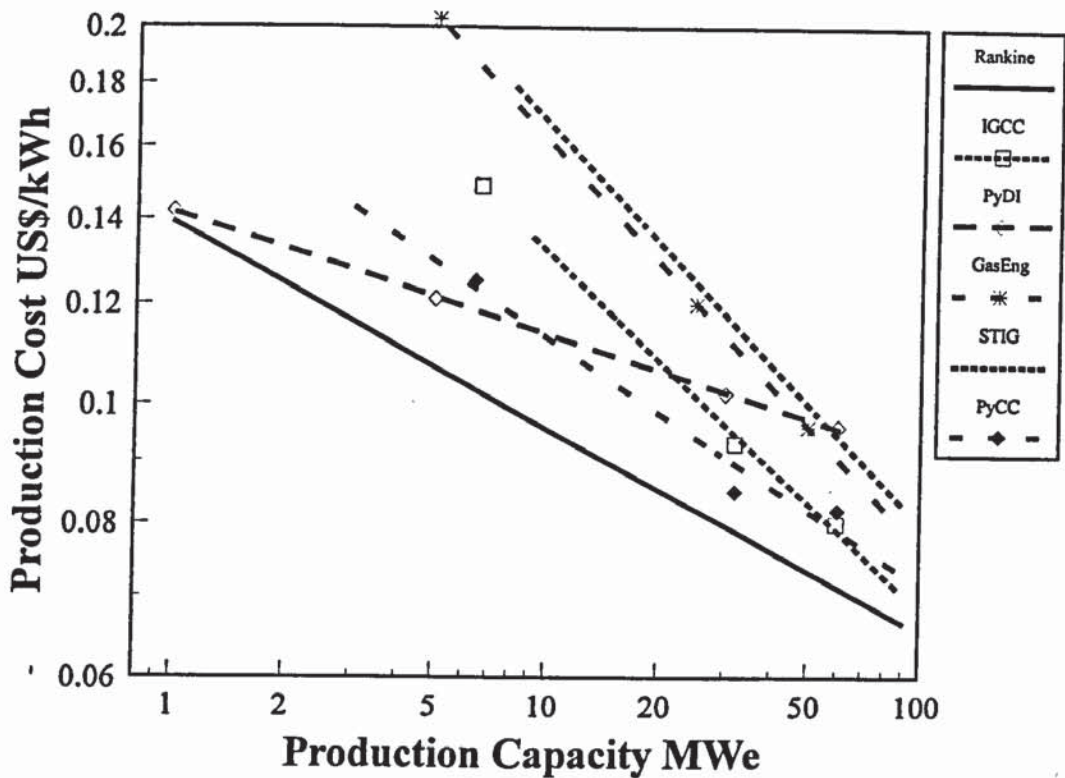


Figure 12-12. COE for intermediate operating time, 5000 h/a. Wood 2.8 US\$/GJ, pyrolysis liquid 8.6 US\$/GJ, annuity factor 0.08.

In base load service, the Rankine cycle is most economical at capacities below 50 MWe, above which IGCC has a lower COE (Figure 12-13). Note that only above 100 MWe does the IGCC COE approach the estimated COE for the new capacity from market fuels and current technologies (around 0.03 - 0.05 US\$/kWh) in the EU.

Of the new concepts, IGCC has the lowest COE above about 10 MWe. Between 5 and 10 MWe, the pyrolysis CC has the lowest COE among the new cycles. Below 5 MWe, the pyrolysis diesel has the lowest COE.

Figure 12-13 reveals that the new concepts are probably not competitive with the Rankine cycle at base load, except for scales above 50 MWe, where IGCC has the lowest COE.

The competitiveness of the pyrolysis concepts is derived from the assumption that the pyrolysis liquid is produced in a larger facility serving several power plants. Therefore, the handling of solids, a stage where small-scale operation is a distinct disadvantage, does not burden pyrolysis as it does gasification-based concepts.

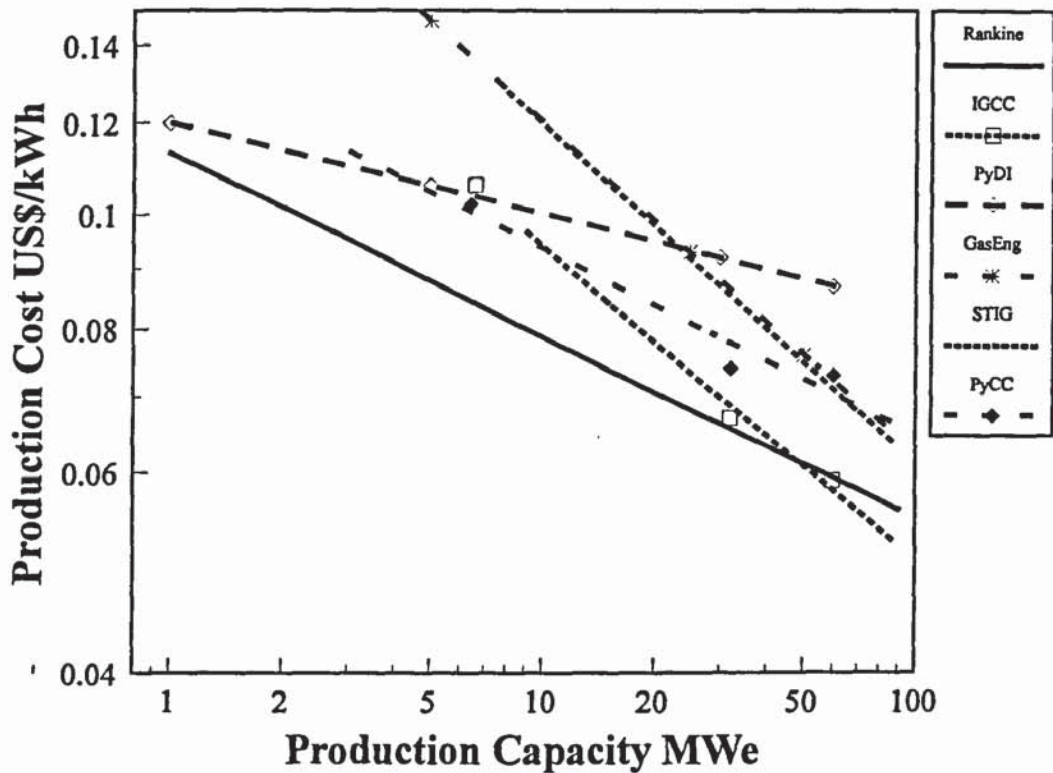


Figure 12-13. COE for base load, 7000 h/a. Wood 2.8 US\$/GJ, pyrolysis liquid 8.6 US\$/GJ, capital cost recovery factor 0.08.

12.5.5 Fuel cost

Bio-power is being developed for future energy markets. It is assumed that all fuel prices will be higher than they are today. If the future fuel costs are below those of today, the new bio-power concepts will certainly be uneconomic. The sensitivity of fuel costs is analysed in two parts: Firstly, the variation of biomass fuel is studied to analyse competition between the bio-power concepts. Secondly, the increase in fossil fuel costs is studied to analyse competition between the fossil fuel and biomass power plant concepts.

The considered cost-sensitivity range of biomass fuel is from 100 to 200%. The rather wide range is used to make differences between concepts clearer, and to compare alternatives in a future situation. Using a more traditional sensitivity of $\pm 30\%$ would neither reveal enough differences between the cases, nor would it change the preferred order of the alternatives. The wood cost is increased from 2.8 to 5.6 US\$/GJ, and the COEs for the alternatives is shown for a 7000 h/a operating time in Figure 12-14. The cost of pyrolysis liquid is

defined on the basis of the relationship shown in Figure 12-2, where the wood feed cost is doubled.

It is seen that at present fuel prices the new systems do not compete with the Rankine cycle. The only exception is the IGCC, which has the lowest COE in base load service at high capacities.

When the wood cost doubles, the IGCC becomes the lowest cost alternative above 10 MWe. Between 10 and 3 MWe, the pyrolysis CC yields the lowest cost. Below 3 MWe, the pyrolysis diesel power plant has the lowest COE. The result suggests that each of the technologies may find markets if they become industrially available.

As expected, the Rankine cycle becomes much less competitive at a high wood cost due to its low efficiency. However, it is still clearly cheaper than the STIG and gasification gas engine concepts.

A presentation similar to that in Figure 12-14 is shown for the intermediate annual operating time in Figure 12-15. The Rankine cycle shows the lowest cost within a wider margin than in base load, which is due to the higher fixed costs of the new concepts. When the wood cost is doubled, the IGCC has the lowest COE above 50 MWe. Between around 50 and 7 MWe the pyrolysis CC has the lowest COE. Below 7 MWe, the pyrolysis diesel has the lowest cost. The result suggests, as in the previous figure, that each of the technologies studied may find markets if the current technical uncertainties can be solved. However, the Rankine cycle is not much more expensive than the new cycles between 5 and 50 MWe at an operating time of 4 700 h/a.

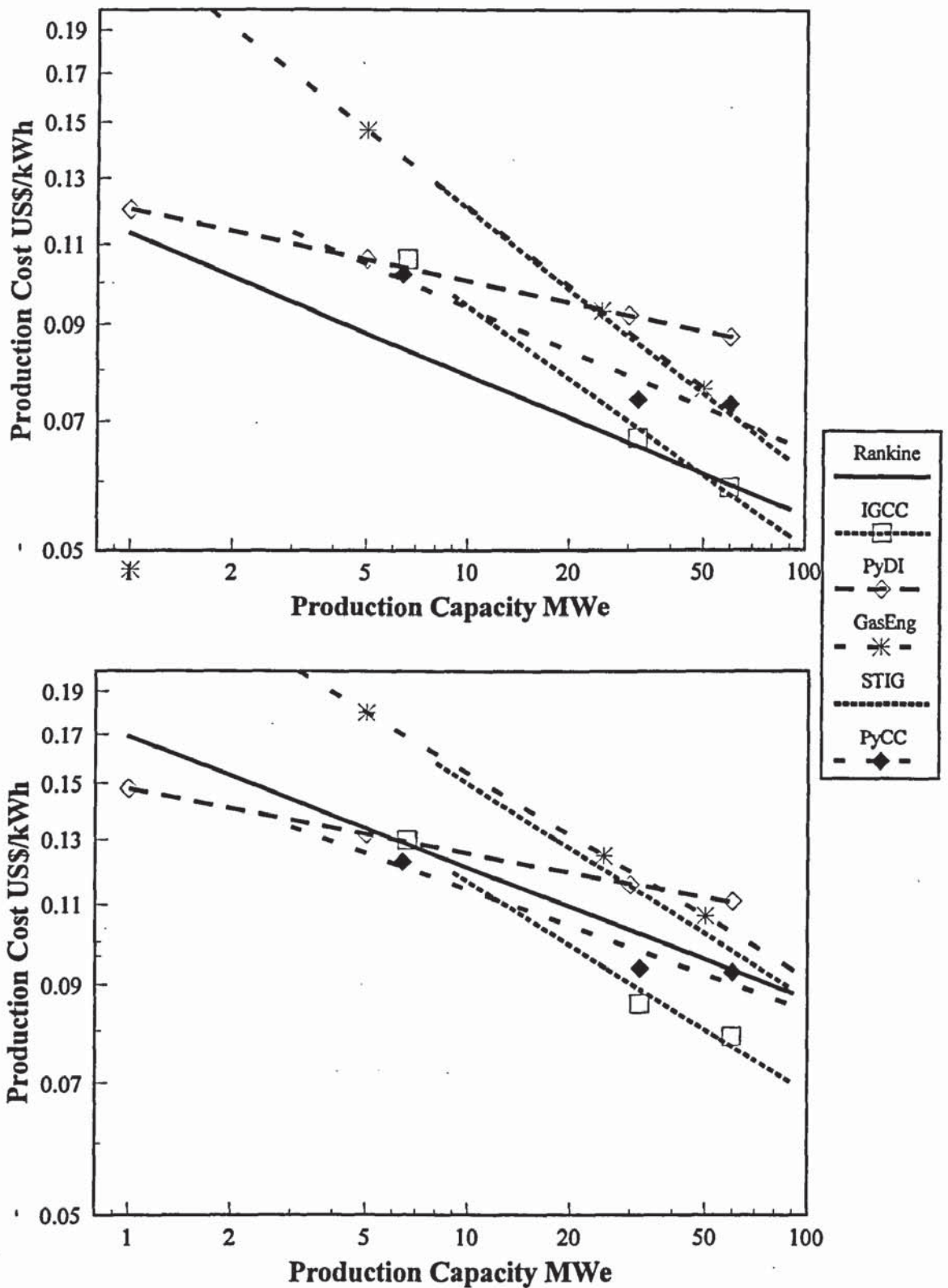


Figure 12-14. A summary of power production costs as a function of power plant capacity at 7000 h/a. Production in condensing mode. Wood cost varied from 2.8 (top) to 5.6 (bottom) US\$/GJ (corresponding pyrolysis liquid costs 8.6 and 11.8 US\$/GJ), annuity for capital costs 0.08 (20-year service life, 5% rate of interest).

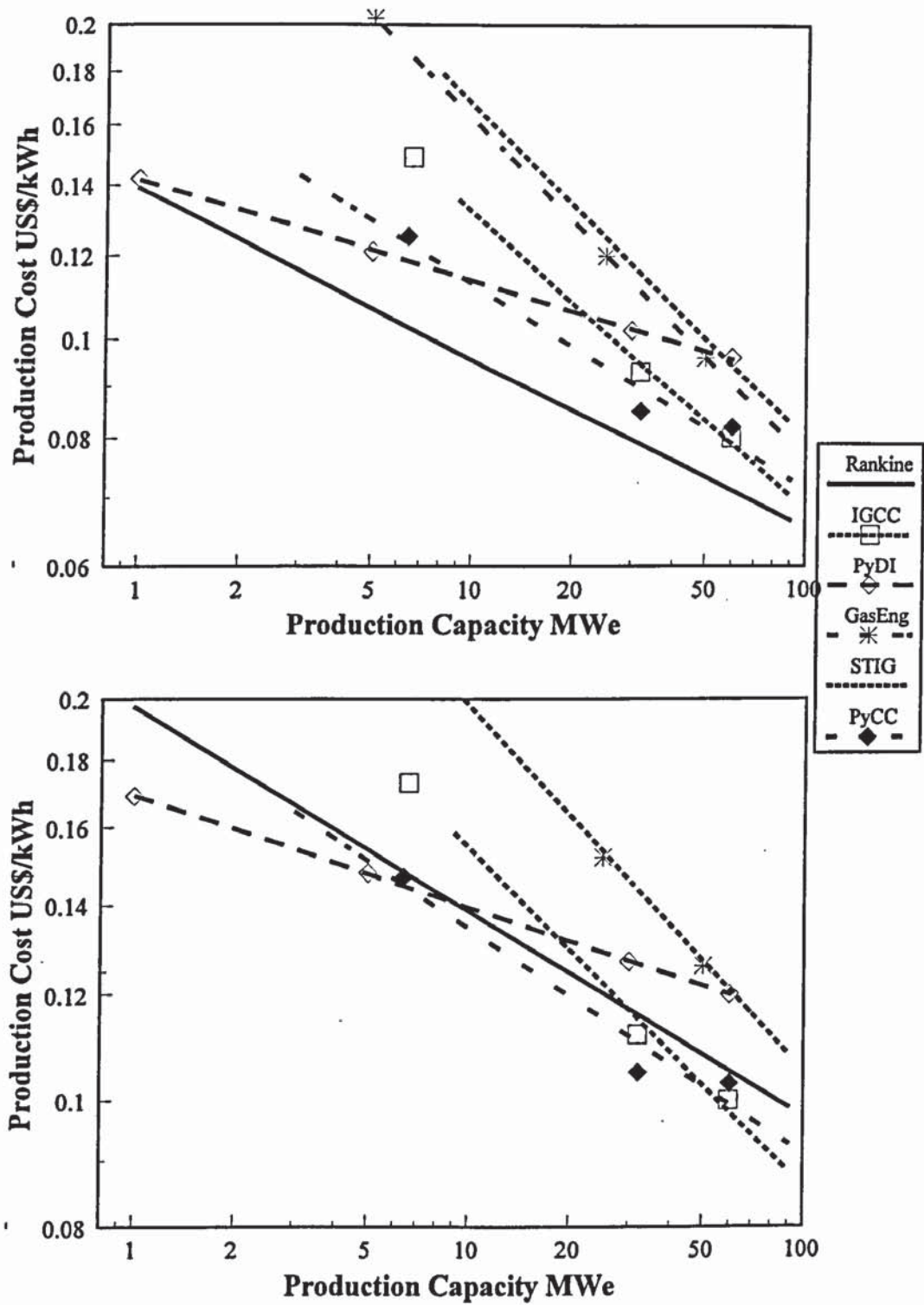


Figure 12-15. Power production costs as a function of power plant capacity at 4 700 h/a. Fuel cost varied from 2.8 (top) to 5.6 (bottom) US\$/GJ (corresponding pyrolysis liquid costs 8.6 and 11.8 US\$/GJ), annuity factor for capital costs 0.08 (20-year service life, 5% rate of interest).

The COE for fossil fuel power plants on three scales is compared to the best bio-power concepts (based on Figures 12-14 and 15) in Figures 12-16 to 12-18. Natural gas (small, medium, and large scale) and coal (large scale) are used as reference fuels. Their cost is varied between 100 and 200%, while the cost of biomass is kept constant. Again, the cost range is selected to compare the alternatives in a future situation. For example, CO₂-taxes may change the relationship between fossil fuels and biofuels.

The fossil fuel power plant concepts are selected to represent commercial technologies as follows:

- Gas turbine and gas engine using natural gas on a small scale
- Gas engine using natural gas on a medium scale
- Combined-cycle using natural gas and the Rankine cycle using coal on a large scale

The analysis is carried out to study the conditions under which bio-power may become competitive in the future, when fossil fuel costs are expected to increase.

On a small scale (Figure 12-16), the gas turbine power plant fired with natural gas loses its competitiveness against the pyrolysis diesel when the gas cost is doubled. However, the natural gas fired gas engine has the lowest cost in both cases, although the difference is not great in the latter case. It is concluded that small-scale power production will be a difficult market to penetrate if natural gas is available.

The gas engine power plant fuelled with natural gas has the lowest COE at all operating times on a medium scale (Figure 12-17). The gas engine at 15 MWe has a lower cost than Rankine at 25, the pyrolysis CC at 30, and the IGCC at 30 MWe. However, with a 100% increase in fossil fuel costs (no increase in wood cost), all of the concepts have almost the same COE above 4 000 h/a. The results suggest that biomass may become competitive on a medium scale if the costs of fossil fuels increase. However, none of the bio-power concepts has a clear advantage over the other concepts.

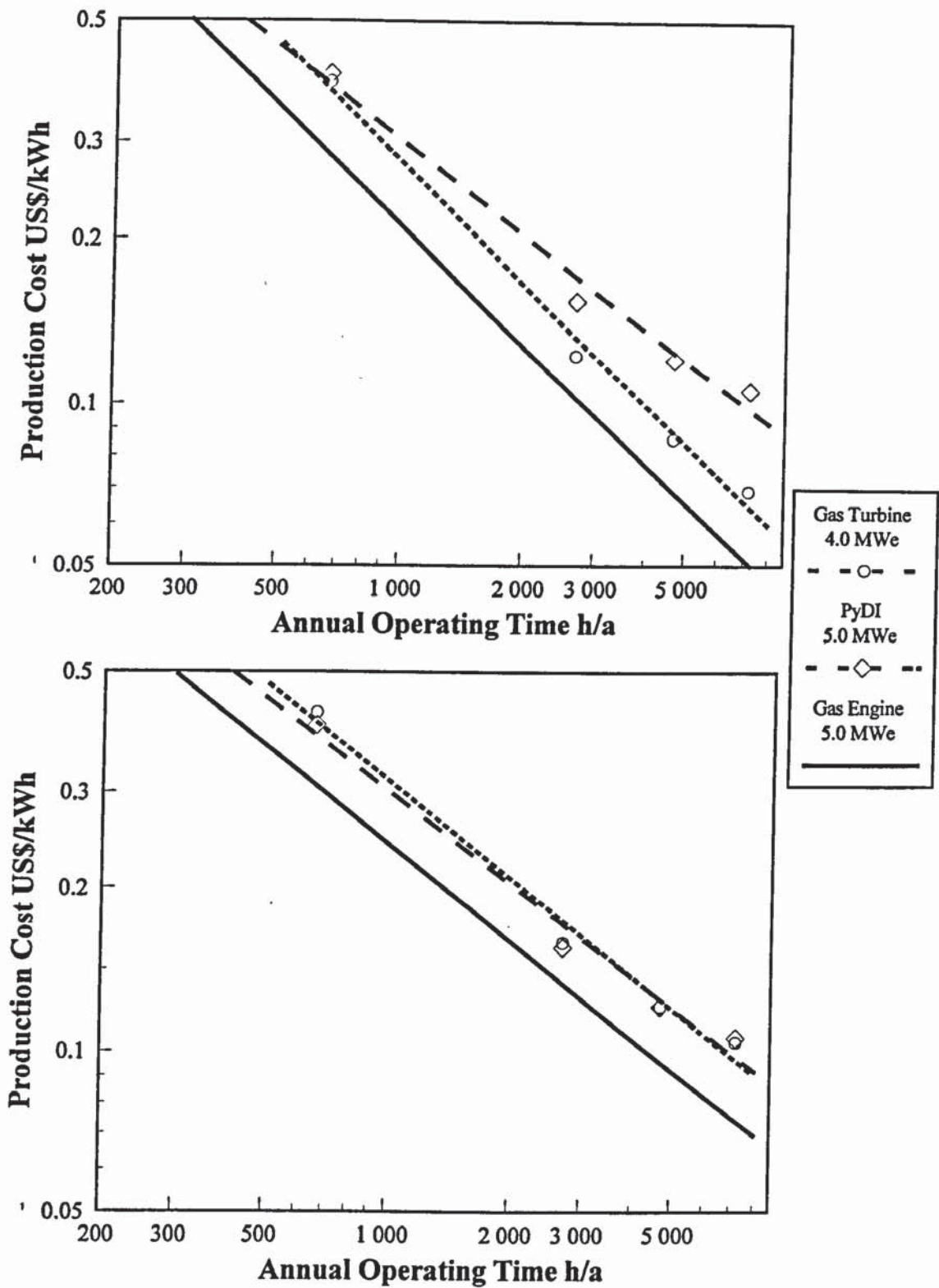


Figure 12-16. Power production costs, small-scale power plants (capacity shown in the legend), effect of variation in fossil fuel cost, natural gas 2.8 (top), 5.6 (bottom) US\$/GJ in gas turbine and gas engine power plants. COE as a function of annual peak operating time. Wood 2.8 US\$/GJ, pyrolysis liquid 8.6 US\$/GJ, annuity factor 0.08.

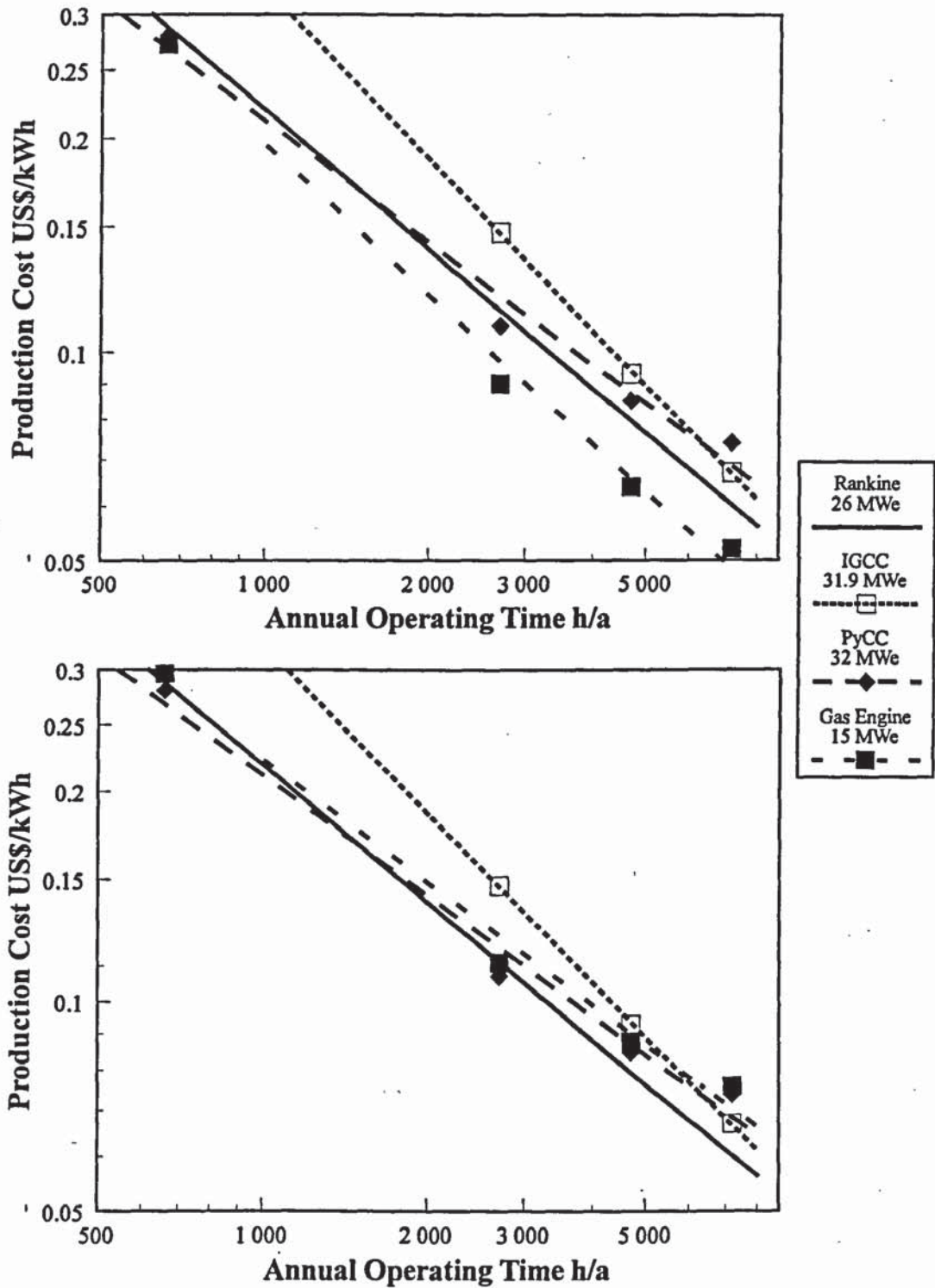


Figure 12-17. Power production costs, medium-scale power plants (capacity shown in the legend in MWe), effect of variation in fossil fuel, cost natural gas 2.8 (top), 5.6 (bottom) US\$/GJ in gas engine power plant. COE as a function of annual peak operating time. Wood 2.8 US\$/GJ, pyrolysis liquid 8.6 US\$/GJ, annuity factor 0.08.

On a larger scale (Figure 12-18), from 40 to 60 MWe, the variation between fossil and renewable alternatives is much larger than on a smaller scale. With the base fossil fuel cost, the coal CFB (60 MWe) yields the lowest COE, followed by the natural gas CC (40 MWe)

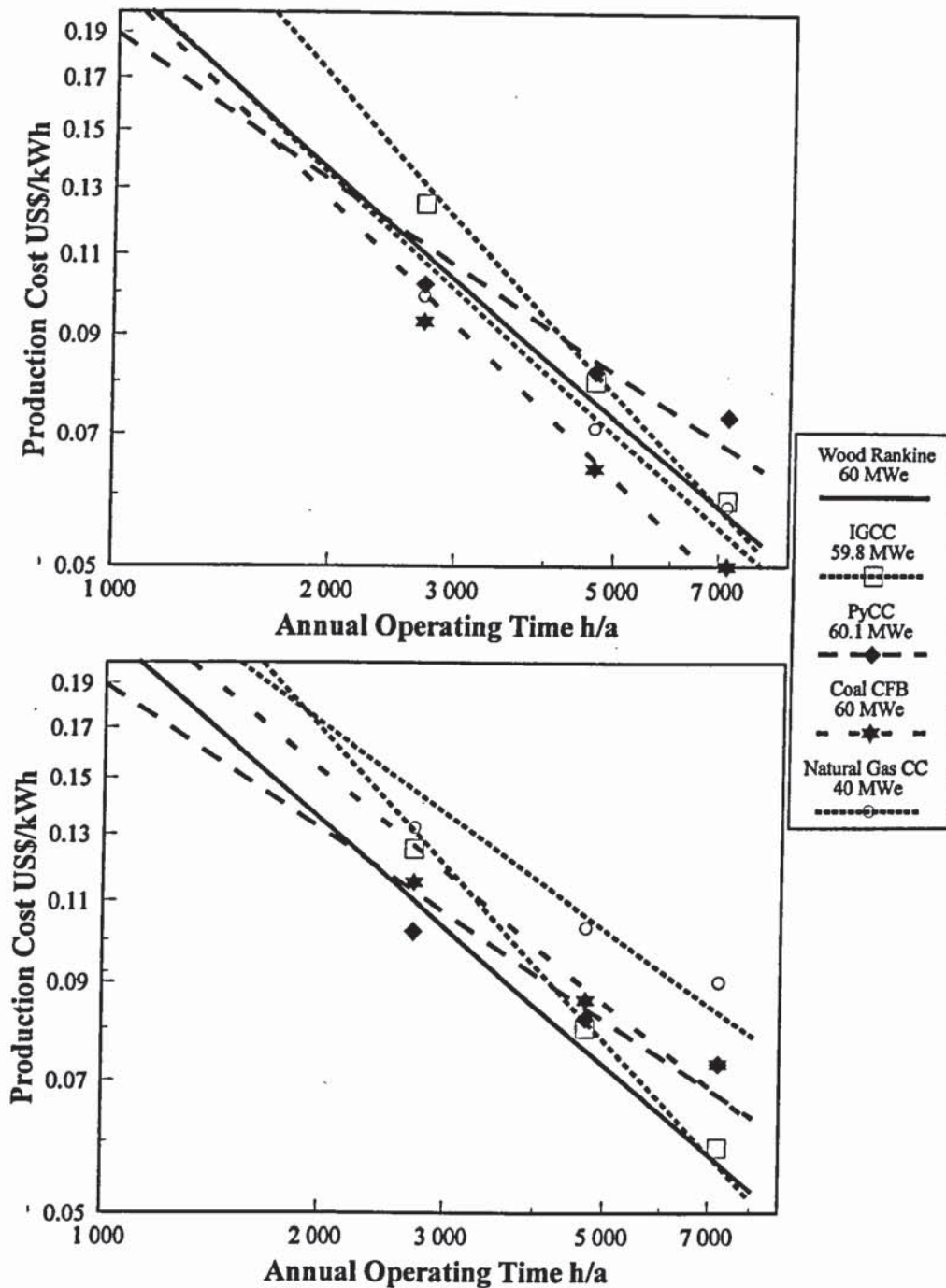


Figure 12-18. Power production costs, large-scale power plants (capacity shown in the legend in MWe), effect of variation in fossil fuel cost (natural gas 2.8, coal 1.9 (top), 5.6 and 3.8 (bottom) US\$/GJ). COE as a function of annual peak operating time. Wood 2.8, pyrolysis liquid 8.6 US\$/GJ, annuity factor 0.08.

and the wood Rankine (60 MWe), except at a very short operation time. With the fossil fuel costs doubled, the COE for both fossil fuel power plants increases considerably. Overall, the IGCC has the lowest cost above 7 000 h/a, the Rankine has the lowest COE between 2 500 and 7 000 h/a, and the pyrolysis CC the lowest below 2 500 h/a. The results suggest that bio-power may become competitive with fossil power plants if fossil fuel costs double. The results display potentially viable applications for the new concepts: peak load for the PyCC, and base load operation for the IGCC.

12.5.6 Rate of interest and contingency

As discussed in section 12.4, risk may be taken into account either by increasing the rate of interest, or by using the contingency for capital investment. In this work, a low interest rate of 5 % together with a contingency has been used. However, to illustrate the effect of increasing the rate of interest from 5 % to 15 % in the annuity method, Figure 12-19 is shown. By increasing the rate of interest in this way, a 10 % profit is effectively included in the COE.

Power production costs for plants of the same medium-scale are shown in Figure 12-17. Base fuel costs are used. It is seen that the IGCC as a capital-intensive power plant loses its competitiveness against the Rankine cycle at high operating times. Similarly, the PyCC loses its competitiveness against the Rankine power plant at low operating times. The natural gas fired gas engine power plant improves its position further. The COE from the gas engine power plant is clearly the lowest over the whole operation range. It may therefore be seen that the advanced cycles will hardly compete against existing alternatives when the return on investment is increased. This suggests that the new systems are not likely candidates for private investors when industrial investment projects are being considered in this size class. The Rankine cycle's COE is throughout 30 % higher than that of the natural gas engine power plant when a 15 % interest rate is used. The new concepts yield COEs which are from 50 to 70 % (PyCC) or from 110 to 90 % (IGCC) more expensive than the fossil fuel generated COE at the medium operation time.

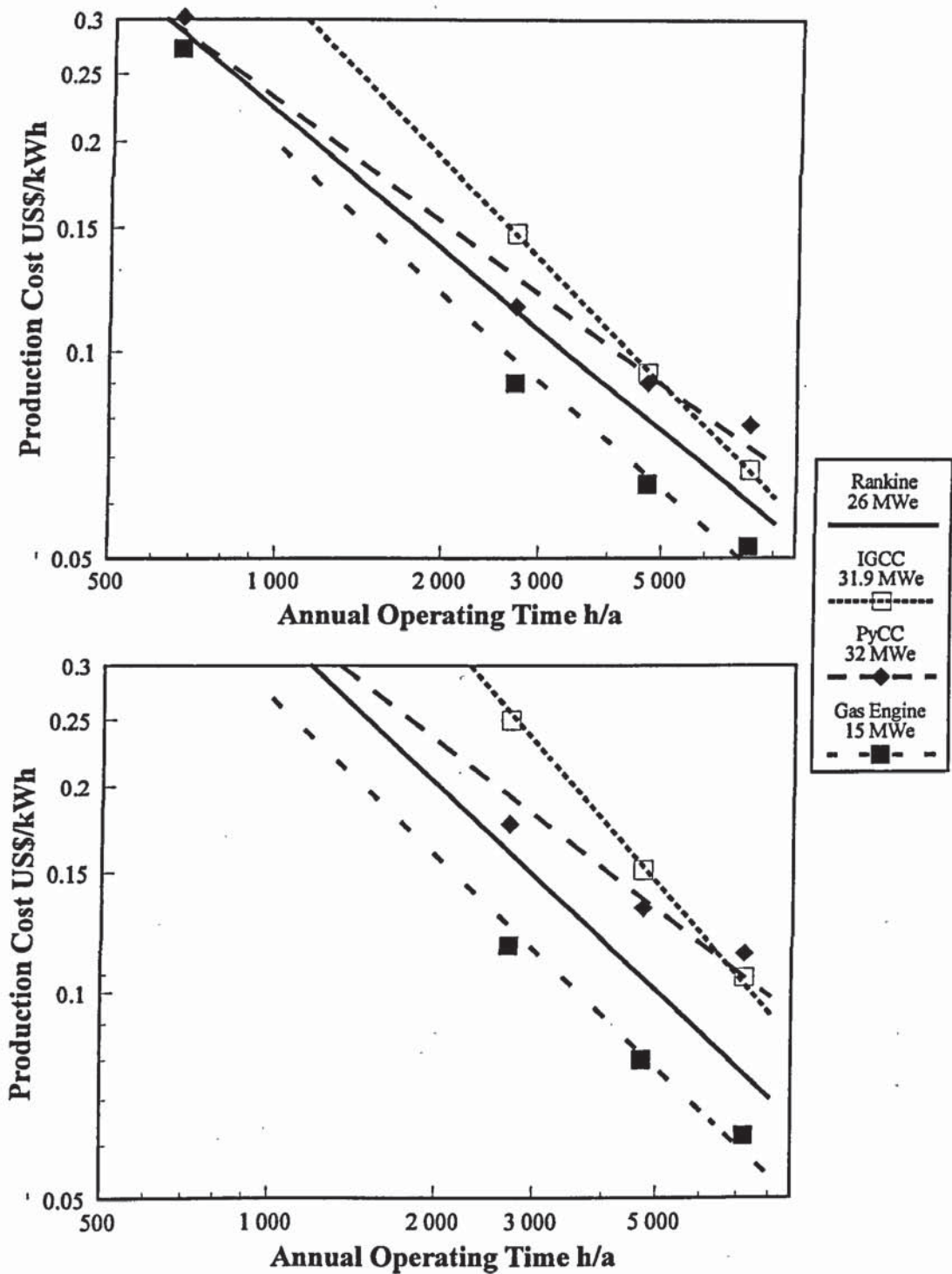


Figure 12-19. Power production costs, medium-scale power plants (capacity shown in the legend in MWe), effect of increasing the rate of interest from 5% (top) to 15% (bottom) in the annuity method, annuity factors 0.08 and 0.16, respectively. COE as a function of annual peak operating time. Wood 2.8 US\$/GJ, pyrolysis liquid 8.6 US\$/GJ, natural gas 2.8 US\$/GJ.

The same comparison is made in Figure 12-20 without considering contingencies for the advanced concepts, but using a 15% interest rate in the lower graph. In this case, the new concepts yield COEs which are from 30 to 50 % (PyCC) or from 75 to 55 % (IGCC) more expensive than the fossil fuel generated COE at the medium operation time. The PyCC and IGCC compete better with the Rankine cycle than in the previous case. However, it should

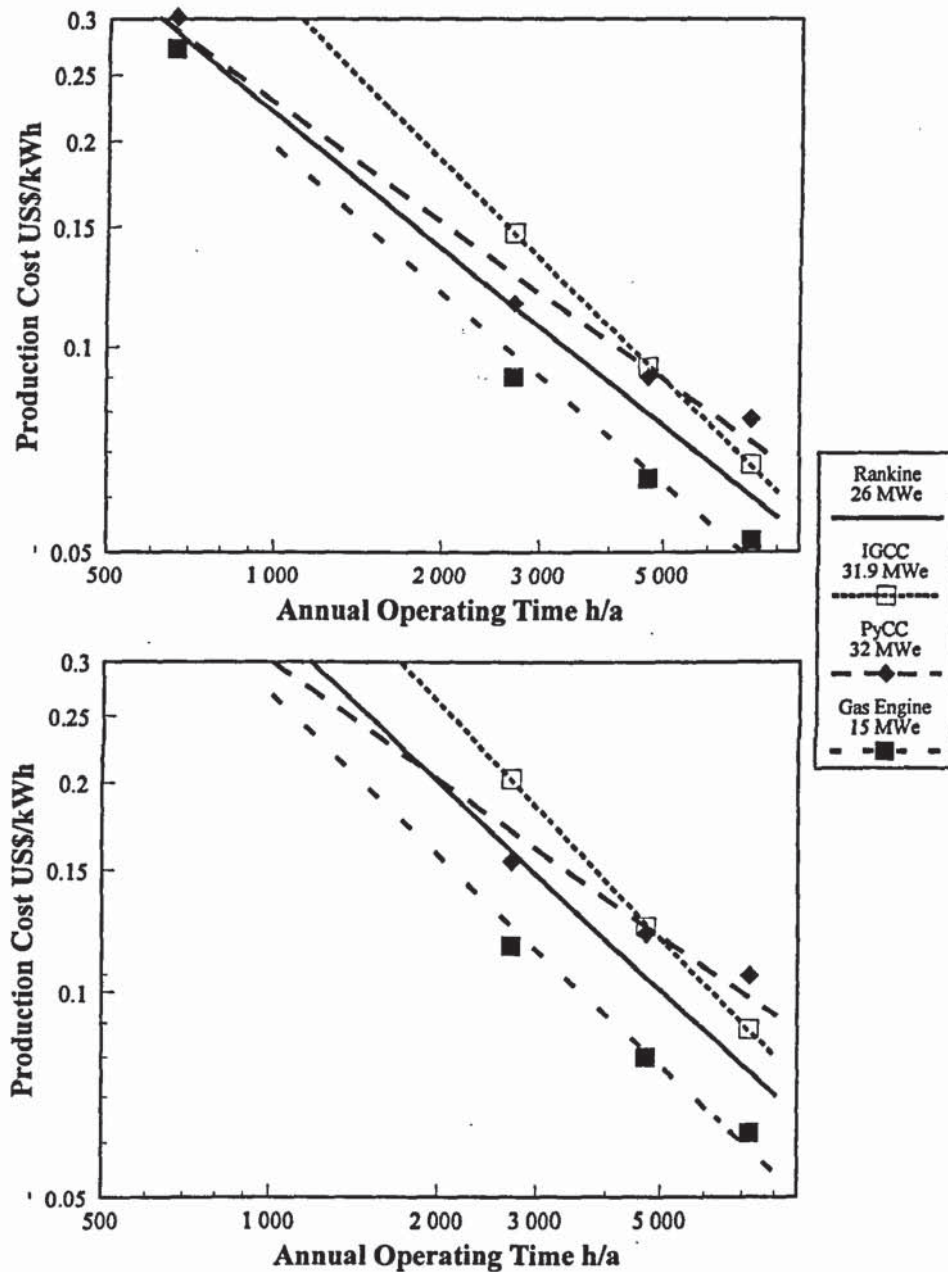


Figure 12-20. Power production costs, medium-scale power plants (capacity shown in the legend in MWe), effect of increasing the rate of interest from 5% (top) to 15% (bottom) in the annuity method, annuity factors 0.08 and 0.16, respectively. No contingencies applied for the bottom case. COE as a function of annual peak operating time. Wood 2.8 US\$/GJ, pyrolysis liquid 8.6 US\$/GJ, natural gas 2.8 US\$/GJ.

be pointed out that all the options, including the least expensive case, yield high COEs. The COE is from 100% (natural gas engine power plant) to 150 - 300% (bio-power cases) higher than the current market price of electricity in the Nordic countries, when a 15% interest rate that is representative of private funding (without considering contingencies for capital investment) is used.

12.5.7 Combined heat and power (CHP)

The COE may be reduced in CHP production. It is employed in many industries in the co-generation of steam or heat and electricity, but also in residential heating (district heating networks). The significance of CHP is also discussed in section 10.15.1.

The significant role of co-generation in the economics of bio-power was shown in chapter 2.3.4 (Figure 2-14). This aspect is depicted in Figure 12-21, where the COEs of the Rankine cycle and IGCC concept in power-only and co-gen are shown. A commercial cost structure typical of district heat in Scandinavia has been employed. It has a fixed cost of 30000 US\$/MW_a and a variable cost component of 11 US\$/MWh /34/.

At high annual operating times Rankine has a COE that is less than 50% of the COE of the power-only case. The IGCC concept is even more favoured because of its high power-to-heat ratio: it has a higher COE in condensing mode (except above 5 000 h/a), but it is equal in co-gen above 3 000 h/a. Note, however, that the two cases are not directly comparable because of the different production scales (marked in Figure 12-21).

It may be seen that co-generation could play an important role in introducing a successful bio-power project. However, the co-generation projects are very site-specific. Industrial co-gen applications may be found in many industries throughout Europe. District heat applications are more difficult to establish, although they are especially widespread in Finland, Denmark, Austria and Sweden.

A co-generation system is designed and sized on the basis of the heat load available (section 10.15). Generally speaking, an increasing power output in co-generation improves the economy of operation.

It is possible to increase the power output from a co-generation system by two distinct approaches. The first one involves adopting a new technology with a higher power-to-heat ratio (α) (section 10.15), which will enable the production of more power per existing heat load. The result of the increased electricity production in co-generation is a reduction in the

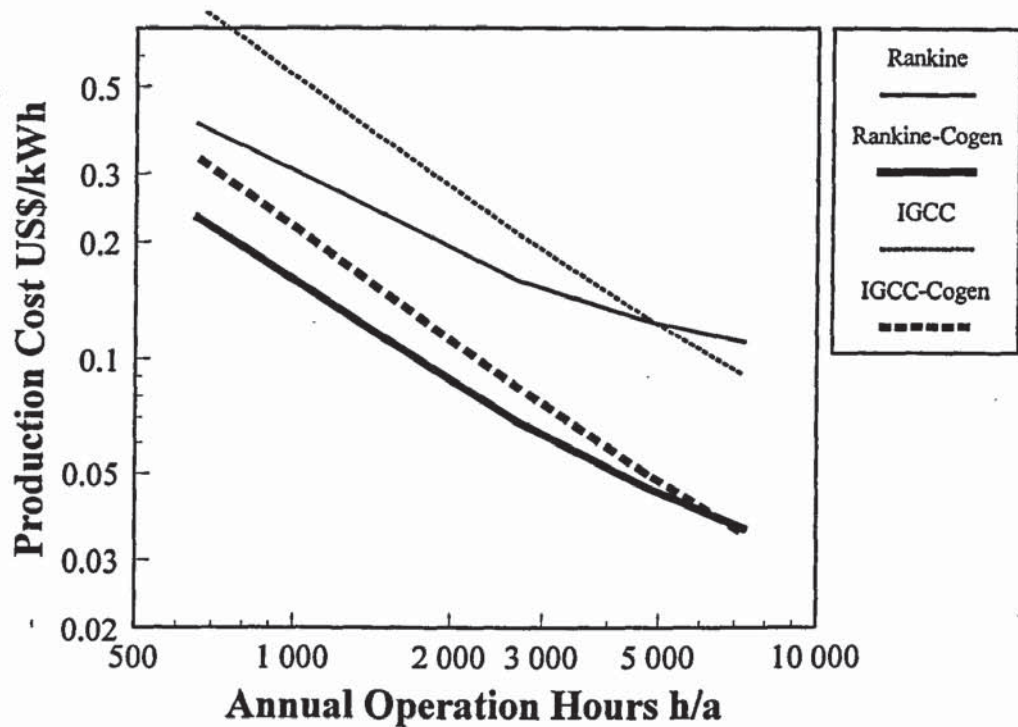


Figure 12-21. COE in power-only and co-generation. Rankine cycle 17 MWe, in co-generation 17 MWe and 40 MW_{th}. IGCC 32 MWe, in co-generation 30 MWe and 33 MW_{th}. Wood 2.8 US\$/GJ, annuity factor 0.08.

need for separate condensing power production, and an improved overall utilisation efficiency of fuels. An example is an integrated gasification combined cycle (IGCC). A conventional steam-cycle co-generation boiler plant has an α of about 0.3 to 0.5, whereas an IGCC has an α of about 1.

In the second approach, technologies are adapted that make co-generation economic in smaller plant sizes than those presently feasible. An example is a diesel or a gas engine power plant, which may be applied to fossil fuels above approximately 0.5 MWe, corresponding to a heat load of about 0.5 MW_{th}. In the future, it may be possible to employ biomass-derived fuels in a diesel or a gas engine. The current conventional co-generation units

employing solid fuels are seldom feasible below 3 to 5 MWe, corresponding to a heat load of about $10 \text{ MW}_{\text{th}}$. However, a feasible scale of operation for biomass applications should be assessed on a case-by-case basis.

As an example, Ekono Energy has estimated /X 232 joku vanha jalo/ that the potential market in Finland for co-generation capacity applying a new power plant technology (unit capacities around 30 - 60 MWe) will be more than 3 000 MWe by the year 2025. An additional co-generation potential in small municipalities in Finland (unit capacities around 2 - 10 MWe) has been estimated /233/ to be around 250 MWe. Lack of heat loads limits the potential additional capacity. The latter potential has been calculated employing low power-to-heat ratios. If new technologies were employed, the potential for small new power plant capacity would be approximately 500 MWe. For reference, the total power generation capacity of Finland in 1999 was around 13 000 MWe.

12.5.8 Scale of pyrolysis liquid production

The production capacity of pyrolysis liquid (PL) is critical for the competitiveness of pyrolysis power plants. Two pyrolysis and two gasification power plant concepts are compared in Figure 12-22. Two scales of liquid production are considered: 30 and $70 \text{ MW}_{\text{th}}$, measured as wood input into the pyrolysis plant with the corresponding cost of liquid fuel.

When pyrolysis liquid is produced on a smaller scale, the pyrolysis concepts have a lower COE only below about 5 MWe. However, with pyrolysis liquid production at $70 \text{ MW}_{\text{th}}$, the pyrolysis power plants have a lower COE below 10 MWe.

Figure 12-22 reveals the considerable effect that PL production capacity (and the corresponding PL cost) has on the pyrolysis power plant COE. Purely from the viewpoint of power plant economy, it is evident that the larger the PL production plants, the better. However, the biomass resources will set an upper limit for the plant size in practice. It should also be borne in mind that when producing PL on a small scale, the pyrolysis power plants may not be competitive.

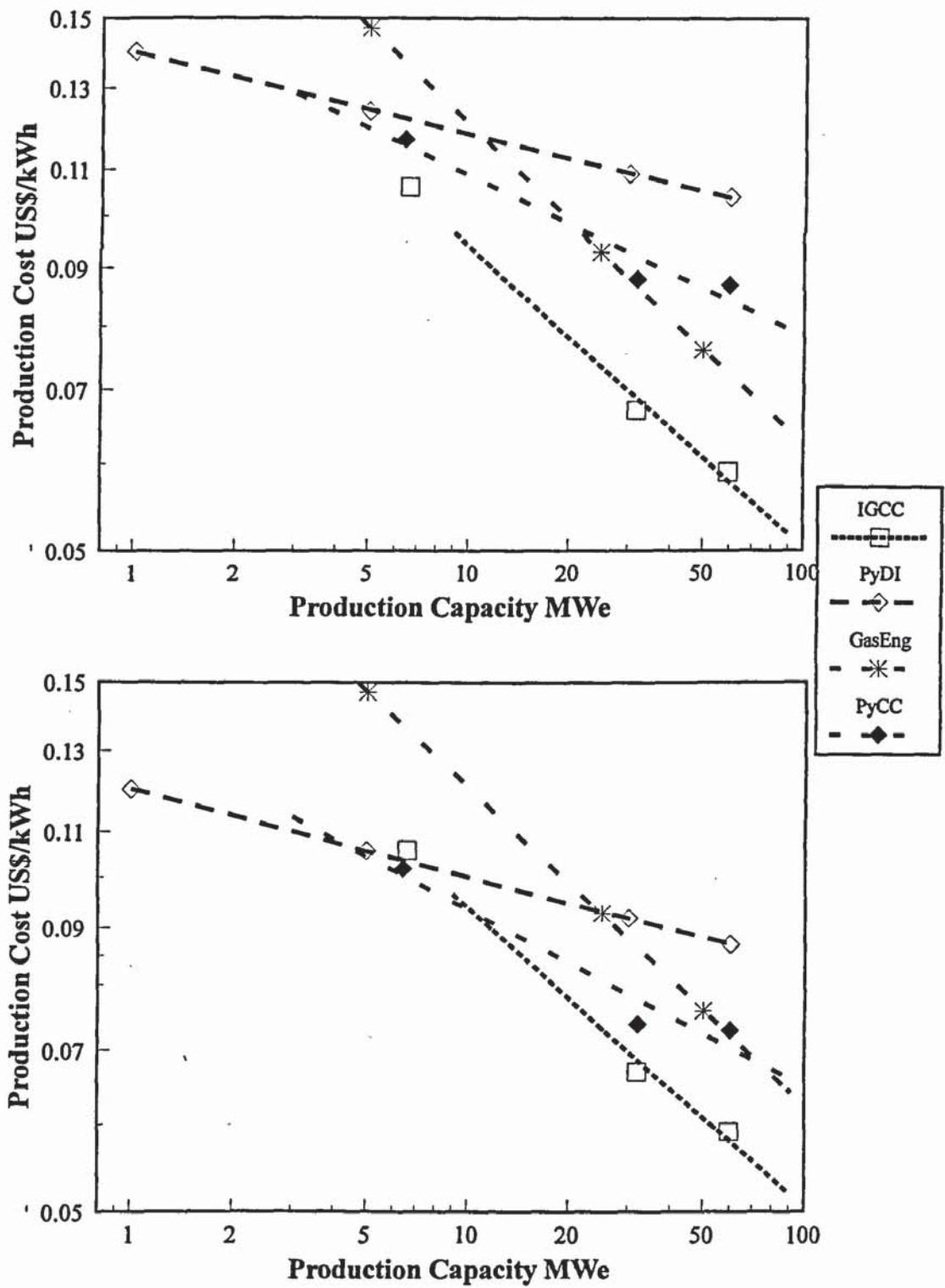


Figure 12-22. COE in power-only and co-generation. Rankine cycle 17 MWe, in co-generation 17 MWe and 40 MW_{th} . IGCC 32 MWe, in co-generation 30 MWe and 33 MW_{th} . Wood 2.8 US\$/GJ, annuity factor 0.08.

12.6 Examples of using the cost and performance models in an industrial evaluation

Two examples of using the models in industrial evaluations are summarised in this section. The first example illustrates the advantages of the IGCC technology in co-generation. In the second example, gas cleaning options in an IGCC are studied on an economic basis.

Co-generation for industry or for district heat is common especially in the Nordic countries. An example of a case with a $55 \text{ MW}_{\text{th}}$ heat load is shown in figures 12-23 and 12-24, where a co-gen IGCC is compared with a conventional Rankine plant. To compare their economic viability, several tasks are carried out. For the assessment:

- Process concepts are designed
- Aspen performance models are built
- Power plant concepts are sized
- Investment costs are estimated

Finally, the COE is calculated for both cases. Note that the co-generation plant is sized on the basis of the heat demand, in this case $55 \text{ MW}_{\text{th}}$. This will make the IGCC power output about double that of the Rankine power plant.

There is no great difference between the power production costs of the two systems, which are compared in Figure 12-23. However, as shown in Figure 12-24, the situation appears different when the annual savings for a power plant operator are shown against the electricity tariff valid in Finland in 1995. The savings are higher for the IGCC, which at the same heat load has about double the power output compared with conventional technology. In fact, the annual savings are of the order of US\$ 2 million at 5000 h/a, while a conventional co-gen plant would only break even against the tariff. This operating time is quite typical of residential co-gen plants. However, note that the capacity shown is fairly high for a biomass power plant. Although feasible in some locations in the Nordic countries, both the heat load and the biomass may not be available in other parts of Europe.

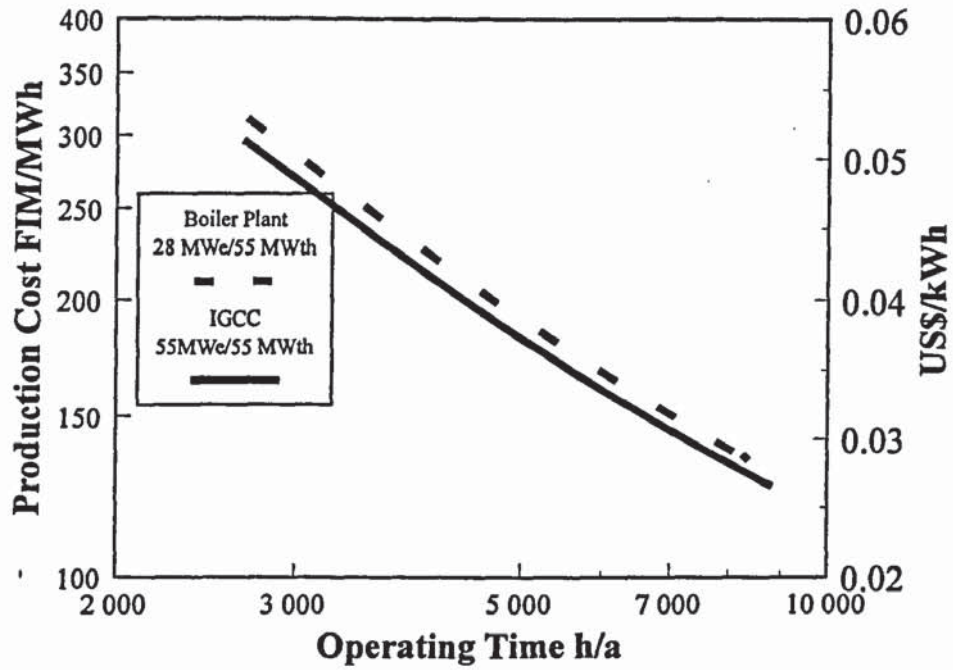


Figure 12-23. Comparison of conventional and IGCC co-generation. Power production costs, co-generation of power and district heat. Biomass 50 FIM/MWh (2.8 US\$/GJ), annuity factor for capital costs 0.08.

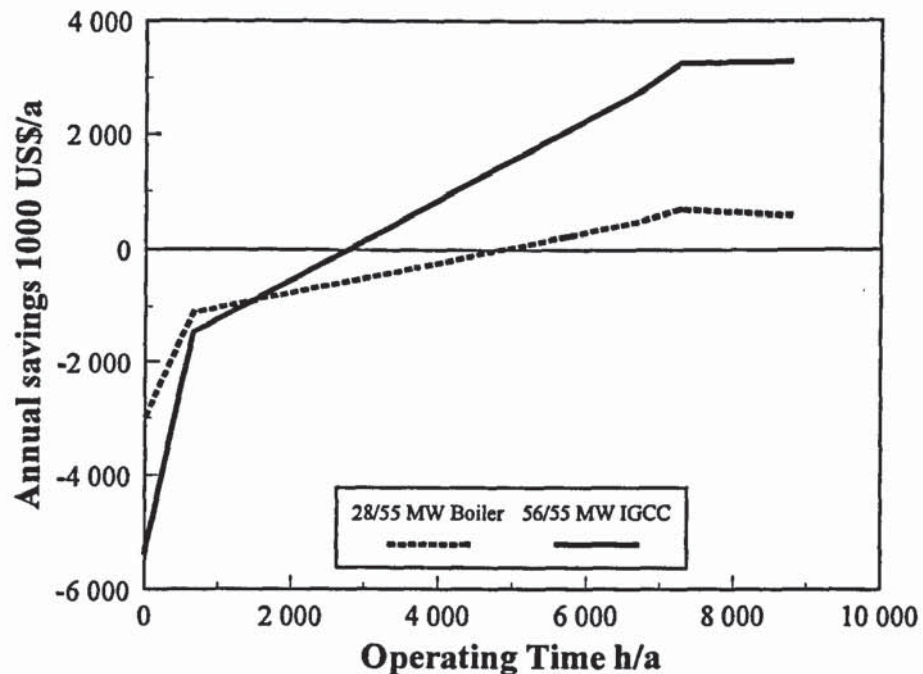


Figure 12-24. Comparison of conventional and IGCC co-generation. Annual operating savings compared with the Finnish purchase tariff for electricity in 1995, co-generation of power and district heat. Biomass 50 FIM/MWh (2.8 US\$/GJ), annuity factor for capital costs 0.08.

In the second example, the applicability of a specific sub-model in Aspen was utilised in studying the **gas cleaning** options related to a biomass IGCC /234/. A catalytic gas cleaning concept has been developed, and the viability of the concept integrated into an IGCC power plant is studied. Two concepts were compared: a base IGCC assuming no catalytic cleaning necessary, and an IGCC concept with a catalytic gas cleaning stage. The catalytic unit converts tars in the gasification gas to CO and H₂, and NH₃ to N₂. Gas cleaning may be necessary to improve gas utilisation and to reduce power plant emissions. The question was therefore asked, under which circumstances would the IGCC concept with gas cleaning be competitive with the IGCC concept with no gas cleaning. In this case it is assumed that gas cleaning is not a problem, and emissions from the IGCC plant are acceptable.

The effect of the catalyst's service life on the overall power production economics is studied in Figure 12-25. Assuming different service lives for the catalyst, respective annual savings against the tariff were calculated. It may be seen that increasing the service life

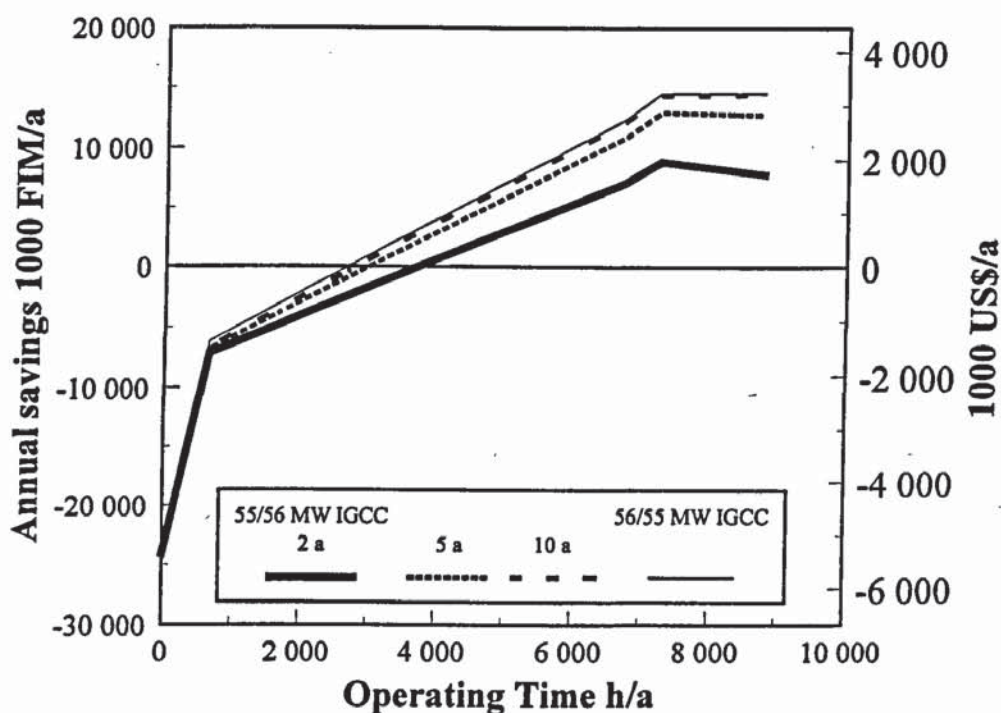


Figure 12-25. Annual operating savings (compared with the Finnish purchase tariff for electricity in 1995) in co-generation of power and district heat, when different service lives are assumed for the gas cleaning catalyst. Biomass 50 FIM/MWh (2.8 US\$/GJ), annuity factor for capital costs 0.08.

from 2 to 5 years would improve the economics considerably. However, only a service life of 10 years would make the catalytic concept competitive with the base IGCC concept. The result indicates that for the gas cleaning stage to be viable, the catalyst lifetime should be at least five years. The result may be used as a criterion in developing and testing the catalytic process.

13. CONCLUSIONS

The conclusions drawn from the work are summarised in three sections. Firstly, issues related to the modelling approach are summarised. Secondly, technical issues related to the technologies are reviewed. Finally, further modelling work is proposed.

13.1 Modelling

The objective of the thesis was to analyse several process configurations producing electricity from biomass. Process simulation models aimed at calculating the industrial performance of power plant concepts were built, tested, and used for analysis. The modelling tool was a state-of-the-art simulation software application (AspenPlus), which has the necessary physical property calculation methods and the unit operation models needed for the work.

The simulation models developed in this work were used:

- To calculate on a consistent basis the mass and energy balances for new bio-power concepts which have not been operated industrially. Models for 21 complete advanced power plant concepts of specific size and configuration were built and employed in determining steady-state performance balances. In addition, investment and operating costs were estimated for all of the systems. It will be easy to add more concepts using the existing model library, when new advanced concepts need to be assessed. As a reference, a model for the conventional Rankine cycle power plant together with investment and operating costs was also built.
- To vary a process input, process parameter or process configuration within a power plant concept to study the affects on the overall performance. Examples of these technical sensitivities are included in chapters 4 (Rankine cycle), 6 (gasification), 7 (fast pyrolysis), 10 (gasification-engine and IGCC concepts), and 12 (using a catalyst in gas cleaning). It is shown that the models may be used to study: the effect of steam cycle parameter variation on the Rankine cycle performance, the effect of the air/feed ratio on gas composition in gasification, the effect of feed moisture on the overall performance

of fast pyrolysis, the effect of engine characteristics on overall power plant performance, and the effect of unit operation variation within the IGCC on the cost of electricity.

These are individual examples of technical sensitivity studies which may be carried out. It is concluded that numerous similar technical sensitivity studies are possible and easily carried out with the models built.

- To gain an insight into interactions between unit operations within an advanced process. Complete systems must be studied to see how unit operation modifications and improvements influence the overall competitiveness of a new system. It is shown in chapter 10 how projected improvements in dryer, gas turbine and steam cycle performance further increase the efficiency of the IGCC concept. Dryer types are also compared in co-generation in chapter 10, and it may be seen that the differences in the performance of the two dryers are significant.
- To compare advanced systems with each other, and ultimately, to compare them with a conventional power plant, which was also modelled. It is concluded that the models were adequate for the purpose of comparison. Modelling the Rankine cycle on a comparable basis with the advanced cycles is considered successful and important.
- To produce information to serve as the basis for the setting of priorities when selecting further R&D work. It is concluded that important aspects related to the competitiveness of these systems are revealed. These are discussed further in the next section.

The process analysis includes two criteria: performance and cost. Rigorous performance analysis is emphasised in this work for two major reasons:

- System performance can be more accurately defined than cost.
- All cost analyses are eventually based on performance data.

Performance rather than cost analysis is therefore believed to offer more useful data for future developments. Cost estimates can never be more accurate than performance analysis: the sizing and costing of equipment is based on calculated mass and energy balances.

It is emphasised in the work that the cost estimation in this or any similar work is necessarily only of an order-of-magnitude at best. The issue is emphasised because it has been shown in the literature how uncertain cost estimation is for new systems. On the other hand, it is believed that the predictive performance analysis carried out is rather accurate. The results in this work agree well with the most advanced work in the literature.

The advanced power plant concepts analysed in this work employ gasification and pyrolysis of biomass. The following specific issues were emphasised in the work due to an inadequacy or lack of consistent previous work:

- The integration of gasification and gas cleaning into the power module is analysed in detail.
- The fast pyrolysis process is modelled in greater detail than in any previous work documented in the public domain.
- Conventional Rankine technology is modelled and analysed in a manner that is consistent with the new systems currently under developed. The lack of consistent treatment with regard to conventional technology has been a considerable deficiency in many previous studies on advanced systems.

The last issue is especially significant. A wide variation in the performance of conventional boiler - steam cycles was reported in the literature. Not all of the differences are explained because of the different investment cost levels (and the respective variation in performance) assumed in the studies. Most of the assessments reviewed did not include a detailed model for the boiler - steam cycle option.

The comparison of new alternatives with existing technology is one of the critical issues in this study. New systems being developed should eventually compete successfully against existing, industrially proven processes. Models with a similar level of detail were built for both new and existing concepts. It is believed that a comparable process analysis has been carried out with the models built.

There is a danger of handling the conventional reference case differently from the new system being studied. Careful consideration should be given to trying to match the cost of a

unit of a new system to its performance. There appears to be a tendency among the groups developing these systems to downplay uncertainties and to be too optimistic concerning the investment costs of new units. At the same time the existing systems are often considered low-efficiency in comparison with the high efficiencies of advanced systems. However, conventional power plants are often built for low efficiency, because their fuels are cheap today and investing in higher efficiency often does not pay off.

The accuracy of the models built is good. By adding up all the chemical energy and sensible heat from the process, and comparing the value with total energy input (which is usually only fuel chemical energy, as internal power consumption is generated in-house), typically more than 99.8% is recovered. The run time of a typical IGCC model would be around 1 to 2 minutes with AspenPlus version 9.3 on a PC with a 133 MHz Pentium processor and 32 Mb of RAM. However, the run time is heavily dependent on the model steam cycle. With good initial values the convergence is fast, but if the initial values are far away from the final ones, the run time could be up to 5 minutes. Aspen is a sequential modular program, and as such it is not perfect for steam-cycle analysis due to the large number of recycle loops generated in the calculation. These are typically easier to analyse with a software application based on an equation solver. On the other hand, other features of the concepts modelled (i.e., solids handling, gasification, pyrolysis, fuel gas treatment, and extensive requirements for chemical compound physical properties) exclude the use of simulation software developed for power plant analysis. *It is concluded that Aspen is a proper and appropriate tool for the work carried out.*

13.2 Technologies studied

Conclusions related to individual technologies are reviewed in this section. New technologies are primarily compared with each other. The most promising concepts are also compared to the commercial reference, the Rankine power plant. In addition, some of the most promising new concepts are compared with the lowest-cost fossil power plants.

Gasification concepts

Pressurised gasification combined-cycles (P-IGCC) appear to be the most competitive of the advanced cycles studied. This technology is best suited for large-scale (above 50 MWe), base load operation. The overall efficiency approaches 50% with wood feedstock and a large gas turbine. Overall, this concept is considered to be the most feasible of all the advanced power plant concepts compared. However, it should be noted that the amount of biomass needed for a 50 MWe power plant is considerable (about 50 t/h, or about 350 000 t/a on a 50% wet basis in base load operation). This quantity will probably not be available except in a few locations (e.g. large forest products industry sites). Other alternatives are energy plantations for biomass, but no large-scale plantation sites have so far been established. It is concluded that although the IGCC concept appears to be the most competitive of the new alternatives, its current market potential is rather limited.

Atmospheric gasification combined-cycles (A-IGCC) are at current fuel prices as economic as the pressurized IGCC (P-IGCC). However, the A-IGCC concept lacks the inherent advantage of the P-IGCC, i.e. high efficiency. When fuel costs rise, the cost of electricity (COE) for A-IGCC will increase more than the COE of P-IGCC. The A-IGCC concept is not competitive on a scale smaller than P-IGCC, a potential advantage usually claimed for A-IGCC. Therefore, it is concluded that the development of the P-IGCC should be preferred over the A-IGCC.

Steam-injected gas turbine (STIG) cycles employing pressurised gasification are not competitive compared with other new concepts. The amount of steam injection allowed in turbines fired with low heating value gas is relatively small, and the additional power output due to steam injection is minor. The conclusion is that the concept is of no interest if current turbines are used.

Gasification coupled to a gas engine appears to be the least viable of all the cases studied. It is concluded that considerable improvements in performance or/and cost are necessary to justify further development of this concept.

Pyrolysis concepts

All new systems include uncertainties, but this is especially true in the production of fast pyrolysis liquid. The technical uncertainties are taken into account in this analysis by using appropriate contingencies in investment cost estimates.

Pyrolysis power plant concepts have some distinct advantages, because the primary stage of liquid production may be de-coupled from the power plant. Firstly, liquid fuels are easier and less expensive to use in a power plant than are solid fuels. Secondly, the solids handling stage may be carried out in large pyrolysis units, which reduces liquid production costs and thus the COE. Pyrolysis diesels are also potentially capable of intermittent operation. This is a distinct advantage in areas where the value of electricity varies greatly, for example, from day to night. Moreover, of the bio-power cases studied, *pyrolysis diesel* power plants are the only alternatives which appear well-suited to peak load operation. It is concluded that pyrolysis is an interesting alternative due to its potential flexibility.

The pyrolysis diesel power plant concept is competitive with other new concepts on a small scale (below 2 MWe) and at a low total number of annual operating hours.

A combined cycle using pyrolysis liquid appears competitive with other advanced systems on a medium scale (around 5 to 20 MWe), and typically in intermediate peak operating mode. The relative success of the pyrolysis concepts is largely related to the high liquid production scale considered. If large-scale (around 70 MW_{th}, corresponding to about 30 t/h wet biomass) feed to pyrolysis liquid production is not available, the potential advantage of pyrolysis power plant concepts diminishes.

Sensitivity analysis

Fuel prices were varied to study the effects on the relative competitiveness of new power plant concepts. In this study, only increases in prices were considered. Lower fuel prices would undermine the need for a R&D programme in this field. Three variations were considered in this section: an increase in wood costs, an increase in fossil fuel costs, and an increase in the rate of interest used in evaluating capital costs.

Higher wood costs improve the competitiveness of all of the advanced cycles compared with the Rankine cycle. At an annual operating time of 5000 h/a, the IGCC has a lower COE than the Rankine cycle above 50 MWe if the cost of wood is doubled from 2.8 to 5.6 USD/GJ. Pyrolysis power plants have roughly the same COE as the Rankine cycle (pyrolysis CC over the whole capacity, pyrolysis diesel < about 15 MWe). If the annual operating time is increased, the advantage of IGCC increases.

Around 4 MWe, even if fossil fuel costs are doubled, the bio-power plants do not compete against the lowest-cost fossil power plant, which is a natural gas fired gas engine. It is concluded that on this scale no viable bio-power concepts were identified.

Around 15 to 30 MWe, if the price of natural gas is doubled, the estimated COE for bio-power plants is very close to that of the natural gas engine power plant. The Rankine cycle remains with the lowest cost, but overall the differences between the Rankine, the IGCC, the PyCC, and the natural gas power plant are fairly small.

On a larger scale, around 50 to 60 MWe, the consequences of a rise in fossil fuel prices are much greater than they are on a smaller scale. At the base cost of fossil fuel, the natural gas CC (40 MWe) yields the lowest COE, followed by the coal CFB (60 MWe) and the wood Rankine (60 MWe). When fossil fuel costs are doubled, the Rankine and the IGCC have the lowest COE, followed by the pyrolysis CC. In particular, the COE of the gas CC increases considerably when the price of fossil fuel rises.

The third sensitivity analysis was carried out to study the effect of increasing the rate of interest used in evaluating capital costs. Effectively, the increase corresponds to raising the required rate of return on investment. The result undoubtedly demonstrates how difficult it will be to establish viable bio-power projects. When the rate of interest in the annuity is raised from the low base value of 5 % to 15 %, the competitiveness of bio-power concepts compared with natural gas engine power plant is considerably reduced.

It is concluded that the new concepts will have a hard time competing with both existing biomass and fossil fuel technologies on the market. On the other hand, the co-generation of heat and power appears to offer a potential market for new bio-power concepts.

Combined heat and power (CHP) production already makes wood-fired power plants feasible in situations where a heat sink is available. It is shown that the COE may be reduced to 50% in co-generation. The new cycles have an important advantage over the Rankine cycle in co-generation: their power-to-heat ratio is much higher.

CHP production is currently the only industrial area of application in which bio-power costs can be considerably reduced to make them competitive. CHP applications will provide a potential market for advanced systems in the near future. The importance of co-generation will probably only increase in the future due to its potential for reducing greenhouse gas emissions and contributing to sustainability. Fuel utilisation will increase to around 90% in co-generation from the present 40% in condensing power production.

Summary

At current fuel prices, the study revealed only one concept case (the IGCC with a capacity above 50 MWe and an operating time of 7000 h/a) that yields a lower COE than the Rankine cycle. Bio-power is not expected to be employed in peak operation. However, if the annual operating time is short, the pyrolysis concepts start to compete with the Rankine cycle. Two extremes thus appear to be potentially interesting for bio-power: larger, base load IGCCs, and small, intermediate to peak load pyrolysis power plants.

It is of interest to see that although the previous results are based on economics, a similar result may also be derived from the performance analysis. The highest power production efficiency is the IGCC on a large scale (above 30 MWe), the pyrolysis CC on a medium scale (from about 5 to 20 MWe), and the pyrolysis diesel on a small scale (below 3 MWe).

The successful reduction of capital costs would appear to be the key to the introduction of the new systems. Capital costs account for a considerable, often dominant, part of the cost of electricity in these concepts. At the present time all of the systems have higher specific investment costs than the conventional industrial alternative, i.e. the Rankine power plant. High efficiencies do not reduce fuel costs enough to compensate for the high capital costs of advanced concepts.

13.3 Further modelling work

There are numerous other biomass-to-electricity systems which have been proposed but not analysed in this work. Systems employing indirectly heated gas turbines, and gas turbines fired with solid fuels are examples of such proposed technologies. These configurations should be modelled in detail, and their feasibility assessed on a comparable basis, once relevant experimental data is available.

Based on the results of this work, AspenPlus is an appropriate simulation platform to be employed. However, several unit operations could be modelled in more detail to expand the usefulness of the models. Dryer, gasifier, fast pyrolysis, gas engine and gas turbine models could be improved.

As the **dryer** is a critical unit in all advanced cycles, its performance and especially emissions should be studied in more detail. It also consumes a considerable amount of energy, and has a relatively high investment cost. As an example, variation in the heat requirement of the dryer integrated into an IGCC was studied in the work. The specific heat requirement has a considerable effect on the efficiency of the system.

Modelling the **gasification** of biofuels other than wood should also be carried out. Biomasses other than wood are important in many areas of the world. Simple models capable of taking into account the specific features of, for instance, grass-type biomasses would be useful in assessing the feasibility of using energy crops. Pre-treatment (handling, milling, pelletizing, drying) of these materials is important for their use in gasifiers, and this aspect should be included in the study. The gasification model employed in this work could be further improved by including empirical correlations for the amounts of tars in the product gas when other biomasses are used. Tars are known to be one of the primary sources of operational difficulties in gasification.

The model built in this work for **fast pyrolysis** should be improved as soon as more experimental data becomes available. Liquid composition as a function of reaction temperature is needed to be able to study the product properties. Data on the performance of a large-scale pyrolysis reactor would be needed. So far, most of the data used in the con-

struction of the model is based on experiments carried out on a laboratory scale. Additionally, reactor yields for organic liquid, water, gas, and char that are relevant to different biomasses other than wood could be included. It is estimated that the current pyrolysis performance model includes considerable uncertainties, particularly as some of the units employed have not been proven in continuous industrial operation. It is also recognised that the liquid recovery stage is modelled with an equilibrium model describing a tray-tower. As no equilibrium is reached in industrial units, the recovery model should be improved.

The gas engine model is only a black box model. Once the injection pressure, losses, and electricity efficiency are defined, the model calculates the temperature of the exhaust gas. However, a model for an internal combustion engine should actually be able to take into account rather complicated phenomena in order to predict the engine performance with LHV gas. In addition, the performance would nevertheless be accurate only for one specific engine at a time. A model would have to be tuned with empirical parameters to reproduce the performance of other engines.

The gas turbine modelling tool employed, GateCycle, is appropriate for the modelling of gas turbines using LHV gas. However, a model integrated into Aspen would be preferable. Such an example has recently been published /235/. It is suggested that this approach should also be tested and integrated into these models.

It has been suggested that small-scale decentralised generating systems (around 50 to 200 kW_e) using fossil fuels may become competitive in the future /236/. If new small industrial fossil fuel power plants gain a market share, there may also be an opportunity for bio-power plants. However, such a generation and transmission network will set special requirements related to load variation and start-up characteristics of the power plant. This scale was not included in the present work as it is considerably below the scale currently used by utilities, and the logistics and operation of these plants are distinct from larger plants.

13.4 Use of the models prepared

The primary uses for the models constructed are envisioned as:

- The effects of the characteristics of single unit operation on overall plant performance and cost may be studied
- Optimising process concepts using the cost of electricity or efficiency as the criterion
- Priorities within a process concept may be established for experimental R&D work

The models can also be used to select process concepts for further experimental work. R&D organisations, universities, funding agencies and private industry, including both contractors and manufacturing industry, could utilise the models for this purpose.

REFERENCES

- 1 Energy Statistics 1996. Ministry of Trade and Industry, Helsinki. Energy 1997:1.
- 2 The evolution of the world's energy system. Shell brochure. London, 1996.
- 3 Energy in Europe. EC DGXVII, Luxembourg 1996.
- 4 Johansson, T., Kelly, H., Reddy, A., Williams, R. Renewable fuels and electricity for a growing world economy. In: Johansson, T., Kelly, H., Reddy, A., Williams, R. (eds.). Renewables for fuel and electricity. Island Press, Washington, DC, 1993. Ch. 1.
- 5 Nakicenovic, N. et al. Long term strategies for mitigating global warming. Energy, vol. 18, 1993, pp. 97-193.
- 6 WEC (World Energy Council Commission), New renewable energy resources. Kogan Page, London, 1994.
- 7 Hall, D., House, J. Biomass: a modern and environmentally acceptable fuel. Solar Energy Materials and Solar Cells, vol. 38, 1995, pp. 521-542.
- 8 Wilen, C., Moilanen, A., Kurkela, E. Biomass feedstock analyses. VTT, Espoo, Finland, 1996. VTT Publications 282.
- 9 Intergovernmental Panel on Climate Change (IPCC), Climate Change 1992: The supplementary report to the IPCC Scientific Assessment. Cambridge University Press, 1992.
- 10 U.S. Department of Energy, Electricity from biomass. NTIS, US Department of Commerce, Springfield, VA, 1992.
- 11 Maniatis, K., Ferrero, G.L. The THERMIE Programme: The Energy from Biomass and Waste Sector and Targeted Projects on CHP Production by Biomass Gasification, In: Proc. European Workshop on Market Penetration of Biomass Technologies at Vienna, Austria, October 5, 1994. Energiesparverband, Linz, Austria.
- 12 Non-nuclear energy, JOULE II, project synopses. EC DGXII, Luxembourg, 1994.
- 13 AIR Agriculture, agro-industry, fisheries. Non-food projects. EC DGVI, XII, and XIV. Luxembourg, 1995.
- 14 Larson, E. Biomass-gasifier/gas-turbine applications in the pulp and paper industry: an initial strategy for reducing electric utility CO₂ emissions. Ninth Annual EPRI Conference on Gasification Power Plants, 16 - 19 October, 1990. Palo Alto, CA, USA.

-
- 15 Larson, E. Biomass-gasifier/gas-turbine cogeneration in the pulp and paper industry. 36th ASME International Gas Turbine and Aeroengine Congress and Exhibition, Orlando, FLA, June 3-6, 1991.
 - 16 Grassi, G. R&D biomass programme of the C.E.C. In: Proceedings of Energy from Biomass Thermochemical Contractors' Meeting, Gent, Belgium, October 29-31, 1991. Bridgwater, A. V., Grassi, G. (eds.). Commission of the European Communities. 13-22.
 - 17 Keränen, H., Salo, K. Feasibility and potential of biomass IGCC in energy production. Enviropower Inc., Espoo, 1995.
 - 18 World Energy Council, Report 1992: International energy data. Imediaprint, London, UK, 1992.
 - 19 Energy in Europe: A view to the future, Special issue. September 1992, Commission of the European Communities.
 - 20 Hislop, D., Hall, D. The export potential of biomass gasification equipment. September 10, 1994. Intermediate report for EC DGXII.
 - 21 Solantausta, Y., Kurkela, E., Wilén, C., Barbucci, P., Neri, G., de Lange, H., Hulkkonen, S., Heinonen, O., Äijälä, M. Feasibility of electricity production from biomass based on gasification. In: Chartier, A., Beenackers, A., Grassi, G. (eds.). Biomass for energy, environment, agriculture, and industry. Elsevier Science, Kidlington, 1995. Pp. 1579-1590.
 - 22 Trebbi, G. , Power production options from biomass: the vision of a southern European utility. Bioresource Technology, vol. 46, Nos 1-2, 1993, pp. 23-30.
 - 23 Kinnula, T., Suutela, J. Electricity production potential integrated to a new pulp plant. Bioenergy Programme 1993-98, vol. 3, p. 303-310. (in Finnish)
 - 24 Overend, R., Milne, T., Mudge, L. (eds.). Fundamentals of thermochemical biomass conversion. Elsevier Applied Science Publishers, London and New York, 1985.
 - 25 Bridgwater, A.V., Kuester, J.L. (eds.). Research in Thermochemical Biomass Conversion. Elsevier Applied Science Publishers, London and New York, 1988.
 - 26 Bridgwater, A.V. (ed.). Advances in thermochemical biomass conversion. Glasgow, UK: Blackie, 1993.
 - 27 Sipilä, K., Korhonen, M. (eds.). Power production from biomass. Bioresource Technology, vol. 46, Nos 1-2, 1993.

-
- 28 Sipilä, K., Korhonen, M. (eds.). Seminar on Power Production from Biomass II. Espoo, Finland, 27-28 March 1995. VTT, Espoo, 1996. VTT Symposium Series 164.
 - 29 Bridgwater, A.V., Boocock, D. (eds.). Developments in thermochemical biomass conversion, Glasgow, UK: Blackie, 1997.
 - 30 Merrow, E., Chapel, S., Worthing, C. A review of cost estimation in new technologies: Implications for energy process plants. Prepared by RAND Corporation for the U.S. Department of Energy. Santa Monica, CA. RAND-R-2481-DOE. July 1979.
 - 31 Solantausta, Y., Bridgwater, T., Beckman, D. Electricity production by advanced biomass power systems. VTT, Espoo, Finland, 1997. VTT Research Notes 1729. 115 p. + app. 79 p.
 - 32 Small-scale power production is viable: Domestic fuels and clear basic solutions. Energy Magazine, vol. 11, No. 3, 1996, pp. 10-12.
 - 33 The competitiveness of domestic fuels. Energia-Ekono Oy for the Ministry of Trade and Industry. Reports, Helsinki, 1986.
 - 34 Kosunen, P., Leino, P. The competitiveness of biofuels in heat and power production. Energia-Ekono Oy for the Ministry of Trade and Industry, Reports 99/1995, Helsinki 1995.
 - 35 Mitchell, C., Bridgwater, A., Toft, A., Watters, M., Stevens, D., Aumonier, S., Ellen-der, R. Technoeconomic assessment of biomass to energy. The BEAM report. Aber-deen University, Forestry Research Paper 1996:1.
 - 36 McMullan, J., Williams, B., Campbell, P., McIlveen-Wright, D., Bemtgen, J. Techno-economic assessment studies of fossil fuel and fuel wood power generation technologies. R&D in Clean Coal Technology. EC DG XII, Brussels, Belgium. 1995.
 - 37 Toft, A. A comparison of integrated biomass to electricity systems. PhD thesis. University of Aston, Birmingham, October 1996.
 - 38 Marrison, C., Larson, E. Cost versus scale for advanced plantation-based biomass energy systems in the USA and Brazil. In: Proceedings of the Second Biomass Con-ference of the Americas. NREL/CP-200-8098 (DE95009230). Portland, OR, August 1995.
 - 39 McGowin, C., Wiltsee, G. Strategic analysis of biomass and waste fuels for electric power generation. Biomass and Bioenergy, vol. 10, Nos 2-3, 1996, pp. 167-175.

-
- 40 Ståhl, K. & Neergaard, M. Experiences from the Värnamo IGCC Demonstration Plant. In: Sipilä, K., Korhonen, M. (eds.). Proc. Seminar on Power Production from Biomass III. Gasification and pyrolysis R&D&D for Industry, Espoo, 14 - 15 Sept. 1998. VTT, Espoo, 1999. Pp. 73-86.
 - 41 Ståhl, K., Neergaard, M., Nieminen, J., Stratton, P. IGCC power plant for biomass utilisation Värnamo, Sweden. In: Developments in Thermochemical Biomass Conversion, Bridgwater, A., Boocock, D., (eds). Chapman & Hall, London, 1997. pp. 1006-1015.
 - 42 Maniatis, K. Overview of EU Thermo gasification projects. In: Sipilä, K., Korhonen, M. (eds.). Proc. Seminar on power production from biomass III. Gasification and pyrolysis R&D&D for Industry, Espoo, 14 - 15 Sept. 1998. VTT, Espoo, 1999. Pp. 9-34.
 - 43 Paisley, M., Farris, G. Development and commercialization of a biomass gasification/power generation system. Proceedings 2nd Biomass Conference of the Americas. Portland, Oregon, August 21-24 1995. NREL, Golden CO, 1995.
 - 44 Kinoshita, C., et al. Power generation potential of biomass gasification systems. In: Proceedings of the 1996 American Power Conference, Chicago, Illinois, April 9-11 1996.
 - 45 Farris, M., Paisley, M. A., Irving, J. & Overend, R. The Battelle/FERCO Biomass Gasification Process. In: Sipilä, K., Korhonen, M. (eds.). Proc. Seminar on Power Production from Biomass III. Gasification and Pyrolysis R&D for Industry, Espoo, 14 - 15 Sept. 1998, Espoo:VTT, 1999. Pp. 87 - 102.
 - 46 Salo, K., Keränen, H. Biomass IGCC. In: Sipilä, K., Korhonen, M. (eds.). Seminar on Power Production from Biomass II. Espoo, Finland, 27-28 March 1995. VTT, Espoo, 1996. VTT Symposium Series 164.
 - 47 Graig, K., Mann, M. Cost and performance analysis of three integrated biomass gasification combined cycle power systems. NREL, Golden Colorado. On the Internet at <http://www.eren.doe.gov/ower/snowpap.html>.
 - 48 Consonni, S., Larson, E. Biomass gasifier/aero-derivative gas turbine combined cycles. Cogen Turbo Power '94, Portland, Oregon 25-27, October 1994.
 - 49 de Biasi, V. Next generation gas turbine designs taking shape in ATS, CAGT programs. Gas Turbine World, Nov-Dec, 1993, pp. 14-20.
 - 50 McIlveen-Wright, D., Williams, B., McMullan, J. Electricity generation from wood-fired power plants: The principal technologies reviewed. In: Bridgwater, A., Boo-

-
- cock, D. (eds). *Developments in Thermochemical Biomass Conversion*, Chapman & Hall, London, 1997. Pp. 1525-1538.
- 51 Van Ree, R., Oudhuis, A., Faaij, A., Curvers, A. Modelling of a biomass-integrated-gasifier/combined-cycle (BIG/CC) system with the flowsheet simulation programme AspenPlus. ECN-C--95-041, Petten, the Netherlands. June 1995.
 - 52 Faaij, A., van Ree, R., Oudhuis, A. Gasification of biomass wastes and residues for electricity production. Utrecht University, Report 95035, Utrecht, June 1995.
 - 53 Solantausta, Y., Bridgwater, A., Beckman, D. , Feasibility of power production with pyrolysis and gasification systems. In: Bridgwater, A., Boocock, D., (eds). *Developments in Thermochemical Biomass Conversion*, Chapman & Hall, London, 1997. Pp. 1539-1555.
 - 54 Craig, K., Bain, R., Overend, R. Biomass power systems - Where are we going, and how do we get there? The role of gasification. Presented at EPRI Conference on New Power Generation Technology. October 25-27, 1995, San Francisco, California.
 - 55 Graig, K., Mann, M., Bain, R. Cost and performance potential of advanced integrated biomass gasification combined cycle power systems. Published in ASME Cogen Turbo Power 94, 8th Congress & Exposition on Gas Turbines in Cogeneration and Utility, Industrial and Independent Power Generation. Portland, OR. ISBN No. 0-7918-1213-8. October 1994.
 - 56 Elliott, P., Booth, R. Brazilian Biomass Demonstration Project. Special project brief. Shell International, London, UK, 1993.
 - 57 Economic development through biomass system integration. Northern States Power et al. Final report for subcontract AAC-4-13326-02. US DOE/NREL 1995.
 - 58 New Bern Biomass to Energy Project, Phase 1 Feasibility Study. Weyerhaeuser et al. Final report for subcontract ZAU-4-13326-04. US DOE/NREL 1995.
 - 59 Williams, R., Larson, E. Biomass gasifier gas turbine power generating technology. *Biomass and Bioenergy* 10(1996)2-3, 149-166.
 - 60 Electric Power Research Institute. TAG - Technical Assessment Guide. EPRI TR-102276-V1R7 Volume 1: Rev 7. Palo Alto, CA, June 1993.
 - 61 Nieminen, J. Biomass CFB gasifier connected to a 350 MWth steam boiler fired with coal and natural gas - Thermie demonstration project in Lahti, Finland. In: Sipilä, K. & Korhonen, M. (eds.). Proc. Seminar on power production from biomass III. Gasification and Pyrolysis R&D for Industry, Espoo, 14 - 15 Sept. 1998. Espoo: VTT, 1999. Pp. 181 - 194. VTT Symposium 192.

-
- 62 Garrett, D., Mallan, G. Pyrolysis process for solid wastes. US patent 4,153,514, May 8, 1979. Occidental Petroleum Corp.
 - 63 Scott, D. S. & Piskorz, J. The flash pyrolysis of aspen-poplar wood. *Can. J. Chem. Eng.*, 1982. Vol. 60, pp. 666 - 674.
 - 64 Diebold, J. & Power, A. Engineering aspects of the Vortex pyrolysis reactor to produce primary pyrolysis oil vapors for use in resins and adhesives. In: Bridgwater, A. V. & Kuester, J. L. (eds.). *Research in thermochemical biomass conversion*. New York: Elsevier Applied Science, 1988. Pp. 609 - 628.
 - 65 Trebbi, G., Rossi, C., Pedrelli, G. Plans for the production and utilization of bio-oil from biomass fast pyrolysis. In: *Developments in Thermochemical Biomass Conversion*, Bridgwater, A., Boocock, D., (eds). Chapman & Hall, London, 1997. Pp. 378-390.
 - 66 Solantausta, Y., Nylund, N.O., Gust, S. Use of pyrolysis oil in a test diesel engine to study the feasibility of a diesel power plant concept. *Biomass and Bioenergy* 7(1994)1-6, pp.297-306.
 - 67 McKeough, P., Nissilä, M., Solantausta, Y., Beckman, D., Östman, A., Bergholm, A., Kannel, A. Techno-economic assessment of direct biomass liquefaction processes. VTT Research Report 337. Espoo 1985.
 - 68 Roy, C., Morin, D., Dube, F. Electricity production from biomass using the integrating pyrolysis combined-cycle process. In: *Making a business from biomass in energy, environment, chemicals, fibers, and materials*. In: Overend, R., Chornet, E. (eds). *Proc. of the 3rd Biomass Conference of the Americas*. Elsevier Science Ltd., 1997.
 - 69 Gregoire, C. & Bain, R. Technoeconomic analysis of the production of biocrude from wood. *Biomass and Bioenergy*, 1994. Vol. 7, No. 1 - 6, pp. 275 - 283.
 - 70 Williams, B., McMullan, J. Techno-economic analysis of fuel conversion and power generation systems - the development of a portable chemical process simulator with capital cost and economic performance analysis capabilities. *International Journal of Energy Research*, 20(1996)125-145.
 - 71 Peters, M., Timmerhaus, K., *Plant design and economics for chemical engineers*. McGraw-Hill Ltd, Tokyo 1968.
 - 72 Anon. *A guide to capital cost estimation*. Institution of Chemical Engineers, UK, 1988.

-
- 73 Modern Power Systems Magazine, Gas Turbine Handbook 1998.
 - 74 Smith, D., Ultra-supercritical chp: getting more competitive. Modern Power Systems 19(1999)1, pp. 21-30.
 - 75 Kotschenreuther, H., Advanced coal-fired power plants exploit high temperature technology. Modern Power Systems vol. 14, 1994, 10, pp. 43-39.
 - 76 Skærbæk goes supercritical for high efficiency. Modern Power Systems vol. 17, 1997, 6, pp. 41-50.
 - 77 Eurlings, J., The future for the IGCC: scale, fuels and products. Modern Power Systems, vol. 17, 1997, 11, pp. 39-44.
 - 78 Susta, M., Luby, P., Combined cycle power plant efficiency: a prognostic extrapolation. Modern Power Systems, vol. 17, 1997, 4, pp. 21-24.
 - 79 Basta, N., Process simulation: new mountains to conquer. Chemical Engineering, vol. 103, 1996, 5, pp. 149-152.
 - 80 AspenPlus™ User Guide Volume 1, release 9. Aspen Technology, Inc., Cambridge, MA, 1994.
 - 81 Tistelgren, S., The efficiency comparison of combined cycles based on the pressurised fluidised bed partial gasification and the pressurised fluidised bed combustion. Helsinki University of Technology, Laboratory of Energy Technology. TKK/EVO, Otaniemi, Finland, 1993. 86 + 8 p. (in Finnish).
 - 82 Grønli, M., A theoretical and experimental study of the thermal degradation of biomass. Ph.D. dissertation. The Norwegian University of Science and Technology, Trondheim, Norway, 1989.
 - 83 Sakari Suontaka, Energy Ekono, January 1995.
 - 84 Goater, G., et al. A comparative assessment of forest biomass conversion to energy forms. Phase I - Proven and near proven technology, Volume III - Data book of unit processes for fuel preparation and handling. H.A. Simons (International) Ltd, B.H. Levelton & Associates Ltd. ENFOR Project C-258. Ottawa, Ont., 1983.
 - 85 Fagernäs, L. Peat and bark extractives and their behaviour in drying processes. VTT, Espoo, 1992. VTT Publications 121.
 - 86 Burnett, D., et al. Hog fuel drying: Status of existing systems in the Canadian pulp and paper industry. Neill and Gunter Ltd. Energy, Mines and Resources Canada. Ottawa, Ont., 1988.

-
- 87 Isoniemi, M., et al. Applying a magnetite fluidized-bed to steam drying of milled peat. Helsinki University of Technology, Department of Mechanical Engineering, Espoo, 1988. Publication 27.(In Finnish)
 - 88 Kaltschmitt, M. & Babu, S. (eds.). State of the art report on biomass gasification in several countries. Prepared by EU AIR3-CT94-2284 and IEA Bioenergy Task XIII Gasification. November 1997.
 - 89 Kurkela, E., Ståhlberg, P. Air gasification of peat, wood and brown coal in a pressurized fluidized-bed reactor. 1. Carbon conversion, gas yields, and tar formation. *Fuel Processing Technol.*, Vol. 31, 1992, pp. 1 -21.
 - 90 Kurkela, E., Koljonen, J. Experiences in the operation of the HTW process at the peat ammonia plant of Kemira Oy. Korhonen, M. (edm.). *Low grade fuels*. Helsinki, 12 - 16 June 1989. Vol. 1. VTT, Espoo, 1990 . Pp. 361 - 372. VTT Symposium 107.
 - 91 Kurkela, E. Status of peat and biomass gasification in Finland. *Biomass*, vol. 18, 1989, pp. 287-292.
 - 92 Lyytinen, H. Biomass gasification as a fuel supply for lime kilns: description of recent installations. *Tappi Journal*, 1987, July, pp. 77 - 80.
 - 93 Ma, R., et al. Modelling a pilot-scale fluidized bed coal gasification reactor. *Fuel Processing Technol.*, vol. 19, 1988, pp. 265-290.
 - 94 Bolthrunis, C. An industrial perspective on fluid bed reactor models. *Chemical Engineering Progress*, vol. 85, No. 5, 1989, pp. 51-54.
 - 95 Van der Aarsen, F. Fluidised bed wood gasifier performance and modelling. Ph.D. dissertation. Technische Hogeschool Twente, Enschede, 1985. 156 p.
 - 96 Buekens, A. & Schoeters, J. Modelling of biomass gasification. In: Overend, R., Milne, T. & Mudge, L. (eds.). *Fundamentals of thermochemical biomass conversion 1982*. London: Elsevier Appl. Sci., 1985. Pp. 619-689.
 - 97 Belleville, P. & Capart, R. A model for predicting outlet gas concentrations from wood gasifier. In: Bridgwater, A. (ed.). *Thermochem. Process. biomass (Evolved Eur. Workshop) 1st*. Butterworths, London, :1983. Pp. 217-228.
 - 98 De Souza-Santos, M. L. Modelling and simulation of fluidized-bed boilers and gasifiers for carbonaceous solids. Ph.D. dissertation. University of Sheffield, Department of Chemical Engineering and Fuel Technology, Sheffield, 1987.

-
- 99 Nilsson, T. Modelling of fluidized-bed gasification. Ph.D. dissertation. The Royal University of Technology, Stockholm, 1 984.
 - 100 Bacon, D. Modelling of fluidized bed wood gasifiers. In: Overend, R., Milne, T. & Mudge, L. (eds.). Fundamentals of thermochemical biomass conversion. Elsevier Applied Science Publishers, London, 1985.
 - 101 <http://www.basinelectric.com/dgc/dgchome.htm>
 - 102 Espenal, M., Britt, H. & Evans, L. System of multiphase reactor models for the ASPEN process simulator and their applications to coal conversion reactors. New York: AIChE (Chem. Eng. Progr.), 1980. Pp. 223-225.
 - 103 Ringard, I. & Benjamin, B. Great Plains ASPEN model development, gasifier model. Literature review and model specification. DOE/MC/19163-1782. NTIS/DE85003388. 1985. 60 p.
 - 104 Denn, M. Steady-state and dynamic simulation of moving-bed gasifiers. In: Proc. Coal Gasification Workshop, Morgantown 1982. Washington D. C: U.S. Department of Energy, 1982. Pp. 391-414.
 - 105 Denn, M. et al. Detailed simulation of a moving-bed gasifier. Electric Power Research Institute, Palo Alto, CA, 1982. AP-2576.
 - 106 Desai, P. & Wen, C. Computer modelling of the Morgantown Energy Research Center's fixed-bed gasifier. Morgantown Energy Research Center, Morgantown, 1978. 136 p. Report MERC/CR-78/3. 136 p.
 - 107 Wen, C. et al. User's manual for computer simulation and design of the moving bed coal gasifier. Final report. Morgantown Energy Research Center, U.S. Department of Energy, Morgantown, 1982.
 - 108 Stillman, R. Simulation of a moving bed gasifier for a Western coal. IBM J. Res. Develop., vol. 23, No 3, 1979, pp. 240 - 252.
 - 109 Daniel, K. Transient model of a moving-bed coal gasifier. Coal Process Technology, vol. 7. AIChE, New York, 1981, Pp. 9- 1. CEP Technical Manual.
 - 110 Kosky, P. & Floess, J. Global model of countercurrent coal gasifiers. Ind. Eng. Chem. Process Des. Dev., vol. 19, No. 4, 1980, pp. 586-592.
 - 111 Cho, Y. & Joseph, B. Heterogeneous model for moving-bed coal gasification reactors. Ind. Eng. Chem. Process Des. Dev., vol. 20, No. 2, 1981, pp. 314 - 318.

-
- 112 Amundson, N. & Arri, L. Char gasification in a counter-current reactor. *AIChE Journal*, vol. 24, No.1, 1978, pp. 87 - 101.
 - 113 Stefano, J. M. Evaluation and modification of ASPEN fixed-bed gasifier models for inclusion in an integrated gasification combined-cycle power plant simulation. U.S. DOE, Morgantown Energy Technology Center, Morgantown, 1985. WV, DOE/METC--85/4013.
 - 114 Benjamin, B. Great Plains ASPEN model development, gasifier model. DOE, Washington, 1985. 175 p. DOE/MC/19163-1787. NTIS/DE85003389.
 - 115 Wen, C. et al. User's manual for computer simulation and design of the moving bed coal gasifier. DOE, Washington, 1982. 91 p. DOE/MC/16474-1390. NTIS/DE 83007533.
 - 116 Transfer of ASPEN technology to METC. Final technical report. Massachusetts Institute of Technology, 1981. DOE/MC/14739-final.
 - 117 Barker, R. et al. ASPEN modelling of the Tri-State Indirect Liquefaction Process. Oak Ridge, Tennessee, 1983. ORNL/TM-8611 and ORNL/TM-8611/S1.
 - 118 Stone, K. R. ASPEN simulation of fluidized-bed and entrained-flow integrated gasification combined-cycle power plants. U.S. DOE & Morgantown Energy Technology Center, Morgantown, 1985. WV, DOE/METC--85/4027.
 - 119 Stone, K.R. ASPEN simulation of fixed-bed integrated gasification combined-cycle power plant. U.S. DOE & Morgantown Energy Technology Center, Morgantown, 1986. (WV, DOE/METC--86/4063.
 - 120 Kurkela, E. Formation and removal of biomass-derived contaminants in fluidized-bed gasification processes. VTT Energy, Espoo, 1996. 47 p. + app. 103 p. VTT Publications 287.
 - 121 Kurkela, E., Ståhlberg, P. Air gasification of peat, wood and brown coal in a pressurized fluidized-bed reactor. *Fuel Processing Technology*, vol. 31, 1992, pp. 1-21.
 - 122 Scott, D. S. & Piskorz, J. The continuous flash pyrolysis of biomass. *Can. J. Chem. Eng.*, vol. 62, 1984, pp. 404 - 412.
 - 123 Scott, D. S., Piskorz, J., Bergougnou, M. A., Graham, R. & Overend, R. P. The role of temperature in the fast pyrolysis of cellulose and wood. *Ind. & Eng. Chem. Res.*, vol. 27, 1988, pp. 8-15.

-
- 124 Meier, D., Oasmaa, A., Peacocke, G. Properties of fast pyrolysis liquids: status of test methods. In: Bridgwater, A.V., Boocock, D. (eds.). *Developments in thermochemical biomass conversion*. Blackie, Glasgow, 1997. Pp. 391-408.
 - 125 Graham, R., Freel, B., Bergougnou, M. Rapid thermal processing (RTP): Biomass fast pyrolysis overview. In: *Biomass thermal processing*. In: Proc. of the 1st Canada/EC R&D Contractors Meeting, Ottawa, 23 - 25 October 1990. CPL Press, London, 1992. Pp. 52-63.
 - 126 Piskorz, J., Scott, D. S., Radlein, D. & Czernik, S. New applications of the Waterloo fast pyrolysis process. In: *Biomass thermal processing*. Proc. of the 1st Canada/EC R&D Contractors Meeting, Ottawa, 23 - 25 October 1990. CPL Press, London, 1992. Pp. 64-73.
 - 127 Graham, B. & Rossi, C. RTP fast pyrolysis. In: Kaltschmitt, M. & Bridgwater, A. (eds.). *Gasification and pyrolysis of biomass. State of the art and future prospects*. CPL Press, Newbury, 1997.
 - 128 Rossi, C. Pyrolysis at the ENEL Bastardo pyrolysis plant. JOULE contractor's meeting, Brussels, 26 March 1999.
 - 129 Cuevas, A. Advances and developments at the Union Fenosa pyrolysis pilot plant. 8th European Conference on Biomass for Energy, Environment, Agriculture, and Industry. Vienna, 3 - 5 October 1994.
 - 130 Peacock, C. Ablative pyrolysis of biomass. PhD thesis. Aston University, Birmingham, 1994.
 - 131 Wagenaar, et al. The rotating cone flash pyrolysis reactor. In: Bridgwater, A.V. (ed.). *Advances in thermochemical biomass conversion*. Blackie, Glasgow, 1994. Pp. 1122-1133.
 - 132 Boukis, I. & Bridgwater, A. Design concept and hydrodynamics of an air-blown CFB reactor for flash pyrolysis. In: Proc. Biomass Pyrolysis Oil Properties and Combustion Meeting, Estes Park, CO, 26 - 28 September 1994. NREL, Golden CO, 1995. P. 343.
 - 133 Meier, D. Fast pyrolysis liquids characteristics. Gasification and pyrolysis of biomass. An international conference, Stuttgart, 9-11 April 1997.
 - 134 Samolada, M. & Vasalos, I. Catalytic cracking of biomass flash pyrolysis liquids. In: Bridgwater, A.V., Boocock, D. (eds.). *Developments in thermochemical biomass conversion*. Blackie, Glasgow, 1997. Pp. 657 - 671.

-
- 135 Sipilä, K., Oasmaa, A., Arpiainen, V., Westerholm, M., Solantausta, Y., Anger, A., Gros, S., Nyrönen, T., Gust, S. Pyrolysis oils for power plants and boilers. In: Chartier, P. et al. (eds). Biomass for energy and the environment. Proc.9th European Conf. on Bioenergy. Copenhagen, 24 - 27 June 1996. Vol 1. Elsevier, London, 1996. Pp. 302- 07.
 - 136 Radlein, D., Production of chemicals from bio-oil. Gasification and pyrolysis of biomass. An international conference, Stuttgart, 9-11 April 1997.
 - 137 Diebold, J., Scahill, J. Improvements in the Vortex reactor design. In: Bridgwater, A.V. & Boocock, D. (eds.). Developments in thermochemical biomass conversion. Blackie, Glasgow, 1997. Pp. 242 - 252.
 - 138 Roy, C., Morin, D., Dube, F. Electricity production from biomass using the integrating pyrolysis combined-cycle process. In: Overend, R. & Chornet, E. (eds). Making a business from biomass in energy, environment, chemicals, fibers, and materials. Proc. 3rd Biomass Conference of the Americas. New York: Elsevier Science Ltd., 1997.
 - 139 Elliott, D. C. IEA Co-operative Project D1, Biomass Liquefaction Test Facility Project, Vol. 4: Analysis and upgrading of biomass liquefaction products. DOE/NBM--1062 Vol. 4. National Technical Information Service, Springfield, VA, 1988.
 - 140 McKinley, J. Biomass liquefaction: centralized analysis. Final Report. DSS File No. 232-4-6192. Energy, Mines and Resources Ministry, Ottawa, 1988.
 - 141 Rick, F., Vix, U. Product standards for pyrolysis products for use as fuel in industrial firing plants. In: Bridgwater, A. & Grassi, G. (eds.). Biomass pyrolysis liquids upgrading and utilisation. Elsevier Applied Science, Barking . Pp. 177-218.
 - 142 Fagernäs, L. Chemical and physical characterisation of biomass-based pyrolysis oils. Literature review. VTT, Espoo, 1995. 113 p. VTT Research Notes 1706.
 - 143 Oasmaa, A., Leppämäki, E., Koponen, P., Levander, J., Tapola, E. Physical characterisation of biomass-based pyrolysis liquids. Application of standard fuel oil analyses. VTT, Espoo, 1997. 46 p. + app. 30 p. VTT Publications 306.
 - 144 Diebold, J., Milne, T., Czernik, S., Oasmaa, A., Bridgwater, T., Cuevas, A., Gust, S., Huffman, D., Piskorz, J. Proposed specifications for various grades of pyrolysis oils. In: Bridgwater, A.V. & Boocock, D. (eds.). Developments in thermochemical biomass conversion. Blackie Glasgow, 1997. Pp. 433-447.
 - 145 Gust, S. Combustion of pyrolysis liquids. Gasification and pyrolysis of biomass. An international conference, Stuttgart, 9-11 April 1997.

-
- 146 Sipilä, K. Bio fuel oil power plants and boilers. JOULE contractor's meeting. Brussels, 26 March 1999.
- 147 Oasmaa, A., Sipilä, K. Pyrolysis oil properties: use of pyrolysis oil as fuel in medium-speed diesel engines. In: Bridgwater, A. V. & Hogan, E. N. (eds.). Bio-oil production & utilization. Proc. 2nd EU-Canada Workshop on Thermal Biomass Processing. CPL Press, Newbury, 1996. Pp. 175-185.
- 148 Jay, D., C., Rantanen, O., Sipilä, K., Nylund, N.-O. Wood pyrolysis oil for diesel engines. In: Proc. 1995 Fall Technical Conference, Milwaukee, Wisconsin, 24 - 27 Sept 1995. ASME, Internal Combustion Engine Division, New York, 1995.
- 149 Leech, J. Running a dual fuel engine on pyrolysis oil. In: Kaltschmitt, M., Bridgwater, A., (eds). Biomass gasification and pyrolysis, State of the art and future prospects. CPL Press, Newbury, 1997.
- 150 Solantausta, Y., Nylund, N-O., Westerholm, M., Koljonen, T., Oasmaa, A. Wood pyrolysis oil as fuel in a diesel power plant. Bioresource Technology, vol. 46, 1993, pp. 177-188
- 151 Casanova, J. Comparative study of various physical and chemical aspects of pyrolysis bio-oils versus conventional fuels, regarding their use in engines. In: Proc. Biomass Pyrolysis Oil Properties and Combustion Meeting, Estes Park, CO, 26-28 September 1994. NREL, Golden, CO, 1995. P. 343.
- 152 Suppes, G. et al. Autoignition of selected oxygenate fuels in a simulated diesel engine environment. AIChE 1996 National Meeting, New Orleans, LA, 26 February 1996.
- 153 Andrews, R., Fuleki, D., Zukowski, S. & Patnaik, P. Results of industrial gas turbine tests using a biomass-derived fuel. In: Overend; R. & Chornet, E. (eds). Making a business from biomass in energy, environment, chemicals, fibers, and materials. Proc. 3rd Biomass Conference of the Americas. Elsevier Science Ltd., New York, 1997.
- 154 McKeough, P., Nissilä, M., Solantausta, Y., Beckman, D., Östman, A., Bergholm, A., Kannel, A. Techno-economic assessment of direct biomass liquefaction processes. IEA Cooperative Project D1, Biomass Liquefaction Test Facility Project, Final Report, #DOE/NBM-1062-Vol. 5, National Technical Information Service, Springfield, Virginia, 1988.
- 155 Beckman, D., Elliott, D., Gevert, B., Hörmell, K., Kjellström, B., Östman, A., Solantausta, Y., Tulenheimo, V. Techno-economic Assessment of Selected Biomass Liquefaction Processes. VTT, Espoo, 1990. 161 p. + app. 95 p. VTT Research Reports 697.

-
- 156 Solantausta, Y., Diebold, J. P., Elliott, D. C., Bridgwater, T. & Beckman, D. Assessment of liquefaction and pyrolysis systems. VTT, Espoo, 1994. 230 p. + app. 79 p. VTT Research Notes 1573.
- 157 Black, J. Preliminary eEvaluation of the Waterloo Fast Pyrolysis Process. BBC Engineering & Research Ltd. Markham, Ont, June 1986. Energy, Mines and Resources Canada, Ottawa, 1986.
- 158 Wan, E. Technical and economic evaluation of biomass-based fuel processes. In: Proc. 1985 Biomass Thermochemical Conversion Contractors Meeting, Minneapolis, MI, 15 - 16 October 1985. Richland, WA, 1985. PNL-SA-13571.
- 159 Beckman, D. & Graham, R. Economic assessment of a wood fast pyrolysis plant. In: Bridgwater, A.V. (ed.). Advances in thermochemical biomass conversion. Blackie, Glasgow, 1992. Pp. 1314 - 1324.
- 160 Cottam, M. Technical and economic simulation of biomass pyrolysis processes for fuels and electricity. Final report. EU contracts JOUB0035 and JOUB0022. Aston University, Birmingham, 1994.
- 161 Piskorz, J., Radlein, D. St. A. G., Scott, D. S., Czernik, S. Liquid products from the fast pyrolysis of wood and cellulose. In: Bridgwater, A. V. & Kuester, J. L. (eds.). Research in thermochemical biomass conversion. Elsevier Applied Science, London, 1988. Pp. 557-571.
- 162 Piskorz, J., Scott, D. S., Radlein, D., Czernik, S. New applications of the Waterloo fast pyrolysis process. In: Hogan, E., Robert, J., Grassi, G. & Bridgwater, A. V. (eds.). Biomass thermal processing. Proc. 1st Canada/European Community R&D Contractors Meeting. CPL Press, Newbury, 199 . Pp. 64-73.
- 163 Oasmaa, A. Pyrolyysiöljyjen analyysejä (Fuel oil analysis of different biomass flash pyrolysis oils). VTT Energy, Espoo, October 1997. (in Finnish)
- 164 Solantausta, Y., Mäkinen, T., Koljonen, T. Modelling of a flash pyrolysis process. EU AIR Contract AIR2-CT94-1162. VTT Energy, Espoo, 1997.
- 165 Graham, R. G., Freel, B. A., Huffman, D. R., Bergougnou, M. A. Applications of rapid thermal processing of biomass. In: Bridgwater, A.V. (ed.). Advances in thermochemical biomass conversion. Blackie, Glasgow, 1992. Pp. 1275 - 1288.
- 166 Glessner, J. Gas turbine technology. Course held at the Hague, the Netherlands, October 12-14, 1992. Center for Professional Advancement, Amsterdam, 1992.

-
- 167 Clark, W., Litzinger, R., Straughan, I., Cool Water: Performance and economics. Presented at the American Institute of Chemical Engineers, Boston National Meeting. 24-27 August, 1986
 - 168 Sundstrom, D., Dow coal gasification progress report. Paper presented at the Alternative Energy '89, Tucson, Arizona. April 18, 1989.
 - 169 IGCC future under test at Buggenum. *Modern Power Systems*, vol. 10, No. 10, 1990, pp. 39-45.
 - 170 Richards, R., European IGCC tilts at windmills in La Mancha. *Modern Power Systems*, vol. 12, No. 8, 1992, pp. 14-26.
 - 171 100-MW Nevada IGCC to go operational late next year. *Gas Turbine World*, vol. 25, No. 5, 1995, p. 38.
 - 172 Wabash IGCC to be on line by the end of this year. *Gas Turbine World*. vol. 25, No. 5, 1995, p. 36.
 - 173 Italy is pioneering the application of commercial heavy oil IGCC plants. *Gas Turbine World*, vol. 25, No. 3, 1995, p. 22.
 - 174 Texaco refinery powered by syngas fueled gas turbine. *Gas Turbine World*, vol. 24 No. 4, 1994, p. 6.
 - 175 Start 6 MWe, 9 MWth biofuel gasification cogen in Sweden. *Gas Turbine World*, vol. 25, No. 6, 1995, p. 41.
 - 176 Karlsson, G., Ekström, C., Liinanki, L. The development of a biomass IGCC process for power and heat production. In: Chartier, A., Beenackers, A., Grassi, G. (eds.) *Biomass for Energy, Environment, Agriculture, and Industry*. Elsevier Science, Kidlington, 1995. Pp. 1538-1549.
 - 177 Naccarati, R., de Lange, H. The use of biomass-derived fuel in a gas turbine for the Energy Farm Project. In: Sipilä, K. & Korhonen, M. (eds.). *Power Production from Biomass III. Gasification and Pyrolysis RD&D for Industry*. VTT, Espoo, 1999. Pp. 141 -150. VTT Symposium 192.
 - 178 Palmer, C., Erbes, M. Performance Predictions of the Frame 6 Engine Fired on Low Btu Fuels. Final Report for VTT, Enter Software, Inc., December 14, 1993.
 - 179 Moses, C., Bernstein, H. Impact study on the use of biomass-derived fuels in gas turbines for power generation. SRI, San Antonio, TX, USA. January 1994. Published by NREL, Golden, CO. NREL/TP-6085.

-
- 180 Arnold, M., Kelsall, G., Hudson, D. Clean and efficient electric power generation for the next century - the British Gas Topping Cycle. Presented at the 1st International Conference on Combustion Technologies for a Clean Environment. Vilamoura, 1991.
 - 181 Kelsall, G., Smith, M., Todd, H., Burrows, M. Combustion of LCV coal derived gas for high temperature, low emissions gas turbines in the British Cola Topping Cycle. 36th ASME International Gas Turbine and Aeroengine Congress and Exhibition, Orlando, FLA, June 3-6, 1991. 91-GT-384.
 - 182 Kelsall, G., Cannon, M. Combustion of low heating value gas in a gas turbine. In: Sipilä, K. & Korhonen, M. (eds.). Power Production from Biomass II, Espoo 1995. VTT, Espoo, 1996. Pp. 109-126. VTT Symposium 164.
 - 183 Boothe, W., McMullen, J. Heavy duty gas turbine design changes for use with low Btu coal gas. Presented at the Gas Turbine Conference & Exhibit & Solar Energy Conference, San Diego, California, March 12-15, 1979. ASME 79-GT-198.
 - 184 Bahr, D., et al. Small industrial gas turbine combustor performance with low BTU gas fuels. Presented at the 1985 Beijing International Gas Turbine Symposium and Exposition, Beijing, People's Republic of China, September 1-7, 1985. ASME 85-IGT-125.
 - 185 Sabla, P., Kutzko, G. Combustion characteristics of the GE LM2500 combustor with hydrogen-carbon monoxide-based low btu fuels. Presented at the 1985 Gas Turbine Conference and Exhibit, Houston, Texas, March 18-21, 1985. ASME 85-GT-179.
 - 186 Williams, R., Larson, E. , Biomass gasifier gas turbine power generating technology. Biomass and Bioenergy, vol. 10, No. 2-3, 1996, pp. 149-166.
 - 187 Palmer, C., Erbes, M. LM2500 Fired on Low Btu Fuels. Final Report for VTT. Enter Software, Inc., January 28, 1992.
 - 188 Kasper, J.M., Jasa, G.B., Trauth, R. Use of pyrolysis-derived fuel in gas turbine engine. 83-GT-96 The American Society of Mechanical Engineers, New York, 1983.
 - 189 Andrews, R., Zukowski, S., Patnaik, P., Feasibility of firing an industrial gas turbine using a biomass derived fuel. In: Bridgwater, A., Boocock, D. (eds). Developments in Thermochemical Biomass Conversion. Chapman & Hall, London, 1997.
 - 190 Johnson, M. The effects of gas turbine characteristics on integrated gasification combined-cycle power plant performance. Ph.D. dissertation. Stanford University, Stanford, CA, 1989.

-
- 191 Consonni, S. Performance prediction of gas/steam cycles for power generation. Ph.D. dissertation. Princeton University, Princeton, NJ, 1992.
 - 192 Phillips, J. A study of the off-design performance of integrated coal gasification combined-cycle power plants. Ph.D. dissertation. Stanford University, Stanford, CA, 1986.
 - 193 Erbes, M. Phased construction of integrated coal gasification combined-cycle power plants. Ph.D. dissertation. Stanford University, Stanford, CA, 1987.
 - 194 Paffenbarger, J. Study of a coal gasification combined-cycle power plant with methanol storage. Mechanical Engineering Department, Stanford University. Stanford, 1989.
 - 195 Allen, R., Ross, K. Performance characteristics and ratings for GE industrial gas turbines. GER-2503B, General Electric Co., 1981.
 - 196 Matchak, T., et al., Cost and performance for commercial applications of Texaco-based-gasification-combined-cycle plants. EPRI AP-3486, Final report. Electric Power Research Institute, Palo Alto, CA, April 1984. Fluor Engineers, Inc.
 - 197 Erbes, M. et al. GATE: A simulation code for analysis of gas turbine power plants. IGTI/ASME Gas Turbine Congress, Toronto, Ontario, July 1989.
 - 198 Gas Turbine World, 6/1997.
 - 199 State of the art report on gasification in a number of countries. Prepared by EU Concerted Action (AIR3-CT94-2284) and the IEA Bioenergy Task XIII Gasification Activity. November 1997.
 - 200 Stassen, H. UNDP/WB Small-scale biomass gasifier monitoring report. A report prepared for World Bank/UNDP. Enschede: University of Twente, BTG, September 1993.
 - 201 Waldheim, L., Blackadder, W. Gasification of wood fuel and electricity production with a diesel engine. Studsvik, 1990. Studsvik Report EP-90/16. (in Swedish)
 - 202 Ekono Oy: Competitiveness of gas diesel power plants. Ministry of Trade and Industry, Helsinki, 1984. Publications D:52. (Kaasudieselvoimalaitosten kilpailukykyisyys).
 - 203 Ekström, C. Atmospheric gasification - diesel. Technical evaluation and proposal for future work. Vattenfall, Vällingby, 1991. (in Swedish).

-
- 204 Jenbacher Energiesysteme, Achenseestrasse 1-3, A-6200 Jenbach, Austria, Fax +43 5244 600-548.
- 205 Herdin, G., Wagner, M. Engine use of producer gas, experience and requirements. In: Sipilä, K. & Korhonen, M. (eds.). Power Production from Biomass III. Gasification and Pyrolysis R&D&D for Industry, Espoo, 1998. VTT, Espoo, 1999. Pp. 231-248. VTT Symposium 192.
- 206 Stassen, H., Koele, H. The use of LCV-gas from biomass gasifiers in internal combustion engines. In: Kaltschmitt, M. & Bridgwater, A. (eds.). Biomass gasification and pyrolysis. State of the art and future respects. CPL Scientific Ltd, Newbury, 1997.
- 207 Gros, S. Pyrolysis oil as diesel fuel. In: Sipilä, K. & Korhonen, M. (eds.) Power Production from Biomass II, Espoo, 1995. VTT, Espoo, 1996. Pp. 225-238. VTT Symposium 164.
- 208 Final report, EU AIR2-CT94-1162. VTT Energy, Espoo 1996.
- 209 Bridgwater, A.V. et al. Development of advanced fast pyrolysis processes for power and heat. JOULE contractor's meeting. Brussels, 26 March 1999.
- 210 Stendahle, T. Optimized heat production in a cogeneration application. Power News (Wärtsilä Diesel Customer Journal). No. 1, 1997, pp. 10 - 11. Vaasa 1997.
- 211 Confidential report to VTT, November 1997, Espoo.
- 212 Wärstilä NSD Oy, Reference list. Vaasa, 1998.
- 213 Haar, L., Gallagher, J.S., Kell, J.H. NBS/NRC Steam Tables. Hemisphere Publishing Corporation, Washington, 1984.
- 214 Taylor, J..H., Craven, P..J., Experience curves for chemicals. Process Economics International, vol. 1, No. 1, Autumn 1979, pp. 13-19.
- 215 Hess, R., Myers, C. Assessing initial cost growth and subsequent long-term cost improvement in coal-to-SNG processes. Prepared by RAND Corporation for the Gas Research Institute. Santa Monica, CA. GRI Publication GRI 89/0129. June 1989.
- 216 Milanese, J. Process industry contingency estimation: A study of the ability to account for unforeseen costs. Prepared by RAND Corporation. Santa Monica, CA. N-2386-PSSP. June 1987.

-
- 217 Milanese, J. Process industry contingency estimation: A study of the ability to account for unforeseen costs. Prepared by RAND Corporation. Santa Monica, CA. N-2386-PSSP. June 1987.
- 218 Perry, R., Chilton, C. (eds.). Chemical engineers' handbook. 5th edition. McGraw-Hill Book Co., New York, 1973.
- 219 Clark, F, Lorenzoni, A Applied cost engineering. Marcel Dekker, Inc., New York, 1985.
- 220 Frey, H. Probabilistic modeling of innovative clean coal technologies: implications for technology evaluation and research planning. Ph.D. dissertation. Carnegie-Mellon University, Pittsburgh, Pennsylvania, 1991.
- 221 Merrow, E., Phillips, K., Myers, C. Understanding cost growth and performance shortfalls in pioneer process plants. Prepared by RAND Corporation for the U.S. Department of Energy. Santa Monica, CA. R-2569-DOE. September 1981.
- 222 Merrow, E., Yarossi, M., Managing capital projects. Where have we been - where are we going? Chemical Engineering, vol. 101, No. 10, 1994, pp. 108-111.
- 223 Gas Research Institute (GRI), guide-lines for Evaluation of Commercial Fossil Fuels Gasification Concepts. GRI-83/0003, Chicago, Illinois. March 1983.
- 224 Bernard, D., McBeath Guide-lines for economic evaluation of coal conversion processes. Engineering Societies Commission on Energy, Inc. (ESCOE), DOE/FE-2468-44. Washington, D.C.. April 1979.
- 225 Valle-Riesta, F. Project evaluation in the chemical process industries. McGraw-Hill, New York, 1984.
- 226 Hackney, J. Control and management of capital projects. J. Wiley & Sons, New York, 1966.
- 227 Hess, R. Review of cost improvement literature with emphasis on synthetic fuel facilities and the petroleum and chemical process industries. The RAND Corporation, N-2273-SFC, March 1985a.
- 228 Stobaugh, R., Townsend, P., Price forecasting and strategic planning: The case of petrochemicals. Journal of Marketing Research, February 1975, pp. 19-29.
- 229 Lieberman, M., The learning curve, pricing, and market structure in the chemical processing industries. Ph.D. thesis. Harvard University, Cambridge, Massachusetts, 1982.

-
- 230 Nousiainen, I. Polttopuun hinta. Bioenergia-ohjelma. VTT Energia, Jyväskylä, 1998. (in Finnish).
- 231 Prices for fuels. Energy Review for the Industry. Finnish National Board of Trade and Industry, Helsinki, 1999. (in Finnish)
- 232 Sipilä, K. New power-production technologies: various options for biomass and co-generation. Bioresource Technology, vol. 46, Nos 1-2, 1993, pp. 5-12.
- 233 Helynen, S. The potential of small power plants in Finland. A seminar of small scale power plants. Jyväskylä 16-17 March 1993. Bioenergy Programme (in Finnish)
- 234 Simell, P., Ståhlberg, P., Solantausta, Y., Hepola, J., Kurkela, E. Gasification gas cleaning with nickel monolith catalyst. Bridgewater, A. & Boocock, D. (eds.). Developments in Thermochemical Biomass Conversion, Banff, 20 - 24 May 1996. Vol. 2. Blackie, London, 1997. Pp. 1103 - 1116.
- 235 Ong'iro, A. Techno-economic modelling of integrated advanced power cycles. Ph.D. thesis. Technical University of Nova Scotia, Dec 1996.
- 236 Hamilton, S. Microturbines poised to go commercial. Modern Power Systems, vol. 19, No. 9, 1999, pp. 21-22.

DERIVING THE CORRELATIONS FOR THE STEAM DRYER

Introduction

A model which calculates the performance of a steam dryer is designed and presented (Figure A1-1). It will also calculate some critical sizing data to be employed in cost estimation.

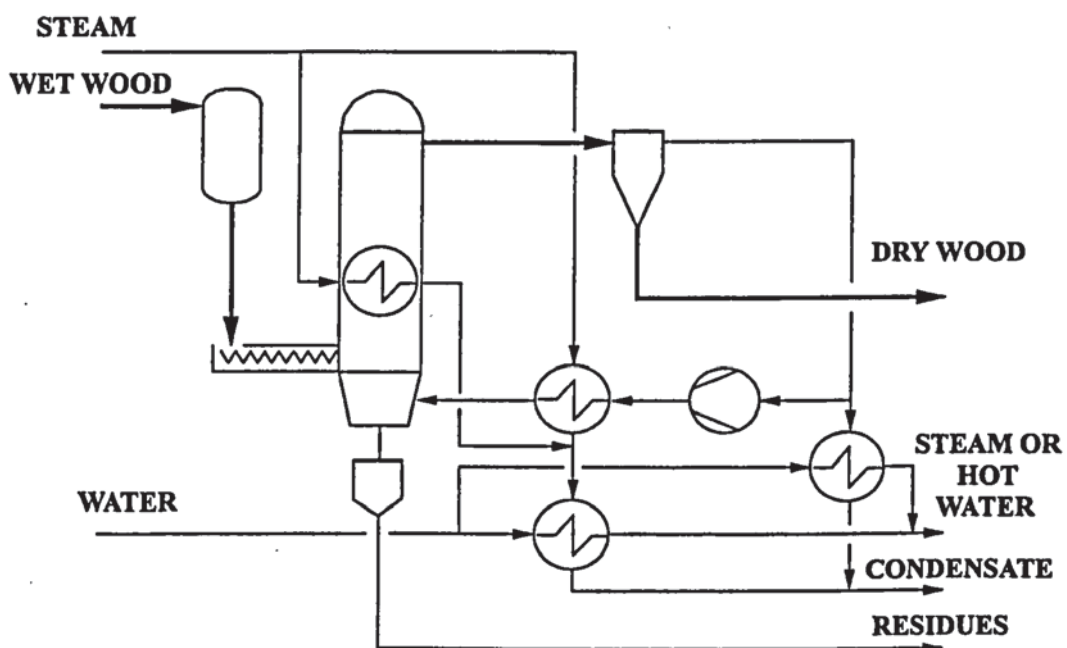


Figure A1-1. Flow diagram of the steam dryer

The purpose of the model is to:

- calculate mass flows for performance analysis
- calculate internal power consumption (recycle vapour blower, dryer feeder) for performance analysis
- size all critical units in the dryer (recycle vapour superheater area, dryer reactor vessel volume, cyclone) for capital cost estimation

The fluidization velocity and the overall heat-transfer coefficient in the model

Two parameters are used in controlling the performance of the model: the fluidization velocity, and the overall heat-transfer coefficient in the fluidized-bed. The flow rate must be sufficiently in excess of the minimum fluidization velocity to maintain fluidization (the recycle flow is controlled), and the heat-transfer coefficient is a function of operating conditions (pressure, temperature). In practical operation a gas velocity three times the minimum fluidization velocity is required, and this value is used here.

The pressure is a critical parameter for fluidization (and subsequently for the heat-transfer coefficient), and therefore model correlations are designed as a function of pressure. Over the operation range considered, temperature may be averaged out. The argumentation is presented in figures A1-2 to A1-5).

Simplified correlations for the fluidization velocity and overall heat-transfer coefficient are used in the Aspen model. The derivation of these is presented. The minimum fluidization velocity is defined by Equation A1-1 [1]. The properties of the gas phase were calculated with Aspen's physical property estimating routines. The sensitivity of the minimum fluidization velocity is depicted as a function of the most important process parameters, i.e. pressure, temperature and particle size, in figures A1-2 and 3. It may be concluded that in the dryer temperature range, temperature has a minor effect on the minimum fluidization velocity. The particle size has a moderate effect on the minimum fluidization velocity. The middle curve from A1-3 is fitted, and the correlation is presented as Equation (A1-2). This correlation is later employed in the Aspen model as the pressure correlation for the minimum fluidization velocity .

$$u = \frac{\mu_g}{d_p \rho_g} \left(\sqrt{33.7^2 + 0.0408 \frac{d_p^3 \rho_g (\rho_p - \rho_g) g}{\mu_g^2}} - 33.7 \right) \quad (\text{A1-1})$$

where

u = gas velocity (corresponding to minimum fluidization), m/s

μ = dynamic viscosity of the gas, kg/sm

d_p = the average particle diameter, m

ρ_g = gas density, kg/m³

ρ_p = solid density, kg/m³

g = gravity constant, 9.81 m/s

$$u = 1.60 * p^{-0.49} \quad (A1-2)$$

where

p = pressure, bar

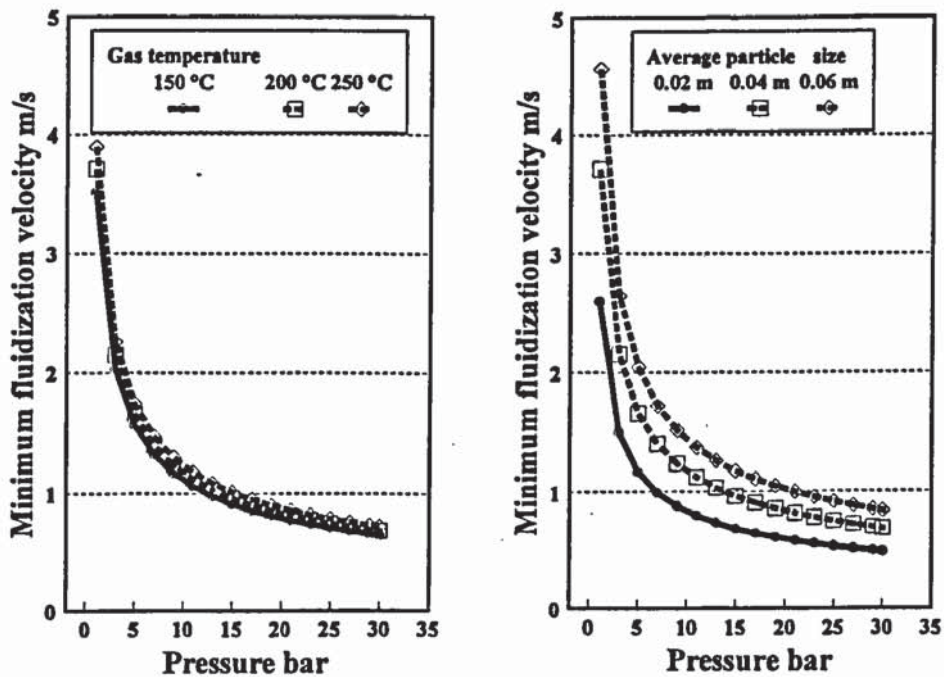


Figure A1-2 (left). The minimum fluidization velocity as a function of pressure, temperature as parameter. Average particle size 0.04 m, solid density 400 kg/m³.

Figure A1-3 (right). The minimum fluidization velocity as a function of pressure, average particle size as parameter. Temperature 200 °C, solid density 400 kg/m³.

Several modes of heat transfer occur in a fluidized-bed dryer. Both heat transfer between the fluidized-bed and the heat exchanger, and the heat transfer between the fluidized-bed and wet particles should be considered. An overall correlation for the heat transfer between the fluidized-bed and the heat exchanger as presented by Denloye and Botterill /2/ is used here, Equation (A1-3). This simplification is made because the heat transfer between the fluidized-bed and the heat exchanger is considered to be the rate-determining step. The heat transfer coefficient is presented as a function of system pressure in Figure A1-4 with temperature as a parameter. Temperature has a minor effect on the coefficient within the range considered. A similar correlation but with the average particle size as a parameter is depicted in Figure A1-5. The particle size has a large effect on the heat transfer coefficient. Equations presented for fluidization have been developed for particles of a regular shape. Correction factors are typically employed for non-spherical particles. Wood chips are far from spherical, and the determination of an "average particle size" is not clear-cut.

It is concluded that a more elaborate analysis of the heat transfer coefficient does not yield more appropriate results, considering the overall objective of the work. It should be noted that Equation (A1-3) expresses the heat transfer coefficient at the optimum fluidization velocity, and the respective correction for the actual velocity has not been made. However, because of the large uncertainties described above in relation to the input data (especially the average particle size), an approximate correlation for the heat transfer coefficient is used. The lower curve in Figure A1-5 is fitted, and the correlation is presented as Equation (A1-4). This correlation is later employed in the Aspen model as the overall heat transfer coefficient for the fluidized-bed heat exchanger. The heat transfer area in the fluidized-bed is then calculated by Aspen.

$$Nu_{\max} = 0.843 Ar^{0.15} + 0.86 d_p^{0.5} Ar^{0.39} \quad (\text{A1-3})$$

where
$$Nu_{\max} = \frac{\alpha d_p}{\lambda_g}$$

$$Ar = \frac{d_p^3 g (\rho_p - \rho_g)}{v_g^2 \rho_g}$$

α = heat transfer coefficient, W/(m²K)

λ_g = heat conductivity of gas, W/(mK)

v_g = kinematic viscosity of gas, m²/s

$$\alpha = 103.1 * p^{0.15}$$

(A1-4)

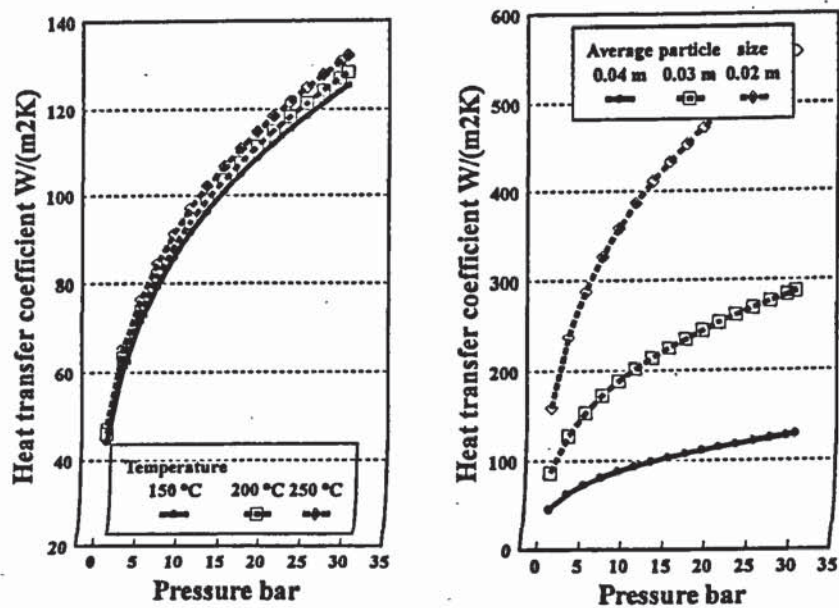


Figure A1-4 (left). The heat transfer coefficient as a function of pressure, temperature as parameter. Average particle size 0.02 m, solid density 400 kg/m³.

Figure A1-5 (right). The heat transfer coefficient as a function of pressure, particle size as parameter. Temperature 200 °C, solid density 400 kg/m³.

Model validation and testing

No experimental data was available to the author concerning the steam drying of wood chips. The overall heat transfer coefficient, which is subject to considerable uncertainty, has not been verified for this application. Therefore, actual verification of the model for wood was not done. However, the model was tested against available data for peat drying. The comparison between the model results and available data is presented below.

Huhtinen et al. have published experimentally determined values for the drying of milled peat /3/. The highest reported heat transfer coefficients were: 88 W/(m²K) (without a distinct bed material, fluidization velocity 1.5 m/s), 179 W/(m²K) (sand as bed material, velocity 1.3 m/s), and 186 W/(m²K) (magnetite as bed material, velocity 1.4 m/s). In approximately similar conditions (5 bar pressure, about 1.5 m/s fluidization velocity) a heat transfer coefficient of about 75 W/(m²K) results from correlation (A1-4). Because of differences in material properties between milled peat and wood chips, the applied correlation may be regarded as pessimistic but reasonable.

The dryer model was tested against performance data for industrial milled peat drying /4/ (Table A1-1). Although the MoDo dryer is not exactly the same as the steam dryer modelled here, their design characteristics are quite analogous. To overcome the differences and to facilitate comparison, the recycle vapour flow and recycle heater steam mass flow were fixed to the same values in the model as in the data report. Thus only the steam consumption and the recycle compressor power were calculated. The calculated steam consumption was predicted to be 5 % higher than in actual operation. The recycle compressor power requirement was estimated to be about 15 % lower than in the real case.

Table A1-1. Comparison of dryer simulation results with design data

	Operation	Simulation
Feed (moist), t/h	41.7	41.7
Feed moisture content, wt-%	60	60
Final moisture, wt-%	10	10
Recycle heat exchanger steam, t/h	7.3	7.3
Recycle vapour flow, t/h	122.4	122.4
Steam consumption, t/h	13.2	13.9
Recycle compressor power, kW	1000	840

In addition, other features of the model were also studied, employing peat as a feedstock. Some results of the technical sensitivity studies are presented below. The results are shown to indicate possibilities of using the model as a tool to optimise process performance. In an IGCC plant for example, increasing the dryer steam pressure reduces the fluidized-bed heat exchanger area (and thus the investment). On the other hand, the increase in steam pressure will reduce the power output from the steam turbine as the steam to the dryer is extracted at a higher pressure. At the same time the power consumption of the recycle compressor is reduced as the recycle ratio decreases.

In the cases below, the feed to the dryer is 148 t/h, and the moisture of feed is 50 wt-%. The correlations for the minimum fluidization velocity and overall heat transfer coefficient are shown in (A1-2) and (A1-4).

The fluidized-bed heat exchanger area is shown in Figure (A1-6) as a function of steam conditions. Increasing the steam pressure from 12 to 30 bar reduces the required area from above 9000 to around 3500 m². Both the recycle ratio and the recycle compressor power requirement decrease (Figure (A1-7)). Increasing the steam pressure from 12 bar to 30 bar decreases the required power from above 4 to around 1.3 MW.

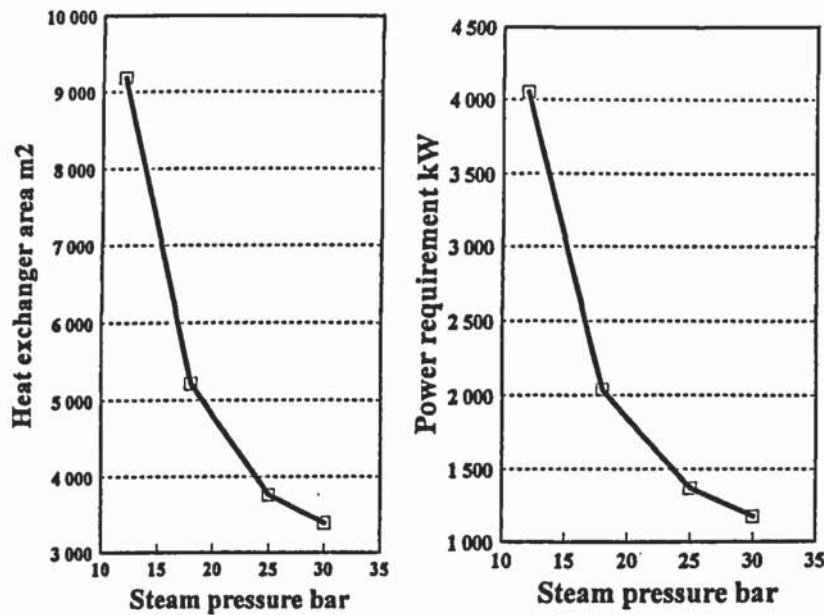


Figure A1-6 (left). Steam drying of peat. The area of the fluidized-bed heat exchanger as a function of steam conditions, superheating 50 °C. Dryer pressure 5 bar, steam mass flow to the fluidized-bed heat exchanger 77 - 85 t/h.

Figure A1-7(right). Steam drying of peat. The power requirement of the recycle compressor as a function of steam conditions, superheating 50 °C. Dryer pressure 5 bar, steam mass flow to the fluidized-bed heat exchanger 77 - 85 t/h.

REFERENCES

- 1 Kunii, D., Levenspiel, O., Fluidization engineering. John Wiley & Sons, Inc. New York, 1969. 534 p.
- 2 Denloye, A., Botterill, S., Bed to surface heat transfer in a fluidized bed of large particles. Powder Technology 19(1978), 197-203.
- 3 Huhtinen, M., et al., Behaviour, dimensioning and profitability of steam fluidized bed dryer based on experiments carried out in pilot dryer. Publication 23. Espoo 1988. Helsinki University of Technology, Department of Mechanical Engineering. 176 p. (In Finnish)
- 4 Mass and energy balances for a MoDo steam dryer. Internal report of VTT. Espoo 1987. (In Finnish)

AspenPlus input file for a steam dryer

```

;
;Input Summary created by ASPEN PLUS Rel. 9.3-1 at 15:35:40 Sun Mar 15, 1998
;Directory D:\Y2\KUI Filename input.001
;
TITLE 'DRYER'

IN-UNITS SI PRESSURE=BAR TEMPERATURE=C

OUT-UNITS SI PRESSURE=BAR TEMPERATURE=C

DEF-STREAMS MIXCINC ALL

SIM-OPTIONS
  IN-UNITS ENG
  SIM-OPTIONS MW-CALC=NO

RUN-CONTROL MAX-TIME=500.0

DATABANKS PURE856 / ASPENPCD

PROP-SOURCES PURE856 / ASPENPCD

COMPONENTS
  H2O H2O H2O /
  BIOMASS * BIOMASS

FLOWSHEET KUI
  BLOCK DRM1 IN=DR11 DR19 OUT=DR12
  BLOCK DRHX1 IN=ST11 DR12 OUT=CO11 DR13
  BLOCK DRCY1 IN=DR13 OUT=DR14 DR20
  BLOCK DRCY2 IN=DR14 OUT=DR15 DR16
  BLOCK DRCO IN=DR16 OUT=DR17 W11
  BLOCK DRM2 IN=CO11 CO12 OUT=CO13
  BLOCK DRX4 IN=CO13 DH11 OUT=CO14 DH12
  BLOCK DRX3 IN=DR15 DH13 OUT=CO15 DH14
  BLOCK DRX2 IN=ST12 DR17 OUT=CO12 DR18

DEF-STREAMS MIXCINC KUI

PROPERTIES SYSOP12

PROP-REPLACE SYSOP12 STEAM-TA
  PROP DLMX DLMX05

NC-COMPS BIOMASS PROXANAL ULTANAL SULFANAL GENANAL

NC-PROPS BIOMASS ENTHALPY HCOALGEN 2 / DENSITY DNSTYGEN

PROP-DATA DATA1
  IN-UNITS SI
  PROP-LIST DENGEN
  PVAL BIOMASS 1.0

STREAM DH11
  SUBSTREAM MIXED TEMP=55.0 PRES=5.0
  MASS-FLOW H2O 27.77778

STREAM DH13
  SUBSTREAM MIXED TEMP=55.0 PRES=5.0
  MASS-FLOW H2O 138.88889

STREAM DR11
  SUBSTREAM MIXED TEMP=.0 PRES=5.0
  MASS-FLOW H2O 11.68
  SUBSTREAM NC TEMP=.0 PRES=5.0
  MASS-FLOW BIOMASS 11.68
  COMP-ATTR BIOMASS PROXANAL (.0 27.5 65.42 7.08 )
  COMP-ATTR BIOMASS ULTANAL ( 7.08 55.21 5.15 2.12 .0 &

```

```

0.31 30.13 )
COMP-ATTR BIOMASS SULFANAL (.0 .0 .31 )
COMP-ATTR BIOMASS GENANAL ( 100.0 )

STREAM DR19
SUBSTREAM MIXED TEMP=200.0 PRES=5.120 MASS-FLOW=10.0
MASS-FRAC H2O 1.0

DEF-STREAMS WORK W11

BLOCK DRMX1 MIXER
PROPERTIES SYSOP12

BLOCK DRMX2 MIXER
PROPERTIES SYSOP12

BLOCK DRCY2 FSPLIT
FRAC DR15 .20
PROPERTIES SYSOP12

BLOCK DRCY1 FLASH2
PARAM PRES=-.20 VFRAC=.82350
FRAC NC .01
PROPERTIES SYSOP12

BLOCK DRHX1 HEATX
PARAM DEGSUB-HOT=10.0 PRES-COLD=-.120 U-OPTION=CONSTANT
FEEDS HOT=ST11 COLD=DR12
PRODUCTS HOT=CO11 COLD=DR13
HEAT-TR-COEF U=300.0
PROPERTIES STEAM-TA / STEAM-TA

BLOCK DRX2 MHEATX
HOT-SIDE IN=ST12 OUT=CO12 DEGSUB=10.0 FREE-WATER=NO
COLD-SIDE IN=DR17 OUT=DR18 FREE-WATER=NO

BLOCK DRX3 MHEATX
HOT-SIDE IN=DR15 OUT=CO15 TEMP=120.0 FREE-WATER=NO
COLD-SIDE IN=DH13 OUT=DH14 FREE-WATER=NO

BLOCK DRX4 MHEATX
HOT-SIDE IN=CO13 OUT=CO14 TEMP=120.0 FREE-WATER=NO
COLD-SIDE IN=DH11 OUT=DH12 FREE-WATER=NO

BLOCK DRCO COMPR
PARAM TYPE=GPSA-POLYTROP DELP=.440 <BAR>
PROPERTIES SYSOP12

DESIGN-SPEC FLUIDVEL
DEFINE A BLOCK-VAR BLOCK=DRHX1 VARIABLE=CALC-AREA &
SENTENCE=RESULTS
DEFINE MF STREAM-VAR STREAM=DR13 SUBSTREAM=MIXED &
VARIABLE=MOLE-FLOW
DEFINE T STREAM-VAR STREAM=DR13 SUBSTREAM=MIXED &
VARIABLE=TEMP
DEFINE P STREAM-VAR STREAM=DR13 SUBSTREAM=MIXED &
VARIABLE=PRES
SPEC &
"(MF*(22.4136*(273+T)/(273*P)))/(A/(3.1416*.0424*4.5)*.08*.08)" &
TO "1.6*P*(-.487)"
TOL-SPEC ".05"
VARY STREAM-VAR STREAM=DR19 SUBSTREAM=MIXED &
VARIABLE=MASS-FLOW
LIMITS "8" "50"

FORTRAN RECYCLE
DEFINE VIN STREAM-VAR STREAM=DR11 SUBSTREAM=MIXED &
VARIABLE=MASS-FLOW
DEFINE VOUT STREAM-VAR STREAM=DR20 SUBSTREAM=MIXED &
VARIABLE=MASS-FLOW
DEFINE V STREAM-VAR STREAM=DR14 SUBSTREAM=MIXED &
VARIABLE=MASS-FLOW

```

```
DEFINE FR BLOCK-VAR BLOCK=DRCY2 SENTENCE=FRAC VARIABLE=FRAC &  
  ID1=DR15  
F FR=(VIN-VOUT)/V  
EXECUTE BEFORE BLOCK DRCY2  
  
FORTRAN U  
DEFINE U BLOCK-VAR BLOCK=DRHX1 VARIABLE=U &  
  SENTENCE=HEAT-TR-COEF  
DEFINE P STREAM-VAR STREAM=DR12 SUBSTREAM=MIXED &  
  VARIABLE=PRES  
F U=103.1*(P-0.12)**0.15  
READ-VARS P  
WRITE-VARS U  
  
CONV-OPTIONS  
PARAM CHECKSEQ=NO  
;
```

AspenPlus input file for a Rankine cycle power plant

```

;
;Input Summary created by ASPEN PLUS Rel. 9.3-1 at 23:55:37 Fri Jan 16, 1998
;Directory C:\ASPEN Filename input.001
;
TITLE conventional boiler
IN-UNITS SI PRESSURE=BAR TEMPERATURE=C PDROP='N/SQM'
DEF-STREAMS MIXCINC ALL
SIM-OPTIONS
  IN-UNITS SI MASS-FLOW='KG/HR' PRESSURE=BAR TEMPERATURE=C &
  PDROP='N/SQM'
  SIM-OPTIONS MW-CALC=NO
RUN-CONTROL MAX-TIME=2000
DATABANKS ASPENPCD / PURE856 / COMBUST / SOLIDS / &
  AQUEOUS / PURECOMP / INORGANIC
PROP-SOURCES ASPENPCD / PURE856 / COMBUST / SOLIDS / &
  AQUEOUS / PURECOMP / INORGANIC
COMPONENTS
  H2 H2 H2 /
  CO CO CO /
  CO2 CO2 CO2 /
  CH4 CH4 CH4 /
  H2S H2S H2S /
  N2 N2 N2 /
  AR AR AR /
  O2 O2 O2 /
  NH3 H3N NH3 /
  H2O H2O H2O /
  SO2 O2S SO2 /
  N2O N2O N2O /
  NO2 NO2 NO2 /
  C6H6 C6H6 C6H6 /
  C2H4 C2H4 C2H4 /
  C2H6 C2H6 C2H6 /
  C C C /
  BIOMASS * BIOMASS /
  S S S /
  FLYASH * FLYASH /
  COS COS COS /
  AIR AIR AIR /
  ASH * ASH /
  OIL * OIL
HENRY-COMPS ALL H2 CO CH4 N2 CO2 NH3
HENRY-COMPS H1 CO CO2 H2 N2 O2
FLOWSHEET BOILER
  BLOCK COMB IN=FUEL AIRCOMB OUT=FLUEGAS Q10
  BLOCK COMB-2 IN=472 495 H2O 483 OUT=ADT QCOMB
  BLOCK CLCH IN=535 OUT=475
  BLOCK B10 IN=KA 504 OUT=472 SPLELEM
  BLOCK B11 IN=ADT OUT=476 TUHKAT QSYKL
  BLOCK B5 IN=SPLELEM OUT=483
  BLOCK B8 IN=QCOMB QSYKL QSENS QCONDFLU QASH 492 GSARMO2 &
    540 OUT=HAVIO
  BLOCK B14 IN=TUHKAT OUT=493 QASH
  BLOCK B15 IN=COMBAIR OUT=495 WBLow
  BLOCK B17 IN=499 OUT=500 501
  BLOCK B18 IN=475 OUT=KA H2O 504
DEF-STREAMS MIXCINC BOILER
FLOWSHEET DEA
  BLOCK DEHE1 IN=DE11 ST110 CO110 CO1111 OUT=DE12 Q110
  BLOCK DEFS1 IN=DE12 OUT=DE14 DE13
  BLOCK DEFS2 IN=DE13 OUT=DE15 DE16
  BLOCK DEPU1 IN=DE15 OUT=DE17 W110
  BLOCK DEMX IN=DE111 DE112 OUT=DE11
DEF-STREAMS CONVEN DEA
FLOWSHEET
  BLOCK B7 IN=QLOSS OUT=540
FLOWSHEET HRSG
  BLOCK HRX1 IN=HR24 469 OUT=HR12 HR25

```

BLOCK HRX2 IN=HR12 HR23 OUT=HR13 HR24
 BLOCK HRX3 IN=HR13 HR18 OUT=HR14 HR19
 BLOCK HRFS IN=HR19 OUT=HR23 471
 BLOCK DUMMY IN=D1 OUT=D2 D3 QD
 BLOCK DRDUM IN=DRDUM1 OUT=DRDUM2 QDRDUM
 BLOCK B4 IN=481 OUT=469
 BLOCK B9 IN=HR15 OUT=SAVUK HOYRY 492
 BLOCK B12 IN=SAVUK OUT=489 QSENS
 BLOCK B13 IN=HOYRY OUT=488 QCONDFLU
 BLOCK B20 IN=HR14 OUT=HR15 GSARMO2
 BLOCK 2PDUMMY IN=2PD1 OUT=2PD2 2PD3 2PQD
 BLOCK DUMMY2 IN=D21 OUT=D22 D23 QD2

DEF-STREAMS CONVEN HRSG

FLOWSHEET ST

BLOCK STCO1 IN=HR25B OUT=ST65 W61
 BLOCK STCO3 IN=ST65 OUT=ST66 W63
 BLOCK STPU IN=CO61 OUT=CO110 W64
 BLOCK WTOT IN=W61 W63 OUT=W60
 BLOCK B3 IN=ST66 OUT=CO61 QDH
 BLOCK DST3 IN=ST3IN OUT=ST3OUT WD3
 BLOCK DST1 IN=ST1IN OUT=ST1OUT WD1
 BLOCK B23 IN=ST3OUT OUT=ST3OUT2 633
 BLOCK STFS0 IN=HR25 OUT=HR25B HRDEA0
 BLOCK B24 IN=HRDEA0 OUT=HRDEA

DEF-STREAMS CONVEN ST

PROPERTIES RK-SOAVE FREE-WATER=STEAMNBS
 PROPERTIES STEAMNBS DEA FREE-WATER=STEAMNBS / STEAMNBS ST &
 FREE-WATER=STEAMNBS / STEAMNBS HRSG FREE-WATER=STEAMNBS &
 / STEAMNBS DR FREE-WATER=STEAMNBS
 PROPERTIES IDEAL / SYSOP3 / SYSOP12 / UNIFAC / WILS-RK

PROP-REPLACE SYSOP3 RKS-BM

PROP MUVMX MUVMX02
 PROP MULMX MULMX02
 PROP KVMX KVMX02
 PROP KLMX KLMX01
 PROP DV DV01
 PROP MUL MUL01
 PROP MUV MUV01
 PROP KV KV01
 PROP KL KL01
 TABPOLY-MODE HV / GV

PROP-REPLACE SYSOP12 STEAM-TA

NC-COMPS BIOMASS PROXANAL ULTANAL SULFANAL GENANAL
 NC-PROPS BIOMASS ENTHALPY HCOALGEN 6 / DENSITY DNSTYGEN
 NC-COMPS FLYASH PROXANAL ULTANAL SULFANAL GENANAL
 NC-PROPS FLYASH ENTHALPY HCOALGEN 6 / DENSITY DNSTYGEN
 NC-COMPS ASH PROXANAL ULTANAL SULFANAL GENANAL
 NC-PROPS ASH ENTHALPY HCOALGEN 2 / DENSITY DNSTYGEN
 NC-COMPS OIL PROXANAL ULTANAL SULFANAL GENANAL
 NC-PROPS OIL ENTHALPY HCOALGEN 6 / DENSITY DNSTYGEN

USER-PROPS DRUSR2 1 2 3

STRUCTURES

UNIFAC H2O 1300 1

ESTIMATE ALL

PROP-DATA DATA1

IN-UNITS SI
 PROP-LIST DENGEN
 PVAL ASH 1.0
 PVAL OIL 1

PROP-DATA DATA2

IN-UNITS SI PRESSURE=BAR TEMPERATURE=C PDROP='N/SQM'
 PROP-LIST HCOMB
 PVAL OIL 4.45E7

PROP-DATA DENGEN

IN-UNITS SI TEMPERATURE=C
 PROP-LIST DENGEN
 PVAL BIOMASS 1.0

PVAL FLYASH 1.0

PROP-DATA HHV
 IN-UNITS SI PRESSURE=BAR TEMPERATURE=C PDROP='N/SQM'
 PROP-LIST HCOMB
 PVAL BIOMASS 2.022E+7
 PVAL FLYASH 9.6E+6

PROP-SET LHV QVALNET UNITS='KJ/KG' SUBSTREAM=MIXED

PROP-SET LHV GAS
 IN-UNITS SI MASS-FLOW='KG/HR' PRESSURE=BAR TEMPERATURE=C &
 PDROP='N/SQM'
 PROPNAME-LIS QVALNET UNITS='KJ/KG' SUBSTREAM=MIXED

STREAM 2-IN1
 IN-UNITS SI MASS-FLOW='KG/HR' PRESSURE=BAR TEMPERATURE=C &
 PDROP='N/SQM'
 SUBSTREAM MIXED TEMP=800 PRES=1 MASS-FLOW=1 <KG/SEC>
 MOLE-FRAC H2 .1 / CO .1 / CO2 .15 / CH4 .05 / N2 &
 .44 / H2O .15

STREAM 2PD1
 IN-UNITS SI MASS-FLOW='KG/HR' PRESSURE=BAR TEMPERATURE=C &
 PDROP='N/SQM'
 SUBSTREAM MIXED TEMP=105 PRES=3 MOLE-FLOW=100.0 <KMOL/HR>
 MOLE-FRAC H2O 1.0

STREAM 489-2
 SUBSTREAM MIXED TEMP=15 PRES=1 MASS-FLOW=.2
 MOLE-FRAC H2O 1

STREAM 499
 SUBSTREAM MIXED TEMP=1000 PRES=1 MASS-FLOW=1
 MOLE-FRAC CO2 .1 / N2 .75 / O2 .05 / H2O .1

STREAM ADT
 SUBSTREAM MIXED TEMP=1000 PRES=120 MASS-FLOW=.0005
 MOLE-FRAC H2 .1 / CO .15 / CO2 .2 / CH4 .05 / N2 &
 .4 / H2O .1

STREAM AIRCOMB
 IN-UNITS SI MASS-FLOW='KG/HR' PRESSURE=BAR TEMPERATURE=C &
 PDROP='N/SQM'
 SUBSTREAM MIXED TEMP=15 PRES=1 MASS-FLOW=30 <KG/SEC>
 MOLE-FRAC N2 .79 / O2 .21

STREAM CO1111
 IN-UNITS SI MASS-FLOW='KG/HR' PRESSURE=BAR TEMPERATURE=C &
 PDROP='N/SQM'
 SUBSTREAM MIXED TEMP=120 PRES=5 MASS-FLOW=.000001 <KG/SEC>
 MASS-FRAC H2O 1

STREAM COMBAIR
 SUBSTREAM MIXED TEMP=15 PRES=1 MASS-FLOW=2.4
 MOLE-FRAC N2 .79 / O2 .21

STREAM D1
 IN-UNITS SI MASS-FLOW='KG/HR' PRESSURE=BAR TEMPERATURE=C &
 PDROP='N/SQM'
 SUBSTREAM MIXED TEMP=120.0 PRES=100 MOLE-FLOW=100.0 <KMOL/HR>
 MOLE-FRAC H2O 1.0

STREAM D21
 IN-UNITS SI MASS-FLOW='KG/HR' PRESSURE=BAR TEMPERATURE=C &
 PDROP='N/SQM'
 SUBSTREAM MIXED TEMP=200 PRES=20 MOLE-FLOW=100 <KMOL/HR>
 MOLE-FRAC H2O 1

STREAM DE15
 SUBSTREAM MIXED TEMP=100 PRES=5 MASS-FLOW=2
 MOLE-FRAC H2O 1

STREAM DE111
 IN-UNITS SI MASS-FLOW='KG/HR' PRESSURE=BAR TEMPERATURE=C &
 PDROP='N/SQM'
 SUBSTREAM MIXED TEMP=15 PRES=5.0 MASS-FLOW=.000001 <KG/SEC>
 MASS-FRAC H2O 1.0

STREAM DE112
 IN-UNITS SI MASS-FLOW='KG/HR' PRESSURE=BAR TEMPERATURE=C &
 PDROP='N/SQM'
 SUBSTREAM MIXED TEMP=120 PRES=5.0 MASS-FLOW=.6 <KG/SEC>
 MASS-FRAC H2O 1.0

STREAM DR11
 IN-UNITS SI MASS-FLOW='KG/HR' PRESSURE=BAR TEMPERATURE=C &

PDROP='N/SQM'
 SUBSTREAM MIXED TEMP=15.0 PRES=1
 MASS-FLOW H2O .266667 <KG/SEC>
 SUBSTREAM NC TEMP=15.0 PRES=1
 MASS-FLOW BIOMASS .4 <KG/SEC>
 COMP-ATTR BIOMASS PROXANAL (0 59.5 40 .5)
 COMP-ATTR BIOMASS ULTANAL (.5 50 6 1 0 0 42.5)
 COMP-ATTR BIOMASS SULFANAL (0 0 0)
 COMP-ATTR BIOMASS GENANAL (100.0 0 0 0 0 0 0 0 0 0 &
 0 0 0 0 0 0 0 0 0)

STREAM DRDUM1
 IN-UNITS SI MASS-FLOW='KG/HR' PRESSURE=BAR TEMPERATURE=C &
 PDROP='N/SQM'
 SUBSTREAM MIXED TEMP=254 PRES=1.05 MASS-FLOW=145 <KG/SEC> &
 NPHASE=1
 MOLE-FRAC CO2 .0725 / N2 .7275 / AR .008 / O2 .1205 / &
 H2O .0715

STREAM FEED
 SUBSTREAM MIXED TEMP=15 PRES=1
 MASS-FLOW H2O .212
 SUBSTREAM NC TEMP=15 PRES=1
 MASS-FLOW BIOMASS .318
 COMP-ATTR BIOMASS PROXANAL (0 30 69.5 .5)
 COMP-ATTR BIOMASS ULTANAL (.5 50 6 1 0 0 42.5)
 COMP-ATTR BIOMASS SULFANAL (0 0 0)
 COMP-ATTR BIOMASS GENANAL (100 0 0 0 0 0 0 0 0 0 &
 0 0 0 0 0 0 0 0 0)

STREAM FUEL
 IN-UNITS SI MASS-FLOW='KG/HR' PRESSURE=BAR TEMPERATURE=C &
 PDROP='N/SQM'
 SUBSTREAM MIXED TEMP=15 PRES=1
 MOLE-FLOW CO 1

STREAM GASAIR
 IN-UNITS SI MASS-FLOW='KG/HR' PRESSURE=BAR TEMPERATURE=C &
 PDROP='N/SQM'
 SUBSTREAM MIXED TEMP=15 PRES=1 MASS-FLOW=.5 <KG/SEC>
 MOLE-FRAC N2 .79 / O2 .21

STREAM HR18
 SUBSTREAM MIXED TEMP=120 PRES=100 MASS-FLOW=2.5
 MASS-FRAC H2O 1.0

STREAM IN1
 IN-UNITS SI MASS-FLOW='KG/HR' PRESSURE=BAR TEMPERATURE=C &
 PDROP='N/SQM'
 SUBSTREAM MIXED TEMP=800 PRES=1 MASS-FLOW=1 <KG/SEC>
 MOLE-FRAC H2 .1 / CO .1 / CO2 .15 / CH4 .05 / N2 &
 .44 / H2O .15

STREAM ST1IN
 SUBSTREAM MIXED TEMP=100 PRES=10 MASS-FLOW=1
 MOLE-FRAC H2O 1

STREAM ST3IN
 SUBSTREAM MIXED TEMP=100 PRES=10 MASS-FLOW=1
 MOLE-FRAC H2O 1

STREAM ST110
 IN-UNITS SI MASS-FLOW='KG/HR' PRESSURE=BAR TEMPERATURE=C &
 PDROP='N/SQM'
 SUBSTREAM MIXED TEMP=190.0 PRES=5.0 &
 MASS-FLOW=1.000E-05 <KG/SEC>
 MASS-FRAC H2O 1.0

BLOCK B22 MIXER
 PROPERTIES RK-SOAVE
 BLOCK-OPTION SIM-LEVEL=4 PROP-LEVEL=4 STREAM-LEVEL=4

BLOCK DEMX MIXER
 IN-UNITS SI MASS-FLOW='KG/HR' PRESSURE=BAR TEMPERATURE=C &
 PDROP='N/SQM'
 PARAM PRES=0
 PROPERTIES SYSOP12

BLOCK MIX1 MIXER
 IN-UNITS SI MASS-FLOW='KG/HR' PRESSURE=BAR TEMPERATURE=C &
 PDROP='N/SQM'

BLOCK RAWGAS MIXER
 IN-UNITS SI MASS-FLOW='KG/HR' PRESSURE=BAR TEMPERATURE=C &
 PDROP='N/SQM'
 PARAM PRES=0 NPHASE=1

BLOCK WTOT MIXER
 IN-UNITS SI MASS-FLOW='KG/HR' PRESSURE=BAR TEMPERATURE=C &
 PDROP='N/SQM'

BLOCK DEFS1 FSPLIT
 IN-UNITS SI MASS-FLOW='KG/HR' PRESSURE=BAR TEMPERATURE=C &
 PDROP='N/SQM'
 FRAC DE14 .000000001

BLOCK DEFS2 FSPLIT
 IN-UNITS SI MASS-FLOW='KG/HR' PRESSURE=BAR TEMPERATURE=C &
 PDROP='N/SQM'
 FRAC DE16 .000000001

BLOCK FEEDMOIS FSPLIT
 FRAC WATGIBB .15

BLOCK HRFS FSPLIT
 IN-UNITS SI MASS-FLOW='KG/HR' PRESSURE=BAR TEMPERATURE=C &
 PDROP='N/SQM'
 FRAC 471 .000000001
 PROPERTIES SYSOP12

BLOCK STFS0 FSPLIT
 FRAC HRDEA0 .05

BLOCK SULJEPUU FSPLIT
 FRAC WOODCOMB .000000001

BLOCK SULJKAAS FSPLIT
 FRAC POLTTOON .999999999

BLOCK B9 SEP
 PARAM
 FRAC STREAM=SAVUK SUBSTREAM=MIXED COMPS=H2 CO CO2 CH4 &
 H2S N2 AR O2 NH3 H2O SO2 N2O NO2 C6H6 C2H4 C2H6 &
 COS C2H2 C10H8 C6H6O AIR FRACS=1 1 1 1 1 1 1 1 &
 1 0 1 1 1 1 1 1 1 1 1 1 1 1 1 1

BLOCK B11 SEP
 PARAM
 FRAC STREAM=TUHKAT SUBSTREAM=MIXED COMPS=H2 CO CO2 CH4 &
 H2S N2 AR O2 NH3 H2O SO2 N2O NO2 C6H6 C2H4 C2H6 &
 COS C2H2 C10H8 C6H6O AIR FRACS=0 0 0 0 0 0 0 0 &
 0 0 0 0 0 0 0 0 0 0 0 0 0 0 0 0
 FRAC STREAM=TUHKAT SUBSTREAM=CISOLID COMPS=C S FRACS=1 &
 1
 FRAC STREAM=TUHKAT SUBSTREAM=NC COMPS=BIOMASS FLYASH &
 FRACS=1 1

BLOCK B18 SEP
 PARAM
 FRAC STREAM=KA SUBSTREAM=MIXED COMPS=H2 CO CO2 CH4 H2S &
 N2 AR O2 NH3 H2O SO2 N2O NO2 C6H6 C2H4 C2H6 COS &
 C2H2 C10H8 C6H6O AIR FRACS=0 0 0 0 0 0 0 0 0 0 &
 0 0 0 0 0 0 0 0 0 0 0 0 0 0 0 0
 FRAC STREAM=KA SUBSTREAM=CISOLID COMPS=C S FRACS=1 1
 FRAC STREAM=KA SUBSTREAM=NC COMPS=BIOMASS FLYASH FRACS=1 &
 1

BLOCK CCON SEP
 IN-UNITS SI MASS-FLOW='KG/HR' PRESSURE=BAR TEMPERATURE=C &
 PDROP='N/SQM'
 PARAM
 FRAC STREAM=LOSS SUBSTREAM=MIXED COMPS=H2 CO CO2 CH4 N2 &
 O2 NH3 H2O C6H6 C2H4 C2H6 C10H8 C6H6O FRACS=0 0 0 &
 0 0 0 0 0 0 0 0 0 0
 FRAC STREAM=LOSS SUBSTREAM=CISOLID COMPS=C FRACS=.005
 FRAC STREAM=LOSS SUBSTREAM=NC COMPS=BIOMASS FLYASH FRACS=&
 0 0
 PROPERTIES SYSOP3

BLOCK DSWAT SEP
 IN-UNITS SI MASS-FLOW='KG/HR' PRESSURE=BAR TEMPERATURE=C &
 PDROP='N/SQM'
 PARAM
 FRAC STREAM=WATER SUBSTREAM=MIXED COMPS=H2 CO CO2 CH4 &
 N2 O2 NH3 H2O C6H6 C2H4 C2H6 C10H8 C6H6O FRACS=0 0 &
 0 0 0 0 0 1 0 0 0 0 0
 FRAC STREAM=WATER SUBSTREAM=CISOLID COMPS=C FRACS=0
 FRAC STREAM=WATER SUBSTREAM=NC COMPS=BIOMASS FLYASH &
 FRACS=0 0
 PROPERTIES SYSOP0

BLOCK HYCASEP SEP
 IN-UNITS SI MASS-FLOW='KG/HR' PRESSURE=BAR TEMPERATURE=C &
 PDROP='N/SQM'

PARAM
 FRAC STREAM=HYCA SUBSTREAM=MIXED COMPS=H2 CO CO2 CH4 N2 &
 O2 NH3 H2O C6H6 C2H4 C2H6 C10H8 C6H6O FRACS=0 0 0 &
 1 0 0 1 0 1 1 0 0 1
 FRAC STREAM=HYCA SUBSTREAM=CISOLID COMPS=C FRACS=0
 FRAC STREAM=HYCA SUBSTREAM=NC COMPS=BIOMASS FLYASH FRACS= &
 0 0
 PROPERTIES SYSOP3

BLOCK A3 HEATER
 PARAM TEMP=15 PRES=0
 PROPERTIES STEAMNBS

BLOCK B3 HEATER
 PARAM PRES=0 VFRAC=0 NPHASE=2
 PROPERTIES STEAMNBS

BLOCK B12 HEATER
 PARAM TEMP=15 PRES=0

BLOCK B13 HEATER
 PARAM TEMP=15 PRES=0
 PROPERTIES STEAMNBS

BLOCK B14 HEATER
 PARAM TEMP=15 PRES=0
 PROPERTIES IDEAL

BLOCK B17 HEATER
 PARAM TEMP=15 PRES=0

BLOCK B20 HEATER
 PARAM PRES=0 DUTY=1

BLOCK B23 HEATER
 PARAM PRES=1 VFRAC=1

BLOCK DEHE1 HEATER
 IN-UNITS SI MASS-FLOW='KG/HR' PRESSURE=BAR TEMPERATURE=C &
 PDROP='N/SQM'
 PARAM TEMP=105 VFRAC=.0

BLOCK DRDUM HEATER
 IN-UNITS SI MASS-FLOW='KG/HR' PRESSURE=BAR TEMPERATURE=C &
 PDROP='N/SQM'
 PARAM PRES=0 DUTY=0 NPHASE=1
 PROPERTIES SYSOP3

BLOCK TERVAT HEATER
 PARAM TEMP=825 PRES=0 NPHASE=1

BLOCK 2PDUMMY FLASH2
 IN-UNITS SI MASS-FLOW='KG/HR' PRESSURE=BAR TEMPERATURE=C &
 PDROP='N/SQM'
 PARAM PRES=3 VFRAC=1.0
 PROPERTIES SYSOP12

BLOCK AIRMOIST FLASH2
 PARAM TEMP=60 PRES=0

BLOCK DUMMY FLASH2
 PARAM PRES=20 VFRAC=1.0
 PROPERTIES SYSOP12

BLOCK DUMMY2 FLASH2
 IN-UNITS SI MASS-FLOW='KG/HR' PRESSURE=BAR TEMPERATURE=C &
 PDROP='N/SQM'
 PARAM PRES=20 VFRAC=1
 PROPERTIES SYSOP12

BLOCK HRX1 MHEATX
 COLD-SIDE IN=HR24 OUT=HR25 TEMP=460 NPHASE=1 FREE-WATER=NO
 HOT-SIDE IN=469 OUT=HR12 FREE-WATER=NO
 STREAM-PROPE HR24 RK-SOAVE FREE-WATER=STEAMNBS

BLOCK HRX2 MHEATX
 HOT-SIDE IN=HR12 OUT=HR13 FREE-WATER=NO
 COLD-SIDE IN=HR23 OUT=HR24 VFRAC=1 NPHASE=2 FREE-WATER=NO
 PARAM NPOINT=5
 STREAM-PROPE HR12 RK-SOAVE FREE-WATER=STEAMNBS
 STREAM-PROPE HR23 STEAMNBS FREE-WATER=STEAMNBS

BLOCK HRX3 MHEATX
 HOT-SIDE IN=HR13 OUT=HR14 FREE-WATER=NO
 COLD-SIDE IN=HR18 OUT=HR19 TEMP=306 FREE-WATER=NO
 PARAM NPOINT=5
 STREAM-PROPE HR13 RK-SOAVE FREE-WATER=STEAMNBS

STREAM-PROPE HR18 STEAMNBS FREE-WATER=STEAMNBS
 BLOCK COMB RSTOIC
 IN-UNITS SI MASS-FLOW='KG/HR' PRESSURE=BAR TEMPERATURE=C &
 PDROP='N/SQM'
 PARAM TEMP=800 PRES=0 NPHASE=1
 STOIC 1 MIXED C -1 / O2 -1 / CO2 1
 STOIC 2 MIXED H2 -1 / O2 -.5 / H2O 1
 CONV 1 MIXED C 1
 CONV 2 MIXED H2 1
 PROPERTIES SYSOP3

 BLOCK B10 RYIELD
 PARAM TEMP=15 PRES=0
 MASS-YIELD MIXED H2 .06 / N2 .01 / O2 .425 / CISOLID &
 C .5 / NC FLYASH .005
 PROPERTIES IDEAL
 COMP-ATTR NC FLYASH PROXANAL (0 75 5 20)
 COMP-ATTR NC FLYASH ULTANAL (20 70 0 5 0 0 5)
 COMP-ATTR NC FLYASH SULFANAL (0 0 0)
 COMP-ATTR NC FLYASH GENANAL (100 0 0 0 0 0 0 0 0 &
 0 0 0 0 0 0 0 0 0 0)

 BLOCK ELEM RYIELD
 PARAM TEMP=15 PRES=0 NPHASE=1
 MASS-YIELD CISOLID C .5 / MIXED H2 .06 / N2 .01 / O2 &
 .425 / NC FLYASH .005
 PROPERTIES SYSOP3
 COMP-ATTR NC FLYASH GENANAL (100 0 0 0 0 0 0 0 0 &
 0 0 0 0 0 0 0 0 0 0)
 COMP-ATTR NC FLYASH PROXANAL (0 40 10 50)
 COMP-ATTR NC FLYASH ULTANAL (50 40 0 0 0 0 10)
 COMP-ATTR NC FLYASH SULFANAL (0 0 0)

 BLOCK DEPU1 PUMP
 PARAM PRES=50

 BLOCK STPU PUMP
 IN-UNITS SI MASS-FLOW='KG/HR' PRESSURE=BAR TEMPERATURE=C &
 PDROP='N/SQM'
 PARAM PRES=3.0
 PROPERTIES SYSOP12
 BLOCK-OPTION FREE-WATER=NO

 BLOCK B15 COMPR
 PARAM TYPE=ISENTROPIC PRES=1.2

 BLOCK B16 COMPR
 PARAM TYPE=ISENTROPIC DELP=.2 <BAR>

 BLOCK DST1 COMPR
 PARAM TYPE=ISENTROPIC PRES=25 SEFF=.8

 BLOCK DST3 COMPR
 PARAM TYPE=ISENTROPIC PRES=0.04 SEFF=.8 NPHASE=2

 BLOCK STCO1 COMPR
 IN-UNITS SI MASS-FLOW='KG/HR' PRESSURE=BAR TEMPERATURE=C &
 PDROP='N/SQM'
 PARAM TYPE=ISENTROPIC PRES=25.0 SEFF=.8
 PROPERTIES SYSOP12

 BLOCK STCO3.COMPR
 IN-UNITS SI MASS-FLOW='KG/HR' PRESSURE=BAR TEMPERATURE=C &
 PDROP='N/SQM'
 PARAM TYPE=ISENTROPIC PRES=.53 SEFF=.8 NPHASE=2
 PROPERTIES SYSOP12

 BLOCK B2 CLCHNG

 BLOCK B4 CLCHNG

 BLOCK CLCH CLCHNG

 BLOCK CLCH1 CLCHNG

 BLOCK B24 VALVE
 PARAM P-OUT=1.3

 DESIGN-SPEC DEA
 IN-UNITS SI MASS-FLOW='KG/HR' PRESSURE=BAR TEMPERATURE=C &
 PDROP='N/SQM'
 DEFINE QD BLOCK-VAR BLOCK=DEHEI VARIABLE=QCALC &
 SENTENCE=PARAM
 SPEC "QD" TO "0"
 TOL-SPEC "100"
 VARY BLOCK-VAR BLOCK=STFS0 SENTENCE=FRAC VARIABLE=FRAC &

```

ID1=HRDEA0
LIMITS *.01* *.99*

FORTRAN EFF-C
  DEFINE F1 STREAM-VAR STREAM=ST65 SUBSTREAM=MIXED &
    VARIABLE=MASS-FLOW
  DEFINE E3 BLOCK-VAR BLOCK=STCO3 VARIABLE=SEFF &
    SENTENCE=PARAM
  DEFINE XIN STREAM-VAR STREAM=ST65 SUBSTREAM=MIXED &
    VARIABLE=LFRAC
  DEFINE XOUT STREAM-VAR STREAM=ST3OUT SUBSTREAM=MIXED &
    VARIABLE=LFRAC
  DEFINE D1 STREAM-VAR STREAM=ST65 SUBSTREAM=MIXED &
    VARIABLE=MASS-DENSITY
  DEFINE D2 STREAM-VAR STREAM=ST3OUT2 SUBSTREAM=MIXED &
    VARIABLE=MASS-DENSITY
F  FA=F1/D1*60
F  FB=F1/D2*60
F  E3=0.0517*DLOG((FA+FB)/2)+0.515-(XIN+XOUT)/2
  READ-VARS XIN XOUT F1 D1 D2
  WRITE-VARS E3

FORTRAN PBFW-DUM
  DEFINE PDEPU1 BLOCK-VAR BLOCK=DEPU1 VARIABLE=PRES &
    SENTENCE=PARAM
  DEFINE PD1 BLOCK-VAR BLOCK=DUMMY VARIABLE=PRES &
    SENTENCE=PARAM
F  PD1=PDEPU1
  READ-VARS PDEPU1
  WRITE-VARS PD1

TRANSFER ST1
  SET STREAM ST1IN
  EQUAL-TO STREAM HR25B
  EXECUTE BEFORE BLOCK STCO1

TRANSFER ST3
  SET STREAM ST3IN
  EQUAL-TO STREAM ST65
  EXECUTE BEFORE BLOCK STCO3

TRANSFER STDEA
  SET STREAM DE112
  EQUAL-TO STREAM HRDEA

TRANSFER STOIC
  SET STREAM FUEL
  EQUAL-TO STREAM 472

CONV-OPTIONS
  SECANT MAXIT=40

SEQUENCE S-1 ST1 DST1 EFF-A STCO1

SEQUENCE S-3 ST3 DST3 EFF-C STCO3

STREAM-REPOR MOLEFLOW MOLEFRAC NOMASSFRAC PROPERTIES=LHV
PROPERTY-REP NOCOMPS

PROP-TABLE LHV GAS1 PROPS
  IN-UNITS SI MASS-FLOW='KG/HR' PRESSURE=BAR TEMPERATURE=C &
    PDROP='N/SQM'
  STREAM RAWGAS
  VARY TEMP
  RANGE LIST=15
  TABULATE PROPERTIES=LHV GAS
:
:
:
:
:

```

TESTING OF THE DEPARTURE-FROM-EQUILIBRIUM MODEL

An approach reported by Stone /118/ to modelling the gasification of biomass in a fluidized-bed reactor with Aspen is tested. The approach calls for determination of equilibrium reactions for the gas mixture. Departures from equilibrium will be controlled with departure (from equilibrium) temperatures, which may be defined for each reaction separately. A simple model was designed (Figure A4-1), and characteristics of the model were studied.

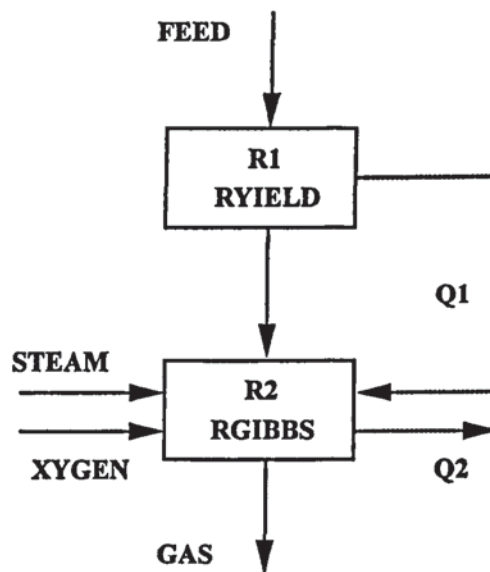


Figure A4-1. Aspen block diagram for a simple gasification model.

The following components of the product gas were considered: H_2 , CO , CO_2 , CH_4 , H_2O , O_2 , N_2 , H_2S , COS , C , NH_3 , C_6H_6 , C_2H_4 , C_2H_6 . As the equilibrium reactions have to be linearly independent, and there were five elements present, a total of nine equilibrium reactions has to be considered. The selected reactions were:





Inputs to the model are mass flows of feed, steam and oxygen, and the composition of the feed. In the model, the feed is first split into its elements in a RYIELD reactor module. In the subsequent RGIBBS reactor module, the mixture of feedstock elements, steam, and oxygen is allowed to reach equilibrium in accordance with the given specifications (pressure, departure-from-equilibrium temperatures for reactions). The RGIBBS is defined as adiabatic, and the model determines the gasification temperature and the gas yield.

The model was tested against data provided by Uhde /1/. The data is based on gasification experiments with peat carried out in a 1 t/h HTW unit in Wachtberg, Germany. This case was chosen as the reference, because the results are based on large-scale tests, the feed resembles biomass (high volatile content), and the experiments were carried out under pressure (a requirement for an IGCC). No industrial data was available to the author concerning the pressure gasification of wood or other biomass.

The selection of departure temperatures for reactions proved laborious. All departure temperatures (except for reaction (A4-2)) had an effect on the gas composition and temperature, and they also changed the amount of other gas components. However, a good agreement was eventually found between the model results and experimental data (Table A4-1). The largest difference is in the gasification temperature. That may be explained by heat losses, which are not taken into account in the simple model. The difference corresponds to an approximately 3% heat loss in the gasifier, which is not far from industrial experience.

Comparison between another study by Uhde /2/ and the Aspen model results is presented in figures A1-1 to 3 for variation of the feed moisture content. These results from Uhde are based on further experiments, which were carried out with the pilot gasifier. Two distinct versions of the model are tested: in one the gasification temperature is kept constant by varying the oxygen feed, and in the other the oxygen feed (and other feeds) is kept constant, and the gas temperature is allowed to vary. Dry gas compositions are compared.

Table A4-1. Comparison between experimental data and the results of a simple Aspen gasification model. Feed 20.5 kg/s (ds.), feed moisture content 15 w-%, steam 5.59 kg/s, oxygen 11.0 kg/s, pressure 15 bar.

Component	Uhde /129/		Aspen		Difference %
	mol%	kmol/h	mol%	kmol/h	
H ₂	29.8	1 985	29.5	1 968	- 0.8
CO	27.3	1 816	27.4	1 828	+ 0.7
CO ₂	18.5	1 229	18.3	1 219	- 0.8
CH ₄	2.2	144	2.1	139	- 3.5
H ₂ O	21.3	1 417	21.5	1 436	+ 1.3
N ₂	0.6	43	0.8	52	+ 23
H ₂ S	0.1	6.7	0.1	6.4	- 4.5
COS	0.01	0.5	0.01	0.7	+ 40
NH ₃	0.13	8.6	0.13	8.4	- 2.3
C ₆ H ₆	0.11	7.1	0.12	7.8	+ 9.9
Product gas kmol/h		6 663		6 664	
Temperature °C		920		1 003	+ 9
Chemical efficiency %		67.3		67.2	- 0.1

Gas yield (CO + H₂) as a function of feed moisture content is shown in Figure A4-1. It may be concluded that the first alternative better describes the system performance. However, gas yields predicted by the model are higher than reported by Uhde. The distribution of major gas components is shown as a function of feed moisture content in Figure A4-2. The variation predicted by the model is not far off, but the predictions of hydrogen and carbon dioxide with the model are too high, whereas that of carbon monoxide is too low. The methane content of the gas and the chemical efficiency are shown in Figure A4-3. The model result for the efficiency is too low, and so is the amount of methane predicted by the model.

As was pointed out earlier, the pyrolysis of biomass causes the error in the amount of methane and other hydrocarbons, when estimated with an equilibrium gasification model. These compounds have high heating values, and consequently they have a considerable effect on model estimates for the chemical efficiency of gasification. It is concluded that the equilibrium model is not quite appropriate for biomass gasification.

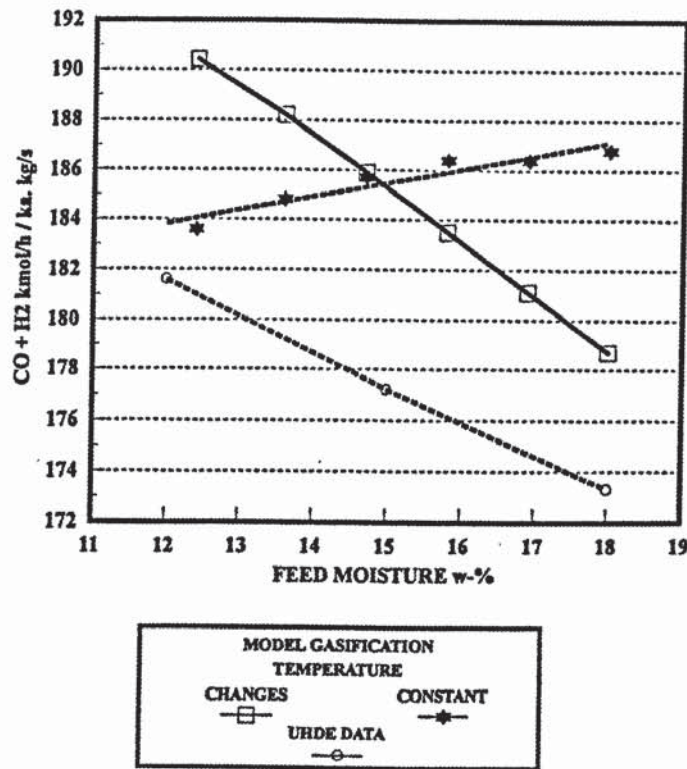


Figure A4-1. Hydrogen and carbon monoxide yield as a function of feed moisture content, comparison of Uhde data with results from two versions of a simple Aspen model.

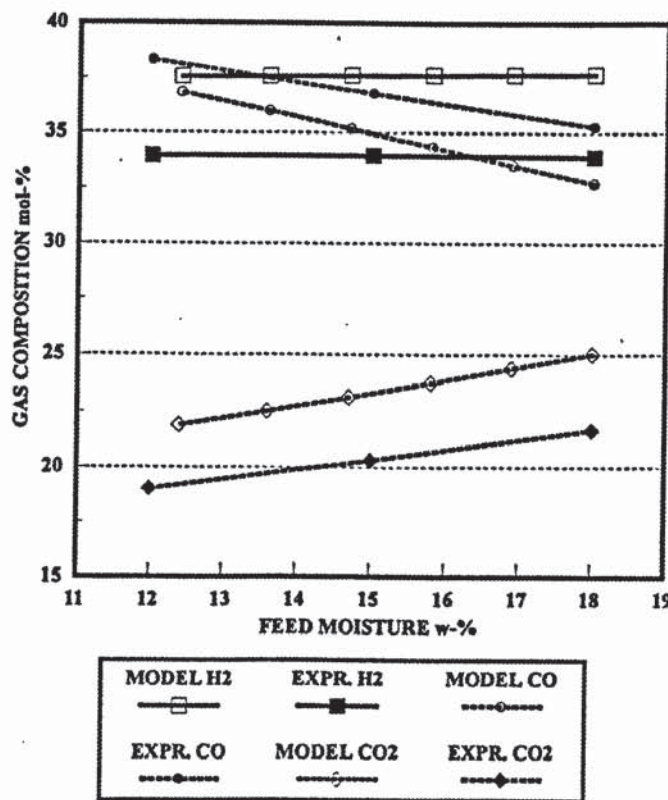


Figure A4-2. Product gas composition as a function of feed moisture content (major components), comparison of Uhde data with results from a simple Aspen model.

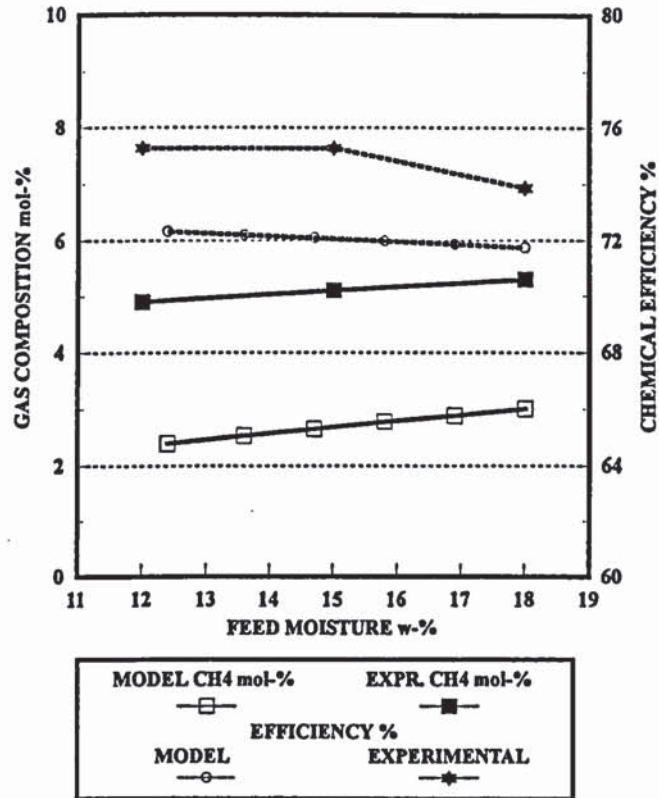


Figure A4-3. Methane content of the product gas and chemical efficiency, comparison of Uhde data with results from a simple Aspen model.

REFERENCES

- 1 A report to Kemira Oy and VTT, Uhde GmbH 1985.
- 2 A report to Kemira Oy, Uhde GmbH 1986.

AspenPlus input file for a gasifier

```

;
;Input Summary created by ASPEN PLUS Rel. 9.3-1 at 15:54:08 Sun Mar 15, 1998
;Directory D:\Y2\KUI Filename D:\Y3\GASIF97\gas.inp
;
TITLE gasification

IN-UNITS SI PRESSURE=BAR TEMPERATURE=C PDROP='N/SQM'

OUT-UNITS SI PRESSURE=BAR TEMPERATURE=C PDROP='N/SQM'

DEF-STREAMS CONVEN ALL

RUN-CONTROL MAX-TIME=1500

DATABANKS ASPENPCD / PURECOMP / COMBUST / SOLIDS / &
  AQUEOUS / INORGANIC

PROP-SOURCES ASPENPCD / PURECOMP / COMBUST / SOLIDS / &
  AQUEOUS / INORGANIC

COMPONENTS
H2 H2 H2 /
CO CO CO /
CO2 CO2 CO2 /
CH4 CH4 CH4 /
H2S H2S H2S /
COS COS COS /
N2 N2 N2 /
AR AR AR /
O2 O2 O2 /
NH3 H3N NH3 /
H2O H2O H2O /
SO2 O2S SO2 /
N2O N2O N2O /
NO2 NO2 NO2 /
C6H6 C6H6 C6H6 /
C2H4 C2H4 C2H4 /
C2H2 C2H2 C2H2 /
C10H8 C10H8 C10H8 /
C2H6 C2H6 C2H6 /
C6H6O C6H6O C6H6O /
BIOMASS * BIOMASS /
ASH * ASH /
C C C /
S S S

FLOWSHEET GAS
BLOCK DRIER IN=DR11 OUT=DR12 GS11 Q1
BLOCK ASHSEP IN=GS14 WATER OUT=ASH C1 Q5
BLOCK ELEM IN=GS13 OUT=GS14 Q3
BLOCK COMB IN=FUEL AIRCOMB OUT=FLUEGAS Q10

DEF-STREAMS MIXCINC GAS

FLOWSHEET MIX
BLOCK INIT IN=IN1 OUT=IN2 QIN

DEF-STREAMS CONVEN MIX

FLOWSHEET NONC
BLOCK B1 IN=C1 OUT=C2
BLOCK CCON IN=C2 OUT=LOSS C3 Q6
BLOCK HYCASEP IN=C4 OUT=HYCA C5 Q8
BLOCK GIBBS IN=C5 AIR Q2 Q3 Q5 Q6 Q8 Q7 OUT=C6 &
  QADIAB
BLOCK RAWGAS IN=C6 HYCA OUT=RAWGAS

DEF-STREAMS MIXCISLD NONC

PROPERTIES RK-SOAVE

```

PROPERTIES SYSOP0

NC-COMPS BIOMASS PROXANAL ULTANAL SULFANAL GENANAL

NC-PROPS BIOMASS ENTHALPY HCOALGEN 6 / DENSITY DNSTYGEN

NC-COMPS ASH PROXANAL ULTANAL SULFANAL GENANAL

NC-PROPS ASH ENTHALPY HCOALGEN 2 / DENSITY DNSTYGEN

PROP-DATA DATA1

IN-UNITS SI TEMPERATURE=C

PROP-LIST DENGEN

PVAL BIOMASS 1.0

PVAL ASH 1.0

PROP-DATA DATA2

IN-UNITS SI PRESSURE=BAR TEMPERATURE=C PDROP=N/SQM

PROP-LIST HCOMB

PVAL BIOMASS 2.022E+7

PVAL ASH 9.6E+7

PROP-DATA RKSKIJ-1

IN-UNITS ENG

PROP-LIST RKSKIJ

BPVAL H2 CO .0804000000

BPVAL H2 CO2 -.3426000000

BPVAL H2 CH4 -.0222000000

BPVAL H2 N2 .0978000000

BPVAL H2 C2H4 -.0681000000

BPVAL H2 C2H6 -.1667000000

BPVAL CO CH4 .0322000000

BPVAL CO N2 .0374000000

BPVAL CO C2H6 -.0278000000

BPVAL CO H2 .0804000000

BPVAL CO H2S .0367000000

BPVAL CO2 CH4 .0933000000

BPVAL CO2 N2 -.0315000000

BPVAL CO2 C2H4 .0533000000

BPVAL CO2 C2H6 .1363000000

BPVAL CO2 H2 -.3426000000

BPVAL CO2 H2S .0989000000

BPVAL CO2 H2O .0737000000

BPVAL CO2 N2O 2.20000000E-3

BPVAL CO2 C6H6 .0767000000

BPVAL CH4 CO .0322000000

BPVAL CH4 CO2 .0933000000

BPVAL CH4 N2 .0278000000

BPVAL CH4 C2H4 .0189000000

BPVAL CH4 C2H6 -7.8000000E-3

BPVAL CH4 H2 -.0222000000

BPVAL CH4 N2O .0211000000

BPVAL CH4 C6H6 .0209000000

BPVAL CH4 COS .0252000000

BPVAL CH4 AR .0252000000

BPVAL CH4 SO2 .1279000000

BPVAL H2S CO .0367000000

BPVAL H2S CO2 .0989000000

BPVAL H2S N2 .1696000000

BPVAL H2S C2H6 .0852000000

BPVAL H2S H2O .0100000000

BPVAL COS CH4 .0252000000

BPVAL N2 CO .0374000000

BPVAL N2 CO2 -.0315000000

BPVAL N2 CH4 .0278000000

BPVAL N2 C2H4 .0798000000

BPVAL N2 C2H6 .0407000000

BPVAL N2 H2 .0978000000

BPVAL N2 H2S .1696000000

BPVAL N2 N2O -.0110000000

BPVAL N2 C6H6 .1530000000

BPVAL N2 AR 0.0

BPVAL N2 SO2 .0578000000
 BPVAL N2 O2 -7.8000000E-3
 BPVAL N2 NH3 .2222000000
 BPVAL AR CH4 .0252000000
 BPVAL AR N2 0.0
 BPVAL AR O2 .0178000000
 BPVAL AR NH3 -.2200000000
 BPVAL O2 N2 -7.8000000E-3
 BPVAL O2 N2O .0433000000
 BPVAL O2 AR .0178000000
 BPVAL NH3 N2 .2222000000
 BPVAL NH3 H2O -.2800000000
 BPVAL NH3 AR -.2200000000
 BPVAL H2O CO2 .0737000000
 BPVAL H2O H2S .0100000000
 BPVAL H2O NH3 -.2800000000
 BPVAL SO2 CH4 .1279000000
 BPVAL SO2 N2 .0578000000
 BPVAL SO2 C6H6 9.30000000E-3
 BPVAL N2O CO2 2.20000000E-3
 BPVAL N2O CH4 .0211000000
 BPVAL N2O N2 -.0110000000
 BPVAL N2O O2 .0433000000
 BPVAL C6H6 CO2 .0767000000
 BPVAL C6H6 CH4 .0209000000
 BPVAL C6H6 N2 .1530000000
 BPVAL C6H6 C2H4 .0241000000
 BPVAL C6H6 C2H6 .0289000000
 BPVAL C6H6 SO2 9.30000000E-3
 BPVAL C2H4 CO2 .0533000000
 BPVAL C2H4 CH4 .0189000000
 BPVAL C2H4 N2 .0798000000
 BPVAL C2H4 C2H6 8.90000000E-3
 BPVAL C2H4 H2 -.0681000000
 BPVAL C2H4 C6H6 .0241000000
 BPVAL C2H4 C2H2 .0596000000
 BPVAL C2H2 C2H4 .0596000000
 BPVAL C2H6 CO -.0278000000
 BPVAL C2H6 CO2 .1363000000
 BPVAL C2H6 CH4 -7.8000000E-3
 BPVAL C2H6 N2 .0407000000
 BPVAL C2H6 C2H4 8.90000000E-3
 BPVAL C2H6 H2 -.1667000000
 BPVAL C2H6 H2S .0852000000
 BPVAL C2H6 C6H6 .0289000000

PROP-SET LHVCIS QVALNET UNITS='KJ/KG' SUBSTREAM=CISOLID

PROP-SET LHVGAS QVALNET UNITS='KJ/KG' SUBSTREAM=MIXED

PROP-SET LHVMIX QVALNET UNITS='KJ/KG' SUBSTREAM=MIXED

STREAM AIR

SUBSTREAM MIXED TEMP=15 PRES=1 MASS-FLOW=7.2
MOLE-FRAC N2 .79 / O2 .21

STREAM AIRCOMB

SUBSTREAM MIXED TEMP=15 PRES=1 MASS-FLOW=30
MOLE-FRAC N2 .79 / O2 .21

STREAM DR11

SUBSTREAM MIXED TEMP=15 PRES=1
MASS-FLOW H2O 4.1274
SUBSTREAM NC TEMP=15 PRES=1
MASS-FLOW BIOMASS 4.1274
COMP-ATTR BIOMASS PROXANAL (.0 25 74.5 .5)
COMP-ATTR BIOMASS ULTANAL (.5 50.4 5.97 .1 0 0 43.03 &
)
COMP-ATTR BIOMASS SULFANAL (.0 .0 0)
COMP-ATTR BIOMASS GENANAL (100 0 0 0 0 0 0 0 0 0)

STREAM FUEL

SUBSTREAM MIXED TEMP=15 PRES=1
 SUBSTREAM CISOLID TEMP=15 PRES=1 MASS-FLOW=1
 MASS-FLOW C 1

DEF-STREAMS HEAT Q1

DEF-STREAMS HEAT Q2

DEF-STREAMS HEAT Q3

DEF-STREAMS HEAT Q5

DEF-STREAMS HEAT Q6

DEF-STREAMS HEAT Q7

DEF-STREAMS HEAT Q8

DEF-STREAMS HEAT Q10

DEF-STREAMS HEAT QADIAB

DEF-STREAMS HEAT QIN

BLOCK RAWGAS MIXER
 PARAM PRES=0 NPHASE=1

BLOCK ASHSEP SEP
 PARAM PRES=0 NPHASE=1
 FRAC STREAM=ASH SUBSTREAM=MIXED COMPS=H2 CO CO2 CH4 H2S &
 COS N2 AR O2 NH3 H2O SO2 N2O NO2 C6H6 C2H4 C2H2 &
 C10H8 C2H6 C6H6O FRACS=0 0 0 0 0 0 0 0 0 0 0 &
 0 0 0 0 0 0 0 0
 FRAC STREAM=ASH SUBSTREAM=CISOLID COMPS=C FRACS=0
 FRAC STREAM=ASH SUBSTREAM=NC COMPS=BIOMASS ASH FRACS=0 &
 1
 PROPERTIES SYSOP0

BLOCK CCON SEP
 FRAC STREAM=LOSS SUBSTREAM=MIXED COMPS=H2 CO CO2 CH4 &
 H2S COS N2 AR O2 NH3 H2O SO2 N2O NO2 C6H6 C2H4 &
 C2H2 C10H8 C2H6 C6H6O FRACS=0 0 0 0 0 0 0 0 0 0 &
 0 0 0 0 0 0 0 0
 FRAC STREAM=LOSS SUBSTREAM=CISOLID COMPS=C FRACS=.005
 PROPERTIES RK-SOAVE

BLOCK HYCASEP SEP
 FRAC STREAM=HYCA SUBSTREAM=MIXED COMPS=H2 CO CO2 CH4 &
 H2S COS N2 AR O2 NH3 H2O SO2 N2O NO2 C6H6 C2H4 &
 C2H2 C10H8 C2H6 C6H6O FRACS=0 0 0 1 0 0 0 0 1 &
 0 0 0 0 1 1 0 0 0 1
 FRAC STREAM=HYCA SUBSTREAM=CISOLID COMPS=C FRACS=0
 PROPERTIES RK-SOAVE

BLOCK INIT HEATER
 PARAM TEMP=900 PRES=0 NPHASE=1

BLOCK COMB RSTOIC
 PARAM TEMP=800 PRES=0 NPHASE=1
 STOIC 1 CISOLID C -1 / MIXED O2 -1 / CO2 1
 STOIC 2 MIXED H2 -1 / O2 -.5 / H2O 1
 CONV 1 CISOLID C 1
 CONV 2 MIXED H2 1
 PROPERTIES RK-SOAVE

BLOCK HYCACON RSTOIC
 PARAM TEMP=600 PRES=0 NPHASE=1
 STOIC 1 CISOLID C -1 / MIXED H2 -2 / CH4 1
 STOIC 2 CISOLID C -2 / MIXED H2 -2 / C2H4 1
 STOIC 3 CISOLID C -5 / MIXED H2 -3 / C6H6 1
 STOIC 4 CISOLID C -6 / MIXED H2 -3 / O2 -.5 / C6H6O &
 1

```

STOIC 5 MIXED N2 -.5 / H2 -1.5 / NH3 1
CONV 1 CISOLID C .1
CONV 2 CISOLID C .05
CONV 3 CISOLID C .03
CONV 4 CISOLID C .02
CONV 5 MIXED N2 .1
PROPERTIES RK-SOAVE

BLOCK ELEM RYIELD
PARAM TEMP=600 PRES=0 NPHASE=1
MASS-YIELD CISOLID C .504 / MIXED H2 .0597 / N2 .001 / &
O2 .4303 / NC ASH .005
PROPERTIES RK-SOAVE
COMP-ATTR NC ASH PROXANAL ( 0 0 0 100 )
COMP-ATTR NC ASH ULTANAL ( 100 0 0 0 0 0 )
COMP-ATTR NC ASH SULFANAL ( 0 0 0 )
COMP-ATTR NC ASH GENANAL ( 100 0 0 0 0 0 0 0 )

BLOCK GIBBS RGIBBS
PARAM TEMP=850 PRES=0 NPHASE=1 NREAC=2
PROD H2 / CO / CO2 / H2O / CH4 / N2
STOIC 1 CO2 -1 / H2 -4 / CH4 1 / H2O 2
STOIC 2 CO -1 / H2O -1 / H2 1 / CO2 1
TAPP-SPEC 2 -50
PROPERTIES RK-SOAVE

BLOCK B1 CLCHNG

DESIGN-SPEC C
DEFINE O MOLE-FRAC STREAM=FLUEGAS SUBSTREAM=MIXED &
COMPONENT=O2
SPEC "O" TO ".005"
TOL-SPEC ".0001"
VARY STREAM-VAR STREAM=AIRCOMB SUBSTREAM=MIXED &
VARIABLE=MASS-FLOW
LIMITS "5" "35"

FORTRAN C2H4
DEFINE B BLOCK-VAR BLOCK=HYCACON VARIABLE=CONV &
SENTENCE=CONV ID1=2
DEFINE T BLOCK-VAR BLOCK=INIT VARIABLE=TEMP SENTENCE=PARAM
READ-VARS T
WRITE-VARS B

FORTRAN C6H6
DEFINE C BLOCK-VAR BLOCK=HYCACON VARIABLE=CONV &
SENTENCE=CONV ID1=3
DEFINE T BLOCK-VAR BLOCK=INIT VARIABLE=TEMP SENTENCE=PARAM
READ-VARS T
WRITE-VARS C

FORTRAN C6H6O
DEFINE D BLOCK-VAR BLOCK=HYCACON VARIABLE=CONV &
SENTENCE=CONV ID1=4
DEFINE T BLOCK-VAR BLOCK=INIT VARIABLE=TEMP SENTENCE=PARAM
READ-VARS T
WRITE-VARS D

TRANSFER FUEL
SET STREAM FUEL
EQUAL-TO STREAM GS14

TRANSFER PRES
SET STREAM-VAR STREAM=DR11 SUBSTREAM=MIXED VARIABLE=PRES
SET STREAM-VAR STREAM=DR11 SUBSTREAM=NC VARIABLE=PRES
SET STREAM-VAR STREAM=AIR SUBSTREAM=MIXED VARIABLE=PRES
EQUAL-TO STREAM-VAR STREAM=IN1 SUBSTREAM=MIXED VARIABLE=PRES

TRANSFER TEMP
SET BLOCK-VAR BLOCK=INIT VARIABLE=TEMP SENTENCE=PARAM
EQUAL-TO BLOCK-VAR BLOCK=GIBBS VARIABLE=TEMP SENTENCE=PARAM

```

CONV-OPTIONS

PARAM TEAR-METHOD=BROYDEN CHECKSEQ=YES

STREAM-REPOR MOLEFLOW MOLEFRAC

PROP-TABLE LHVCIS PROPS

STREAM C1

VARY TEMP

RANGE LIST=15

TABULATE PROPERTIES=LHVCIS

PROP-TABLE LHVGAS1 PROPS

STREAM RAWGAS

VARY TEMP

RANGE LIST=15

TABULATE PROPERTIES=LHVGAS

PROP-TABLE LHVMIX PROPS

STREAM C1

VARY TEMP

RANGE LIST=15

TABULATE PROPERTIES=LHVMIX

PHYSICAL PROPERTY CALCULATION FOR PYROLYSIS

The selection of the physical property calculation method for the process model, especially for the absorber, is difficult because the system is highly non-ideal and there is no experimental vapour-liquid equilibrium data available. The pyrolysis products fed to the absorber comprise a mixture of non-condensable gases and polar organic compounds. Some of the organic compounds associate with each other chemically /164/.

The calculation methods based on activity coefficient models are better at representing highly non-ideal systems than the methods based on equations-of-state. The Wilson activity coefficient model was considered to be the most appropriate for the calculation of liquid-phase properties. The Redlich-Kwong equation of state was used for the vapour-phase properties. The Wilson binary parameters, which are not available from the Aspen Plus™ databanks, were estimated using the UNIFAC method. Two components, hydroxyacetaldehyde and levoglucosan, are missing from the Aspen Plus™ databanks, and their physical property parameters were estimated using group-contribution methods.

The only physical properties calculated for non-conventional components are enthalpy and density. The enthalpy of a non-conventional component is calculated by combining the standard heat of formation with the change in sensible heat. The standard heat of formation of a component can be obtained from the heat of combustion. The sensible heat is calculated using heat capacities.

Physical property parameters for the other non-conventional components employed in the model are presented in Table A6-1.

Table A6-1. Physical property parameters for non-conventional components, C_p = heat capacity, H_v = heat of vaporisation, hc = heavy component.

Parameter	Value
Heat capacity of wood	1.88 kJ/kg °C
Heat capacity of char	calculated using the Kirov* correlation for coal (1.47 kJ/kg °C at 500 °C)
Heat capacity of sand/ash	calculated using the Kirov correlation for coal (1.05 kJ/kg °C at 500 °C)
Liquid C_p of the hc	2.50 kJ/kg °C
Vapour C_p of the hc	calculated using a function for anthracene (2.24 kJ/kg °C at 500 °C)
H_v of the hc	1.0 MJ/kg at 25 °C

* The Kirov correlation treats the heat capacity of coal as a weighed sum of the heat capacities of the following constituents: moisture, fixed carbon, primary volatile matter, secondary volatile matter, and ash.

The heating value of char was calculated from its elemental analysis using the following formula for fuels /1/.

$$hhv = 0.3491C + 1.1783 H + 0.1005 S - 0.1034 O - 0.0151 N - 0.0211 \text{ Ash}$$

where hhv = higher heating value, MJ/kg
 C = amount of carbon in a fuel, wt%
 H = amount of hydrogen in a fuel, wt%
 S = amount of sulphur in a fuel, wt%
 O = amount of oxygen in a fuel, wt%
 N = amount of nitrogen in a fuel, wt%
 Ash = amount of ash in a fuel, wt%.

Heat of pyrolysis is defined in this work as the heat needed (or produced) when dry feed-stock decomposes into vaporised products and char at the reaction temperature. As the estimates published for the heat of biomass pyrolysis range from 370 J/g (endothermic) to -1 700 J/g (exothermic) /2, 3/, the value for the heat of pyrolysis was difficult to determine. In this work, 200 kJ/kg wood m.f. at 380 °C was used for the heat of pyrolysis. It was concluded on the basis of the literature that biomass pyrolysis is slightly endothermic. The heat

of pyrolysis was considered to be dependent on char yields: pyrolysis reactions are more exothermic with higher char yields. This dependence is based on the research work carried out by Mok and Antal /4/.

REFERENCES

- 1 Channiwala, S. A. On biomass gasification process and technology development. PhD Thesis. Bombay: Indian Inst. of Techn. Bombay, 1992.
2. Roberts, A. F. The heat of reaction during the pyrolysis of wood. *Combustion and flame*, 1991., Vol. 17, pp. 79 - 86.
3. Atreya, A. Heat of composition in wood pyrolysis. *Chem. Phys. Processes Combust.*, 1983, Paper 37. 4 p.
4. Mok, W. S.-L. & Antal, M. J. Effects of pressure on biomass pyrolysis. II. Heats of reaction of cellulose pyrolysis. *Thermochimica Acta*, 1983. Vol. 68, pp. 165 - 186.

AspenPlus input file for a pyrolyser

```

;
;Input file created by ModelManager Rel. 3.3-4 on Tue Aug 11 10:30:13 1992
;Directory E:\PYREC Runid PYROL
;

TITLE 'PUU-ITP'

IN-UNITS SI MASS-FLOW='KG/HR' PRESSURE='BAR' TEMPERATURE='C' &
  PDROP='N/SQM'

DEF-STREAMS MIXNC ALL

RUN-CONTROL MAX-TIME=2000

DATABANKS ASPENPCD / PURE856 / COMBUST / SOLIDS / &
  AQUEOUS / PURECOMP / INORGANIC

PROP-SOURCES ASPENPCD / PURE856 / COMBUST / SOLIDS / &
  AQUEOUS / PURECOMP / INORGANIC

COMPONENTS
H2 H2 H2 /
CO CO CO /
CO2 CO2 CO2 /
CH4 CH4 CH4 /
H2S H2S H2S /
N2 N2 N2 /
AR AR AR /
O2 O2 O2 /
NH3 H3N NH3 /
H2O H2O H2O /
SO2 O2S SO2 /
N2O N2O N2O /
NO2 NO2 NO2 /
C6H6 C6H6 C6H6 /
C2H4 C2H4 C2H4 /
C2H6 C2H6 C2H6 /
C C C /
BIOMASS * BIOMASS /
S S S /
FLYASH * FLYASH /
COS COS COS /
C2H2 C2H2 C2H2 /
C10H8 C10H8 C10H8 /
C6H6O C6H6O C6H6O /
AIR AIR AIR /
HCOOH CH2O2 HCOOH /
CH3COOH C2H4O2-1 CH3COOH /
OHASEALD * OHASEALD /
ASETOLI C3H6O2-D1 ASETOLI /
SOKERIT C6H14O6 SOKERIT /
GLYOXAL C2H2O2 GLYOXAL /
GLYKOLI C2H6O2 GLYKOLI /
FORMALD CH2O FORMALD /
PYRENE C16H10-D2 PYRENE /
KOKSI * KOKSI /
TUHKA * TUHKA /
HEAVY2 * HEAVY2 /
WOOD * WOOD /
HEAVY * HEAVY /
HEAVY3 * HEAVY3 /
LEVOGLUK * LEVOGLUK /
FURFURAL C5H4O2 FURFURAL /
GUAIACOL C7H8O2-E1 GUAIACOL

HENRY-COMPS H1 CO CO2 H2 N2 O2

HENRY-COMPS HE1 CO CO2 H2 N2 O2

```

FLOWSHEET

BLOCK COMB-2 IN=472 495 H2O 637 639 643 SPLELEM 638 &
 QHIE3 644 H3 OUT=ADT QCOMB
 BLOCK B10 IN=KA 504 OUT=472 SPLELEM
 BLOCK B11 IN=ADT OUT=476 TUHKAT QSYKL
 BLOCK B8 IN=QCOMB QSYKL QCONDFLU QASH 492 GSARMO2 OUT= &
 HAVIO
 BLOCK B14 IN=TUHKAT OUT=493 QASH
 BLOCK B15 IN=COMBAIR OUT=495 WBLow
 BLOCK B18 IN=WOODCOMB OUT=KA H2O 504
 BLOCK KHIE3 IN=KHIE3 OUT=KHIE4 H3
 BLOCK B6 IN=WBLow OUT=WNET

FLOWSHEET HRSG

BLOCK HRX1 IN=HR24 469 OUT=HR12 HR25
 BLOCK HRX2 IN=HR12 HR23 OUT=HR13 HR24
 BLOCK B4 IN=476 OUT=469
 BLOCK B9 IN=HR15 OUT=SAVUK HOYRY 492
 BLOCK B13 IN=HOYRY OUT=488 QCONDFLU
 BLOCK B20 IN=HR14 OUT=HR15 GSARMO2

DEF-STREAMS CONVEN HRSG

FLOWSHEET KUIV

BLOCK KUIV1 IN=1A2 H2 OUT=F2 2 H4
 BLOCK POLTTO3C IN=151 152 OUT=HHVM
 BLOCK MILL1 IN=WOODPYRO 164 OUT=1A2

DEF-STREAMS MIXNC KUIV

FLOWSHEET PYROL

BLOCK PYRYIE IN=P2 OUT=Y4 H8
 BLOCK HEAT4 IN=Y4B LEIJU1 H18 H8 QHIE2 OUT=5 H28
 BLOCK AINET IN=Y4 OUT=Y4B H18
 BLOCK SSEP2A IN=Y4C OUT=8 CHAR1
 BLOCK HEAVYV IN=5 OUT=Y4C H08
 BLOCK HEAVYL IN=8 OUT=81 H90
 BLOCK WOOD1 IN=2 OUT=P2
 BLOCK HIEKKA2 IN=HIEKKA2 OUT=HIEKKA3 QHIE2
 BLOCK HIEKKA3 IN=HIEKKA3 OUT=HIEKKA4 QHIE3
 BLOCK HIEKKA1 IN=HIEKKA1 OUT=HIEKKA2 QHIE1

DEF-STREAMS MIXNC PYROL

FLOWSHEET TALTO

BLOCK PUMPT1 IN=ROIL2 OUT=ROIL3 WP1
 BLOCK HEATT1 IN=ROIL1 OUT=ROIL2 QRO1
 BLOCK POLTTO3 IN=K302M 154 OUT=148 151
 BLOCK SPLK302 IN=K302 OUT=K302M K302NC
 BLOCK COMPR4 IN=11 OUT=112 WC4
 BLOCK POILSEP IN=POILO 110B OUT=POILI HENTR POILSEP
 BLOCK 11SEP IN=110 OUT=110B 110A
 BLOCK 11HEAT IN=110A HENTR OUT=11 11HEAT
 BLOCK BOUTSEP2 IN=OUT2 OUT=8TERVA LOPUT2
 BLOCK B2 IN=BY4C2 OUT=OUT2 8LAU

DEF-STREAMS MIXNC TALTO

PROPERTIES RK-SOAVE FREE-WATER=STEAMNBS
 PROPERTIES RK-SOAVE HRSG / SYSOP0 KUIV / WILS-RK PYROL / &
 WILS-RK TALTO
 PROPERTIES IDEAL / UNIFAC

NC-COMPS BIOMASS PROXANAL ULTANAL SULFANAL GENANAL

NC-PROPS BIOMASS ENTHALPY HCOALGEN 6 / DENSITY DNSTYGEN

NC-COMPS FLYASH PROXANAL ULTANAL SULFANAL GENANAL

NC-PROPS FLYASH ENTHALPY HCOALGEN 6 / DENSITY DNSTYGEN

NC-COMPS KOKSI PROXANAL ULTANAL SULFANAL GENANAL

NC-PROPS KOKSI ENTHALPY HCOALGEN 6 / DENSITY DNSTYGEN
 NC-COMPS TUHKA PROXANAL ULTANAL SULFANAL GENANAL
 NC-PROPS TUHKA ENTHALPY HCOALGEN 2 / DENSITY DNSTYGEN
 NC-COMPS HEAVY2 PROXANAL ULTANAL SULFANAL GENANAL
 NC-PROPS HEAVY2 ENTHALPY HCOALGEN 6 1 2 / DENSITY DNSTYGEN
 NC-COMPS WOOD PROXANAL ULTANAL SULFANAL GENANAL
 NC-PROPS WOOD ENTHALPY HCOALGEN 6 1 2 / DENSITY DNSTYGEN
 NC-COMPS HEAVY PROXANAL ULTANAL SULFANAL GENANAL
 NC-PROPS HEAVY ENTHALPY HCOALGEN 2 / DENSITY DNSTYGEN
 NC-COMPS HEAVY3 GENANAL
 NC-PROPS HEAVY3 ENTHALPY ENTHGEN / DENSITY DNSTYGEN
 USER-PROPS DRUSR2 1 2 3

STRUCTURES

STRUCTURES ASETOLI O1 C2 S / C2 C3 S / C3 C4 S / C3 &
 O5 D
 UNIFAC CH3COOH 1015 1 / 1955 1
 UNIFAC FORMALD 1610 1
 UNIFAC FURFURAL 2450 1
 UNIFAC GLYKOLI 2500 1
 UNIFAC GLYOXAL 1450 2
 UNIFAC H2O 1300 1
 UNIFAC HCOOH 1950 1
 STRUCTURES LEVOGLUK C1 C2 S / C2 C3 S / C3 O4 S / &
 C3 C5 S / C5 O6 S / C5 C7 S / C7 O8 S / C7 &
 C9 S / C9 O10 S / O10 C2 S / C9 O11 S / O11 &
 C1 S
 STRUCTURES OHASEALD O1 C2 S / C2 C3 S / C3 O4 D
 UNIFAC SOKERIT 1005 4 / 1010 2 / 1200 6

ESTIMATE ALL

WILSON H2O OHASEALD UNIFAC
 WILSON H2O ASETOLI UNIFAC
 WILSON H2O SOKERIT UNIFAC
 WILSON H2O GLYOXAL UNIFAC
 WILSON H2O GLYKOLI UNIFAC
 WILSON H2O FORMALD UNIFAC
 WILSON H2O PYRENE UNIFAC
 WILSON H2O LEVOGLUK UNIFAC
 WILSON H2O FURFURAL UNIFAC
 WILSON H2O GUAIACOL UNIFAC
 WILSON HCOOH OHASEALD UNIFAC
 WILSON HCOOH ASETOLI UNIFAC
 WILSON HCOOH SOKERIT UNIFAC
 WILSON HCOOH GLYOXAL UNIFAC
 WILSON HCOOH GLYKOLI UNIFAC
 WILSON HCOOH FORMALD UNIFAC
 WILSON HCOOH PYRENE UNIFAC
 WILSON HCOOH LEVOGLUK UNIFAC
 WILSON HCOOH FURFURAL UNIFAC
 WILSON HCOOH GUAIACOL UNIFAC
 WILSON CH3COOH OHASEALD UNIFAC
 WILSON CH3COOH ASETOLI UNIFAC
 WILSON CH3COOH SOKERIT UNIFAC
 WILSON CH3COOH GLYOXAL UNIFAC
 WILSON CH3COOH GLYKOLI UNIFAC
 WILSON CH3COOH FORMALD UNIFAC
 WILSON CH3COOH PYRENE UNIFAC
 WILSON CH3COOH LEVOGLUK UNIFAC
 WILSON CH3COOH FURFURAL UNIFAC

WILSON CH3COOH GUAIACOL UNIFAC
 WILSON OHASEALD ASETOLI UNIFAC
 WILSON OHASEALD SOKERIT UNIFAC
 WILSON OHASEALD GLYOXAL UNIFAC
 WILSON OHASEALD GLYKOLI UNIFAC
 WILSON OHASEALD FORMALD UNIFAC
 WILSON OHASEALD PYRENE UNIFAC
 WILSON OHASEALD LEVOGLUK UNIFAC
 WILSON OHASEALD FURFURAL UNIFAC
 WILSON OHASEALD GUAIACOL UNIFAC
 WILSON ASETOLI SOKERIT UNIFAC
 WILSON ASETOLI GLYOXAL UNIFAC
 WILSON ASETOLI GLYKOLI UNIFAC
 WILSON ASETOLI FORMALD UNIFAC
 WILSON ASETOLI PYRENE UNIFAC
 WILSON ASETOLI LEVOGLUK UNIFAC
 WILSON ASETOLI FURFURAL UNIFAC
 WILSON ASETOLI GUAIACOL UNIFAC
 WILSON SOKERIT GLYOXAL UNIFAC
 WILSON SOKERIT GLYKOLI UNIFAC
 WILSON SOKERIT FORMALD UNIFAC
 WILSON SOKERIT PYRENE UNIFAC
 WILSON SOKERIT LEVOGLUK UNIFAC
 WILSON SOKERIT FURFURAL UNIFAC
 WILSON SOKERIT GUAIACOL UNIFAC
 WILSON GLYOXAL GLYKOLI UNIFAC
 WILSON GLYOXAL FORMALD UNIFAC
 WILSON GLYOXAL PYRENE UNIFAC
 WILSON GLYOXAL LEVOGLUK UNIFAC
 WILSON GLYOXAL FURFURAL UNIFAC
 WILSON GLYOXAL GUAIACOL UNIFAC
 WILSON GLYKOLI FORMALD UNIFAC
 WILSON GLYKOLI PYRENE UNIFAC
 WILSON GLYKOLI LEVOGLUK UNIFAC
 WILSON GLYKOLI FURFURAL UNIFAC
 WILSON GLYKOLI GUAIACOL UNIFAC
 WILSON FORMALD PYRENE UNIFAC
 WILSON FORMALD LEVOGLUK UNIFAC
 WILSON FORMALD FURFURAL UNIFAC
 WILSON FORMALD GUAIACOL UNIFAC
 WILSON PYRENE LEVOGLUK UNIFAC
 WILSON PYRENE FURFURAL UNIFAC
 WILSON PYRENE GUAIACOL UNIFAC
 WILSON LEVOGLUK FURFURAL UNIFAC
 WILSON LEVOGLUK GUAIACOL UNIFAC
 WILSON FURFURAL GUAIACOL UNIFAC

PROP-DATA DATA1

IN-UNITS SI MASS-FLOW='KG/HR' PRESSURE=BAR TEMPERATURE=C &
 PDROP='N/SQM'
 PROP-LIST TB / HCOM
 PVAL OHASEALD 97 / -1.04886E9
 PROP-LIST HCOM
 PVAL LEVOGLUK -2.89799E9

PROP-DATA CP

IN-UNITS ENG
 PROP-LIST CP2C
 PVAL HEAVY2 0.597 0 0 0
 PVAL WOOD 0.45 0 0 0

PROP-DATA DENGEN

IN-UNITS SI TEMPERATURE=C
 PROP-LIST DENGEN
 PVAL BIOMASS 1.0
 PVAL FLYASH 1.0

PROP-DATA DENS

IN-UNITS SI PRESSURE=BAR TEMPERATURE=C PDROP='N/SQM'
 PROP-LIST DENGEN
 PVAL TUHKA 1.0
 PVAL KOKSI 1.0

PVAL WOOD 1.0
 PVAL HEAVY 1
 PVAL HEAVY2 1

PROP-DATA HCOM
 IN-UNITS SI
 PROP-LIST HCOMB
 PVAL WOOD 2.02E+07
 PVAL HEAVY2 3.9625E7
 PVAL KOKSI 2.115E7

PROP-DATA HHV
 IN-UNITS SI PRESSURE=BAR TEMPERATURE=C PDROP='N/SQM'
 PROP-LIST HCOMB
 PVAL BIOMASS 2.022E+7
 PVAL FLYASH 9.6E+6

PROP-DATA WILSON-1
 IN-UNITS SI
 PROP-LIST WILSON
 BPVAL H2O GLYKOLI -.045700000 152.3582000 0.0 0.0 &
 303.5500000 469.8500000
 BPVAL GLYKOLI H2O -.337700000 -12.85750000 0.0 0.0 &
 303.5500000 469.8500000
 BPVAL H2O FURFURAL 4.700100000 -2074.369400 0.0 0.0 &
 331.3500000 526.9500000
 BPVAL FURFURAL H2O -2.203200000 -559.8826000 0.0 0.0 &
 331.3500000 526.9500000
 BPVAL H2O HCOOH 9.852072 -3345.572 0.0 0.0 0.0 1000.000
 BPVAL HCOOH H2O -22.84918 7873.398 0.0 0.0 0.0 1000.000
 BPVAL HCOOH CH3COOH 4.224637 -1984.777 0.0 0.0 0.0 &
 1000.000
 BPVAL CH3COOH HCOOH -0.9275674 556.2599 0.0 0.0 0.0 &
 1000.000
 BPVAL H2O CH3COOH -3.972805 1553.363 0.0 0.0 0.0 1000.000
 BPVAL CH3COOH H2O 0.5566518 -666.1200 0.0 0.0 0.0 &
 1000.000

DEF-STREAMS CONVEN 469

STREAM 5
 SUBSTREAM MIXED TEMP=500.0 PRES=1.0130
 MASS-FLOW H2 5.0 / CO 450.0 / CO2 600.0 / CH4 20.0 / &
 N2 8587.0 / H2O 1600.0 / C2H4 13.0 / HCOOH 200.0 / &
 CH3COOH 500.0 / OHASEALD 900.0 / ASETOLI 100.0 / &
 SOKERIT 800.0 / GLYOXAL 200.0 / GLYKOLI 100.0 / &
 FORMALD 100.0 / PYRENE 800.0
 SUBSTREAM NC TEMP=500.0 PRES=1.0130
 MASS-FLOW KOKSI 1100.0
 COMP-ATTR KOKSI PROXANAL (1.1 75.0 20.7 3.6)
 COMP-ATTR KOKSI ULTANAL (3.6 75.0 2.5 0 0 0 18.9)
 COMP-ATTR KOKSI SULFANAL (0 0 0)
 COMP-ATTR KOKSI GENANAL (100 0 0 0 0 0 0 0 0 0 &
 0 0 0 0 0 0 0 0)

STREAM 143
 SUBSTREAM MIXED TEMP=91.77 PRES=1.01 MASS-FLOW=1.55E5
 MASS-FRAC H2O 1

STREAM 154
 SUBSTREAM MIXED TEMP=25 PRES=1.01 MASS-FLOW=80000
 MOLE-FRAC N2 0.79 / O2 0.21

STREAM ADT
 IN-UNITS SI PRESSURE=BAR TEMPERATURE=C PDROP='N/SQM'
 SUBSTREAM MIXED TEMP=1000 PRES=120 MASS-FLOW=.0005
 MOLE-FRAC H2 .1 / CO .15 / CO2 .2 / CH4 .05 / N2 &
 .4 / H2O .1

STREAM COMBAIR
 IN-UNITS SI PRESSURE=BAR TEMPERATURE=C PDROP='N/SQM'
 SUBSTREAM MIXED TEMP=15 PRES=1 MASS-FLOW=2.4

MOLE-FRAC N2 .79 / O2 .21

STREAM D1

IN-UNITS SI PRESSURE=BAR TEMPERATURE=C PDROP='N/SQM'
SUBSTREAM MIXED TEMP=120.0 PRES=100 MOLE-FLOW=.0277777
MOLE-FRAC H2O 1.0

STREAM HR18

IN-UNITS SI PRESSURE=BAR TEMPERATURE=C PDROP='N/SQM'
SUBSTREAM MIXED TEMP=140 PRES=110 MASS-FLOW=2.5
MASS-FRAC H2O 1.0

STREAM WOODCOMB

SUBSTREAM MIXED TEMP=15 PRES=1
MASS-FLOW H2O 46850
SUBSTREAM NC TEMP=15 PRES=1
MASS-FLOW BIOMASS 46850
COMP-ATTR BIOMASS PROXANAL (0 59.5 40.0 0.5)
COMP-ATTR BIOMASS ULTANAL (0.5 50.6 1 0 0 42.5)
COMP-ATTR BIOMASS SULFANAL (0 0 0)
COMP-ATTR BIOMASS GENANAL (100 0 0 0 0 0 0 0 0 0 &
0 0 0 0 0 0 0 0 0)

STREAM WOODPYRO

SUBSTREAM MIXED TEMP=15 PRES=1.0130
MASS-FLOW H2O 9854
SUBSTREAM NC TEMP=15 PRES=1.0130
MASS-FLOW WOOD 9854
COMP-ATTR WOOD PROXANAL (0.0 19.5 80.0 0.5)
COMP-ATTR WOOD ULTANAL (0.5 50.4 6.0 * * * 43.1)
COMP-ATTR WOOD SULFANAL (.0 .0 .0)
COMP-ATTR WOOD GENANAL (100 0 0 0 0 0 0 0 0 0 &
0 0 0 0 0 0 0 0 0)

DEF-STREAMS HEAT 11HEAT

DEF-STREAMS HEAT 151

DEF-STREAMS HEAT 152

DEF-STREAMS HEAT 164

STREAM 164

INFO HEAT DUTY=492700

DEF-STREAMS HEAT 492

DEF-STREAMS HEAT 504

DEF-STREAMS HEAT 638

DEF-STREAMS HEAT 644

DEF-STREAMS HEAT FLUESENS

DEF-STREAMS HEAT GSARMO2

DEF-STREAMS HEAT H1

DEF-STREAMS HEAT H2

DEF-STREAMS HEAT H3

DEF-STREAMS HEAT H4

DEF-STREAMS HEAT H08

DEF-STREAMS HEAT H8

DEF-STREAMS HEAT H18

DEF-STREAMS HEAT H28

DEF-STREAMS HEAT H90
 DEF-STREAMS HEAT HAVIO
 DEF-STREAMS HEAT HHVM
 DEF-STREAMS HEAT POILSENS
 DEF-STREAMS HEAT POILSEP
 DEF-STREAMS HEAT QASH
 DEF-STREAMS HEAT QCOMB
 DEF-STREAMS HEAT QCONDFLU
 DEF-STREAMS HEAT QD
 DEF-STREAMS HEAT QHIE1
 DEF-STREAMS HEAT QHIE2
 DEF-STREAMS HEAT QHIE3
 DEF-STREAMS HEAT QRO1
 DEF-STREAMS HEAT QSYKL
 DEF-STREAMS HEAT SPLELEM
 DEF-STREAMS WORK 144
 DEF-STREAMS WORK WBLOW
 DEF-STREAMS WORK WC4
 DEF-STREAMS WORK WCTOT
 DEF-STREAMS WORK WNET
 DEF-STREAMS WORK WP1
 BLOCK B6 MIXER
 IN-UNITS SI PRESSURE=BAR TEMPERATURE=C PDROP='N/SQM'
 BLOCK B8 MIXER
 IN-UNITS SI PRESSURE=BAR TEMPERATURE=C PDROP='N/SQM'
 BLOCK BIN MIXER
 BLOCK POLTTO3C MIXER
 BLOCK WTOTPY MIXER
 BLOCK ABSSPL FSPLIT
 MASS-FLOW 11A 16424
 BLOCK HRFS FSPLIT
 IN-UNITS SI PRESSURE=BAR TEMPERATURE=C PDROP='N/SQM'
 FRAC 471 .000000001
 BLOCK SSPL1 FSPLIT
 FRAC ROIL1 0.98
 BLOCK POILSEP SEP
 PARAM
 FRAC STREAM=HENTR SUBSTREAM=MIXED COMPS=H2 CO CO2 CH4 &
 H2S N2 AR O2 NH3 H2O SO2 N2O NO2 C6H6 C2H4 C2H6 C &
 S COS C2H2 C10H8 C6H6O AIR HCOOH CH3COOH OHASEALD &
 ASETOLI SOKERIT GLYOXAL GLYKOLI FORMALD LEVOGLUK &
 FURFURAL GUAIACOL FRACS=0 0 0 0 0 0 0 0 0 0 0 &

APPENDIX 7

```

00000000000000000000000000000000 &
0
MASS-FLOW STREAM=HENTR SUBSTREAM=MIXED COMPS=PYRENE FLOWS=&
156
FRAC STREAM=HENTR SUBSTREAM=NC COMPS=BIOMASS FLYASH KOKSI &
TUHKA HEAVY2 WOOD HEAVY HEAVY3 FRACS=000000 &
01

```

BLOCK POLTTO3B SEP

```

PARAM
FRAC STREAM=149 SUBSTREAM=MIXED COMPS=H2 CO CO2 CH4 H2S &
N2 AR O2 NH3 H2O SO2 N2O NO2 C6H6 C2H4 C2H6 C S &
COS C2H2 C10H8 C6H6O AIR HCOOH CH3COOH OHASEALD &
ASETOLI SOKERIT GLYOXAL GLYKOLI FORMALD PYRENE LEVOGLUK &
FURFURAL GUAIACOL FRACS=000000000100 &
00000000000000000000000000000000 &
00
FRAC STREAM=149 SUBSTREAM=NC COMPS=BIOMASS FLYASH KOKSI &
TUHKA HEAVY2 WOOD HEAVY HEAVY3 FRACS=000000 &
00
FLASH-SPECS 149 TEMP=25 PRES=1.01
FLASH-SPECS 150 TEMP=25 PRES=1.01

```

BLOCK SSEP1 SEP

```

PARAM
FRAC STREAM=VESI2 SUBSTREAM=MIXED COMPS=H2 CO CO2 CH4 &
H2S N2 AR O2 NH3 H2O SO2 N2O NO2 C6H6 C2H4 C2H6 C &
S COS C2H2 C10H8 C6H6O AIR HCOOH CH3COOH OHASEALD &
ASETOLI SOKERIT GLYOXAL GLYKOLI FORMALD PYRENE LEVOGLUK &
FURFURAL GUAIACOL FRACS=000000000100 &
00000000000000000000000000000000 &
00
FRAC STREAM=VESI2 SUBSTREAM=NC COMPS=BIOMASS FLYASH KOKSI &
TUHKA HEAVY2 WOOD HEAVY HEAVY3 FRACS=000000 &
00
FLASH-SPECS K302 TEMP=15 PRES=1.01
FLASH-SPECS VESI2 TEMP=15 PRES=1.01

```

BLOCK SSEP2A SEP

```

PARAM
FRAC STREAM=CHAR1 SUBSTREAM=MIXED COMPS=H2 CO CO2 CH4 &
H2S N2 AR O2 NH3 H2O SO2 N2O NO2 C6H6 C2H4 C2H6 C &
S COS C2H2 C10H8 C6H6O AIR HCOOH CH3COOH OHASEALD &
ASETOLI SOKERIT GLYOXAL GLYKOLI FORMALD PYRENE LEVOGLUK &
FURFURAL GUAIACOL FRACS=000000000000 &
00000000000000000000000000000000 &
00
FRAC STREAM=CHAR1 SUBSTREAM=NC COMPS=BIOMASS FLYASH KOKSI &
TUHKA HEAVY2 WOOD HEAVY HEAVY3 FRACS=000.9900 &
000

```

BLOCK 11HEAT HEATER

```

PARAM TEMP=72.0 PRES=1.01 MAXIT=50

```

BLOCK B13 HEATER

```

IN-UNITS SI PRESSURE=BAR TEMPERATURE=C PDROP='N/SQM'
PARAM TEMP=15 PRES=0
PROPERTIES STEAMNBS

```

BLOCK B14 HEATER

```

IN-UNITS SI PRESSURE=BAR TEMPERATURE=C PDROP='N/SQM'
PARAM TEMP=15 PRES=0
PROPERTIES IDEAL

```

BLOCK B20 HEATER

```

IN-UNITS SI PRESSURE=BAR TEMPERATURE=C PDROP='N/SQM'
PARAM PRES=0 DUTY=1

```

BLOCK BIN1 HEATER

```

PARAM TEMP=380 PRES=1.01

```

BLOCK BIN2 HEATER

APPENDIX 7

PARAM TEMP=380 PRES=1.01

BLOCK BOUT HEATER
PARAM TEMP=380 PRES=1.01

BLOCK HEAT4 HEATER
PARAM TEMP=500 PRES=1.0130

BLOCK HEAT1 HEATER
PARAM TEMP=45 PRES=1.0130

BLOCK HIEKKA1 HEATER
PARAM TEMP=640 PRES=0

BLOCK HIEKKA2 HEATER
PARAM TEMP=600 PRES=0

BLOCK HIEKKA3 HEATER
PARAM TEMP=650 PRES=0

BLOCK KHIE1 HEATER
PARAM TEMP=640 PRES=0

BLOCK KHIE2 HEATER
PARAM PRES=0 DUTY=-4E7

BLOCK KHIE3 HEATER
PARAM TEMP=650 PRES=0

BLOCK MILL1 HEATER
PARAM PRES=0

BLOCK WOOD1 HEATER
PARAM PRES=0 DUTY=0

BLOCK B2 FLASH2
PARAM TEMP=40 PRES=1

BLOCK ABS RADFRAC
PARAM NSTAGE=4 MAXOL=40
FEEDS 81 4 ON-STAGE / ROIL3 1 ON-STAGE
PRODUCTS 110 1 V / 9 4 L
P-SPEC 1 1.010
COL-SPECS Q1=0 QN=0 MOLE-RDV=1.0

BLOCK AINET RSTOIC
PARAM TEMP=500 PRES=0
STOIC 1 NC HEAVY -1 / HEAVY2 1
CONV 1 NC HEAVY 1
COMP-ATTR NC HEAVY2 PROXANAL (0 75 25 0)
COMP-ATTR NC HEAVY2 ULTANAL (0 66.377 5.937 0 0 0 &
27.676)
COMP-ATTR NC HEAVY2 SULFANAL (0 0 0)
COMP-ATTR NC HEAVY2 GENANAL (100 0 0 0 0 0 0 0 0 &
0 0 0 0 0 0 0 0 0)

BLOCK COMB-2 RSTOIC
IN-UNITS SI PRESSURE=BAR TEMPERATURE=C PDROP='N/SQM'
PARAM TEMP=1000 PRES=0 NPHASE=1
STOIC 1 MIXED H2 -2 / O2 -1 / H2O 2
STOIC 2 MIXED C -1 / O2 -1 / CO2 1
STOIC 3 MIXED CO -1 / O2 -.5 / CO2 1
STOIC 4 MIXED CH4 -1 / O2 -2 / CO2 1 / H2O 2
STOIC 5 MIXED NH3 -1 / O2 -1.75 / NO2 1 / H2O 1.5
STOIC 6 MIXED C6H6 -1 / O2 -7.5 / CO2 6 / H2O 3
STOIC 7 MIXED C2H4 -1 / O2 -3 / CO2 2 / H2O 2
STOIC 8 MIXED C6H6O -1 / O2 -7 / CO2 6 / H2O 3
STOIC 9 MIXED HCOOH -2 / O2 -1 / CO2 2 / H2O 2
STOIC 10 MIXED CH3COOH -1 / O2 -2 / CO2 2 / H2O 2
STOIC 11 MIXED OHASEALD -1 / O2 -2 / CO2 2 / H2O 2
STOIC 12 MIXED ASETOLI -2 / O2 -7 / CO2 6 / H2O 6
STOIC 13 MIXED GLYOXAL -2 / O2 -3 / CO2 4 / H2O 2

STOIC 14 MIXED GLYKOLI -2 / O2 -5 / CO2 4 / H2O 6
 STOIC 15 MIXED FORMALD -1 / O2 -1 / CO2 1 / H2O 1
 STOIC 16 MIXED SOKERIT -2 / O2 -13 / CO2 12 / H2O 14
 STOIC 17 MIXED PYRENE -2 / O2 -37 / CO2 32 / H2O 10
 STOIC 18 MIXED FURFURAL -1 / O2 -5 / CO2 5 / H2O 2
 STOIC 19 MIXED GUAIACOL -1 / O2 -8 / CO2 7 / H2O 4
 STOIC 20 MIXED LEVOGLUK -1 / O2 -6 / H2O 5 / CO2 6
 CONV 1 MIXED H2 1
 CONV 2 MIXED C 1
 CONV 3 MIXED CO 1
 CONV 4 MIXED CH4 1
 CONV 5 MIXED NH3 .6
 CONV 6 MIXED C6H6 1
 CONV 7 MIXED C2H4 1
 CONV 8 MIXED C6H6O 1
 CONV 9 MIXED HCOOH 1
 CONV 10 MIXED CH3COOH 1
 CONV 11 MIXED OHASEALD 1
 CONV 12 MIXED ASETOLI 1
 CONV 13 MIXED GLYOXAL 1
 CONV 14 MIXED GLYKOLI 1
 CONV 15 MIXED FORMALD 1
 CONV 16 MIXED SOKERIT 1
 CONV 17 MIXED PYRENE 1
 CONV 18 MIXED FURFURAL 1
 CONV 19 MIXED GUAIACOL 1
 CONV 20 MIXED LEVOGLUK 1

BLOCK HEAVYL RSTOIC
 PARAM PRES=0 DUTY=0
 STOIC 1 NC HEAVY3 -1 / HEAVY2 1
 CONV 1 NC HEAVY3 0.95

BLOCK HEAVYV RSTOIC
 PARAM PRES=0 DUTY=0
 STOIC 1 NC HEAVY2 -1 / HEAVY3 1
 CONV 1 NC HEAVY2 0.999
 COMP-ATTR NC HEAVY3 GENANAL (100 0 0 0 0 0 0 0 0 &
 0 0 0 0 0 0 0 0 0 0)

BLOCK B10 RYIELD
 IN-UNITS SI PRESSURE=BAR TEMPERATURE=C PDROP='N/SQM'
 PARAM TEMP=15 PRES=0
 MASS-YIELD MIXED H2 .06 / N2 .01 / O2 .425 / C .5 / &
 NC FLYASH .005
 PROPERTIES IDEAL
 COMP-ATTR NC FLYASH PROXANAL (0 75 5 20)
 COMP-ATTR NC FLYASH ULTANAL (20 70 0 5 0 0 5)
 COMP-ATTR NC FLYASH SULFANAL (0 0 0)
 COMP-ATTR NC FLYASH GENANAL (100 0 0 0 0 0 0 0 0 &
 0 0 0 0 0 0 0 0 0 0)

BLOCK RYGASNC RYIELD
 PARAM TEMP=500 PRES=1
 MASS-YIELD MIXED C 0.8719 / H2 0.0760 / O2 0.0521

BLOCK COMPR4 COMPR
 PARAM TYPE=ISENTROPIC PRES=1.5 NPHASE=2

BLOCK B5 SSPLIT
 FRAC MIXED NC 0
 FRAC NC NC 1

BLOCK SPLK302 SSPLIT
 MASS-FLOW MIXED K302M 1 <KG/SEC> *
 FRAC NC K302M 0

BLOCK B4 CLCHNG
 IN-UNITS SI PRESSURE=BAR TEMPERATURE=C PDROP='N/SQM'

DESIGN-SPEC AIRT1
 PROPRIETARY INFORMATION

DESIGN-SPEC ROIL
 PROPRIETARY INFORMATION

DESIGN-SPEC TEMPI
 PROPRIETARY INFORMATION

TRANSFER LEIJU1
 SET STREAM BLEIJU1
 EQUAL-TO STREAM LEIJU1

TRANSFER P2
 SET STREAM BP2
 EQUAL-TO STREAM P2

TRANSFER STR8
 SET STREAM BY4C2
 EQUAL-TO STREAM 11A

TRANSFER Y4C
 SET STREAM BY4C
 EQUAL-TO STREAM Y4C

CONV-OPTIONS
 WEGSTEIN MAXIT=80
 SECANT MAXIT=40

CONVERGENCE C-2 BROYDEN
 TEAR 9
 SPEC ROIL
 PARAM MAXIT=300

STREAM-REPOR MOLEFLOW MASSFLOW MOLEFRAC MASSFRAC PROPERTIES=H25 &
 H25S HHVPY HT HTS LHPY VISK SH SC SO H500 H500S &
 H350 H350S CPM CPM15 CPNC CPMX3 CPMX5
 SUPPLEMENTAR 1 PROPERTIES=CPNC CPNC3 CPNC5 CPMX3 CPMX5 &
 INCL-STREAMS=HIEKKA1 HIEKKA2 HIEKKA3 8
 SUPPLEMENTAR 2 PROPERTIES=CPMX40 CPMX80 INCL-STREAMS=8TERVA
 SUPPLEMENTAR 3 PROPERTIES=CPNC1 CPNC3 CPNC5 &
 INCL-STREAMS=CHAR1 P2

PROP-TABLE TABLE1 PROPS
 STREAM K302
 VARY TEMP
 RANGE LIST=30.0
 TABULATE "KUIVA TUOTEOLJY" PROPERTIES=LIST1

PROP-TABLE TABLE2 PROPS
 STREAM POIL1
 VARY TEMP
 RANGE LIST=30.0
 TABULATE "TUOTEOLJY+VESI" PROPERTIES=LIST1

AspenPlus input file for a gas turbine

```

;
;Input file created by ModelManager Rel. 3.3-4 on Tue Nov 02 11:06:09 1993
;Directory D:\Y1\GT Runid PHDRY
;

TITLE "GT"

IN-UNITS SI PRESSURE=BAR TEMPERATURE=C

OUT-UNITS SI PRESSURE=BAR TEMPERATURE=C

DEF-STREAMS CONVEN ALL

DATABANKS ASPENPCD / DIPRPCD / COMBUST

PROP-SOURCES ASPENPCD / DIPRPCD / COMBUST

COMPONENTS
H2 H2 H2 /
CO CO CO /
CO2 CO2 CO2 /
CH4 CH4 CH4 /
H2S H2S H2S /
COS COS COS /
N2 N2 N2 /
AR AR AR /
O2 O2 O2 /
NH3 H3N NH3 /
H2O H2O H2O /
SO2 O2S SO2 /
N2O N2O N2O /
NO2 NO2 NO2 /
C6H6 C6H6 C6H6 /
C2H4 C2H4 C2H4 /
C2H2 C2H2 C2H2 /
C10H8 C10H8 C10H8

FLOWSHEET
BLOCK GTCO1 IN=GT42 OUT=GT43 W41
BLOCK GTRE IN=GT44 GT45 OUT=GT46
BLOCK GTLO2 IN=GT47 OUT=GT48 GTQ1
BLOCK GTCO2 IN=GT46 OUT=GT47 W42
BLOCK GTMX IN=W41 W42 OUT=W40
BLOCK GTEX IN=GT43 OUT=GT431 GT44
BLOCK GTLO1 IN=GT41 OUT=GT42
BLOCK GTLO3 IN=GT48 OUT=GT49

PROPERTIES SYSOP3

MODEL-PARAME ESRKS / APIRKS

STREAM GT41
SUBSTREAM MIXED TEMP=15 PRES=1.013250 &
MASS-FLOW=230799 <KG/HR>
MOLE-FRAC N2 .7770 / AR .010 / O2 .20920 / H2O &
3.800E-03

STREAM GT45
SUBSTREAM MIXED TEMP=480 PRES=22.0 MASS-FLOW=43185 <KG/HR> &
NPHASE=1
MOLE-FRAC H2 .1242 / CO .1855 / CO2 .1162 / CH4 .0442 &
/N2 .4108 / NH3 0 / H2O .1129 / C2H4 .0062

DEF-STREAMS HEAT GTQ1

DEF-STREAMS WORK W40

DEF-STREAMS WORK W41

```

DEF-STREAMS WORK W42

BLOCK GTMX MIXER

BLOCK GTEX FSPLIT

PARAM NPHASE=1

MASS-FLOW GT431 25851 <KG/HR>

BLOCK GTLO1 HEATER

PARAM PRES=-4 <IN-WATER> DUTY=0 NPHASE=1

BLOCK GTLO2 HEATER

PARAM PRES=-0 DELT=-10 NPHASE=1

BLOCK GTLO3 HEATER

PARAM PRES=-10 <IN-WATER> DUTY=0 NPHASE=1

BLOCK GTRE RSTOIC

PARAM PRES=-.50 DUTY=0.0 NPHASE=1

STOIC 1 MIXED H2 -2.0 / O2 -1.0 / H2O 2.0

STOIC 2 MIXED CO -2.0 / O2 -1.0 / CO2 2.0

STOIC 3 MIXED CH4 -1.0 / O2 -2.0 / CO2 1.0 / H2O 2.0

STOIC 4 MIXED H2S -2.0 / O2 -3.0 / H2O 2.0 / SO2 2.0

STOIC 5 MIXED COS -1.0 / O2 -1.50 / CO2 1.0 / SO2 &

1.0

STOIC 6 MIXED NH3 -2.0 / O2 -3.50 / NO2 2.0 / H2O &

3.0

STOIC 7 MIXED C6H6 -1.0 / O2 -7.50 / CO2 6.0 / H2O &

3.0

STOIC 8 MIXED C2H4 -1.0 / O2 -3.0 / CO2 2.0 / H2O &

2.0

STOIC 9 MIXED C2H2 -1.0 / O2 -2.50 / CO2 2.0 / H2O &

1.0

STOIC 10 MIXED C10H8 -1.0 / O2 -12.0 / CO2 10.0 / H2O &

4.0

STOIC 11 MIXED NH3 -2.0 / O2 -1.50 / N2 1.0 / H2O &

3.0

CONV 1 MIXED H2 1.0

CONV 2 MIXED CO 1.0

CONV 3 MIXED CH4 1.0

CONV 4 MIXED H2S 1.0

CONV 5 MIXED COS 1.0

CONV 6 MIXED NH3 .50

CONV 7 MIXED C6H6 1.0

CONV 8 MIXED C2H4 1.0

CONV 9 MIXED C2H2 1.0

CONV 10 MIXED C10H8 1.0

CONV 11 MIXED NH3 .50

BLOCK GTCO1 COMPR

PARAM TYPE=ISENTROPIC PRES=18.23 SEFF=.841

BLOCK GTCO2 COMPR

PARAM TYPE=ISENTROPIC DELP=-16.7 SEFF=.8662375 MEFF=1.0

SENSITIVITY 1

DEFINE TOUT STREAM-VAR STREAM=GT49 SUBSTREAM=MIXED &

VARIABLE=TEMP

DEFINE W INFO-VAR INFO=WORK VARIABLE=POWER STREAM=W40

DEFINE TIN STREAM-VAR STREAM=GT43 SUBSTREAM=MIXED &

VARIABLE=TEMP

TABULATE 1 "W"

TABULATE 2 "TOUT"

TABULATE 3 "TIN"

VARY BLOCK-VAR BLOCK=GTLO2 VARIABLE=DELT SENTENCE=PARAM

RANGE LOWER="0" UPPER="20" NPOINT="5"

;
;
;
;
;
;

AspenPlus input file for an internal combustion engine

```

;
;Input file created by ModelManager Rel. 3.3-4 on Tue Mar 09 09:59:58 1993
;Directory D:\Y1\GT Runid FUEL2
;

TITLE 'Gas engine'

IN-UNITS SI PRESSURE=BAR TEMPERATURE=C PDROP='N/SQM'

OUT-UNITS SI PRESSURE=BAR TEMPERATURE=C PDROP='N/SQM'

DEF-STREAMS CONVEN ALL

DATABANKS ASPENPCD / PURE856 / AQUEOUS / COMBUST / &
  SOLIDS / PURECOMP / INORGANIC

PROP-SOURCES ASPENPCD / PURE856 / AQUEOUS / COMBUST / &
  SOLIDS / PURECOMP / INORGANIC

COMPONENTS
  H2 H2 H2 /
  CO CO CO /
  CO2 CO2 CO2 /
  CH4 CH4 CH4 /
  H2S H2S H2S /
  COS COS COS /
  N2 N2 N2 /
  AR AR AR /
  O2 O2 O2 /
  NH3 H3N NH3 /
  H2O H2O H2O /
  SO2 O2S SO2 /
  N2O N2O N2O /
  NO2 NO2 NO2 /
  C6H6 C6H6 C6H6 /
  C2H4 C2H4 C2H4 /
  C2H6 C2H6 C2H6 /
  C2H2 C2H2 C2H2 /
  C10H8 C10H8 C10H8 /
  C C C /
  C6H6O C6H6O C6H6O /
  BIOMASS * BIOMASS /
  FLYASH * FLYASH /
  S S S /
  ASH * ASH /
  OIL * OIL /
  C3H6 C3H6-2 C3H6 /
  COAL * COAL /
  NH4+ NH4+ NH4+ /
  NH2COO- NH2COO- NH2COO- /
  HCO3- HCO3- HCO3- /
  HS- HS- HS- /
  OH- OH- OH- /
  CO3- CO3-2 CO3- /
  S- S-2 S- /
  H3O+ H3O+ H3O+ /
  CAO CAO CAO /
  CAS CAS CAS

HENRY-COMPS ALL H2 CO CH4 N2 CO2 NH3

HENRY-COMPS GLOBAL CO2 H2S NH3

CHEMISTRY GLOBAL
IN-UNITS ENG
STOIC 1 H2O -2 / H3O+ 1 / OH- 1
STOIC 2 H2S -1 / H2O -1 / H3O+ 1 / HS- 1
STOIC 3 HS- -1 / H2O -1 / H3O+ 1 / S- 1
STOIC 4 CO2 -1 / H2O -2 / H3O+ 1 / HCO3- 1

```

STOIC 5 HCO3- -1 / H2O -1 / H3O+ 1 / CO3- 1
 STOIC 6 NH3 -1 / H2O -1 / NH4+ 1 / OH- 1
 STOIC 7 NH3 -1 / HCO3- -1 / NH2COO- 1 / H2O 1
 K-STOIC 1 A=132.89888 B=-13445.9 C=-22.4773 D=0
 K-STOIC 2 A=214.582443 B=-12995.4 C=-33.5471 D=0
 K-STOIC 3 A=-9.741963 B=-8585.47 C=0 D=0
 K-STOIC 4 A=231.465439 B=-12092.1 C=-36.7816 D=0
 K-STOIC 5 A=216.05043 B=-12431.7 C=-35.4819 D=0
 K-STOIC 6 A=-1.256563 B=-3335.7 C=1.4971 D=-0.0370566
 K-STOIC 7 A=-4.583437 B=2900 C=0 D=0

FLWSHEET DIESEL

BLOCK DICOMB IN=DI12 1467 Q44 OUT=DI6 Q43
 BLOCK DICLCH IN=DI3 OUT=DI4
 BLOCK DIMX3 IN=DI11 G6 OUT=DI12
 BLOCK DIHX4 IN=DI6 OUT=DI7 QP
 BLOCK B9 IN=DI7 OUT=DI9 QENGLOS
 BLOCK QDILOSS IN=Q43 QENGLOS OUT=QDILOSS
 BLOCK QLOSSTOT IN=QGASLOSS QDILOSS QL120 Q110 Q61 1506 &
 OUT=646
 BLOCK B34 IN=DI4 OUT=1467 DISLPUMP

DEF-STREAMS MIXCISLD DIESEL

FLWSHEET GASSENS

BLOCK B18 IN=1485 OUT=1486
 BLOCK B19 IN=1486 OUT=1488 1487

DEF-STREAMS CONVEN GASSENS

FLWSHEET NC

BLOCK OILULTIM IN=DI1 OUT=DI3 Q44

DEF-STREAMS MIXCINC NC

PROPERTIES ELECNRTL HENRY-COMPS=GLOBAL CHEMISTRY=GLOBAL &
 FREE-WATER=STEAMNBS TRUE-COMPS=NO
 PROPERTIES RK-SOAVE STOIAR FREE-WATER=STEAMNBS / RK-SOAVE &
 GASSENS FREE-WATER=STEAMNBS / STEAMNBS DEA &
 FREE-WATER=STEAMNBS / STEAMNBS ST FREE-WATER=STEAMNBS / &
 RK-SOAVE HRSG FREE-WATER=STEAMNBS
 PROPERTIES SYSOP0 / IDEAL / SYSOP3 / SYSOP12

PROP-REPLACE SYSOP3 RK-SOAVE

PROP VLMX VLMX48
 PROP MUVMX MUVMX02
 PROP MULMX MULMX02
 PROP KVMX KVMX02
 PROP SIGLMX SIGLMX01
 PROP VL VL09
 PROP DV DV01

PROP-REPLACE SYSOP12 STEAM-TA

NC-COMPS BIOMASS PROXANAL ULTANAL SULFANAL GENANAL

NC-PROPS BIOMASS ENTHALPY HCOALGEN 6 / DENSITY DNSTYGEN

NC-COMPS FLYASH PROXANAL ULTANAL SULFANAL GENANAL

NC-PROPS FLYASH ENTHALPY HCOALGEN 2 / DENSITY DNSTYGEN

NC-COMPS ASH PROXANAL ULTANAL SULFANAL GENANAL

NC-PROPS ASH ENTHALPY HCOALGEN 2 / DENSITY DNSTYGEN

NC-COMPS OIL PROXANAL ULTANAL SULFANAL GENANAL

NC-PROPS OIL ENTHALPY HCOALGEN 6 / DENSITY DNSTYGEN

NC-COMPS COAL PROXANAL ULTANAL SULFANAL GENANAL

NC-PROPS COAL ENTHALPY HCOALGEN 6 / DENSITY DNSTYGEN

USER-PROPS DRUSR2 1 2 3

PROP-DATA DATA1
IN-UNITS SI
PROP-LIST DENGEN
PVAL ASH 1.0
PVAL OIL 1

PROP-DATA DATA2
IN-UNITS SI PRESSURE=BAR TEMPERATURE=C PDROP='N/SQM'
PROP-LIST HCOMB
PVAL OIL 4.45E7

PROP-DATA DENGEN
IN-UNITS SI
PROP-LIST DENGEN
PVAL BIOMASS 1.0
PVAL FLYASH 1.0
PVAL ASH 1
PVAL OIL 1

PROP-DATA DENS
IN-UNITS SI TEMPERATURE=C
PROP-LIST DENGEN
PVAL BIOMASS 1.0
PVAL ASH 1.0

PROP-DATA HHV
IN-UNITS SI PRESSURE=BAR TEMPERATURE=C PDROP='N/SQM'
PROP-LIST HCOMB
PVAL BIOMASS 2.014E+7

PROP-DATA HHVBIO
IN-UNITS SI PRESSURE=BAR TEMPERATURE=C PDROP='N/SQM'
PROP-LIST HCOMB
PVAL BIOMASS 2.050E+7

PROP-DATA HHVOIL
IN-UNITS SI PRESSURE=BAR TEMPERATURE=C PDROP='N/SQM'
PROP-LIST HCOMB
PVAL OIL 4E+7

PROP-SET LHV QVALNET UNITS='KJ/KG' SUBSTREAM=MIXED

PROP-SET LHVCIS QVALNET UNITS='KJ/KG' SUBSTREAM=CISOLID

PROP-SET LHV GAS QVALNET UNITS='KJ/KG' SUBSTREAM=MIXED

PROP-SET LHVMIX QVALNET UNITS='KJ/KG' SUBSTREAM=MIXED

STREAM 1485
SUBSTREAM MIXED TEMP=15 PRES=1 MASS-FLOW=1
MOLE-FRAC H2 .1 / CO .1 / N2 .8

STREAM DII
SUBSTREAM NC TEMP=15 PRES=3.0 MASS-FLOW=.000000001
MASS-FRAC OIL 1.0
COMP-ATTR OIL PROXANAL (.0 20.0 80.0 .0)
COMP-ATTR OIL ULTANAL (.0 92.0 8.0 .0 .0 .0)
COMP-ATTR OIL SULFANAL (.0 .0 .0)
COMP-ATTR OIL GENANAL (100.0 .0 .0 .0 .0 .0 .0 .0 &
.000000000000)

STREAM DII1
SUBSTREAM MIXED TEMP=15.0 PRES=1.0 MOLE-FLOW=.44 NPHASE=1
MOLE-FRAC N2 .790 / O2 .210

DEF-STREAMS HEAT 646

DEF-STREAMS HEAT 1506

DEF-STREAMS HEAT Q43
 DEF-STREAMS HEAT Q44
 DEF-STREAMS HEAT Q61
 DEF-STREAMS HEAT Q110
 DEF-STREAMS HEAT QDILOSS
 DEF-STREAMS HEAT QENGL0S
 DEF-STREAMS HEAT QGASLOSS
 DEF-STREAMS HEAT QL120
 DEF-STREAMS HEAT QP
 DEF-STREAMS WORK DISLPUMP
 BLOCK DIMX3 MIXER
 PARAM PRES=-.001 NPHASE=1
 PROPERTIES RK-SOAVE FREE-WATER=STEAMNBS
 BLOCK QDILOSS MIXER
 BLOCK QLOSSTOT MIXER
 BLOCK B9 HEATER
 PARAM TEMP=418 PRES=0
 PROPERTIES RK-SOAVE FREE-WATER=STEAMNBS
 BLOCK B18 HEATER
 PARAM TEMP=100 PRES=2
 BLOCK DIHX4 HEATER
 PARAM PRES=0 DUTY=-100 NPHASE=1
 PROPERTIES RK-SOAVE FREE-WATER=STEAMNBS
 BLOCK B19 FLASH2
 PARAM PRES=0 DUTY=0
 BLOCK DICOMB RSTOIC
 PARAM PRES=0 DUTY=0 NPHASE=1
 STOIC 1 MIXED H2 -2.0 / O2 -1 / H2O 2.0
 STOIC 2 CISOLID C -1.0 / MIXED O2 -1.0 / CO2 1.0
 STOIC 3 MIXED CO -1.0 / O2 -.50 / CO2 1.0
 STOIC 4 MIXED CH4 -1.0 / O2 -2.0 / CO2 1.0 / H2O 2.0
 STOIC 5 MIXED C2H4 -1 / O2 -3 / CO2 2 / H2O 2
 STOIC 6 MIXED C6H6 -1 / O2 -7.5 / CO2 6 / H2O 3
 STOIC 7 MIXED C2H2 -1 / O2 -2.5 / CO2 2 / H2O 1
 STOIC 8 MIXED C2H6 -1 / O2 -3.5 / CO2 2 / H2O 3
 STOIC 9 MIXED NH3 -1 / O2 -1.75 / NO2 1 / H2O 1.5
 STOIC 10 MIXED H2S -1 / O2 -1.5 / H2O 1 / SO2 1
 CONV 1 MIXED H2 1.0
 CONV 2 CISOLID C 1.0
 CONV 3 MIXED CO 1.0
 CONV 4 MIXED CH4 1.0
 CONV 5 MIXED C2H4 1
 CONV 6 MIXED C6H6 1
 CONV 7 MIXED C2H2 1
 CONV 8 MIXED C2H6 1
 CONV 9 MIXED NH3 .5
 CONV 10 MIXED H2S .3
 PROPERTIES RK-SOAVE FREE-WATER=STEAMNBS
 BLOCK OILULTIM RYIELD
 PARAM TEMP=80.0 PRES=3.0
 MASS-YIELD MIXED H2 .080 / CISOLID C .920
 PROPERTIES RK-SOAVE FREE-WATER=STEAMNBS

BLOCK B34 PUMP
 DESCRIPTION "DIESEL PAINEISTUS "
 PARAM PRES=600
 PROPERTIES RK-SOAVE FREE-WATER=STEAMNBS

BLOCK B11 CLCHNG

BLOCK DICLCH CLCHNG

DESIGN-SPEC CHARCOMB
 DEFINE O2 MOLE-FRAC
 SPEC "O2" TO ".01"
 TOL-SPEC ".001"
 VARY STREAM-VAR
 LIMITS ".005" ".008"

DESIGN-SPEC COMBAIR
 DEFINE V1 MOLE-FRAC STREAM=DI6 SUBSTREAM=MIXED COMPONENT=O2
 SPEC "V1" TO ".08"
 TOL-SPEC ".0001"
 VARY STREAM-VAR STREAM=DI11 SUBSTREAM=MIXED &
 VARIABLE=MASS-FLOW
 LIMITS "2" "40"

DESIGN-SPEC COMBO2
 DEFINE O MOLE-FRAC
 SPEC "O" TO ".002"
 TOL-SPEC ".0005"
 VARY STREAM-VAR
 LIMITS ".33" ".45"

DESIGN-SPEC P-EFF
 DEFINE QP INFO-VAR INFO=HEAT VARIABLE=DUTY STREAM=QP
 DEFINE A11 STREAM-VAR STREAM=DI4 SUBSTREAM=MIXED &
 VARIABLE=MASS-FLOW
 DEFINE Q11 STREAM-PROP STREAM=DI4 PROPERTY=LHV
 DEFINE A13 STREAM-VAR STREAM=G6 SUBSTREAM=MIXED &
 VARIABLE=MASS-FLOW
 DEFINE Q13 STREAM-PROP STREAM=G6 PROPERTY=LHV
 DEFINE A12 STREAM-VAR STREAM=DI4 SUBSTREAM=CISOLID &
 VARIABLE=MASS-FLOW
 DEFINE Q12 STREAM-PROP STREAM=DI4 PROPERTY=LHVCIS
 F Q1=A11*Q11+A12*Q12
 F Q2=A13*Q13
 SPEC "QP" TO ".43*(Q1+Q2)*1000"
 TOL-SPEC "100"
 VARY BLOCK-VAR BLOCK=DIHX4 VARIABLE=DUTY SENTENCE=PARAM
 LIMITS "-20000000" "-1000"

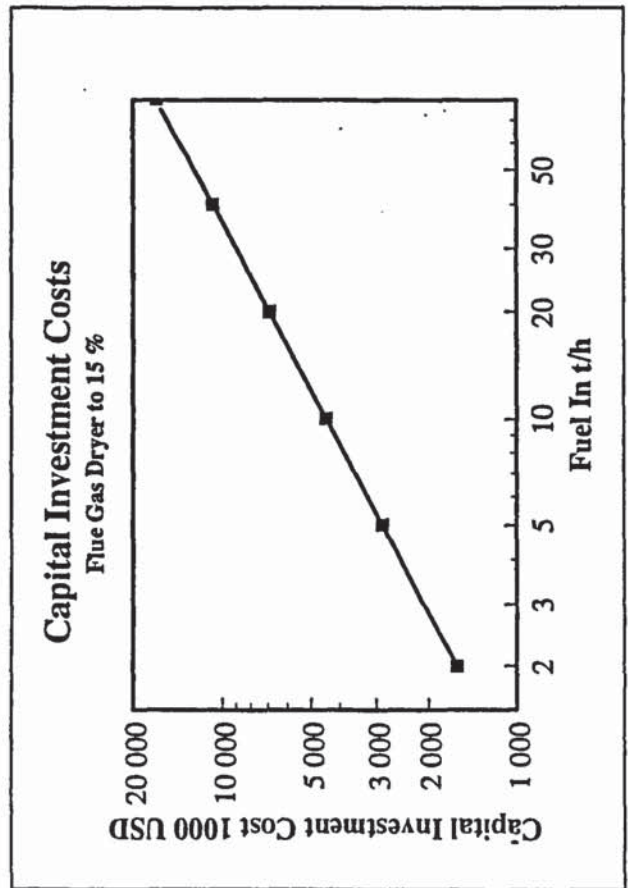
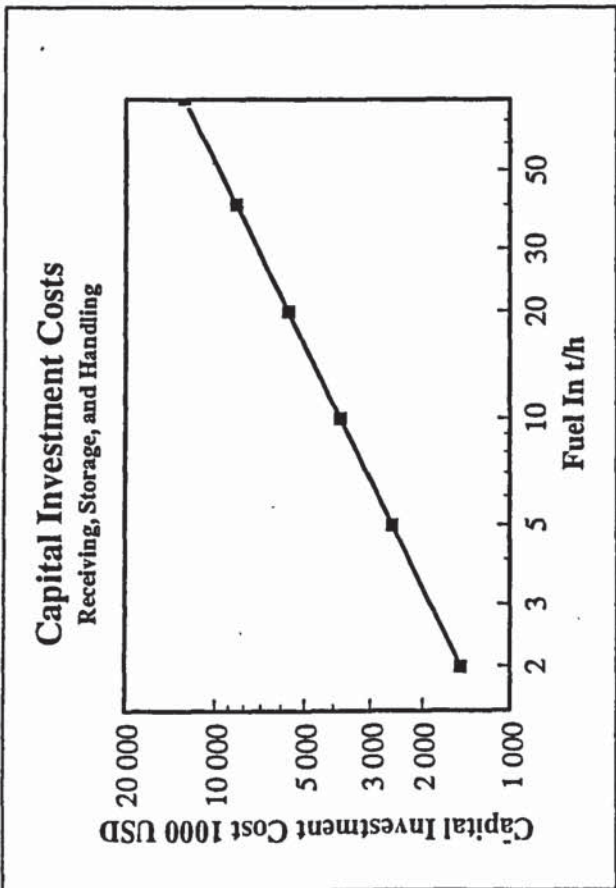
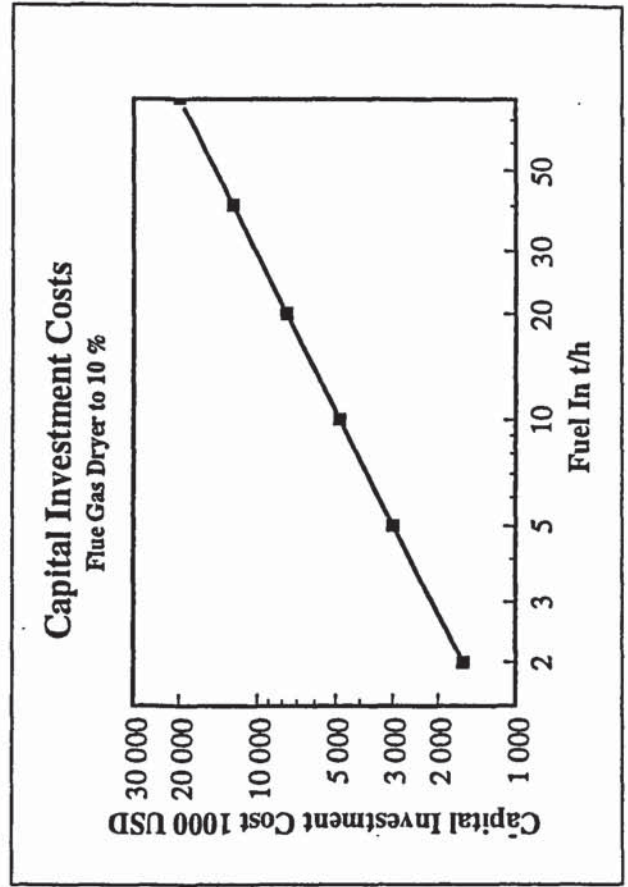
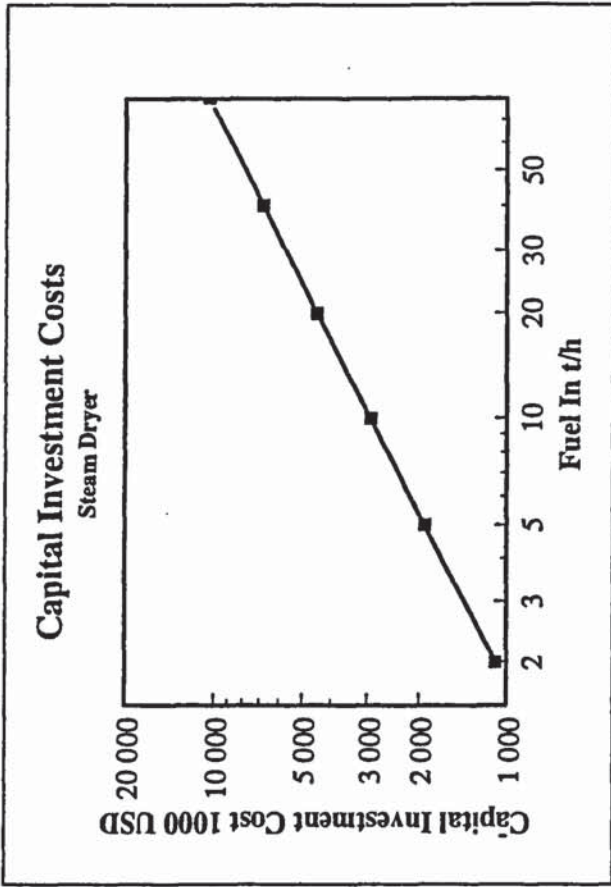
DESIGN-SPEC STOIC-2
 DEFINE O2 MOLE-FRAC
 SPEC "O2" TO ".01"
 TOL-SPEC ".001"
 VARY STREAM-VAR
 LIMITS ".15" ".28"

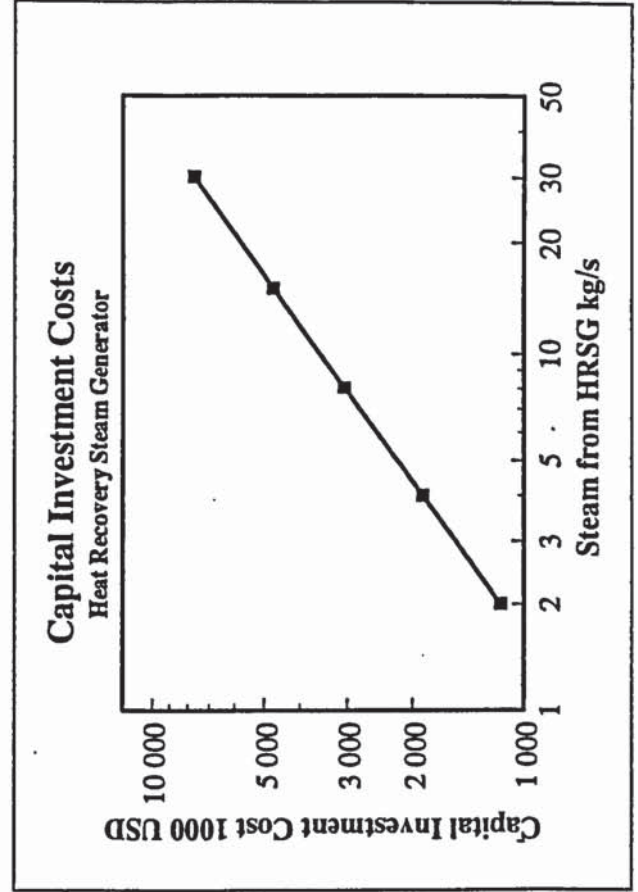
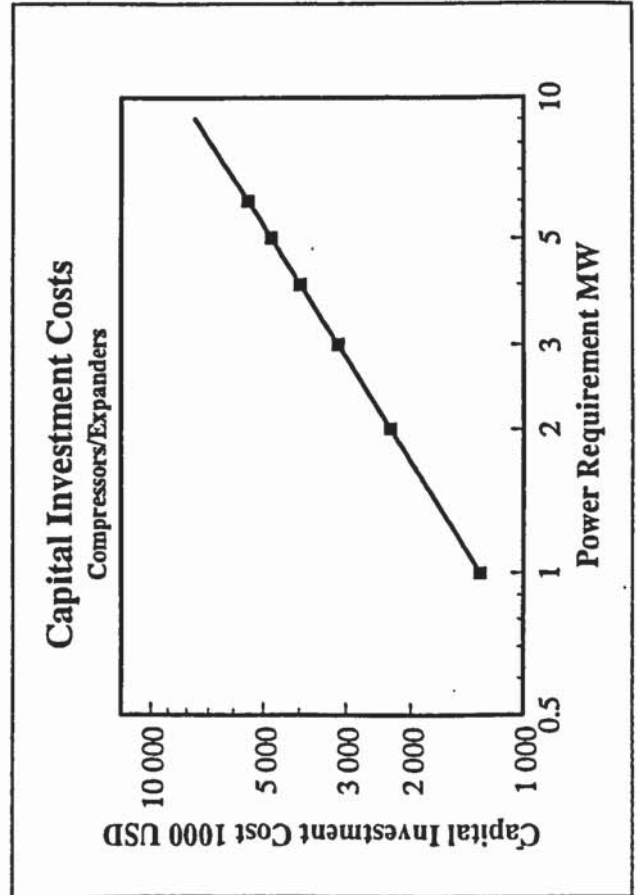
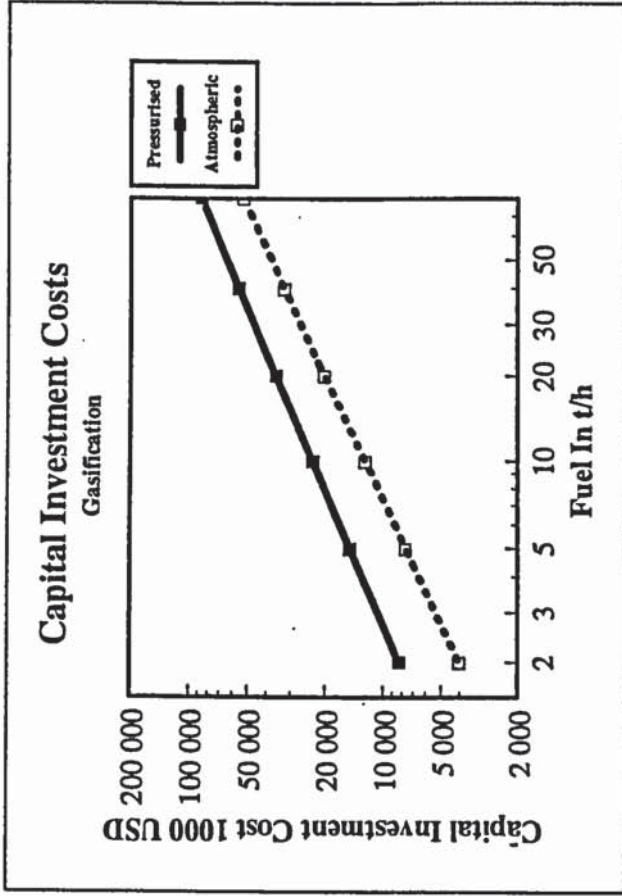
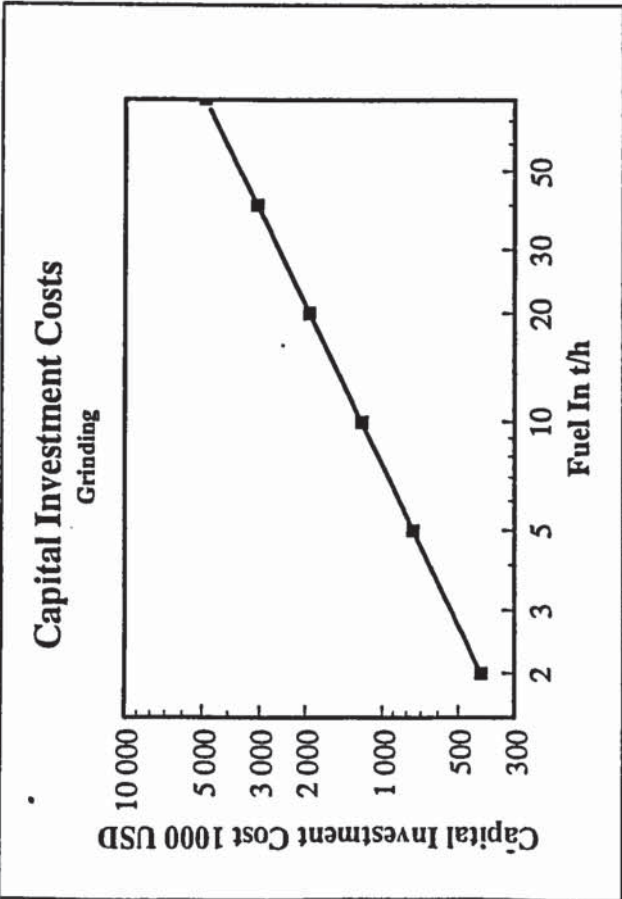
DESIGN-SPEC WORKFIX
 DEFINE Q45 INFO-VAR INFO=HEAT VARIABLE=DUTY STREAM=QP
 SPEC "Q45" TO "10000000"
 TOL-SPEC "100"
 VARY STREAM-VAR
 LIMITS ".5" "2.5"

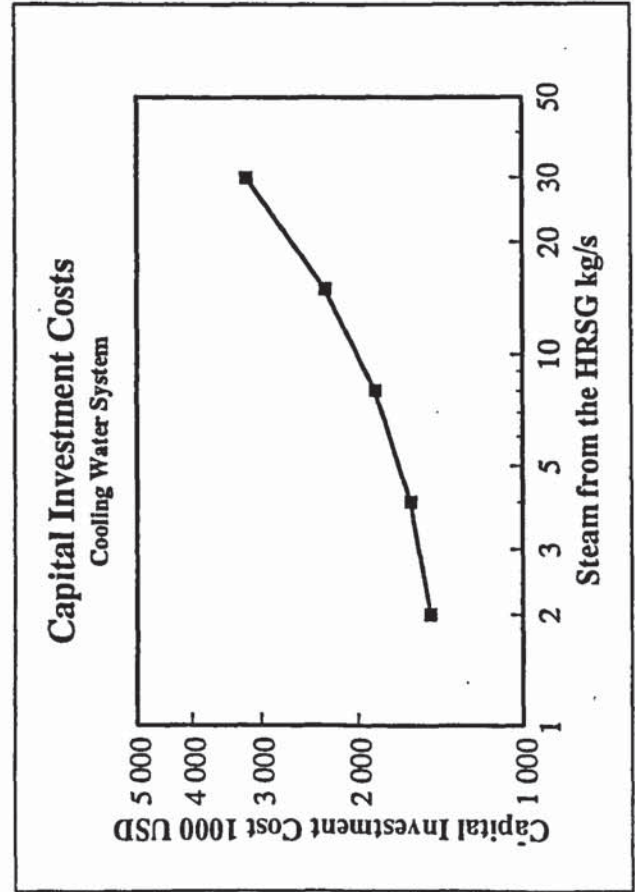
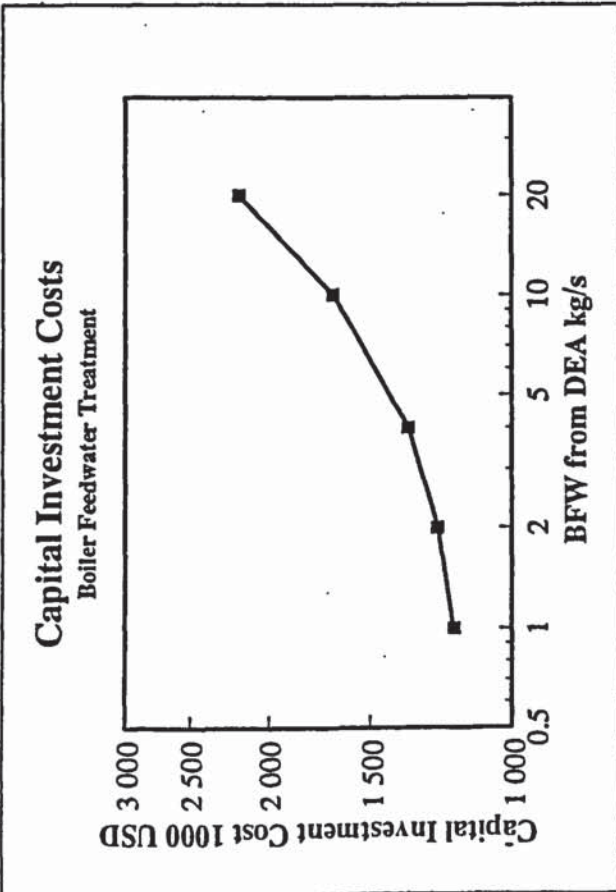
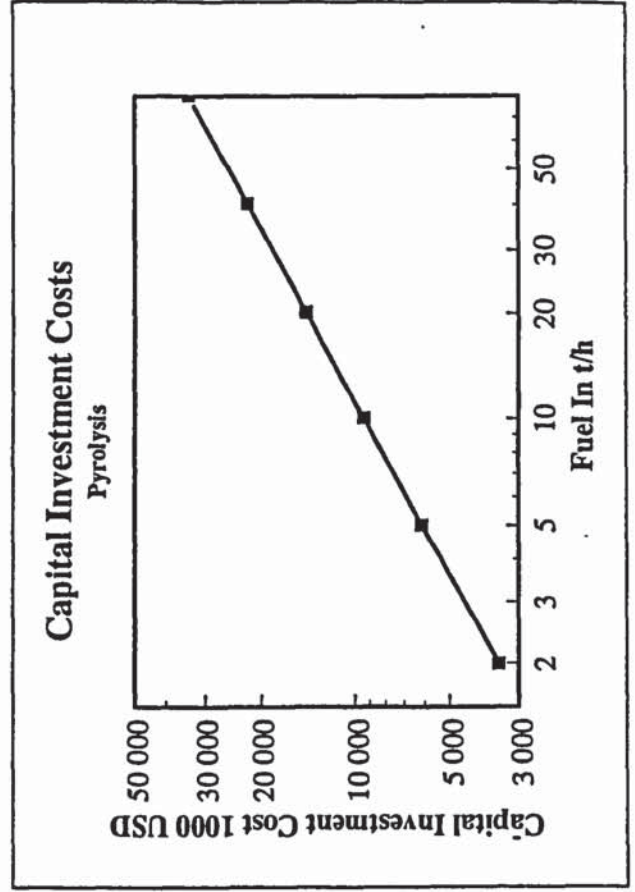
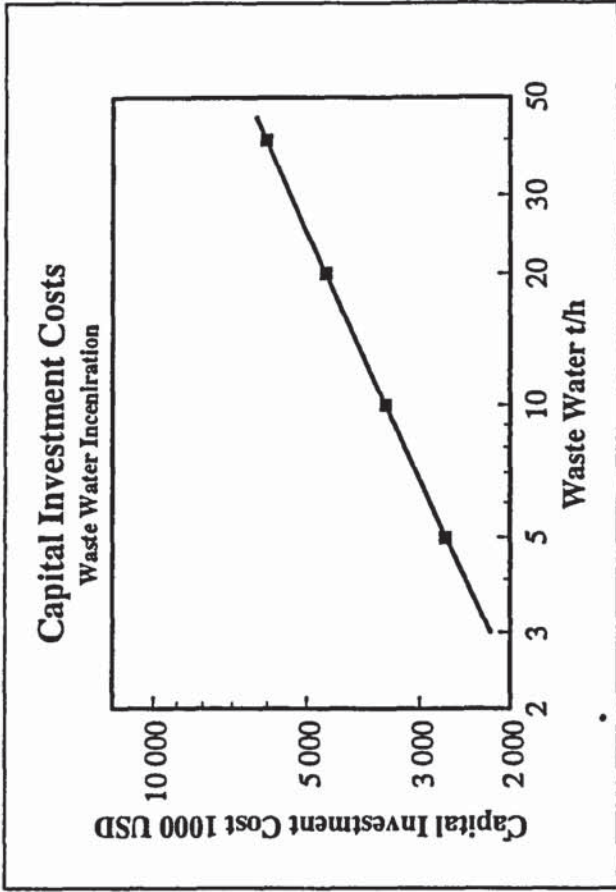
CONV-OPTIONS
 PARAM TEAR-METHOD=BROYDEN CHECKSEQ=YES

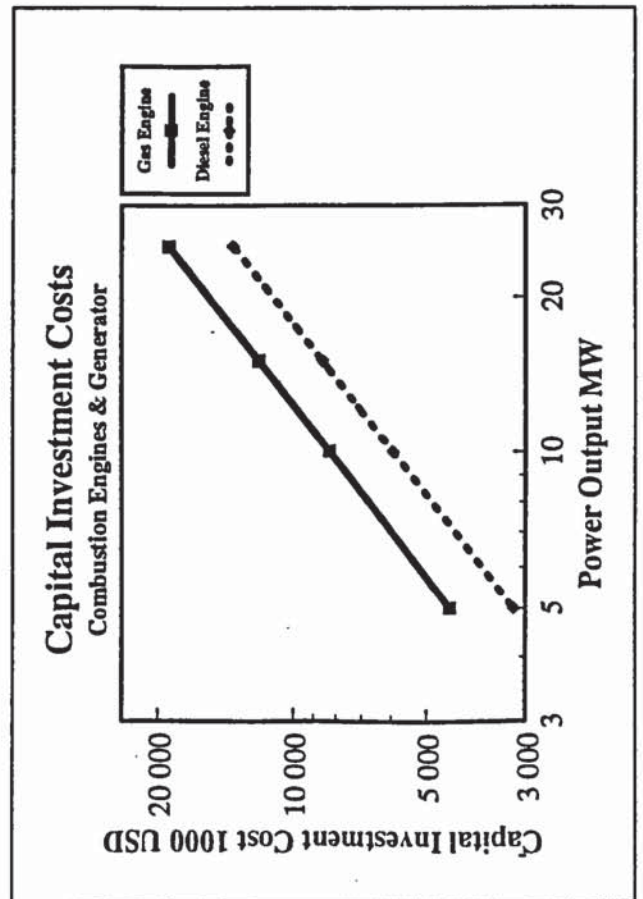
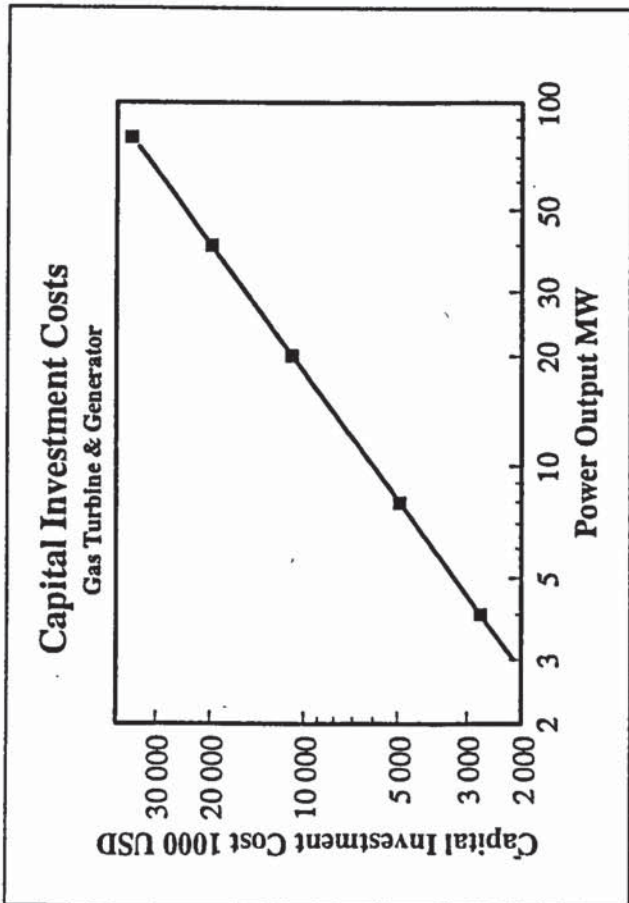
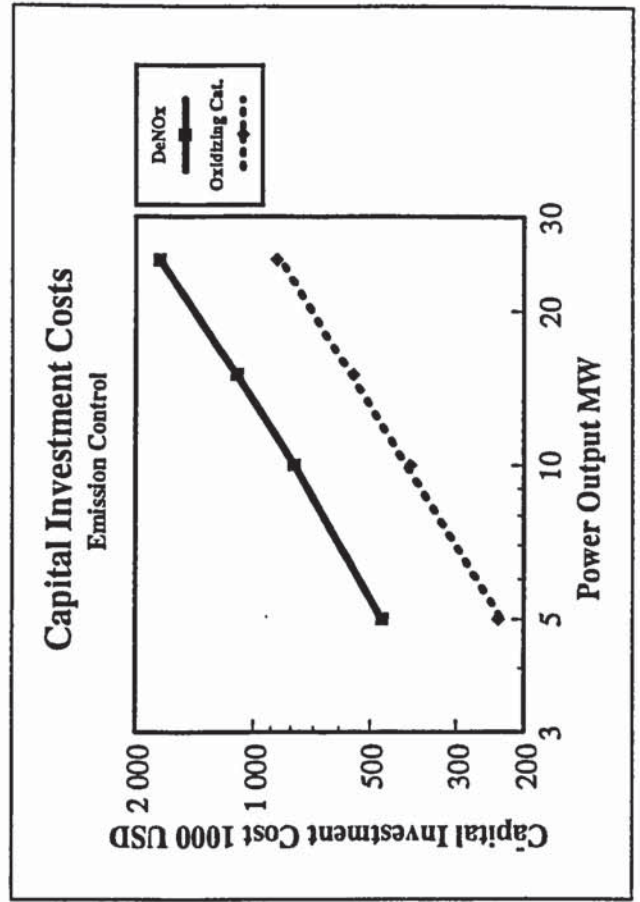
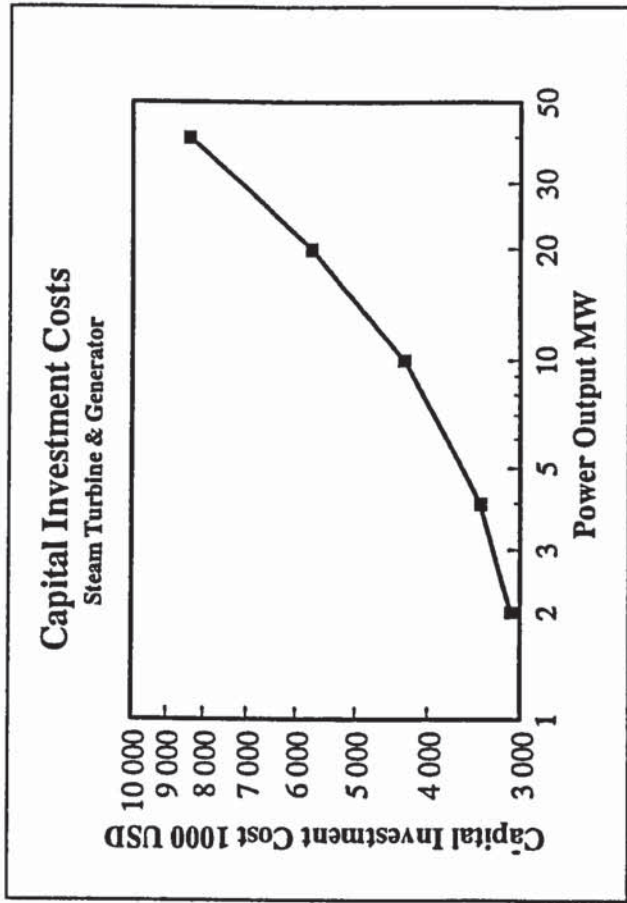
STREAM-REPOR NOSORT MOLEFLOW NOMASSFLOW MOLEFRAC PROPERTIES=LHV

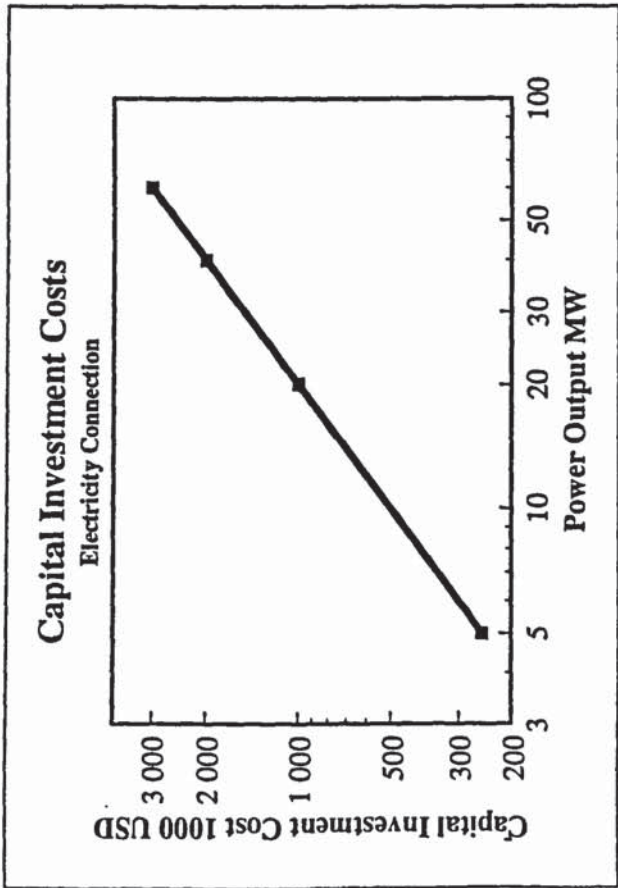
Bases for the unit investment costs











TESTING OF THE METC MODEL

The gas turbine performance model presented by Stone /118/ is tested in this section. The Aspen block flow diagram of the model is depicted in Figure 8-2. The model was used to generate data, which was then compared to the data provide by Fluor and published by EPRI /196/. The engine employed to design the model, although not specified by Stone, was probably the GE MS7001E.

It was observed in this study that if the heat loss for the gas turbine combustor was kept as defined by Stone, the output power would be well below Fluor data (about 370 MW versus 397 MW). Stone defined the heat loss as 4 % of the fuel gas's lower heating value. The amount corresponds to a temperature drop of approximately 60 °C between the combustor and first turbine blades. However, it was found in this work that with a temperature drop of about 18 °C (Figure A12-1), a correct output power is achieved.

Another test with the model is shown in Table A12-1, where model flue gas flow, temperature and output power are compared with the Fluor data at different ambient temperatures. Note that such a calculation cannot be carried out with the original model presented by Stone. The model was modified in this study to include a design specification, whereby the combustion temperature was kept constant by varying the fuel gas flow. Air flows for each temperature were taken from the Fluor data. Although the gas turbine combustion temperature does not remain exactly constant under these circumstances, Palmer and Erbes /178/ show that the firing temperature is essentially the same between 20 and 100 % load with another industrial turbine (Frame 6). It is therefore concluded that this modification is appropriate for the Stone model.

A comparison of the reported values with the model results reveals that the deviations are not major except for the flue gas temperature. However, it is concluded that the studied model is not appropriate for other engines, and another approach is needed in this work. The modelling procedure presented here may produce relatively accurate results with a

certain industrial gas turbine, if critical input parameters are chosen correctly. However, these parameters are not known for other engines. The applicability of this model to the modelling of aero-derivative engines is not known either.

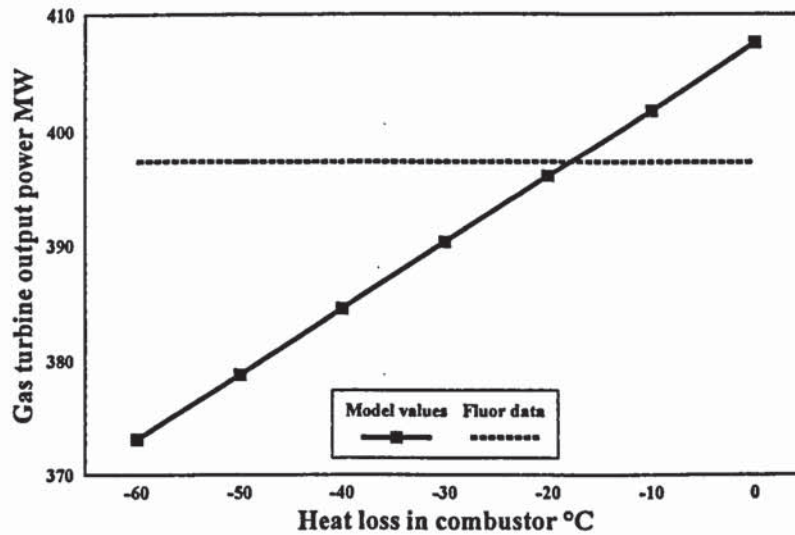


Figure A12-1. Gas turbine output power as a function of heat loss in combustion, testing of the model presented by Stone /118/.

Table A12-1. The effect of ambient temperature on gas turbine performance, comparison of model results with published results /196/.

	Fluor	Ambient temperature °C				
		- 6.7 Model	Fluor	15.0 Model	Fluor	31.1 Model
Air kg/s	1139.8		1049.3		981.6	
Gas turbine MW	461.79	467.07	397.35	397.04	355.68	348.67
Deviation %		+ 1.1		- 0.1		- 2.0
Flue gas kg/s	1269.0	1272.6	1165.2	1165.1	1088.7	1085.6
Deviation %		+ 0.3		- 0.0		- 0.3
Flue gas °C	552.2	579.0	567.7	577.7	580.0	576.8
Deviation %		+ 4.8		+ 1.7		- 0.6

AspenPlus input file for an IGCC

```

;
;Input file created by ModelManager Rel. 3.3-4 on Wed Nov 10 11:43:08 1993
;Directory D:\Y3\IEAEY Runid IEACOGEN
;
TITLE &
  "WOOD GASIFICATION COMBINED-CYCLE, LM2500-PH, HOT GAS CLEAN-UP"

IN-UNITS SI PRESSURE=BAR TEMPERATURE=C

OUT-UNITS SI PRESSURE=BAR TEMPERATURE=C

DEF-STREAMS CONVEN ALL

RUN-CONTROL MAX-TIME=1500

DATABANKS ASPENPCD / DIPRPCD / COMBUST / SOLIDS / AQUEOUS &
  / BINARY

PROP-SOURCES ASPENPCD / DIPRPCD / COMBUST / SOLIDS / &
  AQUEOUS / BINARY

COMPONENTS
H2 H2 H2 /
CO CO CO /
CO2 CO2 CO2 /
CH4 CH4 CH4 /
H2S H2S H2S /
COS COS COS /
N2 N2 N2 /
AR AR AR /
O2 O2 O2 /
NH3 H3N NH3 /
H2O H2O H2O /
SO2 O2S SO2 /
N2O N2O N2O /
NO2 NO2 NO2 /
C6H6 C6H6 C6H6 /
C2H4 C2H4 C2H4 /
C2H2 C2H2 C2H2 /
C10H8 C10H8 C10H8 /
C2H6 C2H6 C2H6 /
C C C /
C6H6O C6H6O C6H6O /
BIOMASS * BIOMASS /
FLYASH * FLYASH /
S S S /
ASH * ASH

FLOWSHEET DEA
BLOCK DEHE1 IN=DE11 ST110 DE21 CO110 DE191 CO1111 OUT= &
  DE12 Q110
BLOCK DEFS1 IN=DE12 OUT=DE14 DE13
BLOCK DEFS2 IN=DE13 OUT=DE15 DE16
BLOCK DEPU1 IN=DE15 OUT=DE17 W110
BLOCK DEPU3 IN=DE16 OUT=DE161 W111
BLOCK DEHE3 IN=DE19 OUT=DE191 Q111
BLOCK DEMX IN=DE112 DE111 OUT=DE11
BLOCK DEHE4 IN=DE141 OUT=DE142 Q112

DEF-STREAMS CONVEN DEA

FLOWSHEET GAS
BLOCK GAS1 IN=GS11 ST31 GA16 OUT=GS12 Q31
BLOCK GSX1 IN=GS12 OUT=GS13 Q32
BLOCK GSCY IN=GS13 OUT=GS14 GS15
BLOCK LOGS4 IN=LO110 OUT=LO111 QL16

```

BLOCK LOGS1 IN=LO111 LO112 LO101 QL16 OUT=LO102 QL12
 BLOCK GSDU IN=GSD1 OUT=GSD2 GSD3

DEF-STREAMS MIXCINC GAS

FLOWSHEET GT

BLOCK GTHE1 IN=GT431 OUT=GT432 GT476 Q41
 BLOCK GTCO3 IN=GT433 OUT=GT434 W43
 BLOCK GTMX5 IN=CL15 OUT=CL16
 BLOCK GTCO1 IN=GT42 OUT=GT43 W41
 BLOCK GTLO2 IN=GT47 OUT=GT48 QL41
 BLOCK GTCO2 IN=GT46 OUT=GT47 W42
 BLOCK GTMX IN=W41 W42 OUT=W40
 BLOCK GTEX IN=GT43 OUT=GT431 GT44
 BLOCK GTLO1 IN=GT41 OUT=GT42
 BLOCK GSCO IN=GS101 OUT=GS102 W21
 BLOCK DR2 IN=CO14 OUT=CO141

DEF-STREAMS CONVEN GT

FLOWSHEET HRSG

BLOCK HRX1 IN=HR24 HR21 GT49 OUT=HR12 HR25 HR22
 BLOCK HRX2 IN=HR12 HR23 OUT=HR13 HR24
 BLOCK HRX3 IN=HR13 HR18 OUT=HR14 HR19
 BLOCK HRX4 IN=HR14 DE142 OUT=HR15 DE18
 BLOCK GASX IN=GS17 HR20 OUT=GS18 HR21
 BLOCK HRFS IN=HR19 OUT=HR20 HR23
 BLOCK HRMX IN=HR25 HR22 OUT=HR26
 BLOCK LOSC1 IN=HR17 OUT=LO107 QL15
 BLOCK HRDU IN=GSD2 OUT=HRD1

DEF-STREAMS CONVEN HRSG

FLOWSHEET KUI

BLOCK DRMX1 IN=DR11 DR19 OUT=DR12
 BLOCK DRHX1 IN=ST11 DR12 OUT=CO11 DR13
 BLOCK DRMX2 IN=CO11 CO12 OUT=CO13
 BLOCK DRX4 IN=CO13 DH11 OUT=CO14 DH12
 BLOCK DRX3 IN=DR15 DH13 OUT=CO15 DH14
 BLOCK DRX2 IN=ST12 DR17 OUT=CO12 DR18
 BLOCK DRVE IN=DR20 OUT=GS11 Q11
 BLOCK LODR1 IN=CO15 OUT=LO100 QL10

DEF-STREAMS MIXCINC KUI

FLOWSHEET ST

BLOCK STCO1 IN=HR26 OUT=ST62 W61
 BLOCK STFS1 IN=ST62 OUT=ST622 ST63
 BLOCK STCO2 IN=ST63 OUT=ST64 W62
 BLOCK STFS2 IN=ST64 OUT=ST642 ST65
 BLOCK STCO3 IN=ST65 OUT=ST66 W63
 BLOCK STHX IN=ST66 DH61 OUT=CO61 DH62
 BLOCK WTOT IN=W61 W62 W63 OUT=W60

DEF-STREAMS CONVEN ST

PROPERTIES SYSOP3

PROPERTIES SYSOP12 DEA / SYSOP12 ST / SYSOP3 HRSG / &
 SYSOP3 SYS15 / SYSOP12 KUI
 PROPERTIES SYSOP0

NC-COMPS BIOMASS PROXANAL ULTANAL SULFANAL GENANAL

NC-PROPS BIOMASS ENTHALPY HCOALGEN 6 / DENSITY DNSTYGEN

NC-COMPS FLYASH PROXANAL ULTANAL SULFANAL GENANAL

NC-PROPS FLYASH ENTHALPY HCOALGEN 6 / DENSITY DNSTYGEN

NC-COMPS ASH PROXANAL ULTANAL SULFANAL GENANAL

NC-PROPS ASH ENTHALPY HCOALGEN 2 / DENSITY DNSTYGEN

PROP-DATA DATA1

IN-UNITS SI
 PROP-LIST DENGEN
 PVAL BIOMASS 1.0
 PVAL FLYASH 1.0
 PVAL ASH 1

PROP-DATA DATA2

IN-UNITS SI PRESSURE=BAR TEMPERATURE=C
 PROP-LIST HCOMB
 PVAL BIOMASS 2.022E+7
 PVAL FLYASH 9.6E+7

MODEL-PARAME ESRKS / APIRKS

STREAM CO1111

SUBSTREAM MIXED TEMP=120 PRES=5 MASS-FLOW=11
 MASS-FRAC H2O 1

STREAM D1

SUBSTREAM MIXED TEMP=120.0 PRES=100 MOLE-FLOW=100.0 <KMOL/HR>
 MOLE-FRAC H2O 1.0

STREAM DE111

SUBSTREAM MIXED TEMP=15 PRES=5.0 MASS-FLOW=.00001
 MASS-FRAC H2O 1.0

STREAM DH51

SUBSTREAM MIXED TEMP=55 PRES=4.0 MASS-FLOW=10.0
 MOLE-FRAC H2O 1.0

STREAM DH61

SUBSTREAM MIXED TEMP=55 PRES=4.0 MASS-FLOW=129
 MASS-FRAC H2O 1.0

STREAM DR11

SUBSTREAM MIXED TEMP=15 PRES=1.5
 MASS-FLOW H2O 4.1274
 SUBSTREAM NC TEMP=15 PRES=1.5
 MASS-FLOW BIOMASS 4.1274
 COMP-ATTR BIOMASS PROXANAL (.0 25 74.5 .5)
 COMP-ATTR BIOMASS ULTANAL (.5 50.4 5.97 .1 0 0 43.03 &
)
 COMP-ATTR BIOMASS SULFANAL (.0 0 0)
 COMP-ATTR BIOMASS GENANAL (100.0)

STREAM DR19

SUBSTREAM MIXED TEMP=200.0 PRES=5.120 MASS-FLOW=10.0
 MASS-FRAC H2O 1.0

STREAM GS101

SUBSTREAM MIXED TEMP=30 PRES=1 MOLE-FLOW=1
 MOLE-FRAC N2 1

STREAM GS17

SUBSTREAM MIXED TEMP=850 PRES=25.0 MOLE-FLOW=.4817514 &
 NPHASE=1
 MOLE-FRAC H2 .1242 / CO .1854 / CO2 .1162 / CH4 .0442 &
 / H2S 0 / N2 .4109 / NH3 0 / H2O .1129 / C6H6 &
 0 / C2H4 .0062 / C2H2 0

STREAM GT41

SUBSTREAM MIXED TEMP=15 PRES=1.013250 MASS-FLOW=64.1108
 MOLE-FRAC N2 .7770 / AR .010 / O2 .20920 / H2O &
 3.800E-03

STREAM GT45

SUBSTREAM MIXED TEMP=480.0 PRES=22.0 MASS-FLOW=11.9958 &
 NPHASE=1
 MOLE-FRAC H2 .12420 / CO .18550 / CO2 .11620 / CH4 &
 .04420 / N2 .41080 / NH3 .0 / H2O .11290 / C2H4 &

6.200E-03

STREAM HR18

SUBSTREAM MIXED TEMP=140 PRES=100 MASS-FLOW=12.4
MASS-FRAC H2O 1.0

STREAM LO101

SUBSTREAM MIXED TEMP=15 PRES=1 MASS-FLOW=4.5
MOLE-FRAC N2 .79 / O2 .21

STREAM ST11

SUBSTREAM MIXED TEMP=327.8 PRES=25.0
MASS-FLOW H2O 5

STREAM ST110

SUBSTREAM MIXED TEMP=190.0 PRES=5.0 MASS-FLOW=1.000E-05
MASS-FRAC H2O 1.0

STREAM ST12

SUBSTREAM MIXED TEMP=327.8 PRES=25.0
MASS-FLOW H2O .50

STREAM ST31

SUBSTREAM MIXED TEMP=327.8 PRES=25.0 MASS-FLOW=2.8554167
MASS-FRAC H2O 1.0

DEF-STREAMS HEAT QD

DEF-STREAMS HEAT QL10

DEF-STREAMS HEAT QL11

DEF-STREAMS HEAT QL12

DEF-STREAMS HEAT QL15

DEF-STREAMS HEAT QL16

DEF-STREAMS HEAT QL41

DEF-STREAMS WORK W11

DEF-STREAMS WORK W110

DEF-STREAMS WORK W111

DEF-STREAMS WORK W112

DEF-STREAMS WORK W21

DEF-STREAMS WORK W40

DEF-STREAMS WORK W41

DEF-STREAMS WORK W42

DEF-STREAMS WORK W63

DEF-STREAMS WORK W64

BLOCK DEMX MIXER

PARAM PRES=.0
PROPERTIES SYSOP12

BLOCK DRMX1 MIXER

PROPERTIES SYSOP12

BLOCK DEFS2 FSPLIT

FRAC DE16 .010

BLOCK DEFS3 FSPLIT

MASS-FLOW DE20 .0

BLOCK DRCY2 FSPLIT
 FRAC DR15 .20
 PROPERTIES SYSOP12

BLOCK GTEX FSPLIT
 PARAM NPHASE=1
 MASS-FLOW GT431 7.1808

BLOCK HRFS FSPLIT
 FRAC HR20 .3580286
 PROPERTIES SYSOP12

BLOCK STFS1 FSPLIT
 PARAM NPHASE=1
 MASS-FLOW ST622 13
 PROPERTIES SYSOP12

BLOCK STFS2 FSPLIT
 PARAM NPHASE=1
 FRAC ST642 1.000E-05
 PROPERTIES SYSOP12

BLOCK GSCY SEP
 FRAC STREAM=GS14 SUBSTREAM=MIXED COMPS=H2 CO CO2 CH4 &
 H2S COS N2 AR O2 NH3 H2O SO2 N2O NO2 C6H6 C2H4 &
 C2H2 C10H8 C2H6 C6H6O FRACS=1 1 1 1 1 0 1 0 0 1 &
 1 0 0 0 0 1 1 0 0 0
 FRAC STREAM=GS14 SUBSTREAM=CISOLID COMPS=C S FRACS=0 0
 FRAC STREAM=GS14 SUBSTREAM=NC COMPS=BIOMASS FLYASH FRACS=&
 0 0

BLOCK LOGS3 SEP
 FRAC STREAM=LO110 SUBSTREAM=MIXED COMPS=H2 CO CO2 CH4 &
 H2S COS N2 AR O2 NH3 H2O SO2 N2O NO2 C6H6 C2H4 &
 C2H2 C10H8 C2H6 C6H6O FRACS=0 0 0 0 0 0 0 0 0 0 &
 0 0 0 0 0 0 0 0 0 0
 FRAC STREAM=LO110 SUBSTREAM=CISOLID COMPS=C S FRACS=0 0
 FRAC STREAM=LO110 SUBSTREAM=NC COMPS=BIOMASS FLYASH &
 FRACS=0 1

BLOCK DEHE1 HEATER
 PARAM TEMP=140 VFRAC=.0

BLOCK DEHE3 HEATER
 PARAM TEMP=90 PRES=2.0
 PROPERTIES SYSOP12

BLOCK DEHE4 HEATER
 PARAM TEMP=130 PRES=.0
 PROPERTIES SYSOP12

BLOCK DRVE HEATER
 PARAM PRES=25 DELT=-.50

BLOCK GSX1 HEATER
 PARAM TEMP=500 PRES=0

BLOCK GTHE1 HEATER
 PARAM TEMP=100.0 PRES=.0
 PROPERTIES SYSOP3
 BLOCK-OPTION FREE-WATER=YES

BLOCK DRCY1 FLASH2
 PARAM PRES=-.20 VFRAC=.82350
 PROPERTIES SYSOP12

BLOCK DUMMY FLASH2
 PARAM PRES=60.0 VFRAC=1.0
 PROPERTIES SYSOP12

BLOCK DRHX1 HEATX

PARAM DEGSUB-HOT=10.0 PRES-COLD=-.120
 FEEDS HOT=ST11 COLD=DR12
 PRODUCTS HOT=CO11 COLD=DR13
 HEAT-TR-COEF U=300.0
 PROPERTIES SYSOP12 / SYSOP12

BLOCK STHX HEATX
 PARAM VFRAC-HOT=.0 PRES-HOT=.0 PRES-COLD=.0
 FEEDS HOT=ST66 COLD=DH61
 PRODUCTS HOT=CO61 COLD=DH62
 PROPERTIES SYSOP12 / SYSOP12

BLOCK DRX2 MHEATX
 HOT-SIDE IN=ST12 OUT=CO12 DEGSUB=10.0
 COLD-SIDE IN=DR17 OUT=DR18

BLOCK DRX3 MHEATX
 HOT-SIDE IN=DR15 OUT=CO15 TEMP=95
 COLD-SIDE IN=DH13 OUT=DH14

BLOCK DRX4 MHEATX
 HOT-SIDE IN=CO13 OUT=CO14 DELT=-120
 COLD-SIDE IN=DH11 OUT=DH12 NPHASE=1 PHASE=L
 STREAM-PROPE DH11 SYSOP12

BLOCK HRX1 MHEATX
 COLD-SIDE IN=HR24 OUT=HR25 TEMP=485 NPHASE=1
 COLD-SIDE IN=HR21 OUT=HR22 TEMP=485 NPHASE=1
 HOT-SIDE IN=GT49 OUT=HR12

BLOCK HRX2 MHEATX
 HOT-SIDE IN=HR12 OUT=HR13
 COLD-SIDE IN=HR23 OUT=HR24 VFRAC=1.0
 STREAM-PROPE HR23 SYSOP12
 STREAM-PROPE HR12 SYSOP3

BLOCK HRX5 MHEATX
 HOT-SIDE IN=HR15 OUT=HR16
 COLD-SIDE IN=DE161 OUT=DE21 VFRAC=.30
 STREAM-PROPE HR15 SYSOP3
 STREAM-PROPE DE161 SYSOP12

BLOCK HRX6 MHEATX
 HOT-SIDE IN=HR16 OUT=HR17
 COLD-SIDE IN=DH51 OUT=DH52 TEMP=85.0
 STREAM-PROPE HR16 SYSOP3
 STREAM-PROPE DH51 SYSOP12

BLOCK GTRE RSTOIC
 PARAM PRES=-.50 DUTY=0 NPHASE=1
 STOIC 1 MIXED H2 -2.0 / O2 -1.0 / H2O 2.0
 STOIC 2 MIXED CO -2.0 / O2 -1.0 / CO2 2.0
 STOIC 3 MIXED CH4 -1.0 / O2 -2.0 / CO2 1.0 / H2O 2.0
 STOIC 4 MIXED H2S -2.0 / O2 -3.0 / H2O 2.0 / SO2 2.0
 STOIC 5 MIXED COS -1.0 / O2 -1.50 / CO2 1.0 / SO2 &
 1.0
 STOIC 6 MIXED NH3 -2.0 / O2 -3.50 / NO2 2.0 / H2O &
 3.0
 STOIC 7 MIXED C6H6 -1.0 / O2 -7.50 / CO2 6.0 / H2O &
 3.0
 STOIC 8 MIXED C2H4 -1.0 / O2 -3.0 / CO2 2.0 / H2O &
 2.0
 STOIC 9 MIXED C2H2 -1.0 / O2 -2.50 / CO2 2.0 / H2O &
 1.0
 STOIC 10 MIXED C10H8 -1.0 / O2 -12.0 / CO2 10.0 / H2O &
 4.0
 STOIC 11 MIXED NH3 -2.0 / O2 -1.50 / N2 1.0 / H2O &
 3.0
 CONV 1 MIXED H2 1.0
 CONV 2 MIXED CO 1.0
 CONV 3 MIXED CH4 1.0
 CONV 4 MIXED H2S 1.0

CONV 5 MIXED COS 1.0
 CONV 6 MIXED NH3 .50
 CONV 7 MIXED C6H6 1.0
 CONV 8 MIXED C2H4 1.0
 CONV 9 MIXED C2H2 1.0
 CONV 10 MIXED C10H8 1.0
 CONV 11 MIXED NH3 .50

BLOCK GAS1 RYIELD

PARAM TEMP=850.0 PRES=25.0
 MASS-YIELD MIXED H2 .01 / CO .2073 / CO2 .2042 / CH4 &
 .0283 / H2O .0812 / NC FLYASH .0025 / MIXED N2 &
 .45916 / C2H4 5.600E-03 / NH3 .00034
 COMP-ATTR NC FLYASH PROXANAL (.0 28.4 .0 71.6)
 COMP-ATTR NC FLYASH ULTANAL (71.6 28.4 .0 .0 .0 .0 &
 .0)
 COMP-ATTR NC FLYASH SULFANAL (.0 .0 .0)

BLOCK LOGS4 RYIELD

PARAM TEMP=320 PRES=0
 MASS-YIELD CISOLID C .284 / NC ASH .716
 COMP-ATTR NC ASH PROXANAL (0 0 0 100)
 COMP-ATTR NC ASH ULTANAL (100 0 0 0 0 0)
 COMP-ATTR NC ASH SULFANAL (0 0 0)
 COMP-ATTR NC ASH GENANAL (100)

BLOCK DEPU1 PUMP

PARAM PRES=61

BLOCK DEPU2 PUMP

PARAM PRES=25.0
 PROPERTIES SYSOP12

BLOCK DEPU3 PUMP

PARAM PRES=5
 PROPERTIES SYSOP12

BLOCK STPU PUMP

PARAM PRES=3.0
 PROPERTIES SYSOP12
 BLOCK-OPTION FREE-WATER=NO

BLOCK DRCO COMPR

PARAM TYPE=POLYTROPIC DELP=.440
 PROPERTIES SYSOP12

BLOCK GSCO COMPR

PARAM TYPE=ISENTROPIC PRES=25

BLOCK GTCO1 COMPR

PARAM TYPE=ISENTROPIC PRES=18.23 SEFF=.841

BLOCK GTCO2 COMPR

PARAM TYPE=ISENTROPIC DELP=-16.7 SEFF=.8662375 MEFF=1.0

BLOCK GTCO3 COMPR

PARAM TYPE=ISENTROPIC PRES=28 SEFF=.850

DESIGN-SPEC DEAQ

DEFINE Q BLOCK-VAR BLOCK=DEHE1 VARIABLE=QCALC &
 SENTENCE=PARAM
 SPEC "Q" TO "0"
 TOL-SPEC "1310"
 VARY BLOCK-VAR BLOCK=DEFS2 SENTENCE=FRAC VARIABLE=FRAC &
 ID1=DE16
 LIMITS ".01" ".4"

DESIGN-SPEC GSQT00

DEFINE Q BLOCK-VAR BLOCK=GAS1 VARIABLE=QCALC SENTENCE=PARAM
 SPEC "Q" TO "0"
 TOL-SPEC "100"
 VARY BLOCK-VAR BLOCK=GAS1 VARIABLE=TEMP SENTENCE=PARAM

```

LIMITS "400" "1200"

DESIGN-SPEC STEAM
  DEFINE Q BLOCK-VAR BLOCK=DRCY1 VARIABLE=QCALC &
    SENTENCE=PARAM
  SPEC "Q" TO "0"
  TOL-SPEC "500"
  VARY STREAM-VAR STREAM=ST11 SUBSTREAM=MIXED &
    VARIABLE=MASS-FLOW
  LIMITS "3" "15"

DESIGN-SPEC WHB
  DEFINE T1 STREAM-VAR STREAM=HR21 SUBSTREAM=MIXED &
    VARIABLE=TEMP
  DEFINE T2 STREAM-VAR STREAM=D2 SUBSTREAM=MIXED &
    VARIABLE=TEMP
  SPEC "T1" TO "T2+.2"
  TOL-SPEC ".1"
  VARY BLOCK-VAR BLOCK=HRFS SENTENCE=FRAC VARIABLE=FRAC &
    ID1=HR20
  LIMITS ".05" ".9"

FORTRAN D2
  DEFINE PP BLOCK-VAR BLOCK=DEPU1 VARIABLE=PRES &
    SENTENCE=PARAM
  DEFINE DP BLOCK-VAR BLOCK=DUMMY VARIABLE=PRES &
    SENTENCE=PARAM
  F DP=PP
  EXECUTE BEFORE BLOCK DUMMY

FORTRAN DE112
  DEFINE HDE20 BLOCK-VAR BLOCK=DEFS3 SENTENCE=MASS-FLOW &
    VARIABLE=FLOW ID1=DE20
  DEFINE HST31 MASS-FLOW STREAM=ST31 SUBSTREAM=MIXED &
    COMPONENT=H2O
  DEFINE HDE112 MASS-FLOW STREAM=DE112 SUBSTREAM=MIXED &
    COMPONENT=H2O
  F HDE112=HDE20+HST31
  EXECUTE BEFORE BLOCK DEMX

FORTRAN FEED
  DEFINE MDS STREAM-VAR STREAM=DR11 SUBSTREAM=NC &
    VARIABLE=MASS-FLOW
  DEFINE MH2O STREAM-VAR STREAM=DR11 SUBSTREAM=MIXED &
    VARIABLE=MASS-FLOW
  F MH2O=MDS
  EXECUTE BEFORE BLOCK DRM1

FORTRAN GSSTBA
  DEFINE MS STREAM-VAR STREAM=ST31 SUBSTREAM=MIXED &
    VARIABLE=MASS-FLOW
  DEFINE MD STREAM-VAR STREAM=GS11 SUBSTREAM=NC &
    VARIABLE=MASS-FLOW
  F MS=.0*MD
  READ-VARS MD
  WRITE-VARS MS

FORTRAN HR18
  DEFINE PDEPU1 BLOCK-VAR BLOCK=DEPU1 VARIABLE=PRES &
    SENTENCE=PARAM
  DEFINE PHR18 STREAM-VAR STREAM=HR18 SUBSTREAM=MIXED &
    VARIABLE=PRES
  F PHR18=PDEPU1
  EXECUTE BEFORE BLOCK $HRX3H02

FORTRAN MOIST
  DEFINE P STREAM-VAR STREAM=DR13 SUBSTREAM=NC &
    VARIABLE=MASS-FLOW
  DEFINE V STREAM-VAR STREAM=DR13 SUBSTREAM=MIXED &
    VARIABLE=MASS-FLOW
  DEFINE VF BLOCK-VAR BLOCK=DRCY1 VARIABLE=VFRAC &
    SENTENCE=PARAM

```

F VF=1-0.15*P/(V*.85)

READ-VARS P V

WRITE-VARS VF

TRANSFER CO14

SET STREAM CO1111

EQUAL-TO STREAM CO141

TRANSFER GS17

SET STREAM GS17

EQUAL-TO STREAM HRD1

TRANSFER GSD

SET STREAM GSD1

EQUAL-TO STREAM GS12

CONVERGENCE BFW SECANT

SPEC WHB

PARAM BRACKET=YES

SEQUENCE SEQ2 DEFS3 DEMX

STREAM-REPOR MOLEFLOW MOLEFRAC NOATTR-DESC NOCOMP-ATTR &

NOSUBS-ATTR EXCL-STREAMS=LO100 LO110 LO112 LO111 LO102 &

LO103 D1 D2 D3 LO107

;

Building an AspenPlus model

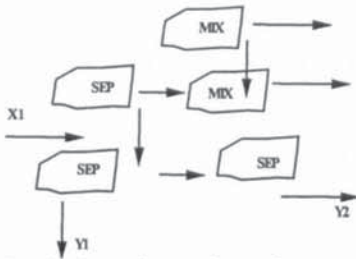
Introduction

In this Appendix building an AspenPlus model is described.

Key steps

The key steps in building a model are:

1. Define the process flowsheet to be modeled and the purpose of the model.



2. Select the units of measurement for input data and output reports (Figure A14-1). There is three build-in alternatives within Aspen, English engineering units, metric units, and SI units.

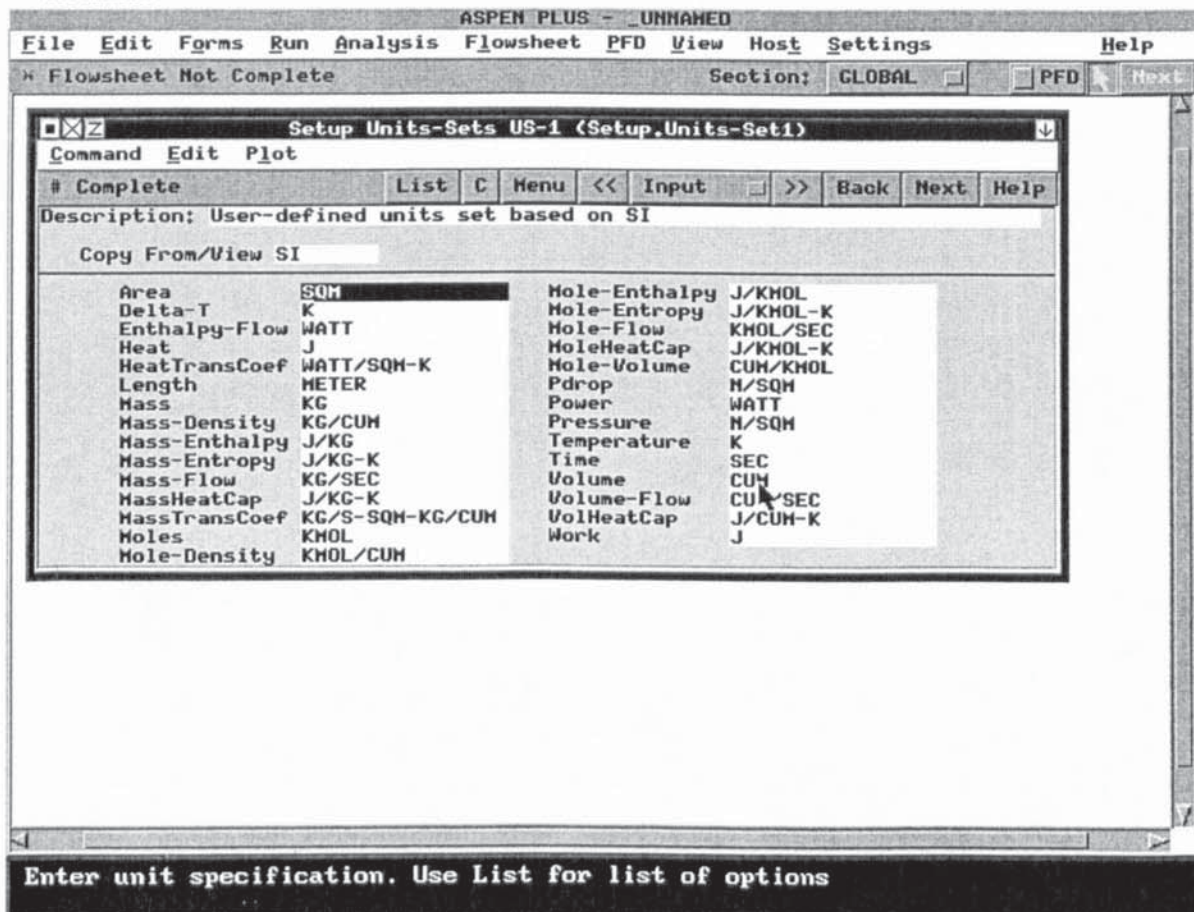


Figure A14-1

3. Specify the participating chemical components which will be present in the streams of the flowsheet (Figure A14-2). There are two types of compounds, mixed and non-conventional. The last are not pure chemical species, solid fuels being examples. Only enthalpy and density are calculated for non-conventional compounds.

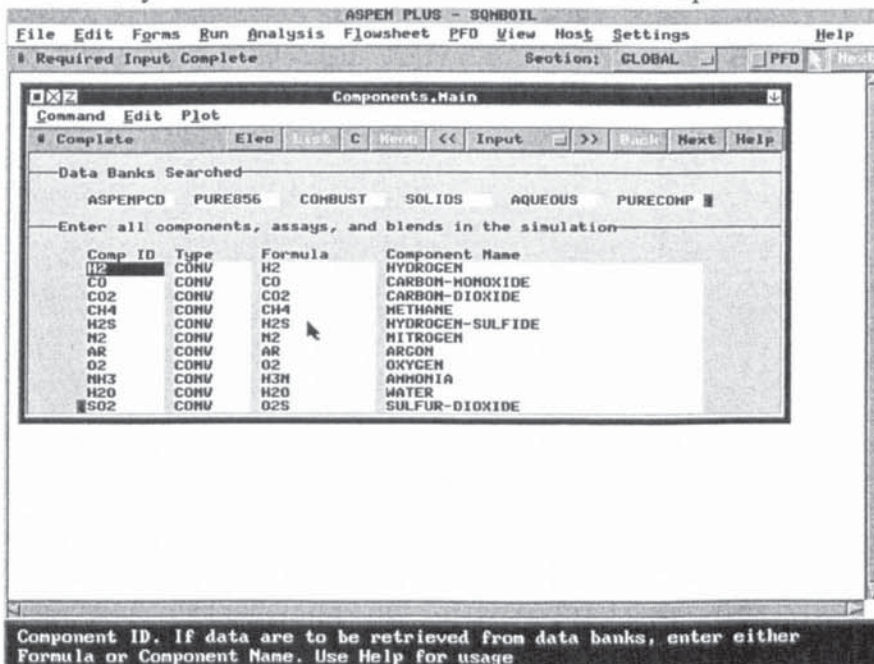


Figure A14-2

4. Specify the models and methods to be used for calculating the physical properties (Figure A14-3). Models and methods used to calculate thermodynamic and transport properties are packaged in AspenPlus in built-in option sets. Physical property parameters have to be supplied for the option sets. Much is available directly in AspenPlus.

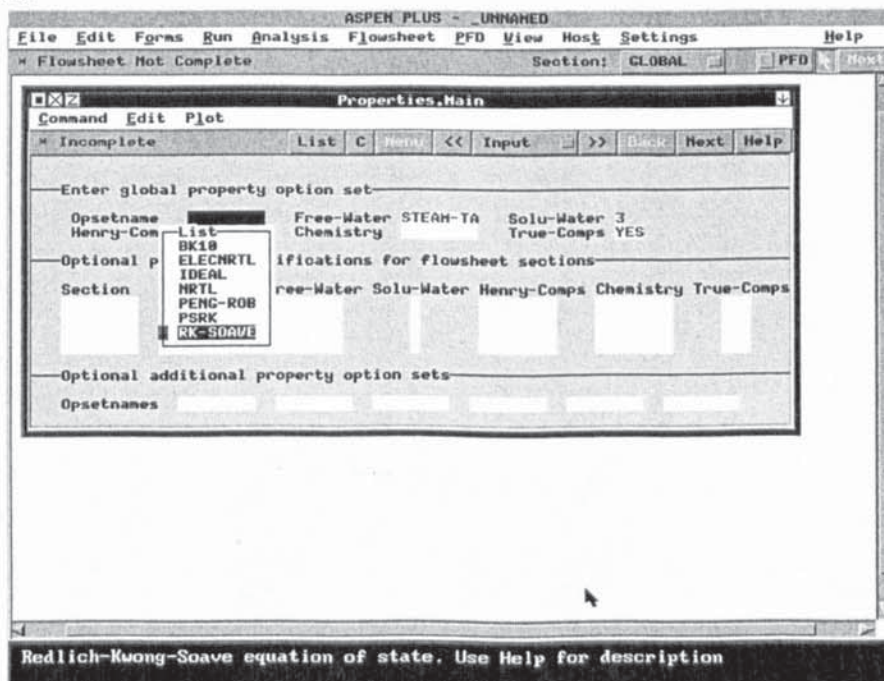


Figure A14-3

- Flowsheet connectivity. Using built-in unit operation blocks, process model connectivity is established in a graphical user interface (Figure A14-4). Unit operation models include turbines, chemical reactors, absorber columns, heat exchangers etc.

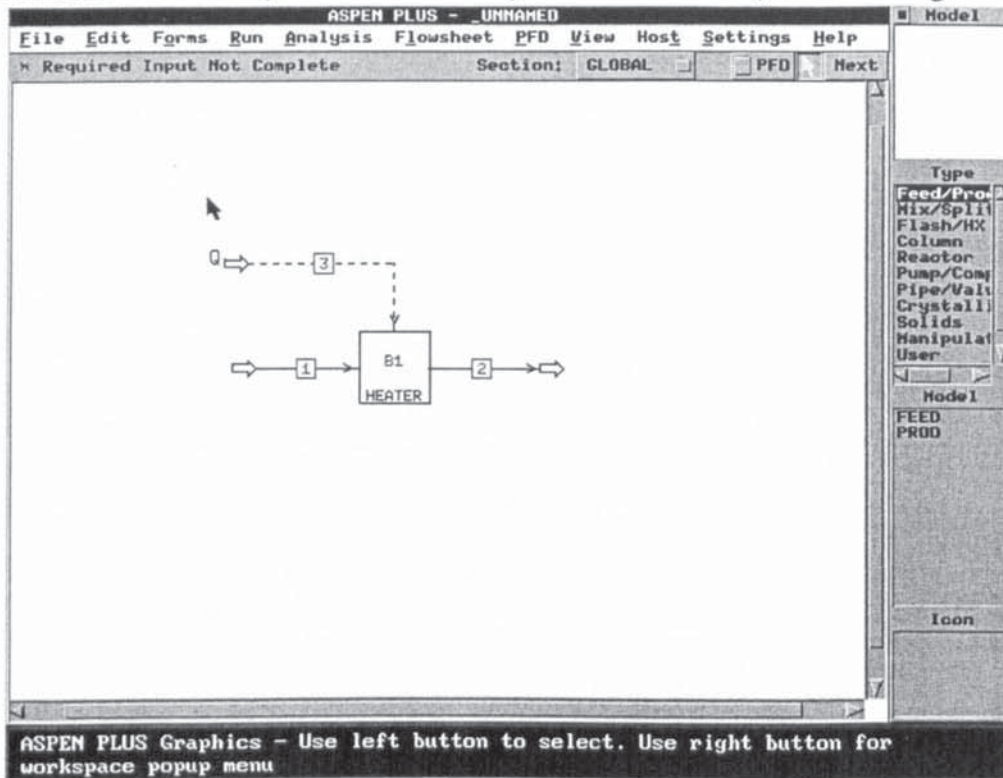


Figure A14-4

- Input streams are defined (Figure A14-5). This includes mass (or mole) flow, flow composition, temperature, and pressure.

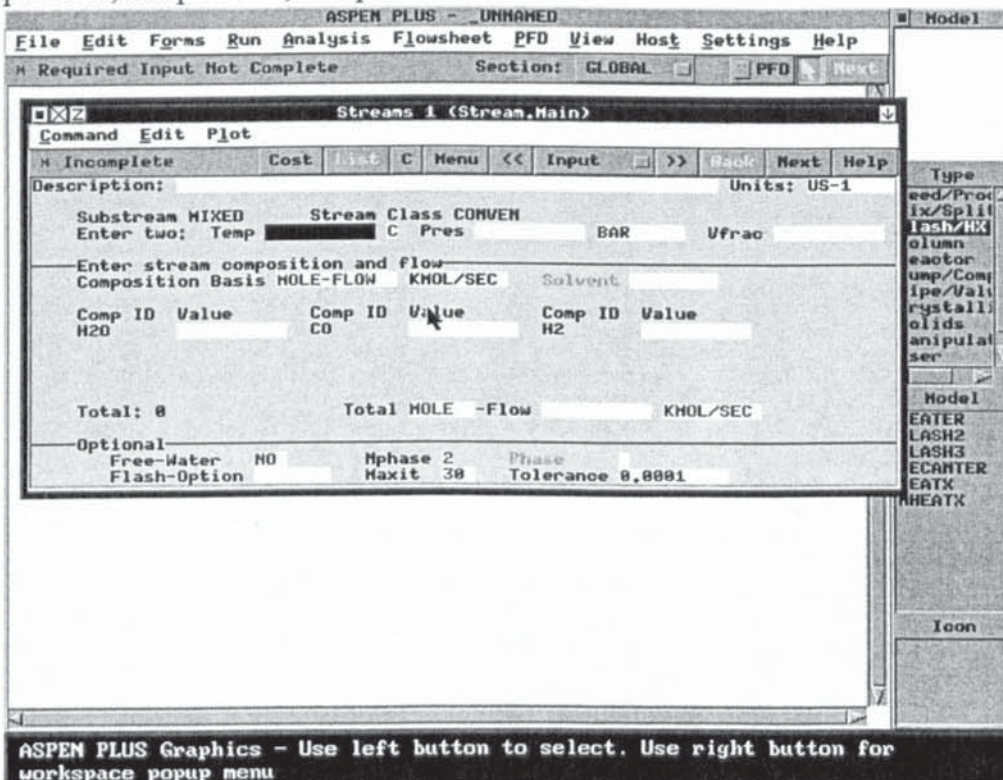


Figure A14-5

7. Unit operation blocks are defined (Figure A14-6). An example would be stream temperature out from a heat exchanger, or pressure after a pump.

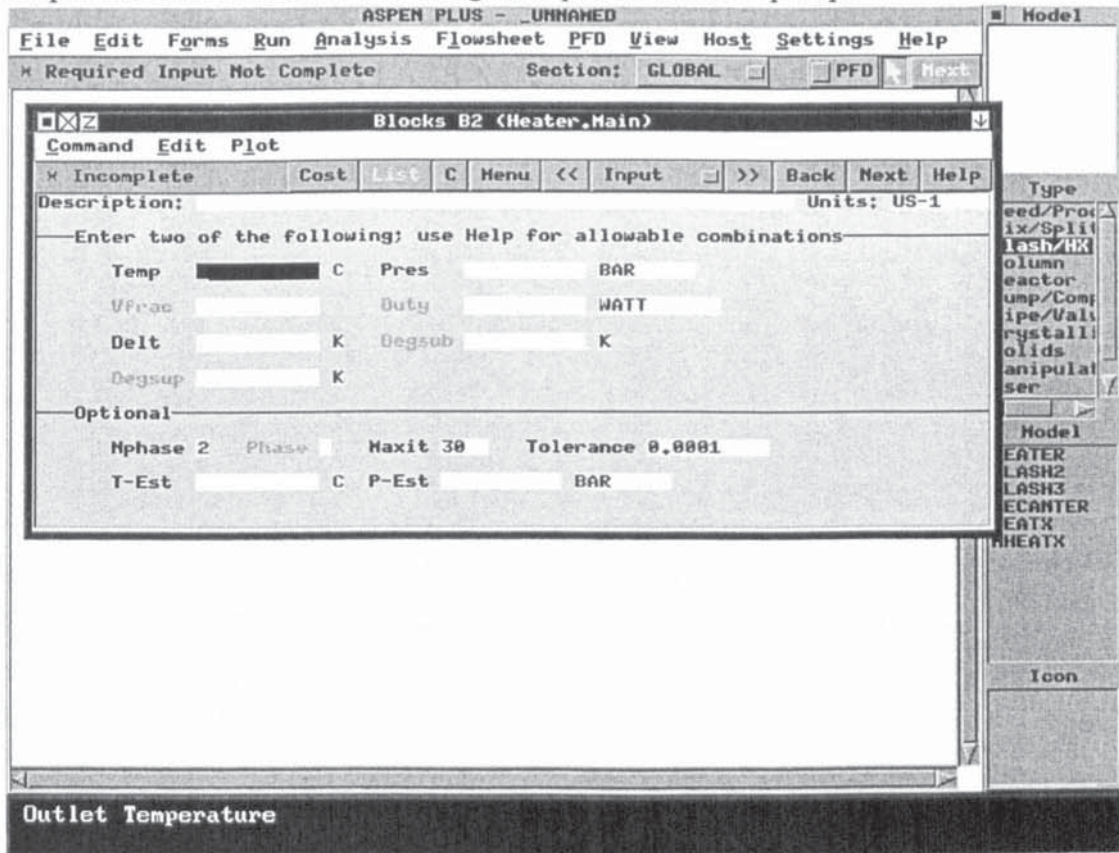


Figure A14-6

8. Impose design specifications (Figure A14-7).

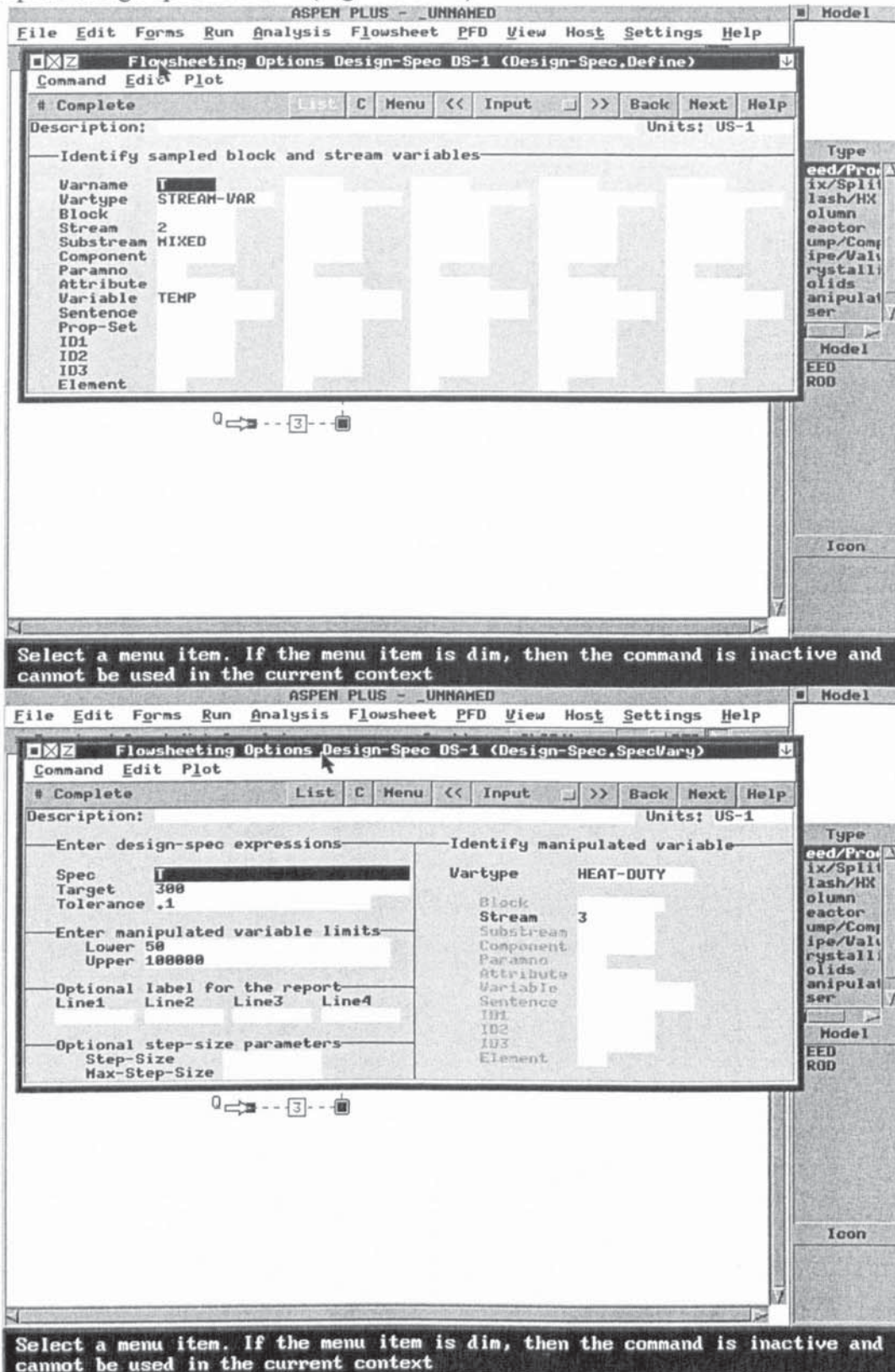


Figure A14-7

Once the connectivity and definitions are complete, calculation may be carried out (Figure A14-8).

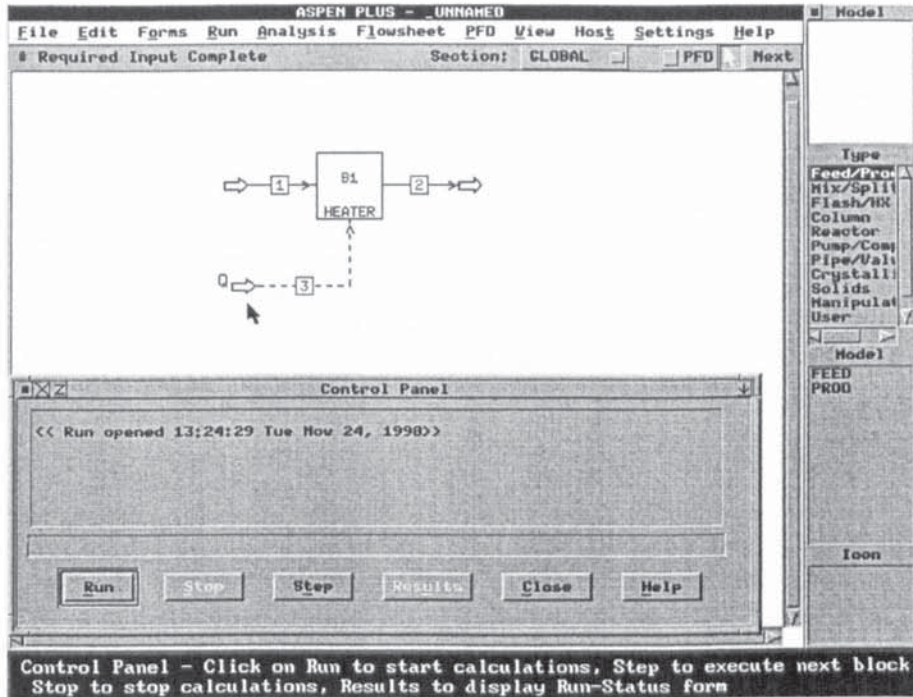


Figure A14-9

An example of running a model

An example of running a model is summarised. An Aspen flowsheet of a Rankine cycle power plant is shown in Figure A14-10. Three main sections (combustion of wood, heat recovery, and steam cycle) of the model are shown.

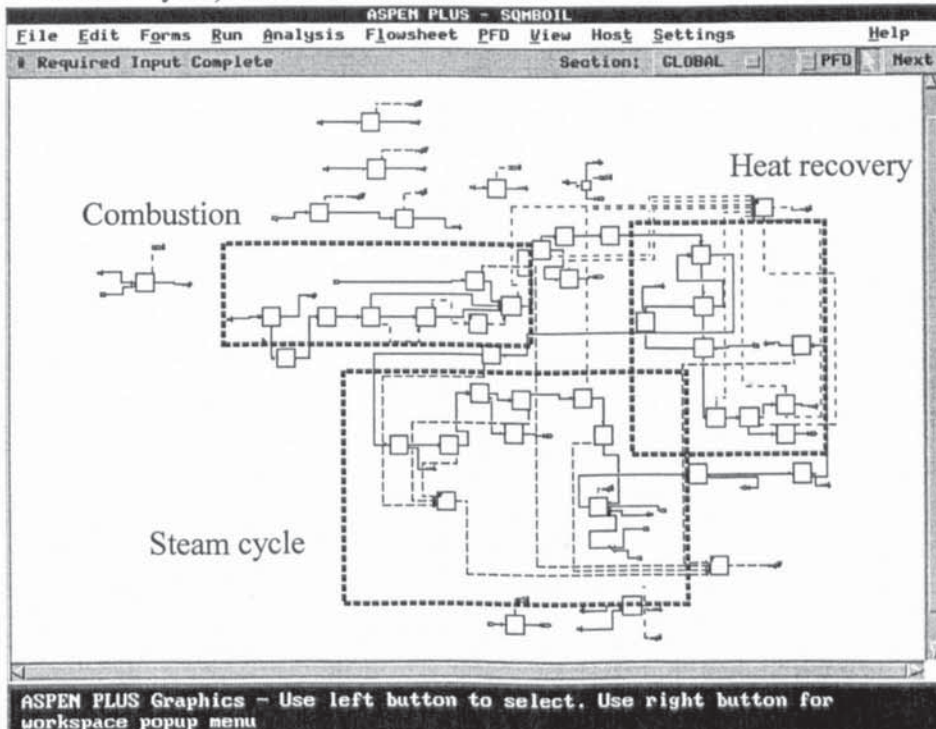


Figure A14-10

Once the model is completed, it may be run in Aspen. Aspen expert system next checks the input, and analysis it for calculation (Figure A14-11). Iterative loops are generated by Aspen.

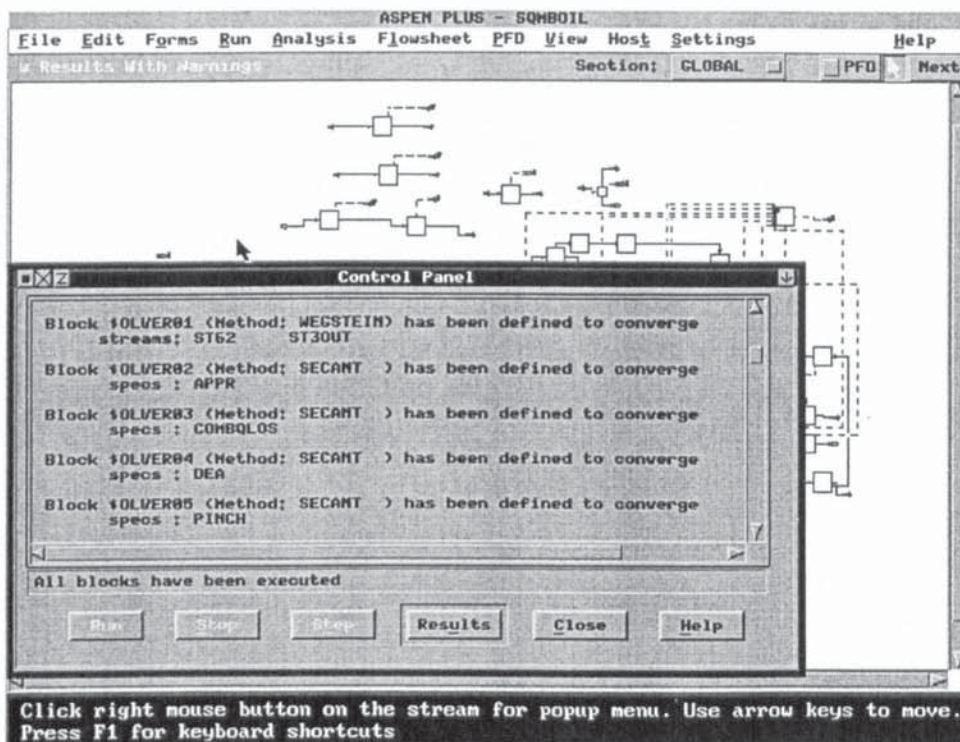


Figure A14-11

Calculation order is determined, and reported (Figure A14-12).

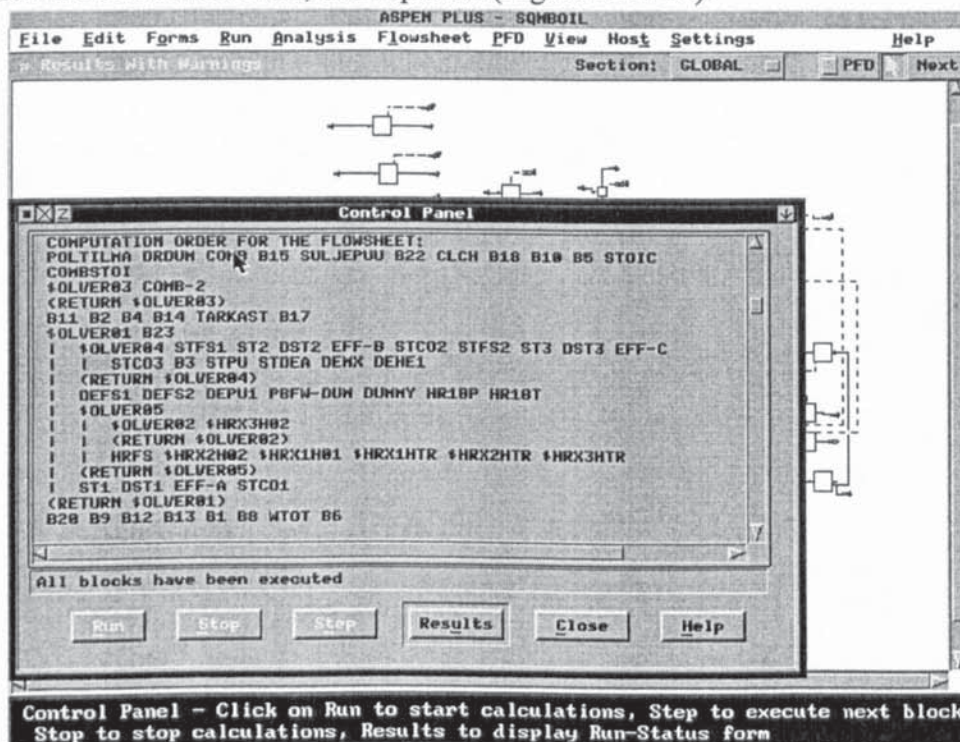


Figure A14-12

Aspen then proceeds in carrying out the simulation. A report is produced while the simulation is in progress (Figure A14-13).

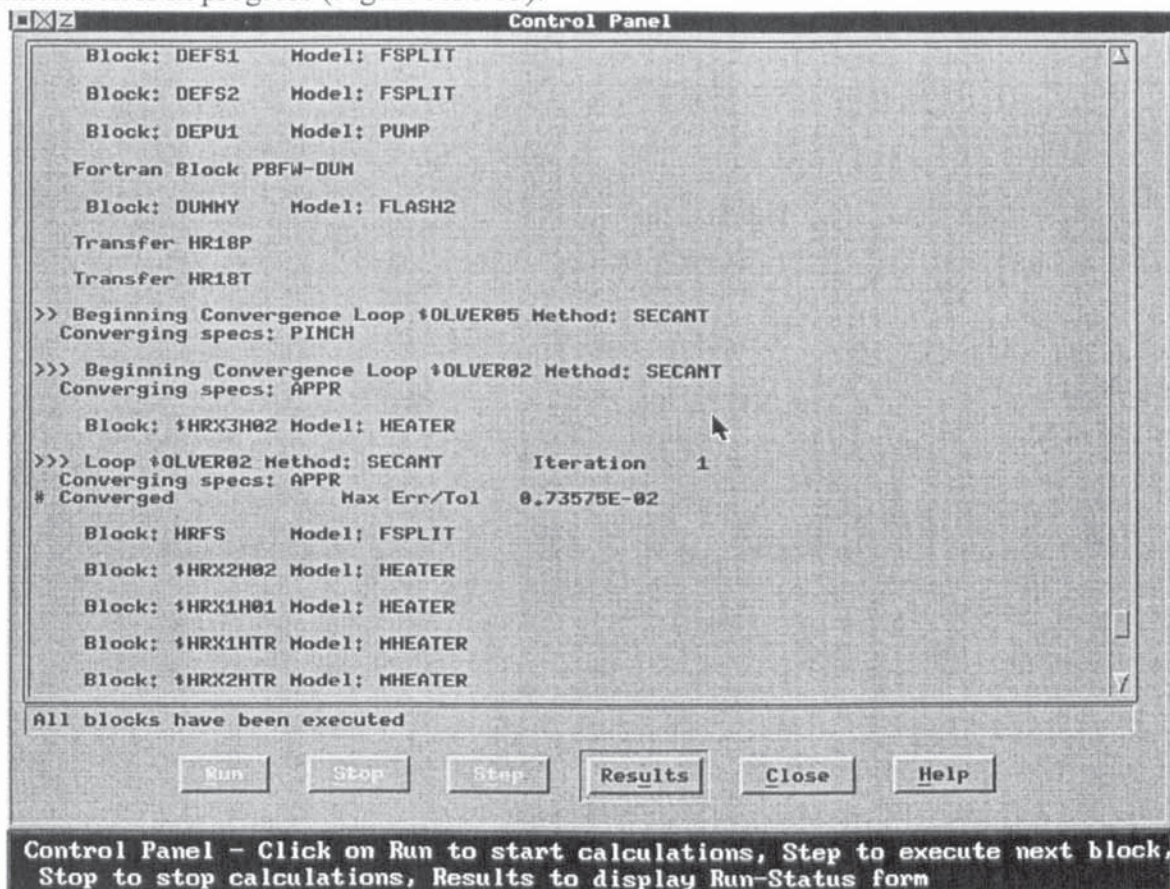


Figure A14-13

After simulation, a number of reports is produced. One fundamental report (Figure A14-14) summarises data on convergency of design-specification and tear streams.

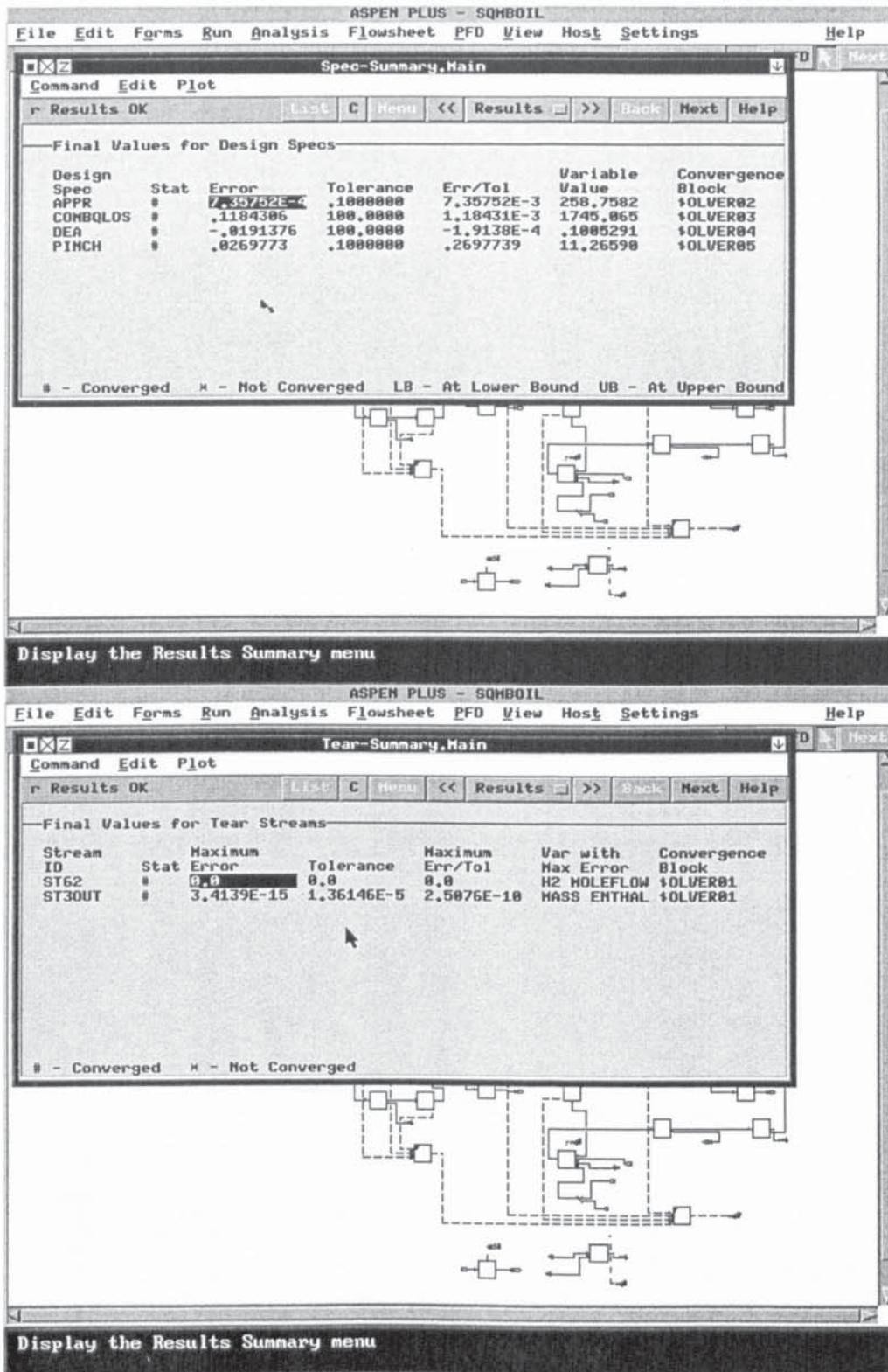


Figure A14-14

Convergency may also be studied graphically (Figure A14-15). This feature may for example be used in selecting initial values for tear streams.

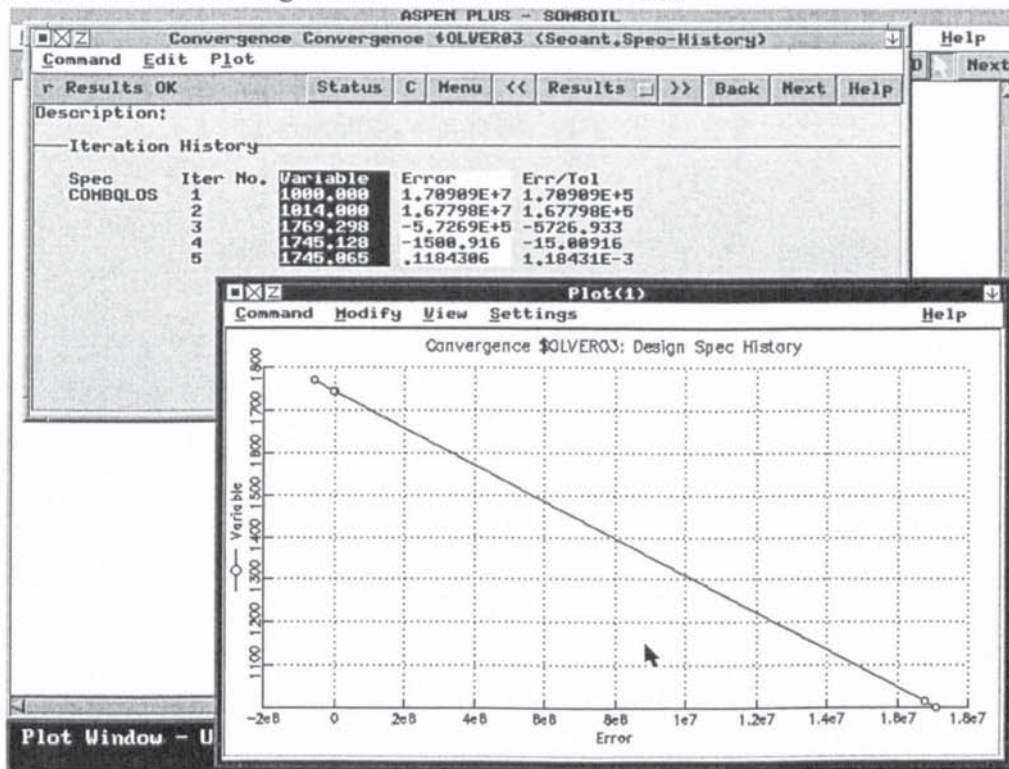


Figure A14-15

Aspen produces a full stream report, where all the flows are shown with their conditions (Figure A14-16). Block reports are also generated. An example is shown in Figure A14-17, where temperature gradients of streams in a heat exchanger are shown.

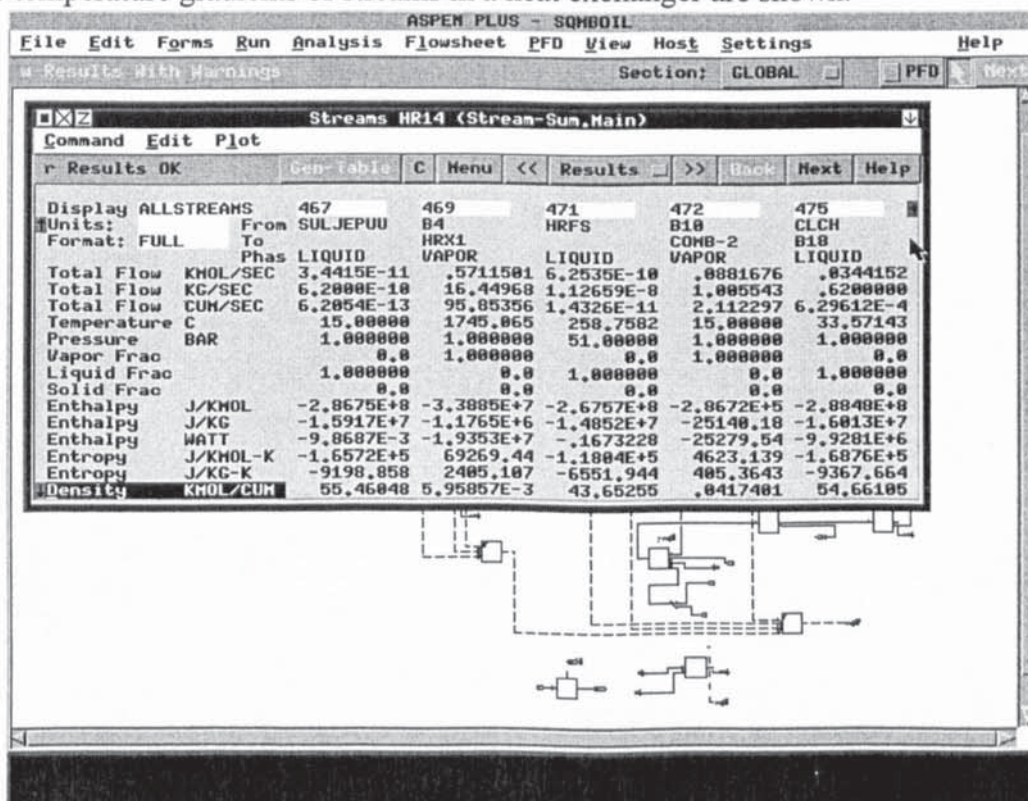


Figure A14-16

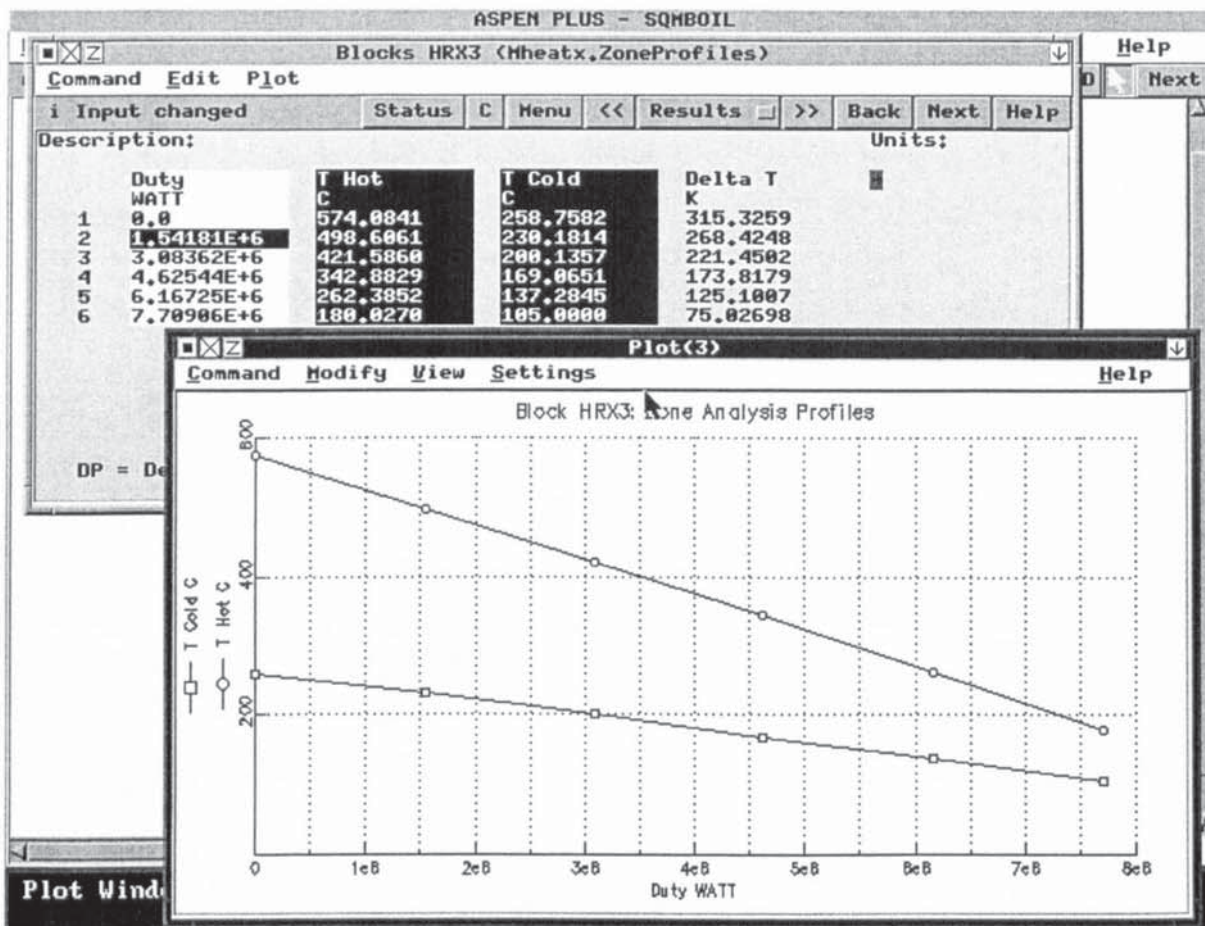


Figure A14-17

Solantausta, Y., Bridgwater, T. & Beckman, D. The performance and economics of power from biomass. In: Bridgwater, A. & Boocock, D. (eds.). Developments in thermochemical biomass conversion. London: Chapman & Hall, 1997. Pp. 1539 - 1555.

Pages removed for copyright restrictions.